frontiers | Research Topics

Targeting pulmonary endothelium in acute lung injury and acute respiratory distress syndrome

Edited by
Lulong Bo, You Shang and Guochang Hu

Published in
Frontiers in Cell and Developmental Biology
Frontiers in Pharmacology
Frontiers in Immunology

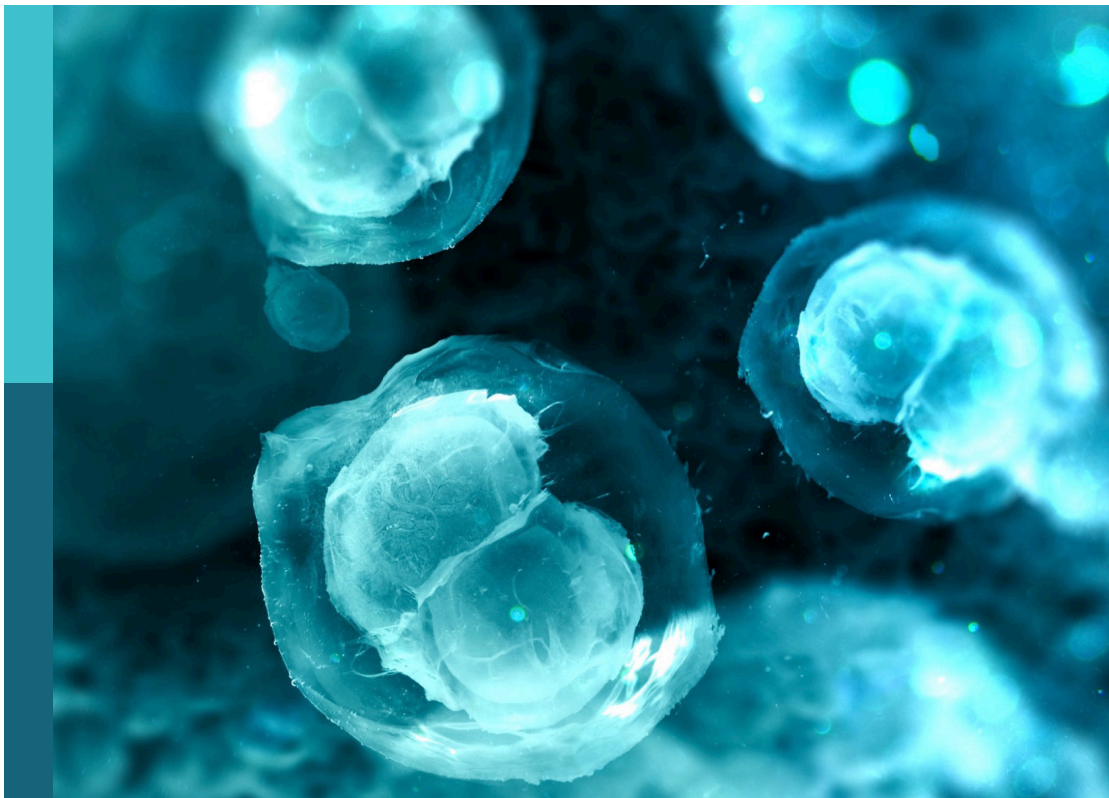

ISSN 1664-8714
ISBN 978-2-8325-7041-8
DOI 10.3389/978-2-8325-7041-8

Generative AI statement
Any alternative text (Alt text) provided alongside figures in the articles in this ebook has been generated by Frontiers with the support of artificial intelligence and reasonable efforts have been made to ensure accuracy, including review by the authors wherever possible. If you identify any issues, please contact us.

About Frontiers

Frontiers is more than just an open access publisher of scholarly articles: it is a pioneering approach to the world of academia, radically improving the way scholarly research is managed. The grand vision of Frontiers is a world where all people have an equal opportunity to seek, share and generate knowledge. Frontiers provides immediate and permanent online open access to all its publications, but this alone is not enough to realize our grand goals.

Frontiers journal series

The Frontiers journal series is a multi-tier and interdisciplinary set of open-access, online journals, promising a paradigm shift from the current review, selection and dissemination processes in academic publishing. All Frontiers journals are driven by researchers for researchers; therefore, they constitute a service to the scholarly community. At the same time, the *Frontiers journal series* operates on a revolutionary invention, the tiered publishing system, initially addressing specific communities of scholars, and gradually climbing up to broader public understanding, thus serving the interests of the lay society, too.

Dedication to quality

Each Frontiers article is a landmark of the highest quality, thanks to genuinely collaborative interactions between authors and review editors, who include some of the world's best academicians. Research must be certified by peers before entering a stream of knowledge that may eventually reach the public - and shape society; therefore, Frontiers only applies the most rigorous and unbiased reviews. Frontiers revolutionizes research publishing by freely delivering the most outstanding research, evaluated with no bias from both the academic and social point of view. By applying the most advanced information technologies, Frontiers is catapulting scholarly publishing into a new generation.

What are Frontiers Research Topics?

Frontiers Research Topics are very popular trademarks of the *Frontiers journals series*: they are collections of at least ten articles, all centered on a particular subject. With their unique mix of varied contributions from Original Research to Review Articles, Frontiers Research Topics unify the most influential researchers, the latest key findings and historical advances in a hot research area.

Find out more on how to host your own Frontiers Research Topic or contribute to one as an author by contacting the Frontiers editorial office: frontiersin.org/about/contact

Targeting pulmonary endothelium in acute lung injury and acute respiratory distress syndrome

Topic editors

Lulong Bo — Navy Medical University, China

You Shang — Huazhong University of Science and Technology, China

Guochang Hu — University of Illinois Chicago, United States

Citation

Bo, L., Shang, Y., Hu, G., eds. (2025). *Targeting pulmonary endothelium in acute lung injury and acute respiratory distress syndrome*. Lausanne: Frontiers Media SA. doi: 10.3389/978-2-8325-7041-8

Table of contents

frontiers | Frontiers in Cell and Developmental Biology

TYPE Editorial
PUBLISHED 08 October 2025
DOI 10.3389/fcell.2025.1714104

OPEN ACCESS

EDITED AND REVIEWED BY
Ana Cuenda,
Spanish National Research Council (CSIC), Spain

*CORRESPONDENCE
Lulong Bo,
bartbo@smmu.edu.cn

†These authors have contributed equally to this work

RECEIVED 27 September 2025
ACCEPTED 30 September 2025
PUBLISHED 08 October 2025

CITATION
Bo L, Shang Y and Hu G (2025) Editorial: Targeting pulmonary endothelium in acute lung injury and acute respiratory distress syndrome.
Front. Cell Dev. Biol. 13:1714104.
doi: 10.3389/fcell.2025.1714104

Editorial: Targeting pulmonary endothelium in acute lung injury and acute respiratory distress syndrome

Lulong Bo[1*†], You Shang[2†] and Guochang Hu[3,4†]

[1]Department of Anesthesiology, Changhai Hospital, Naval Medical University, Shanghai, China, [2]Department of Critical Care Medicine, Union Hospital, Tongji Medical College, Huazhong University of Science and Technology, Wuhan, Hubei, China, [3]Department of Anesthesiology, University of Illinois College of Medicine, Chicago, IL, United States, [4]Department of Pharmacology and Regenerative Medicine, University of Illinois College of Medicine, Chicago, IL, United States

KEYWORDS

acute lung injury, pulmonary endothelium, biomarker, heparin-binding protein, endothelial barrier function

Editorial on the Research Topic
Targeting pulmonary endothelium in acute lung injury and acute respiratory distress syndrome

Acute lung injury (ALI) and acute respiratory distress syndrome (ARDS) remain major causes of mortality in critical care, despite advances in mechanical ventilation and supportive care (Ma et al., 2025; Al-Husinat et al., 2025). The pulmonary endothelium, a thin, semipermeable barrier lining the pulmonary vasculature, plays a central role in the pathogenesis of ALI/ARDS. Endothelial dysfunction drives vascular leak, inflammation, and coagulation abnormalities—hallmark features of ALI/ARDS that culminate in alveolar edema and hypoxemia (Su et al., 2024; Qiao et al., 2024). This Research Topic, "*Targeting Pulmonary Endothelium in Acute Lung Injury and Acute Respiratory Distress Syndrome*," brings together 13 articles that dissect the molecular mechanisms of endothelial injury, identify novel biomarkers, and explore endothelial-targeted therapeutic strategies, addressing critical gaps in our understanding of these devastating conditions.

A central theme of this Research Topic is elucidating the diverse mechanisms driving endothelial dysfunction in ALI/ARDS, including epigenetic regulation, programmed cell death, and inflammatory signaling crosstalk. Klein underscores the pivotal role of the vascular endothelium in acute pathological conditions, while clarifying the key concepts of endothelial activation, dysfunction, and damage, along with their complex, context-dependent interactions. Cheng et al. highlight the role of histone deacetylases (HDACs)—key epigenetic regulators—in mediating endothelial–mesenchymal interactions during lung fibrosis, a frequent sequela of ARDS. They report that specific HDAC isoforms (*e.g.*, HDAC3, HDAC6) are aberrantly upregulated in pulmonary endothelial cells and fibroblasts from patients with idiopathic pulmonary fibrosis, where they activate transforming growth factor β (TGF-β)/SMAD3 signaling and promote extracellular matrix deposition. Notably, selective HDAC inhibition reduces endothelial-to-mesenchymal transition and extracellular matrix production, underscoring the therapeutic potential of epigenetic modulation in restoring endothelial homeostasis.

Complementing this epigenetic perspective, Han et al. investigate the interplay between the renin–angiotensin system (RAS) and programmed cell death in hyperbaric hyperoxic lung injury. In a rat model of hyperoxic lung injury, they demonstrate that RAS activation triggers necroptosis in type I alveolar epithelial cells, leading to secondary injury of adjacent endothelial cells. Pretreatment with RAS inhibitors reduces angiotensin I expression, suppresses necroptosis-related proteins (receptor interacting protein kinase-1/3, and mixed lineage kinase domain-like protein), and preserves endothelial barrier integrity, thereby establishing a mechanistic link between RAS-mediated cell death and endothelial dysfunction.

Xiao et al. further advance our understanding of cell death pathways by focusing on caspase-mediated pyroptosis, apoptosis, and necroptosis in ALI. Their review highlights caspase-11 (in murine) and caspase-4/5 (in humans) as critical mediators of endothelial pyroptosis in response to lipopolysaccharide (LPS). Upon activation, these caspases cleave gasdermin D (GSDMD), leading to the formation of membrane pores that compromise endothelial barrier integrity. In contrast, caspase inhibitors (*e.g.*, Ac-FLTD-CMK) or GSDMD-targeted agents (*e.g.*, disulfiram) have been shown to preserve endothelial barrier function. Complementing this, Yao et al. systematically review therapeutic strategies targeting ferroptosis in the management of ARDS, emphasizing the use of antioxidants, glutathione peroxidase 4 activators, iron chelators, and lipid peroxidation inhibitors. These interventions aim to mitigate oxidative stress overload, restore the endogenous antioxidant defense system of pulmonary cells, and inhibit iron-mediated ferroptotic cell death, thereby preserving alveolar-endothelial barrier function.

Accurate diagnosis and prognosis of ALI/ARDS remain challenging; however, studies in this Research Topic identify endothelial-derived molecules as promising biomarkers. Liu et al. investigate heparin-binding protein—a neutrophil-derived inflammatory mediator—in bronchoalveolar lavage fluid and plasma of ARDS patients. Their animal and human studies demonstrate that heparin-binding protein levels in bronchoalveolar lavage fluid are significantly elevated in ARDS compared with cardiogenic pulmonary edema and show a stronger correlation with lung injury severity than plasma heparin-binding protein. Xiao et al. further identify CMTM3 (CKLF-like MARVEL transmembrane domain-containing 3), as both a biomarker and therapeutic target. Using LPS- or hypoxia/reoxygenation-stimulated human umbilical vein endothelial cells, they demonstrate that CMTM3 expression is upregulated in injured endothelial cells, enhancing vascular permeability and interleukin (IL)-6/tissue necrosis factor (TNF)-α production. In CMTM3 knockout mice with ARDS, pulmonary vascular permeability and lung injury scores are reduced, while survival is improved—establishing CMTM3 as a critical mediator of endothelial dysfunction with diagnostic and therapeutic potential.

Translational studies in this Research Topic bridge preclinical findings to clinical practice, highlighting strategies to restore endothelial function in ALI/ARDS. Xu et al. perform a network meta-analysis of 26 clinical trials (5,071 patients) to compare the efficacy of corticosteroids, neuromuscular blocking agents, and inhaled nitric oxide—three commonly used interventions—on ARDS outcomes related to endothelial function. Their analysis revels that dexamethasone reduces new infection events (a surrogate for endothelial barrier integrity) and increases ventilator-free days, while vecuronium bromide decreases 28-day mortality, likely by reducing endothelial inflammation and oxidative stress.

In addition, studies examining other key mechanisms of endothelial dysfunction in ALI/ARDS further enhance the scope of this Research Topic. For instance, review by Xu et al. focuses on specific signaling pathways, such as phosphatidylinositol 3-kinase (PI3K)/AKT and Notch1 show that their aberrant activation disrupts endothelial junctions and increases vascular permeability. In preclinical ALI models, pharmacologic inhibition of these overactivated pathways restores endothelial integrity, offering additional therapeutic avenues.

Heat stroke is a life-threatening condition with increasing incidence and mortality driven by global warming. Wang et al. review recent advances in understanding the pathogenesis of heat stroke-induced endothelial injury, including glycocalyx degradation and cell death activation and discuss potential therapeutic approaches. They emphasize the central role of the endothelium and highlight related biomarkers with diagnostic and prognostic value.

Although the studies in this Research Topic advance our understanding of endothelial targeting in ALI/ARDS, several critical gaps remain. First, most preclinical studies rely on homogeneous endothelial cell populations or animal models that fail to recapitulate the heterogeneity of human pulmonary endothelium (Mora et al., 2025). As Yang et al. review, future work should harness single-cell RNA sequencing to delineate subtype-specific endothelial responses. Second, the long-term outcomes of endothelial-targeted therapies, such as fibrosis, and vascular remodeling, remain poorly studied; longitudinal studies are needed to determine whether restoring endothelial function reduces late-stage ARDS sequelae (Cusack et al., 2023). Finally, clinical translation of preclinical findings is limited by the absence of endothelial-specific drug delivery systems. Nanoparticle-based targeting of endothelial markers holds promise for enhancing both the efficacy and safety of existing therapies.

In conclusion, this Research Topic underscores the pulmonary endothelium as a central player in ALI/ARDS pathophysiology and a promising therapeutic target. The articles herein unravel epigenetic, cell death, and inflammatory mechanisms of endothelial dysfunction, validate novel biomarkers, and confirm the efficacy of

endothelial-targeted therapies. By bridging basic and translational research, this Research Topic offers a roadmap for advancing precision medicine strategies aimed at restoring endothelial homeostasis and improving outcomes in ALI/ARDS.

Author contributions

LB: Supervision, Writing – review and editing, Conceptualization, Writing – original draft, Project administration. YS: Validation, Conceptualization, Writing – original draft, Resources, Visualization, Writing – review and editing. GH: Supervision, Writing – original draft, Visualization, Funding acquisition, Validation, Conceptualization, Investigation, Writing – review and editing.

Funding

The author(s) declare that financial support was received for the research and/or publication of this article. GH is supported by the National Heart, Lung, and Blood Institute of the National Institutes of Health under Award Numbers R01HL152696 and R01HL173334.

Conflict of interest

The authors declare that the research was conducted in the absence of any commercial or financial relationships that could be construed as a potential conflict of interest.

Generative AI statement

The author(s) declare that no Generative AI was used in the creation of this manuscript.

Any alternative text (alt text) provided alongside figures in this article has been generated by Frontiers with the support of artificial intelligence and reasonable efforts have been made to ensure accuracy, including review by the authors wherever possible. If you identify any issues, please contact us.

Publisher's note

References

Al-Husinat, L., Azzam, S., Al Sharie, S., Araydah, M., Battaglini, D., Abushehab, S., et al. (2025). A narrative review on the future of ARDS: evolving definitions, pathophysiology, and tailored management. *Crit. Care* 29 (1), 88. doi:10.1186/s13054-025-05291-0

Cusack, R., Bos, L. D., Povoa, P., and Martin-Loeches, I. (2023). Endothelial dysfunction triggers acute respiratory distress syndrome in patients with sepsis: a narrative review. *Front. Med. (Lausanne)* 10. doi:10.3389/fmed.2023.1203827

Ma, W., Tang, S., Yao, P., Zhou, T., Niu, Q., Liu, P., et al. (2025). Advances in acute respiratory distress syndrome: focusing on heterogeneity, pathophysiology, and therapeutic strategies. *Signal Transduct. Target Ther.* 10 (1), 75. doi:10.1038/s41392-025-02127-9

Mora, M. K., Dai, Z., Petrache, I., Ventetuolo, C. E., and Lahm, T. (2025). Lung endothelial cell heterogeneity in health and pulmonary vascular disease. *Am. J. Physiol. Lung Cell. Mol. Physiol.* 328 (6), L877–L884. doi:10.1152/ajplung.00296.2024

Qiao, X., Yin, J., Zheng, Z., Li, L., and Feng, X. (2024). Endothelial cell dynamics in sepsis-induced acute lung injury and acute respiratory distress syndrome: pathogenesis and therapeutic implications. *Cell. Commun. Signal* 22 (1), 241. doi:10.1186/s12964-024-01620-y

Su, Y., Lucas, R., Fulton, D. J. R., and Verin, A. D. (2024). Mechanisms of pulmonary endothelial barrier dysfunction in acute lung injury and acute respiratory distress syndrome. *Chin. Med. J. Pulm. Crit. Care Med.* 2 (2), 80–87. doi:10.1016/j.pccm.2024.04.002

frontiers | Frontiers in Cell and Developmental Biology

TYPE Review
PUBLISHED 13 August 2024
DOI 10.3389/fcell.2024.1426508

OPEN ACCESS

EDITED BY
Kwang Won Jeong,
Gachon University, Republic of Korea

REVIEWED BY
Zhe Yang,
Wayne State University, United States
Inwha Baek,
Kyung Hee University, Republic of Korea

*CORRESPONDENCE
Dan-dan Feng,
fengdandanph@163.com
Xiao-hong Li,
li1989@csu.edu.cn

RECEIVED 01 May 2024
ACCEPTED 03 July 2024
PUBLISHED 13 August 2024

CITATION
Cheng H-p, Jiang S-h, Cai J, Luo Z-q, Li X-h and Feng D-d (2024), Histone deacetylases: potential therapeutic targets for idiopathic pulmonary fibrosis.
Front. Cell Dev. Biol. 12:1426508.
doi: 10.3389/fcell.2024.1426508

Histone deacetylases: potential therapeutic targets for idiopathic pulmonary fibrosis

Hai-peng Cheng[1,2], Shi-he Jiang[1,2], Jin Cai[1,2], Zi-qiang Luo[3,4], Xiao-hong Li[1,2]* and Dan-dan Feng[3]*

[1]Department of Pathology, The Second Xiangya Hospital, Central South University, Changsha, Hunan, China, [2]Hunan Clinical Medical Research Center for Cancer Pathogenic Genes Testing and Diagnosis, Changsha, Hunan, China, [3]Department of Physiology, Xiangya School of Medicine, Central South University, Changsha, Hunan, China, [4]Hunan Key Laboratory of Organ Fibrosis, Central South University, Changsha, Hunan, China

Idiopathic pulmonary fibrosis (IPF) is a chronic progressive disease of unknown origin and the most common interstitial lung disease. However, therapeutic options for IPF are limited, and novel therapies are urgently needed. Histone deacetylases (HDACs) are enzymes that participate in balancing histone acetylation activity for chromatin remodeling and gene transcription regulation. Increasing evidence suggests that the HDAC family is linked to the development and progression of chronic fibrotic diseases, including IPF. This review aims to summarize available information on HDACs and related inhibitors and their potential applications in treating IPF. In the future, HDACs may serve as novel targets, which can aid in understanding the etiology of PF, and selective inhibition of single HDACs or disruption of HDAC genes may serve as a strategy for treating PF.

KEYWORDS

histone deacetylase, idiopathic pulmonary fibrosis, histone acetylation, fibroblasts, HDAC inhibitors

1 Introduction

Pulmonary fibrosis (PF) is a progressive lung disease with high mortality and disability rates worldwide because other effective treatments aside from lung transplantation are unavailable (Richeldi et al., 2017). Its common manifestation is progressive lung scarring and usual interstitial pneumonia, which can lead to respiratory failure and death (Martinez et al., 2017). With the continuous spread of SARS-CoV-2, the cumulative number of infections worldwide has exceeded 130 million. PF is a potential long-term complication of coronavirus infection (Cocconcelli et al., 2021; Faverio et al., 2022). Therefore, now that the COVID-19 pandemic is controlled, PF prevention and treatment are expected to become an important global issue.

PF involves a complex interplay of genetic susceptibility, aging, and environmental factors; however, its exact etiology remains unclear. Large-scale studies have demonstrated that 75% of individuals with PF have a history of smoking and that genetic background plays a critical role in PF development (Wolters et al., 2014; Wolters et al., 2018). Epigenetic factors also contribute to PF development (Coward et al., 2009; Coward et al., 2010; Sanders et al., 2012; Yang et al., 2014; Sehgal et al., 2022). Specifically, epigenetic mechanisms alter gene expression through DNA methylation, histone modifications, and non-coding RNAs.

The HDAC-derived deacetylated chromatin is a crucial driving force behind the influence of epigenetics on the pathophysiology of PF (Korfei et al., 2022).

Several histone deacetylases (HDACs), including HDAC1, HDAC2, HDAC3, HDAC4, HDAC5, HDAC6, HDAC7, and HDAC8, play vital roles in PF progression (Shan et al., 2008; Pang and Zhuang, 2010; Huang et al., 2013; Khalil et al., 2015; Rubio et al., 2019; Zhang et al., 2020; Jeong et al., 2022; Hua et al., 2023). However, the relationship between newly discovered HDAC subtypes, such as HDAC9, HDAC10, and HDAC11, and PF progression has received little attention. Furthermore, pan-HDAC inhibitors have shown therapeutic potential in preclinical models of lung fibrosis (Zhang et al., 2013; Ye et al., 2014; Ota et al., 2015; Rao et al., 2016; Korfei et al., 2018). Selective effects on single HDACs, such as HDAC3, HDAC6, and HDAC8, may trigger an effective therapeutic response (Saito et al., 2017; Saito et al., 2019; Chen et al., 2021). However, the roles, mechanisms, and inhibitors of HDACs in PF remain unclear. Thus, this review aims to discuss the role of each HDAC subtype and its inhibitors in PF development. It serves as a basis for using HDACs as novel molecular targets and selective inhibition of single HDACs as a potential treatment for PF. Due to their unique structural and mechanistic properties, sirtuins stand apart from the other histone deacetylase classes, including HDAC1-11. Given that sirtuins do not rely on Zn^{2+} for their catalytic activity and are thus unaffected by the common Zn^{2+}-dependent HDAC inhibitors, this review will not encompass a discussion on the sirtuin family members.

2 Overview of HDACs

Transcription regulation in eukaryotes occurs in the chromatin environment and is deeply influenced by posttranslational modifications of histones, such as methylation, phosphorylation, and acetylation (Attwood et al., 2002; Kim et al., 2022). The steady state of acetylation depends on the balance between histone acetyltransferases and HDACs. HDACs contain 18 genes and are classified as I–IV based on their respective yeast homologs. Classes I, II, and IV form the "classic" HDACs, which include 11 family members, namely, HDAC1–11. Class III, called sirtuins, consists of seven family members, namely, SIRT1–7. HDAC1–11 require zinc (Zn^{2+}) for catalysis, whereas SIRT1–7 relies on oxidized nicotinamide adenine dinucleotide (Haberland et al., 2009; Witt et al., 2009). The Zn^{2+}-dependent HDACs (Classes I, II, and IV) are recognized as "classical HDACs" and common targets for therapy. However, sirtuins are structurally and mechanistically distinct from these Zn^{2+}-dependent HDAC classes and are not inhibited by the widely used Zn^{2+}-dependent HDAC inhibitors. As a result, the Class III sirtuins and their inhibitors are not in the scope of this review.

Class I HDACs, including HDAC1–3 and HDAC8, are mainly located in the nucleus and are widely expressed in various tissues. The deacetylation of nucleosomal histones by Class I HDACs is primarily carried out through the formation of enzymatically active complexes (Xu et al., 2007; Sanaei and Kavoosi, 2019). Class II HDACs, including HDAC4–7, HDAC9, and HDAC10, are located in the cytoplasm but can shuttle to the nucleus (Xu et al., 2007; Sanaei and Kavoosi, 2019). HDAC11, the sole representative of Class IV enzymes, is expressed in various tissues such as the brain, heart, kidney, testis, and skeletal muscle, where it is primarily localized in the nucleus. Notably, HDAC11 stands out for its exceptional catalytic efficiency as a fatty acid acylase, harboring a catalytic activity center that is shared by both Class I and Class II enzymes (Chen et al., 2022). HDAC proteins in the histone deacetylase family share a common ancestor, resulting in similar 3D structure, function, and sequence homology. HDAC typically has a 350-amino-acid core domain with two conserved isoforms: the N-terminal and central domains. In contrast, the C-terminal domain is more diverse. The HDAC domain contains catalytic sites, like zinc ions and arginine residues, essential for its activity (Figure 1). Moreover, HDAC can form complexes with regulatory proteins and transcription factors (Wang et al., 2016).

3 Roles of HDACs in PF development

3.1 Class I HDACs in PF

3.1.1 HDAC1 and HDAC2

The human HDAC1 gene is located on chromosome 1p34, whereas the mouse HDAC1 gene is located on chromosome 4D2. The HDAC1 protein comprises 482 amino acids (de Ruijter et al., 2003). The human HDAC2 gene is located on chromosome 6q21, whereas the mouse HDAC2 gene is located on chromosome 10B1. HDAC1 and HDAC2 share 85% global sequence identity (Segré and Chiocca, 2011). Moreover, they share similar structures and many binding partners in macromolecular complexes (Brunmeir et al., 2009; Segré and Chiocca, 2011). The nuclear localization of HDAC1 and HDAC2 suggests that their primary role is regulating gene expression (Johnstone, 2002). HDAC1 and HDAC2 mediate lysine deacetylation within histone tails. This process enhances the affinity of histones for the negatively charged DNA backbone, effectively suppressing transcription by impeding the access of transcriptional machinery and transcription factors to gene promoter regions. This phenomenon has led to the classical understanding of the role of HDAC1 and HDAC2 in suppressing transcription. Furthermore, the expression levels of HDAC1 and HDAC2 are significantly elevated in fibrotic lesions of idiopathic pulmonary fibrosis (IPF) lung tissues and primary IPF fibroblasts (Korfei et al., 2015). This finding has also been demonstrated in numerous rodent models of PF (Huang et al., 2013; Li et al., 2017). Several studies have reported the antifibrotic properties of HDAC inhibitors. Primary IPF fibroblasts treated with the pan-HDAC inhibitor LBH589 and the Class I HDAC inhibitor valproic acid (VPA) can considerably reduce the profibrotic and antiapoptotic phenotypes owing to the regulatory effect of Class I HDACs, such as HDAC1, HDAC2, and/or HDAC3, on the expression of various key molecules that are antiapoptotic and profibrotic in lung fibroblasts (Korfei et al., 2015). Furthermore, LBH589 inhibits HDACs and inactivates HDAC1 and HDAC2 via significant proteolysis, which abrogates profibrotic STAT3 phosphorylation and activates downstream signaling pathways, consequently decreasing cell proliferation, survivin expression, and the expression of genes associated with extracellular matrix (ECM) in IPF fibroblasts (Korfei et al., 2018). Meanwhile, the HDAC inhibitor suberoylanilide hydroxamic acid induces the apoptosis of primary myofibroblasts, decreases

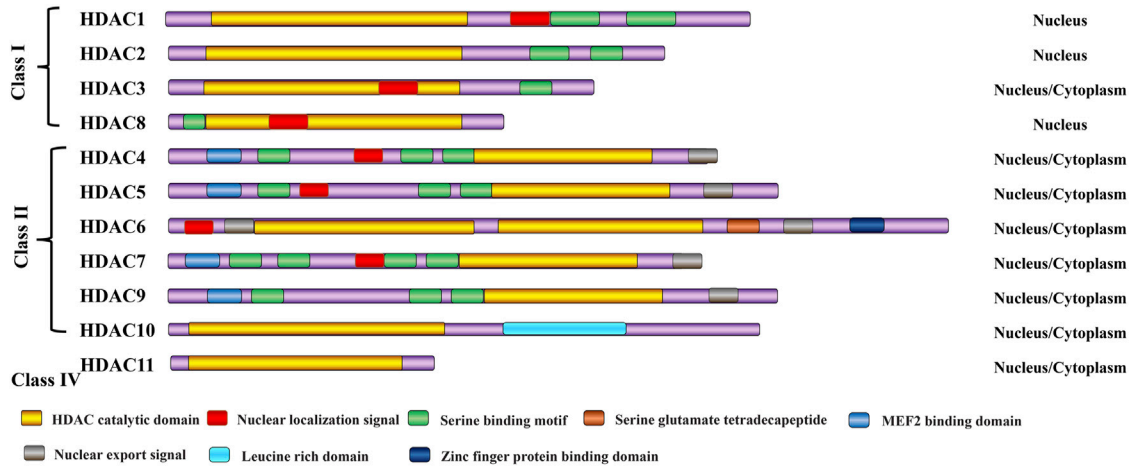

FIGURE 1
Classification of HDAC enzymes. All HDAC proteins of the histone deacetylase family share a common ancestor, resulting in similar 3D structure, function, and sequence homology. H3/H4: histone H3/H4; Ac: acetylation.

bleomycin (BLM)- stimulated murine model lung fibrosis, and improves lung function by modifying the susceptibility of myofibroblasts to apoptosis (Sanders et al., 2014). The proliferation of IPF fibroblasts is effectively reduced, and the expression of interstitial collagen is suppressed *in vitro* through the selective inhibition of spiruchostatin A, which exhibits a distinct activity profile toward Class I HDACs (Davies et al., 2012). Profibrotic signaling through STAT3 phosphorylation and activation is associated with epigenetic alterations while inducing cell cycle arrest and apoptosis in IPF fibroblasts (Korfei et al., 2018), and it may be enhanced by the lysine deacetylation of STAT3 depending on HDAC1, HDAC2, and HDAC3 (O'Shea et al., 2005; Gupta et al., 2012). Consistently, BG45 is a novel Class I HDAC inhibitor that participates in the activation of the JAK2/STAT3 pathway (Tang et al., 2018). Taken together, these studies indicate that the upregulation of HDAC1 and HDAC2 expression is linked to survivin expression, cell proliferation, myofibroblast transformation, and ECM-associated genes in IPF fibroblasts.

3.1.2 HDAC3

The human HDAC3 gene is located on chromosome 5q31, whereas the mouse HDAC3 gene is located on chromosome 18B3 (de Ruijter et al., 2003). The predicted amino acid sequence of HDAC3 comprises a 49 kDa molecular mass open reading frame, encompassing 428 amino acids (Yang et al., 2002). However, information about the role of HDAC3 in IPF is limited. Korfei et al. found that HDAC3 expression is significantly upregulated in alpha-smooth muscle actin (α-SMA) positive-expressing myofibroblasts and ciliated bronchial cells in IPF (Korfei et al., 2015). Recent studies have highlighted that microenvironmental signals, particularly stiffness, in progressive fibrosing interstitial lung diseases serve as media to integrate the contribution of epigenetics to direct persistent fibroblast activation (Toscano-Marquez et al., 2023). Matrix stiffness reduces nuclear HDAC3 expression in fibroblasts, resulting in chromatin opening and hyperacetylation. This phenomenon consequently upregulates the expression of profibrotic genes, including *Col1A1*, *α-SMA*, and *p21* (Toscano-Marquez et al., 2023). Additionally, HDAC3 promotes epithelial–mesenchymal transition (EMT), inflammation, and PF development by activating Notch intracellular domain one and signal transducer and activator of transcription one signaling to upregulate the expression of inflammasome components, including AIM2 and ASC (Zheng et al., 2022). Aberrant HDAC3 elevation and its suppression of Nrf2 decrease the expression of catalase and superoxide dismutase 3, leading to an insufficient capacity of antioxidant stress and antifibrosis capacities and consequently promoting PF progression (Chen et al., 2021). HDAC3 regulates the hypoxia-induced EMT in response to the increasing of hypoxia-inducible factor-1α via the AKT signaling pathway and HDAC3-miR224-FOXA1 axis, enhancing the migratory and invasive properties of fibroblasts (Jeong et al., 2022). HDAC3 upregulates the expression of miR-19a-3p-mediated interleukin 17 receptor A. This phenomenon downregulates the expression of fibrosis marker genes, such as COL1A1, COL3A1, and FN, which facilitate the development of rheumatoid arthritis-associated interstitial lung disease or fibrosis (Yuan et al., 2020). Recent studies have shown that increased expression of histone deacetylase three in alveolar type 2 epithelial cells promotes EMT and PF progression. This process is associated with the activation of the TGF-β1/SMAD3 signaling pathway (Xiong et al., 2023). Taken together, these findings indicate that the abnormal overexpression of HDAC3 in fibroblasts/myofibroblasts plays a crucial role in mediating fibrogenic signaling, particularly in IPF, and can be mitigated by the targeted inhibition of HDAC3.

3.1.3 HDAC8

The human HDAC8 gene is located on chromosome Xq13, whereas the mouse HDAC8 gene exists on chromosome XD (de Ruijter et al., 2003). HDAC8 consists of 377 amino acids (Buggy et al., 2000). The expression of HDAC8 increases in IPF lung cell types, such as fibroblast foci, smooth muscle cells, and vascular smooth muscle cells (Korfei et al., 2015). Furthermore, HDAC8 is expressed in the cytoplasm and nucleus of the aforementioned cell

types (Korfei et al., 2015). However, little is known about the role of HDAC8 in PF. Previous studies found that HDAC8 most efficiently influences the formation of the SMA cytoskeleton and the contractility of smooth muscle cells (Waltregny et al., 2004; Waltregny et al., 2005). Zhao et al. have recently reported that treatment with the HDAC8 selective inhibitor PCI34051 and knockdown of HDAC8 expression mitigate cardiac fibrosis by inhibiting the tumor growth factor (TGF)-β1/Smad2/3 pathway in rat cardiac fibroblasts (Zhao et al., 2022). Notably, silencing HDAC8 can significantly inhibit the activation of the TGF-β signaling pathway and suppress ACTA2 expression in human skin fibroblasts (Glenisson et al., 2007). Moreover, the selective inhibition of HDAC8 has recently been verified as an effective therapeutic schedule in BLM-induced PF (Saito et al., 2019). Shigeki et al. reported that the specific deacetylation of structural maintenance of chromosomes protein three by HDAC8 induces the inhibition of antifibrotic PPARγ-signaling, production of ECM proteins, and formation of stress fiber in TGF-β-stimulated IPF fibroblasts. This process can be abrogated by silencing HDAC8 with RNAi or using the HDAC8 selective inhibitor NCC170 (Saito et al., 2019). These studies suggest a need for further research on HDAC8 as a risk factor for fibrotic lung disease. A novel two-stage screen platform has recently been reported to accelerate the development of HDAC6, HDAC8, or dual HDAC6/8 inhibitors, which can alleviate PF progression in various animal models (Yu et al., 2023).

In conclusion, these studies consistently demonstrate the potent antifibrotic effect of Class I selective HDAC inhibitors in PF. This evidence further highlights the key role of Class I HDACs in mediating profibrotic signal transduction in progressive fibrosing interstitial lung diseases.

3.2 Class II HDACs in PF

3.2.1 HDAC4

The human HDAC4 gene, which comprises 1084 amino acids, is located on chromosome 2q37, whereas the mouse HDAC4 gene exists on chromosome 1D1 (Wang et al., 2014). The localization of HDAC4 is shuttling between cytoplasm and nucleus based on the state of phosphorylation; for instance, dephosphorylated HDAC4 is translocated to the nucleus (Wu et al., 2016).

Aberrant expression of HDAC4 drives fibrogenesis via the HDAC4-miR-206-MRTF-A axis in hepatic stellate cells (Han et al., 2017). Furthermore, the pan-HDAC inhibitor trichostatin A inhibits TGF-β1-mediated fibroblast-myofibroblast transdifferentiation, and this process is dependent on the cytoplasmic localization of HDAC4 and requires the phosphorylation of Akt but not SMAD2/3 (Guo et al., 2009). Silencing HDAC4 efficiently abrogates the TGF-β-induced differentiation of fibroblasts into myofibroblasts by enhancing endogenous repressors of the TGF-β signaling pathway instead of Smad7 (Glenisson et al., 2007). Additionally, TGF-β increases NADPH oxidase 4-derived reactive oxygen species production and promotes HDAC4 nucleus-to-cytoplasm translocation, exerting profibrotic effects by promoting fiber formation and enhancing cell contraction in lung fibroblasts (Guo et al., 2017). Moreover, silencing HDAC4 upregulates miR-29 expression, which reduces the expression of activation markers α-SMA, lysyl oxidase, and collagens (both type I and type III) in fibrotic mesenchymal cells and inhibits cell proliferation (Mannaerts et al., 2013). HDAC4 shows a complex distribution in various types of IPF bronchiolar cells, such as basal cells of hyperplastic (in the cytoplasm) or luminal ciliated bronchial cells (in the nucleus) (Korfei et al., 2015). These results indicate that HDAC4 is widely expressed in IPF fibroblasts and shows an array of intracellular signal transduction pathways, including but not limited to HDAC4/AKT/α-SMA, HDAC4/TGIF/α-SMA, and HDAC4/NOX4/α-SMA, depending on its subcellular localization.

3.2.2 HDAC5

The human HDAC5 gene is located on chromosome 17q21, whereas the mouse HDAC5 gene exists on chromosome 11D11 (Verdel and Khochbin, 1999). HDAC5, with a molecular weight of 121.9 kDa, comprises 1122 amino acids and consists of C-terminal deacetylase and N-terminal adapter domains (Yang et al., 2021).

Currently, the role and function of HDAC5 in lung fibrosis are poorly understood. Korfei et al. showed that the expression of Class I and II HDACs, including HDAC5, is increased significantly in fibroblast foci and abnormal bronchiolar epithelium (Korfei et al., 2015). Aberrant down-expression of HDACs, especially HDAC2, HDAC5, and HDAC8, regulates the production of proinflammatory cytokines in alveolar macrophages in patients with chronic obstructive pulmonary disease (Ito et al., 2005). HDAC5 knockdown significantly inhibits the phosphorylation of Smad2/3 but upregulates Smad7 expression in TGF-β1-stimulated fibroblasts. This process relies on the interaction with myocyte enhancer 2A (Gao et al., 2022). Chromatin immunoprecipitation studies showed that nuclear factor erythroid 2-related factor 2 is an important antifibrotic gene and that its suppression state can be restored by HDAC inhibitor treatment in fibroblasts (Sanders et al., 2011). Increased HDAC5 expression in pathological cardiomyocyte hypertrophy decreases cardiomyocyte oxidative stress and represses NRF2 activation (Hu et al., 2019). Moreover, the downregulation of HDAC5 expression upregulates α-SMA expression in TGF-β1-induced IPF fibroblasts (Jones et al., 2019). Taken together, these studies showed that HDAC5 promotes the activation of fibroblasts and production of fibrotic factors; however, its role in IPF remains to be evaluated in experimental fibrosis.

3.2.3 HDAC6

The human HDAC6 gene is located on chromosome Xp11, whereas the mouse HDAC6 gene exists on chromosome XA1. HDAC6 is the largest HDAC protein, with 1216 amino acids (Grozinger et al., 1999). It is a unique HDAC enzyme composed exclusively of two functional N-terminal catalytic domains and a C-terminal binding domain (Li et al., 2011).

HDAC6 is generally located in the cytoplasm but can shuttle into the nucleus. It is a cytoplasmic and cytoskeleton-associated HDAC that regulates the deacetylation of peroxiredoxin, β-catenin, and heat shock protein 90 (Parmigiani et al., 2008; Li et al., 2013; Liu et al., 2021). PRDX1 deficiency enhances EMT, lung fibroblast proliferation, and fibrosis progression through the PI3K/Akt and JNK/Smad signaling pathways (Sun et al., 2023). Heat shock protein 90 contributes to the TGF-β signaling activation-induced ECM synthesis causing fibrosis, increased inflammatory response, and

lung impairment (Štorkánová et al., 2021; Roque, 2022). Remarkable HDAC6 upregulation and α-tubulin deacetylation occur in primary IPF fibroblasts (Korfei et al., 2015). HDAC6 expression is also significantly upregulated, along with a significant degree of α-tubulin deacetylation, in TGF-β1-stimulated fibroblasts (Saito et al., 2017). HDAC6 inhibitors (trichostatin A [TSA]), TSA is classified in Class 1/2 or pan HDAC inhibitor, are innovative and targeted disease-modifying agents in rare diseases, including IPF (Brindisi et al., 2020). Campiani et al. also reported that novel hHDAC6 inhibitors (6a-m) can effectively inhibit fibrotic sphere formation and cell viability, reversing the IPF phenotype (Campiani et al., 2021). In summary, these results suggest that HDAC6 overexpression in lung fibroblasts induces PF.

3.2.4 HDAC7

The human HDAC7 gene is located on chromosome 12q13 and encodes a polypeptide of 912 amino acids, whereas the mouse HDAC7 gene is found on chromosome 15F1 and shares 95% similarity of amino acid sequence with human HDAC7 (Fischle et al., 1999; Fischle et al., 2001).

Recently, HDAC7 has been viewed as a key risk factor in enhancing the TGF-β-mediated transdifferentiation of fibroblasts into myofibroblasts during PF progression. Dakota et al. demonstrated that silencing HDAC7 significantly decreases the expression of profibrotic mediators NOX4 and CTGF but increases the expression of PGC1A in TGF-β-induced IPF fibroblasts (Jones et al., 2019). Additionally, HDAC7 knockdown can effectively inhibit SMAD signaling activation, fibroblast-myofibroblast transdifferentiation, and ECM production in TGF-β induced fibroblasts (Kang et al., 2018). HDAC7 could play a key role in airway fibrosis, which consists of p300 and AP-1 to form the transcriptional complex and increase CTGF expression in lung fibroblasts (Hua et al., 2021). Darren et al. reported that HDAC7 plays a vital role in cystic fibrosis by influencing the function of the cystic fibrosis transmembrane conductance regulator in human primary airway epithelia (Hutt et al., 2010). Silencing HDAC-7 significantly decreases the production of collagen-I, collagen-III, and profibrotic mediators ICAM-1 and CTGF in TGF-β-treated skin fibroblasts (Hemmatazad et al., 2009). Taken together, these findings suggest that HDAC7 plays a crucial role in the aberrant expression of profibrotic molecules during fibrogenesis.

3.2.5 HDAC9

The human HDAC9 is located on human chromosome 7p21, whereas the mouse HDAC9 gene exists on chromosome 12A3 (Zhou et al., 2001). The HDAC9 protein is composed of 1069 amino acids and can be subjected to alternative splicing to form at least 29 variant isoforms (Mahlknecht et al., 2002; Brancolini et al., 2021).

HDAC9 is important in the human physiological system and is involved in the development of various diseases, such as cancer, diabetes, atherosclerosis, cardiovascular diseases, and liver fibrosis (Das et al., 2023). Zhang et al. demonstrated that HDAC9 expression increases in mouse and human fibrotic kidneys, where it deacetylates STAT1, while promoting G2/M phase arrest and activating fibroblasts. Macrophage accumulation, G2/M phase arrest, and ECM protein production play crucial roles in this process, and treatment with the high-affinity HDAC9 inhibitor TMP195 can effectively alleviate the above phenomena (Zhang et al., 2023). These studies show that HDAC9 is a powerful target for developing novel treatment methods for organ fibrosis. Currently, the functions of HDAC9 in PF remain unclear. HDAC9 is located in the cytoplasm but can shuttle to the nucleus, and its expression is significantly increased in the cytoplasm of lung myofibroblasts. Immunohistochemical analysis revealed that HDAC9 expression regulates vascular smooth muscle cells and is significantly upregulated in IPF (Korfei et al., 2015). Silencing HDAC9 remarkably increases the expression levels of ACTA2 in TGF-β-induced IPF fibroblasts (Jones et al., 2019). Moreover, HDAC9 and isoform HDAC-related proteins play important roles in the transdifferentiation of fibroblasts into myofibroblasts and cell apoptosis resistance in lung fibroblasts. These studies suggest that HDAC9 plays crucial roles in lung fibrosis; however, further research is warranted to specify these roles.

3.2.6 HDAC10

The human HDAC10 gene is located on chromosome 22q13, whereas the mouse HDAC11 gene exists on chromosome 15E3 (de Ruijter et al., 2003). HDAC10 is composed of 20 exons, including the N-terminal catalytic domain and the C-terminal domain rich in leucine, and 669 amino acids (Cheng et al., 2021). It is widely expressed in human tissues and cultured mammalian cells, including the liver, kidney, pancreas, spleen, heart, and lungs (Tong et al., 2002).

The Class IIB member HDAC10 is pancellular. Zhang et al. demonstrated that HDAC10 plays an important role in asthma-induced eosinophil airway inflammation (Zhang et al., 2016). It is also a potential pathogenic gene for emphysema (Choi et al., 2009). Thus, HDAC10 may be a potential therapeutic target for treating respiratory system diseases. Immunohistochemical analysis has shown that HDAC10 is highly expressed in myofibroblasts within fibroblast foci in IPF (Korfei et al., 2015). Surprisingly, silencing HDAC10 with RNAi has shown no significant effect on the expression of profibrotic genes, such as α-SMA and collagen-I, in TGF-β1-stimulated fibroblasts (Saito et al., 2017). Furthermore, Tian et al. demonstrated that the upregulation of HDAC10 expression can significantly improve PF and lung function in silicosis by attenuating oxidative stress, inflammation, and fibrotic lesions via the ROS/NF-κB pathway (Tian et al., 2023). However, the effects of HDAC10 overexpression in IPF fibroblasts need further investigation.

In summary, the potential effects of significantly upregulated expression of all six Class II HDACs in fibroblasts remain poorly elucidated. Studies using Class II HDAC selective inhibitors in various experimental models of PF have contributed to further understanding of the functions of overexpressed Class II HDACs in fibrotic lung fibroblasts. Novel inhibitors targeting HDAC6 are promising drugs for treating IPF.

3.3 Class IV HDACs in PF

3.3.1 HDAC11

Since its first discovery in 2002, HDAC11 is the smallest and unique member of the HDAC family (Yanginlar and Logie, 2018).

The human HDAC11 gene is located on chromosome 3p25, whereas the mouse HDAC11 gene exists on chromosome 6D1 (de Ruijter et al., 2003). HDAC11 has 347 amino acids and similar sequences to the catalytic core regions of Class I and II HDAC proteins (Gao et al., 2002; Thangapandian et al., 2012). HDAC11 is expressed in several organs and tissues. It is mainly distributed in the heart, kidneys, smooth muscles, skeletal muscles, and testes (Chen et al., 2022). Immunoblot analyses revealed robust HDAC11 upregulation in IPF *versus* control fibroblasts (Korfei et al., 2015). However, reports on the mechanism by which HDAC11 influences PF development are rare. Notably, HDAC11 suppresses the transcription of Kruppel-like factor 15 by activator protein two to mitigate unilateral ureteral obstruction-induced renal fibrosis (Mao et al., 2020). Further, the upregulation of HDAC11 is involved in the mechanisms by which glucocorticoid relieves allergen-driven airway inflammation in mice (Zhang et al., 2016). Taken together, these studies suggest that little is known about the functions of HDAC11 in IPF and that further attention is needed in the future.

4 Potential regulatory network of HDACs involved in PF

IPF is a fatal lung disease of unknown etiology and is viewed as an epithelial-driven disease. Specifically, aging alveolar epithelial cells, which are dysfunctional and constantly subjected to microinjuries, experience regenerative defects due to these persistent insults. This triggers abnormal interactions between the damaged epithelium and mesenchymal cells, ultimately causing an imbalance in the levels of pro-fibrotic and antifibrotic mediators. This imbalance inhibits the natural repair mechanisms for chronic fibrosis, fostering an environment that encourages excessive proliferation and hyperactivity of fibroblasts and myofibroblasts, thus affecting the normal repair process of chronic fibrosis (Stella and Balestro, 2015; Spagnolo et al., 2021). The profound biological complexity of IPF lies in the diverse array of cell types and signaling pathways that are intricately intertwined with the disease's pathogenesis. These mechanisms include, but are not limited to, the dysregulation of epithelial repair functions, imbalance in host defense mechanisms, accelerated cellular senescence, skewed immune responses (particularly the abnormal activation of macrophage subsets), fibrogenic reactions closely linked to abnormal kinase activation, transforming growth factor-β (TGF-β) and its downstream profibrotic signaling cascades, and reactivation of developmental pathways. These biological processes collectively contribute to the onset and progression of IPF.

Within the realm of IPF, a critical function in fibrosis progression is played by the aberrant overexpression of Class I HDACs in fibroblasts and myofibroblasts. This abnormal expression is intricately linked to the activation of the TGF-β/SMAD2/3 signaling cascade and its downstream pathways, resulting in fibroblasts acquiring enhanced apoptosis resistance and transforming into myofibroblasts. During this transformation, a substantial amount of ECM, primarily represented by Col1A1 and α-SMA, is synthesized. Concurrently, the activation of the TGF-β1/SMAD3 and HIF-1 signaling pathways expedites the EMT of alveolar type 2 epithelial cells, thereby advancing the progression of lung fibrosis. Notably, in IPF fibroblasts, both the fibrotic-inducing activation of STAT3 and its lysine deacetylation exhibit a remarkable upregulation (Figure 2A). Compared to normal lung tissue, the myofibroblasts within the fibrotic lesions of IPF have significantly upregulated the protein levels of Class II HDACs. Under the stimulation of TGF-β, the lung fibroblasts enhance their a-SMA fiber formation and cell contractile ability, which is considered a crucial mechanism for promoting fibrosis. Class II HDACs play a significant role in the transdifferentiation process of fibroblasts into myofibroblasts and the apoptosis resistance of lung fibroblasts. This process involves the activation of multiple signaling pathways, including TGF-β/SMAD2/3, AKT/α-SMA, TGIF/α-SMA, NOX4/CTGF/α-SMA, and TGF-PI3K-Akt, which further promote the excessive production of ECM. Additionally, SMAD3 activation mediates the TGF-β-induced EMT, a process that is accompanied by the deacetylation of α-tubulin and the formation of mesenchymal stress fibers (Figure 2B). In contrast to Class I and Class II HDACs, our knowledge regarding the role and function of Class IV HDAC (HDAC11) in lung fibrosis is limited. Current research indicates that HDAC11 may be linked to the progression of lung fibrosis by suppressing the transcription of Kruppel-like factor 15 (KLF15) via the activation of protein 2 (Figure 2C).

5 HDAC inhibitors in IPF

Currently, several natural and synthetic compounds are known to exhibit inhibitory effects on HDACs. However, because HDAC inhibitors do not exhibit the same level of inhibition across all HDAC enzymes, these agents can be classified into pan-inhibitors, Class II-specific inhibitors, and Class I-specific inhibitors (Han et al., 2024). Moreover, due to their potent antitumor mechanisms, numerous pan-inhibitors and type I specific inhibitors have been hailed as successful anticancer drugs. These mechanisms primarily involve inducing apoptosis and autophagy (Gilardini Montani et al., 2017), thereby halting tumor cell cycles (Zhang et al., 2013), inhibiting angiogenesis (Mottamal et al., 2015), diminishing tumor cell mobility and migration, and ultimately enhancing the susceptibility of tumor cells to radiotherapy and chemotherapy (Lee et al., 2010). Since 2006, vorinostat (SAHA), the first-approved HDAC inhibitor for cancer treatment by FDA, has been utilized in clinical settings. Concurrently, significant research has been devoted to exploring various HDAC inhibitors in preclinical models of lung fibrosis/IPF. These inhibitors encompass: (a) hydroxamic acids such as TSA (a naturally occurring compound), SAHA, panobinostat (LBH589), and parcinostat (SB939); (b) cyclic peptides, notably romidepsin (FK228); (c) synthetic compounds such as 4-phenylbutyrate sodium, benzamide MS-275 (entinostat), and CG-745; and (d) subtype-specific HDAC inhibitors, including the short-chain fatty acid VPA, RGFP966, NCC170, tubacin, and tubastatin A. Table 1 encapsulates the overarching therapeutic impacts of diverse HDAC inhibitors on preclinical models pertaining to lung fibrosis/IPF. Overall, HDAC inhibitors either globally or selectively suppress the activity of HDACs, altering the acetylation levels of proteins such as SMAD7, STAT3, tubulin, and Hsp90 through both histone and non-histone acetyltransferases. This modulation regulates the activation of downstream signaling pathways, including TGF-β/SMAD2/3, JAK2/p-STAT3, PI3K/AKT, PI3K/ERK, Notch1, p38, and P53-p21. Subsequently, it affects processes like EMT, oxidative stress levels, apoptosis resistance in fibroblasts/myofibroblasts, the

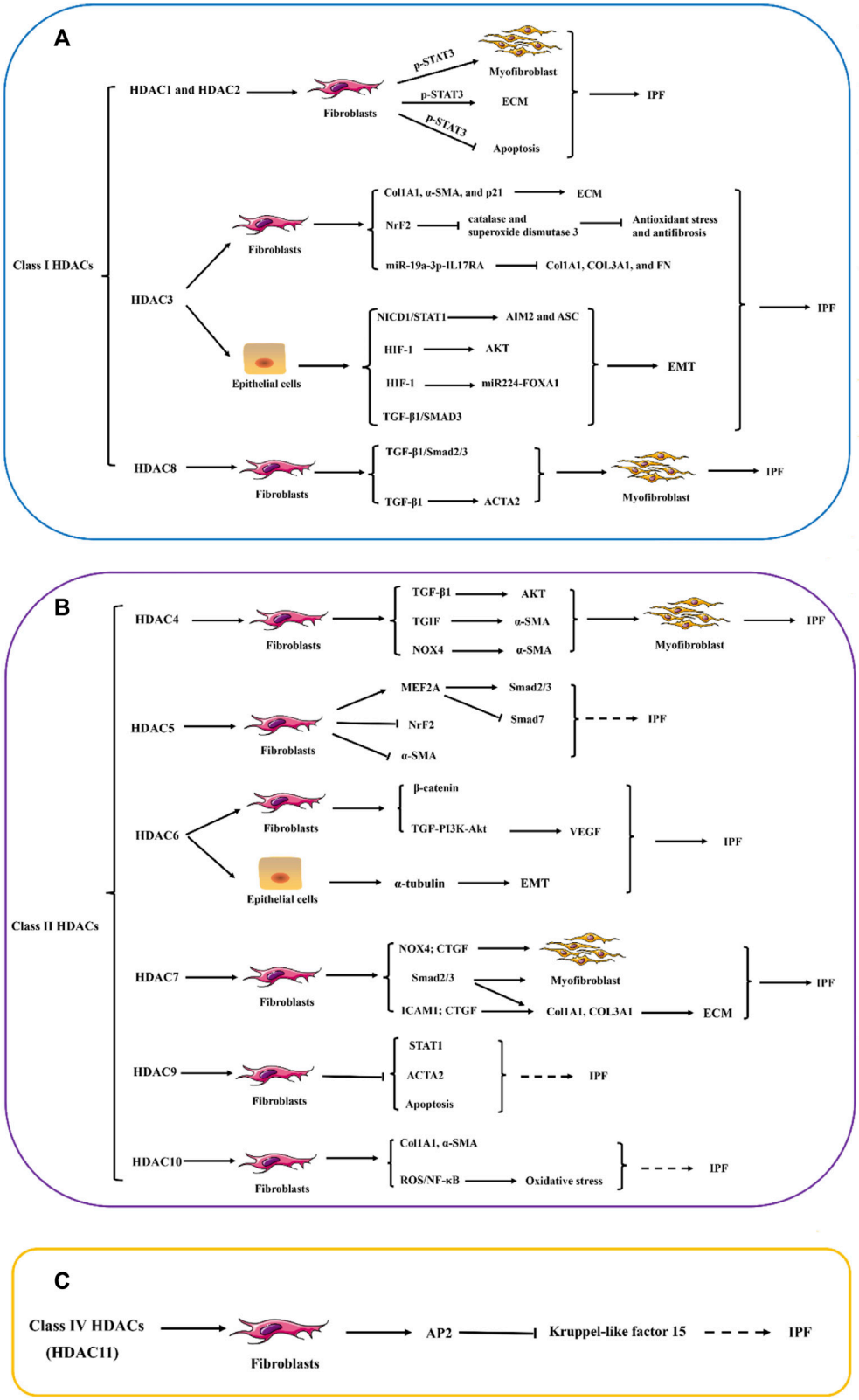

FIGURE 2
The potential role of HDAC enzymes in Idiopathic pulmonary fibrosis (IPF). **(A–C)** Abnormal increases in the expression of histone deacetylases (HDACs) in fibroblasts and myofibroblasts, as well as the aberrant expression of certain types of HDACs in epithelial cells, are believed to play a significant role in the pathogenesis of pulmonary fibrosis. These alterations in HDAC expression primarily influence the expression of numerous genes related to the ECM and anti-apoptotic pathways within cells. The dysregulation of HDACs affects the delicate balance of cellular processes, including EMT and FMD, which is a key feature of fibrotic lesions in the lungs. STAT1, signal transducer and activator of transcription 1; STAT3, signal transducer and activator of transcription 3; Col1A1, Collagen I; Col3A1, Collagen III; α-SMA, α-smooth muscle actin; NrF2, Nuclear factor erythroid 2-related factor 2; IL17RA, (*Continued*)

FIGURE 2 (Continued)
Interleukin 17 Receptor A; NICD1, Notch intracellular domain 1; AIM2, Absent in melanoma 2; ASC, Apoptosis-related Dot-like Protein ASC; HIF-1, hypoxia inducible factor-1; FOXA1, Forkhead Box Protein A1; TGF-β1, Transforming growth factor beta 1; SMAD3, SMAD family member 3; ACTA2, actin alpha 2; TGIF, TGFB-induced factor; NOX4, NADPH oxidase 4; MEF2A, MADS box transcription enhancer factor 2; PI3K: Phosphatidylinositol 3-kinase; VEGF, vascular endothelial growth factor; CTGF, connective tissue growth factor; ICAM1, intercellular cell adhesion molecule-1; AP2, activator protein 2; NF-κB, nuclear factor kappa-B; ROS, reactive oxygen species; ECM, extracellular matrix; EMT, epithelial–mesenchymal transition FMD, Fibroblast-to-myofibroblast differentiation.

TABLE 1 HDAC inhibitors for treatment of pulmonary fibrosis.

HDAC inhibiton	Cells or tissue	Type of HDACs	Proposed function	Refs
trichostatin A (TSA)	lung fibroblasts of bleomycin mice, primary IPF fibroblasts, blood monocyte derived macrophages, TGF-β-treated human normal lung fibroblasts	pan-HDAC	Fas/FAS↓, Thy1 (CD90)↓, ACTA2↓, α-SMA ↓; EMT↓, HMGB1↑; FMD↓; alleviation of lung fibrosis	Glenisson et al. (2007), Guo et al. (2009), Sanders et al. (2011), Huang et al. (2013), Sanders et al. (2014), Ye et al. (2014), Ota et al. (2015), Zheng et al. (2024)
panobinostat (LBH589)	primary IPF fibroblast, TGF-β-treated IPF fibroblasts	pan-HDAC	COX2↓, PGC1A↓, CXCL10↓, STAT3↓; ECM↓; FMD↓	Coward et al. (2009), Coward et al. (2010), Korfei et al. (2015), Korfei et al. (2018)
vorinostat (SAHA)	primary IPF fibroblasts, TGF-β-treated normal human lung fibroblasts (HFL1), bleomycin mouse model	pan-HDAC	BAK↑, BID↑, BCL2L1↓, COL3A1↓; FMD ↓; SMAD7 acetylation and stabilization; SMAD3 dephosphorylation; alleviation of lung fibrosis s	Zhang et al. (2013a), Sanders et al. (2014), Rao et al. (2016)
4-phenyl-butyrate (4-PBA)	bleomycin mouse/rat model A549 cells, alveolar epithelial cells	Class I- and Class IIA-HDAC	IL6↓, TGF-β↓, TNF-α↓, α-SMA↓, Col1a1↓, Col1a2 ↓; oxidative stress ↓; EMT↓; alleviation of lung fibrosis	Zhao et al. (2015), Kabel et al. (2016), Delbrel et al. (2019), Gong et al. (2020), Qin et al. (2021)
CG-745	bleomycin mouse model, PHMG-induced lung fibrosis	Class I-HDAC + HDAC6	α-SMA↓, Col1a1↓; alleviation of lung fibrosis	Kim et al. (2019)
pracrinostat	TGF-β-treated primary IPF fibroblasts	pan-HDAC, except HDAC6	PGC1A↓, ACTA2↓, IL6↓, PDGFA↓; FMD↓	Jones et al. (2019)
valproic acid (VPA)	primary IPF fibroblasts, TGF-β-treated A549 cells, bleomycin mouse/rat model	HDAC1, HDAC2	BIRC5↓, Col1a1↓, SMAD2/3↓; cell proliferation ↓; oxidative stress ↓; EMT↓; alleviation of lung fibrosis	Korfei et al. (2015), Noguchi et al. (2015), Kabel et al. (2016), Chen et al. (2021b)
romidepsin (FK228)	TGF-β-treated primary IPF fibroblasts, bleomycin mouse model	HDAC1, HDAC2	ACTA2↓, COL3A1↓, LOX↓; FMD↓; ECM↓; alleviation of lung fibrosis	Conforti et al. (2017)
entinostat (MS-275)	TGF-β-treated embryonic mouse fibroblasts, TGF-β-treated normal human lung fibroblasts	HDAC1, HDAC3	Adam12↓, Timp1↓, SPARC↓; Inhibition of PI3K and ERK pathways	Barter et al. (2010), Kamio et al. (2017), Wang et al. (2020)
RGFP966	bleomycin mouse model	HDAC3	NrF2↑; E-cadherin↑; ECM↓; EMT↓	Chen et al. (2021a), Xiong et al. (2023)
NCC170	TGF-β-treated normal human lung fibroblasts, Bleomycin mouse model	HDAC8	PPARG↑, ECM↓; alleviation of lung fibrosis	Saito et al. (2019)
tubacin	TGF-β-stimulated A549 cells	HDAC6	E-cadherin↑, PAI1↓, COL1A1↓; Notch1 signaling↓, p38 pathway↓	Shan et al. (2008), Deskin et al. (2016)
tubastatin A	TGF-β-stimulated human normal lung fibroblasts, Bleomycin mouse model	HDAC6	PI3K-AKT pathway↓, FMD ↓ ECM ↓; alleviation of lung fibrosis	(Saito et al., 2017)
6a-m	TGF-β-stimulated human normal lung fibroblasts	HDAC6	α-SMA ↓, COL1A1↓, COL3A1↓	Campiani et al. (2021)
HDAC4 siRNA	TGF-β-treated human normal lung fibroblasts	HDAC4	ACTA2 ↓, α-SMA ↓ TGF-β signaling↓, FMD↓ AKT phosphorylation↓	Glenisson et al. (2007), Guo et al. (2009)
HDAC7 siRNA	TGF-β-treated primary IPF fibroblasts; TGF-β/endothelin-treated fibroblasts	HDAC7	ACTA2↓, CTGF↓, NOX4↓ PGC1A↓, AP-1↓, α-SMA ↓ FMD↓; ECM↓	Kang et al. (2018), Jones et al. (2019), Hua et al. (2021)

IPF: idiopathic pulmonary fibrosis; EMT: epithelial–mesenchymal transition; ECM: extracellular matrix; FMD: fibroblast-to-myofibroblast differentiation; siRNA: small interfering RNA; ↑: upregulation; ↓: downregulation.

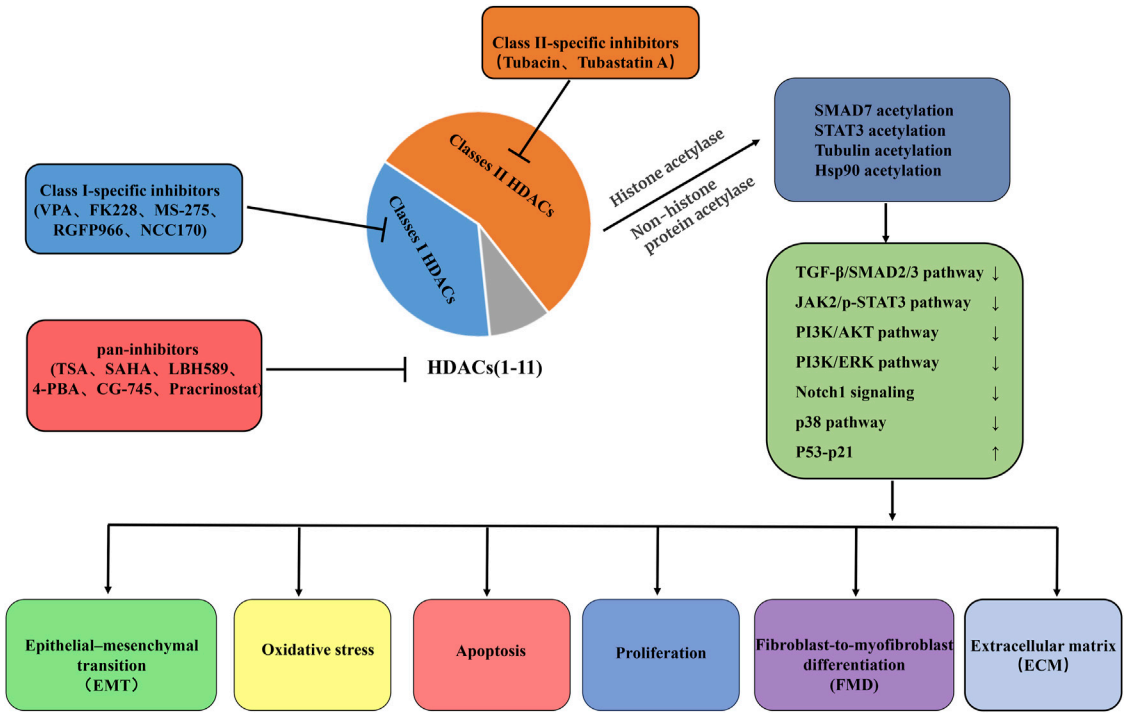

FIGURE 3
Summary of putative therapeutic effects of HDAC-inhibitor treatment on IPF. Pan-HDAC inhibition, Class I-specific inhibitors, and Class II-specific inhibitors influence the delicate balance of cell fate decisions, such as EMT, oxidative stress, cell proliferation, apoptosis, and FMD, processes that are critical in the remodeling of the ECM and the development of fibrosis. These beneficial effects were mediated largely through chromatin hyperacetylation and mechanisms involving non-histone protein acetylation. VPA, valproic acid; FK228, romidepsin; MS-275, entinostat; TSA, trichostatin A; SAHA, vorinostat; LBH589, panobinostat; 4-PBA, 4-phenyl-butyrate; TGF-β1, Transforming growth factor beta 1; SMAD3, SMAD family member 3; JAK2, Janus kinase 2; STAT3, signal transducer and activator of transcription 3; PI3K, Phosphatidylinositol 3-kinase; Notch1, Notch homolog 1; EMT, epithelial–mesenchymal transition; FMD, Fibroblast-to-myofibroblast differentiation; ECM, extracellular matrix.

transdifferentiation of fibroblasts into myofibroblasts, and the excessive formation of ECM to varying degrees (Figure 3).

In summary, the targeted inhibition of a specific HDAC has the potential to provide therapeutic advantages, whereas employing pan-HDAC inhibitors could elicit a more robust therapeutic response. Furthermore, HDAC inhibitors that are FDA-approved for cancer treatment may emerge as promising candidates for the treatment of IPF.

6 Conclusions and future perspectives

FDA-approved antifibrotic drugs, such as nintedanib and pirfenidone, can alleviate the progression of IPF to some extent. However, IPF cannot be completely cured, and novel therapeutic drugs or targets are needed. As a family of enzymes crucial for gene transcription and chromatin remodeling, HDACs have been considered a potential molecular target for treating PF. FDA-approved HDAC inhibitors have shown antifibrotic effects in BLM-induced PF animal models; however, their use in fibrotic diseases has not yet been approved (Lyu et al., 2019; Yoon et al., 2019). Additionally, the research and development of single HDAC selective inhibitors is still in its early stages. The effectiveness and selectivity of HDAC inhibitors need to be evaluated, and relevant lead compounds need to be modified to produce highly selective and powerful inhibitors. Despite their many limitations, HDACs remain attractive targets in developing strategies and drugs for treating PF owing to their therapeutic potential and effectiveness.

Author contributions

H-pC: Conceptualization, Data curation, Funding acquisition, Investigation, Visualization, Writing–original draft, Writing–review and editing. S-hJ: Project administration, Resources, Supervision, Writing–original draft. JC: Funding acquisition, Software, Supervision, Validation, Writing–original draft. Z-qL: Funding acquisition, Supervision, Writing–review and editing. X-hL: Project administration, Resources, Writing–review and editing. D-dF: Project administration, Resources, Writing–review and editing.

Funding

The author(s) declare that financial support was received for the research, authorship, and/or publication of this article. The authors gratefully acknowledge financial support from the National Natural Sciences Foundation of China (Grant numbers: 82200086, 82370077, and 81900070), the Hunan Provincial Natural Science Foundation of China (Grant numbers: 2022JJ40678 and 2023JJ40807). This work was supported by the Scientific

Research Launch Project for new employees of the Second Xiangya Hospital of Central South University.

Conflict of interest

The authors declare that the research was conducted in the absence of any commercial or financial relationships that could be construed as a potential conflict of interest.

Publisher's note

References

Attwood, J. T., Yung, R. L., and Richardson, B. C. (2002). DNA methylation and the regulation of gene transcription. *Cell Mol. Life Sci.* 59 (2), 241–257. doi:10.1007/s00018-002-8420-z

Barter, M. J., Pybus, L., Litherland, G. J., Rowan, A. D., Clark, I. M., Edwards, D. R., et al. (2010). HDAC-mediated control of ERK- and PI3K-dependent TGF-β-induced extracellular matrix-regulating genes. *Matrix Biol.* 29 (7), 602–612. doi:10.1016/j.matbio.2010.05.002

Brancolini, C., Di Giorgio, E., Formisano, L., and Gagliano, T. (2021). Quis custodiet ipsos custodes (who controls the controllers)? Two decades of studies on HDAC9. *Life (Basel)* 11 (2), 90. doi:10.3390/life11020090

Brindisi, M., Saraswati, A. P., Brogi, S., Gemma, S., Butini, S., and Campiani, G. (2020). Old but gold: tracking the new guise of histone deacetylase 6 (HDAC6) enzyme as a biomarker and therapeutic target in rare diseases. *J. Med. Chem.* 63 (1), 23–39. doi:10.1021/acs.jmedchem.9b00924

Brunmeir, R., Lagger, S., and Seiser, C. (2009). Histone deacetylase HDAC1/HDAC2-controlled embryonic development and cell differentiation. *Int. J. Dev. Biol.* 53 (2-3), 275–289. doi:10.1387/ijdb.082649rb

Buggy, J. J., Sideris, M. L., Mak, P., Lorimer, D. D., McIntosh, B., and Clark, J. M. (2000). Cloning and characterization of a novel human histone deacetylase, HDAC8. *Biochem. J.* 350 Pt 1 (Pt 1), 199–205. doi:10.1042/0264-6021:3500199

Campiani, G., Cavella, C., Osko, J. D., Brindisi, M., Relitti, N., Brogi, S., et al. (2021). Harnessing the role of HDAC6 in idiopathic pulmonary fibrosis: design, synthesis, structural analysis, and biological evaluation of potent inhibitors. *J. Med. Chem.* 64 (14), 9960–9988. doi:10.1021/acs.jmedchem.1c00184

Chen, F., Gao, Q., Zhang, L., Ding, Y., Wang, H., and Cao, W. (2021a). Inhibiting HDAC3 (histone deacetylase 3) aberration and the resultant Nrf2 (nuclear factor erythroid-derived 2-related factor-2) repression mitigates pulmonary fibrosis. *Hypertension* 78 (2), e15–e25. doi:10.1161/hypertensionaha.121.17471

Chen, H., Xie, C., Chen, Q., and Zhuang, S. (2022). HDAC11, an emerging therapeutic target for metabolic disorders. *Front. Endocrinol. (Lausanne)* 13, 989305. doi:10.3389/fendo.2022.989305

Chen, L., Alam, A., Pac-Soo, A., Chen, Q., Shang, Y., Zhao, H., et al. (2021b). Pretreatment with valproic acid alleviates pulmonary fibrosis through epithelial-mesenchymal transition inhibition *in vitro* and *in vivo*. *Lab. Invest.* 101 (9), 1166–1175. doi:10.1038/s41374-021-00617-2

Cheng, F., Zheng, B., Wang, J., Zhao, G., Yao, Z., Niu, Z., et al. (2021). Histone deacetylase 10, a potential epigenetic target for therapy. *Biosci. Rep.* 41 (6). doi:10.1042/bsr20210462

Choi, J. S., Lee, W. J., Baik, S. H., Yoon, H. K., Lee, K. H., Kim, Y. H., et al. (2009). Array CGH reveals genomic aberrations in human emphysema. *Lung* 187 (3), 165–172. doi:10.1007/s00408-009-9142-x

Cocconcelli, E., Bernardinello, N., Giraudo, C., Castelli, G., Giorgino, A., Leoni, D., et al. (2021). Characteristics and prognostic factors of pulmonary fibrosis after COVID-19 pneumonia. *Front. Med. (Lausanne)* 8, 823600. doi:10.3389/fmed.2021.823600

Conforti, F., Davies, E. R., Calderwood, C. J., Thatcher, T. H., Jones, M. G., Smart, D. E., et al. (2017). The histone deacetylase inhibitor, romidepsin, as a potential treatment for pulmonary fibrosis. *Oncotarget* 8 (30), 48737–48754. doi:10.18632/oncotarget.17114

Coward, W. R., Watts, K., Feghali-Bostwick, C. A., Jenkins, G., and Pang, L. (2010). Repression of IP-10 by interactions between histone deacetylation and hypermethylation in idiopathic pulmonary fibrosis. *Mol. Cell Biol.* 30 (12), 2874–2886. doi:10.1128/mcb.01527-09

Coward, W. R., Watts, K., Feghali-Bostwick, C. A., Knox, A., and Pang, L. (2009). Defective histone acetylation is responsible for the diminished expression of cyclooxygenase 2 in idiopathic pulmonary fibrosis. *Mol. Cell Biol.* 29 (15), 4325–4339. doi:10.1128/mcb.01776-08

Das, T., Khatun, S., Jha, T., and Gayen, S. (2023). HDAC9 as a privileged target: reviewing its role in different diseases and structure-activity relationships (SARs) of its inhibitors. *Mini Rev. Med. Chem.* 24, 767–784. doi:10.2174/0113895575267301230919165827

Davies, E. R., Haitchi, H. M., Thatcher, T. H., Sime, P. J., Kottmann, R. M., Ganesan, A., et al. (2012). Spiruchostatin A inhibits proliferation and differentiation of fibroblasts from patients with pulmonary fibrosis. *Am. J. Respir. Cell Mol. Biol.* 46 (5), 687–694. doi:10.1165/rcmb.2011-0040OC

Delbrel, E., Uzunhan, Y., Soumare, A., Gille, T., Marchant, D., Planès, C., et al. (2019). ER stress is involved in epithelial-to-mesenchymal transition of alveolar epithelial cells exposed to a hypoxic microenvironment. *Int. J. Mol. Sci.* 20 (6), 1299. doi:10.3390/ijms20061299

de Ruijter, A. J., van Gennip, A. H., Caron, H. N., Kemp, S., and van Kuilenburg, A. B. (2003). Histone deacetylases (HDACs): characterization of the classical HDAC family. *Biochem. J.* 370 (Pt 3), 737–749. doi:10.1042/bj20021321

Deskin, B., Lasky, J., Zhuang, Y., and Shan, B. (2016). Requirement of HDAC6 for activation of Notch1 by TGF-β1. *Sci. Rep.* 6, 31086. doi:10.1038/srep31086

Faverio, P., Luppi, F., Rebora, P., D'Andrea, G., Stainer, A., Busnelli, S., et al. (2022). One-year pulmonary impairment after severe COVID-19: a prospective, multicenter follow-up study. *Respir. Res.* 23 (1), 65. doi:10.1186/s12931-022-01994-y

Fischle, W., Dequiedt, F., Fillion, M., Hendzel, M. J., Voelter, W., and Verdin, E. (2001). Human HDAC7 histone deacetylase activity is associated with HDAC3 *in vivo*. *J. Biol. Chem.* 276 (38), 35826–35835. doi:10.1074/jbc.M104935200

Fischle, W., Emiliani, S., Hendzel, M. J., Nagase, T., Nomura, N., Voelter, W., et al. (1999). A new family of human histone deacetylases related to *Saccharomyces cerevisiae* HDA1p. *J. Biol. Chem.* 274 (17), 11713–11720. doi:10.1074/jbc.274.17.11713

Gao, L., Cueto, M. A., Asselbergs, F., and Atadja, P. (2002). Cloning and functional characterization of HDAC11, a novel member of the human histone deacetylase family. *J. Biol. Chem.* 277 (28), 25748–25755. doi:10.1074/jbc.M111871200

Gao, Y., Liu, Y., Zheng, D., Ho, C., Wen, D., Sun, J., et al. (2022). HDAC5-mediated Smad7 silencing through MEF2A is critical for fibroblast activation and hypertrophic scar formation. *Int. J. Biol. Sci.* 18 (15), 5724–5739. doi:10.7150/ijbs.76140

Gilardini Montani, M. S., Granato, M., Santoni, C., Del Porto, P., Merendino, N., D'Orazi, G., et al. (2017). Histone deacetylase inhibitors VPA and TSA induce apoptosis and autophagy in pancreatic cancer cells. *Cell Oncol. (Dordr)* 40 (2), 167–180. doi:10.1007/s13402-017-0314-z

Glenisson, W., Castronovo, V., and Waltregny, D. (2007). Histone deacetylase 4 is required for TGFbeta1-induced myofibroblastic differentiation. *Biochim. Biophys. Acta* 1773 (10), 1572–1582. doi:10.1016/j.bbamcr.2007.05.016

Gong, L., Liu, G., Zhu, H., Li, C., Li, P., Liu, C., et al. (2020). IL-32 induces epithelial-mesenchymal transition by triggering endoplasmic reticulum stress in A549 cells. *BMC Pulm. Med.* 20 (1), 278. doi:10.1186/s12890-020-01319-z

Grozinger, C. M., Hassig, C. A., and Schreiber, S. L. (1999). Three proteins define a class of human histone deacetylases related to yeast Hda1p. *Proc. Natl. Acad. Sci. U. S. A.* 96 (9), 4868–4873. doi:10.1073/pnas.96.9.4868

Guo, W., Saito, S., Sanchez, C. G., Zhuang, Y., Gongora Rosero, R. E., Shan, B., et al. (2017). TGF-β1 stimulates HDAC4 nucleus-to-cytoplasm translocation and NADPH oxidase 4-derived reactive oxygen species in normal human lung fibroblasts. *Am. J. Physiol. Lung Cell Mol. Physiol.* 312 (6), L936–l944. doi:10.1152/ajplung.00256.2016

Guo, W., Shan, B., Klingsberg, R. C., Qin, X., and Lasky, J. A. (2009). Abrogation of TGF-beta1-induced fibroblast-myofibroblast differentiation by histone deacetylase inhibition. *Am. J. Physiol. Lung Cell Mol. Physiol.* 297 (5), L864–L870. doi:10.1152/ajplung.00128.2009

Gupta, M., Han, J. J., Stenson, M., Wellik, L., and Witzig, T. E. (2012). Regulation of STAT3 by histone deacetylase-3 in diffuse large B-cell lymphoma: implications for therapy. *Leukemia* 26 (6), 1356–1364. doi:10.1038/leu.2011.340

Haberland, M., Montgomery, R. L., and Olson, E. N. (2009). The many roles of histone deacetylases in development and physiology: implications for disease and therapy. *Nat. Rev. Genet.* 10 (1), 32–42. doi:10.1038/nrg2485

Han, H., Feng, X., He, T., Wu, Y., He, T., Yue, Z., et al. (2024). Discussion on structure classification and regulation function of histone deacetylase and their inhibitor. *Chem. Biol. Drug Des.* 103 (1), e14366. doi:10.1111/cbdd.14366

Han, X., Hao, C., Li, L., Li, J., Fang, M., Zheng, Y., et al. (2017). HDAC4 stimulates MRTF-A expression and drives fibrogenesis in hepatic stellate cells by targeting miR-206. *Oncotarget* 8 (29), 47586–47594. doi:10.18632/oncotarget.17739

Hemmatazad, H., Rodrigues, H. M., Maurer, B., Brentano, F., Pileckyte, M., Distler, J. H., et al. (2009). Histone deacetylase 7, a potential target for the antifibrotic treatment of systemic sclerosis. *Arthritis Rheum.* 60 (5), 1519–1529. doi:10.1002/art.24494

Hu, T., Schreiter, F. C., Bagchi, R. A., Tatman, P. D., Hannink, M., and McKinsey, T. A. (2019). HDAC5 catalytic activity suppresses cardiomyocyte oxidative stress and NRF2 target gene expression. *J. Biol. Chem.* 294 (21), 8640–8652. doi:10.1074/jbc.RA118.007006

Hua, H. S., Wen, H. C., Lee, H. S., Weng, C. M., Yuliani, F. S., Kuo, H. P., et al. (2023). Endothelin-1 induces connective tissue growth factor expression in human lung fibroblasts by disrupting HDAC2/Sin3A/MeCP2 corepressor complex. *J. Biomed. Sci.* 30 (1), 40. doi:10.1186/s12929-023-00931-5

Hua, H. S., Wen, H. C., Weng, C. M., Lee, H. S., Chen, B. C., and Lin, C. H. (2021). Histone deacetylase 7 mediates endothelin-1-induced connective tissue growth factor expression in human lung fibroblasts through p300 and activator protein-1 activation. *J. Biomed. Sci.* 28 (1), 38. doi:10.1186/s12929-021-00735-5

Huang, S. K., Scruggs, A. M., Donaghy, J., Horowitz, J. C., Zaslona, Z., Przybranowski, S., et al. (2013). Histone modifications are responsible for decreased Fas expression and apoptosis resistance in fibrotic lung fibroblasts. *Cell Death Dis.* 4 (5), e621. doi:10.1038/cddis.2013.146

Hutt, D. M., Herman, D., Rodrigues, A. P., Noel, S., Pilewski, J. M., Matteson, J., et al. (2010). Reduced histone deacetylase 7 activity restores function to misfolded CFTR in cystic fibrosis. *Nat. Chem. Biol.* 6 (1), 25–33. doi:10.1038/nchembio.275

Ito, K., Ito, M., Elliott, W. M., Cosio, B., Caramori, G., Kon, O. M., et al. (2005). Decreased histone deacetylase activity in chronic obstructive pulmonary disease. *N. Engl. J. Med.* 352 (19), 1967–1976. doi:10.1056/NEJMoa041892

Jeong, S. H., Son, E. S., Lee, Y. E., Kyung, S. Y., Park, J. W., and Kim, S. H. (2022). Histone deacetylase 3 promotes alveolar epithelial-mesenchymal transition and fibroblast migration under hypoxic conditions. *Exp. Mol. Med.* 54 (7), 922–931. doi:10.1038/s12276-022-00796-y

Johnstone, R. W. (2002). Histone-deacetylase inhibitors: novel drugs for the treatment of cancer. *Nat. Rev. Drug Discov.* 1 (4), 287–299. doi:10.1038/nrd772

Jones, D. L., Haak, A. J., Caporarello, N., Choi, K. M., Ye, Z., Yan, H., et al. (2019). TGFβ-induced fibroblast activation requires persistent and targeted HDAC-mediated gene repression. *J. Cell Sci.* 132 (20), jcs233486. doi:10.1242/jcs.233486

Kabel, A. M., Omar, M. S., and Elmaaboud, M. A. A. (2016). Amelioration of bleomycin-induced lung fibrosis in rats by valproic acid and butyrate: role of nuclear factor kappa-B, proinflammatory cytokines and oxidative stress. *Int. Immunopharmacol.* 39, 335–342. doi:10.1016/j.intimp.2016.08.008

Kamio, K., Azuma, A., Usuki, J., Matsuda, K., Inomata, M., Nishijima, N., et al. (2017). XPLN is modulated by HDAC inhibitors and negatively regulates SPARC expression by targeting mTORC2 in human lung fibroblasts. *Pulm. Pharmacol. Ther.* 44, 61–69. doi:10.1016/j.pupt.2017.03.003

Kang, D. H., Yin, G. N., Choi, M. J., Song, K. M., Ghatak, K., Minh, N. N., et al. (2018). Silencing histone deacetylase 7 alleviates transforming growth factor-β1-induced profibrotic responses in fibroblasts derived from peyronie's plaque. *World J. Mens. Health* 36 (2), 139–146. doi:10.5534/wjmh.170005

Khalil, W., Xia, H., Bodempudi, V., Kahm, J., Hergert, P., Smith, K., et al. (2015). Pathologic regulation of collagen I by an aberrant protein phosphatase 2A/histone deacetylase C4/MicroRNA-29 signal Axis in idiopathic pulmonary fibrosis fibroblasts. *Am. J. Respir. Cell Mol. Biol.* 53 (3), 391–399. doi:10.1165/rcmb.2014-0150OC

Kim, J., Lee, H., Yi, S. J., and Kim, K. (2022). Gene regulation by histone-modifying enzymes under hypoxic conditions: a focus on histone methylation and acetylation. *Exp. Mol. Med.* 54 (7), 878–889. doi:10.1038/s12276-022-00812-1

Kim, Y. S., Cha, H., Kim, H. J., Cho, J. M., and Kim, H. R. (2019). The anti-fibrotic effects of CG-745, an HDAC inhibitor, in bleomycin and PHMG-induced mouse models. *Molecules* 24 (15), 2792. doi:10.3390/molecules24152792

Korfei, M., Mahavadi, P., and Guenther, A. (2022). Targeting histone deacetylases in idiopathic pulmonary fibrosis: a future therapeutic option. *Cells* 11 (10), 1626. doi:10.3390/cells11101626

Korfei, M., Skwarna, S., Henneke, I., MacKenzie, B., Klymenko, O., Saito, S., et al. (2015). Aberrant expression and activity of histone deacetylases in sporadic idiopathic pulmonary fibrosis. *Thorax* 70 (11), 1022–1032. doi:10.1136/thoraxjnl-2014-206411

Korfei, M., Stelmaszek, D., MacKenzie, B., Skwarna, S., Chillappagari, S., Bach, A. C., et al. (2018). Comparison of the antifibrotic effects of the pan-histone deacetylase-inhibitor panobinostat versus the IPF-drug pirfenidone in fibroblasts from patients with idiopathic pulmonary fibrosis. *PLoS One* 13 (11), e0207915. doi:10.1371/journal.pone.0207915

Lee, J. H., Choy, M. L., Ngo, L., Foster, S. S., and Marks, P. A. (2010). Histone deacetylase inhibitor induces DNA damage, which normal but not transformed cells can repair. *Proc. Natl. Acad. Sci. U. S. A.* 107 (33), 14639–14644. doi:10.1073/pnas.1008522107

Li, G., Jiang, H., Chang, M., Xie, H., and Hu, L. (2011). HDAC6 α-tubulin deacetylase: a potential therapeutic target in neurodegenerative diseases. *J. Neurol. Sci.* 304 (1-2), 1–8. doi:10.1016/j.jns.2011.02.017

Li, M., Zheng, Y., Yuan, H., Liu, Y., and Wen, X. (2017). Effects of dynamic changes in histone acetylation and deacetylase activity on pulmonary fibrosis. *Int. Immunopharmacol.* 52, 272–280. doi:10.1016/j.intimp.2017.09.020

Li, Y., Shin, D., and Kwon, S. H. (2013). Histone deacetylase 6 plays a role as a distinct regulator of diverse cellular processes. *Febs J.* 280 (3), 775–793. doi:10.1111/febs.12079

Liu, P., Xiao, J., Wang, Y., Song, X., Huang, L., Ren, Z., et al. (2021). Posttranslational modification and beyond: interplay between histone deacetylase 6 and heat-shock protein 90. *Mol. Med.* 27 (1), 110. doi:10.1186/s10020-021-00375-3

Lyu, X., Hu, M., Peng, J., Zhang, X., and Sanders, Y. Y. (2019). HDAC inhibitors as antifibrotic drugs in cardiac and pulmonary fibrosis. *Ther. Adv. Chronic Dis.* 10, 2040622319862697. doi:10.1177/2040622319862697

Mahlknecht, U., Schnittger, S., Will, J., Cicek, N., and Hoelzer, D. (2002). Chromosomal organization and localization of the human histone deacetylase 9 gene (HDAC9). *Biochem. Biophys. Res. Commun.* 293 (1), 182–191. doi:10.1016/s0006-291x(02)00193-6

Mannaerts, I., Eysackers, N., Onyema, O. O., Van Beneden, K., Valente, S., Mai, A., et al. (2013). Class II HDAC inhibition hampers hepatic stellate cell activation by induction of microRNA-29. *PLoS One* 8 (1), e55786. doi:10.1371/journal.pone.0055786

Mao, L., Liu, L., Zhang, T., Qin, H., Wu, X., and Xu, Y. (2020). Histone deacetylase 11 contributes to renal fibrosis by repressing KLF15 transcription. *Front. Cell Dev. Biol.* 8, 235. doi:10.3389/fcell.2020.00235

Martinez, F. J., Collard, H. R., Pardo, A., Raghu, G., Richeldi, L., Selman, M., et al. (2017). Idiopathic pulmonary fibrosis. *Nat. Rev. Dis. Prim.* 3, 17074. doi:10.1038/nrdp.2017.74

Mottamal, M., Zheng, S., Huang, T. L., and Wang, G. (2015). Histone deacetylase inhibitors in clinical studies as templates for new anticancer agents. *Molecules* 20 (3), 3898–3941. doi:10.3390/molecules20033898

Noguchi, S., Eitoku, M., Moriya, S., Kondo, S., Kiyosawa, H., Watanabe, T., et al. (2015). Regulation of gene expression by sodium valproate in epithelial-to-mesenchymal transition. *Lung* 193 (5), 691–700. doi:10.1007/s00408-015-9776-9

O'Shea, J. J., Kanno, Y., Chen, X., and Levy, D. E. (2005). Cell signaling. Stat acetylation--a key facet of cytokine signaling? *Science* 307 (5707), 217–218. doi:10.1126/science.1108164

Ota, C., Yamada, M., Fujino, N., Motohashi, H., Tando, Y., Takei, Y., et al. (2015). Histone deacetylase inhibitor restores surfactant protein-C expression in alveolar-epithelial type II cells and attenuates bleomycin-induced pulmonary fibrosis *in vivo*. *Exp. Lung Res.* 41 (8), 422–434. doi:10.3109/01902148.2015.1060275

Pang, M., and Zhuang, S. (2010). Histone deacetylase: a potential therapeutic target for fibrotic disorders. *J. Pharmacol. Exp. Ther.* 335 (2), 266–272. doi:10.1124/jpet.110.168385

Parmigiani, R. B., Xu, W. S., Venta-Perez, G., Erdjument-Bromage, H., Yaneva, M., Tempst, P., et al. (2008). HDAC6 is a specific deacetylase of peroxiredoxins and is involved in redox regulation. *Proc. Natl. Acad. Sci. U. S. A.* 105 (28), 9633–9638. doi:10.1073/pnas.0803749105

Qin, X., Lin, X., Liu, L., Li, Y., Li, X., Deng, Z., et al. (2021). Macrophage-derived exosomes mediate silica-induced pulmonary fibrosis by activating fibroblast in an endoplasmic reticulum stress-dependent manner. *J. Cell Mol. Med.* 25 (9), 4466–4477. doi:10.1111/jcmm.16524

Rao, S. S., Zhang, X. Y., Shi, M. J., Xiao, Y., Zhang, Y. Y., Wang, Y. Y., et al. (2016). Suberoylanilide hydroxamic acid attenuates paraquat-induced pulmonary fibrosis by preventing Smad7 from deacetylation in rats. *J. Thorac. Dis.* 8 (9), 2485–2494. doi:10.21037/jtd.2016.08.08

Richeldi, L., Collard, H. R., and Jones, M. G. (2017). Idiopathic pulmonary fibrosis. *Lancet* 389 (10082), 1941–1952. doi:10.1016/s0140-6736(17)30866-8

Roque, W. (2022). Heat shock proteins in pulmonary fibrosis: pawns of cell homeostasis. *Am. J. Physiol. Cell Physiol.* 322 (6), C1105–c1109. doi:10.1152/ajpcell.00073.2022

Rubio, K., Singh, I., Dobersch, S., Sarvari, P., Günther, S., Cordero, J., et al. (2019). Inactivation of nuclear histone deacetylases by EP300 disrupts the MiCEE complex in idiopathic pulmonary fibrosis. *Nat. Commun.* 10 (1), 2229. doi:10.1038/s41467-019-10066-7

Saito, S., Zhuang, Y., Shan, B., Danchuk, S., Luo, F., Korfei, M., et al. (2017). Tubastatin ameliorates pulmonary fibrosis by targeting the TGFβ-PI3K-Akt pathway. *PLoS One* 12 (10), e0186615. doi:10.1371/journal.pone.0186615

Saito, S., Zhuang, Y., Suzuki, T., Ota, Y., Bateman, M. E., Alkhatib, A. L., et al. (2019). HDAC8 inhibition ameliorates pulmonary fibrosis. *Am. J. Physiol. Lung Cell Mol. Physiol.* 316 (1), L175–l186. doi:10.1152/ajplung.00551.2017

Sanaei, M., and Kavoosi, F. (2019). Histone deacetylases and histone deacetylase inhibitors: molecular mechanisms of action in various cancers. *Adv. Biomed. Res.* 8, 63. doi:10.4103/abr.abr_142_19

Sanders, Y. Y., Ambalavanan, N., Halloran, B., Zhang, X., Liu, H., Crossman, D. K., et al. (2012). Altered DNA methylation profile in idiopathic pulmonary fibrosis. *Am. J. Respir. Crit. Care Med.* 186 (6), 525–535. doi:10.1164/rccm.201201-0077OC

Sanders, Y. Y., Hagood, J. S., Liu, H., Zhang, W., Ambalavanan, N., and Thannickal, V. J. (2014). Histone deacetylase inhibition promotes fibroblast apoptosis and ameliorates pulmonary fibrosis in mice. *Eur. Respir. J.* 43 (5), 1448–1458. doi:10.1183/09031936.00095113

Sanders, Y. Y., Tollefsbol, T. O., Varisco, B. M., and Hagood, J. S. (2011). Epigenetic regulation of thy-1 by histone deacetylase inhibitor in rat lung fibroblasts. *Am. J. Respir. Cell Mol. Biol.* 45 (1), 16–23. doi:10.1165/rcmb.2010-0154OC

Segré, C. V., and Chiocca, S. (2011). Regulating the regulators: the post-translational code of class I HDAC1 and HDAC2. *J. Biomed. Biotechnol.* 2011, 690848. doi:10.1155/2011/690848

Sehgal, M., Jakhete, S. M., Manekar, A. G., and Sasikumar, S. (2022). Specific epigenetic regulators serve as potential therapeutic targets in idiopathic pulmonary fibrosis. *Heliyon* 8 (8), e09773. doi:10.1016/j.heliyon.2022.e09773

Shan, B., Yao, T. P., Nguyen, H. T., Zhuo, Y., Levy, D. R., Klingsberg, R. C., et al. (2008). Requirement of HDAC6 for transforming growth factor-beta1-induced epithelial-mesenchymal transition. *J. Biol. Chem.* 283 (30), 21065–21073. doi:10.1074/jbc.M802786200

Spagnolo, P., Kropski, J. A., Jones, M. G., Lee, J. S., Rossi, G., Karampitsakos, T., et al. (2021). Idiopathic pulmonary fibrosis: disease mechanisms and drug development. *Pharmacol. Ther.* 222, 107798. doi:10.1016/j.pharmthera.2020.107798

Stella, G. M., and Balestro, E. (2015). Idiopathic pulmonary fibrosis landscapes: looking glass from pathology to therapy. *Minerva Med.* 106 (4 Suppl. 3), 17–24.

Štorkánová, H., Oreská, S., Špiritović, M., Heřmánková, B., Bubová, K., Komarc, M., et al. (2021). Plasma Hsp90 levels in patients with systemic sclerosis and relation to lung and skin involvement: a cross-sectional and longitudinal study. *Sci. Rep.* 11 (1), 1. doi:10.1038/s41598-020-79139-8

Sun, H. N., Ren, C. X., Lee, D. H., Wang, W. H., Guo, X. Y., Hao, Y. Y., et al. (2023). PRDX1 negatively regulates bleomycin-induced pulmonary fibrosis via inhibiting the epithelial-mesenchymal transition and lung fibroblast proliferation *in vitro* and *in vivo*. *Cell Mol. Biol. Lett.* 28 (1), 48. doi:10.1186/s11658-023-00460-x

Tang, S., Cheng, B., Zhe, N., Ma, D., Xu, J., Li, X., et al. (2018). Histone deacetylase inhibitor BG45-mediated HO-1 expression induces apoptosis of multiple myeloma cells by the JAK2/STAT3 pathway. *Anticancer Drugs* 29 (1), 61–74. doi:10.1097/cad.0000000000000568

Thangapandian, S., John, S., Lee, Y., Arulalapperumal, V., and Lee, K. W. (2012). Molecular modeling study on tunnel behavior in different histone deacetylase isoforms. *PLoS One* 7 (11), e49327. doi:10.1371/journal.pone.0049327

Tian, Y., Shi, H., Zhang, D., Wang, C., Zhao, F., Li, L., et al. (2023). Nebulized inhalation of LPAE-HDAC10 inhibits acetylation-mediated ROS/NF-κB pathway for silicosis treatment. *J. Control Release* 364, 618–631. doi:10.1016/j.jconrel.2023.10.018

Tong, J. J., Liu, J., Bertos, N. R., and Yang, X. J. (2002). Identification of HDAC10, a novel class II human histone deacetylase containing a leucine-rich domain. *Nucleic Acids Res.* 30 (5), 1114–1123. doi:10.1093/nar/30.5.1114

Toscano-Marquez, F., Romero, Y., Espina-Ordoñez, M., and Cisneros, J. (2023). Absence of HDAC3 by matrix stiffness promotes chromatin remodeling and fibroblast activation in idiopathic pulmonary fibrosis. *Cells* 12 (7), 1020. doi:10.3390/cells12071020

Verdel, A., and Khochbin, S. (1999). Identification of a new family of higher eukaryotic histone deacetylases. Coordinate expression of differentiation-dependent chromatin modifiers. *J. Biol. Chem.* 274 (4), 2440–2445. doi:10.1074/jbc.274.4.2440

Waltregny, D., De Leval, L., Glénisson, W., Ly Tran, S., North, B. J., Bellahcène, A., et al. (2004). Expression of histone deacetylase 8, a class I histone deacetylase, is restricted to cells showing smooth muscle differentiation in normal human tissues. *Am. J. Pathol.* 165 (2), 553–564. doi:10.1016/s0002-9440(10)63320-2

Waltregny, D., Glénisson, W., Tran, S. L., North, B. J., Verdin, E., Colige, A., et al. (2005). Histone deacetylase HDAC8 associates with smooth muscle alpha-actin and is essential for smooth muscle cell contractility. *Faseb J.* 19 (8), 966–968. doi:10.1096/fj.04-2303fje

Wang, R., Xin, M., Li, Y., Zhang, P., and Zhang, M. (2016). The functions of histone modification enzymes in cancer. *Curr. Protein Pept. Sci.* 17 (5), 438–445. doi:10.2174/1389203717666160122120521

Wang, Y., Yella, J. K., Ghandikota, S., Cherukuri, T. C., Ediga, H. H., Madala, S. K., et al. (2020). Pan-transcriptome-based candidate therapeutic discovery for idiopathic pulmonary fibrosis. *Ther. Adv. Respir. Dis.* 14, 1753466620971143. doi:10.1177/1753466620971143

Wang, Z., Qin, G., and Zhao, T. C. (2014). HDAC4: mechanism of regulation and biological functions. *Epigenomics* 6 (1), 139–150. doi:10.2217/epi.13.73

Witt, O., Deubzer, H. E., Milde, T., and Oehme, I. (2009). HDAC family: what are the cancer relevant targets? *Cancer Lett.* 277 (1), 8–21. doi:10.1016/j.canlet.2008.08.016

Wolters, P. J., Blackwell, T. S., Eickelberg, O., Loyd, J. E., Kaminski, N., Jenkins, G., et al. (2018). Time for a change: is idiopathic pulmonary fibrosis still idiopathic and only fibrotic? *Lancet Respir. Med.* 6 (2), 154–160. doi:10.1016/s2213-2600(18)30007-9

Wolters, P. J., Collard, H. R., and Jones, K. D. (2014). Pathogenesis of idiopathic pulmonary fibrosis. *Annu. Rev. Pathol.* 9, 157–179. doi:10.1146/annurev-pathol-012513-104706

Wu, Y., Hou, F., Wang, X., Kong, Q., Han, X., and Bai, B. (2016). Aberrant expression of histone deacetylases 4 in cognitive disorders: molecular mechanisms and a potential target. *Front. Mol. Neurosci.* 9, 114. doi:10.3389/fnmol.2016.00114

Xiong, R., Geng, B., Jiang, W., Hu, Y., Hu, Z., Hao, B., et al. (2023). Histone deacetylase 3 deletion in alveolar type 2 epithelial cells prevents bleomycin-induced pulmonary fibrosis. *Clin. Epigenetics* 15 (1), 182. doi:10.1186/s13148-023-01588-5

Xu, W. S., Parmigiani, R. B., and Marks, P. A. (2007). Histone deacetylase inhibitors: molecular mechanisms of action. *Oncogene* 26 (37), 5541–5552. doi:10.1038/sj.onc.1210620

Yang, I. V., Pedersen, B. S., Rabinovich, E., Hennessy, C. E., Davidson, E. J., Murphy, E., et al. (2014). Relationship of DNA methylation and gene expression in idiopathic pulmonary fibrosis. *Am. J. Respir. Crit. Care Med.* 190 (11), 1263–1272. doi:10.1164/rccm.201408-1452OC

Yang, J., Gong, C., Ke, Q., Fang, Z., Chen, X., Ye, M., et al. (2021). Insights into the function and clinical application of HDAC5 in cancer management. *Front. Oncol.* 11, 661620. doi:10.3389/fonc.2021.661620

Yang, W. M., Tsai, S. C., Wen, Y. D., Fejer, G., and Seto, E. (2002). Functional domains of histone deacetylase-3. *J. Biol. Chem.* 277 (11), 9447–9454. doi:10.1074/jbc.M105993200

Yanginlar, C., and Logie, C. (2018). HDAC11 is a regulator of diverse immune functions. *Biochim. Biophys. Acta Gene Regul. Mech.* 1861 (1), 54–59. doi:10.1016/j.bbagrm.2017.12.002

Ye, Q., Li, Y., Jiang, H., Xiong, J., Xu, J., Qin, H., et al. (2014). Prevention of pulmonary fibrosis via trichostatin A (TSA) in bleomycin induced rats. *Sarcoidosis Vasc. Diffuse Lung Dis.* 31 (3), 219–226.

Yoon, S., Kang, G., and Eom, G. H. (2019). HDAC inhibitors: therapeutic potential in fibrosis-associated human diseases. *Int. J. Mol. Sci.* 20 (6), 1329. doi:10.3390/ijms20061329

Yu, W. C., Yeh, T. Y., Ye, C. H., Chong, P. C. T., Ho, Y. H., So, D. K., et al. (2023). Discovery of HDAC6, HDAC8, and 6/8 inhibitors and development of cell-based drug screening models for the treatment of TGF-β-induced idiopathic pulmonary fibrosis. *J. Med. Chem.* 66 (15), 10528–10557. doi:10.1021/acs.jmedchem.3c00644

Yuan, H., Jiao, L., Yu, N., Duan, H., Yu, Y., and Bai, Y. (2020). Histone deacetylase 3-mediated inhibition of microRNA-19a-3p facilitates the development of rheumatoid arthritis-associated interstitial lung disease. *Front. Physiol.* 11, 549656. doi:10.3389/fphys.2020.549656

Zhang, H. P., Wang, L., Fu, J. J., Fan, T., Wang, Z. L., and Wang, G. (2016). Association between histone hyperacetylation status in memory T lymphocytes and allergen-induced eosinophilic airway inflammation. *Respirology* 21 (5), 850–857. doi:10.1111/resp.12774

Zhang, W., Zhang, Y., Tu, T., Schmull, S., Han, Y., Wang, W., et al. (2020). Dual inhibition of HDAC and tyrosine kinase signaling pathways with CUDC-907 attenuates TGFβ1 induced lung and tumor fibrosis. *Cell Death Dis.* 11 (9), 765. doi:10.1038/s41419-020-02916-w

Zhang, X., Liu, H., Hock, T., Thannickal, V. J., and Sanders, Y. Y. (2013a). Histone deacetylase inhibition downregulates collagen 3A1 in fibrotic lung fibroblasts. *Int. J. Mol. Sci.* 14 (10), 19605–19617. doi:10.3390/ijms141019605

Zhang, Y., Yang, Y., Yang, F., Liu, X., Zhan, P., Wu, J., et al. (2023). HDAC9-mediated epithelial cell cycle arrest in G2/M contributes to kidney fibrosis in male mice. *Nat. Commun.* 14 (1), 3007. doi:10.1038/s41467-023-38771-4

Zhang, Z., Hao, C., Wang, L., Liu, P., Zhao, L., Zhu, C., et al. (2013b). Inhibition of leukemic cells by valproic acid, an HDAC inhibitor, in xenograft tumors. *Onco Targets Ther.* 6, 733–740. doi:10.2147/ott.S46135

Zhao, H., Qin, H. Y., Cao, L. F., Chen, Y. H., Tan, Z. X., Zhang, C., et al. (2015). Phenylbutyric acid inhibits epithelial-mesenchymal transition during bleomycin-induced lung fibrosis. *Toxicol. Lett.* 232 (1), 213–220. doi:10.1016/j.toxlet.2014.10.013

Zhao, T., Kee, H. J., Kee, S. J., and Jeong, M. H. (2022). Hdac8 inhibitor alleviates transverse aortic constriction-induced heart failure in mice by downregulating Ace1. *Oxid. Med. Cell Longev.* 2022, 6227330. doi:10.1155/2022/6227330

Zheng, Q., Lei, Y., Hui, S., Tong, M., and Liang, L. (2022). HDAC3 promotes pulmonary fibrosis by activating NOTCH1 and STAT1 signaling and up-regulating inflammasome components AIM2 and ASC. *Cytokine* 153, 155842. doi:10.1016/j.cyto.2022.155842

Zheng, S., Bulut, G. B., Kummarapurugu, A. B., Ma, J., and Voynow, J. A. (2024). Neutrophil elastase degrades histone deacetylases and sirtuin 1 in primary human monocyte derived macrophages. *Int. J. Mol. Sci.* 25 (8), 4265. doi:10.3390/ijms25084265

Zhou, X., Marks, P. A., Rifkind, R. A., and Richon, V. M. (2001). Cloning and characterization of a histone deacetylase, HDAC9. *Proc. Natl. Acad. Sci. U. S. A.* 98 (19), 10572–10577. doi:10.1073/pnas.191375098

frontiers | Frontiers in Medicine

TYPE Systematic Review
PUBLISHED 03 February 2025
DOI 10.3389/fmed.2025.1507805

OPEN ACCESS

EDITED BY
Lulong Bo,
Navy Medical University, China

REVIEWED BY
Quanguang Zhang,
Augusta University, United States
Wentao Ji,
Naval Medical University, China

*CORRESPONDENCE
Xiao Liu
docliuxiao@163.com
Liang Zhang
zhangl1203@sina.com
Xianliang Yan
docyxl@163.com

RECEIVED 08 October 2024
ACCEPTED 13 January 2025
PUBLISHED 03 February 2025

CITATION
Xu Z, Liu X, Zhang L and Yan X (2025) Comparative outcomes of corticosteroids, neuromuscular blocking agents, and inhaled nitric oxide in ARDS: a systematic review and network meta-analysis.
Front. Med. 12:1507805.
doi: 10.3389/fmed.2025.1507805

Comparative outcomes of corticosteroids, neuromuscular blocking agents, and inhaled nitric oxide in ARDS: a systematic review and network meta-analysis

Zhiyuan Xu[1], Xiao Liu[2]*, Liang Zhang[1]* and Xianliang Yan[2,3]*

[1]Department of Emergency Medicine, Xuzhou No. 1 People's Hospital, Xuzhou, Jiangsu, China, [2]Department of Emergency Medicine, Affiliated Hospital of Xuzhou Medical University, Xuzhou, Jiangsu, China, [3]Department of Emergency Medicine, Suining County People's Hospital, Xuzhou, Jiangsu, China

Objectives: Acute respiratory distress syndrome (ARDS) is associated with high rates of morbidity and mortality. However, the evidence regarding the effectiveness of commonly used treatments, including corticosteroids, neuromuscular blocking agents (NMBAs), and inhaled nitric oxide (iNO), remains uncertain. Therefore, this study aimed to compare and rank these three treatments to identify the most effective option.

Data sources: We searched PubMed, Embase, Cochrane Library, and Web of Science for clinical trials from the earliest records to 1 May 2024.

Study selection and data extraction: Clinical trials evaluating three interventions compared with the control group for ARDS were included, with restrictions on any language. Data were extracted by two independent reviewers. Frequentist network meta-analysis (NMA) was performed to identify the most effective intervention, and treatments were ranked using the surface under the cumulative ranking (SUCRA) curve. The primary outcome was 28-day mortality, while secondary outcomes included ventilator-free days up to 28 days, ICU mortality, in-hospital mortality, and the incidence of new infection events.

Data synthesis: Data from 26 clinical trials encompassing 5,071 patients were analyzed. Vecuronium bromide was the most effective strategy for reducing 28-day mortality compared to conventional treatment, iNO, methylprednisolone, and placebo (OR 0.38, 95% CI 0.15–1.00, and OR 0.30, 95% CI 0.10–0.85 and OR 0.25, 95% CI 0.08–0.74 and OR 0.23, 95% CI 0.08–0.65; SUCRA: 96.6%). Dexamethasone was identified as the most effective treatment option for increasing ventilator-free days at 28 days compared to conventional therapy and cisatracurium (MD 3.60, 95% CI 1.77–5.43, and MD 3.40, 95% CI 0.87–5.92; SUCRA: 93.2%). Methylprednisolone demonstrated the highest effectiveness for preventing ICU mortality (SUCRA: 88.5%). Although dexamethasone, cisatracurium, conventional therapy, methylprednisolone, and iNO treatment did not show significant superiority in reducing in-hospital mortality, dexamethasone showed the highest probability of being the most effective treatment option (SUCRA: 79.7%). Furthermore, dexamethasone treatment showed the highest safety in reducing the incidence of new infection events

compared with placebo and iNO (OR 0.61, 95% CI 0.42–0.88, and OR 0.33, 95% CI 0.19–0.58; SUCRA: 91.8%).

Conclusion: This NMA suggests that corticosteroids may provide benefits to patients with ARDS. While the application of NMBAs may reduce 28-day mortality, iNO did not demonstrate a significant beneficial effect as a therapeutic measure.

Systematic review registration: PROSPERO, CRD42022333165 https://www.crd.york.ac.uk/PROSPERO/.

KEYWORDS

ARDS, corticosteroids, NMBAs, iNO, network meta-analysis

Introduction

Acute respiratory distress syndrome (ARDS) is a severe global health issue characterized by high morbidity and mortality. It is defined as chronic respiratory failure caused by non-hemodynamic pulmonary edema due to inflammatory cytokines (1, 2). The COVID-19 pandemic has further underscored the severity of ARDS, increased its incidence, and revealed the critical need for effective treatments (3). Globally, ARDS affects 10.4% of intensive care unit patients and 23.4% of intubated patients, with an associated hospital mortality rate of 40% (2). Since its initial description in 1967 (4), numerous management strategies for ARDS have been clinically evaluated (5, 6). Despite over 50 years of research, none of the available treatments directly target the pathophysiological mechanisms underlying acute respiratory failure (7).

Recent guidelines on ARDS management (8), developed following the National Institute for Health and Care Excellence (NICE) methodology, emphasize evidence-based interventions. Based on existing recommendations and expert consensus, corticosteroids, neuromuscular blocking agents (NMBAs), and inhaled nitric oxide (iNO) were identified as key focus areas. Corticosteroids target the inflammatory cascade central to ARDS pathophysiology with their anti-inflammatory and antifibrotic properties. NMBAs improve oxygenation and reduce ventilator-induced lung injury by enhancing patient–ventilator synchrony. At the same time, iNO, a selective pulmonary vasodilator, is often used to improve oxygenation in severe cases despite its controversial efficacy. Although these treatments are widely utilized, systematic reviews and meta-analyses (SR/MAs) have produced mixed results regarding their effectiveness and safety. Some evidence suggests that corticosteroids reduce mortality and increase ventilator-free days (VFD) (9), while other analyses indicate that early and prolonged corticosteroid use may further improve outcomes (10). Studies show potential benefits of NMBAs, including improved oxygenation, reduced ventilator-induced lung injury, and decreased 28-day mortality rates (11). The role of iNO in ARDS management has been evaluated through multiple randomized controlled trials (RCTs) and subsequent SR/MAs, though its efficacy remains debated.

The COVID-19 pandemic has amplified the global relevance of ARDS, with the SARS-CoV-2 outbreak driving a sharp increase in ARDS-related mortality (3). This highlights the urgent need to synthesize existing evidence to inform current critical care practices. We conducted a network meta-analysis (NMA) of high-quality trials to evaluate the efficacy of corticosteroids, NMBAs, and iNO in ARDS management, with the goal of informing treatment strategies and improving patient outcomes.

Materials and methods

Literature review

We conducted a systematic search of PubMed, Embase, Cochrane Library, and Web of Science from their inception to 1 May 2024. Details of the search strategy are provided in Appendix 1. This meta-analysis adhered to guidelines outlined in the Preferred Reporting Items for Systematic Reviews and Meta-Analyses (PRISMA) and was registered on PROSPERO (CRD42022333165).

Inclusion and exclusion criteria

Eligible studies met the following inclusion criteria: (I) adult patients (aged ≥18 years) who had ARDS treated with the three interventions, as outlined in the 2019 Guidelines on the Management of ARDS (8); (II) interventions involving corticosteroids, iNO, or NMBAs in the treatment group, with a matched placebo or conventional therapy in the control group. Studies were excluded if they met any of the following criteria: (I) publication types such as letters, case reports, reviews, or editorials; (II) *in vitro* or animal studies; (III) insufficient or unavailable data. No language restrictions were applied.

Data collection and outcomes

Two reviewers (Zhiyuan Xu and Xiao Liu) independently extracted data using a standardized form. Any disagreements were resolved through consensus or, when necessary, a third reviewer (Pro Yan). The primary outcome was 28-day mortality, defined as the mortality rate on the 28th day of treatment. The secondary outcomes included ventilator-free days at 28 days (the number of days without ventilator use by day 28), ICU mortality, in-hospital mortality, and the occurrence of new infections.

Risk of bias assessment and quality assessment

Two reviewers (Zhiyuan Xu and Liang Zhang) independently screened articles and assessed studies for inclusion. Discrepancies were resolved through discussion with a third reviewer (Pro Yan). The reviewers evaluated the risk of bias using the Cochrane assessment tool, considering seven domains such as random sequence generation,

allocation concealment, blinding of participants and personnel, blinding of outcome assessment, incomplete outcome data, selective reporting, and other potential biases (12). Each domain was graded as low, high, or unclear risk of bias. Any disagreements regarding the quality assessment were resolved through consensus with the third reviewer.

Statistical analysis

We performed a frequentist NMA using the mvmeta command in Stata 16.0. All treatment comparisons were presented using a network graph for each outcome. The nodes in the evidence diagram represented different intervention measures, and the lines between these nodes represented different head-to-head comparisons. Dichotomous variables were summarized as odds ratios (ORs) with 95% confidence intervals (CIs), while continuous variables were expressed as mean differences (MDs) with 95% CIs. Statistical heterogeneity was initially assessed in each comparison using the I^2 statistic, which categorizes heterogeneity as low (<25%), moderate (25–50%), or high (>50%) (13).

To provide a more comprehensive assessment of heterogeneity, we also calculated τ^2 values, which were categorized based on established guidelines as low (<0.04), low-to-moderate (0.04–0.16), moderate-to-high (0.16–0.36), and high (>0.36). Model selection was guided by heterogeneity measures: a random-effects model was adopted when $I^2 > 50\%$ or when τ^2 values suggested notable heterogeneity; otherwise, a fixed-effects model was applied (14). Residual deviance was assessed using a chi-squared (chi^2) test to evaluate the model adequacy. The residual deviance was compared to its degrees of freedom (df), with values closer to the df indicating a better model fit.

We presented rank probabilities for each intervention and determined the treatment hierarchy using the surface under the cumulative ranking curve (SUCRA) (15). Higher SUCRA probabilities indicate a higher likelihood of being the most effective treatment. Ranking results were interpreted in the context of relative risk estimates and their corresponding 95% CIs for each comparison. To assess the robustness of our findings, sensitivity analyses were conducted to evaluate the impact of risk of bias on the overall study outcomes. We visually inspected funnel plots for publication bias, focusing on primary outcomes and adverse events. No substantial asymmetry was detected, suggesting minimal risk of publication bias.

Results

Characteristics, risk of bias, and consistency

The risk of bias assessments for the studies included in each outcome analysis are detailed in Supplementary Figure 1. A total of 7,136 reports were screened, of which 26 trials involving 5,071 participants met the eligibility criteria (Figure 1). These trials comprised 24 studies published in English (16–39) and 2 high-quality studies published in Chinese (40, 41).

Among the 26 included studies, 12 (16, 17, 20, 22, 24, 26, 29–31, 33, 34, 37) reported ventilator-free days at 28 days, and 17 (18, 20–22, 26, 27, 29, 30, 32–34, 36–41) provided data on 28-day mortality. ICU mortality was assessed in 10 studies (16, 20, 21, 24, 25, 30–33, 35), while 14 studies (16, 18–20, 23–25, 28–30, 32, 33, 35, 36) reported in-hospital mortality. Additionally, 13 studies (16, 17, 19–21, 24–28, 36, 37, 40) provided data on new infection events. The baseline characteristics of all included studies are summarized in Table 1.

The consistency analyses for all outcomes showed *p*-values greater than 0.05, indicating good consistency (Supplementary Table 1). Additionally, only two outcomes, in-hospital mortality and new infection events, formed closed loops, allowing for further node-splitting analysis. The results of the node-splitting method also indicated *p*-values greater than 0.05, confirming good consistency (Supplementary Tables 2, 3). Heterogeneity, assessed using τ^2, suggested that overall heterogeneity was low to moderate across all outcomes (Supplementary Table 1). Furthermore, funnel plots showed good symmetry, indicating no significant publication bias (Supplementary Figure 2).

28-day mortality

Data regarding the efficiency of corticosteroids, iNO, and NMBAs on 28-day mortality were available from 17 trials (18, 20–22, 26, 27, 29, 30, 32–34, 36–41) involving 3,930 patients. As shown in Figures 2, 3, vecuronium bromide was more effective than conventional therapy (OR 0.38, 95% CI 0.15–1.00), iNO (OR 0.30, 95% CI 0.10–0.85), methylprednisolone (OR 0.25, 95% CI 0.08–0.74), and placebo (OR 0.23, 95% CI 0.08–0.65). Dexamethasone was only better than placebo (OR 0.47, 95% CI 0.24–0.93). Cisatracurium was found to be superior to methylprednisolone (OR 0.59, 95% CI 0.38–0.90) and placebo (OR 0.53, 95% CI 0.33–0.85). Conventional therapy also showed an advantage over placebo (OR 0.59, 95% CI 0.38–0.91). However, no treatment has shown significant advantages over the others when comparing hydrocortisone, iNO, methylprednisolone, and placebo. The effects of all drugs were ranked based on SUCRA probabilities (Figure 4). Vecuronium bromide had the greatest probability (SUCRA 96.6%) of being the best treatment option for reducing 28-day mortality in patients with ARDS, followed by dexamethasone (SUCRA 73.8%), cisatracurium (SUCRA 67.3%), conventional therapy (SUCRA 57.7%), hydrocortisone (SUCRA 47.4%), iNO (SUCRA 32.4%), methylprednisolone (SUCRA 17.4%), and placebo, which ranked last (SUCRA 7.4%).

Ventilator-free days at 28 days

A total of 12 studies (16, 17, 20, 22, 24, 26, 29–31, 33, 34, 37) involving 3,119 patients evaluated the effect of these drugs on ventilator-free days at 28 days. Compared to placebo, both dexamethasone and methylprednisolone increased ventilator-free days at 28 days (MD 5.50, 95% CI 1.91–9.08 and MD 4.31, 95% CI 2.37–6.26) (Figures 2, 3). Dexamethasone and methylprednisolone also have a significant benefit for ventilator-free days at 28 days (MD 4.97, 95% CI 0.74–9.21) and (MD 3.79, 95% CI 0.94–6.64) compared to the iNO group. Compared to conventional therapy and cisatracurium, dexamethasone showed a significant superiority (MD 3.60, 95% CI 1.77–5.43, and MD 3.40, 95% CI 0.87–5.92) in ventilator-free days at 28 days. However, iNO, cisatracurium, and hydrocortisone exhibited no superiority of ventilator-free days at 28 days over placebo or conventional therapy. As shown in Figure 5, dexamethasone had the highest probability of being

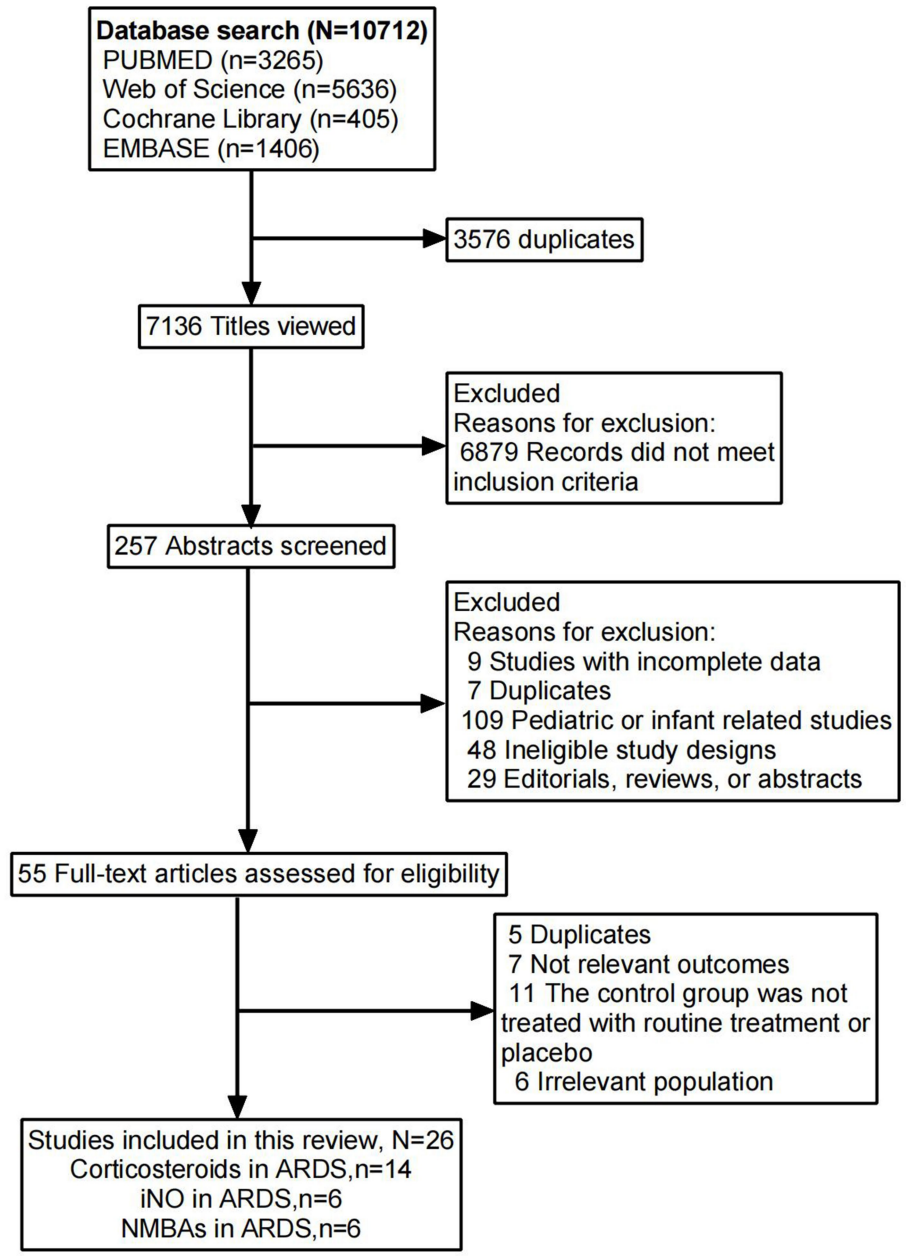

FIGURE 1
Flowchart for identifying studies eligible for the meta-analysis.

the best treatment option for increasing ventilator-free days at 28 days (SUCRA 93.2%), followed by methylprednisolone (SUCRA 82.4%). Hydrocortisone (SUCRA 51.6%) and cisatracurium (SUCRA 48.5%) ranked third and fourth, respectively, followed by conventional therapy (SUCRA 43.1%), iNO (SUCRA 21.7%), and placebo (SUCRA 9.4%).

ICU mortality

ICU mortality was reported from a total of 10 studies (16, 20, 21, 24, 25, 30–33, 35) of 1,244 patients. Methylprednisolone significantly decreased the mortality in ICU compared with placebo (OR 0.48, 95% CI 0.33–0.72), as shown in Figures 2, 3. The therapy of methylprednisolone, cisatracurium, and dexamethasone was superior to conventional therapy in reducing ICU mortality (OR 0.34, 95% CI 0.13–0.90; OR 0.46, 95% CI 0.21–0.99; and OR 0.58, 95% CI 0.34–1.00). The therapy of iNO had no advantages in reducing mortality in the ICU over other treatments. Our results (Figure 6) suggested that, regarding prevention of ICU mortality, methylprednisolone (SUCRA 88.5%) was most effective, followed by cisatracurium (SUCRA 69.4%), dexamethasone (SUCRA 53.7%), iNO (SUCRA 42.3%), placebo (SUCRA 33.6%), and conventional therapy (SUCRA 12.4%).

In-hospital mortality

A total of 14 studies (16, 18–20, 23–25, 28–30, 32, 33, 35, 36) involving 3,327 participants assessed in-hospital mortality. As shown

TABLE 1 Characteristics of the included studies.

Study	Year	Country	Research type	Sample size	Treatment group (PaO_2/FiO_2, mm Hg)	Control group (PaO_2/FiO_2, mm Hg)	Primary outcome	Secondary outcome	Score of NOS	Score of Jadad
Villar (16)	2020	Spain	Randomized controlled trial	277	142.4 ± 37·3	143.5 ± 33.4	Ventilator-free days at 28 days	All-cause mortality 60 days	–	5
Steinberg (17)	2006	USA	Randomized controlled trial	180	126 ± 42	126 ± 40	Mortality at 60 days	Ventilator-free days at 28 days	–	5
Liu J (18)	2020	China	Retrospective study	774	168 (IQR 99–237)	168 (IQR 99–237)	28-day all-cause mortality.	In-hospital mortality	8	–
Bernard (19)	1987	USA	Randomized controlled trial	99	–	–	Mortality at 45 days	New infection events	–	5
Annane (20)	2006	France	Retrospective study	177	104 ± 42	108 ± 45	Ventilator-free days at 28 days	Mortality in ICU	7	–
Meduri (21)	2018	USA	Retrospective study	180	–	–	Mortality at 28 days	New infection events	8	–
Tongyoo (22)	2016	Thailand	Randomized controlled trial	197	175.4 ± 6.9	172.4 ± 6.7	28-day all-cause mortality	Ventilator-free days at 28 days	–	5
HS Lee (23)	2005	Korea	Retrospective study	20	142.5 ± 23.7	143.4 ± 23.9	In-hospital mortality	Hospital stay days	7	–
Meduri (24)	2007	USA	Randomized controlled trial	91	118.4 ± 51.2	125.9 ± 38.6	Ventilator-free days at 28 days	Mortality in ICU	–	4
Meduri (25)	1998	USA	Randomized controlled trial	24	161 ± 14	141 ± 19	Lung function and mortality	MODS scores	–	5
Tomazini (26)	2020	Brazil	Randomized controlled trial	299	131.1 ± 46.2	132.6 ± 45.7	Ventilator-free days at 28 days	All-cause mortality at 28 days	–	5
Liu L (40)	2012	China	Randomized controlled trial	26	138.2 (87.0, 171.0)	157.0 (88.7, 176.3)	Mortality at 28 days	New infection events	–	4
Varpula (27)	2000	Finland	Retrospective study	31	126.3 ± 52.4	107 ± 41.4	Mortality at 28 days	New infection events	7	–
Buisson (28)	2011	French	Retrospective study	208	101 (73–174)	107 (78–144)	In-hospital mortality	New infection events	9	–
Moss (29)	2019	USA	Randomized controlled trial	1,006	98.7 ± 27.9	99.5 ± 27.9	In-hospital mortality	Organ dysfunction	–	5
Gainnier (30)	2004	France	Randomized controlled trial	56	130 ± 34	119 ± 31	Ventilator-free days at 28 days	Mortality in ICU	–	4
Guervilly (31)	2016	France	Randomized controlled trial	24	158 (131; 185)	150 (121; 187)	Ventilator-free days at 28 days	Mortality in ICU	–	5
Forel (32)	2006	France	Randomized controlled trial	36	105 ± 22	125 ± 20	Mortality at 28 days	Mortality in ICU	–	4
Papazian (33)	2010	France	Randomized controlled trial	340	106.0 ± 36.0	115.0 ± 41.0	The 90-day mortality	The day-28 mortality	–	5
Lyu (41)	2014	China	Randomized controlled trial	96	141.0 ± 26.1	144.3 ± 24.1	Mortality at 28 days	APACHE 1I scores	–	4
Dellinger (34)	1998	USA	Randomized controlled trial	177	135 ± 41.0	129.0 ± 38.0	Ventilator-free days at 28 days	The day-28 mortality	–	4

(Continued)

10.3389/fmed.2025.1507805

TABLE 1 (Continued)

Study	Year	Country	Research type	Sample size	Treatment group (PaO_2/FiO_2, mm Hg)	Control group (PaO_2/FiO_2, mm Hg)	Primary outcome	Secondary outcome	Score of NOS	Score of Jadad
Gerlach (35)	2003	Germany	Randomized controlled trial	40	113.0 ± 28.0	104.0 ± 26.0	Duration of ventilation	Mortality in ICU	–	4
Lundin (36)	1999	UK	Randomized controlled trial	268	102.8 ± 32.3	100.5 ± 33.0	The day-28 mortality	New infection events	–	4
Taylor (37)	2004	USA	Randomized controlled trial	385	133.0 ± 42.0	138.0 ± 43.0	Ventilator-free days at 28 days	The day-28 mortality	–	5
Troncy (38)	1998	Canada	Randomized controlled trial	30	–	–	The day-28 mortality	APACHE II scores	–	4
Cuthbertson (39)	2000	UK	Randomized controlled trial	30	–	–	The day-28 mortality	APACHE II scores		4

in Figures 2, 3, compared with the conventional treatment or placebo, dexamethasone, cisatracurium, methylprednisolone, and iNO showed no significant advantages in reducing hospital mortality. As shown in Figure 7, dexamethasone reduced the incidence of in-hospital mortality at the top-ranking position (SUCRA 79.7%), followed by cisatracurium (SUCRA 72.1%), conventional therapy (SUCRA 47.6%), methylprednisolone (SUCRA 45.6%), iNO (SUCRA 42.1%), and placebo (SUCRA 13.0%).

New infection events

Data regarding new infection events were available from 13 trials (16, 17, 19–21, 24–28, 36, 37, 40) involving 2,157 patients. Dexamethasone significantly decreased the rate of new infection events compared to hydrocortisone and iNO (OR 0.46, 95% CI 0.24–0.89, and OR 0.25, 95% CI 0.10–0.59), as shown in Figures 2, 3. Methylprednisolone had advantages in protecting against new infection events compared to placebo and iNO (OR 0.61, 95% CI 0.42–0.88 and OR 0.33, 95% CI 0.19–0.58). Conventional therapy also significantly reduced new infection events (OR 0.59, 95% CI 0.35–1.00 and OR 0.32, 95% CI 0.15–0.69) compared to hydrocortisone and iNO. In addition, placebo significantly decreased the rate of new infection events compared to iNO (OR 0.53, 95% CI 0.34–0.83). For decreasing the incidence of new infection events, dexamethasone showed the highest safety ranking (Figure 8, SUCRA 91.8%), followed by methylprednisolone (SUCRA 72.3%) and conventional therapy (SUCRA 70.9%). Placebo (SUCRA 32.5%) and hydrocortisone (SUCRA 31.2%) ranked fourth and fifth, respectively, while iNO ranked last (SUCRA 1.2%).

Discussion

This is the first NMA to directly compare the efficacy and safety of corticosteroids, iNO, and NMBAs in adult patients with ARDS. Our findings suggest that vecuronium may be the most effective treatment for reducing 28-day mortality in these patients. However, its effect was not significantly different from dexamethasone, cisatracurium, or hydrocortisone. Dexamethasone and methylprednisolone demonstrated significant benefits in increasing ventilator-free days at 28 days. Additionally, methylprednisolone, cisatracurium, and dexamethasone showed significant efficacy in reducing ICU mortality, with methylprednisolone ranking highest. Dexamethasone and methylprednisolone were also effective in preventing new infections in ARDS patients. However, no intervention demonstrated superiority over others in reducing in-hospital mortality.

While our findings provide important insights, the applicability of these treatments may vary across different patient subgroups. ARDS is a highly heterogeneous syndrome with diverse causes, such as sepsis, trauma, and pneumonia, which may influence treatment response. For instance, corticosteroids may be more effective in treating ARDS caused by systemic inflammation (e.g., sepsis), given their anti-inflammatory and antifibrotic properties. In contrast, their benefits might be less pronounced in trauma-induced ARDS due to differences in inflammatory profiles. Similarly, age and comorbidities could impact treatment efficacy. Younger patients with greater physiological resilience may respond better to corticosteroids or NMBAs, while older patients or

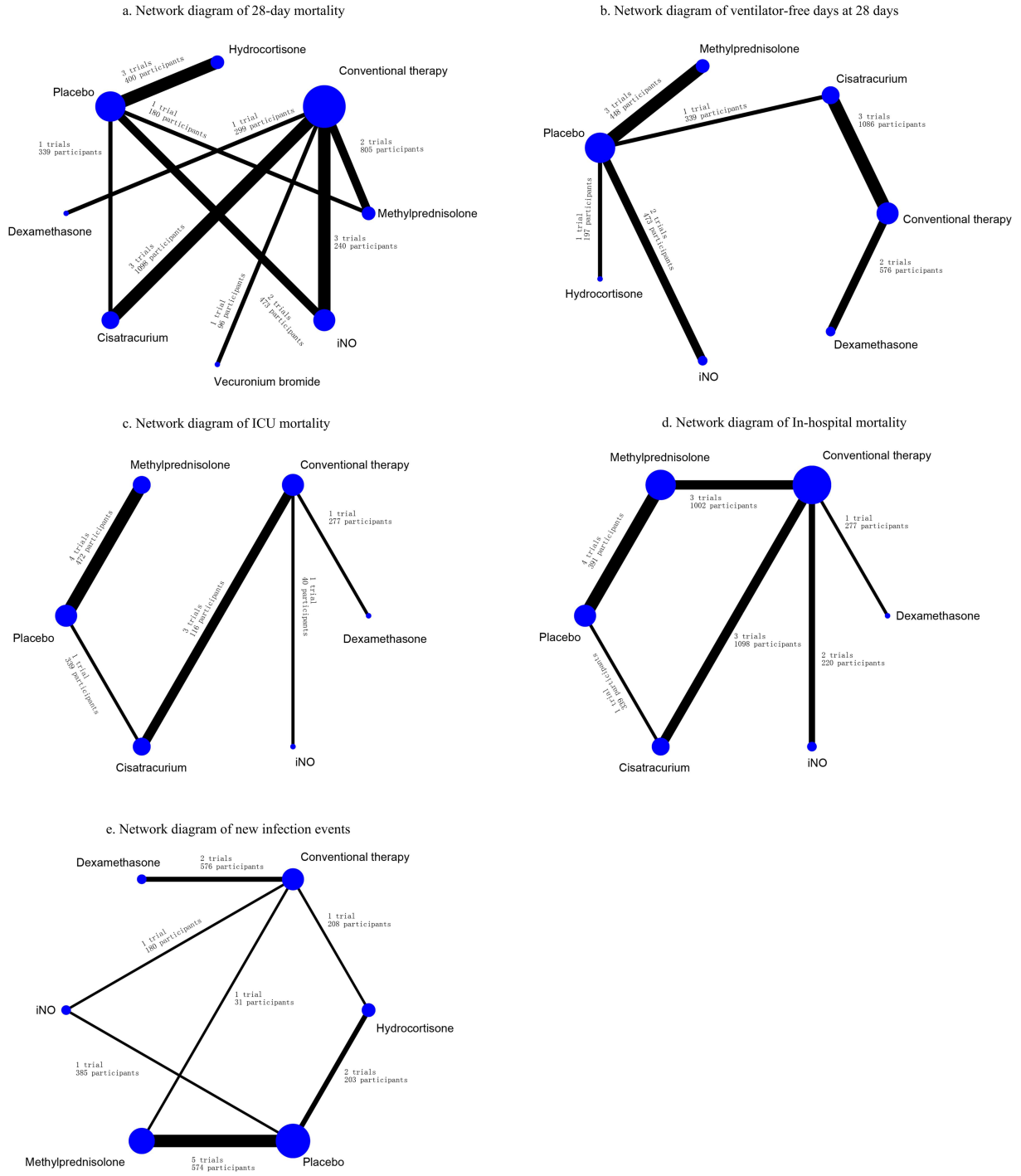

FIGURE 2
Network diagrams for the association between interventions and outcomes. **(A)** Network diagram of 28-day mortality. **(B)** Network diagram of ventilator-free days at 28 days. **(C)** Network diagram of ICU mortality. **(D)** Network diagram of in-hospital mortality. **(E)** Network diagram of new infection events. Network diagrams showing ARDS treatment comparisons in clinical trials with respect to the number of studies and sample sizes. The width of the line is proportional to the number of trials directly comparing each pair of treatments, and the size of each node is proportional to the sample size of randomized participants.

those with significant comorbidities, such as chronic kidney disease or diabetes, may be more susceptible to adverse effects, such as infections or myopathy. Future studies should explore these subgroups to further refine treatment recommendations.

Two recent studies (10) demonstrated that corticosteroids may reduce short-term mortality and the duration of mechanical ventilation in patients with ARDS. Corticosteroids, with their anti-inflammatory properties, help maintain endothelial integrity, reduce pro-inflammatory cytokines, and inhibit nitric oxide synthases, making them effective in managing various inflammatory conditions (10). Additionally, their antifibrotic properties, achieved by inhibiting fibroblast growth and collagen deposition, further support their

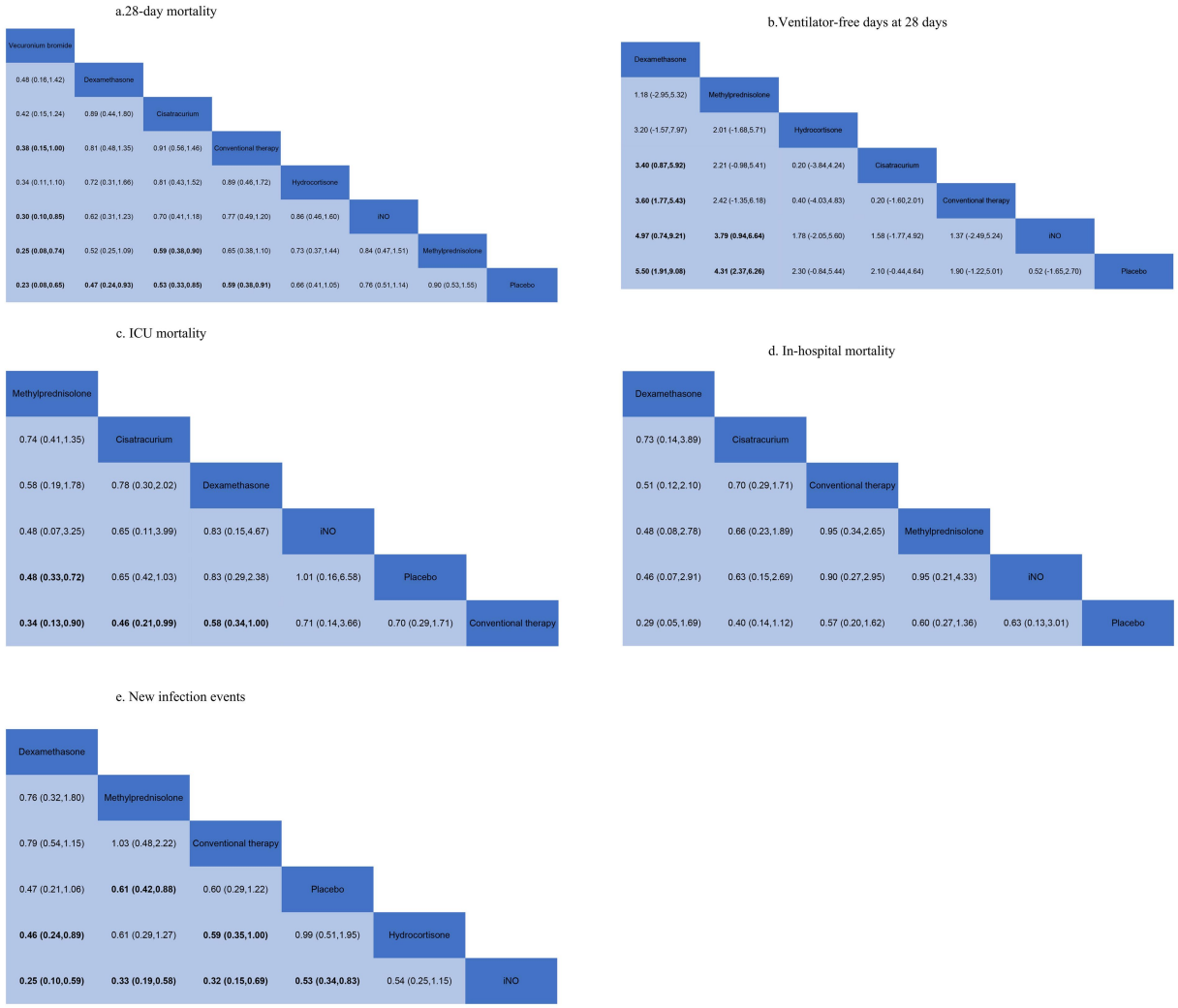

FIGURE 3
Summary of results from network meta-analysis. **(A)** 28-day mortality. **(B)** Ventilator-free days at 28 days. **(C)** ICU mortality. **(D)** In-hospital mortality. **(E)** New infection events.

therapeutic role (42). Another study (43) suggested that the effectiveness of corticosteroids in ARDS may vary depending on the specific medication used, a finding consistent with our results. The long-standing hypothesis that corticosteroid therapy benefits ARDS patients (17, 25) is strongly supported by the findings of our NMA. Our analysis confirmed that corticosteroids reduce short-term mortality and the duration of mechanical ventilation in ARDS patients. These results suggest that clinicians can consider corticosteroids to mitigate the immediate life-threatening risks associated with ARDS and to reduce the incidence of infections. Additionally, corticosteroids reduce ventilator dependency, promote the recovery of spontaneous breathing, and improve lung function, thereby contributing to overall patient recovery.

Muscle relaxation therapy, a common non-ventilatory strategy, is frequently employed by clinicians to treat moderate-to-severe ARDS (33). The benefits of NMBAs are primarily attributed to their pharmacological ability to control tidal volume and improve ventilator synchronization (44). NMBAs enhance patient–ventilator coordination by relaxing skeletal muscles and enabling better tidal volume management (45). The efficacy of NMBAs in ARDS is well documented. Numerous studies indicate that NMBAs can reduce ventilator-induced lung injury by improving man–machine synchronization, lowering oxygen consumption, and potentially exerting indirect anti-inflammatory effects. Over the past two decades, multiple clinical trials have evaluated the role of NMBAs in ARDS management (30–33, 41, 46). However, the results have often been inconsistent, complicating clinical decisions regarding their use. Our study provides new insights showing that NMBAs effectively reduce the 28-day mortality and ICU mortality of ARDS patients. These findings are more robust and innovative than those of some previous studies (11, 47–50), offering valuable evidence to guide clinical judgment on using NMBAs in ARDS management.

Nitric oxide was first identified as an endogenous vasodilator in 1987 (51), leading to its application in treating pulmonary hypertension and lung diseases (52, 53). Currently, iNO is commonly used to manage pulmonary hypertension, ARDS, and hypoxic respiratory failure in children (54–56). However, unlike corticosteroids and NMBAs, using iNO in ARDS has been highly controversial. In

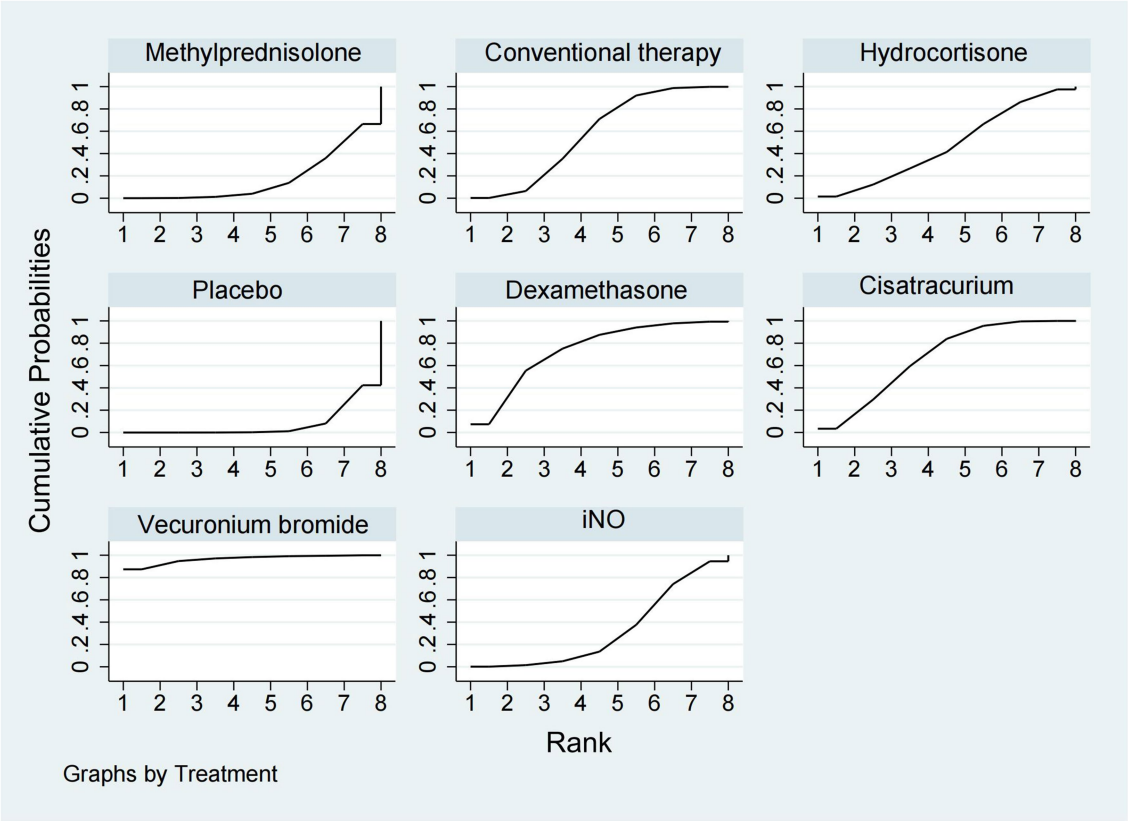

FIGURE 4
Ranking of treatment strategies based on the probability of their protective effects on outcomes of 28-day mortality according to the cumulative ranking area (SUCRA).

2007, Adhikari et al. reported that iNO was associated with renal insufficiency in ARDS patients, with limited metabolic improvements and potential harm (57). A follow-up study in 2014 (58) reached similar conclusions, showing that iNO does not reduce mortality in adults or children with ARDS. Consistent with these findings, our NMA demonstrated that iNO does not improve mortality rates or ventilator-free days in ARDS patients. Several factors may explain why iNO fails to improve outcomes. First, the prolonged fixed-dosing regimens used in most trials may diminish their benefits over time, as increased sensitivity can inhibit oxygenation improvements while exposing patients to potential toxic effects, such as oxidative damage (59). Second, even in severe cases of hypoxemia, ARDS patients often succumb to primary respiratory failure rather than multiple organ failure. In such cases, the modest oxygenation benefits of iNO may be outweighed by the harmful effects of mechanical ventilation strategies employed in most trials, which often lack strict limitations on tidal volume or airway pressure.

Strengths and limitations of the study

This NMA is the first to directly compare the effectiveness and safety of three treatments for ARDS patients. Building on prior research, we included new and relevant studies while excluding low-quality or ineligible ones, aiming to provide a robust evidence base for ARDS treatment. However, several limitations, including potential confounders and variability in study quality, warrant a detailed discussion.

The quality of the included studies varied which may have influenced the results. While most included studies were RCTs, a few non-RCTs were included to ensure comprehensive data coverage. Non-RCTs, lacking methodological rigor such as randomization and blinding, are prone to selection, performance, and detection biases. For example, open-label designs may introduce observer bias, particularly in subjective outcomes like infection rates or ventilator-free days. Additionally, inconsistencies in trial protocols, including randomization methods, blinding, and follow-up duration, further complicate result interpretation. Double-blind studies minimize bias, but unblinded designs may inflate perceived treatment effects. Shorter follow-up periods may underestimate adverse effects or fail to capture long-term treatment benefits.

Including studies with varying designs, such as observational and non-RCTs, introduces additional complexity. Observational studies, while valuable for hypothesis generation, are prone to confounding due to the absence of randomization. Variations in baseline characteristics, such as ARDS severity, comorbidities, and treatment settings, may disproportionately influence outcomes, particularly in studies with smaller sample sizes. Although network meta-analyses accommodate data from diverse study designs, including heterogeneous designs raises concerns about comparing populations, interventions, and outcomes. Such heterogeneity may contribute to variations in effect sizes and confidence intervals, potentially limiting the generalizability of findings.

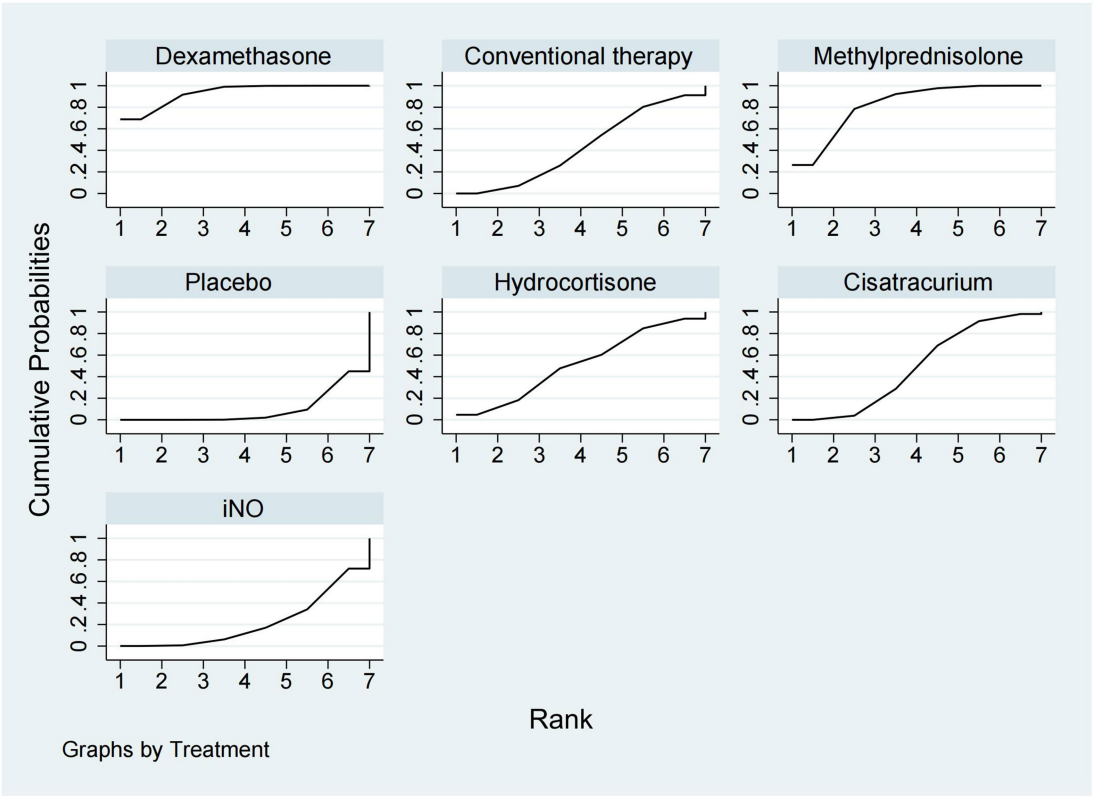

FIGURE 5
Ranking of treatment strategies based on the probability of their protective effects on outcomes of ventilator-free days at 28 days according to the surface under the cumulative ranking area (SUCRA).

Despite efforts to control for confounders, residual confounding likely influenced the results. Differences in baseline patient characteristics, such as age, sex, comorbidities, and immune status, may affect treatment efficacy and safety. For example, younger ARDS patients often exhibit better immune resilience, potentially amplifying the perceived benefits of corticosteroids or neuromuscular blocking agents in studies involving younger populations. Similarly, comorbidities such as diabetes or chronic kidney disease may impact outcomes such as infection rates or mortality. Geographical differences and variations in healthcare systems further contribute to confounding factors. Patients in countries with advanced critical care infrastructure may experience better outcomes irrespective of the intervention, due to higher baseline care quality. For instance, studies conducted in high-income countries may report lower mortality rates than those from low- or middle-income countries, reflecting differences in supportive care rather than the effectiveness of interventions themselves.

Variations in patient recruitment criteria, particularly in PaO_2/FiO_2 thresholds, introduced heterogeneity in ARDS severity among included studies. Some trials exclusively enrolled patients with severe ARDS, while others included a broader spectrum of disease severity. These differences may skew the results, as treatments exhibit varying efficacy across different ARDS severities. For instance, Herwig Gerlach's study focused on severe ARDS, potentially overstating the benefits of treatments that may not perform as effectively in milder cases.

Our analysis of adverse effects was limited to new infections, and infection definitions varied across studies. This inconsistency may have introduced additional bias and underestimated other adverse events, such as renal insufficiency or neuromuscular complications. Furthermore, inconsistent reporting of adverse effects across trials restricted the evaluation of comprehensive safety profiles for each intervention.

This study primarily evaluated short-term outcomes, such as 28-day mortality and ventilator-free days. Still, it did not assess long-term outcomes such as functional recovery, quality of life, or survival beyond 28 days. While short-term metrics are relevant for acute interventions, they do not capture the full impact of treatments on patient outcomes. Future studies should explore long-term implications, particularly as ARDS survivors often face prolonged morbidity and impaired lung function.

To address these limitations, future studies should focus on well-designed, high-quality RCTs with consistent recruitment criteria, rigorous randomization, and standardized outcome reporting, covering both short- and long-term metrics. Meta-analyses of individual patient data (IPD) could provide more granular insights by enabling subgroup analyses based on age, severity, and comorbidities. Additionally, further research is needed to comprehensively evaluate the safety profiles of the interventions, particularly for rare but serious adverse events, and to better understand their long-term effects.

Conclusion

This NMA indicates that corticosteroids improve short-term survival, increase ventilator-free days, and reduce infection rates in patients with ARDS. NMBAs may also minimize 28-day mortality, while iNO offers no significant benefit. Based on these findings, we recommend the use of corticosteroids or NMBAs in the treatment

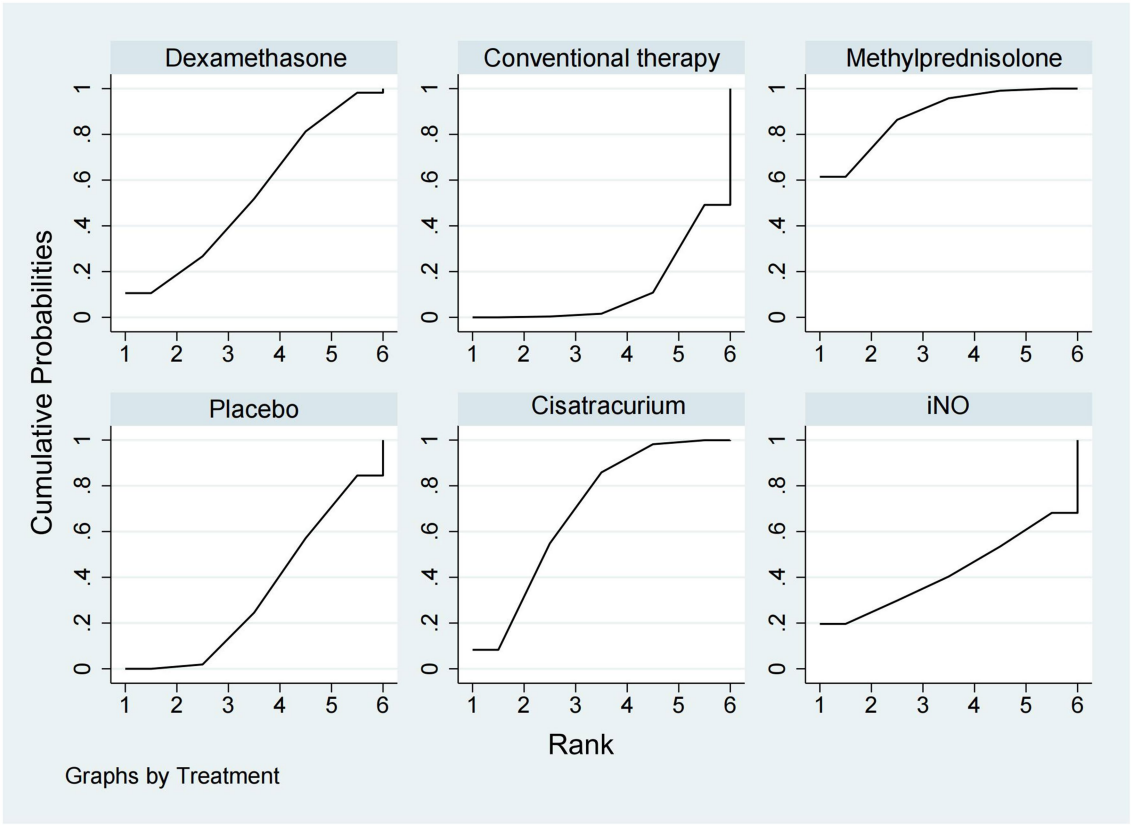

FIGURE 6
Ranking of treatment strategies based on the probability of their protective effects on outcomes of ICU mortality according to the surface under the cumulative ranking area (SUCRA).

of ARDS. However, important questions remain, including the long-term survival benefits, variations in treatment efficacy based on the underlying cause of ARDS, and optimal protocols for the type, dosage, and duration of corticosteroid or NMBA use. Future trials should address these critical gaps to refine treatment strategies further.

Data availability statement

The original contributions presented in the study are included in the article/Supplementary material, further inquiries can be directed to the corresponding authors.

Author contributions

ZX: Data curation, Software, Writing – original draft, Methodology, Writing – review & editing. XL: Conceptualization, Formal analysis, Investigation, Methodology, Project administration, Supervision, Writing – review & editing. LZ: Methodology, Project administration, Resources, Software, Supervision, Validation, Writing – review & editing, Formal analysis. XY: Conceptualization, Funding acquisition, Project administration, Resources, Supervision, Validation, Visualization, Writing – review & editing.

Funding

The author(s) declare that financial support was received for the research, authorship, and/or publication of this article. This research was supported by the Excellent Teaching Team of "Qinglan Project" in Jiangsu, Xuzhou National Clinical Key Specialty Cultivation Project (2018ZK004), Jiangsu Provincial Commission of Health and Family Planning (LGY2019085), the excellent young and middle-age talents project of the affiliated hospital of Xuzhou medical university (2019128009), National keypoint research and invention program (2020YFC151270).

Acknowledgments

We thank Pro Yan for administrative, technical, and material support, and we thank Liang Zhang for statistical analysis.

Conflict of interest

The authors declare that the research was conducted in the absence of any commercial or financial relationships that could be construed as a potential conflict of interest.

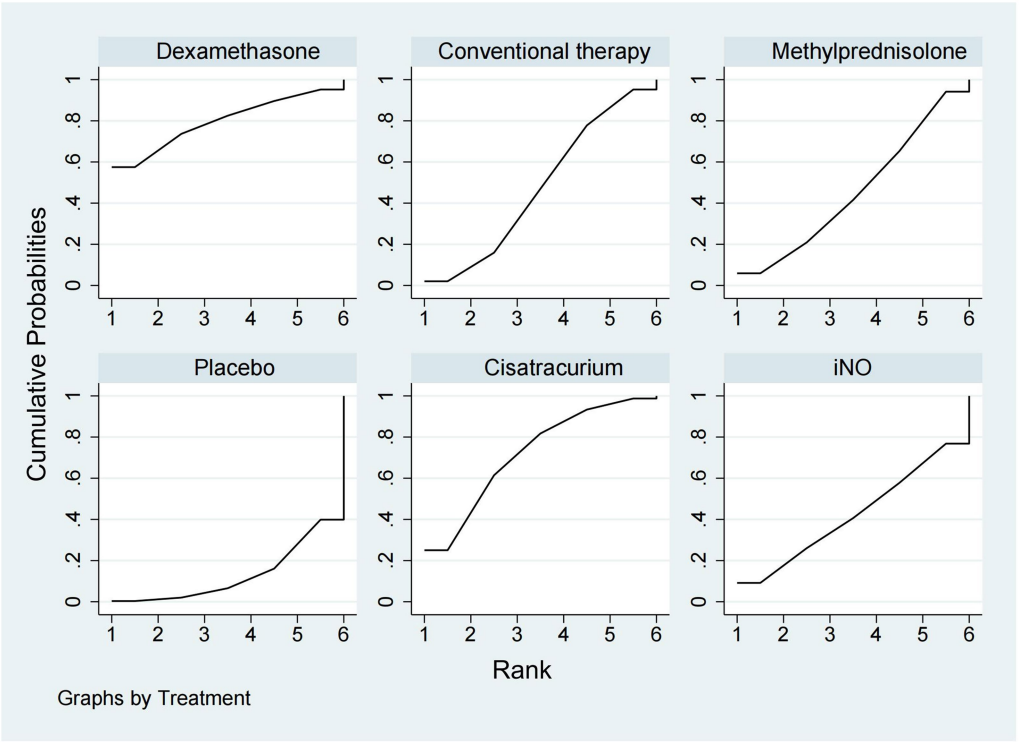

FIGURE 7
Ranking of treatment strategies based on the probability of their protective effects on outcomes of in-hospital mortality according to the surface under the cumulative ranking area (SUCRA).

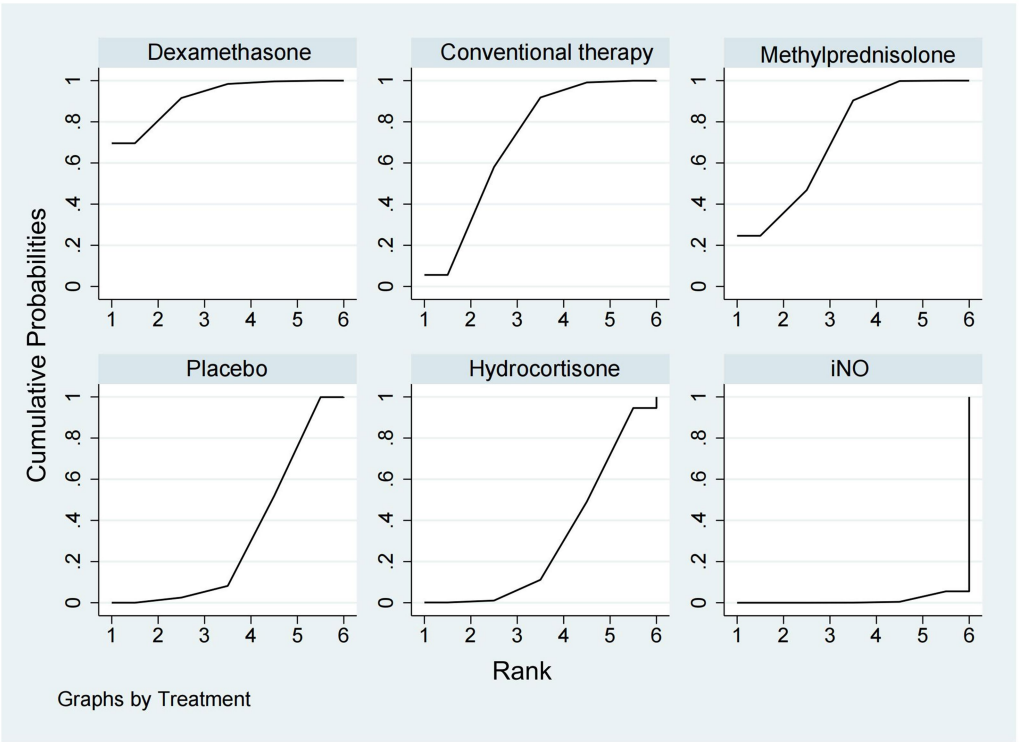

FIGURE 8
Ranking of treatment strategies based on the probability of their protective effects on outcomes of new infection events according to the surface under the cumulative ranking area (SUCRA).

Generative AI statement

The authors declare that no Gen AI was used in the creation of this manuscript.

Publisher's note

Supplementary material

The Supplementary material for this article can be found online at: https://www.frontiersin.org/articles/10.3389/fmed.2025.1507805/full#supplementary-material

References

1. Villar J, Blanco J, Añón JM, Santos-Bouza A, Blanch L, Ambrós A, et al. The ALIEN study: incidence and outcome of acute respiratory distress syndrome in the era of lung protective ventilation. *Intensive Care Med*. (2011) 37:1932–41. doi: 10.1007/s00134-011-2380-4

2. Bellani G, Laffey JG, Pham T, Fan E, Brochard L, Esteban A, et al. Epidemiology, patterns of care, and mortality for patients with acute respiratory distress syndrome in intensive care units in 50 countries. *JAMA*. (2016) 315:788–800. doi: 10.1001/jama.2016.0291

3. Meyer NJ, Gattinoni L, Calfee CS. Acute respiratory distress syndrome. *Lancet*. (2021) 398:622–37. doi: 10.1016/S0140-6736(21)00439-6

4. Ashbaugh DG, Bigelow DB, Petty TL, Levine BE. Acute respiratory distress in adults. *Lancet*. (1967) 2:319–23. doi: 10.1016/S0140-6736(67)90168-7

5. Fan E, Brodie D, Slutsky AS. Acute respiratory distress syndrome: advances in diagnosis and treatment. *JAMA*. (2018) 319:698–710. doi: 10.1001/jama.2017.21907

6. Thompson BT, Chambers RC, Liu KD. Acute respiratory distress syndrome. *N Engl J Med*. (2017) 377:562–72. doi: 10.1056/NEJMra1608077

7. Aoyama H, Uchida K, Aoyama K, Pechlivanoglou P, Englesakis M, Yamada Y, et al. Assessment of therapeutic interventions and lung protective ventilation in patients with moderate to severe acute respiratory distress syndrome: a systematic review and network Meta-analysis. *JAMA Netw Open*. (2019) 2:e198116. doi: 10.1001/jamanetworkopen.2019.8116

8. Griffiths, MJD, McAuley, DF, Perkins, GD, Barrett, N, Blackwood, B, Boyle, A, et al. Guidelines on the management of acute respiratory distress syndrome. *BMJ Open Respir Res*. (2019) 6:e000420. doi: 10.1136/bmjresp-2019-000420

9. Sud S, Friedrich JO, Adhikari NKJ, Fan E, Ferguson ND, Guyatt G, et al. Comparative effectiveness of protective ventilation strategies for moderate and severe acute respiratory distress syndrome. A network Meta-analysis. *Am J Respir Crit Care Med*. (2021) 203:1366–77. doi: 10.1164/rccm.202008-3039OC

10. Chaudhuri D, Sasaki K, Karkar A, Sharif S, Lewis K, Mammen MJ, et al. Corticosteroids in COVID-19 and non-COVID-19 ARDS: a systematic review and meta-analysis. *Intensive Care Med*. (2021) 47:521–37. doi: 10.1007/s00134-021-06394-2

11. Hirano Y, Madokoro S, Kondo Y, Okamoto K, Tanaka H. Corticosteroid treatment for early acute respiratory distress syndrome: a systematic review and meta-analysis of randomized trials. *J Intensive Care*. (2020) 8:91. doi: 10.1186/s40560-020-00510-y

12. Hutton B, Salanti G, Caldwell DM, Chaimani A, Schmid CH, Cameron C, et al. The PRISMA extension statement for reporting of systematic reviews incorporating network meta-analyses of health care interventions: checklist and explanations. *Ann Intern Med*. (2015) 162:777–84. doi: 10.7326/M14-2385

13. Cumpston M, Li T, Page MJ, Chandler J, Welch VA, Higgins JPT, et al. Updated guidance for trusted systematic reviews: a new edition of the Cochrane handbook for systematic reviews of interventions. *Cochrane Database Syst Rev*. (2019) 10:ED000142. doi: 10.1002/14651858.ED000142

14. Lin L. Comparison of four heterogeneity measures for meta-analysis. *J Eval Clin Pract*. (2020) 26:376–84. doi: 10.1111/jep.13159

15. Riley RD, Higgins JP, Deeks JJ. Interpretation of random effects meta-analyses. *BMJ*. (2011) 342:d549. doi: 10.1136/bmj.d549

16. Villar J, Ferrando C, Martínez D, Ambrós A, Muñoz T, Soler JA, et al. Dexamethasone treatment for the acute respiratory distress syndrome: a multicentre, randomised controlled trial. *Lancet Respir Med*. (2020) 8:267–76. doi: 10.1016/S2213-2600(19)30417-5

17. Steinberg KP, Hudson LD, Goodman RB, Hough CL, Lanken PN, Hyzy R, et al. Efficacy and safety of corticosteroids for persistent acute respiratory distress syndrome. *N Engl J Med*. (2006) 354:1671–84. doi: 10.1056/NEJMoa051693

18. Liu J, Zhang S, Dong X, Li Z, Xu Q, Feng H, et al. Corticosteroid treatment in severe COVID-19 patients with acute respiratory distress syndrome. *J Clin Invest*. (2020) 130:6417–28. doi: 10.1172/JCI140617

19. Bernard GR, Luce JM, Sprung CL, Rinaldo JE, Tate RM, Sibbald WJ, et al. High-dose corticosteroids in patients with the adult respiratory distress syndrome. *N Engl J Med*. (1987) 317:1565–70. doi: 10.1056/NEJM198712173172504

20. Annane D, Sébille V, Bellissant E; Ger-Inf-05 Study Group. Effect of low doses of corticosteroids in septic shock patients with or without early acute respiratory distress syndrome. *Crit Care Med*. (2006) 34:22–30. doi: 10.1097/01.CCM.0000194723.78632.62

21. Meduri GU, Bridges L, Siemieniuk RAC, Kocak M. An exploratory reanalysis of the randomized trial on efficacy of corticosteroids as rescue therapy for the late phase of acute respiratory distress syndrome. *Crit Care Med*. (2018) 46:884–91. doi: 10.1097/CCM.0000000000003021

22. Tongyoo S, Permpikul C, Mongkolpun W, Vattanavanit V, Udompanturak S, Kocak M, et al. Hydrocortisone treatment in early sepsis-associated acute respiratory distress syndrome: results of a randomized controlled trial. *Crit Care*. (2016) 20:329. doi: 10.1186/s13054-016-1511-2

23. Lee HS, Lee JM, Kim MS, Kim HY, Hwangbo B, Zo JI. Low-dose steroid therapy at an early phase of postoperative acute respiratory distress syndrome. *Ann Thorac Surg*. (2005) 79:405–10. doi: 10.1016/j.athoracsur.2004.07.079

24. Meduri GU, Golden E, Freire AX, Taylor E, Zaman M, Carson SJ, et al. Methylprednisolone infusion in early severe ARDS: results of a randomized controlled trial. *Chest*. (2007) 131:954–63. doi: 10.1378/chest.06-2100

25. Meduri GU, Headley AS, Golden E, Carson SJ, Umberger RA, Kelso T, et al. Effect of prolonged methylprednisolone therapy in unresolving acute respiratory distress syndrome: a randomized controlled trial. *JAMA*. (1998) 280:159–65. doi: 10.1001/jama.280.2.159

26. Tomazini BM, Maia IS, Cavalcanti AB, Berwanger O, Rosa RG, Veiga VC, et al. Effect of dexamethasone on days alive and ventilator-free in patients with moderate or severe acute respiratory distress syndrome and COVID-19: the CoDEX randomized clinical trial. *JAMA*. (2020) 324:1307–16. doi: 10.1001/jama.2020.17021

27. Varpula T, Pettilä V, Rintala E, Takkunen O, Valtonen V. Late steroid therapy in primary acute lung injury. *Intensive Care Med*. (2000) 26:526–31. doi: 10.1007/s001340051199

28. Brun-Buisson C, Richard JC, Mercat A, Thiébaut AC. Brochard L; REVA-SRLF a/H1N1v 2009 registry group. Early corticosteroids in severe influenza a/H1N1 pneumonia and acute respiratory distress syndrome. *Am J Respir Crit Care Med*. (2011) 183:1200–6. doi: 10.1164/rccm.201101-0135OC

29. National Heart, Lung, and Blood Institute PETAL Clinical Trials NetworkMoss M, Huang DT, Brower RG, Ferguson ND, Ginde AA, et al. Early neuromuscular blockade in the acute respiratory distress syndrome. N Engl J Med (2019);380:1997–2008, doi: 10.1056/NEJMoa1901686

30. Gainnier M, Roch A, Forel JM, Thirion X, Arnal JM, Donati S, et al. Effect of neuromuscular blocking agents on gas exchange in patients presenting with acute respiratory distress syndrome. *Crit Care Med*. (2004) 32:113–9. doi: 10.1097/01.CCM.0000104114.72614.BC

31. Guervilly C, Bisbal M, Forel JM, Mechati M, Lehingue S, Bourenne J, et al. Effects of neuromuscular blockers on transpulmonary pressures in moderate to severe acute respiratory distress syndrome. *Intensive Care Med*. (2017) 43:408–18. doi: 10.1007/s00134-016-4653-4

32. Forel JM, Roch A, Marin V, Michelet P, Demory D, Blache JL, et al. Neuromuscular blocking agents decrease inflammatory response in patients presenting with acute respiratory distress syndrome. *Crit Care Med*. (2006) 34:2749–57. doi: 10.1097/01.CCM.0000239435.87433.0D

33. Papazian L, Forel JM, Gacouin A, Penot-Ragon C, Perrin G, Loundou A, et al. Neuromuscular blockers in early acute respiratory distress syndrome. *N Engl J Med*. (2010) 363:1107–16. doi: 10.1056/NEJMoa1005372

34. Dellinger RP, Zimmerman JL, Taylor RW, Straube RC, Hauser DL, Criner GJ, et al. Effects of inhaled nitric oxide in patients with acute respiratory distress syndrome: results of a randomized phase II trial. Inhaled nitric oxide in ARDS study group. *Crit Care Med*. (1998) 26:15–23. doi: 10.1097/00003246-199801000-00011

35. Gerlach H, Keh D, Semmerow A, Busch T, Lewandowski K, Pappert DM, et al. Dose-response characteristics during long-term inhalation of nitric oxide in patients with severe acute respiratory distress syndrome: a prospective, randomized, controlled study. *Am J Respir Crit Care Med*. (2003) 167:1008–15. doi: 10.1164/rccm.2108121

36. Lundin S, Mang H, Smithies M, Stenqvist O, Frostell C. Inhalation of nitric oxide in acute lung injury: results of a European multicentre study. The European study Group of Inhaled Nitric Oxide. *Intensive Care Med*. (1999) 25:911–9. doi: 10.1007/s001340050982

37. Taylor RW, Zimmerman JL, Dellinger RP, Straube RC, Criner GJ, Davis K Jr, et al. Low-dose inhaled nitric oxide in patients with acute lung injury: a randomized controlled trial. *JAMA*. (2004) 291:1603–9. doi: 10.1001/jama.291.13.1603

38. Troncy E, Collet JP, Shapiro S, Guimond JG, Blair L, Ducruet T, et al. Inhaled nitric oxide in acute respiratory distress syndrome. *Am J Respir Crit Care Med*. (1998) 157:1483–8. doi: 10.1164/ajrccm.157.5.9707090

39. Cuthbertson BH, Galley HF, Webster NR. Effect of inhaled nitric oxide on key mediators of the inflammatory response in patients with acute lung injury. *Crit Care Med*. (2000) 28:1736–41. doi: 10.1097/00003246-200006000-00006

40. Ling L, Jia L, Yingzi H, Yang CS, Guo FM, Qiu HB, et al. The effect of stress dose glucocorticoid on patients with acute respiratory distress syndrome combined with critical illness-related corticosteroid insufficiency. *Zhonghua Nei Ke Za Zhi*. (2012) 51:599–603.

41. Lyu G, Wang X, Jiang W, Cai T, Zhang Y. Clinical study of early use of neuromuscular blocking agents in patients with severe sepsis and acute respiratory distress syndrome. *Zhonghua Wei Zhong Bing Ji Jiu Yi Xue*. (2014) 26:325–9. doi: 10.3760/cma.j.issn.2095-4352.2014.05.008

42. Thompson BT. Glucocorticoids and acute lung injury. *Crit Care Med*. (2003) 31:S253–7. doi: 10.1097/01.CCM.0000057900.19201.55

43. Yoshihiro S, Hongo T, Ohki S, Kaneko T, Ishikawa J, Ihara S, et al. Steroid treatment in patients with acute respiratory distress syndrome: a systematic review and network meta-analysis. *J Anesth*. (2022) 36:107–21. doi: 10.1007/s00540-021-03016-5

44. Freebairn R. How relaxed should we be with acute respiratory distress syndrome? *Crit Care Med*. (2004) 32:296–8. doi: 10.1097/01.CCM.0000104925.62805.D9

45. Bourenne J, Hraiech S, Roch A, Gainnier M, Papazian L, Forel JM. Sedation and neuromuscular blocking agents in acute respiratory distress syndrome. *Ann Transl Med*. (2017) 5:291. doi: 10.21037/atm.2017.07.19

46. Zhengyi, R, Junwei, L, Yan, M, Xingxiang, L, Jia, X, Lu, T, et al. To retain spontaneous breathing or eliminate spontaneous breathing with neuromuscular blockers in acute respiratory distress syndrome patients? Eds. Zhonghua Wei Zhong Bing Ji Jiu Yi Xue. (2016) 28:973–7.

47. Lyu T, Lee YS, Dhanvijay S, Freebairn R. The effect of neuromuscular blocking agents uses in acute respiratory distress syndrome: a systematic review and meta-analysis of randomized controlled trials. *Minerva Anestesiol*. (2021) 87:341–50. doi: 10.23736/S0375-9393.20.14783-7

48. Wei XB, Wang ZH, Liao XL, Guo WX, Qin TH, Wang SH. Role of neuromuscular blocking agents in acute respiratory distress syndrome: an updated Meta-analysis of randomized controlled trials. *Front Pharmacol*. (2020) 10:1637. doi: 10.3389/fphar.2019.01637

49. Tao W, Yang LQ, Gao J, Shao J. Neuromuscular blocking agents for adult patients with acute respiratory distress syndrome: a meta-analysis of randomized controlled trials. *J Trauma Acute Care Surg*. (2018) 85:1102–9. doi: 10.1097/TA.0000000000002057

50. Shao S, Kang H, Tong Z. Early neuromuscular blocking agents for adults with acute respiratory distress syndrome: a systematic review, meta-analysis, and meta-regression. *BMJ Open*. (2020) 10:e037737. doi: 10.1136/bmjopen-2020-037737

51. Palmer RM, Ferrige AG, Moncada S. Nitric oxide release accounts for the biological activity of endothelium-derived relaxing factor. *Nature*. (1987) 327:524–6. doi: 10.1038/327524a0

52. Pepke-Zaba J, Higenbottam TW, Dinh-Xuan AT, Stone D, Wallwork J. Inhaled nitric oxide as a cause of selective pulmonary vasodilatation in pulmonary hypertension. *Lancet*. (1991) 338:1173–4. doi: 10.1016/0140-6736(91)92033-X

53. Griffiths MJ, Evans TW. Inhaled nitric oxide therapy in adults. *N Engl J Med*. (2005) 353:2683–95. doi: 10.1056/NEJMra051884

54. Spieth PM, Zhang H. Pharmacological therapies for acute respiratory distress syndrome. *Curr Opin Crit Care*. (2014) 20:113–21. doi: 10.1097/MCC.0000000000000056

55. Gayat E, Mebazaa A. Pulmonary hypertension in critical care. *Curr Opin Crit Care*. (2011) 17:439–48. doi: 10.1097/MCC.0b013e32834a7619

56. Kumar PCommittee on Fetus and Newborn; American Academy of Pediatrics. Use of inhaled nitric oxide in preterm infants. *Pediatrics*. (2014) 133:164–70. doi: 10.1542/peds.2013-3444

57. Adhikari NK, Burns KE, Friedrich JO, Granton JT, Cook DJ, Meade MO. Effect of nitric oxide on oxygenation and mortality in acute lung injury: systematic review and meta-analysis. *BMJ*. (2007) 334:779. doi: 10.1136/bmj.39139.716794.55

58. Adhikari NK, Dellinger RP, Lundin S, Payen D, Vallet B, Gerlach H, et al. Inhaled nitric oxide does not reduce mortality in patients with acute respiratory distress syndrome regardless of severity: systematic review and meta-analysis. *Crit Care Med*. (2014) 42:404–12. doi: 10.1097/CCM.0b013e3182a27909

59. Lamb NJ, Quinlan GJ, Westerman ST, Gutteridge JM, Evans TW. Nitration of proteins in bronchoalveolar lavage fluid from patients with acute respiratory distress syndrome receiving inhaled nitric oxide. *Am J Respir Crit Care Med*. (1999) 160:1031–4. doi: 10.1164/ajrccm.160.3.9810048

frontiers | Frontiers in Medicine

TYPE Original Research
PUBLISHED 17 February 2025
DOI 10.3389/fmed.2025.1537680

OPEN ACCESS

EDITED BY
Lulong Bo,
Navy Medical University, China

REVIEWED BY
Guo-wei Tu,
Fudan University, China
Jianguo Zhang,
Linyi People's Hospital, China

*CORRESPONDENCE
Shao-lin Ma
✉ mslin@sohu.com

†These authors have contributed equally to this work

RECEIVED 01 December 2024
ACCEPTED 03 February 2025
PUBLISHED 17 February 2025

CITATION
Liu Y, Zhou W, Xu W, Lv X-p, Wang F-f, Wang X-b and Ma S-l (2025) The value of heparin-binding protein in bronchoalveolar lavage fluid in acute respiratory distress syndrome.
Front. Med. 12:1537680.
doi: 10.3389/fmed.2025.1537680

The value of heparin-binding protein in bronchoalveolar lavage fluid in acute respiratory distress syndrome

Yang Liu†, Wei Zhou†, Wei Xu, Xing-ping Lv, Fei-fei Wang, Xue-bin Wang and Shao-lin Ma*

Department of Critical Care Medicine, Shanghai East Hospital, Tongji University School of Medicine, Shanghai, China

Background: Heparin-binding protein (HBP) is recognized as a significant factor in the development of Acute Respiratory Distress Syndrome (ARDS). Although plasma levels of HBP have been identified as a predictive biomarker for ARDS, the role and value of HBP in bronchoalveolar lavage fluid (BALF) remain unexplored.

Methods: Our study utilized a cecum ligation and puncture (CLP) method to induce an ARDS model in mice, examining the correlations between plasma and BALF HBP levels, lung injury severity, lung wet-to-dry (WD) ratio, and BALF total protein levels. Additionally, we conducted a comparative analysis of BALF and plasma HBP levels in 44 ARDS patients and 38 patients with cardiogenic pulmonary edema (CPE), investigating their correlations.

Results: In the animal study, CLP-induced mice demonstrated significantly higher lung WD ratios, BALF protein, BALF HBP, and plasma HBP levels compared to the control group. Notably, both BALF and plasma HBP levels were significantly correlated with lung injury severity. In human subjects, significant differences in BALF HBP, BALF protein, and plasma HBP levels were observed between ARDS and CPE patients, along with notable correlations between these markers and the severity of lung injury. Particularly, BALF HBP levels exhibited a stronger correlation with lung injury compared to plasma HBP levels.

Conclusion: The study indicates that both BALF and plasma HBP levels are significantly elevated in the context of lung injury in both animal models and human ARDS patients. More importantly, BALF HBP levels show a stronger correlation with the severity of lung injury, suggesting that BALF HBP could serve as a valuable biomarker for diagnosing and guiding the treatment of ARDS.

KEYWORDS

heparin-binding protein, bronchoalveolar lavage fluid, ARDS, prognosis, ALI/ARDS

1 Introduction

Acute respiratory distress syndrome (ARDS) presents a critical challenge in intensive care units globally, characterized by sudden respiratory failure. Despite extensive research, the precise mechanisms underlying ARDS remain partially understood. It is commonly accepted that ARDS represents a severe form of the systemic inflammatory response syndrome (SIRS) manifesting within the lungs. The condition is marked by the damage to pulmonary vascular endothelial cells and alveolar epithelia, which triggers an overwhelming inflammatory response. This results in increased capillary permeability, allowing fluid and proteins to leak

into the alveolar and interstitial spaces, thereby compromising lung function. Understanding the dynamics of pulmonary vascular permeability is, therefore, pivotal in ARDS research.

Neutrophils are key players in modulating capillary permeability, with their accumulation and subsequent cytokine release being critical in the pathogenesis of ARDS, contributing to alveolar capillary damage and enhanced permeability (1). Among the potent inflammatory mediators released by activated neutrophils is the heparin-binding protein (HBP), which is a versatile modulator of inflammation. It promotes monocyte recruitment, adhesion, and transmigration (2), serving as a vital signal to vascular endothelial cells and playing a significant role in the vascular leakage and pulmonary edema characteristic of ARDS (3). In sepsis cases, plasma HBP levels are significantly elevated and associated with the development of hypotension and organ dysfunction. Rapid assessment of HBP concentration is valuable for early diagnosis and prognostic evaluation of severe sepsis (4).

Clinical investigations have demonstrated a significant elevation in plasma HBP levels in ARDS patients, correlating with the syndrome's onset (5). Plasma HBP levels of ALI/ARDS patients were significantly higher than that of CPE patients. HBP was a strong prognostic marker for short-term mortality in ALI/ARDS (6). In animal studies of ventilator-associated lung injury, although the increase in HBP in plasma was not significant compared to the control group, there was a significant increase in HBP in BALF, which gradually increased over time (7). HBP is implicated as a critical effector in the etiology of transfusion-related acute lung injury and sepsis-induced ARDS (8). Our previous research has established a concurrent rise in neutrophil counts and HBP levels in ARDS cases, highlighting HBP's predictive value for the syndrome's development. Furthermore, we have identified the β2 integrin-PI3K signaling pathway as a key mechanism in HBP release from PMNs, offering new avenues for therapeutic intervention (9).

Despite the recognized significance of plasma HBP levels, the investigation into bronchoalveolar lavage fluid (BALF) HBP and its connection to ARDS is lacking. Given that BALF directly samples the alveolar surface, it may contain higher concentrations of cytokines, including HBP. HBP levels in the BALF of lung injury patients have not previously been studied, and whether HBP plays a role in VILI has, to our knowledge, not been studied previously. We hypothesize that BALF HBP levels are significantly elevated in ARDS patients, aiming to explore its levels and implications in both animal models of acute lung injury (ALI) and human ARDS cases. By examining HBP levels in BALF and blood in a CLP-induced rat model of ALI and comparing these markers in ARDS patients and individuals with cardiogenic pulmonary edema, we seek to elucidate BALF HBP's role in ARDS. The assessment of lung injury severity through the wet/dry lung weight ratio and BALF total protein levels further complements our investigation.

2 Methods

2.1 Animal studies

2.1.1 Animals

Male C57BL/6 mice aged 6–8 weeks and weighing 22–25 g were sourced from the Experimental Animal Centre of Tongji University Medical College, Shanghai, China. These mice were accommodated in a pathogen-free environment with wood shavings, under a controlled 12-h light cycle, and had unrestricted access to food and water. All procedures adhered to international, national, and institutional guidelines for animal care and use.

2.1.2 Grouping and treatment

We divided 24 mice randomly into two groups: sham and cecum ligation and puncture (CLP). Mice in the CLP group underwent the CLP procedure, whereas Sham group mice underwent a similar procedure without cecal ligation or puncture.

2.1.3 Cecal ligation and puncture procedure

Under anesthesia with 1.5% pentobarbital sodium, a 1 cm abdominal incision was made to expose the cecum, which was then ligated below the ileocecal junction with 4-0 silk and punctured using an 18-gauge needle. A small amount of fecal material was expelled to verify puncture patency before the cecum was repositioned and the incision sutured. Within approximately 6–12 h after the CLP procedure in mice, the lungs begin to show signs of acute injury, including shortness of breath, cyanosis around the mouth, reduced activity, and refusal to eat. The above symptoms worsen further within about 24 h, and there is a peak period of death within 24–48 h. No mechanical ventilation was given to the mice during the operation.

Twenty-four hours after CLP or sham operation, mice were anesthetized for plasma HBP extraction and bronchoalveolar lavage. The left lungs were reserved for wet/dry weight ratio analysis.

2.1.4 Bronchoalveolar lavage

Anesthetized mice had an 18-gauge catheter inserted into the right bronchus for PBS instillation (0.5 mL). This process was repeated twice, pooling effluents for protein quantification. Half of the bronchoalveolar lavage fluid (BALF) was allocated for protein measurement via BCA Protein Assay, while the remainder was frozen at −80°C for HBP analysis.

2.1.5 Blood and BALF HBP measurement

Blood was collected from an arterial line into EDTA vacutainer tubes and immediately chilled and centrifuged at 2,000 RCF for 10 min. The plasma was then stored at −80°C until HBP measurement.

To address changes in HBP and protein concentration levels caused by variability in BALF sampling, we used urea dilution method to correct HBP and protein concentration. The urea dilution method utilizes the principle that urea in plasma can freely diffuse into the alveoli to measure the concentration of urea in plasma and BALF, calculate how many times the lavage fluid has been diluted, and use this multiple to correct the protein concentration in the lavage fluid. All BALF and plasma were simultaneously measured for urea levels.

The calculation formula is: corrected concentration = uncorrected concentration * plasma urea concentration/BALF urea concentration. All statistical analyses were performed using the corrected protein concentrations.

2.1.6 Wet/dry lung weight ratio

To assess pulmonary edema, the left lung was weighed for its wet weight, dried at 55°C for 48 h for dry weight, and the wet/dry ratio calculated.

2.1.7 Enzyme-linked immunosorbent assay

HBP levels in plasma and BALF were quantified using an Azurocidin (HBP) Enzyme-linked immunosorbent assay (ELISA) kit (Boster, Wuhan, China) as per the manufacturer's instructions. Briefly, 100 μL of each sample was added to anti-human HBP antibody-coated wells, incubated, followed by the addition of a biotin-conjugated secondary antibody and subsequent incubation steps. After adding the avidin-biotin complex and tetramethylbenzidine (TMB), the reaction was stopped and read at 450 nm on a microtiter plate reader to determine HBP concentrations.

2.2 Human studies

We embarked on a prospective observational study to examine the significance of bronchoalveolar lavage fluid (BALF) HBP in patients with acute respiratory distress syndrome (ARDS), using individuals with cardiogenic pulmonary edema (CPE) as a comparator. The main endpoint of the study is to determine whether there is a significant increase in HBP in BALF of ARDS patients. The secondary endpoint is to determine whether the elevated level of HBP in BALF is consistent with the severity of lung injury in patients, and whether it is consistent with the elevated protein in bronchoalveolar lavage fluid.

2.3 Study population

The study included patients admitted to the intensive care units (ICUs) of Tongji University Shanghai East Hospital from May 2018 to October 2020, who were screened for ARDS onset. Eligible participants were those aged 18 to 89 years, diagnosed with ARDS, underwent fiberoptic bronchoscopy in the ICU, and provided informed consent. Exclusion criteria encompassed pregnancy, history of malignant tumors, post-cardiopulmonary resuscitation status, supporting with mechanical circular support, chronic interstitial lung disease or COPD, pulmonary embolism, immunosuppression due to medication or disease, severe renal insufficiency and ongoing hemodialysis. Prior to the study, sample size estimation was conducted based on the preliminary experimental results. At least 35 patients were included in each group, and the recruitment target was ultimately targeted at 35–45 patients. All patients in the CPE group were those who received endotracheal intubation and mechanical ventilation due to cardiogenic pulmonary edema which is not induce by infection. All patients with ARDS were treated with low tidal volume ventilation, low plateau pressure, and appropriate PEEP (set using the optimal compliance method). After intubation, appropriate sedation was administered. If there was obvious respiratory distress (such as respiratory rate >30 times/min), muscle relaxants were used for treatment. Patients with CPE were supported with PEEP levels of 5–10 cmH_2O.

ARDS patients met the criteria of the ARDS Berlin definition, which include: (1) onset within 1 week of a known clinical insult or new/worsening respiratory symptoms; (2) bilateral opacities on chest radiograph or CT scan not fully accounted for by effusions, lobar/lung collapse, or nodules; (3) categorized as mild (PaO_2/FiO_2 >200 mmHg and ≤300 mmHg with PEEP or CPAP ≥5 cm H_2O), Moderate (PaO_2/FiO_2 >100 mmHg and ≤200 mmHg with PEEP or CPAP ≥5 cm H_2O), or Severe (PaO_2/FiO_2 ≤ 100 mmHg); and (4) respiratory failure not solely attributable to cardiac failure or fluid overload, or objective assessment to rule out hydrostatic edema if no risk factor is present.

2.4 BALF and blood HBP measurement

Fiberoptic bronchoscopy was performed on all patients within 24 h of enrollment. During the procedure, patients were intubated and ventilated. A 15-min preoxygenation was carried out before the bronchoscope was inserted through the tracheal tube into a bronchus of the middle or lingual lobe. Three aliquots of 20 mL of sterile 0.9% NaCl at room temperature were instilled (totaling 60 mL) and subsequently recovered via gentle suction. The lavage fluid was processed and half of the supernatant was used for BALF protein analysis using the BCA Protein Assay kit protocol, while the remainder was preserved at −80°C for HBP level assessment.

Blood samples were drawn from arterial lines into EDTA vacutainer tubes, immediately chilled, and centrifuged at 3,500 rpm for 10 min. The plasma obtained was then stored at −80°C until further analysis.

HBP concentrations in both BALF and plasma were quantified using an enzyme-linked immunosorbent assay (ELISA).

2.5 P/F ratio calculation

Arterial blood gas analysis was conducted on all patients before the bronchoscopy to calculate the P/F ratio, defined as the ratio of arterial oxygen partial pressure (PaO_2 in mmHg) to the fraction of inspired oxygen (FiO_2, expressed as a percentage).

2.6 Statistical methods

Statistical analyses were performed using SPSS version 26.0 and GraphPad Prism 9 software. For categorical variables, differences were assessed using Fisher's exact test. Quantitative data are presented as mean ± standard deviation (SD), and comparisons between groups were conducted using the independent samples *t*-test. The S–W test is used to verify whether the data is normally distributed, and logarithmic comparison is performed on non-normally distributed data. Correlation analyses were carried out employing the Pearson method. The association between plasma and BALF HBP levels was examined through logistic regression analysis. A *p*-value of less than 0.05 was considered statistically significant.

3 Results

3.1 Animal studies

In comparison to the sham group, mice in the CLP group exhibited significantly higher lung wet/dry (WD) ratios (4.72 ± 0.26 vs. 6.81 ± 0.52, $p = 0.0017$) and bronchoalveolar lavage fluid (BALF) protein levels (0.32 ± 0.05 vs. 0.74 ± 0.08, $p = 0.0003$). Similarly, levels of BALF HBP (50.75 ± 5.17 vs. 545.81 ± 182.92, $p = 0.013$) and plasma

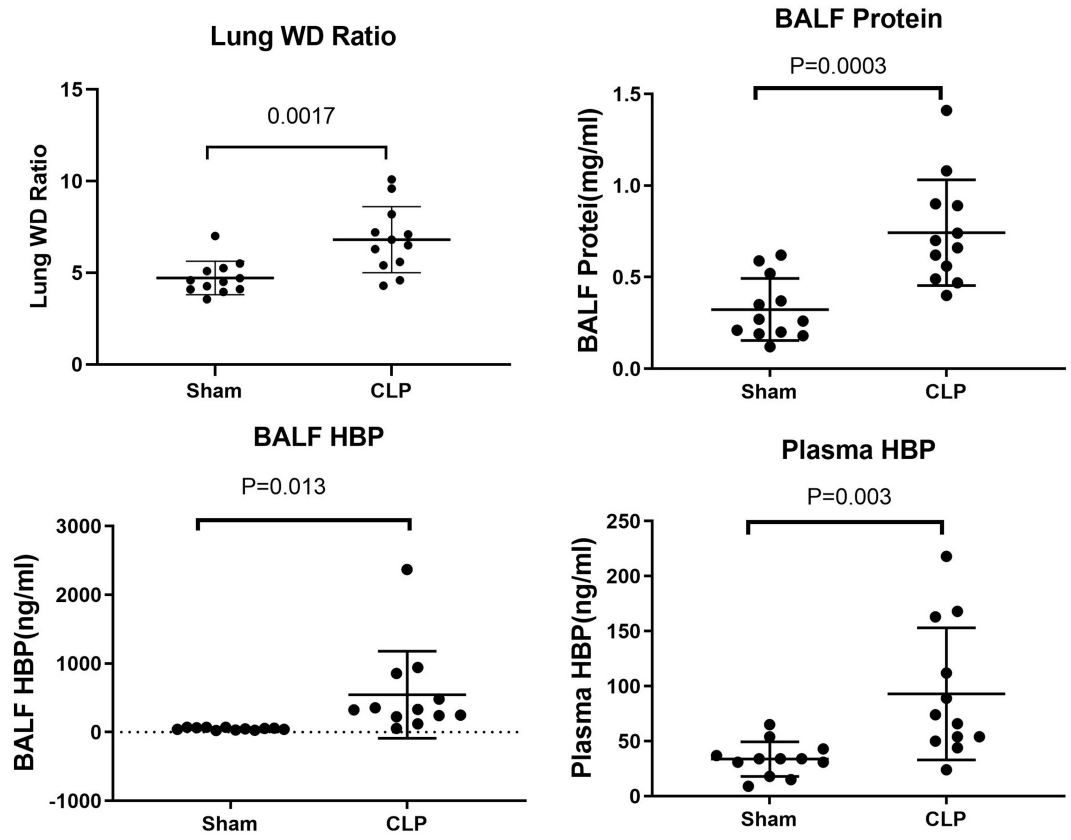

FIGURE 1
Comparison of lung WD ratio, BALF protein, BALF HBP, and plasma HBP between sham and CLP group mice.

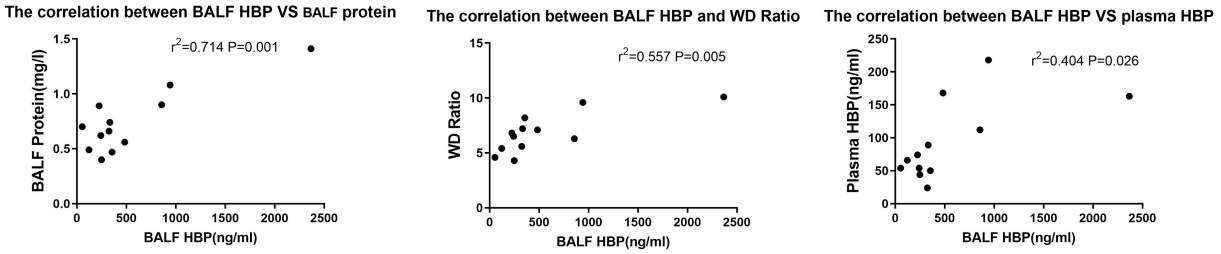

FIGURE 2
Correlation between BALF HBP, plasma HBP, and P/F ratio in CLP group mice.

HBP (33.75 ± 4.53 vs. 93.00 ± 17.34, $p = 0.003$) were also significantly elevated in the CLP group compared to the sham group (see Figure 1).

The BALF protein and lung WD ratio is considered an important indicator of the severity of lung injury. We conducted a correlation analysis between animal BALF HBP with BALF protein and WD ratio to clarify the relationship between HBP and lung injury. Previous studies have suggested that plasma HBP is elevated during ARDS, so the correlation of BALF HBP and plasma HBP were also analyzed. Analysis revealed a significant correlation between BALF HBP with BALF protein ($r^2 = 0.714$, $p = 0.001$) and WD ratio ($r^2 = 0.557$, $p = 0.005$) in CLP group mice. Additionally, a significant correlation was observed between plasma and BALF HBP ($r^2 = 0.404$, $p = 0.026$) (see Figure 2).

3.1.1 Characteristics of the study population

Ultimately, 44 ARDS patients and 38 cardiogenic pulmonary edema (CPE) patients who were intubated and mechanical ventilation in ICU were included in the study (see Figure 3). Necessary vasoactive drugs were used to maintain patients' mean arterial pressure above 65 mmHg. The patients had oxygen saturation above 90% 25 with the support of a ventilator, and PEEP was used appropriately according to their condition. The patients were given appropriate sedation. After completing the signing of the informed consent form, patients drew blood samples within 24 h after a clear diagnosis was made, and underwent fiberoptic bronchoscopy examination.

Both groups had comparable age (mean age 60.5 vs. 55.6 years) and gender distribution (male 54.5% vs. 52.4%). In the ARDS

group, there were 10 cases (22.7%) of abdominal infection, 6 cases (13.6%) of urinary infection, 24 cases (54.5%) of pulmonary infection, 4 cases (9.1%) of soft tissue infection, and 2 cases of blood transfusion. The CPE group consisted of patients with cardiogenic pulmonary edema and hypoxic endotracheal intubation. There was no significant difference in age, gender and ventilator drive pressure between the two groups of patients. Except for CPE patients who have a higher history of coronary heart disease, there is no significant difference in other medical histories (see Table 1).

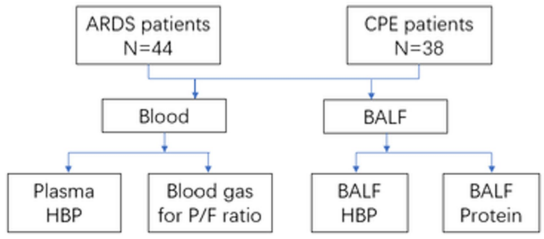

FIGURE 3
The process of obtaining patient research data.

3.1.2 Comparison between two groups

The levels of BALF HBP and plasma HBP between the ARDS and CPE groups were compared. There were significant differences in BALF HBP (24.532 ± 39.349 vs. 240.583 ± 366.403, $t = 6.298$, $p < 0.001$), BALF protein (0.675 ± 0.492 vs. 1.387 ± 1.017, $t = 5.846$, $p < 0.001$), and plasma HBP (27.403 ± 47.175 vs. 233.180 ± 310.502, $t = 7.034$, $p < 0.001$) between the two groups (see Figure 4).

TABLE 1 Patient characteristics.

	ARDS group	CPE group	*F/t*	*p*
Patients, *n*	44	38		
Gender, % male	24/20	20/18	0.020	0.89
Age (mean ± SD)	60.5 ± 13.3	55.6 ± 12.4	7.86	0.76
Medical history				
Hypertension	20	24	2.570	0.109
Diabetes mellitus	12	16	1.995	0.158
Coronary heart disease	29	34	6.360	0.012
COPD	1	1	0.011	0.916
Chronic renal insufficiency	2	4	1.076	0.300
P/F ratio				
200–300 mmHg	21	/		
100–200 mmHg	12	/		
<100 mmHg	11	/		
Parameters of ventilator				
Tidal volume (mL)	393.9 ± 36.5	411.3 ± 50.6	1.806	0.075
Respiratory rate (breaths/min)	30.1 ± 4.9	31.6 ± 5.3	1.313	0.193
Driving pressure (cmH_2O)	12.8 ± 1.3	12.6 ± 1.7	0.582	0.562
Positive end expiratory pressure (cmH_2O)	9.2 ± 2.7	8.2 ± 1.4	1.947	0.055
Peak pressure	22.3 ± 2.5	20.9 ± 2.1	0.523	0.643
Etiology of ARDS, *n*				
Intra-abdominal infection	10			
Urinary system infection	6			
Lung infections	24			
Soft tissue infection	4			
Blood transfusion	2			
Severity of ARDS, *n*				
PaO_2/FiO_2 200–300 mmHg	21			
PaO_2/FiO_2 100–200 mmHg	12			
PaO_2/FiO_2 <100 mmHg	11			

Data are presented as the median ± standard deviation.

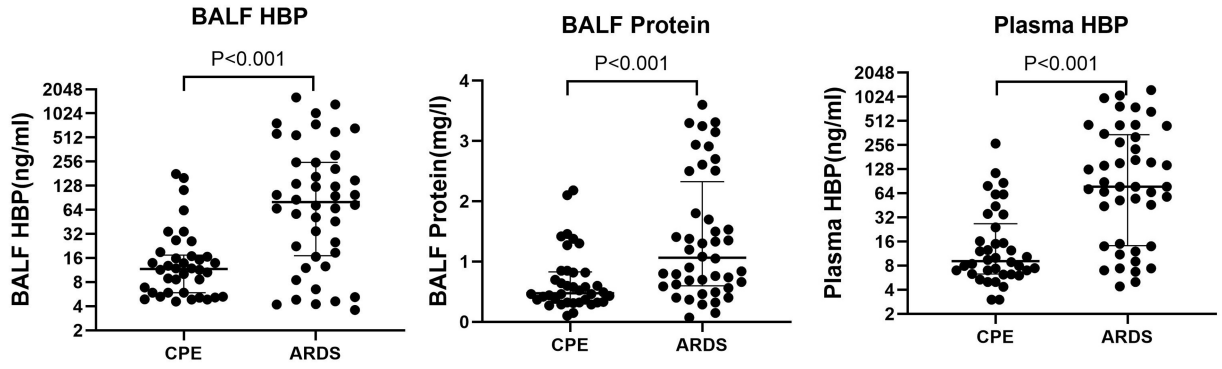

FIGURE 4
Comparison of BALF HBP, BALF protein, and plasma HBP between ARDS and CPE groups.

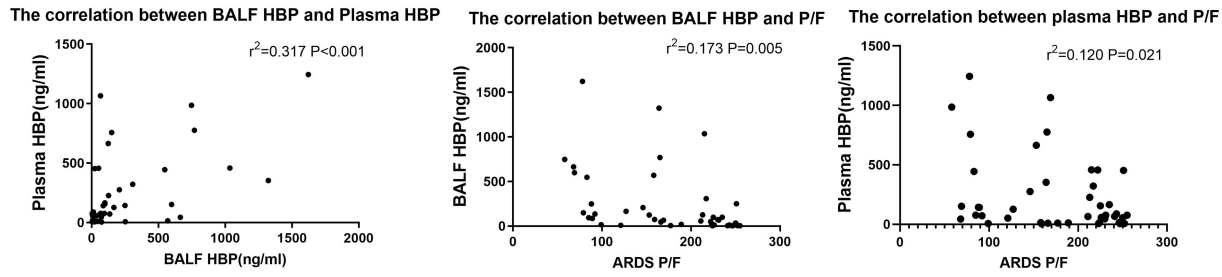

FIGURE 5
Correlation between BALF HBP, plasma HBP, and P/F ratio in ARDS patients.

3.1.3 BALF HBP and lung injury severity in patients

The P/F ratio is considered a severity index of lung injury. To clarify the relationship between HBP in BALF and plasma HBP with the degree of lung injury, we analyzed their correlation with P/F index. Results showed there were P/F ratio have significant correlations with BALF HBP ($r^2 = 0.173$, $p = 0.005$) and plasma HBP ($r^2 = 0.120$, $p = 0.021$). Additionally, a significant correlation was found between BALF HBP and plasma HBP ($r^2 = 0.317$, $p < 0.001$) (see Figure 5).

4 Discussion

While the precise mechanisms underlying acute lung injury (ALI) and acute respiratory distress syndrome (ARDS) remain to be fully elucidated, the prevailing view among scholars is that these conditions are predominantly driven by a systemic inflammatory response syndrome (SIRS) triggered by infection. In response to infectious stimuli, the immune system releases a vast array of inflammatory mediators, leading to neutrophil degranulation, the release of proteolytic enzymes, and increased capillary endothelial cell permeability. This sequence of events facilitates the leakage of fluid and protein into the interstitial spaces and alveoli, culminating in ARDS. The damage induced by neutrophils to the lung's endothelial and epithelial barriers is deemed a primary contributor to ARDS.

HBP, a cytokine released by activated immune cells, has been implicated in inducing lung inflammation and oxidative stress. As a key component of granules in polymorphonuclear neutrophils (PMNs), HBP plays a pivotal role in initiating the cascade of inflammation and enhancing vascular permeability (10). Secreted by emigrating PMNs, HBP attaches to the endothelial glycocalyx, presenting itself to circulating leukocytes. It activates monocytes rolling along the endothelium, leading to stable monocyte arrest, adhesion, transendothelial extravasation, and targeted migration to injury sites. HBP also triggers a swift increase in cytosolic free Ca^{2+} in adjacent endothelial cells, the formation of actin stress fibers, and heightened paracellular permeability (11, 12). Immunoneutralization of HBP in neutrophil-derived secretions effectively inhibits these activities, underscoring HBP's crucial role in mediating neutrophil-induced changes in vascular permeability.

In this study, HBP levels surged and were closely linked with the lung wet/dry ratio and BALF protein levels, reflecting the compromised alveolar-capillary barrier that facilitates leukocyte migration and protein influx. The results are consistent with the changes in vascular permeability in the pathophysiology of ARDS. Numerous clinical studies have explored the relationship between HBP and ARDS. HBP is posited as a potential mediator of sepsis-induced ALI through its impact on endothelial permeability (13). In ARDS research, patients have displayed significantly elevated plasma HBP levels compared to those with cardiogenic pulmonary edema, with HBP serving as a potent prognostic marker for short-term mortality and hypoxemia severity (14). Moreover, in studies on transfusion-related ALI, PMNs were shown to release substantial HBP amounts in response to human antibodies, without concurrent interleukin-6 or tumor necrosis factor-alpha release, highlighting

HBP's role as a primary effector molecule in such cases (8). Our previous work has indicated that early-stage HBP elevation is a reliable biomarker for predicting sepsis-associated ARDS onset (9).

HBP's association with infection has been well-documented, with plasma HBP levels serving as a robust indicator for distinguishing severe sepsis with circulatory failure from less severe infections (15). However, investigations into HBP levels in body fluids other than plasma have been scarce. A multicenter study in Sweden on the diagnostic and predictive value of HBP in urinary tract infections found HBP to be an effective diagnostic marker, suggesting its potential utility in identifying adult patients with suspected UTIs (16). Considering BALF as a marker of pulmonary exudation due to vascular leakage, its HBP levels are likely closely linked to lung injury severity. Previous ARDS research has predominantly focused on plasma HBP as a marker of systemic inflammation, with little attention to BALF HBP levels directly from the lungs. This study aimed to fill that gap by evaluating BALF HBP levels in both animal models and patients with ALI/ARDS.

In our animal studies, we utilized the lung wet/dry ratio and BALF protein levels as indicators of lung injury severity. Both plasma and BALF HBP levels were elevated in lung injury models compared to controls, with injury severity positively correlating with BALF HBP levels. Clinical findings revealed higher BALF and plasma HBP levels in ARDS patients versus those with cardiogenic pulmonary edema, establishing a significant correlation between BALF HBP, plasma HBP, and ARDS severity.

These findings underscore that BALF HBP levels in ARDS patients are markedly higher than in cases of cardiogenic pulmonary edema due to elevated hydrostatic pressure. The concurrent elevation of HBP in BALF and plasma aligns with the pathological mechanisms of pulmonary neutrophil aggregation and HBP release, leading to vascular leakage and impaired pulmonary oxygen exchange in ARDS. Thus, lung-derived HBP levels appear more intimately linked to lung injury severity, offering insights into the pathophysiological processes underlying ARDS.

4.1 Limitations

1) This study was conducted at a single institution and involved a relatively small cohort. To further substantiate these findings, larger-scale studies encompassing a greater number of participants are necessary.
2) While our study identified elevated HBP levels in BALF, the precise mechanisms driving this increase require clarification through further basic research.

5 Conclusion

In summary, our investigation reveals that HBP levels in bronchoalveolar lavage fluid (BALF) are markedly elevated in both animal models and humans experiencing lung injury, displaying a significant correlation with the injury's severity. Notably, BALF HBP demonstrated a stronger association with lung injury compared to plasma HBP. These findings enhance our understanding of HBP's pathological significance in acute respiratory distress syndrome (ARDS) and lay a theoretical foundation for targeted interventions aimed at modulating HBP levels in the lungs to mitigate or prevent ARDS.

Data availability statement

The original contributions presented in the study are included in the article/supplementary material, further inquiries can be directed to the corresponding author.

Ethics statement

The studies involving humans were approved by the Ethics Committee of Shanghai East Hospital, Tongji University School of Medicine. The studies were conducted in accordance with the local legislation and institutional requirements. The participants provided their written informed consent to participate in this study. The animal study was approved by the Ethics Committee of Shanghai East Hospital, Tongji University School of Medicine. The study was conducted in accordance with the local legislation and institutional requirements.

Author contributions

YL: Conceptualization, Writing – original draft. WZ: Writing – original draft. WX: Data curation, Methodology, Writing – original draft. X-pL: Resources, Writing – original draft. F-fW: Investigation, Writing – original draft. X-bW: Conceptualization, Writing – review & editing. S-lM: Project administration, Writing – review & editing.

Funding

The author(s) declare that financial support was received for the research, authorship, and/or publication of this article. This study was supported by the Pudong New Area Health Commission Clinical Peak Discipline Construction (Emergency and Critical Care Unit, No. PWYgf2021-03). National Natural Science Foundation of China (Grant No. 82102288) and Project of Shanghai Municipal Health Commission (The Role of Mechanical Ventilation Simulation Teaching in Resident Training, No.: 201740159).

Conflict of interest

The authors declare that the research was conducted in the absence of any commercial or financial relationships that could be construed as a potential conflict of interest.

Generative AI statement

The authors declare that no Gen AI was used in the creation of this manuscript.

Publisher's note

References

1. Matthay MA, Zemans RL. The acute respiratory distress syndrome: pathogenesis and treatment. *Annu Rev Pathol*. (2011) 6:147–63. doi: 10.1146/annurev-pathol-011110-130158

2. Chang M, Guo F, Zhou Z, Huang X, Yi L, Dou Y, et al. HBP induces the expression of monocyte chemoattractant protein-1 via the FAK/PI3K/AKT and p38 MAPK/NF-kappaB pathways in vascular endothelial cells. *Cell Signal*. (2018) 43:85–94. doi: 10.1016/j.cellsig.2017.12.008

3. Bentzer P, Fisher J, Kong HJ, Mörgelin M, Boyd JH, Walley KR, et al. Heparin-binding protein is important for vascular leak in sepsis. *Intensive Care Med Exp*. (2016) 4:33. doi: 10.1186/s40635-016-0104-3

4. Fisher J, Linder A. Heparin-binding protein: a key player in the pathophysiology of organ dysfunction in sepsis. *J Intern Med*. (2017) 281:562–74. doi: 10.1111/joim.12604

5. Johansson J, Brattström O, Sjöberg F, Lindbom L, Herwald H, Weitzberg E, et al. Heparin-binding protein (HBP): an early marker of respiratory failure after trauma? *Acta Anaesthesiol Scand*. (2013) 57:580–6. doi: 10.1111/aas.12070

6. Lin Q, Shen J, Shen L, Zhang Z, Fu F. Increased plasma levels of heparin-binding protein in patients with acute respiratory distress syndrome. *Crit Care*. (2013) 17:R155. doi: 10.1186/cc12834

7. Tydén J, Larsson N, Lehtipalo S, Herwald H, Hultin M, Walldén J, et al. Heparin-binding protein in ventilator-induced lung injury. *Intensive Care Med Exp*. (2018) 6:33. doi: 10.1186/s40635-018-0198-x

8. Yasui K, Furuta RA, Matsuyama N, Fukumori Y, Kimura T, Tani Y, et al. Possible involvement of heparin-binding protein in transfusion-related acute lung injury. *Transfusion*. (2008) 48:978–87. doi: 10.1111/j.1537-2995.2007.01632.x

9. Liu Y, Ma S, Wang X, Feng Y, Zhang S, Wang S, et al. The role of beta2 integrin associated heparin-binding protein release in ARDS. *Life Sci*. (2018) 203:92–8. doi: 10.1016/j.lfs.2018.04.029

10. Linder A, Soehnlein O, Akesson P. Roles of heparin-binding protein in bacterial infections. *J Innate Immun*. (2010) 2:431–8. doi: 10.1159/000314853

11. Di Gennaro A, Kenne E, Wan M, Soehnlein O, Lindbom L, Haeggström JZ. Leukotriene B4-induced changes in vascular permeability are mediated by neutrophil release of heparin-binding protein (HBP/CAP37/azurocidin). *FASEB J*. (2009) 23:1750–7. doi: 10.1096/fj.08-121277

12. Persson B, Halldorsdottir H, Lindbom L, Rossi P, Herwald H, Weitzberg E, et al. Heparin-binding protein (HBP/CAP37)—a link to endothelin-1 in endotoxemia-induced pulmonary oedema? *Acta Anaesthesiol Scand*. (2014) 58:549–59. doi: 10.1111/aas.12301

13. Liu Y, Ma S, Wang X. The predictive value of early serum heparin-binding protein level on septic shock. *Chin J Emerg Med*. (2014) 23:79–83. doi: 10.3760/cma.j.issn.1671-0282.2014.01.019

14. Sterner N, Fisher J, Thelaus L, Ketteler C, Lemež Š, Dardashti A, et al. The dynamics of heparin-binding protein in cardiothoracic surgery—a pilot study. *J Cardiothorac Vasc Anesth*. (2021) 35:2640–50. doi: 10.1053/j.jvca.2020.12.033

15. Wu YL, Yo CH, Hsu WT, Qian F, Wu BS, Dou QL, et al. Accuracy of heparin-binding protein in diagnosing sepsis: a systematic review and meta-analysis. *Crit Care Med*. (2021) 49:e80–90. doi: 10.1097/CCM.0000000000004738

16. Kjolvmark C, Pahlman LI, Akesson P, Linder A. Heparin-binding protein: a diagnostic biomarker of urinary tract infection in adults. *Open Forum Infect Dis*. (2014) 1:ofu004. doi: 10.1093/ofid/ofu004

frontiers | Frontiers in Medicine

TYPE Original Research
PUBLISHED 21 February 2025
DOI 10.3389/fmed.2025.1521729

OPEN ACCESS

EDITED BY
Lulong Bo,
Navy Medical University, China

REVIEWED BY
Xinru Liu,
Shanghai University, China
Yanfei Mao,
Shanghai Jiao Tong University, China

*CORRESPONDENCE
ShiFeng Wang
✉ wangsf23@hotmail.com
WenWu Liu
✉ 13661966681@hotmail.com

†These authors have contributed equally to this work

RECEIVED 02 November 2024
ACCEPTED 27 January 2025
PUBLISHED 21 February 2025

CITATION
Han CH, Zhang PX, Liu Y, Xu JJ, Yu XH, Wen YK, Wang SF and Liu WW (2025) Inhibition of renin-angiotensin system attenuates type I alveolar epithelial cell necroptosis in rats after hyperbaric hyperoxic exposure. *Front. Med.* 12:1521729. doi: 10.3389/fmed.2025.1521729

Inhibition of renin-angiotensin system attenuates type I alveolar epithelial cell necroptosis in rats after hyperbaric hyperoxic exposure

CuiHong Han[1†], PeiXi Zhang[2†], Ying Liu[3†], JiaJun Xu[4], XuHua Yu[4], YuKun Wen[4], ShiFeng Wang[4*] and WenWu Liu[4*]

[1]Department of Pathology, Jining No 1 People's Hospital, Jining, Shandong, China, [2]Department of Cardiothoracic Surgery, Jining No 1 People's Hospital, Jining, Shandong, China, [3]Department of Pathology, Yantaishan Hospital, Yantai, Shandong, China, [4]Department of Diving and Hyperbaric Medicine, Naval Medical Center, Shanghai, China

Objective: There is evidence showing both necroptosis and activation of renin-angiotensin system (RAS) are involved in the pathogenesis of hyperbaric hyperoxic lung injury (HLI). This study aimed to investigate whether RAS activation can induce lung cell necroptosis and the cell specificity of necroptosis in the lung in case of hyperbaric HLI.

Methods: Male SD rats were randomly assigned into control group (n = 12), HLI group (n = 18), captopril group (n = 18), and valsartan group (n = 18). Rats were pre-treated with intraperitoneal captopril (50 mg/kg) or intragastrical valsartan (30 mg/kg) for 3 days before hyperbaric exposure. Then, animals were exposed to 99.9% oxygen at 250 kPa for 6 h to induce HLI. After hyperbaric exposure, lung function was non-invasively detected, and then animals were sacrificed for the detection of wet to dry ratio of the lung, blood gas and lung inflammatory factors, and lung tissues were collected for double immunofluorescence staining. Statistical analysis was performed with one way analysis of variance.

Results: Either valsartan or captopril pre-treatment could inhibit lung edema, improve blood gas (0 h) and lung function (48 h), and reduce pro-inflammatory factors in the lung. In addition, valsartan or captopril pre-treatment could inhibit AGT1 expression and lung cell necroptosis, and type I alveolar epithelial cells (AECs) were the major cell type experiencing necroptosis after hyperbaric hyperoxic exposure.

Conclusion: Our study indicates inhibition of RAS can suppress the hyperbaric HLI, which may be, at least partially, related to the inhibition of type I AECs

necroptosis. Our findings provide new mechanism for the protective effects of RAS inhibition on hyperbaric HLI.

KEYWORDS

hyperbaric hyperoxic lung injury, necroptosis, renin-angiotensin system, type I alveolar epithelial cells, inflammation

1 Introduction

It has been confirmed that long term exposure to hyperoxic environment is toxic to human body (1). When the oxygen partial pressure is higher than 50 kPa (but lower than about 200 kPa), persistent exposure to this hyperoxic environment may cause damage to the lung, which is also known as pulmonary oxygen toxicity. In routine clinical practice, premature neonates are exposed to hyperoxic environment as a treatment, but it is a normobaric hyperoxic environment (2). There is high-quality evidence supporting that liberal oxygen exposure is associated with a dose-dependent increased risk in short-term and long-term mortality (3). However, in diving, divers are often exposed to a hyperbaric hyperoxic environment (4). There is evidence showing that the mechanism of hyperoxic lung injury (HLI) after normobaric hyperoxic exposure is different from that after hyperbaric hyperoxic exposure (5).

To date, numerous studies have been conducted to investigate the mechanisms underlying the pathogenesis of HLI, and some mechanisms have been proposed (1). The renin-angiotensin system (RAS) is a peptidergic system with endocrine characteristics, and involved in the regulation of blood pressure and fluid balance (6). Some studies have indicated that RAS is closely related to the pathogenesis of some lung diseases such as acute lung injury (ALI), chronic obstructive pulmonary disease (COPD), and asthma (7). In our previous study, results also showed hyperbaric hyperoxic exposure could activate the RAS in rats, which was related to the pathogenesis of prolonged exposure to hyperbaric hyperoxic lung injury (8, 9).

There is evidence showing that cell death plays an important role in the pathogenesis of HLI (10). Our previous study indicated that oxidative stress induced necroptosis, a type of programmed cell death, was involved in the pathogenesis of HLI, and inhibition of necroptosis was protective against HLI (11). In recent years, studies have shown that angiotensin II, an important part of RAS, may activate necroptosis in some disease models (12). However, whether angiotensin II can induce necroptosis in case of HLI has not been reported so far. In this study, the relationship between angiotensin and necroptosis and the cell specificity of necroptosis were investigated in a rat model of hyperbaric hyperoxic exposure.

2 Materials and methods

2.1 Animals and grouping

A total of 66 Sprague Dawley rats weighing 200–220 g were purchased from Shanghai SLAC Experimental Animal Co., Ltd. This study was approved by the Naval Medical Center of Naval Medical University. Animals were randomly divided into control group (n = 12), HLI group (n = 18), captopril group (n = 18), and valsartan group (n = 18). This study was approved by the Ethics Committee of Naval Medical Center.

2.2 Establishment of animal model

Animals were housed for a week in a humidity and temperature control environment. They were placed in a small chamber which was then flushed with 99.9% oxygen for 5 min until the oxygen concentration in the chamber was higher than 96%. Then, the chamber was pressurized with 99.9% oxygen to 250 kPa within 3 min. Soda lime was placed at the bottom to remove carbon dioxide, the chamber was ventilated continuously with 99.9% oxygen, and the oxygen concentration in the chamber was continuously monitored and maintained at >96% during the hyperbaric exposure. Animals received hyperbaric exposure at 250 kPa for 6 h and then the chamber was depressurized to atmospheric pressure (100 kPa) within 5 min. In the control group, animals were placed in the chamber which was flushed with room air, but it was not pressurized.

2.3 Treatments

Animals in the captopril group were intraperitoneally treated with captopril (50 mg/kg) for 3 days before hyperbaric exposure (13). In the valsartan group, animals were orally treated with valsartan (30 mg/kg) for 3 days before hyperbaric exposure (14). In the HLI group, animals were intraperitoneally treated with normal saline.

2.4 Detection of lung function

Lung function was detected with a whole-body plethysmograph (WBP-8R; TOW-INT Tech, Shanghai, China). Briefly, the rat was allowed to stay in the detection chamber for at least 5 min until the parameters remained stable. The parameters of lung function were detected automatically and stored in Excel for further analysis. Detection was done at least three times and average was obtained. The parameters included inspiration time (TI), expiration time (TE), peak inspiratory flow (PIF), peak expiratory flow (PEF), respiratory frequency (f), tidal volume (Vt), and minute ventilation (MV).

2.5 Blood gas analysis

Rats were intraperitoneally anesthetized with 3% sodium pentobarbital (40 mg/kg) at specific time points. Arterial blood was collected from the abdominal aorta and added to the test cartridge. Blood gas analysis was done with a blood analyzer (i-STAT blood analyzer, Abbott, CA, USA). The parameters included the pH value, carbon dioxide partial pressure (PCO_2), oxygen partial pressure (PO_2), extracellular fluid base excess (BEecf), bicarbonate radical (HCO_3^-), total carbon dioxide (TCO_2), oxygen saturation (SO_2), hemoglobin (Hb) and hematocrit (Hct).

2.6 Detection of wet to dry ratio

Immediately after hyperbaric exposure, rats were intraperitoneally anesthetized with 3% sodium pentobarbital (40 mg/kg), and the lung tissues were collected and weighed. Then, the lung tissues were dried in an oven and weighed until the weight remained stable (3 days later). The wet to dry ratio was calculated as follow: (wet weight – dry weight) / dry weight × 100%.

2.7 Enzyme linked immunosorbent assay

Immediately after hyperbaric exposure, animals were intraperitoneally anesthetized with 3% sodium pentobarbital (40 mg/kg), and the lung was harvested and processed for enzyme linked immunosorbent assay (ELISA) with corresponding kits (interleukin-1β [IL-1β; EK301B] and tumor necrosis factor α [TNF-α; EK382HS]; Multi Sciences, China).

2.8 Western blotting

Lung tissues were collected and stored at −80°C for further use. In brief, lung tissues were homogenized in lysis buffer and then centrifuged. The supernatant was collected and the protein concentration was determined by using BCA method. Then, total proteins (20 mg) were loaded for separation on 15% SDS-polyacrylamide gel electrophoresis and transferred onto polyvinylidene fluoride (PVDF) membranes (Bio-Rad, USA). The membranes were blocked with 5% non-fat milk, followed by incubation with primary antibodies at 4°C overnight: AGT1 (Affinity, DF4910, 1:1000), RIP1 (Bioss, bs-5805R, 1:1000), RIP3 (Bioss, bs-3551R, 1:1000) and MLKL (Abcam, ab243142, 1:1000). The secondary antibody was HRP conjugated goat anti-rat GAPDH (1:10000). The images of protein bands were captured and the band density was analyzed with Image J software (NIH, Bethesda, MD, USA).

2.9 Pathological scoring

After hyperbaric exposure, animals were anesthetized and thoracotomy was performed. Animals were perfused with normal saline via the left ventriculus and then with 4% paraformaldehyde. Lung tissues were collected, fixed in 4% paraformaldehyde, embedded in paraffin and sectioned. Lung sections were processed for HE staining, and then observed under a light microscope. Pathological scoring was based on the alveolar congestion, alveolar hemorrhage, and infiltration or aggregation of neutrophils in the alveolar space or vascular wall, alveolar wall thickening, and/or hyaline membrane formation. These pathological features were independently scored using a four-point scale: 1 indicates normal and 4 represents the most severe injury.

2.10 Immunohistochemistry

In brief, lung sections (4 μm) were processed for HE staining and immunofluorescence staining. Surfactant C (SPC) (Proteintech 10774-1-ap; 1:1000) was used to stain type II alveolar epithelial cells (AEC), aquaporin 5 (AQP5) (ab315856; 1:2000) was employed to stain type I AEC and MLKL was used to mark necroptotic cells. In brief, lung sections were deparaffinized and rehydrated in gradient alcohol. After antigen retrieval, sections were treated with 2.5% normal serum and then with anti-MLKL/SPC/AQP5 antibody at 4°C, overnight. Sections were rinsed with PBS, and then treated with fluorescent secondary antibody. In negative controls, sections were incubated with PBS instead of primary antibody. Finally, sections were observed under a fluorescence microscope.

2.11 Statistical analysis

Statistical analysis was performed with GraphPad Prism 8 (GraphPad Software, Boston, MA, USA). Data are expressed as mean ± standard deviation and compared with one way analysis of variance (ANOVA) among groups, followed by Tukey's *post hoc* test. A value of $P < 0.05$ was considered statistically significant.

3 Results

3.1 Effects of captopril and valsartan on the wet to dry ratio and lung structure after hyperbaric exposure

Animals were sacrificed immediately after hyperbaric exposure and lung tissues were collected for the detection of wet to dry ratio. Our results showed both captopril and valsartan pre-treatment could reduce the wet to dry ratio of the lung tissues ($P = 0.0021$ and 0.0358; Figure 1A), but there was no significant difference between two treatment groups. As shown in Figure 1B, the lung structure was significantly damaged after hyperoxic exposure, which was characterized by the thickening of alveolar septum, alveolar hemorrhage, infiltration of inflammatory cells and rupture of alveolar septum. In addition, both captopril and valsartan pre-treatment attenuated the lung injury secondary to hyperoxic exposure which was manifested as the improvement of pathological scores (Figure 1C).

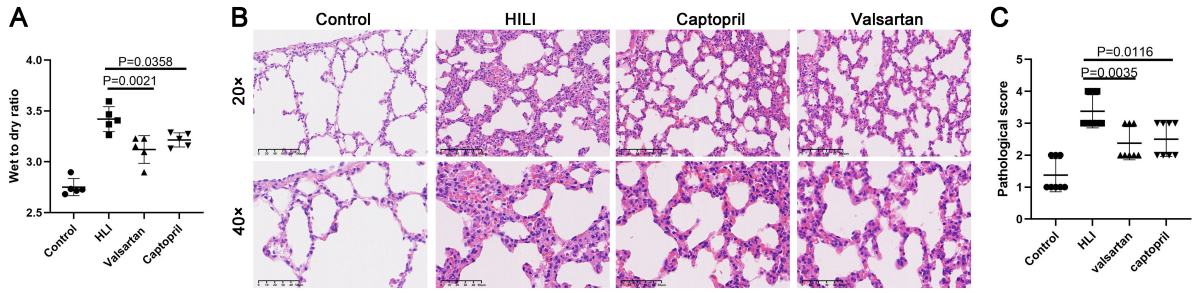

FIGURE 1
Wet to dry ratio and lung histological examination. **(A)** Wet to dry ratio immediately after hyperbaric hyperoxic exposure; **(B)** HE staining of lung tissues in different groups. **(C)** Histological scores of lung microstructure in different groups. ANOVA was used for comparisons among groups followed by Tukey's *post hoc*.

3.2 Effects of captopril and valsartan on the blood gas after hyperbaric exposure

The blood gas was detected immediately after hyperbaric exposure. Our results showed the pH value, SO_2, PO_2, BEecf, Hb and Hct increased, but PCO_2 reduced after hyperbaric exposure (Figure 2). In addition, captopril pre-treatment significantly reduced the pH value, Hb and Hct and markedly increased PCO_2, and BEecf slightly reduced after captopril treatment; valsartan pre-treatment reduced pH value, BEecf, Hb and Hct, but increased PCO_2, and significant difference was noted in Hb and Hct.

3.3 Effects of captopril and valsartan on the lung function after hyperbaric exposure

In this study, lung function was non-invasively detected after hyperbaric exposure. TI and Vt increased significantly and the respiratory frequency reduced markedly after hyperbaric exposure. However, either captopril or valsartan pre-treatment failed to improve the lung function immediately after hyperbaric exposure except for the respiratory frequency. Therefore, the lung function was further detected at 48 h after hyperbaric exposure. Results indicated captopril pre-treatment significantly reduced TI and markedly increased Vt; valsartan pre-treatment significantly reduced TI and PEF and markedly increased Vt and MV at 48 h after hyperbaric exposure (Figure 3).

3.4 Effects of captopril and valsartan on the inflammation after hyperbaric exposure

Inflammation is involved in the pathogenesis of HLI. In this study, we detected the pro-inflammatory factors IL-1β and TNF-α in the lung after hyperbaric exposure. Our results indicated the contents of IL-1β ($P < 0.001$) and TNF-α ($P < 0.001$) increased significantly in the lung after hyperoxic exposure (Figure 4). However, either captopril or valsartan pre-treatment could significantly inhibit the production of pro-inflammatory factors in the lung ($P = 0.0004$ and $P < 0.0001$, respectively), but there were no marked differences in the contents of IL-1β and TNF-α in the lung between captopril group and valsartan group ($P > 0.05$; Figure 4).

3.5 Cell-specific necroptosis in the lung after hyperbaric exposure

Although our previous study showed necroptosis was involved in the pathogenesis of HLI, but the cell-specificity of necroptosis is still unclear. In the present study, double immunofluorescence staining was employed to investigate the cell-specificity of necroptosis in the lung. MLKL was used to indicate necroptosis. Our results showed most type II AECs and endothelial cells were negative to MLKL (Figures 5A, B), but type I AECs were positive to MLKL (Figure 5C). The number of MLKL positive cells increased significantly after hyperbaric exposure as compared to the control group, but either captopril or valsartan pre-treatment could markedly reduce the number of MLKL positive cells in the lung as compared to the HLI group (Figure 5C).

3.6 Protein expression of AGT1, MLKL, RIP1 and RIP3

Our results showed AGT1 expression increased significantly in the lung after hyperbaric exposure, but either captopril or valsartan pre-treatment could markedly reduce the expression of AGT1 in the lung ($P = 0.019$ and $P = 0.0106$, respectively; Figure 5A). In the lung, the protein expression of MLKL, RIP3 and RIP1 increased markedly after hyperoxic exposure. However, either captopril or valsartan pre-treatment decreased the protein expression of MLKL, RIP3 and RIP1 in the lung as compared to the HLI group (Figures 6B–D).

4 Discussion

In recent years, RAS has been found to possess pro-inflammatory, hypertrophic, pro-fibrotic, and pro-oxidative

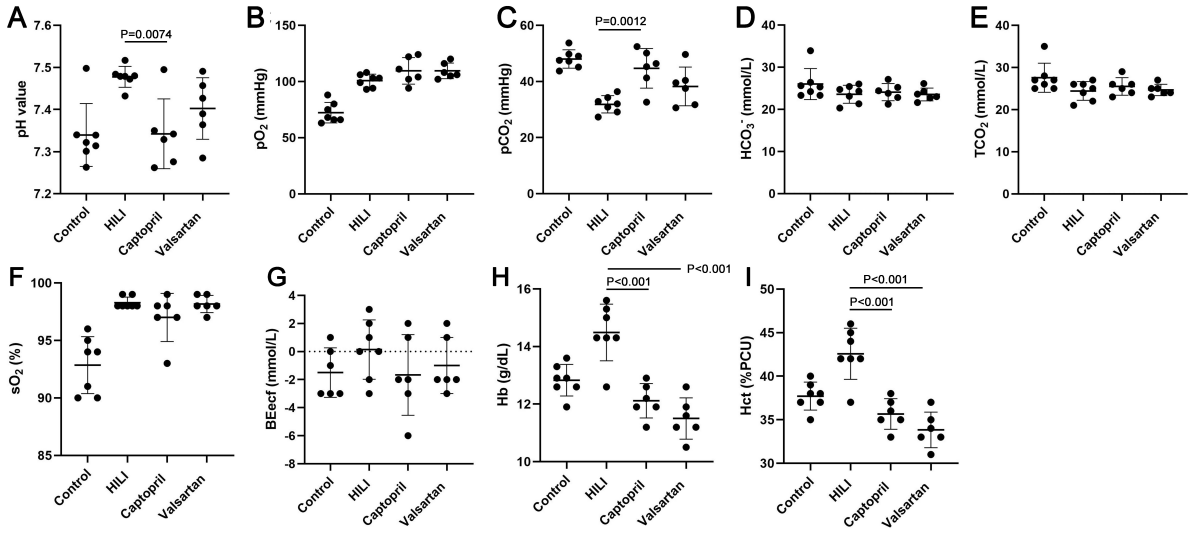

FIGURE 2
Blood gas in different groups immediately after hyperbaric exposure. **(A)** pH value; **(B)** oxygen partial pressure (PO_2); **(C)** carbon dioxide partial pressure (PCO_2); **(D)** bicarbonate radical (HCO_3^-); **(E)** total carbon dioxide (TCO_2); **(F)** oxygen saturation (SO_2), **(G)** extracellular fluid base excess (BEecf); **(H)** hemoglobin (Hb); **(I)** hematocrit (Hct). ANOVA was used for comparisons among groups followed by Tukey's *post hoc*.

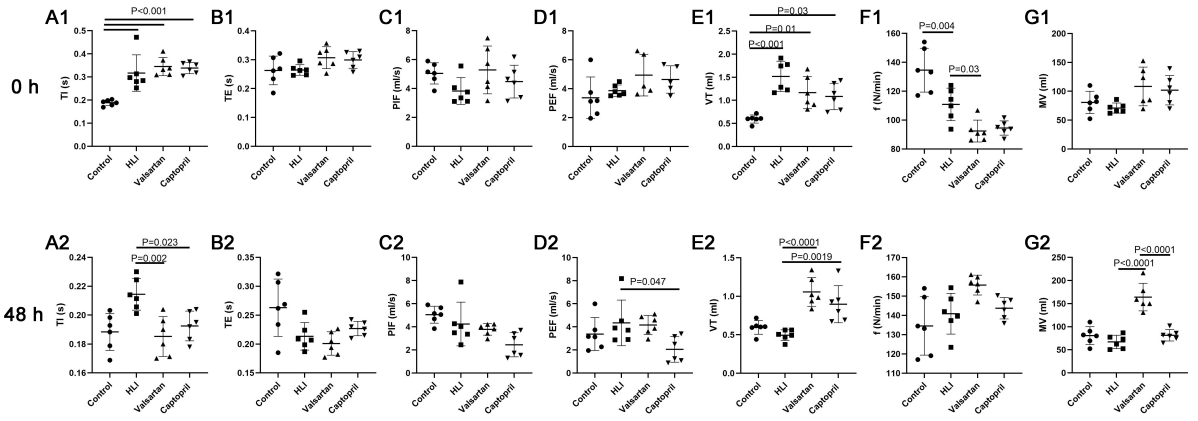

FIGURE 3
Lung function in different groups at 0 and 48 h after hyperbaric exposure. **(A1,A2)** Inspiration time (TI); **(B1,B2)** expiration time (TE); **(C1,C2)** peak inspiratory flow (PIF); **(D1,D2)** peak expiratory flow (PEF); **(E1,E2)** tidal volume (VT); **(F1,F2)** respiratory frequency (f); **(G1,G2)** minute ventilation (MV). ANOVA was used for comparisons among groups followed by Tukey's *post hoc*.

activities, and the dysregulations in the RAS is involved in the pathogenesis of many diseases, including lung diseases (7). Our previous study has indicated that the angiotensin II and angiotensin-converting enzyme (ACE) increased in the lung after hyperbaric HLI (8), which suggests the activation of RAS in the lung after hyperbaric HLI. It has been shown that cell death is involved in the pathogenesis of HLI and RAS activation may induce necroptosis, a type of programmed cell death (10, 12). Our group for the first time found that necroptosis is involved in the pathogenesis of HLI because inhibition of necroptosis is able to attenuate lung injury secondary to hyperbaric hyperoxic exposure (11). However, whether the activation of RAS can induce necroptosis in the lung in case of hyperbaric HLI has not been reported. In this study, we investigated the relationship between RAS activation and necroptosis in the lung after hyperbaric HLI. Valsartan and captopril were used to independently inhibit RAS activation. Valsartan is an angiotensin II receptor blocker (ARB) and can block angiotensin II from binding to the AT1 receptor in many tissues. Captopril is an ACE inhibitor (ACEI) and can suppress the conversion of angiotensin I into angiotensin II in tissues.

In the present study, animals were pre-treated with valsartan or captopril for 3 days before the hyperbaric hyperoxic exposure, and the protective effects were first evaluated by the wet to dry ratio, lung function and blood gas. Wet to dry ratio is a common indicator of lung edema. Wet to dry ratio analysis in the present study showed both valsartan and captopril could suppress lung edema secondary to hyperbaric hyperoxic exposure. The lung is responsible for gas exchange and thus lung injury is easy to cause the change in blood gas. Therefore, blood gas analysis is

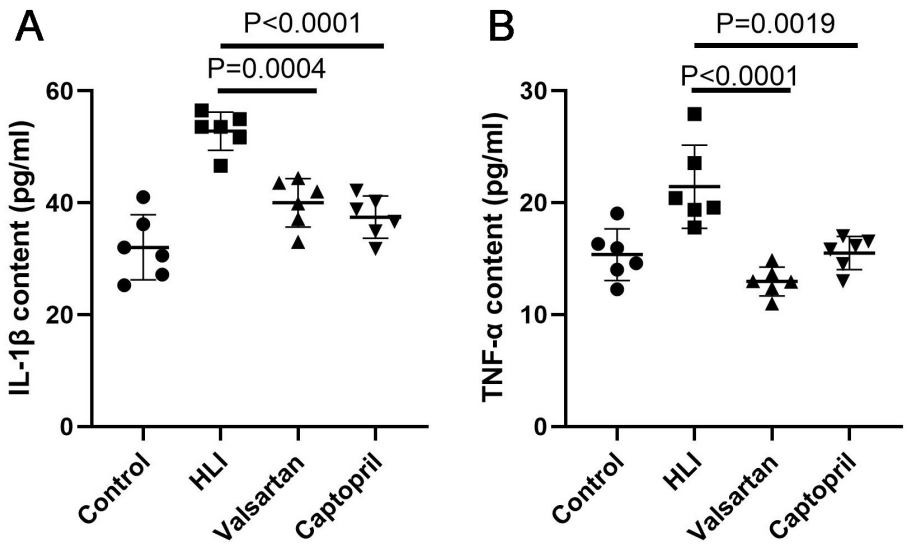

FIGURE 4
Contents of pro-inflammatory factors in the lung of different groups immediately after hyperbaric exposure. **(A)** IL-1β content of the lung; **(B)** TNF-α content of the lung. ANOVA was used for comparisons among groups followed by Tukey's *post hoc*.

often employed to evaluate the severity of lung injury. In the present study, arterial blood was collected for blood gas analysis, and results showed both valsartan and captopril could improve the changes in blood gas after hyperbaric exposure: significantly reduced pH value, Hb and Hct, and slightly reduced BEecf, but markedly increased PCO_2 after hyperbaric hyperoxic exposure. Lung injury is often translated to the change in lung function, and lung function detection can identify the mild lung injury if the clinical symptoms are not evident. In diving medicine, the reduction in tidal volume is closely related to the HLI (15). There is evidence showing that hyperoxic exposure could increase airway resistance and decrease pulmonary compliance (16). To further understand the protective effects of valsartan and captopril on the lung function, non-invasive lung function detection was performed immediately after hyperbaric exposure. However, the lung function largely remained unchanged immediately after hyperbaric exposure (except for respiratory frequency). Therefore, lung function was detected at 48 h after hyperbaric exposure. Increase in TI (increased resistance of inspiration) and decrease in respiratory frequency (deep breath) were the most common changes in the lung function after hyperbaric exposure and both valsartan and captopril could significantly reduce TI and increase respiratory frequency after hyperbaric exposure. In addition, both valsartan and captopril increased Vt, leading to the elevation of MV after hyperbaric exposure. These indicate valsartan and captopril pre-treatment may improve the lung function. All these findings indicate both valsartan and captopril (inhibition of RAS) are able to inhibit the lung injury secondary to prolonged exposure to hyperbaric hyperoxic environment.

It has been reported that lung cell death (including apoptosis, necrosis, autophagy and pyroptosis) plays an important role in the pathogenesis of HLI (17–19). In our previous study, results indicated necroptosis was involved in the pathogenesis of hyperbaric HLI (11). However, whether the necroptosis is cell-specific is still unclear. In this study, double immunofluorescence staining was employed to investigate the cell specificity of necroptosis in lung tissues after hyperbaric hyperoxic exposure. Type I ACEs are the most common type of cells in the lung and responsible for the gas exchange in the lung. In addition, they serve as the first-line defense against environment and therefore are susceptible to the damage due to the environmental change. In our study, immunofluorescence staining not only indicated the necroptosis increased after hyperbaric hyperoxic exposure, but also type I ACEs were found to be the major cells experiencing necroptosis secondary to hyperoxic exposure, and few type II ACEs and endothelial cells were necroptotic in the lung. After hyperoxic exposure, there was an evident loss of healthy capillary endothelial cells in the lung (20), which was different from our findings. This might be ascribed to the difference in the animal model.

In 2006, Bhandari et al reported that hyperoxia could cause angiopoietin 2-mediated acute lung injury and necrotic cell death (21). Whether inhibition of RAS may inhibit the necroptosis in the lung is poorly understood. Immunofluorescence staining and Western blotting were employed to detect the expression of major proteins in the necroptosis process. Both detections confirmed the expression of necroptosis related proteins reduced after hyperbaric hyperoxic exposure in case of valsartan or captopril pre-treatment. Further examination indicated either valsartan or captopril pre-treatment significantly reduced the contents of pro-inflammatory factors in the lung after hyperbaric hyperoxic exposure. A study on the normobaric hyperoxic exposure indicated inflammatory activation is the major driver of the observed transcriptional changes in hyperoxia (20). These findings suggest either valsartan or captopril can inhibit cell necroptosis and subsequent inflammation in the lung, leading to the improvement of lung edema, lung function and blood gas. However, the exact mechanism underlying Ang II induced necroptosis is still unclear. It has been reported that the binding of Ang II to its receptor can induce the increase in intracellular calcium (22, 23), and the increased intracellular calcium may further

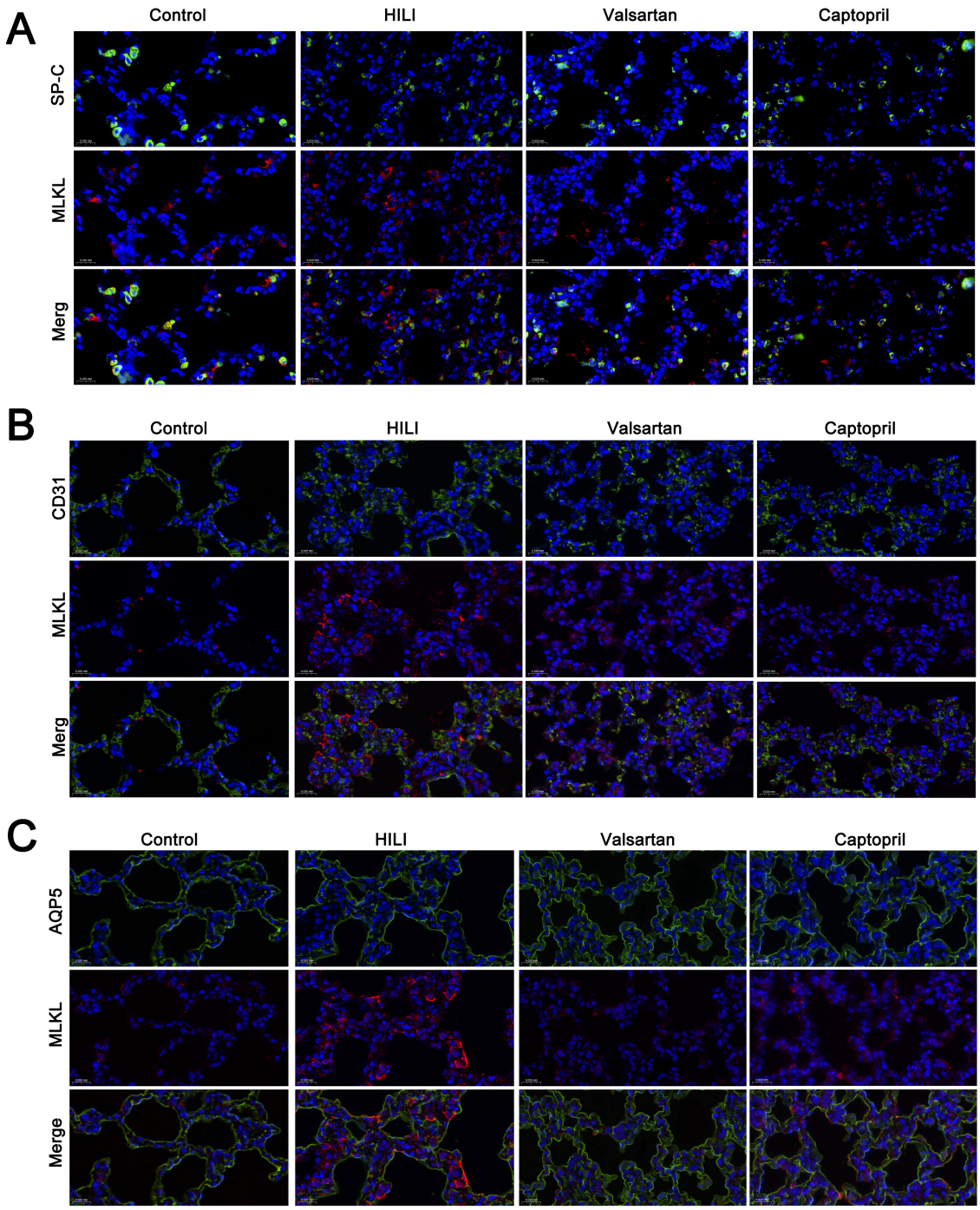

FIGURE 5
Cell-specificity of necroptosis in the lung. **(A)** Double immunofluorescence staining of type II alveolar epithelial cells (SP-C) and necroptosis (MLKL); **(B)** double immunofluorescence staining of blood vessels (CD31) and necroptosis (MLKL); **(C)** double immunofluorescence staining of type I alveolar epithelial cells (AQP5). Magnification: 40×.

induce RIP1/RIP3 complex-dependent necroptosis (24). Whether intracellular calcium mediates the Ang II induced necroptosis is warranted to be further elucidated in more studies.

Taken together, the novelty of this study was that our group for the first time investigated the relationship between RAS activation and necroptosis in the lung after hyperbaric hyperoxic exposure and further explored the cell-specificity of necroptosis in case of HLI. Our results show hyperbaric hyeroxic exposure mainly induces the necroptosis of type I AECs, and inhibition of RAS with valsartan or captopril before exposure can effectively prevent the lung against hyperbaric HLI. Both valsartan and captopril have pleiotropic activities and have been widely used in the clinical treatment of diseases with favorable safety. Thus, both valsartan and captopril have the promise to become a preventive strategy for hyperbaric HLI. However, there were still limitations in this study. In our previous study, the blood gas was analyzed immediately and

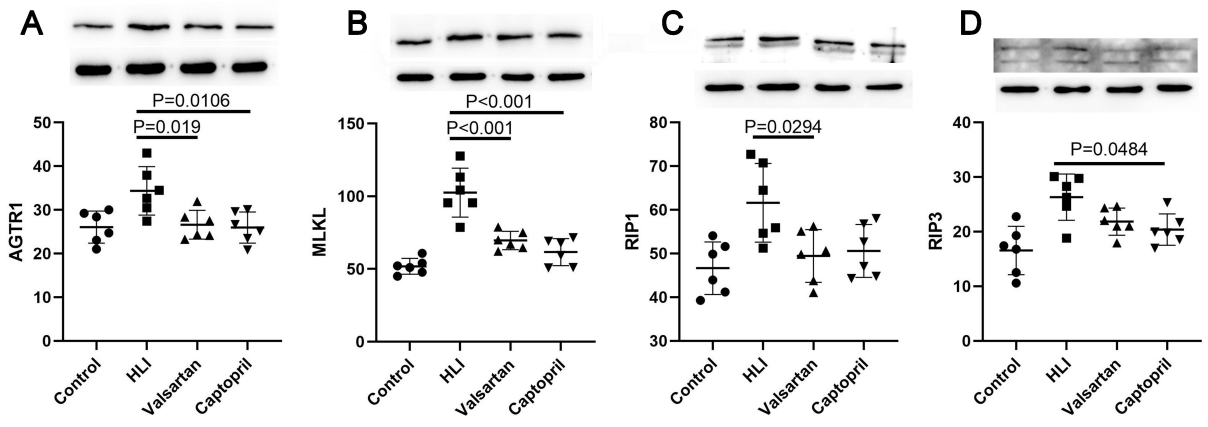

FIGURE 6
Expression of AGTR1 and necroptosis related molecules in different groups (Western blotting). **(A)** AGTR1 protein expression; **(B)** MLKL protein expression; **(C)** RIP1 protein expression; **(D)** RIP3 protein expression. ANOVA was used for comparisons among groups followed by Tukey's *post hoc*.

at 48 h after hyperbaric hyperoxic exposure, and results showed the blood gas nearly returned to the levels in the control group at 48 h after hyperbaric exposure. Thus, in this study, blood gas at 48 h after exposure was not detected. As previously reported, valsartan and captopril can exert some bioeffects beyond their primordial role in the cardiovascular system, and the signaling pathway by which valsartan and captopril inhibit lung cell necroptosis is still unclear and was not further explored in this present study. In our study, the dose dependent response was not investigated for valsartan and captopril although protective effects of valsartan and captopril were indicated, and thus the optimal dose at which preventive effect is achieved with few adverse effects is still unclear. Thus, more studies are needed to further elucidate this in the future.

Data availability statement

The raw data supporting the conclusions of this article will be made available by the authors, without undue reservation.

Ethics statement

The animal study was approved by Ethics Committee of Naval Medical Center. The study was conducted in accordance with the local legislation and institutional requirements.

Author contributions

WL: Conceptualization, Investigation, Writing – original draft, Writing – review and editing. CH: Data curation, Funding acquisition, Methodology, Project administration, Writing – review and editing. YL: Funding acquisition, Methodology, Project administration, Supervision, Writing – review and editing. PZ: Methodology, Project administration, Writing – review and editing. SW: Conceptualization, Funding acquisition, Methodology, Supervision, Writing – review and editing. JX: Methodology, Data Curation, Writing – review and editing. XY: Methodology, Data Curation, Writing – review and editing. YW: Methodology, Data Curation, Writing – review and editing.

Funding

The author(s) declare that financial support was received for the research, authorship, and/or publication of this article. This study was supported by the Key R&D Program of Jining City (2022YXNS112) and the Program of Medical Health Science and Technology of Shandong Province (202303020676).

Conflict of interest

The authors declare that the research was conducted in the absence of any commercial or financial relationships that could be construed as a potential conflict of interest.

Generative AI statement

The authors declare that no Generative AI was used in the creation of this manuscript.

Publisher's note

References

1. Alva R, Mirza M, Baiton A, Lazuran L, Samokysh L, Bobinski A, et al. Oxygen toxicity: Cellular mechanisms in normobaric hyperoxia. *Cell Biol Toxicol.* (2023) 39:111–43. doi: 10.1007/s10565-022-09773-7

2. Rao T, Zhou Y, Chen C, Chen J, Zhang J, Lin W, et al. Recent progress in neonatal hyperoxic lung injury. *Pediatr Pulmonol.* (2024) 59:2414–27. doi: 10.1002/ppul.27062

3. Chu D, Kim L, Young P, Zamiri N, Almenawer S, Jaeschke R, et al. Mortality and morbidity in acutely ill adults treated with liberal versus conservative oxygen therapy (IOTA): A systematic review and meta-analysis. *Lancet.* (2018) 391:1693–705. doi: 10.1016/S0140-6736(18)30479-3

4. Wingelaar T, van Ooij P, van Hulst R. Oxygen toxicity and special operations forces diving: Hidden and dangerous. *Front Psychol.* (2017) 8:1263. doi: 10.3389/fpsyg.2017.01263

5. Demchenko I, Welty-Wolf K, Allen B, Piantadosi C. Similar but not the same: Normobaric and hyperbaric pulmonary oxygen toxicity, the role of nitric oxide. *Am J Physiol Lung Cell Mol Physiol.* (2007) 293:L229–38. doi: 10.1152/ajplung.00450.2006

6. Paul M, Poyan Mehr A, Kreutz R. Physiology of local renin-angiotensin systems. *Physiol Rev.* (2006) 86:747–803. doi: 10.1152/physrev.00036.2005

7. Gan P, Liao W, Linke K, Mei D, Wu X, Wong W. Targeting the renin angiotensin system for respiratory diseases. *Adv Pharmacol.* (2023) 98:111–44. doi: 10.1016/bs.apha.2023.02.002

8. Han C, Zhang P, Liu Y, Zheng J, Liu K, Wei D, et al. Changes in angiotensin II and angiotensin-converting enzyme of different tissues after prolonged hyperoxia exposure. *Undersea Hyperb Med.* (2017) 44:39–44. doi: 10.22462/1.2.2017.7

9. Zhang P, Han C, Zhou F, Li L, Zhang H, Liu W. Renin-angiotensin system and its role in hyperoxic acute lung injury. *Undersea Hyperb Med.* (2016) 43:239–46.

10. Pagano A, Barazzone-Argiroffo C. Alveolar cell death in hyperoxia-induced lung injury. *Ann N Y Acad Sci.* (2003) 1010:405–16. doi: 10.1196/annals.1299.074

11. Han C, Guan Z, Zhang P, Fang H, Li L, Zhang H, et al. Oxidative stress induced necroptosis activation is involved in the pathogenesis of hyperoxic acute lung injury. *Biochem Biophys Res Commun.* (2018) 495:2178–83. doi: 10.1016/j.bbrc.2017.12.100

12. Zhu Y, Cui H, Lv J, Li G, Li X, Ye F, et al. Angiotensin II triggers RIPK3-MLKL-mediated necroptosis by activating the Fas/FasL signaling pathway in renal tubular cells. *PLoS One.* (2020) 15:e0228385. doi: 10.1371/journal.pone.0228385

13. Dong X, Fan J, Lin D, Wang X, Kuang H, Gong L, et al. Captopril alleviates epilepsy and cognitive impairment by attenuation of C3-mediated inflammation and synaptic phagocytosis. *J Neuroinflammation.* (2022) 19:226. doi: 10.1186/s12974-022-02587-8

14. Ulutas Z, Ermis N, Ozhan O, Parlakpinar H, Vardi N, Ates B, et al. The protective effects of compound 21 and valsartan in isoproterenol-induced myocardial injury in rats. *Cardiovasc Toxicol.* (2021) 21:17–28. doi: 10.1007/s12012-020-09590-6

15. Risberg J, van Ooij P. Hyperoxic exposure monitoring in diving: A farewell to the UPTD. *Undersea Hyperb Med.* (2022) 49:395–413. doi: 10.22462/07.08.2022.1

16. Qin H, Zhuang W, Liu X, Wu J, Li S, Wang Y, et al. Targeting CXCR1 alleviates hyperoxia-induced lung injury through promoting glutamine metabolism. *Cell Rep.* (2023) 42:112745. doi: 10.1016/j.celrep.2023.112745

17. Mantell L, Lee P. Signal transduction pathways in hyperoxia-induced lung cell death. *Mol Genet Metab.* (2000) 71:359–70. doi: 10.1006/mgme.2000.3046

18. Wang M, Zhang F, Ning X, Wu C, Zhou Y, Gou Z, et al. Regulating NLRP3 inflammasome-induced pyroptosis via Nrf2: TBHQ limits hyperoxia-induced lung injury in a mouse model of bronchopulmonary Dysplasia. *Inflammation.* (2023) 46:2386–401. doi: 10.1007/s10753-023-01885-4

19. Ren Y, Qin S, Liu X, Feng B, Liu J, Zhang J, et al. Hyperoxia can induce lung injury by upregulating AECII autophagy and apoptosis via the mTOR pathway. *Mol Biotechnol.* (2023) 66(11):3357–68. doi: 10.1007/s12033-023-00945-2

20. Hurskainen M, Mižíková I, Cook D, Andersson N, Cyr-Depauw C, Lesage F, et al. Single cell transcriptomic analysis of murine lung development on hyperoxia-induced damage. *Nat Commun.* (2021) 12:1565. doi: 10.1038/s41467-021-21865-2

21. Bhandari V, Choo-Wing R, Lee C, Zhu Z, Nedrelow J, Chupp G, et al. Hyperoxia causes angiopoietin 2-mediated acute lung injury and necrotic cell death. *Nat Med.* (2006) 12(11):1286–93. doi: 10.1038/nm1494

22. Batra V, Gopalakrishnan V, McNeill J, Hickie R. Angiotensin II elevates cytosolic free calcium in human lung adenocarcinoma cells via activation of AT1 receptors. *Cancer Lett.* (1994) 76:19–24. doi: 10.1016/0304-3835(94)90129-5

23. Griendling K, Berk B, Socorro L, Tsuda T, Delafontaine P, Alexander R. Secondary signalling mechanisms in angiotensin II-stimulated vascular smooth muscle cells. *Clin Exp Pharmacol Physiol.* (1988) 15:105–12. doi: 10.1111/j.1440-1681.1988.tb01051.x

24. Sun W, Wu X, Gao H, Yu J, Zhao W, Lu J, et al. Cytosolic calcium mediates RIP1/RIP3 complex-dependent necroptosis through JNK activation and mitochondrial ROS production in human colon cancer cells. *Free Radic Biol Med.* (2017) 108:433–44. doi: 10.1016/j.freeradbiomed.2017.04.010

frontiers | Frontiers in Pharmacology

TYPE Review
PUBLISHED 21 March 2025
DOI 10.3389/fphar.2025.1559659

OPEN ACCESS

EDITED BY
Guochang Hu,
University of Illinois Chicago, United States

REVIEWED BY
Zoran Todorovic,
University of Belgrade, Serbia
Thangavel Muthusamy,
Sree Balaji Medical College and Hospital, India

*CORRESPONDENCE
Ana Hou,
houan@sj-hospital.org

RECEIVED 13 January 2025
ACCEPTED 03 March 2025
PUBLISHED 21 March 2025

CITATION
Xiao J, Wang L, Zhang B and Hou A (2025) Cell death in acute lung injury: caspase-regulated apoptosis, pyroptosis, necroptosis, and PANoptosis.
Front. Pharmacol. 16:1559659.
doi: 10.3389/fphar.2025.1559659

Cell death in acute lung injury: caspase-regulated apoptosis, pyroptosis, necroptosis, and PANoptosis

Jun Xiao, Lichuan Wang, Bohan Zhang and Ana Hou*

Department of Pediatrics, Shengjing Hospital of China Medical University, Shenyang, China

There has been abundant research on the variety of programmed cell death pathways. Apoptosis, pyroptosis, and necroptosis under the action of the caspase family are essential for the innate immune response. Caspases are classified into inflammatory caspase-1/4/5/11, apoptotic caspase-3/6/7, and caspase-2/8/9/10. Although necroptosis is not caspase-dependent to transmit cell death signals, it can cross-link with pyroptosis and apoptosis signals under the regulation of caspase-8. An increasing number of studies have reiterated the involvement of the caspase family in acute lung injuries caused by bacterial and viral infections, blood transfusion, and ventilation, which is influenced by noxious stimuli that activate or inhibit caspase engagement pathways, leading to subsequent lung injury. This article reviews the role of caspases implicated in diverse programmed cell death mechanisms in acute lung injury and the status of research on relevant inhibitors against essential target proteins of the described cell death mechanisms. The findings of this review may help in delineating novel therapeutic targets for acute lung injury.

KEYWORDS

caspase, NLRP3, RIPK, mlkl, inflammation, acute lung injury

1 Introduction

Acute Lung Injury (ALI) and its severe variant, Acute Respiratory Distress Syndrome (ARDS), are prevalent critical illnesses marked by the compromise of the alveolar-capillary barrier, pulmonary edema, and an unregulated inflammatory response, with a fatality rate of 30%–40% (Bos and Ware, 2022; Mokrá, 2020). The etiology is multifaceted, encompassing various causal variables including infection, trauma, and shock; nonetheless, the fundamental pathological mechanism remains ambiguous (Brower et al., 2000; Lentini et al., 2023; Land, 2013).

Recently, the caspase family of proteins has been involved in the regulation of programmed cell death (PCD), including apoptosis, pyroptosis, necroptosis, and PANoptosis (Kesavardhana et al., 2020). PANoptosis has been a central theme in studies exploring ALI processes and treatment approaches, due to its dual role in regulating tissue homeostasis and the immune microenvironment (He et al., 2025). In the context of *Francisella* infection, AIM2-PANoptosis offers immunoprotection (Lee et al., 2021), while ZBP-PANoptosis is a fuel for the cytokine storm observed in COVID-19 patients (Karki et al., 2022).

Traditionally, apoptosis curtails inflammation by caspase-3/7-mediated "silent" death (Fettucciari et al., 2003), while localized and necroptosis depends on hole creation by

gasdermin proteins or MLKL-mediated membrane rupture, resulting in the release of many damage-associated molecular patterns (DAMPs) that drive alveolar macrophage overactivation with neutrophil infiltration (Chen et al., 2016). Bronchial epithelial cells, alveolar epithelial cells (AEC), and macrophages express various pattern recognition receptors (PRRs) that effectively identify pathogen-associated molecular patterns (PAMPs) linked to bacterial, viral, or nonspecific infections (Sundaram et al., 2024a). This recognition initiates the synergistic activation of PCD, including necroptosis, pyroptosis, and apoptosis, which collectively contribute to the inflammatory cascade response and disrupt tissue repair processes (Wang et al., 2023). Caspase-8 cleaves GSDMD, facilitating the conversion from apoptosis to pyroptosis, and also regulates necroptosis via the RIPK1-RIPK3-MLKL axis (Schwarzer et al., 2020a). The intersectionality of PCD indicates that inhibiting a single pathway may be inadequate for reversing ALI progression. Targeting core molecules, such as caspase-8 in PANoptosis, or employing combined strategies across death pathways is necessary (Fritsch et al., 2019).

Nonetheless, the precise regulation and functional, focused intervention mechanisms of PCD in ALI remain inadequately clarified. This review will systematically consolidate recent research on the molecular mechanisms of PCD and targeted pharmacological inhibitors, focusing on caspase-regulated cell death. It aims to investigate the dynamic regulation of PCD in ALI and its potential as a therapeutic target, to offer novel insights to overcome the constraints of conventional anti-inflammatory treatment.

2 Inflammatory caspases

2.1 The structure and function of inflammatory caspases

Caspase can specifically cleave the peptide chain on the aspartate residue of the target protein. The caspase family members are mainly divided into two categories in terms of function (Ai et al., 2024). The first category is inflammatory caspases, including caspase1/4/5/11, which are related to inflammatory cytokine signaling and pyroptosis (de Vasconcelos and Lamkanfi, 2020). In 1989, the discovery of a novel protease sensitive to the activation of pro-IL-1β was documented and named interleukin (IL)-1β converting enzyme (ICE), also known as caspase-1 (Kostura et al., 1989). Caspase-1, the most widely studied member of the caspase family, plays a vital role in processing cytokines, particularly IL-1β and IL-18. In the resting state, caspase exists in the form of inactive pro-caspase-1 and participates in the inflammasome through ASC (Huang et al., 2021). Mouse caspase-11 is a homolog of human caspase-4/5 (Rathinam et al., 2019). Caspase-1/4/11 acquires protease activity through dimerization, with the functional difference between the three lying in the self-processing of the interdomain linker (IDL). The IDL and the CARD domain linker (CDL) between the caspase-1 catalytic subunits undergo autoproteolytic cleavage to produce the active fragment p20/p10, whereas caspase-1 IDL autoprocessing is necessary for cleaving cytokines (Broz et al., 2010). Unlike caspase-1, caspase-11 does not cleave the precursor of IL-1β but can still generate mature cytokines through the N-GSDMD channel. This is mainly because, during GSDMD maturation, other cell-intrinsic signals trigger NLRP3-dependent caspase-1 activation (Kayagaki et al., 2015). Interestingly, the structure and function of human caspase-4 complement its downstream inflammatory targets. First, caspase-4 dimerizes to acquire basal protease activity. Second, caspase-4 D289/D270 IDL site undergoes self-cleavage to generate fully active protease fragments cleave GSDMD to induce pyroptosis, but only the protease fragment generated by autoproteolysis at the D289 site can cleave pro-IL-1β. Importantly, caspase-4/IL-1β signaling is independent of NLRP3 in human macrophages and epithelial cells (Chan et al., 2023). Meanwhile, the structure of pro-IL-18 has an autoinhibitory interaction between the propeptide and the post-cleavage site, but the loss of the propeptide upon caspase-4/5 cleavage facilitates the conformational maturation of IL-18. Caspase-4/5-IL-1β/IL-18 complements the non-inflammasome pathway for pathological inflammatory responses (Shi et al., 2023).

Inflammatory caspases are not only responsible for the processing of inflammatory factors but also for the targeted cleavage of gasdermin protein. Gasdermins are the executors of pyroptosis and are widely expressed throughout the human body with tissue specificity. In humans, the gasdermin family includes DFNB59 and gasdermin A-E (GSDMA-E), the last five of which have gasdermin-N and -C dual domains (Vasudevan et al., 2023). They are implicated in a variety of biological functions and pathological conditions, such as cell proliferation and death, coagulation and thrombosis, and inflammation (Chen and Broz, 2024). GSDMD is the most studied gasdermin, which uses two routes to mediate pyroptosis (Rathinam and Fitzgerald, 2016).

2.2 Caspase-1 and inflammasomes

The dominant and canonical mechanism is the NLRP3 inflammasome-dependent pyroptosis pathway, primarily observed in macrophages (Wei et al., 2022). During the innate immune response, inflammasomes serve as responders to intracellular danger signals. Inflammasome sensor molecule is a type of PRR, including Nod-like receptor (NLR) family protein (such as NLRP1/3/12, NLRC4/5) and HIN200 family protein (such as AIM2) (Fu and Wu, 2023; Le et al., 2023).

NLRs are structurally divided into three parts: N-terminal, C-terminal, and middle NACHT. Except for NLRP10, the C-terminals of other NLR family members contain leucine-rich repeat sequences (LRR) (Sundaram et al., 2024a; Chou et al., 2023). NLRs can be divided into different subtypes based on the different domains contained in the N-terminus, namely NLRBs (baculovirus inhibitor of apoptosis protein repeat, BIR), NLRCs (caspase recruitment domain, CARD), NLRPs (pyrin domain, PYD) (Chen et al., 2021).

Pro-caspase-1 is an effector that contains a CARD. ASC (apoptosis-associated speck-like protein containing a CARD) is a bipartite molecule that contains an N-terminal PYD and a C-terminal CARD (Rathinam and Fitzgerald, 2016). ASC recruits pro-caspase-1 through CARD-CARD interactions. In most cases, the assembly of inflammasomes requires the recruitment of ASC through PYD-PYD or CARD-CARD interactions. ASC serves as a

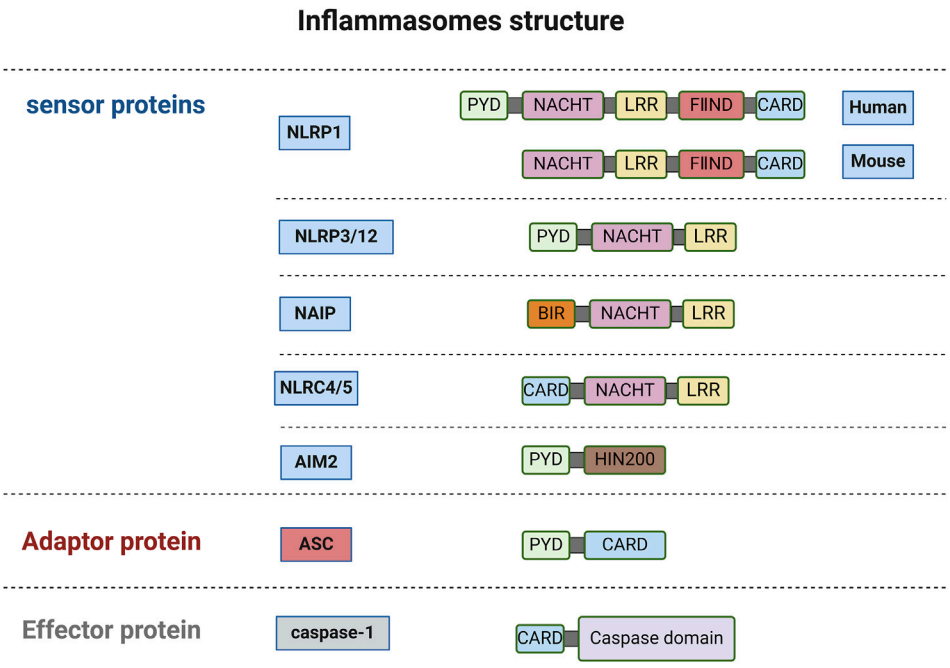

FIGURE 1
The structure of inflammasomes (created with BioRender.com).

bridge protein in the inflammasome to transmit upstream stimulation information to downstream effector proteins.

However, ASC is not required for the assembly of all inflammasomes (Fu et al., 2024). NLRP1 was the first inflammasome discovered that requires ASC to complete its self-assembly. Various viral proteases and Toxoplasma gondii infection can act as NLRP1 activators (Taabazuing et al., 2020). Human NLRP1 relies on its C-terminal CARD to interact with the C-terminal CARD of ASC to recruit ASC. However, mouse homologous NLRP1 (NLRP1a, b, c) can recruit pro-caspase-1 without the presence of ASC. Additionally, the C-terminal domain of NLRP1 has an autoproteolytic domain between LRR and CARD, called FIIND, and its self-cleavage is necessary for NLRP1 activation (Taabazuing et al., 2020; Gong et al., 2021). Human NLRB consists of only one family member, NAIP. After activation by bacterial proteins such as flagellin, it recruits NLRC4 through NACHT interaction, and the N-terminal CARD adapter protein contained in NLRC4 can directly recruit and activate pro-caspase-1, implying that ASC is unnecessary in this process (Fu et al., 2024; Zhang et al., 2015). NLRC5 is structurally similar to NLRC4, but functionally NLRC5 acts both as an innate immunity sensor and regulates NLRP3 activation and PANoptosome formation (Sundaram et al., 2024b; Zhang et al., 2021).

A variety of signals, including entire pathogens, PAMPs/DAMPs, external stimuli that damage lysosomes (e.g., silicon, alum), mitochondrial DNA (mtDNA), and reactive oxygen species (ROS), trigger NLRP3 (Hayward et al., 2018; Yang et al., 2019). Structurally, NLRP3 oligomers transform to monomers or dimers under the regulation of NIMA-related kinase 7 (NEK7); a key process to assemble NLRP3 (Fang et al., 2024). NLRP3 requires expression and assembly signals for activation. PAMPs or DAMPs (such as LPS) first stimulate the TLR/MyD88/NF-κB signaling pathway, which leads to the transcriptional upregulation of NLRP3, ASC, and pro-caspase-1 (Yang et al., 2019). NLRP3 lacks a CARD and recruits ASC through PYD-PYD interactions to form the NLRP3 inflammasome (Fu et al., 2024). Secondly, assembly signals mostly result in K+ efflux that activates NLRP3. Paxillin interacts with NLRP3 and enhances NLRP3 deubiquitination; a process dependent on the ATP release stimulates P2X7R to induce K+ efflux and paxillin phosphorylation, thereby activating the NLRP3 inflammasome (Wang et al., 2020b). The structures and functions of NLRP12 are similar to NLRP3 (Coombs et al., 2024). AIM2 is a cytosolic DNA sensor that recruits pro-caspase-1 through PYD-PYD interactions to promote inflammasome assembly to eliminate harmful pathogenic invasion (Lee et al., 2021) (Figure 1). Consequently, the activated NLRP3 inflammasome activates caspase-1 via ASC signal transduction, cleaving GSDMD, pro-IL-1β, and pro-IL-18 (de Vasconcelos and Lamkanfi, 2020).

2.3 Caspase-4/5/11 and the non-canonical pathway of pyroptosis

The non-canonical pathway of pyroptosis mediated by caspase-4/5/11 is different from the canonical pathway mediated by caspase-1. The formation of LPS monomers by extracellular LPS with the help of LPS binding protein (LBP) is the initial step for toll-like receptor 4 (TLR4) to recognize LPS. Subsequently, the LPS monomers-LBP complex is transported to CD14 and combined with TLR4/MD-2 complex to complete the entire process of TLR4 recognition of extracellular LPS (Mazgaeen and Gurung, 2020). In addition, Vishva Dixit et al. demonstrated that caspase-

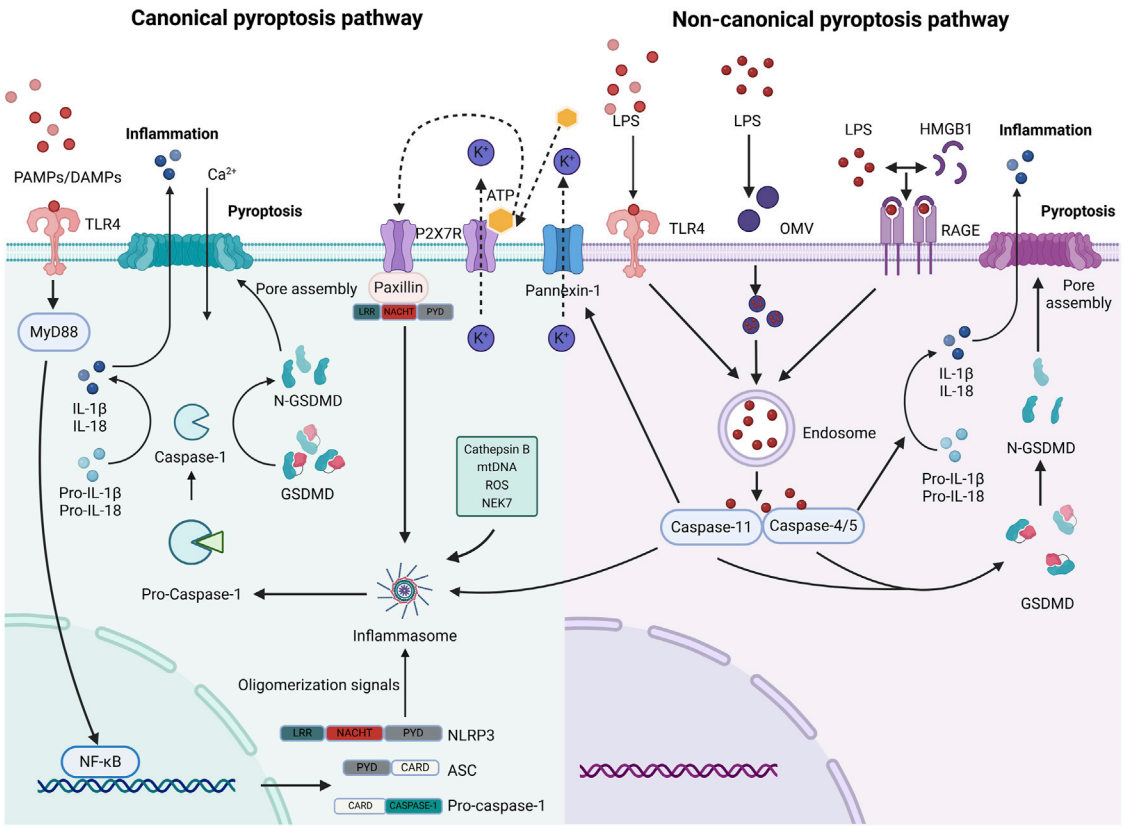

FIGURE 2
The canonical and non-canonical pyroptosis pathways (created with BioRender.com). The classical process involves the activation of caspase-1 through NLRP3 by PAMPs/DAMPs, K+ efflux, Cathepsin B, mitochondrial DNA (mtDNA), ROS, and NEK7, resulting in GSDMD breakage. In the non-classical process, LPS enters cells through multiple pathways, as illustrated in the diagram. It is promptly identified and triggers caspase-4/5/11 to enzymatically degrade GSDMD. There is interference between the signals on these two paths. The Panniexin-1 receptor mediates the signals, including K+ efflux and ATP release, which in turn stimulates the P2X7 receptor to trigger inflammation via the NLRP3 pathway (Zhang et al., 2023). This could potentially be another intracellular signal that facilitates the transmission of NLRP3 when Caspase-11 triggers pyroptosis.

11 could induce pyroptosis by sensing intracellular LPS independent of caspase-1 through an unknown mechanism independent of TLR4. Caspase-11 plays a bigger role than caspase-1 in the lethal inflammatory response (Kayagaki et al., 2011; Kayagaki et al., 2013). LPS can enter the host cytoplasm through a variety of pathways. One mechanism involves LPS binding to high mobility group box 1 protein (HMGB1) and entering cells, which is mediated by the receptor for advanced glycation end products (RAGE) (Matikainen et al., 2020). Contrarily, outer membrane vesicles can serve as carriers for LPS internalization into the cytoplasm (Yi, 2020). Additionally, caspase-4/5/11 directly recognizes cytoplasmic LPS, leading to its oligomerization and activation (Shi et al., 2014). Eventually, caspase-4/5/11 specifically cleaves GSDMD, generating N-GSDMD that disrupts the cell membrane, resulting in the formation of a non-selective transmembrane cavity, the release of cytokines, disruption of water ion balance, and cellular swelling (Wang et al., 2020a) (Figure 2).

3 Apoptotic caspases and apoptosis

Apoptosis is a tightly controlled type of programmed cell death that is essential for illness, tissue homeostasis, and biological growth (Kesavardhana et al., 2020). Apoptotic caspases comprise the primary executors of apoptosis, apoptosis-initiating proteins (caspase-2/8/9/10), and apoptosis effector proteins (caspase-3/6/7) (Van Opdenbosch and Lamkanfi, 2019).

Exogenous and endogenous stimuli activate apoptosis via two pathways. First, exogenous stimuli such as pathogens and inflammatory factors are recognized by death receptors, such as Fas and tumor necrosis factor receptor-1 (TNFR-1) (Kim et al., 2024). The ligand activates the death receptor and binds to the Fas-associated death domain (FADD) to recruit caspase-8/10 to form a complex that initiates the downstream caspase chain reaction (Schwarzer et al., 2020a; Jiang et al., 2021). Next, endoplasmic reticulum stress, oxidative stress, cytochrome c, and other non-receptor stimuli induce mitochondrial membrane permeability and pro-apoptotic genes actively participate in this process. Finally, the endogenous and exogenous pathways complete signal transmission, which is regulated by the apoptotic effector caspase-3/7 (Chen et al., 2019).

To guarantee accurate apoptosis, apoptosis regulatory mechanisms include the mitochondrial/death receptor pathway, zymogen activation cascade, repressor protein antagonism, and calpain cross-regulation (Hengartner, 2000). When the death domain, FADD, or apoptotic body (Apaf-1/cytochrome c

complex) aggregate, caspase-8/9 is activated (Hengartner, 2000). The starting caspases activate caspase-3/6/7, which are then further cleaved and activated to carry out the apoptotic program (Lakhani et al., 2006). Apoptosis inhibitory proteins, such as XIAP and cIAP, bind directly to the active site of caspase-3/7 to prevent its enzymatic action (Scott et al., 2005). Certain IAPs regulate apoptotic homeostasis by ubiquitinating and degrading the pro-apoptotic proteins Smac/DIABLO (Srinivasula et al., 2001). Bcl-2 and Bcl-xL are anti-apoptotic constituents of the Bcl-2 family. They inhibit the triggering of caspase-9 indirectly by obstructing the release of cytochrome c and the permeability of the mitochondrial membrane (Gottschalk et al., 1996).

Calpains, a category of calcium-dependent cysteine proteases, participate in apoptosis via calcium-dependent activation, direct cleavage of apoptosis-executing proteins, awakening of caspase cascades, and modulation of mitochondrial pathways (Momeni, 2011). In instances of calcium ion overload or endoplasmic reticulum stress, calpains facilitate apoptotic execution through the activation of caspase-3 and caspase-12 by cleavage (Tan et al., 2006). While caspases are the primary executors of pyroptosis, calpains can modulate associated signaling pathways. The activation of calpains may impact the processing of pro-caspase-1 or the construction of inflammasomes, thereby affecting the inflammatory response triggered by pyroptosis (Lopez-Castejon et al., 2012). Furthermore, the GSDMD-induced enhancement of plasma membrane permeability facilitates substantial calcium ion influx into the cell, activating calpain, which subsequently propels various responses linked to pyroptosis, such as intermediate filament disruption, cellular swelling, and rupture (Davis et al., 2019). Nevertheless, additional research is required to clarify their particular role in the focused death signaling network.

4 Apoptotic caspases and pyroptosis

Apoptosis and pyroptosis are two separate forms of planned cell death; nevertheless, new research has uncovered intricate interactions between them regarding molecular mechanisms, regulatory networks, and pathogenic processes (Qian et al., 2024). This signaling interference impacts cell fate decisions and is significantly involved in tumor immunity and infection defense. An examination of the architecture and role of inflammatory caspases prompted us to put forward that the primary substrate proteins of caspase-1/4/5/11 are GSDMD, IL-1β, and IL-18. Our investigation into GSDMA-C and GSDME indicated that inflammatory caspase-1, which cleaves GSDMB, can also successfully trigger pyroptosis (Panganiban et al., 2018). We sought to examine whether apoptotic caspases are involved in processing substrate proteins and possess the capability to cleave specific locations, thereby producing active fragments that initiate pyroptosis or other signaling pathways. Caspase-3/8 in apoptotic caspases primarily participates in the pyroptosis pathway by cleaving associated substrate proteins (Jiao et al., 2023; Hou et al., 2020) (Table 1).

More recent studies have proven that caspase3/GSDME constitutes a new route for cell pyroptosis (Jiao et al., 2023). Caspase-3 cleaves GSDME at the D270 site, resulting in the release of N-GSDME, which oligomerizes and integrates into the cell membrane, causing cell enlargement and rupture (Liu et al., 2020a). When GSDME is substantially expressed in cells, the activation of caspase-3 predominantly induces pyroptosis instead of apoptosis, a mechanism that is especially evident in tissue damage caused by chemotherapeutic agents (Li et al., 2023a; Xing et al., 2023). Viruses operate as activators of GSDME, resulting in pyroptosis in epithelial cells, which serve as the initial line of immunological protection against viruses (Guy et al., 2023). Caspase-8 demonstrates intricate and dynamic pathogenic functions in disease models by regulating cellular pyroptosis, characterized by a "double-edged sword" effect in many illness situations (Liang et al., 2024). Hypoxia or chemotherapeutic drugs like cisplatin can cause caspase-8 to cleave GSDMC or GSDMD, which kills tumor cells or helps blood vessels grow and metastasis spread to other parts of the body through inflammation linked to cell death (Hou et al., 2020; Liang et al., 2024; Xia et al., 2024).

5 Caspase-8 and necroptosis

Necroptosis; an alternative pathway of apoptosis, does not form apoptotic bodies and does not require caspase activation for the removal of the damaged cells (Yan et al., 2022). Interestingly, this process can be regulated by caspase-8 (Pang and Vince, 2023). Different stimuli such as TNF, IFN, LPS, DNA, or RNA viruses can trigger necroptosis, which subsequently activates receptor-interacting protein kinase 1 (RIPK1) and RIPK3 and the recruitment of the membrane perforator protein MLKL (mixed lineage kinase domain-like protein) (Yan et al., 2022).

Necroptosis is characterized by a core signaling pathway that includes various protein family members, such as RIPK1/3, the effector protein MLKL, receptor proteins TNFR/ZBP1, and regulatory factors CYLD/cFLIP (Newton and Manning, 2016). The dynamic balance among these components is crucial in determining cell fate. Upon activation of TNFR1 or TLR3/4 and inhibition of the apoptosis key protease caspase-8, RIPK1 interacts with RIPK3 via the RHIM domain to create a necrosome. Subsequently, activated RIPK3 phosphorylates the downstream effector protein MLKL, leading to its oligomerization and insertion into the cell membrane, thereby forming a pore (Alvarez-Diaz et al., 2016). This process compromises membrane integrity, resulting in the release of DAMPs such as HMGB1 and ATP, which in turn initiates a robust inflammatory response (Kao et al., 2014; Tummers and Green, 2017). Furthermore, pathogenic signals like viral RNA can directly activate RIPK3 via ZBP1, circumventing RIPK1 to trigger necroptosis (Yang et al., 2020).

Numerous studies have elucidated the significant role of calpain in necroptosis. Under hypoxia-acidosis conditions, calpain inhibits the caspase-dependent apoptotic pathway by cleaving pro-caspase-3, thereby preventing its activation to active caspase-3 and facilitating necroptosis (Graham et al., 2015). The necroptosis pathway appears to amplify the inflammatory response through the release of DAMPs. In response to cellular DNA damaging agents, the death receptor signaling pathway is activated with calpain's involvement, resulting in mitochondrial damage through the cleavage of BID (Cabon et al., 2012). Concurrently,

TABLE 1 Caspase family substrate proteins in pyroptosis.

Inflammatory caspase	Target proteins	Processing sites	Active fragments? (YES or NO)	Ref
Caspase-1	GSDMB GSDMD IL-1β IL-18	D236 D275 D27 D116 D36	YES YES YES YES	Panganiban et al. (2018) Liu et al. (2020a) Exconde et al. (2023) Exconde et al. (2023), Akita et al. (1997)
Caspase-4	GSDMD IL-1β IL-18	D275 D27 D116 D36	YES YES (weakly) YES	Liu et al. (2020a) Exconde et al. (2023) Exconde et al. (2023)
Caspase-5	GSDMD IL-1β IL-18	D275 D27 D36	YES NO YES	Liu et al. (2020a) Exconde et al. (2023) Exconde et al. (2023)
Caspase-11	GSDMD IL-1β	D276 D27	YES NO	Liu et al. (2020a) Exconde et al. (2023)
Apoptotic caspase	**Target protein**	**Processing sites**	**Active fragments? (YES or NO)**	**Ref**
Caspase-3	GSDMB GSDMD GSDME IL-18	D91 D87 D270 D71 D76	NO NO YES NO	Chao et al. (2017) Chen et al. (2019), Liu et al. (2020a) Kesavardhana et al. (2020), Liu et al. (2020a) Akita et al. (1997)
Caspase-6	GSDMB	D91	NO	Chao et al. (2017)
Caspase-7	GSDMB GSDMD	D91 D87	NO NO	Chao et al. (2017) Taabazuing et al. (2017)
Caspase-8	GSDMC GSDMD IL-1β IL-18	D365 D275 D27 D116 D36	YES YES YES YES	Hou et al. (2020) Kesavardhana et al. (2020), Van Opdenbosch and Lamkanfi (2019), Orning et al. (2018) Exconde et al. (2023), Maelfait et al. (2008) Tummers and Green (2017), Schneider et al. (2017)
Caspase-2/9/10	None	None	None	None

mitochondrial damage induces the release of tAIF from the mitochondria into the cytoplasm and nucleus, leading to chromatin lysis and a decline in cell viability (Delavallée et al., 2011). Calpain serves a crucial regulatory role in this process, integrating signals from various pathways and coordinating the initiation and execution of necroptosis (Cheng et al., 2018).

Necroptosis is primarily regulated by ubiquitination modifications, the deubiquitinating enzyme CYLD, and the dynamics of the apoptosis-necrosis homeostasis protein cFLIP (Newton and Manning, 2016). The ubiquitination of RIPK1, facilitated by cIAP1/2 or LUBAC, enhances NF-κB survival signaling and suppresses necroptosis (Bertrand et al., 2008). The deubiquitinating enzyme CYLD facilitates necroptosis through the removal of the ubiquitin chain from RIPK1, thereby enhancing the binding between RIPK1 and RIPK3 (Moquin et al., 2013). cFLIP and caspase-8 possess two death effector domains (DEDs) each, which interact to form a heterodimer via DED-DED binding. cFLP has two isoforms, cFLPL and cFLPS (Irmler et al., 1997). cFLIPL forms a complex with caspase-8 that is inactive, thereby inhibiting the initiation of apoptosis. cFLIPS can entirely inhibit caspase-8 activation, thereby compelling cells to undergo necroptosis (Zhang et al., 2024). Cleavage of CYLD by Caspase-8 may influence its deubiquitinating enzyme activity, thereby regulating the NF-κB signaling pathway, which impacts the apoptotic and necroptotic states of the cell (Jono et al., 2004). RIPK1/3 serves as a substrate for caspase-8 cleavage. While the direct cleavage of RIPK1/3 by caspase-8 has not been extensively studied, it is evident that this process can reduce inflammation and modulate the interplay between apoptosis and necroptosis (Schwarzer et al., 2020b).

Necroptosis serves a dual function in the context of infection defense and inflammatory diseases, facilitating the elimination of abnormal cells while also potentially intensifying tissue damage. Host detection of viral nucleic acids through ZBP1 initiates MLKL-mediated cell membrane rupture, resulting in the release of viral particles and the activation of an antiviral interferon response (Karki et al., 2022; Li et al., 2023b). Excessive necroptosis results in the release of significant quantities of IL-1α and IL-33 (Li et al., 2020; Karki et al., 2021), which subsequently activate neutrophils and macrophages, thereby contributing to irreversible inflammation in critically ill COVID-19 patients (Li et al., 2020).

6 Caspases and PANoptosis

Recent studies have found that the immune system releases several PAMPs and DAMPs in response to pathogenic infection, which are recognized by numerous inflammasome sensors and cause a variety of programmed cell deaths. Since 1989, when caspase-1 was first characterized as a cysteine-aspartate protease, the caspase family has become integral to the study of programmed

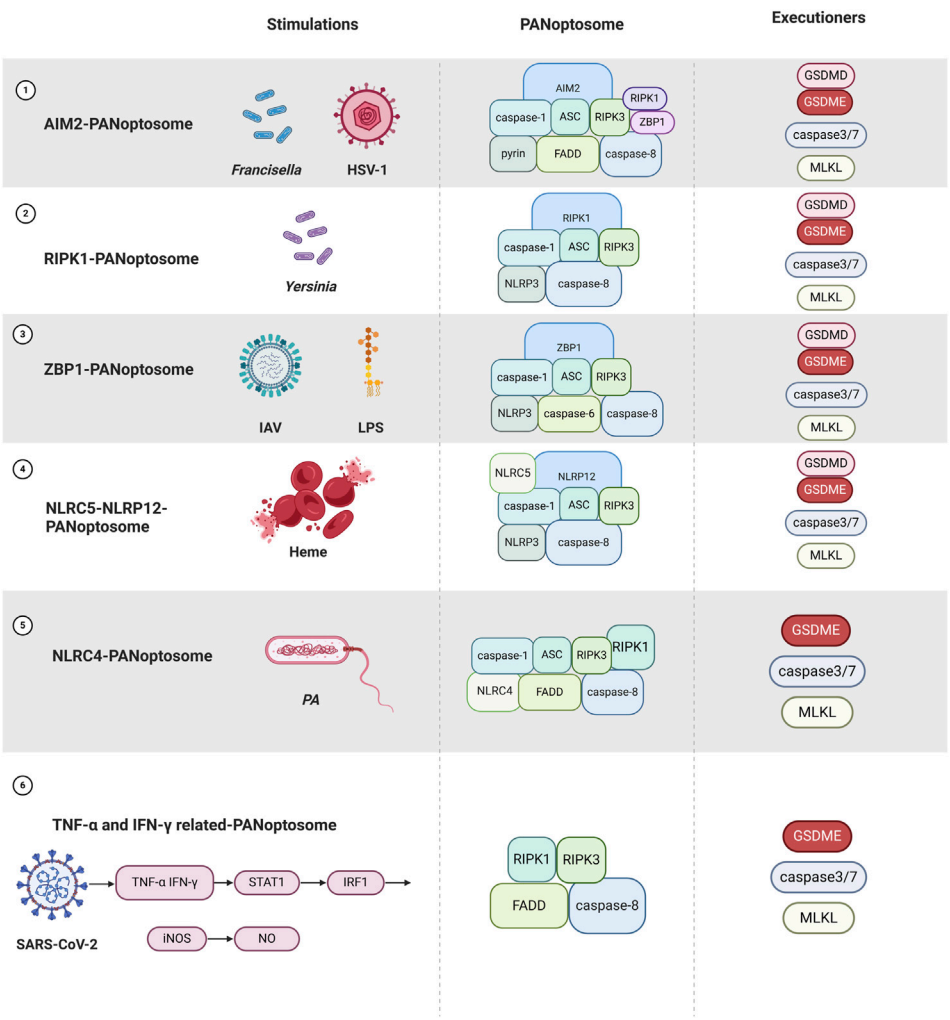

FIGURE 3
Overview of different PANoptosome assemblies in response to different stimuli as well as PANoptosis occurred (Created with BioRender.com).

cell death (Kostura et al., 1989). Their functions have evolved from the original role in apoptosis to encompass the regulation of new forms of cell death, including pyroptosis and necroptosis, thereby establishing a multi-pathway intersecting PANoptosis network (Qi et al., 2023). The caspase family is crucial in regulating and executing PANoptosis, with caspase-1/8 involved in the initiation phase and caspase-3/7 in the execution phase (Pandeya and Kanneganti, 2024).

Caspase-1 cleaves GSDMD, resulting in pore formation in the cell membrane and subsequent cell lysis (Sundaram et al., 2024a). The membrane rupture observed is indicative of pyroptosis, thereby contributing to the lytic characteristics of PANoptosis (Han et al., 2023). Caspase-8, previously considered an apoptosis promoter, is now recognized for its role in activating the pyroptosis pathway through the cleavage of GSDMC/GSDMD (Hou et al., 2020, Xia et al., 2024), similar to the function of caspase-1. The assembly of PANoptosomes facilitates the interaction of caspase-8 with RIPK1 and RIPK3 (Pandeya and Kanneganti, 2024), which are critical molecules in necroptosis, thereby linking the signaling pathways of apoptosis and necroptosis (Schwarzer et al., 2020b).

Caspase-3/7, primarily responsible for executing apoptosis, is also activated during PANoptosis and works in conjunction with caspase-8 to initiate the apoptotic process. This activation results in the cleavage and activation of downstream substrates that facilitate apoptosis-related changes in cellular morphology (Qi et al., 2023; Hengartner, 2000).

Under immunofluorescence visualization, ASC, caspase-8, and RIPK3 are essential components (Wang et al., 2022). Due to differences in other components, PANoptosome is classified into six classes: TNF-α and IFN-γ-, Z-DNA-binding protein 1 (ZBP1-), RIPK1-, NLRC4-, NLRC5-NLRP12-, and AIM2- (Pandeya and Kanneganti, 2024; Sundaram et al., 2024b; Sundaram et al., 2022).

The regulation of PANoptosis is intricate and relies on dynamic interactions within the PANoptosome (He et al., 2025). Upstream sensors, including ZBP1 and AIM2, trigger PANoptosome assembly in response to diverse inflammatory signals, such as PAMPs and DAMPs. ZBP1, upon stimulation, recruits caspase-8 and RIPK3 to assemble the PANoptosome (Lee et al., 2021; Zheng and Kanneganti, 2020). PANoptosome forms the regulatory cell death

molecules GSDME/GSDMD, caspase-3/7, and RIPK3/MLKL, leading to PANoptosis (Qi et al., 2023) (Figure 3).

7 Caspases and ALI

7.1 Bacteria-related ALI

Bacteria invade the lungs causing acute infections in adults or neonates when the body is immunocompromised. Especially in neonates with imperfect immune function, microbial infections bring adverse outcomes. Primarily due to the evolution of multiple mechanisms for pathogens to evade host immune surveillance, inadequate or delayed pathogen clearance leads to pathogen proliferation and an overactive immune response inducing ALI (Blutt et al., 2023).

7.1.1 Group B streptococcal (GBS)

GBS is the main causative agent of intrauterine infections and preterm labor as well as neonatal pneumonia and sepsis and is rich in virulence factors (cell wall surface β-protein, capsular polysaccharide, β-hemolysin/cytolysin, hyaluronidase, and membrane vesicles), which help GBS to evade the recognition of the immune system and are involved in cell death and promotion of inflammatory cell recruitment (Furuta et al., 2022).

GBS immune escape and recognition is the first step in GBS lung invasion. The terminal sialic acid of capsular polysaccharide, as well as the β-protein, can be recognized by sialic acid-binding immunoglobulin-like lectin expressed by different immune cells and can inhibit phagocytosis by immune cells (Carlin et al., 2009; Fong et al., 2018). Apoptosis, a non-inflammatory cell death, favors pathogen survival in large logarithms. β-hemolysin induces macrophage apoptosis in a caspase-independent and caspase-dependent manner, and a reduction in the number of macrophages attenuates or delays the onset of specific immune responses (Fettucciari et al., 2003; Fettucciari et al., 2000). In addition, β-hemolysin-induced cytotoxicity is present in invasively infected lung interstitial cells, a process dependent on apoptosis-associated caspases to drive infection progression (Kling et al., 2013). Hyaluronic acid (HA) is a normal component of lung tissue and facilitates interstitial development. In a variety of lung diseases, such as idiopathic pulmonary fibrosis, higher lung HA content is suggestive of disease progression and severity (Juul et al., 1996). Interestingly, GBS specifically secretes hyaluronidase to break down HA and reduce lung HA content, an unconventional phenomenon that seems to favor lung parenchymal invasion (Coleman et al., 2021). Membrane vesicles are pathogenic structures produced by GBS that carry virulence factors and are classified into hemolytic and common membrane vesicles (Surve et al., 2016; Armistead et al., 2021). Hemolytic membrane vesicles carry mainly β-hemolysin/cytolysin, which is associated with high mortality in neonatal mice, and activation of macrophage pyroptosis signaling during fetal life is detrimental to fetal survival (Armistead et al., 2021; Whidbey et al., 2015). Pore-forming toxins of pathogenic bacteria induce multiple forms of cell death and alter normal cellular function to promote pathogen survival *in vivo* (González-Juarbe et al., 2015). For example, necroptosis occurs in macrophages during *Staphylococcus aureus* and *Serratia marcescens* infections (Kitur et al., 2015). Although it has been shown that GBS common membrane vesicles carry this virulence factor, there appears to be no definitive study indicating whether GBS pore-forming toxins cause necroptosis (Surve et al., 2016).

Pyroptosis dominates the immune defense process. Neutrophils are the main source of IL-1β production in lungs infected with GBS, which is directly recognized and facilitates the amplification of inflammatory signals through the TLR (Mohammadi et al., 2016). Macrophages also bear a part of IL-1β production, acting in a sialic acid-dependent or non-dependent manner to enhance NLRP3 activation (Tsai et al., 2020). Apoptosis, pyroptosis, and necroptosis appear to have their roles during GBS infection, but it should be emphasized that erythrocytes are substrates for β-hemolysin and have a high affinity for cell membrane phospholipids (Whidbey et al., 2015; Rosa-Fraile et al., 2014). Heme released from damaged erythrocytes is a threat to the innate immune system, and NLRP12 is an innate inflammasome sensor for heme and PAMPs in bone marrow-derived macrophages (Henkel and O'Neill, 2023). NLRP12 interacts with NLRP3, ASC, caspase-1, caspase-8, and RIPK3 to form NLRP12-PANptosome complexes in response to heme and PAMPs in the hemolysis model induced by heme and PAMPs (Sundaram et al., 2023; Bernard and Broz, 2023). Furthermore, NLRC5 is also involved in interactions driving inflammatory cell death (Sundaram et al., 2024b).

7.1.2 *Yersinia pestis*

Flagellin secreted by the functional type III secretion system (T3SS) of extracellular opportunistic pathogenic bacteria is required for NLRC4 activation (Schubert et al., 2020). Macrophage NLRC4 activation reduces bacterial clearance in an ALI mouse model.

Yersinia pestis is one of the pathogens of fatal lung infections. In the pre-inflammatory phase, T3SS secretes more than a dozen effector proteins Yops, pore-forming toxins, Pla, and anti-host factors to inhibit the innate immune response, which integrally coordinates the establishment of lung infection (Rosenzweig and Chopra, 2013). This is an extensive process. There is no doubt that neutrophils are the forerunners (Banerjee et al., 2020). Pla, an adhesin produced by *Y. pestis*, inhibits IL-17 expression delaying neutrophil recruitment and degranulation functioning to silence host protective immune defense mechanisms (Theriot et al., 2023). In addition, YopM prevented inflammasome assembly (LaRock and Cookson, 2012), and YopJ inhibited cytokine production by blocking TAK1 with its downstream MAPK and NF-κB inflammatory signaling (Orning et al., 2018; Philip et al., 2014).

In the later stages of infection, there is an explosive increase in pro-inflammatory factors, which manifests as acute pulmonary congestion, edema, and necrosis in the lungs (Chung and Bliska, 2016). As research progresses, it is suggested that *Y. pestis* modulates the innate immune response by inducing cell death. Pla interferes with the Fasl-dependent exogenous apoptotic pathway, effectively suppressing the innate immune response and creating an adaptive environment for bacterial replication (Caulfield et al., 2014). Inhibition of apoptotic signaling appears to alter the direction of the innate immune response. Caspase-8 responds to *Yersinia* infection, an effect that appears to be a combined process of apoptosis, pyroptosis, and necroptosis (Orning et al., 2018; Philip et al., 2014; Malireddi et al., 2020; Zheng et al., 2021). Caspase-8 and

RIPK1 are required for inflammatory cellular focalization induced by YopJ in response to TAK1 inhibition (Orning et al., 2018). Furthermore, another study added that RIPK1-dependent PANoptosis was triggered in TAK1-deficient macrophages, suggesting that *Yersinia* pre-inhibition of an effective innate immune response is followed by a positive host response that initiates caspase-8-dependent immune defense against *Yersinia* infection (Malireddi et al., 2020).

7.1.3 *Pseudomonas aeruginosa* (PA)

Pseudomonas aeruginosa (PA) as an extracellular opportunistic pathogen, T3SS and flagellin, outer membrane vesicles, and pyocyanin are responsible for destructive immunity (Wood et al., 2023). Apoptosis tends to occur early in infection, and pusillanimins are apoptosis-related toxins that inhibit early lung inflammation favoring early bacterial multiplication and respiratory colonization (Allen et al., 2005). Outer membrane vesicles are carriers of multiple virulence factors released by PA that can detach from live bacteria to act as independent virulence factors causing lung inflammation (Park et al., 2013). Primarily contained are fat-soluble virulence factors that bind to membrane lipids to invade the cytoplasm and interfere with airway epithelial cilia to clear pathogens (Bomberger et al., 2009).

Signaling crosstalk between pyroptosis and necroptosis during PA infection is also of interest. RIPK3 kinase-dependent function drives necroptosis in epithelial cells, and NLRP3 activation is dependent on mitochondrial dysfunction and ROS production caused by the onset of necroptosis (Li et al., 2023c). The RIPK3 scaffold structural domain drives destructive lung inflammation and death, which is distinct from necroptosis triggered by the RIPK3 kinase structural domain. In a different way, blocking RIPK3 effectively ameliorates lung inflammation as well as mortality in PA infection (Lyons et al., 2023). Not only that, NLRC4 deletion in macrophages caused deficient caspase-1/3/7/8 activation, and necroptosis compensated for the lack of immune response, underscoring the occurrence of PANoptosis in macrophages in the context of PA infection (Sundaram et al., 2022).

7.1.4 Other gram-negative bacilli

LPS is a virulence factor for Gram-negative bacteria (*Francisella, Klebsiella pneumoniae, Burkholderia thailandensis*) and has been strongly associated with poor sepsis outcome (Mazgaeen and Gurung, 2020). Sepsis-associated acute lung injury (SALI) is the primary cause of mortality in individuals experiencing severe sepsis. The primary mechanism of SALI involves a systemic inflammatory response induced by LPS, resulting in irreversible shock, endothelial cell injury, and ultimately lung failure (Deng et al., 2025). Mechanisms by which LPS induces SALI include synergistic action of RIPK3 with GSDMD (Chen et al., 2020), caspase-8 inhibition impedes apoptosis-dependent macrophage depletion delaying inflammatory clearance (Janssen et al., 2011), and targeting ZBP1 is critical for the regulation of PANoptosis (Guo et al., 2023; Cui et al., 2022a). Uncontrollable body inflammation disrupts normal coagulation mechanisms and systemic multi-organ functional involvement into an irreversible phase of endotoxic shock.

Caspase-11 mediates endothelial cell barrier disruption, and bacterial entry into the bloodstream, and excessive caspase-11 activation triggers shock (Cheng et al., 2017). Endotoxemia after hemorrhagic shock (HS) often promotes the irreversible development of shock, leading to multiple organ dysfunction, which can lead to fatalities (Li et al., 2018; Khazoom et al., 2020; Peitzman et al., 1995). HS induces mitochondrial and lysosomal damage and releases inflammatory mediators to destroy the homeostasis of endothelial cells and macrophages and affect the development of SALI. Two inflammatory mediators, HMGB1 and extracellular cold-inducible RNA-binding protein (eCIRP), are associated with HS and high mortality in endotoxemia (Aziz et al., 2019; Yang et al., 2016a). Initially, LPS triggers mtDNA release via the TLR4/Caspase-11/GSDMD pathway; the cyclic GMP-AMP synthase (cGSA) detects mtDNA in the cytoplasm and triggers an increase in the phosphorylation level of stimulators of the interferon genes (STING) (Platnich et al., 2018). HMGB1/RAGE induces NLRP3 activation by disrupting lysosomes to release cathepsin B (Xiang et al., 2011). Both the pro-inflammatory factors HMGB1 and CIRP can trigger ROS production and are actively involved in this process via TXNIP, a thioredoxin-interacting protein (Aziz et al., 2019; Xiang et al., 2011). Inflammation triggers CIRP from the nucleus to the cytoplasm and its release into the circulation, which can upregulate TNF-α, IL-1β, and surface adhesion molecules in the lung tissue (Yang et al., 2016b). In macrophages, eCIRP has a dual role. It induces mtDNA release through the TLR4-MyD88 pathway and promotes STING activation through the TLR4-TRIF pathway (Aziz et al., 2019; Bortolotti et al., 2018). Importantly, the detection of cytosolic DNA by the cGAS-STING axis initiates K^+ efflux upstream of NLRP3, coordinating the lysosomal cell death program of NLRP3 (Gaidt et al., 2017; Ning et al., 2020). In addition, caspase-11 is activated early during endotoxic shock, which regulates the activity of caspase-3/7 (Kang et al., 2002). Caspase-8 and caspase-11 synergistically coordinate to drive systemic inflammation with no involvement from RIPK1 and RIPK3 (Mandal et al., 2018).

Interestingly, insufficient LPS acylation of *Francisella* is not fully recognized by caspase-11, favoring *Francisella* latency in the organism (Lagrange et al., 2018). A short immune delay is followed by a rapidly developing inflammatory response leading to severe sepsis. However, recent studies have proposed that AIM2-PANoptosis occurs to provide immunoprotection against *Francisella* infection (Wang et al., 2023). First, Pyrin recognizes *Francisella* or *herpes simplex virus-1* in response to AIM2. Deletion of the ZBP1 sensor attenuates caspase-1 processing. Pyrin and ZBP1 act synergistically on AIM2-caspase-1 activation. In response to ASC cohesion, a multiprotein complex of AIM2-PANoptosome is formed, which induces PANoptosis during infection (Lee et al., 2021).

7.2 Viral infection-related ALI

7.2.1 SARS-CoV-2

SARS-CoV-2 is a coronavirus, and its protein components such as N proteins can effectively limit apoptosis to promote viral replication (Pan et al., 2023). Targeting apoptosis reduces disease severity, and studies have demonstrated that caspase-dependent apoptosis of airway epithelial cells occurs commonly and is less symptomatic in children and young patients compared with older adults (Inde et al., 2021).

In addition, pyroptosis can be induced by structural and nonstructural proteins (Momeni, 2011). Inflammation and thrombosis are both clinical phenomena observed during the SARS-CoV-2 infection (Zaid et al., 2020). The spike protein of SARS-CoV-2 interacts with two receptors, angiotensin-converting enzyme 2 and transmembrane serine protease 2, to facilitate virus entry into host cells (Jackson et al., 2022). Moreover, the virus can also be internalized into hematopoietic stem cells and endothelial progenitor cells, activating NLRP3 through the spike protein (Ratajczak et al., 2021). Syncytia, which is formed by the fusion of multiple cells, has been observed in deceased patients with COVID-19. *In vitro* simulations have shown that syncytia undergoes GSDME-dependent pyroptosis, which may occur in infected alveolar type II epithelial cells (Ma et al., 2021).

The role of non-structural proteins (NSP) encoded by SARS-CoV-2 in having a pyroptosis-activating effect requires investigation. There are at least 16 types of non-structural proteins, such as NSP3 and NSP4, that primarily participate in virus replication (Pahmeier et al., 2023). NSP6 targets the inactive form of ATPase H+ transporting accessory protein 1, resulting in defective lysosomal acidification and impaired autophagy. This, in turn, activates NLRP3 and mediates the pyroptosis of epithelial cells (Sun et al., 2022). Contrarily, NSP5 activates the NLRP1 inflammasome. However, in terms of the pyroptosis mechanism, NSP5 inhibits GSDMD and utilizes the caspase-3/GSDME alternative pyroptosis pathway (Planès et al., 2022).

Furthermore, during infection, vascular endothelial cell damage leads to the release of von Willebrand factor, initiating the coagulation cascade and resulting in thrombosis (Eltobgy et al., 2022). Excessive inflammation caused by bacterial or viral infection induces type I IFN, which acts as a procoagulant signal. This signal induces macrophage pyroptosis and the release of tissue factor through the caspase-11 pyroptosis pathway, mediating intravascular coagulation (Ryan et al., 2023).

Different views exist as to whether necroptosis mediates the onset of destructive inflammation during infection. ZBP1-RIPK3-MLKL is one of the important molecular mechanisms by which excessive inflammation leads to irreversible lung injury in critically ill patients (Li et al., 2023b). In contrast, *in vivo* modeling studies in SARS-Cov-2-infected mice pointed out that MLKL defects did not improve lung pathology (Stefanie et al., 2024). However, caspase-8-dependent apoptosis, necroptosis, and typical lung inflammatory features were observed in lung sections from deceased COVID-19 patients (Li et al., 2020).

The release of inflammatory mediators leads to excessive immune response, cell death, and pulmonary pathologic changes. The combination of TNF-α and IFN-γ induces nitric oxide production and drives caspase-8/FADD mediated PANoptosis through the JAK/STAT1/IRF1 axis. Cell death mediated by this mechanism tightly links cytokine storms to lung injury (Karki et al., 2021). Conversely, ZBP1 expression in immune cells was higher in deceased COVID-19 patients. ZBP1 is not only a product of viral RNA, but also a sensor for RNA or DNA viruses (Kao et al., 2014). ZBP1 promotes PANoptosis and promotes the further release of inflammatory factors (Karki et al., 2022). In conclusion, these studies suggest that inflammatory cell death is closely associated with pathological changes in COVID-19 patients.

7.2.2 Influenza A virus (IAV)

In addition to coronaviruses, influenza A viruses (IAV), such as H7N9 and H9N2, induce GSDME-dependent pyroptosis in AEC (Zhang et al., 2023; Wan et al., 2022). Human bronchial epithelial cells can sense IAV dsRNA and activate GSDMD and GSDME. Inflammatory mediators produced by IAV infection are potent activators of ZBP1, and cyclic-promoting effects of necroptosis and disruptive inflammation are found in infected macrophages (Ferreira et al., 2023). However, in the absence of apoptosis, viral infection can be limited by relying independently on necroptosis (Soni et al., 2023; Shubina et al., 2020). Similar to RIPK1-PANoptosome, ZBP1-PANoptosome was discovered in response to an IAV infection. ZBP1 is not only a product of viral RNA but also a sensor of RNA or DNA viruses (Zheng and Kanneganti, 2020). ZBP1 senses Z-RNA produced by influenza viruses and interacts with NLRP3 (Zheng and Kanneganti, 2020). ZBP1-NLRP3 inflammasome is subsequently activated by recruiting RIPK3 and caspase-8; caspase-6 is required for inflammasome activation and promotes RIPK3 binding to ZBP1 (Zheng et al., 2020). Additionally, ZBP1 initiates RIPK3-MLKL, leading to DNA leakage into the cytosol, and ultimately necroptosis (Yang et al., 2020). RIPK3 can interact with RIPK1, which recruits caspase-8 through FADD to initiate apoptosis (Alvarez-Diaz et al., 2016). In response to IAV infection, these components constitute ZBP1-PANoptosom in innate immune cells, thereby protecting the host from viral infection.

7.3 Transfusion-related acute lung injury (TRALI)

Transfusion-related acute lung injury (TRALI) is a severe complication that can occur during or up to 6 h after a transfusion (Barrett and Kam, 2006). While the exact cause of TRALI is not fully understood, in most cases it may involve an immune-directed, antibody-mediated mechanism. This mechanism is frequently triggered by two harmful factors: the first is the patient's underlying injury, which might include infection, sepsis, or surgery, and the second is the infusion of blood components containing antibodies or biological response modifiers (BRM), which cause neutrophils to become excited and generate TRALI symptoms (Silliman, 2006).

Interestingly, the "two-hit" model of TRALI is similar to the two-step activation of NLRP3, both of which may also be linked to each other (Land, 2013). An earlier study revealed that the development of TRALI could be uniquely reliant on polymorphonuclear leukocytes (PMNs). Human leukocyte antigen A2 promotes interaction between PMNs and endothelial cells through Src phosphorylation and increases the pro-inflammatory state through upregulation of NF-κB and NLRP3, ultimately leading to lung tissue injury by releasing more ROS (Le et al., 2022). In addition, ROS release serves as a convergence point for additional antibody-mediated TRALI-related processes (Tung et al., 2022). This could create an ideal setting for inflammasome activation. Pyroptosis-related protein expression is upregulated by ROS and can facilitate inflammasome establishment and activation in response to TXNIP (Abais et al., 2015; Zhou et al., 2010).

Nonetheless, HMGB1 is a risk factor for erythrocyte transfusion, and *in vitro* studies have shown that human lung endothelial cells undergo necroptosis upon exposure to allogeneic erythrocytes and release RIPK3 and HMGB1 (Qing et al., 2014). In the plasma of patients with severe sepsis, RIPK3 levels were increased after transfusion and were higher in non-survivors. In a mouse model, erythrocyte infusion enhanced the susceptibility of mice to LPS-induced lung inflammation by releasing HMGB1 (Ware, 2014). This necroptosis and danger signaling release may explain the mechanism underlying the increased risk of acute respiratory distress syndrome in critically ill patients receiving erythrocyte transfusions (Qing et al., 2014; Ware, 2014).

The prevention of adverse effects of hemolytic transfusion is essential for patients with sickle cell disease (SCD) who are dependent on transfusion for survival (Firth et al., 2003; Suddock and Crookston, 2024). SCD is characterized by chronic hemolytic anemia. Recent studies confirm that NLRC5 interacts with NLRP12-PANoptosome to drive inflammatory cell death in hemolytic models (Sundaram et al., 2024b). Repeated hemolysis in the blood vessels of SCD leads to endothelial dysfunction and ischemia-reperfusion injury (I/RI). SCD-induced I/RI drives organ damage, with the lung being the most vulnerable organ (Ansari and Gavins, 2019). In the context of lung ischemia-reperfusion injury (LI/RI), it is noteworthy that the activation of NF-κB/NLRP3 occurs due to the release of IL-1R by monocytes, resulting in damage to the endothelium cells (Zhou et al., 2021). Pathological tests have demonstrated that renal or intestinal ischemia-reperfusion injury (RI/RI or II/RI) can induce ALI, which is marked by notable inflammation and lung damage (Liu et al., 2020b; Li et al., 2022). Apoptotic signals govern pyroptosis during the investigation of the intestinal ischemia-reperfusion injury. PKR-like ER kinase, a protein found in mitochondria-associated membranes, initiates apoptotic signals. Furthermore, MAMs recruit NLRP3 and facilitate its assembly and activation in response to stimuli. Suppression of PERK can also hinder pyroptosis signaling and mitigate II/RI (Li et al., 2023d). Nrf2 regulates heme-oxygenase 1, a route that safeguards the body against detrimental stimuli and can ameliorate RI/RI (Li et al., 2023e). Similarly, under the influence of recombinant HMGB1, this pathway is stimulated and improves LI/RI (Fei et al., 2020).

7.4 Ventilation-related ALI (VILI)

Mechanical ventilation (MV) is often operated to maintain respiratory function in critically ill patients such as preterm infants with respiratory distress and hemorrhagic shock (Davis et al., 2024). However prolonged high tidal volume MV increases the risk of bronchopulmonary dysplasia in preterm infants. Lung hyperexpansion and hyperoxia are key factors in VILI (van Kaam, 2024).

At the cellular level, VILI is accompanied by various forms of cell death (Kuipers et al., 2012; Shao et al., 2022). Activation of the NLRP3 inflammasome was found to be necessary in a double-hit VILI study model by LPS and MV. Caspase-1 and NLRP3 were expressed in the alveolar lavage fluid of patients with MV, and inhibiting IL-1β could alleviate hypoxemia (Kuipers et al., 2012; Kuipers et al., 2011). Plasma RIPK3 levels were higher in patients with MV compared to those without MV, and mouse RIPK3 deficiency ameliorated VILI (Shao et al., 2022). Patients with ALI are often exposed to hyperoxia before the application of MV. After exposure to hyperoxia, HV activates caspase-8/9, indicating that death receptors or mitochondria mediate the occurrence of endogenous and exogenous apoptosis, causing severe lung injury (Makena et al., 2010). Importantly hyperoxia drives ROS production directly or indirectly involved in cell death (Alva et al., 2023). In many diseases, ROS levels are positively correlated with PANoptosis occurrence. For example, targeting ROS production can alleviate organ damage associated with PANoptosis occurrence in inflammatory diseases such as sepsis (Ding et al., 2024). Existing studies suggest that systemic high inflammation levels as well as extrapulmonary organ damage are observed in the VILI mouse model. For example, the pro-inflammatory mediator HMGB1 promotes hepatic PANoptosis (Ding et al., 2023).

8 Therapeutic agents targeting apoptosis, pyroptosis, necroptosis, and PANoptosis in ALI

8.1 Caspase family inhibitors

Caspase family proteins, which are involved in apoptosis, pyroptosis, PANoptosis, and regulation of necroptosis, were targeted for inhibition to alleviate the severity of ALI.

Inhibitors of caspase-1 include Ac-YVAD-CMK, VX-765, and Ac-YVAD-CHO.The mechanism of action of caspase-1 inhibition differs based on the structural specificity of the inhibitors involved (Kasana et al., 2024). Ac-YVAD-CMK is an irreversible and highly selective inhibitor of caspase-1 (Mathiak et al., 2000). Ac-YVAD-CMK exhibits greater selectivity for caspase-1 compared to the broad-spectrum caspase inhibitor Z-VAD-FMK and does not disrupt apoptosis-related pathways, thereby minimizing off-target effects (Modi et al., 2023). In contrast to the irreversible inhibitor Ac-YVAD-CMK, Ac-YVAD-CHO interacts dynamically with the target through the aldehyde group, resulting in a reduction of the inhibitory effect as concentration decreases (Garcia-Calvo et al., 1998). VX-765, an oral reversible caspase-1 inhibitor entering clinical trials for inflammatory diseases (Modi et al., 2023), met all pharmacokinetic and pharmacodynamic targets in Phase I. In 2005, 68 psoriasis patients participated in a 4-week Phase IIa safety and pharmacokinetic study (Kasana et al., 2024). To date, there have been no new developments in clinical trials involving VX-765.

Experimental modeling studies at ALI have found, that Ac-YVAD-CMK and VX-765, potent inhibitors of caspase-1, were effective in protecting against alveolar macrophage and pulmonary vascular endothelial cells brought on by SARS-CoV-2 infection and LI/RI injury (Pan et al., 2021; Wu et al., 2015; Wu et al., 2021). In addition, for another caspase-1 inhibitor, Ac-YVAD-CHO, it was proposed that nebulized inhalation was effective in alleviating LPS-induced endotoxemia in rats, and this mode of administration is more suitable to be applied to the clinical administration of ARDS (Boost et al., 2007). Moreover, caspase-3 and caspase-8 inhibitors are also targets for alleviating sepsis and

TABLE 2 Caspase family inhibitors in ALI models.

Name	Target	Effects	Experimental models	Ref
Ac-YVAD-CMK	Caspase-1	Targeted inhibition of caspase-1	LPS-induced ALI model in mice, SARS-CoV-2-induced ALI model in mice	Pan et al. (2021), Wu et al. (2015)
VX-765	Caspase-1	Targeted inhibition of caspase-1	LI/RI mouse model	Wu et al. (2021)
Ac-YVAD-CHO	Caspase-1	Targeted inhibition of caspase-1	LPS-induced endotoxemia model in rats	Boost et al. (2007)
Z-DEVD-FMK	Caspase-3	Specific inhibition of caspase-3	Cecal ligation to model sepsis-induced lung injury in mice	Qin et al. (2024)
Z-IETD-FMK	Caspase-8	Selective inhibition of caspase-8	A mouse model of lethal bacterial peritonitis and pneumonia	Lentini et al. (2023)
Wedelolactone	Caspase-11	Inhibition of NF-κB signaling-mediated	Bacterial LPS-stimulated mouse BALB/c 3T3 cell model	Kobori et al. (2004)
Goitrin	Caspase-11	Inhibition of caspase-11	LPS-induced septic shock mouse model	Ruan et al. (2023)
Ac-FLTD-CMK	Caspase-1/4/5/11	Specific inhibition of inflammatory caspases binding to GSDMD at the cleavage site FLTD peptide	LPS-stimulated RAW264.7 cells	Yang et al. (2018)
Q-VD-OPh	Caspase-1/3/7/8/9/10/12	Widespread inhibition of caspase-1/3/7/8/9/10/12	Mouse model of IAV-induced lung inflammation	Soni et al. (2023)
Z-VAD-FMK	Caspase-1/3/4/5/7/8/11	Widespread inhibition of caspase-1/3/4/5/7/8/11	Rat model of LI/RI, LPS-induced ALI model in mice, PA-infected rat lung injury model	Wang et al. (2020c), Kawasaki et al. (2000), Le Berre et al. (2004)

endotoxic shock. Z-DEVD-FMK targets caspase-3 and blocks caspase-3/GSDMD pyroptosis signaling (Qin et al., 2024). Z-IETD-FMK inhibits caspase-8 and induces neutrophil-resident clearance of bacteria to eliminate lung inflammation (Lentini et al., 2023). Importantly, Ac-FLTD-CMK, a caspase-1/4/5/11 specific inhibitor, specifically inhibits FLTD peptide, the cleavage site of inflammatory caspases binding to GSDMD in macrophages (Yang et al., 2018). Inhibition of apoptotic caspases has emerged as a therapeutic target for IAV infection. Q-VD-OPh, which broadly inhibits a wide range of apoptotic caspases, blocks IAV replication in bronchial epithelial cells (Soni et al., 2023). The combined inhibition of apoptotic and inflammatory caspases provides a more comprehensive approach to disease treatment. Z-VAD-FMK, which broadly inhibits caspases, effectively ameliorates LI/RI, inhibits LPS-mediated apoptosis to enhance mouse survival and ameliorates endothelial damage associated with PA infection (Wang et al., 2020c; Kawasaki et al., 2000; Le Berre et al., 2004). In conclusion, targeted inhibition of the caspase family has become an important target for ALI therapy (Table 2).

8.2 Inflammasomes inhibitors (NLRP1/3, NLRC4, AIM2)

The inflammasome is a core member of pyroptosis and an important component of the PANoptosome. MCC950, a small molecule inhibitor of NLRP3 pharmacology, selectively blocks the interaction of NLRP3 with NEK7 and has very significant therapeutic effects in a wide range of inflammatory diseases (Pan et al., 2021). Examples include SARS-CoV-2 and LPS-induced lung infections, acute kidney injury, colitis, and myocardial injury (Pan et al., 2021; Wang et al., 2021).

Britannin and alantolactone, two bioactive natural compounds from traditional Chinese medicine, demonstrate significant inhibitory effects on NLRP3 inflammasome activation via distinct mechanisms (Shao et al., 2024). Both drugs directly target the NACHT domain of NLRP3, which disrupts its oligomerization and subsequent assembly with NEK7, according to structural and functional assessments (Li et al., 2023f). Their inhibitory effects function independently of NLRP3 ATPase activity, setting them apart from traditional ATP-competitive inhibitors like MCC950 (Wang et al., 2021).

The interaction of ADS032 with the NACHT domains of NLRP1 and NLRP3 identifies it as the inaugural dual-specific inhibitor for these inflammasomes. Additionally, it is the first NLRP1-selective compound to exhibit cross-species efficacy in both murine and human cellular models. This property addresses a significant translational barrier resulting from interspecies differences in NLRP1 activation mechanisms (Docherty et al., 2023). In a murine IAV infection model, ADS032 demonstrated broad therapeutic effects over time, protecting during both the early phase of viral replication and the late phase characterized by an inflammatory cytokine storm. MCC950 exhibited time-dependent variations in efficacy; it was effective when administered early, but its delayed application paradoxically heightened susceptibility to low-dose IAV challenge (Tate et al., 2016).

JC2-11, a derivative of benzylideneacetophenone synthesized from the chalcone scaffold, exhibits broad-spectrum inhibitory activity against various inflammasomes, including NLRP3, NLRC4, and AIM2 (Lee et al., 2022). The pan-inflammasome suppression strategy effectively bypasses compensatory activation mechanisms, which is a significant limitation of single-target inhibitors (Heinisch et al., 2022).

Both ADS032 and JC2-11 present innovative strategies for inflammasome modulation; however, their potential for translation into clinical applications has not been thoroughly

TABLE 3 Inflammasome inhibitors in ALI models.

Name	Target	Effects	Experimental models	Ref
ADS032	NLRP1/NLRP3	Dual inhibition of NLRP1 and NLRP3	IAV-induced lung inflammation model in mice	Docherty et al. (2023)
Britannin	NLRP3	Blocking the interaction between NLRP3 and NEK7	LPS-induced ALI mouse model	Shao et al. (2024)
Alantolactone	NLRP3	Binds to the NACHT structural domain of NLRP3 to inhibit the activation and assembly of NLRP3 inflammatory vesicles	LPS-induced ALI mouse model	Li et al. (2023f)
MCC950	NLRP3	Selective inhibition of NLRP3	SARS-CoV-2-induced ALI mouse model, LPS-induced ALI mouse model	Pan et al. (2021), Wang et al. (2021)
JC2-11	NLRP3/NLRC4/AIM2	Pan-inflammasome inhibitors	LPS-induced ALI mouse model	Lee et al. (2022)

investigated. Current limitations encompass inadequate pharmacokinetic profiling in non-rodent species and unvalidated efficacy in complex disease models that exhibit interactions between canonical and non-canonical inflammasome pathways (Docherty et al., 2023; Lee et al., 2022). Systematic structure-activity relationship studies and multi-omics validation are crucial for addressing these gaps and advancing these compounds toward clinical development (Table 3).

8.3 RIPK1/RIPK3 inhibitors

The RIPK1 inhibitors that have been developed can be categorized into three types based on how they bind to RIPK1, type I and type II are ATP-competitive and bind to the ATP-binding site, and type III binds to the allosteric pocket around the ATP-binding site (Shi et al., 2022). Necrostatin-1 and GSK2982772 are both type III RIPK1 inhibitors and GSK2982772 is in phase II clinical trials (Shi et al., 2022). Necrostatin-1 is widely used to inhibit necroptosis in several animal models of inflammation, including LPS and mechanical ventilation-induced ALI, and TNF-induced systemic inflammatory response syndrome (SIRS) (Takahashi et al., 2012; Lin et al., 2020). Necrostatin derivatives, such as Necrostatin −2 and Necrostatin −5, alleviate the harmful inflammation caused by bacteria, SARS-CoV-2, and I/RI (Wang et al., 2007; Hao et al., 2023; Guo et al., 2024).

ZB-R-55 signifies a significant advancement in the development of RIPK1 inhibitors due to its innovative dual-targeting mechanism, which simultaneously interacts with both the allosteric regulatory pocket and the ATP-binding catalytic domain of RIPK1(Yang et al., 2022). This bispecific interaction strategy addresses the limitations of traditional single-mode inhibitors by synergistically stabilizing inactive kinase conformations and competitively inhibiting ATP hydrolysis. In comparison to GSK2982772, a first-generation allosteric RIPK1 inhibitor in Phase II clinical trials, ZB-R-55 demonstrates significantly greater inhibitory potency, improved kinase family selectivity, and optimized oral pharmacokinetic properties (Shi et al., 2022; Yang et al., 2022).

GSK872 is a classic RIPK3-selective inhibitor with favorable therapeutic effects in ALI, Alzheimer's disease, acute kidney injury, spinal cord injury, and systemic inflammatory diseases (Cui et al., 2022b; Zhong et al., 2023).

In addition, UH15-38 addressed the hyperinflammatory state caused by IAV infection without affecting adaptive immunity (Gautam et al., 2024).

Unlike the classical inhibitor GSK872, UH15-38 utilizes a distinct binding mode characterized by significant interactions with both the hinge region and the back pocket of the RIPK3 active site, thereby improving its inhibitory potency and intracellular efficacy (Gautam et al., 2024). The therapeutic potential has been validated in IAV infection models, indicating promising prospects for clinical translation in necroptosis-related diseases (Willson, 2024).

HG-9-91-01, a salt-inducible kinase inhibitor, inhibits TNF/TLRs-mediated necroptosis by promoting the interaction between RIPK1 and RIPK3 while decreasing the binding of RIPK3 to MLKL and the oligomerization of MLKL. The multimodal mechanism inhibits necroptosis while simultaneously activating apoptosis and pyroptosis via cross-regulation of signaling pathways, illustrating its polypharmacological bioactivity and therapeutic potential for inflammatory diseases (Huang et al., 2022). In conclusion, RIPK1/RIPK3 are involved in PANoptosome composition and are important targets for disease intervention (Lee et al., 2022) (Table 4).

8.4 GSDMD/GSDME/MLKL inhibitors

GSDMD/GSDME/MLKL are the ultimate determinants of PANoptosis occurrence. Ac-FLTD-CMK specifically inhibits inflammatory caspases, which is equivalent to being a derivative inhibitor of GSDMD and can control macrophage pyroptosis *in vitro* (Yang et al., 2018). Necrosulfonamide (NSA), Disulfiram, and Dimethyl fumarate (DMF) are known GSDMD inhibitors (Rathkey et al., 2018; Adrover et al., 2022; Humphries et al., 2020). Among them, NAS can inhibit MLKL by binding to Cys86 of MLKL (Hao et al., 2023).

NSA uses a "single agent, dual mechanisms" approach to inhibit GSDMD and MLKL, breaking their synergistic interaction and reducing inflammatory amplification cascades (Hao et al., 2023; Rathkey et al., 2018). Disulfiram, an FDA-approved anti-alcohol, and strong GSDMD inhibitor, reduces mouse pyroptosis and LPS-induced septic mortality (Hu et al., 2020). New research suggests it protects against TRALI models and SARS-CoV-2 infection by inhibiting neutrophil extracellular traps (NETs) formation (Zhao et al., 2023). Reducing pulmonary NETs, neutrophil infiltration, and vascular leakage reduces lung histological damage, suggesting repurposing for inflammatory pulmonary diseases (Adrover et al.,

TABLE 4 RIPK1/RIPK3 inhibitors in ALI models.

Name	Target	Effects	Experimental models	Ref
Necrostatin-1	RIPK1	Type III RIPK1 inhibitor	Ventilator-induced ALI mouse model, TNF-induced SIRS mouse model, LPS-induced ALI model in mice	Takahashi et al. (2012), Lin et al. (2020), Wang et al. (2007)
Necrostatin-2	RIPK1	Pharmacological inhibitor of RIPK1	SARS-CoV-2 stimulates human airway epithelial cells	Hao et al. (2023), Guo et al. (2024)
Necrostatin-5	RIPK1	Non-pharmacological inhibitor of RIPK1 Necrostatin Derivatives	Mouse model of bacterial pneumonia	González-Juarbe et al. (2015), Wang et al. (2007)
GSK2982772	RIPK1	Type III RIPK1 inhibitor	Clinical trial phase (psoriasis, rheumatoid arthritis, and ulcerative colitis)	Shi et al. (2022)
ZB-R-55	RIPK1	Dual-mode RIPK1 inhibitor	LPS-induced SIRS and sepsis mouse model	Yang et al. (2022)
GSK872	RIPK3	Binding of the RIPK3 kinase structural domain	LPS-induced ALI mouse model	Cui et al. (2022b), Zhong et al. (2023)
UH15-38	RIPK3	Targeted inhibition of RIPK3	IAV-induced severe lung injury model in mice	Gautam et al. (2024)
HG-9-91-01	RIPK3	Inhibition of RIPK3 kinase activity	TNF-induced SIRS mouse model	Huang et al. (2022)

TABLE 5 GSDMD/GSDME/MLKL inhibitors in ALI models.

Name	Target	Effects	Experimental model	Ref
Ac-FLTD-CMK	GSDMD	Specific inhibition of inflammatory caspases binding to GSDMD at the cleavage site FLTD peptide	LPS-stimulated RAW264.7 cells	Yang et al. (2018)
NSA	GSDMD	Binding to GSDMD Cys191 inhibits GSDMD	LPS-induced mouse sepsis model	Rathkey et al. (2018)
Disulfiram	GSDMD	Inhibition of GSDMD by binding Cys191 and NETs	LPS-induced mouse model, LPS and anti-H2d antibody-induced TRAIL mouse model, SARS-CoV-2-induced ALI mouse model	Adrover et al. (2022), Hu et al. (2020), Zhao et al. (2023)
DMF	GSDMD	Succinates GSDMD and prevents binding to caspase-1	LPS-induced shock mouse model	Humphries et al. (2020)
Ac-DMLD-CMK	GSDME	A peptide targeting caspase-3/GSDMD signaling	Cecal ligation to model sepsis-induced lung injury in mice	Qin et al. (2024)
GW806742X	MLKL	Targeted inhibition of MLKL	Mouse model of bacterial pneumonia	González-Juarbe et al. (2015)
NSA	MLKL	Inhibition of MLKL by binding to Cys86 of MLKL	SARS-CoV-2 stimulates human airway epithelial cells	Hao et al. (2023)

2022). Through succinylation-mediated functional regulation of GSDMD, DMF, an FDA-approved treatment for multiple sclerosis and associated conditions, reduces inflammation (Humphries et al., 2020). This novel post-translational modification mechanism provides molecular-level validation for the therapeutic efficacy of DMF in inflammatory disease (Bresciani et al., 2023). GW806742X can also target the inhibition of MLKL (González-Juarbe et al., 2015). In addition, it should be added that Ac-DMLD-CMK targets inhibition of caspase-3/GSDME signaling to alleviate sepsis-induced lung injury (Qin et al., 2024). We summarize the inhibition targets and the therapeutic effects exerted in different ALI models in the table (Table 5).

8.5 Calpain inhibitors

The regulation of apoptosis, pyroptosis, necroptosis, and PANoptosis by caspases has been widely studied (Pandeya and Kanneganti, 2024). During our literature survey, we identified another protein family member that also seems to be involved in caspase regulation as well as cell death. Calpains figure among apoptosis (Momeni, 2011), pyroptosis, and necroptosis (Davis et al., 2019; Cheng et al., 2018). Consider whether inhibiting it could also impede PANoptosis and treat ALI and other inflammatory illnesses. More research is needed to prove this conjecture.

Calpain-1 and -2 are the best-researched calpains and are expressed in mammalian tissues (Wang et al., 2020d). Calpain inhibitors diminish neuronal death and limit disease progression (Ono et al., 2016). Calpain inhibitors such as PD150606, SNJ-1945, and MDL28170 are highly selective for calpain and have inhibitory effects on both calpain-1 and calpain-2 (Donkor, 2020; Dókus et al., 2020). PD150606 inhibits calpain activity by binding to the CysPc structural domain of calpain, thereby attenuating neuroinflammation and apoptosis (Wang et al., 1996). SNJ-1945 reduced neuroinflammation, demyelinating lesions, T-cell infiltration, and neuronal damage in the multiple sclerosis model by inhibiting microglia activation and inflammatory factor

production (Trager et al., 2014). Calpain inhibitors may treat other disorders. In myocardial ischemia-reperfusion injury, MDL28170 prevents cardiomyocyte apoptosis, lowers myocardial injury, and maintains mitochondrial function via inhibiting mitochondrial permeability transition pore opening (Thompson et al., 2016).

Calpain hydrolyzes vascular endothelial cadherin in lung microvascular cells, leading to the disruption of the endothelial barrier and the development of pulmonary edema. Additionally, serum calpain levels may serve as a potential biomarker for ALI, which is significant for assessing the severity of lung injury and predicting clinical outcomes (Yi et al., 2022; Song et al., 2023). The administration of MDL28170 to inhibit calpain activity significantly decreased pulmonary edema and alveolar wall thickening, suggesting that calpain is involved in LPS-induced endothelial barrier dysfunction in the pulmonary vasculature during ALI (Song et al., 2023). The involvement of calpains in the regulation of apoptosis, pyroptosis, and necroptosis has been addressed; however, the potential impact of calpain inhibitors on caspase-mediated cell death in ALI remains underexplored. Further discussion and investigation into this area would be beneficial.

9 Conclusion

Caspase-mediated PCDis common in bacterial and viral infections, blood transfusion, and ventilator-inducedALI. Initially, the various programmed death mechanisms were considered to be mutually independent, however, this perspective was challenged by the investigation of PANoptosis, which involves TNF-α and IFN-γ, as well as ZBP1, RIPK1, NLRC4, NLRC5, NLRP12, and AIM2 pathways. We found that the signaling crosstalk of apoptosis, pyroptosis, and necroptosis mediated PANoptosis. Although the three programmed deaths are not comprehensively involved in all lung diseases, there is evidence of the presence of partial caspase signaling crosstalk. The existence of ALIinduced by various causes poses a major threat to human health. Due to the complexity of the mechanisms involved in PCD, therapeutic agents targeting this process remain under development. Numerous studies have investigated various mechanisms of PCD and the impacts of targeted inhibition. This summary outlines the therapeutic mechanisms and effects of five classes of inhibitors: the caspase family, inflammasomes, RIPK1/3, GSDMD/GSMDE/MLKL and calpains in experimental models. Single-targeted inhibitors appear insufficient to fully ameliorate the ALI condition, potentially due to the activation of compensatory mechanisms related to cell death. Different components of SARS-CoV-2 activate NLRP3 and NLRP1 independently, indicating that a single NLRP3 inhibitor cannot inhibit NLRP1. In contrast, the dual NLRP1 and NLRP3 inhibitor ADS032 demonstrates a significant effect solely in the treatment of IAV infection. The development and application of single-agent multi-target inhibitors is forthcoming. The potential role of calpain inhibitors in mitigating caspase-mediated cell death is acknowledged; however, the mechanism by which they regulate PANoptosis remains unclear. The potential effects of calpain inhibitors on caspase-mediated cell death in ALI are not yet fully investigated. Additional exploration and investigation in this domain would be advantageous. Nonetheless, these inhibitors encounter numerous challenges during clinical translation, including target specificity, pharmacokinetic properties, safety, and potential side effects associated with long-term use. Addressing these issues necessitates comprehensive basic research and extensive clinical trials to facilitate the effective transition of these inhibitors from laboratory settings to clinical applications.

Author contributions

JX: Conceptualization, Resources, Supervision, Writing–original draft, Writing–review and editing. LW: Conceptualization, Resources, Writing–review and editing. BZ: Conceptualization, Resources, Writing–review and editing. AH: Conceptualization, Resources, Visualization, Writing–review and editing.

Funding

The author(s) declare that financial support was received for the research and/or publication of this article. This work was supported by the Key Research and Development Program Joint Program of Liaoning Province [2020JH2/10300132]; the Public Welfare Fund of China Foundation for International Medical Exchange [Z-2019-41-2101-04]; the 345 lent Project of China Medical University affiliated Shengjing Hospital and the Social Development Major Projects of Liaoning Province [2020JH1/1030001].

Acknowledgments

We would like to thank the figures created with BioRender and Editage (www.editage.jp) for English language editing services.

Conflict of interest

The authors declare that the research was conducted in the absence of any commercial or financial relationships that could be construed as a potential conflict of interest.

Generative AI statement

The author(s) declare that no Generative AI was used in the creation of this manuscript.

Publisher's note

References

Abais, J. M., Xia, M., Zhang, Y., Boini, K. M., and Li, P. L. (2015). Redox regulation of NLRP3 inflammasomes: ROS as trigger or effector? *Antioxid. Redox Signal* 22 (13), 1111–1129. doi:10.1089/ars.2014.5994

Adrover, J. M., Carrau, L., Daßler-Plenker, J., Bram, Y., Chandar, V., Houghton, S., et al. (2022). Disulfiram inhibits neutrophil extracellular trap formation and protects rodents from acute lung injury and SARS-CoV-2 infection. *JCI Insight* 7 (5), e157342. doi:10.1172/jci.insight.157342

Ai, Y., Meng, Y., Yan, B., Zhou, Q., and Wang, X. (2024). The biochemical pathways of apoptotic, necroptotic, pyroptotic, and ferroptotic cell death. *Mol. Cell* 84 (1), 170–179. doi:10.1016/j.molcel.2023.11.040

Akita, K., Ohtsuki, T., Nukada, Y., Tanimoto, T., Namba, M., Okura, T., et al. (1997). Involvement of caspase-1 and caspase-3 in the production and processing of mature human interleukin 18 in monocytic THP.1 cells. *J. Biol. Chem.* 272 (42), 26595–26603. doi:10.1074/jbc.272.42.26595

Allen, L., Dockrell, D. H., Pattery, T., Lee, D. G., Cornelis, P., Hellewell, P. G., et al. (2005). Pyocyanin production by *Pseudomonas aeruginosa* induces neutrophil apoptosis and impairs neutrophil-mediated host defenses *in vivo*. *J. Immunol.* 174 (6), 3643–3649. doi:10.4049/jimmunol.174.6.3643

Alva, R., Mirza, M., Baiton, A., Lazuran, L., Samokysh, L., Bobinski, A., et al. (2023). Oxygen toxicity: cellular mechanisms in normobaric hyperoxia. *Cell Biol. Toxicol.* 39 (1), 111–143. doi:10.1007/s10565-022-09773-7

Alvarez-Diaz, S., Dillon, C. P., Lalaoui, N., Tanzer, M. C., Rodriguez, D. A., Lin, A., et al. (2016). The pseudokinase MLKL and the kinase RIPK3 have distinct roles in autoimmune disease caused by loss of death-receptor-induced apoptosis. *Immunity* 45 (3), 513–526. doi:10.1016/j.immuni.2016.07.016

Ansari, J., and Gavins, F. N. E. (2019). Ischemia-reperfusion injury in sickle cell disease: from basics to therapeutics. *Am. J. Pathol.* 189 (4), 706–718. doi:10.1016/j.ajpath.2018.12.012

Armistead, B., Quach, P., Snyder, J. M., Santana-Ufret, V., Furuta, A., Brokaw, A., et al. (2021). Hemolytic membrane vesicles of group B Streptococcus promote infection. *J. Infect. Dis.* 223 (8), 1488–1496. doi:10.1093/infdis/jiaa548

Aziz, M., Brenner, M., and Wang, P. (2019). Extracellular CIRP (eCIRP) and inflammation. *J. Leukoc. Biol.* 106 (1), 133–146. doi:10.1002/JLB.3MIR1118-443R

Banerjee, S. K., Crane, S. D., and Pechous, R. D. (2020). A dual role for the plasminogen activator protease during the preinflammatory phase of primary pneumonic plague. *J. Infect. Dis.* 222 (3), 407–416. doi:10.1093/infdis/jiaa094

Barrett, N. A., and Kam, P. C. (2006). Transfusion-related acute lung injury: a literature review. *Anaesthesia* 61 (8), 777–785. doi:10.1111/j.1365-2044.2006.04742.x

Bernard, E. M., and Broz, P. (2023). NLRP12 senses heme and PAMPs to drive necrotic cell death and inflammation. *Mol. Cell* 83 (15), 2621–2623. doi:10.1016/j.molcel.2023.07.005

Bertrand, M. J., Milutinovic, S., Dickson, K. M., Ho, W. C., Boudreault, A., Durkin, J., et al. (2008). cIAP1 and cIAP2 facilitate cancer cell survival by functioning as E3 ligases that promote RIP1 ubiquitination. *Mol. Cell* 30 (6), 689–700. doi:10.1016/j.molcel.2008.05.014

Blutt, S. E., Coarfa, C., Neu, J., and Pammi, M. (2023). Multiomic investigations into lung health and disease. *Microorganisms* 11 (8), 2116. doi:10.3390/microorganisms11082116

Bomberger, J. M., Maceachran, D. P., Coutermarsh, B. A., Ye, S., O'Toole, G. A., and Stanton, B. A. (2009). Long-distance delivery of bacterial virulence factors by *Pseudomonas aeruginosa* outer membrane vesicles. *PLoS Pathog.* 5 (4), e1000382. doi:10.1371/journal.ppat.1000382

Boost, K. A., Hoegl, S., Hofstetter, C., Flondor, M., Stegewerth, K., Platacis, I., et al. (2007). Targeting caspase-1 by inhalation-therapy: effects of Ac-YVAD-CHO on IL-1 beta, IL-18 and downstream proinflammatory parameters as detected in rat endotoxaemia. *Intensive Care Med.* 33 (5), 863–871. doi:10.1007/s00134-007-0588-0

Bortolotti, P., Faure, E., and Kipnis, E. (2018). Inflammasomes in tissue damages and immune disorders after trauma. *Front. Immunol.* 9, 1900. doi:10.3389/fimmu.2018.01900

Bos, L. D. J., and Ware, L. B. (2022). Acute respiratory distress syndrome: causes, pathophysiology, and phenotypes. *Lancet* 400 (10358), 1145–1156. doi:10.1016/S0140-6736(22)01485-4

Bresciani, G., Manai, F., Davinelli, S., Tucci, P., Saso, L., and Amadio, M. (2023). Novel potential pharmacological applications of dimethyl fumarate-an overview and update. *Front. Pharmacol.* 14, 1264842. doi:10.3389/fphar.2023.1264842

Brower, R. G., Matthay, M. A., Morris, A., Schoenfeld, D., Thompson, B. T., Wheeler, A., et al. (2000). Ventilation with lower tidal volumes as compared with traditional tidal volumes for acute lung injury and the acute respiratory distress syndrome. *N. Engl. J. Med.* 342 (18), 1301–1308. doi:10.1056/NEJM200005043421801

Broz, P., Pelegrín, P., and Shao, F. (2020). The gasdermins, a protein family executing cell death and inflammation. *Nat. Rev. Immunol.* 20 (3), 143–157. doi:10.1038/s41577-019-0228-2

Broz, P., von Moltke, J., Jones, J. W., Vance, R. E., and Monack, D. M. (2010). Differential requirement for Caspase-1 autoproteolysis in pathogen-induced cell death and cytokine processing. *Cell Host Microbe* 8 (6), 471–483. doi:10.1016/j.chom.2010.11.007

Cabon, L., Galán-Malo, P., Bouharrour, A., Delavallée, L., Brunelle-Navas, M. N., Lorenzo, H. K., et al. (2012). BID regulates AIF-mediated caspase-independent necroptosis by promoting BAX activation. *Cell Death Differ.* 19 (2), 245–256. doi:10.1038/cdd.2011.91

Carlin, A. F., Chang, Y. C., Areschoug, T., Lindahl, G., Hurtado-Ziola, N., King, C. C., et al. (2009). Group B Streptococcus suppression of phagocyte functions by protein-mediated engagement of human Siglec-5. *J. Exp. Med.* 206 (8), 1691–1699. doi:10.1084/jem.20090691

Caulfield, A. J., Walker, M. E., Gielda, L. M., and Lathem, W. W. (2014). The Pla protease of *Yersinia pestis* degrades fas ligand to manipulate host cell death and inflammation. *Cell Host Microbe* 15 (4), 424–434. doi:10.1016/j.chom.2014.03.005

Chan, A. H., Burgener, S. S., Vezyrgiannis, K., Wang, X., Acklam, J., Von Pein, J. B., et al. (2023). Caspase-4 dimerisation and D289 auto-processing elicit an interleukin-1β-converting enzyme. *Life Sci. Alliance* 6 (10), e202301908. doi:10.26508/lsa.202301908

Chao, K. L., Kulakova, L., and Herzberg, O. (2017). Gene polymorphism linked to increased asthma and IBD risk alters gasdermin-B structure, a sulfatide and phosphoinositide binding protein. *Proc. Natl. Acad. Sci. U. S. A.* 114 (7), E1128–E1137. doi:10.1073/pnas.1616783114

Chen, H., Li, Y., Wu, J., Li, G., Tao, X., Lai, K., et al. (2020). RIPK3 collaborates with GSDMD to drive tissue injury in lethal polymicrobial sepsis. *Cell Death Differ.* 27 (9), 2568–2585. doi:10.1038/s41418-020-0524-1

Chen, K., Zhang, S., Shao, Y., Guo, M., Zhang, W., and Li, C. (2021). A unique NLRC4 receptor from echinoderms mediates Vibrio phagocytosis via rearrangement of the cytoskeleton and polymerization of F-actin. *PLoS Pathog.* 17 (12), e1010145. doi:10.1371/journal.ppat.1010145

Chen, K. W., and Broz, P. (2024). Gasdermins as evolutionarily conserved executors of inflammation and cell death. *Nat. Cell Biol.* 26 (9), 1394–1406. doi:10.1038/s41556-024-01474-z

Chen, K. W., Demarco, B., Heilig, R., Shkarina, K., Boettcher, A., Farady, C. J., et al. (2019). Extrinsic and intrinsic apoptosis activate pannexin-1 to drive NLRP3 inflammasome assembly. *Embo J.* 38 (10), e101638. doi:10.15252/embj.2019101638

Chen, S., Jiang, J., Li, T., and Huang, L. (2023). PANoptosis: mechanism and role in pulmonary diseases. *Int. J. Mol. Sci.* 24 (20), 15343. doi:10.3390/ijms242015343

Chen, X., He, W. T., Hu, L., Li, J., Fang, Y., Wang, X., et al. (2016). Pyroptosis is driven by non-selective gasdermin-D pore and its morphology is different from MLKL channel-mediated necroptosis. *Cell Res.* 26 (9), 1007–1020. doi:10.1038/cr.2016.100

Cheng, K. T., Xiong, S., Ye, Z., Hong, Z., Di, A., Tsang, K. M., et al. (2017). Caspase-11-mediated endothelial pyroptosis underlies endotoxemia-induced lung injury. *J. Clin. Invest* 127 (11), 4124–4135. doi:10.1172/JCI94495

Cheng, S. Y., Wang, S. C., Lei, M., Wang, Z., and Xiong, K. (2018). Regulatory role of calpain in neuronal death. *Neural Regen. Res.* 13 (3), 556–562. doi:10.4103/1673-5374.228762

Chou, W. C., Jha, S., Linhoff, M. W., and Ting, J. P. (2023). The NLR gene family: from discovery to present day. *Nat. Rev. Immunol.* 23 (10), 635–654. doi:10.1038/s41577-023-00849-x

Chu, S. J., Tang, S. E., Pao, H. P., Wu, S. Y., and Liao, W. I. (2021). Protease-activated receptor-1 antagonist protects against lung ischemia/reperfusion injury. *Front. Pharmacol.* 12, 752507. doi:10.3389/fphar.2021.752507

Chung, L. K., and Bliska, J. B. (2016). Yersinia versus host immunity: how a pathogen evades or triggers a protective response. *Curr. Opin. Microbiol.* 29, 56–62. doi:10.1016/j.mib.2015.11.001

Coleman, M., Armistead, B., Orvis, A., Quach, P., Brokaw, A., Gendrin, C., et al. (2021). Hyaluronidase impairs neutrophil function and promotes group B Streptococcus invasion and preterm labor in nonhuman primates. *mBio* 12 (1), e03115–e03120. doi:10.1128/mBio.03115-20

Coombs, J. R., Zamoshnikova, A., Holley, C. L., Maddugoda, M. P., Teo, D. E. T., Chauvin, C., et al. (2024). NLRP12 interacts with NLRP3 to block the activation of the human NLRP3 inflammasome. *Sci. Signal* 17 (820), eabg8145. doi:10.1126/scisignal.abg8145

Cui, Y., Wang, X., Lin, F., Li, W., Zhao, Y., Zhu, F., et al. (2022a). MiR-29a-3p improves acute lung injury by reducing alveolar epithelial cell PANoptosis. *Aging Dis.* 13 (3), 899–909. doi:10.14336/AD.2021.1023

Cui, Y. R., Qu, F., Zhong, W. J., Yang, H. H., Zeng, J., Huang, J. H., et al. (2022b). Beneficial effects of aloperine on inflammation and oxidative stress by suppressing necroptosis in lipopolysaccharide-induced acute lung injury mouse model. *Phytomedicine* 100, 154074. doi:10.1016/j.phymed.2022.154074

Davis, J. A., Manoach, S., Heerdt, P., and Berlin, D. A. (2024). Management of respiratory failure in hemorrhagic shock. *Ann. Am. Thorac. Soc.* 21 (7), 993–997. doi:10.1513/AnnalsATS.202310-905CME

Davis, M. A., Fairgrieve, M. R., Den Hartigh, A., Yakovenko, O., Duvvuri, B., Lood, C., et al. (2019). Calpain drives pyrophoric vimentin cleavage, intermediate filament loss,

and cell rupture that mediates immunostimulation. *Proc. Natl. Acad. Sci. U. S. A.* 116 (11), 5061–5070. doi:10.1073/pnas.1818598116

Delavallée, L., Cabon, L., Galán-Malo, P., Lorenzo, H. K., and Susin, S. A. (2011). AIF-mediated caspase-independent necroptosis: a new chance for targeted therapeutics. *IUBMB Life* 63 (4), 221–232. doi:10.1002/iub.432

Deng, R. M., Huang, G., Wang, T., and Zhou, J. (2025). Regulated programmed cell death in sepsis associated acute lung injury: from pathogenesis to therapy. *Int. Immunopharmacol.* 148, 114111. doi:10.1016/j.intimp.2025.114111

de Vasconcelos, N. M., and Lamkanfi, M. (2020). Recent insights on inflammasomes, gasdermin pores, and pyroptosis. *Cold Spring Harb. Perspect. Biol.* 12 (5), a036392. doi:10.1101/cshperspect.a036392

Ding, N., Xiao, H., Zhen, L., Li, H., Zhang, Z., and Ge, J. (2024). Imp7 siRNA nanoparticles protect against mechanical ventilation-associated liver injury by inhibiting HMGB1 production and NETs formation. *Biochim. Biophys. Acta Mol. Basis Dis.* 1870 (4), 167085. doi:10.1016/j.bbadis.2024.167085

Ding, N., Xiao, H., Zhen, L., Li, H., Zhang, Z., Ge, J., et al. (2023). Systemic cytokines inhibition with Imp7 siRNA nanoparticle ameliorates gut injury in a mouse model of ventilator-induced lung injury. *Biomed. Pharmacother.* 165, 115237. doi:10.1016/j.biopha.2023.115237

Docherty, C. A., Fernando, A. J., Rosli, S., Lam, M., Dolle, R. E., Navia, M. A., et al. (2023). A novel dual NLRP1 and NLRP3 inflammasome inhibitor for the treatment of inflammatory diseases. *Clin. Transl. Immunol.* 12 (6), e1455. doi:10.1002/cti2.1455

Dókus, L. E., Yousef, M., and Bánóczi, Z. (2020). Modulators of calpain activity: inhibitors and activators as potential drugs. *Expert Opin. Drug Discov.* 15 (4), 471–486. doi:10.1080/17460441.2020.1722638

Donkor, I. O. (2020). An update on the therapeutic potential of calpain inhibitors: a patent review. *Expert Opin. Ther. Pat.* 30 (9), 659–675. doi:10.1080/13543776.2020.1797678

Eltobgy, M. M., Zani, A., Kenney, A. D., Estfanous, S., Kim, E., Badr, A., et al. (2022). Caspase-4/11 exacerbates disease severity in SARS-CoV-2 infection by promoting inflammation and immunothrombosis. *Proc. Natl. Acad. Sci. U. S. A.* 119 (21), e2202012119. doi:10.1073/pnas.2202012119

Exconde, P. M., Hernandez-Chavez, C., Bourne, C. M., Richards, R. M., Bray, M. B., Lopez, J. L., et al. (2023). The tetrapeptide sequence of IL-18 and IL-1β regulates their recruitment and activation by inflammatory caspases. *Cell Rep.* 42 (12), 113581. doi:10.1016/j.celrep.2023.113581

Fang, Z. E., Wang, Y., Bian, S., Qin, S., Zhao, H., Wen, J., et al. (2024). Helenine blocks NLRP3 activation by disrupting the NEK7-NLRP3 interaction and ameliorates inflammatory diseases. *Phytomedicine* 122, 155159. doi:10.1016/j.phymed.2023.155159

Fei, L., Jingyuan, X., Fangte, L., Huijun, D., Liu, Y., Ren, J., et al. (2020). Preconditioning with rHMGB1 ameliorates lung ischemia-reperfusion injury by inhibiting alveolar macrophage pyroptosis via the Keap1/Nrf2/HO-1 signaling pathway. *J. Transl. Med.* 18 (1), 301. doi:10.1186/s12967-020-02467-w

Ferreira, A. C., Sacramento, C. Q., Pereira-Dutra, F. S., Fintelman-Rodrigues, N., Silva, P. P., Mattos, M., et al. (2023). Severe influenza infection is associated with inflammatory programmed cell death in infected macrophages. *Front. Cell Infect. Microbiol.* 13, 1067285. doi:10.3389/fcimb.2023.1067285

Fettucciari, K., Fetriconi, I., Bartoli, A., Rossi, R., and Marconi, P. (2003). Involvement of mitogen-activated protein kinases in Group B Streptococcus-induced macrophage apoptosis. *Pharmacol. Res.* 47 (4), 355–362. doi:10.1016/s1043-6618(03)00004-5

Fettucciari, K., Rosati, E., Scaringi, L., Cornacchione, P., Migliorati, G., Sabatini, R., et al. (2000). Group B Streptococcus induces apoptosis in macrophages. *J. Immunol.* 165 (7), 3923–3933. doi:10.4049/jimmunol.165.7.3923

Firth, P. G., Tsuruta, Y., Kamath, Y., Dzik, W. H., Ogilvy, C. S., and Peterfreund, R. A. (2003). Transfusion-related acute lung injury or acute chest syndrome of sickle cell disease? - a case report. *Can. J. Anaesth.* 50 (9), 895–899. doi:10.1007/BF03018735

Fong, J. J., Tsai, C. M., Saha, S., Nizet, V., Varki, A., and Bui, J. D. (2018). Siglec-7 engagement by GBS β-protein suppresses pyroptotic cell death of natural killer cells. *Proc. Natl. Acad. Sci. U. S. A.* 115 (41), 10410–10415. doi:10.1073/pnas.1804108115

Fritsch, M., Günther, S. D., Schwarzer, R., Albert, M. C., Schorn, F., Werthenbach, J. P., et al. (2019). Caspase-8 is the molecular switch for apoptosis, necroptosis and pyroptosis. *Nature* 575 (7784), 683–687. doi:10.1038/s41586-019-1770-6

Fu, J., Schroder, K., and Wu, H. (2024). Mechanistic insights from inflammasome structures. *Nat. Rev. Immunol.* 24, 518–535. doi:10.1038/s41577-024-00995-w

Fu, J., and Wu, H. (2023). Structural mechanisms of NLRP3 inflammasome assembly and activation. *Annu. Rev. Immunol.* 41, 301–316. doi:10.1146/annurev-immunol-081022-021207

Furuta, A., Brokaw, A., Manuel, G., Dacanay, M., Marcell, L., Seepersaud, R., et al. (2022). Bacterial and host determinants of group B streptococcal infection of the neonate and infant. *Front. Microbiol.* 13, 820365. doi:10.3389/fmicb.2022.820365

Gaidt, M. M., Ebert, T. S., Chauhan, D., Ramshorn, K., Pinci, F., Zuber, S., et al. (2017). The DNA inflammasome in human myeloid cells is initiated by a STING-cell death program upstream of NLRP3. *Cell* 171 (5), 1110–1124.e18. doi:10.1016/j.cell.2017.09.039

Garcia-Calvo, M., Peterson, E. P., Leiting, B., Ruel, R., Nicholson, D. W., and Thornberry, N. A. (1998). Inhibition of human caspases by peptide-based and macromolecular inhibitors. *J. Biol. Chem.* 273 (49), 32608–32613. doi:10.1074/jbc.273.49.32608

Gautam, A., Boyd, D. F., Nikhar, S., Zhang, T., Siokas, I., Van de Velde, L. A., et al. (2024). Necroptosis blockade prevents lung injury in severe influenza. *Nature* 628 (8009), 835–843. doi:10.1038/s41586-024-07265-8

Gong, Q., Robinson, K., Xu, C., Huynh, P. T., Chong, K. H. C., Tan, E. Y. J., et al. (2021). Structural basis for distinct inflammasome complex assembly by human NLRP1 and CARD8. *Nat. Commun.* 12 (1), 188. doi:10.1038/s41467-020-20319-5

González-Juarbe, N., Gilley, R. P., Hinojosa, C. A., Bradley, K. M., Kamei, A., Gao, G., et al. (2015). Pore-forming toxins induce macrophage necroptosis during acute bacterial pneumonia. *PLoS Pathog.* 11 (12), e1005337. doi:10.1371/journal.ppat.1005337

Gottschalk, A. R., Boise, L. H., Oltvai, Z. N., Accavitti, M. A., Korsmeyer, S. J., Quintáns, J., et al. (1996). The ability of Bcl-x(L) and Bcl-2 to prevent apoptosis can be differentially regulated. *Cell Death Differ.* 3 (1), 113–118.

Graham, R. M., Thompson, J. W., and Webster, K. A. (2015). BNIP3 promotes calcium and calpain-dependent cell death. *Life Sci.* 142, 26–35. doi:10.1016/j.lfs.2015.10.010

Guo, J., Luo, Y., Zuo, J., Teng, J., Shen, B., and Liu, X. (2023). Echinacea polyphenols inhibit NLRP3-dependent pyroptosis, apoptosis, and necroptosis via suppressing NO production during lipopolysaccharide-induced acute lung injury. *J. Agric. Food Chem.* 71 (19), 7289–7298. doi:10.1021/acs.jafc.2c08382

Guo, Y., Zhou, J., Wang, Y., Wu, X., Mou, Y., and Song, X. (2024). Cell type-specific molecular mechanisms and implications of necroptosis in inflammatory respiratory diseases. *Immunol. Rev.* 321 (1), 52–70. doi:10.1111/imr.13282

Guy, C., Baran, M., Ribó-Molina, P., van den Hoogen, B. G., and Bowie, A. G. (2023). Viral sensing by epithelial cells involves PKR- and caspase-3-dependent generation of gasdermin E pores. *iScience* 26 (9), 107698. doi:10.1016/j.isci.2023.107698

Han, J. H., Karki, R., Malireddi, R. K. S., Mall, R., Sarkar, R., Sharma, B. R., et al. (2024). NINJ1 mediates inflammatory cell death, PANoptosis, and lethality during infection conditions and heat stress. *Nat. Commun.* 15 (1), 1739. doi:10.1038/s41467-024-45466-x

Han, J. H., Tweedell, R. E., and Kanneganti, T. D. (2023). Evaluation of caspase activation to assess innate immune cell death. *J. Vis. Exp.* (191). doi:10.3791/64308

Hao, S., Ning, K., Kuz, C. A., Xiong, M., Zou, W., Park, S. Y., et al. (2023). SARS-CoV-2 infection of polarized human airway epithelium induces necroptosis that causes airway epithelial barrier dysfunction. *J. Med. Virol.* 95 (9), e29076. doi:10.1002/jmv.29076

Hayward, J. A., Mathur, A., Ngo, C., and Man, S. M. (2018). Cytosolic recognition of microbes and pathogens: inflammasomes in action. *Microbiol. Mol. Biol. Rev.* 82 (4), e00015–e00018. doi:10.1128/MMBR.00015-18

He, X., Jiang, X., Guo, J., Sun, H., and Yang, J. (2025). PANoptosis in bacterial infections: a double-edged sword balancing host immunity and pathogenesis. *Pathogens* 14 (1), 43. doi:10.3390/pathogens14010043

Heinisch, O., Zeyen, T., Goldmann, T., Prinz, M., Huber, M., Jung, J., et al. (2022). Erythropoietin abrogates post-ischemic activation of the NLRP3, NLRC4, and AIM2 inflammasomes in microglia/macrophages in a TAK1-dependent manner. *Transl. Stroke Res.* 13 (3), 462–482. doi:10.1007/s12975-021-00948-8

Hengartner, M. O. (2000). The biochemistry of apoptosis. *Nature* 407 (6805), 770–776. doi:10.1038/35037710

Henkel, F. D. R., and O'Neill, L. A. J. (2023). NLRP12 drives PANoptosis in response to heme. *Trends Immunol.* 44 (8), 574–576. doi:10.1016/j.it.2023.06.008

Hou, J., Zhao, R., Xia, W., Chang, C. W., You, Y., Hsu, J. M., et al. (2020). PD-L1-mediated gasdermin C expression switches apoptosis to pyroptosis in cancer cells and facilitates tumour necrosis. *Nat. Cell Biol.* 22 (10), 1264–1275. doi:10.1038/s41556-020-0575-z

Hu, J. J., Liu, X., Xia, S., Zhang, Z., Zhang, Y., Zhao, J., et al. (2020). FDA-approved disulfiram inhibits pyroptosis by blocking gasdermin D pore formation. *Nat. Immunol.* 21 (7), 736–745. doi:10.1038/s41590-020-0669-6

Huang, D., Chen, P., Huang, G., Sun, H., Luo, X., He, C., et al. (2022). Salt-inducible kinases inhibitor HG-9-91-01 targets RIPK3 kinase activity to alleviate necroptosis-mediated inflammatory injury. *Cell Death Dis.* 13 (2), 188. doi:10.1038/s41419-022-04633-y

Huang, Y., Xu, W., and Zhou, R. (2021). NLRP3 inflammasome activation and cell death. *Cell Mol. Immunol.* 18 (9), 2114–2127. doi:10.1038/s41423-021-00740-6

Humphries, F., Shmuel-Galia, L., Ketelut-Carneiro, N., Li, S., Wang, B., Nemmara, V. V., et al. (2020). Succination inactivates gasdermin D and blocks pyroptosis. *Science.* 369 (6511), 1633–1637. doi:10.1126/science.abb9818

Inde, Z., Croker, B. A., Yapp, C., Joshi, G. N., Spetz, J., Fraser, C., et al. (2021). Age-dependent regulation of SARS-CoV-2 cell entry genes and cell death programs correlates with COVID-19 severity. *Sci. Adv.* 7 (34), eabf8609. doi:10.1126/sciadv.abf8609

Irmler, M., Thome, M., Hahne, M., Schneider, P., Hofmann, K., Steiner, V., et al. (1997). Inhibition of death receptor signals by cellular FLIP. *Nature* 388 (6638), 190–195. doi:10.1038/40657

Jackson, C. B., Farzan, M., Chen, B., and Choe, H. (2022). Mechanisms of SARS-CoV-2 entry into cells. *Nat. Rev. Mol. Cell Biol.* 23 (1), 3–20. doi:10.1038/s41580-021-00418-x

Janssen, W. J., Barthel, L., Muldrow, A., Oberley-Deegan, R. E., Kearns, M. T., Jakubzick, C., et al. (2011). Fas determines differential fates of resident and recruited macrophages during resolution of acute lung injury. *Am. J. Respir. Crit. Care Med.* 184 (5), 547–560. doi:10.1164/rccm.201011-1891OC

Jiang, M., Qi, L., Li, L., Wu, Y., Song, D., and Li, Y. (2021). Caspase-8: a key protein of cross-talk signal way in "PANoptosis" in cancer. *Int. J. Cancer* 149 (7), 1408–1420. doi:10.1002/ijc.33698

Jiao, C., Zhang, H., Li, H., Fu, X., Lin, Y., Cao, C., et al. (2023). Caspase-3/GSDME mediated pyroptosis: a potential pathway for sepsis. *Int. Immunopharmacol.* 124 (Pt B), 111022. doi:10.1016/j.intimp.2023.111022

Jono, H., Lim, J. H., Chen, L. F., Xu, H., Trompouki, E., Pan, Z. K., et al. (2004). NF-kappaB is essential for induction of CYLD, the negative regulator of NF-kappaB: evidence for a novel inducible autoregulatory feedback pathway. *J. Biol. Chem.* 279 (35), 36171–36174. doi:10.1074/jbc.M406638200

Juul, S. E., Kinsella, M. G., Truog, W. E., Gibson, R. L., and Redding, G. J. (1996). Lung hyaluronan decreases during group B streptococcal pneumonia in neonatal piglets. *Am. J. Respir. Crit. Care Med.* 153 (5), 1567–1570. doi:10.1164/ajrccm.153.5.8630603

Kang, S. J., Wang, S., Kuida, K., and Yuan, J. (2002). Distinct downstream pathways of caspase-11 in regulating apoptosis and cytokine maturation during septic shock response. *Cell Death Differ.* 9 (10), 1115–1125. doi:10.1038/sj.cdd.4401087

Kao, R. L., Xu, X., Xenocostas, A., Parry, N., Mele, T., Martin, C. M., et al. (2014). Induction of acute lung inflammation in mice with hemorrhagic shock and resuscitation: role of HMGB1. *J. Inflamm. (Lond).* 11 (1), 30. doi:10.1186/s12950-014-0030-7

Karki, R., Lee, S., Mall, R., Pandian, N., Wang, Y., Sharma, B. R., et al. (2022). ZBP1-dependent inflammatory cell death, PANoptosis, and cytokine storm disrupt IFN therapeutic efficacy during coronavirus infection. *Sci. Immunol.* 7 (74), eabo6294. doi:10.1126/sciimmunol.abo6294

Karki, R., Sharma, B. R., Tuladhar, S., Williams, E. P., Zalduondo, L., Samir, P., et al. (2021). Synergism of TNF-α and IFN-γ triggers inflammatory cell death, tissue damage, and mortality in SARS-CoV-2 infection and cytokine shock syndromes. *Cell* 184 (1), 149–168.e17. doi:10.1016/j.cell.2020.11.025

Kasana, S., Kumar, S., Patel, P., Kurmi, B. D., Jain, S., Sahu, S., et al. (2024). Caspase inhibitors: a review on recently patented compounds (2016–2023). *Expert Opin. Ther. Pat.* 34 (10), 1047–1072. doi:10.1080/13543776.2024.2397732

Kawasaki, M., Kuwano, K., Hagimoto, N., Matsuba, T., Kunitake, R., Tanaka, T., et al. (2000). Protection from lethal apoptosis in lipopolysaccharide-induced acute lung injury in mice by a caspase inhibitor. *Am. J. Pathol.* 157 (2), 597–603. doi:10.1016/S0002-9440(10)64570-1

Kayagaki, N., Stowe, I. B., Lee, B. L., O'Rourke, K., Anderson, K., Warming, S., et al. (2015). Caspase-11 cleaves gasdermin D for non-canonical inflammasome signalling. *Nature* 526 (7575), 666–671. doi:10.1038/nature15541

Kayagaki, N., Warming, S., Lamkanfi, M., Vande Walle, L., Louie, S., Dong, J., et al. (2011). Non-canonical inflammasome activation targets caspase-11. *Nature* 479 (7371), 117–121. doi:10.1038/nature10558

Kayagaki, N., Wong, M. T., Stowe, I. B., Ramani, S. R., Gonzalez, L. C., Akashi-Takamura, S., et al. (2013). Noncanonical inflammasome activation by intracellular LPS independent of TLR4. *Science* 341 (6151), 1246–1249. doi:10.1126/science.1240248

Kesavardhana, S., Malireddi, R. K. S., and Kanneganti, T. D. (2020). Caspases in cell death, inflammation, and pyroptosis. *Annu. Rev. Immunol.* 38, 567–595. doi:10.1146/annurev-immunol-073119-095439

Khazoom, F., L'Écuyer, S., Gilbert, K., Gagné, M. A., Bouchard, C., Rose, C. F., et al. (2020). Impact of uric acid on liver injury and intestinal permeability following resuscitated hemorrhagic shock in rats. *J. Trauma Acute Care Surg.* 89 (6), 1076–1084. doi:10.1097/TA.0000000000002868

Kim, R., Kin, T., and Beck, W. T. (2024). Impact of complex apoptotic signaling pathways on cancer cell sensitivity to therapy. *Cancers (Basel)* 16 (5), 984. doi:10.3390/cancers16050984

Kitur, K., Parker, D., Nieto, P., Ahn, D. S., Cohen, T. S., Chung, S., et al. (2015). Toxin-induced necroptosis is a major mechanism of *Staphylococcus aureus* lung damage. *PLoS Pathog.* 11 (4), e1004820. doi:10.1371/journal.ppat.1004820

Kling, D. E., Tsvang, I., Murphy, M. P., and Newburg, D. S. (2013). Group B Streptococcus induces a caspase-dependent apoptosis in fetal rat lung interstitium. *Microb. Pathog.* 61-62, 1–10. doi:10.1016/j.micpath.2013.04.008

Kobori, M., Yang, Z., Gong, D., Heissmeyer, V., Zhu, H., Jung, Y. K., et al. (2004). Wedelolactone suppresses LPS-induced caspase-11 expression by directly inhibiting the IKK complex. *Cell Death Differ.* 11 (1), 123–130. doi:10.1038/sj.cdd.4401325

Kostura, M. J., Tocci, M. J., Limjuco, G., Chin, J., Cameron, P., Hillman, A. G., et al. (1989). Identification of a monocyte specific pre-interleukin 1 beta convertase activity. *Proc. Natl. Acad. Sci. U. S. A.* 86 (14), 5227–5231. doi:10.1073/pnas.86.14.5227

Kuipers, M. T., Aslami, H., Janczy, J. R., van der Sluijs, K. F., Vlaar, A. P., Wolthuis, E. K., et al. (2012). Ventilator-induced lung injury is mediated by the NLRP3 inflammasome. *Anesthesiology* 116 (5), 1104–1115. doi:10.1097/ALN.0b013e3182518bc0

Kuipers, M. T., van der Poll, T., Schultz, M. J., and Wieland, C. W. (2011). Bench-to-bedside review: damage-associated molecular patterns in the onset of ventilator-induced lung injury. *Crit. Care* 15 (6), 235. doi:10.1186/cc10437

Lagrange, B., Benaoudia, S., Wallet, P., Magnotti, F., Provost, A., Michal, F., et al. (2018). Human caspase-4 detects tetra-acylated LPS and cytosolic Francisella and functions differently from murine caspase-11. *Nat. Commun.* 9 (1), 242. doi:10.1038/s41467-017-02682-y

Lakhani, S. A., Masud, A., Kuida, K., Porter, G. A., Jr., Booth, C. J., Mehal, W. Z., et al. (2006). Caspases 3 and 7: key mediators of mitochondrial events of apoptosis. *Science* 311 (5762), 847–851. doi:10.1126/science.1115035

Land, W. G. (2013). Transfusion-related acute lung injury: the work of DAMPs. *Transfus. Med. Hemother* 40 (1), 3–13. doi:10.1159/000345688

LaRock, C. N., and Cookson, B. T. (2012). The Yersinia virulence effector YopM binds caspase-1 to arrest inflammasome assembly and processing. *Cell Host Microbe* 12 (6), 799–805. doi:10.1016/j.chom.2012.10.020

Le, A., Liu, W., Wu, C., Hu, P., Zou, J., Wu, Y., et al. (2022). Polymorphonuclear neutrophil activation by Src phosphorylation contributes to HLA-A2 antibody-induced transfusion-related acute lung injury. *Mol. Immunol.* 150, 9–19. doi:10.1016/j.molimm.2022.04.010

Le, J., Kulatheepan, Y., and Jeyaseelan, S. (2023). Role of toll-like receptors and nod-like receptors in acute lung infection. *Front. Immunol.* 14, 1249098. doi:10.3389/fimmu.2023.1249098

Le Berre, R., Faure, K., Fauvel, H., Viget, N. B., Ader, F., Prangère, T., et al. (2004). Apoptosis inhibition in P. aeruginosa-induced lung injury influences lung fluid balance. *Intensive Care Med.* 30 (6), 1204–1211. doi:10.1007/s00134-004-2165-0

Lee, G., Ahn, H., Yun, J. H., Park, J., Lee, E., Oh, S., et al. (2022). JC2-11, a benzylideneacetophenone derivative, attenuates inflammasome activation. *Sci. Rep.* 12 (1), 22484. doi:10.1038/s41598-022-27129-3

Lee, S., Karki, R., Wang, Y., Nguyen, L. N., Kalathur, R. C., and Kanneganti, T. D. (2021). AIM2 forms a complex with pyrin and ZBP1 to drive PANoptosis and host defence. *Nature* 597 (7876), 415–419. doi:10.1038/s41586-021-03875-8

Lentini, G., Famà, A., De Gaetano, G. V., Coppolino, F., Mahjoub, A. K., Ryan, L., et al. (2023). Caspase-8 inhibition improves the outcome of bacterial infections in mice by promoting neutrophil activation. *Cell Rep. Med.* 4 (7), 101098. doi:10.1016/j.xcrm.2023.101098

Li, C., Han, S., Zhu, J., and Cheng, F. (2023e). MiR-132-3p activation aggravates renal ischemia-reperfusion injury by targeting Sirt1/PGC1alpha axis. *Cell Signal* 110, 110801. doi:10.1016/j.cellsig.2023.110801

Li, H., Guan, J., Chen, J., Sun, W., Chen, H., Wen, Y., et al. (2023c). Necroptosis signaling and NLRP3 inflammasome cross-talking in epithelium facilitate *Pseudomonas aeruginosa* mediated lung injury. *Biochim. Biophys. Acta Mol. Basis Dis.* 1869 (3), 166613. doi:10.1016/j.bbadis.2022.166613

Li, S., Yue, M., Xu, H., Zhang, X., Mao, T., Quan, M., et al. (2023a). Chemotherapeutic drugs-induced pyroptosis mediated by gasdermin E promotes the progression and chemoresistance of pancreatic cancer. *Cancer Lett.* 564, 216206. doi:10.1016/j.canlet.2023.216206

Li, S., Zhang, Y., Guan, Z., Li, H., Ye, M., Chen, X., et al. (2020). SARS-CoV-2 triggers inflammatory responses and cell death through caspase-8 activation. *Signal Transduct. Target Ther.* 5 (1), 235. doi:10.1038/s41392-020-00334-0

Li, S., Zhang, Y., Guan, Z., Ye, M., Li, H., You, M., et al. (2023b). SARS-CoV-2 Z-RNA activates the ZBP1-RIPK3 pathway to promote virus-induced inflammatory responses. *Cell Res.* 33 (3), 201–214. doi:10.1038/s41422-022-00775-y

Li, W., Xu, H., Shao, J., Chen, J., Lin, Y., Zheng, Z., et al. (2023f). Discovery of alantolactone as a naturally occurring NLRP3 inhibitor to alleviate NLRP3-driven inflammatory diseases in mice. *Br. J. Pharmacol.* 180 (12), 1634–1647. doi:10.1111/bph.16036

Li, W., Yang, K., Li, B., Wang, Y., Liu, J., Chen, D., et al. (2022). Corilagin alleviates intestinal ischemia/reperfusion-induced intestinal and lung injury in mice via inhibiting NLRP3 inflammasome activation and pyroptosis. *Front. Pharmacol.* 13, 1060104. doi:10.3389/fphar.2022.1060104

Li, Z., Wang, B., Tian, L., Zheng, B., Zhao, X., and Liu, R. (2023d). Methane-rich saline suppresses ER-mitochondria contact and activation of the NLRP3 inflammasome by regulating the PERK signaling pathway to ameliorate intestinal ischemia–reperfusion injury. *Inflammation* 47, 376–389. doi:10.1007/s10753-023-01916-0

Li, Z. G., Scott, M. J., Brzóska, T., Sundd, P., Li, Y. H., Billiar, T. R., et al. (2018). Lung epithelial cell-derived IL-25 negatively regulates LPS-induced exosome release from macrophages. *Mil. Med. Res.* 5 (1), 24. doi:10.1186/s40779-018-0173-6

Liang, X., Qin, Y., Wu, D., Wang, Q., and Wu, H. (2024). Pyroptosis: a double-edged sword in lung cancer and other respiratory diseases. *Cell Commun. Signal* 22 (1), 40. doi:10.1186/s12964-023-01458-w

Lin, B., Jin, Z., Chen, X., Zhao, L., Weng, C., Chen, B., et al. (2020). Necrostatin-1 protects mice from acute lung injury by suppressing necroptosis and reactive oxygen species. *Mol. Med. Rep.* 21 (5), 2171–2181. doi:10.3892/mmr.2020.11010

Liu, Z., Meng, Y., Miao, Y., Yu, L., and Yu, Q. (2020b). Propofol reduces renal ischemia/reperfusion-induced acute lung injury by stimulating sirtuin 1 and inhibiting pyroptosis. *Aging (Albany NY)* 13 (1), 865–876. doi:10.18632/aging.202191

Liu, Z., Wang, C., Yang, J., Chen, Y., Zhou, B., Abbott, D. W., et al. (2020a). Caspase-1 engages full-length gasdermin D through two distinct interfaces that mediate caspase recruitment and substrate cleavage. *Immunity* 53 (1), 106–114.e5. doi:10.1016/j.immuni.2020.06.007

Lopez-Castejon, G., Corbett, D., Goldrick, M., Roberts, I. S., and Brough, D. (2012). Inhibition of calpain blocks the phagosomal escape of Listeria monocytogenes. *PLoS One* 7 (4), e35936. doi:10.1371/journal.pone.0035936

Lyons, J. D., Mandal, P., Otani, S., Chihade, D. B., Easley, K. F., Swift, D. A., et al. (2023). The RIPK3 scaffold regulates lung inflammation during Pseudomonas aeruginosa pneumonia. *Am. J. Respir. Cell Mol. Biol.* 68 (2), 150–160. doi:10.1165/rcmb.2021-0474OC

Ma, H., Zhu, Z., Lin, H., Wang, S., Zhang, P., Li, Y., et al. (2021). Pyroptosis of syncytia formed by fusion of SARS-CoV-2 spike and ACE2-expressing cells. *Cell Discov.* 7 (1), 73. doi:10.1038/s41421-021-00310-0

Maelfait, J., Vercammen, E., Janssens, S., Schotte, P., Haegman, M., Magez, S., et al. (2008). Stimulation of Toll-like receptor 3 and 4 induces interleukin-1beta maturation by caspase-8. *J. Exp. Med.* 205 (9), 1967–1973. doi:10.1084/jem.20071632

Makena, P. S., Luellen, C. L., Balazs, L., Ghosh, M. C., Parthasarathi, K., Waters, C. M., et al. (2010). Preexposure to hyperoxia causes increased lung injury and epithelial apoptosis in mice ventilated with high tidal volumes. *Am. J. Physiol. Lung Cell Mol. Physiol.* 299 (5), L711–L719. doi:10.1152/ajplung.00072.2010

Malireddi, R. K. S., Gurung, P., Kesavardhana, S., Samir, P., Burton, A., Mummareddy, H., et al. (2020). Innate immune priming in the absence of TAK1 drives RIPK1 kinase activity-independent pyroptosis, apoptosis, necroptosis, and inflammatory disease. *J. Exp. Med.* 217 (3), 20191644. doi:10.1084/jem.20191644

Mandal, P., Feng, Y., Lyons, J. D., Berger, S. B., Otani, S., DeLaney, A., et al. (2018). Caspase-8 collaborates with caspase-11 to drive tissue damage and execution of endotoxic shock. *Immunity* 49 (1), 42–55.e6. doi:10.1016/j.immuni.2018.06.011

Mathiak, G., Grass, G., Herzmann, T., Luebke, T., Zetina, C. C., Boehm, S. A., et al. (2000). Caspase-1-inhibitor ac-YVAD-cmk reduces LPS-lethality in rats without affecting haematology or cytokine responses. *Br. J. Pharmacol.* 131 (3), 383–386. doi:10.1038/sj.bjp.0703629

Matikainen, S., Nyman, T. A., and Cypryk, W. (2020). Function and regulation of noncanonical caspase-4/5/11 inflammasome. *J. Immunol.* 204 (12), 3063–3069. doi:10.4049/jimmunol.2000373

Mazgaeen, L., and Gurung, P. (2020). Recent advances in lipopolysaccharide recognition systems. *Int. J. Mol. Sci.* 21 (2), 379. doi:10.3390/ijms21020379

Modi, P., Shah, B. M., and Patel, S. (2023). Interleukin-1β converting enzyme (ICE): a comprehensive review on discovery and development of caspase-1 inhibitors. *Eur. J. Med. Chem.* 261, 115861. doi:10.1016/j.ejmech.2023.115861

Mohammadi, N., Midiri, A., Mancuso, G., Patanè, F., Venza, M., Venza, I., et al. (2016). Neutrophils directly recognize group B streptococci and contribute to interleukin-1β production during infection. *PLoS One* 11 (8), e0160249. doi:10.1371/journal.pone.0160249

Mokrá, D. (2020). Acute lung injury - from pathophysiology to treatment. *Physiol. Res.* 69 (Suppl. 3), S353–S366. doi:10.33549/physiolres.934602

Momeni, H. R. (2011). Role of calpain in apoptosis. *Cell J.* 13 (2), 65–72.

Moquin, D. M., McQuade, T., and Chan, F. K. (2013). CYLD deubiquitinates RIP1 in the TNFα-induced necrosome to facilitate kinase activation and programmed necrosis. *PLoS One* 8 (10), e76841. doi:10.1371/journal.pone.0076841

Newton, K., and Manning, G. (2016). Necroptosis and inflammation. *Annu. Rev. Biochem.* 85, 743–763. doi:10.1146/annurev-biochem-060815-014830

Ning, L., Wei, W., Wenyang, J., Rui, X., and Qing, G. (2020). Cytosolic DNA-STING-NLRP3 axis is involved in murine acute lung injury induced by lipopolysaccharide. *Clin. Transl. Med.* 10 (7), e228. doi:10.1002/ctm2.228

Ono, Y., Saido, T. C., and Sorimachi, H. (2016). Calpain research for drug discovery: challenges and potential. *Nat. Rev. Drug Discov.* 15 (12), 854–876. doi:10.1038/nrd.2016.212

Orning, P., Weng, D., Starheim, K., Ratner, D., Best, Z., Lee, B., et al. (2018). Pathogen blockade of TAK1 triggers caspase-8-dependent cleavage of gasdermin D and cell death. *Science* 362 (6418), 1064–1069. doi:10.1126/science.aau2818

Pahmeier, F., Lavacca, T. M., Goellner, S., Neufeldt, C. J., Prasad, V., Cerikan, B., et al. (2023). Identification of host dependency factors involved in SARS-CoV-2 replication organelle formation through proteomics and ultrastructural analysis. *J. Virol.* 97, e0087823. doi:10.1128/jvi.00878-23

Pan, P., Ge, W., Lei, Z., Luo, W., Liu, Y., Guan, Z., et al. (2023). SARS-CoV-2 N protein enhances the anti-apoptotic activity of MCL-1 to promote viral replication. *Signal Transduct. Target Ther.* 8 (1), 194. doi:10.1038/s41392-023-01459-8

Pan, P., Shen, M., Yu, Z., Ge, W., Chen, K., Tian, M., et al. (2021). SARS-CoV-2 N protein promotes NLRP3 inflammasome activation to induce hyperinflammation. *Nat. Commun.* 12 (1), 4664. doi:10.1038/s41467-021-25015-6

Pandeya, A., and Kanneganti, T. D. (2024). Therapeutic potential of PANoptosis: innate sensors, inflammasomes, and RIPKs in PANoptosomes. *Trends Mol. Med.* 30 (1), 74–88. doi:10.1016/j.molmed.2023.10.001

Pang, J., and Vince, J. E. (2023). The role of caspase-8 in inflammatory signalling and pyroptotic cell death. *Semin. Immunol.* 70, 101832. doi:10.1016/j.smim.2023.101832

Panganiban, R. A., Sun, M., Dahlin, A., Park, H. R., Kan, M., Himes, B. E., et al. (2018). A functional splice variant associated with decreased asthma risk abolishes the ability of gasdermin B to induce epithelial cell pyroptosis. *J. Allergy Clin. Immunol.* 142 (5), 1469–1478.e2. doi:10.1016/j.jaci.2017.11.040

Park, K. S., Lee, J., Jang, S. C., Kim, S. R., Jang, M. H., Lötvall, J., et al. (2013). Pulmonary inflammation induced by bacteria-free outer membrane vesicles from *Pseudomonas aeruginosa*. *Am. J. Respir. Cell Mol. Biol.* 49 (4), 637–645. doi:10.1165/rcmb.2012-0370OC

Peitzman, A. B., Billiar, T. R., Harbrecht, B. G., Kelly, E., Udekwu, A. O., and Simmons, R. L. (1995). Hemorrhagic shock. *Curr. Probl. Surg.* 32 (11), 925–1002. doi:10.1016/s0011-3840(05)80008-5

Philip, N. H., Dillon, C. P., Snyder, A. G., Fitzgerald, P., Wynosky-Dolfi, M. A., Zwack, E. E., et al. (2014). Caspase-8 mediates caspase-1 processing and innate immune defense in response to bacterial blockade of NF-κB and MAPK signaling. *Proc. Natl. Acad. Sci. U. S. A.* 111 (20), 7385–7390. doi:10.1073/pnas.1403252111

Planès, R., Pinilla, M., Santoni, K., Hessel, A., Passemar, C., Lay, K., et al. (2022). Human NLRP1 is a sensor of pathogenic coronavirus 3CL proteases in lung epithelial cells. *Mol. Cell* 82 (13), 2385–2400.e9. doi:10.1016/j.molcel.2022.04.033

Platnich, J. M., Chung, H., Lau, A., Sandall, C. F., Bondzi-Simpson, A., Chen, H. M., et al. (2018). Shiga toxin/lipopolysaccharide activates caspase-4 and gasdermin D to trigger mitochondrial reactive oxygen species upstream of the NLRP3 inflammasome. *Cell Rep.* 25 (6), 1525–1536.e7. doi:10.1016/j.celrep.2018.09.071

Qi, Z., Zhu, L., Wang, K., and Wang, N. (2023). PANoptosis: emerging mechanisms and disease implications. *Life Sci.* 333, 122158. doi:10.1016/j.lfs.2023.122158

Qian, S., Long, Y., Tan, G., Li, X., Xiang, B., Tao, Y., et al. (2024). Programmed cell death: molecular mechanisms, biological functions, diseases, and therapeutic targets. *MedComm (2020)* 5 (12), e70024. doi:10.1002/mco2.70024

Qin, H., Lu, N., Chen, K., Huang, Y., Rui, Y., Huang, L., et al. (2024). Inhibiting caspase-3/GSDME-mediated pyroptosis ameliorates septic lung injury in mice model. *Mol. Immunol.* 172, 96–104. doi:10.1016/j.molimm.2024.06.007

Qing, D. Y., Conegliano, D., Shashaty, M. G., Seo, J., Reilly, J. P., Worthen, G. S., et al. (2014). Red blood cells induce necroptosis of lung endothelial cells and increase susceptibility to lung inflammation. *Am. J. Respir. Crit. Care Med.* 190 (11), 1243–1254. doi:10.1164/rccm.201406-1095OC

Ratajczak, M. Z., Bujko, K., Ciechanowicz, A., Sielatycka, K., Cymer, M., Marlicz, W., et al. (2021). SARS-CoV-2 entry receptor ACE2 is expressed on very small CD45(-) precursors of hematopoietic and endothelial cells and in response to virus spike protein activates the Nlrp3 inflammasome. *Stem Cell Rev. Rep.* 17 (1), 266–277. doi:10.1007/s12015-020-10010-z

Rathinam, V. A., and Fitzgerald, K. A. (2016). Inflammasome complexes: emerging mechanisms and effector functions. *Cell* 165 (4), 792–800. doi:10.1016/j.cell.2016.03.046

Rathinam, V. A. K., Zhao, Y., and Shao, F. (2019). Innate immunity to intracellular LPS. *Nat. Immunol.* 20 (5), 527–533. doi:10.1038/s41590-019-0368-3

Rathkey, J. K., Zhao, J., Liu, Z., Chen, Y., Yang, J., Kondolf, H. C., et al. (2018). Chemical disruption of the pyroptotic pore-forming protein gasdermin D inhibits inflammatory cell death and sepsis. *Sci. Immunol.* 3 (26), eaat2738. doi:10.1126/sciimmunol.aat2738

Rosa-Fraile, M., Dramsi, S., and Spellerberg, B. (2014). Group B streptococcal haemolysin and pigment, a tale of twins. *FEMS Microbiol. Rev.* 38 (5), 932–946. doi:10.1111/1574-6976.12071

Rosenzweig, J. A., and Chopra, A. K. (2013). Modulation of host immune defenses by Aeromonas and Yersinia species: convergence on toxins secreted by various secretion systems. *Front. Cell Infect. Microbiol.* 3, 70. doi:10.3389/fcimb.2013.00070

Ruan, D., Yang, J., Luo, Q., Shi, Y., Ding, L., Wang, Z., et al. (2023). The protective effects of goitrin on LPS-induced septic shock in C57bl/6J mice via caspase-11 non-canonical inflammasome inhibition. *Molecules* 28 (7), 2883. doi:10.3390/molecules28072883

Ryan, T. A. J., Hooftman, A., Rehill, A. M., Johansen, M. D., Brien, E. C. O., Toller-Kawahisa, J. E., et al. (2023). Dimethyl fumarate and 4-octyl itaconate are anticoagulants that suppress Tissue Factor in macrophages via inhibition of Type I Interferon. *Nat. Commun.* 14 (1), 3513. doi:10.1038/s41467-023-39174-1

Stefanie, M. B., Cooney, J. P., Bhandari, R., Mackiewicz, L., Dayton, M., Sheerin, D., et al. (2024). Necroptosis does not drive disease pathogenesis in a mouse infective model of SARS-CoV-2 *in vivo*. *Cell Death Dis.* 15 (1), 100. doi:10.1038/s41419-024-06471-6

Schneider, K. S., Groß, C. J., Dreier, R. F., Saller, B. S., Mishra, R., Gorka, O., et al. (2017). The inflammasome drives GSDMD-independent secondary pyroptosis and IL-1 release in the absence of caspase-1 protease activity. *Cell Rep.* 21 (13), 3846–3859. doi:10.1016/j.celrep.2017.12.018

Schubert, K. A., Xu, Y., Shao, F., and Auerbuch, V. (2020). The Yersinia type III secretion system as a tool for studying cytosolic innate immune surveillance. *Annu. Rev. Microbiol.* 74, 221–245. doi:10.1146/annurev-micro-020518-120221

Schwarzer, R., Jiao, H., Wachsmuth, L., Tresch, A., and Pasparakis, M. (2020a). FADD and caspase-8 regulate gut homeostasis and inflammation by controlling MLKL- and GSDMD-mediated death of intestinal epithelial cells. *Immunity* 52 (6), 978–993.e6. doi:10.1016/j.immuni.2020.04.002

Schwarzer, R., Laurien, L., and Pasparakis, M. (2020b). New insights into the regulation of apoptosis, necroptosis, and pyroptosis by receptor interacting protein kinase 1 and caspase-8. *Curr. Opin. Cell Biol.* 63, 186–193. doi:10.1016/j.ceb.2020.02.004

Scott, F. L., Denault, J. B., Riedl, S. J., Shin, H., Renatus, M., and Salvesen, G. S. (2005). XIAP inhibits caspase-3 and -7 using two binding sites: evolutionarily conserved mechanism of IAPs. *Embo J.* 24 (3), 645–655. doi:10.1038/sj.emboj.7600544

Shao, J. J., Li, W. F., Sun, J. F., Zhuang, Z. S., Min, J. L., Long, X. H., et al. (2024). Britannin as a novel NLRP3 inhibitor, suppresses inflammasome activation in macrophages and alleviates NLRP3-related diseases in mice. *Acta Pharmacol. Sin.* 45 (4), 803–814. doi:10.1038/s41401-023-01212-5

Shao, R. G., Xie, Q. W., Pan, L. H., Lin, F., Qin, K., Ming, S. P., et al. (2022). Necrostatin-1 attenuates Caspase-1-dependent pyroptosis induced by the RIPK1/ZBP1 pathway in ventilator-induced lung injury. *Cytokine* 157, 155950. doi:10.1016/j.cyto.2022.155950

Shi, J., Zhao, Y., Wang, Y., Gao, W., Ding, J., Li, P., et al. (2014). Inflammatory caspases are innate immune receptors for intracellular LPS. *Nature* 514 (7521), 187–192. doi:10.1038/nature13683

Shi, K., Zhang, J., Zhou, E., Wang, J., and Wang, Y. (2022). Small-molecule receptor-interacting protein 1 (RIP1) inhibitors as therapeutic agents for multifaceted diseases: current medicinal chemistry insights and emerging opportunities. *J. Med. Chem.* 65 (22), 14971–14999. doi:10.1021/acs.jmedchem.2c01518

Shi, X., Sun, Q., Hou, Y., Zeng, H., Cao, Y., Dong, M., et al. (2023). Recognition and maturation of IL-18 by caspase-4 noncanonical inflammasome. *Nature* 624 (7991), 442–450. doi:10.1038/s41586-023-06742-w

Shubina, M., Tummers, B., Boyd, D. F., Zhang, T., Yin, C., Gautam, A., et al. (2020). Necroptosis restricts influenza A virus as a stand-alone cell death mechanism. *J. Exp. Med.* 217 (11), e20191259. doi:10.1084/jem.20191259

Silliman, C. C. (2006). The two-event model of transfusion-related acute lung injury. *Crit. Care Med.* 34 (5 Suppl. l), S124–S131. doi:10.1097/01.CCM.0000214292.62276.8E

Song, L., Shi, X., Kovacs, L., Han, W., John, J., Barman, S. A., et al. (2023). Calpain promotes LPS-induced lung endothelial barrier dysfunction via cleavage of talin. *Am. J. Respir. Cell Mol. Biol.* 69 (6), 678–688. doi:10.1165/rcmb.2023-0009OC

Soni, S., Walton-Filipczak, S., Nho, R. S., Tesfaigzi, Y., and Mebratu, Y. A. (2023). Independent role of caspases and Bik in augmenting influenza A virus replication in airway epithelial cells and mice. *Virol. J.* 20 (1), 78. doi:10.1186/s12985-023-02027-w

Srinivasula, S. M., Hegde, R., Saleh, A., Datta, P., Shiozaki, E., Chai, J., et al. (2001). A conserved XIAP-interaction motif in caspase-9 and Smac/DIABLO regulates caspase activity and apoptosis. *Nature* 410 (6824), 112–116. doi:10.1038/35065125

Suddock, J. T., and Crookston, K. P. (2024). "Transfusion reactions. StatPearls. Treasure island (FL) ineligible companies," in *Disclosure: kendall Crookston declares no relevant financial relationships with ineligible companies*, (St. Petersburg, FL: StatPearls Publishing LLC.).

Sun, X., Liu, Y., Huang, Z., Xu, W., Hu, W., Yi, L., et al. (2022). SARS-CoV-2 non-structural protein 6 triggers NLRP3-dependent pyroptosis by targeting ATP6AP1. *Cell Death Differ.* 29 (6), 1240–1254. doi:10.1038/s41418-021-00916-7

Sun, X., Yang, Y., Meng, X., Li, J., Liu, X., and Liu, H. (2024). PANoptosis: mechanisms, biology, and role in disease. *Immunol. Rev.* 321 (1), 246–262. doi:10.1111/imr.13279

Sundaram, B., Karki, R., and Kanneganti, T. D. (2022). NLRC4 deficiency leads to enhanced phosphorylation of MLKL and necroptosis. *Immunohorizons* 6 (3), 243–252. doi:10.4049/immunohorizons.2100118

Sundaram, B., Pandian, N., Kim, H. J., Abdelaal, H. M., Mall, R., Indari, O., et al. (2024b). NLRC5 senses NAD(+) depletion, forming a PANoptosome and driving PANoptosis and inflammation. *Cell* 187, 4061–4077.e17. doi:10.1016/j.cell.2024.05.034

Sundaram, B., Pandian, N., Mall, R., Wang, Y., Sarkar, R., Kim, H. J., et al. (2023). NLRP12-PANoptosome activates PANoptosis and pathology in response to heme and PAMPs. *Cell* 186 (13), 2783–2801.e20. doi:10.1016/j.cell.2023.05.005

Sundaram, B., Tweedell, R. E., Prasanth Kumar, S., and Kanneganti, T. D. (2024a). The NLR family of innate immune and cell death sensors. *Immunity* 57 (4), 674–699. doi:10.1016/j.immuni.2024.03.012

Surve, M. V., Anil, A., Kamath, K. G., Bhutda, S., Sthanam, L. K., Pradhan, A., et al. (2016). Membrane vesicles of group B Streptococcus disrupt feto-maternal barrier leading to preterm birth. *PLoS Pathog.* 12 (9), e1005816. doi:10.1371/journal.ppat.1005816

Taabazuing, C. Y., Griswold, A. R., and Bachovchin, D. A. (2020). The NLRP1 and CARD8 inflammasomes. *Immunol. Rev.* 297 (1), 13–25. doi:10.1111/imr.12884

Taabazuing, C. Y., Okondo, M. C., and Bachovchin, D. A. (2017). Pyroptosis and apoptosis pathways engage in bidirectional crosstalk in monocytes and macrophages. *Cell Chem. Biol.* 24 (4), 507–514.e4. doi:10.1016/j.chembiol.2017.03.009

Takahashi, N., Duprez, L., Grootjans, S., Cauwels, A., Nerinckx, W., DuHadaway, J. B., et al. (2012). Necrostatin-1 analogues: critical issues on the specificity, activity and *in vivo* use in experimental disease models. *Cell Death Dis.* 3 (11), e437. doi:10.1038/cddis.2012.176

Tan, Y., Dourdin, N., Wu, C., De Veyra, T., Elce, J. S., and Greer, P. A. (2006). Ubiquitous calpains promote caspase-12 and JNK activation during endoplasmic reticulum stress-induced apoptosis. *J. Biol. Chem.* 281 (23), 16016–16024. doi:10.1074/jbc.M601299200

Tate, M. D., Ong, J. D. H., Dowling, J. K., McAuley, J. L., Robertson, A. B., Latz, E., et al. (2016). Reassessing the role of the NLRP3 inflammasome during pathogenic influenza A virus infection via temporal inhibition. *Sci. Rep.* 6, 27912. doi:10.1038/srep27912

Theriot, H. M., Malaviarachchi, P. A., Scott, M. G., Appell, K. T., Banerjee, S. K., and Pechous, R. D. (2023). Pulmonary expression of interleukin-17 contributes to neutrophil infiltration into the lungs during pneumonic plague. *Infect. Immun.* 91 (7), e0013123. doi:10.1128/iai.00131-23

Thompson, J., Hu, Y., Lesnefsky, E. J., and Chen, Q. (2016). Activation of mitochondrial calpain and increased cardiac injury: beyond AIF release. *Am. J. Physiol. Heart Circ. Physiol.* 310 (3), H376–H384. doi:10.1152/ajpheart.00748.2015

Trager, N., Smith, A., Wallace Iv, G., Azuma, M., Inoue, J., Beeson, C., et al. (2014). Effects of a novel orally administered calpain inhibitor SNJ-1945 on immunomodulation and neurodegeneration in a murine model of multiple sclerosis. *J. Neurochem.* 130 (2), 268–279. doi:10.1111/jnc.12659

Tsai, C. M., Riestra, A. M., Ali, S. R., Fong, J. J., Liu, J. Z., Hughes, G., et al. (2020). Siglec-14 enhances NLRP3-inflammasome activation in macrophages. *J. Innate Immun.* 12 (4), 333–343. doi:10.1159/000504323

Tummers, B., and Green, D. R. (2017). Caspase-8: regulating life and death. *Immunol. Rev.* 277 (1), 76–89. doi:10.1111/imr.12541

Tung, J. P., Chiaretti, S., Dean, M. M., Sultana, A. J., Reade, M. C., and Fung, Y. L. (2022). Transfusion-related acute lung injury (TRALI): potential pathways of development, strategies for prevention and treatment, and future research directions. *Blood Rev.* 53, 100926. doi:10.1016/j.blre.2021.100926

van Kaam, A. H. (2024). Optimal strategies of mechanical ventilation: can we avoid or reduce lung injury? *Neonatology* 121, 570–575. doi:10.1159/000539346

Van Opdenbosch, N., and Lamkanfi, M. (2019). Caspases in cell death, inflammation, and disease. *Immunity* 50 (6), 1352–1364. doi:10.1016/j.immuni.2019.05.020

Vasudevan, S. O., Behl, B., and Rathinam, V. A. (2023). Pyroptosis-induced inflammation and tissue damage. *Semin. Immunol.* 69, 101781. doi:10.1016/j.smim.2023.101781

Wan, X., Li, J., Wang, Y., Yu, X., He, X., Shi, J., et al. (2022). H7N9 virus infection triggers lethal cytokine storm by activating gasdermin E-mediated pyroptosis of lung alveolar epithelial cells. *Natl. Sci. Rev.* 9 (1), nwab137. doi:10.1093/nsr/nwab137

Wang, K., Li, J., Degterev, A., Hsu, E., Yuan, J., and Yuan, C. (2007). Structure-activity relationship analysis of a novel necroptosis inhibitor, Necrostatin-5. *Bioorg Med. Chem. Lett.* 17 (5), 1455–1465. doi:10.1016/j.bmcl.2006.11.056

Wang, K., Sun, Q., Zhong, X., Zeng, M., Zeng, H., Shi, X., et al. (2020a). Structural mechanism for GSDMD targeting by autoprocessed caspases in pyroptosis. *Cell* 180 (5), 941–955.e20. doi:10.1016/j.cell.2020.02.002

Wang, K. K., Nath, R., Posner, A., Raser, K. J., Buroker-Kilgore, M., Hajimohammadreza, I., et al. (1996). An alpha-mercaptoacrylic acid derivative is a selective nonpeptide cell-permeable calpain inhibitor and is neuroprotective. *Proc. Natl. Acad. Sci. U. S. A.* 93 (13), 6687–6692. doi:10.1073/pnas.93.13.6687

Wang, L., Chen, B., Xiong, X., Chen, S., Jin, L., and Zhu, M. (2020c). Necrostatin-1 synergizes the Pan caspase inhibitor to attenuate lung injury induced by ischemia reperfusion in rats. *Mediat. Inflamm.* 2020, 7059304. doi:10.1155/2020/7059304

Wang, L., Lei, W., Zhang, S., and Yao, L. (2021). MCC950, a NLRP3 inhibitor, ameliorates lipopolysaccharide-induced lung inflammation in mice. *Bioorg Med. Chem.* 30, 115954. doi:10.1016/j.bmc.2020.115954

Wang, L., Zhu, Y., Zhang, L., Guo, L., Wang, X., Pan, Z., et al. (2023). Mechanisms of PANoptosis and relevant small-molecule compounds for fighting diseases. *Cell Death Dis.* 14 (12), 851. doi:10.1038/s41419-023-06370-2

Wang, W., Hu, D., Feng, Y., Wu, C., Song, Y., Liu, W., et al. (2020b). Paxilla mediates ATP-induced activation of P2X7 receptor and NLRP3 inflammasome. *BMC Biol.* 18 (1), 182. doi:10.1186/s12915-020-00918-w

Wang, Y., Liu, Y., Bi, X., and Baudry, M. (2020d). Calpain-1 and calpain-2 in the brain: new evidence for a critical role of calpain-2 in neuronal death. *Cells* 9 (12), 2698. doi:10.3390/cells9122698

Wang, Y., Pandian, N., Han, J. H., Sundaram, B., Lee, S., Karki, R., et al. (2022). Single cell analysis of PANoptosome cell death complexes through an expansion microscopy method. *Cell Mol. Life Sci.* 79 (10), 531. doi:10.1007/s00018-022-04564-z

Ware, L. B. (2014). Transfusion-induced lung endothelial injury: a DAMP death? *Am. J. Respir. Crit. Care Med.* 190 (12), 1331–1332. doi:10.1164/rccm.201411-2047ED

Wei, S., Feng, M., and Zhang, S. (2022). Molecular characteristics of cell pyroptosis and its inhibitors: a review of activation, regulation, and inhibitors. *Int. J. Mol. Sci.* 23 (24), 16115. doi:10.3390/ijms232416115

Whidbey, C., Vornhagen, J., Gendrin, C., Boldenow, E., Samson, J. M., Doering, K., et al. (2015). A streptococcal lipid toxin induces membrane permeabilization and pyroptosis leading to fetal injury. *EMBO Mol. Med.* 7 (4), 488–505. doi:10.15252/emmm.201404883

Willson, J. (2024). RIPK3 inhibitor prevents lung damage in severe influenza infection. *Nat. Rev. Drug Discov.* 23 (6), 417. doi:10.1038/d41573-024-00072-w

Wood, S. J., Goldufsky, J. W., Seu, M. Y., Dorafshar, A. H., and Shafikhani, S. H. (2023). *Pseudomonas aeruginosa* cytotoxins: mechanisms of cytotoxicity and impact on inflammatory responses. *Cells* 12 (1), 195. doi:10.3390/cells12010195

Wu, D. D., Pan, P. H., Liu, B., Su, X. L., Zhang, L. M., Tan, H. Y., et al. (2015). Inhibition of alveolar macrophage pyroptosis reduces lipopolysaccharide-induced acute lung injury in mice. *Chin. Med. J. Engl.* 128 (19), 2638–2645. doi:10.4103/0366-6999.166039

Wu, S., Li, Z., Ye, M., Liu, C., Liu, H., He, X., et al. (2021). VX765, a specific caspase-1 inhibitor, alleviates lung ischemia reperfusion injury by suppressing endothelial pyroptosis and barrier dysfunction. *Biomed. Res. Int.* 2021, 4525988. doi:10.1155/2021/4525988

Xia, Y., Huang, P., Qian, Y. Y., Wang, Z., Jin, N., Li, X., et al. (2024). PARP inhibitors enhance antitumor immune responses by triggering pyroptosis via TNF-caspase 8-GSDMD/E axis in ovarian cancer. *J. Immunother. Cancer* 12 (10), e009032. doi:10.1136/jitc-2024-009032

Xiang, M., Shi, X., Li, Y., Xu, J., Yin, L., Xiao, G., et al. (2011). Hemorrhagic shock activation of NLRP3 inflammasome in lung endothelial cells. *J. Immunol.* 187 (9), 4809–4817. doi:10.4049/jimmunol.1102093

Xing, G., Yu, X., Zhang, Y., Sheng, S., Jin, L., Zhu, D., et al. (2023). Macrophages-based biohybrid microrobots for breast cancer photothermal immunotherapy by inducing pyroptosis. *Small* 20, e2305526. doi:10.1002/smll.202305526

Yan, J., Wan, P., Choksi, S., and Liu, Z. G. (2022). Necroptosis and tumor progression. *Trends Cancer* 8 (1), 21–27. doi:10.1016/j.trecan.2021.09.003

Yang, D., Liang, Y., Zhao, S., Ding, Y., Zhuang, Q., Shi, Q., et al. (2020). ZBP1 mediates interferon-induced necroptosis. *Cell Mol. Immunol.* 17 (4), 356–368. doi:10.1038/s41423-019-0237-x

Yang, J., Liu, Z., Wang, C., Yang, R., Rathkey, J. K., Pinkard, O. W., et al. (2018). Mechanism of gasdermin D recognition by inflammatory caspases and their inhibition by a gasdermin D-derived peptide inhibitor. *Proc. Natl. Acad. Sci. U. S. A.* 115 (26), 6792–6797. doi:10.1073/pnas.1800562115

Yang, J., Zhao, Y., Zhang, P., Li, Y., Yang, Y., Yang, Y., et al. (2016a). Hemorrhagic shock primes for lung vascular endothelial cell pyroptosis: role in pulmonary inflammation following LPS. *Cell Death Dis.* 7 (9), e2363. doi:10.1038/cddis.2016.274

Yang, W. L., Sharma, A., Wang, Z., Li, Z., Fan, J., and Wang, P. (2016b). Cold-inducible RNA-binding protein causes endothelial dysfunction via activation of Nlrp3 inflammasome. *Sci. Rep.* 6, 26571. doi:10.1038/srep26571

Yang, X., Lu, H., Xie, H., Zhang, B., Nie, T., Fan, C., et al. (2022). Potent and selective RIPK1 inhibitors targeting dual-pockets for the treatment of systemic inflammatory response syndrome and sepsis. *Angew. Chem. Int. Ed. Engl.* 61 (5), e202114922. doi:10.1002/anie.202114922

Yang, Y., Wang, H., Kouadir, M., Song, H., and Shi, F. (2019). Recent advances in the mechanisms of NLRP3 inflammasome activation and its inhibitors. *Cell Death Dis.* 10 (2), 128. doi:10.1038/s41419-019-1413-8

Yi, C., Chen, F., Ma, R., Fu, Z., Song, M., Zhang, Z., et al. (2022). Serum level of calpains product as a novel biomarker of acute lung injury following cardiopulmonary bypass. *Front. Cardiovasc Med.* 9, 1000761. doi:10.3389/fcvm.2022.1000761

Yi, Y. S. (2020). Functional crosstalk between non-canonical caspase-11 and canonical NLRP3 inflammasomes during infection-mediated inflammation. *Immunology* 159 (2), 142–155. doi:10.1111/imm.13134

Zaid, Y., Puhm, F., Allaeys, I., Naya, A., Oudghiri, M., Khalki, L., et al. (2020). Platelets can associate with SARS-cov-2 RNA and are hyperactivated in COVID-19. *Circ. Res.* 127 (11), 1404–1418. doi:10.1161/CIRCRESAHA.120.317703

Zhang, L., Chen, S., Ruan, J., Wu, J., Tong, A. B., Yin, Q., et al. (2015). Cryo-EM structure of the activated NAIP2-NLRC4 inflammasome reveals nucleated polymerization. *Science* 350 (6259), 404–409. doi:10.1126/science.aac5789

Zhang, L., Jiao, C., Liu, L., Wang, A., Tang, L., Ren, Y., et al. (2021). NLRC5: a potential target for central nervous system disorders. *Front. Immunol.* 12, 704989. doi:10.3389/fimmu.2021.704989

Zhang, M., Xu, G., Zhou, X., Luo, M., Ma, N., Wang, X., et al. (2023). Mesenchymal stem cells ameliorate H9N2-induced acute lung injury by inhibiting caspase-3-GSDME-mediated pyroptosis of lung alveolar epithelial cells. *Eur. J. Pharmacol.* 960, 176148. doi:10.1016/j.ejphar.2023.176148

Zhang, W., Zhu, C., Liao, Y., Zhou, M., Xu, W., and Zou, Z. (2024). Caspase-8 in inflammatory diseases: a potential therapeutic target. *Cell Mol. Biol. Lett.* 29 (1), 130. doi:10.1186/s11658-024-00646-x

Zhao, C., Liang, F., Ye, M., Wu, S., Qin, Y., Zhao, L., et al. (2023). GSDMD promotes neutrophil extracellular traps via mtDNA-cGAS-STING pathway during lung ischemia/reperfusion. *Cell Death Discov.* 9 (1), 368. doi:10.1038/s41420-023-01663-z

Zheng, M., and Kanneganti, T. D. (2020). The regulation of the ZBP1-NLRP3 inflammasome and its implications in pyroptosis, apoptosis, and necroptosis (PANoptosis). *Immunol. Rev.* 297 (1), 26–38. doi:10.1111/imr.12909

Zheng, M., Karki, R., Vogel, P., and Kanneganti, T. D. (2020). Caspase-6 is a key regulator of innate immunity, inflammasome activation, and host defense. *Cell* 181 (3), 674–687.e13. doi:10.1016/j.cell.2020.03.040

Zheng, Z., Deng, W., Bai, Y., Miao, R., Mei, S., Zhang, Z., et al. (2021). The lysosomal rag-ragulator complex licenses RIPK1 and caspase-8-mediated pyroptosis by Yersinia. *Science* 372 (6549), eabg0269. doi:10.1126/science.abg0269

Zhong, W. J., Zhang, J., Duan, J. X., Zhang, C. Y., Ma, S. C., Li, Y. S., et al. (2023). TREM-1 triggers necroptosis of macrophages through mTOR-dependent mitochondrial fission during acute lung injury. *J. Transl. Med.* 21 (1), 179. doi:10.1186/s12967-023-04027-4

Zhou, P., Guo, H., Li, Y., Liu, Q., Qiao, X., Lu, Y., et al. (2021). Monocytes promote pyroptosis of endothelial cells during lung ischemia-reperfusion via IL-1R/NF-κB/NLRP3 signaling. *Life Sci.* 276, 119402. doi:10.1016/j.lfs.2021.119402

Zhou, R., Tardivel, A., Thorens, B., Choi, I., and Tschopp, J. (2010). Thioredoxin-interacting protein links oxidative stress to inflammasome activation. *Nat. Immunol.* 11 (2), 136–140. doi:10.1038/ni.1831

frontiers | Frontiers in Immunology

TYPE Original Research
PUBLISHED 24 March 2025
DOI 10.3389/fimmu.2025.1544610

OPEN ACCESS

EDITED BY
Lulong Bo,
Navy Medical University, China

REVIEWED BY
Jin Bin,
Shandong University, China
Lifeng Huang,
Capital Medical University, China

*CORRESPONDENCE
Fengxue Zhu
Fengxue_Zhu@126.com

†These authors have contributed equally to this work

RECEIVED 13 December 2024
ACCEPTED 05 March 2025
PUBLISHED 24 March 2025

CITATION
Xiao Z, Zhou G, Xue H, Chen L, Zhao X, Li S, Fu C, Wang Z and Zhu F (2025) CMTM3 regulates vascular endothelial cell dysfunction by influencing pulmonary vascular endothelial permeability and inflammation in ARDS. *Front. Immunol.* 16:1544610. doi: 10.3389/fimmu.2025.1544610

CMTM3 regulates vascular endothelial cell dysfunction by influencing pulmonary vascular endothelial permeability and inflammation in ARDS

Ziyan Xiao[1,2,3†], Gang Zhou[1,2†], Haiyan Xue[1,2,3], Lihe Chen[1,2,3], Xiujuan Zhao[1], Shu Li[1,2], Chun Fu[1,2], Zhengzhou Wang[1,2] and Fengxue Zhu[1,2*]

[1]Department of Critical Care Medicine, Peking University People's Hospital, Beijing, China, [2]National Center for Trauma Medicine of China, Peking University People's Hospital, Beijing, China, [3]Beijing Key Surgical Basic Research Laboratory of Liver Cirrhosis and Liver Cancer, Peking University People's Hospital, Beijing, China

Introduction: CMTM3 is a member of the human chemokine-like factor superfamily. The mechanistic role of CMTM3 in acute respiratory distress syndrome (ARDS) is not known. This study investigated the role of CMTM3 in the progression of ARDS and its impact on the function of vascular endothelial cells.

Methods: ARDS modeling in human umbilical vascular endothelial cells (HUVECs) was performed by treating with lipopolysaccharide (LPS) or hypoxia/reoxygenation. We assessed CMTM3 expression levels in the LPS- and hypoxia/reoxygenation-stimulated HUVEC cells. Furthermore, we assessed the role of CMTM3 in the permeability function and inflammatory response of the vascular endothelial cells under ARDS conditions using HUVEC cells with CMTM3 overexpression(adCMTM3) or knockdown(shCMTM3). Concurrently, we generated CMTM3 knockout (CMTM3ko) mice and evaluated the differences in pulmonary vascular permeability, inflammatory lung injury, and survival rates between the CMTM3ko-ARDS and WT-ARDS model mice.

Results: HUVECs stimulated with LPS and hypoxia/reoxygenation showed significantly higher CMTM3 expression compared to the control group ($p<0.05$). Compared with the adsham-HUVECs, adCMTM3-HUVECs stimulated with LPS and hypoxia/reoxygenation demonstrated significantly higher cellular permeability ($p<0.05$) as well as IL-6 and TNF-α expression levels ($p<0.05$). Conversely, shCMTM3-HUVECs stimulated with LPS and hypoxia/reoxygenation showed significantly reduced cellular permeability as well as IL-6 and TNF-α expression levels ($p<0.05$). In vivo ARDS modeling experiments demonstrated that CMTM3-knockout ARDS mice exhibited significantly higher survival rates ($p=0.0194$) as well as significantly reduced lung injury and pulmonary vascular permeability ($p<0.05$) compared to the wild-type ARDS mice.

Discussion: These findings demonstrated that CMTM3 played a critical role in the development of ARDS by influencing permeability of the pulmonary vascular endothelial cells and lung inflammation. Therefore, CMTM3 is a potential therapeutic target in ARDS.

KEYWORDS

ARDS, HUVECs, CMTM3, inflammation, immunosuppression

1 Introduction

Acute Respiratory Distress Syndrome (ARDS) is characterized by progressive hypoxemia and respiratory distress (1). The pathophysiology of ARDS involves damage to the pulmonary capillary endothelial cells and alveolar epithelial cells. This leads to increased permeability of the alveolar membranes, destruction of the alveolar surfactants, formation of hyaline membranes, and alveolar atrophy. This causes diffuse interstitial and alveolar edema in the course of non-cardiogenic illnesses such as severe infections, trauma, and shock. ARDS is one of the most common and serious complications during sepsis (2, 3). About 25% to 50% of patients with severe infections develop ARDS (4). The incidence of ARDS increases with the severity of sepsis. The mortality rate of patients with sepsis-related ARDS is 70% to 90% (5).

Barrier dysfunction is the primary mechanism underlying ARDS and is caused by inflammatory mediators and cytokines (6) as well as oxidative stress. The process of ARDS mainly involves dysregulated inflammatory response and excessive production of cytokines, multinucleated cells, monocytes, macrophages, vascular endothelial cells, and the coagulation and fibrinolytic system. In ARDS, acute inflammatory response directly damages the pulmonary capillary endothelial cells and leads to a cascade of events that indirectly damages the lung tissue (7). Pulmonary capillary endothelial cells represent 20%–30% of the total cell population in the lungs. They play an important role in regulating pulmonary vascular tone and maintaining the function and integrity of the alveolar-pulmonary capillary membrane barrier (7). Pulmonary capillary endothelial cells are both the target cells and effector cells in the ARDS-related inflammatory response. Endothelial barrier dysfunction caused by damage to the lung endothelial cells leads to increased permeability of the vascular endothelium to the plasma proteins and inflammatory cells. This results in pulmonary edema, which leads to ventilation dysfunction and the development of ARDS (8). Currently, clinically approved drugs that effectively target the inflammatory response or endothelial damage are not available for patients with ARDS. Therefore, there is an urgent need to characterize the pathogenetic mechanism underlying endothelial dysfunction in ARDS to identify new targets for the treatment of endothelial barrier disruption and vascular inflammation to slow down disease progression during early stages of ARDS and improve the prognosis of patients.

The CKLF-like MARVEL transmembrane structural domain-containing family (CMTM) is a family of genes with immune functions. It consists of nine genes, including chemokine-like factor (CKLF) and CMTM1-8, which share significant protein sequence homology (9, 10).

CMTM3, a key member of the CMTM family, contains a MARVEL structural domain, which regulates membrane penetration and protein secretion (11). CMTM3 is highly conserved during evolution. The human and murine forms of CMTM3 show 91.8% protein sequence homology (9). CMTM3 plays contradictory roles in different tumors. It functions as an oncogene in gastric cancer and hepatocellular carcinoma (12, 13) but plays a pro-carcinogenic role in gliomas (14). This suggests tissue and cellular heterogeneity in the expression and function of CMTM3. Furthermore, CMTM3 mediates angiogenesis by regulating the levels of VE-cadherin on the surface of endothelial cells at the adherens junction cells, thereby impacting vascular endothelial cell permeability (15). Vascular endothelial function plays a significant role in the pathogenesis of ARDS, but the role and mechanism of CMTM3 in ARDS are not known. Therefore, in this study, we investigated whether CMTM3 played a role in ARDS by affecting vascular endothelial function. Our aim was to provide a scientific basis for CMTM3 as a novel diagnostic biomarker and therapeutic target in ARDS.

2 Materials and methods

2.1 Mice

We obtained 6- to 8-week-old CMTM3 knockout mice and wild-type (WT) mice with the same genetic background from the laboratory of Prof. Wenling Han, Department of Immunology, Peking University School of Medicine. These mice underwent a controlled breeding program to ensure genetic uniformity. All the mice were housed under specific pathogen-free (SPF) conditions at the Animal Center of the People's Hospital of Peking University (Table 1). The environmental conditions were strictly controlled with a temperature range of 22°C–25°C, humidity of 50%–60%, and a 12-h light-dark cycle. The mice were provided free access to food and water. For the experiments, we selected 8- to 10-week-old mice weighing 18–20 g. The mouse experiments adhered to all ethical and moral guidelines for animal experimentation. The experimental

TABLE 1 Mice, cell lines, and reagents.

Reagent/resource	Reference or source	Identifier or catalog number
Experimental models		
Cmtm3$^{-/-}$ C57/BL6 mice	Professor Han Wenling's laboratory at Peking University Health Science Center	N/A
Cmtm3$^{+/+}$ C57/BL6 mice	Professor Han Wenling's laboratory at Peking University Health Science Center	N/A
Experimental cells		
HUVECs	Meisen (CTCC)	N/A
Chemicals, Enzymes and other reagents		
Endothelial Cell Medium	ScienCell	1001
CMTM3 overexpression Lentivirus	Shanghai Jikai Gene Chemistry Co. China	N/A
CMTM3 knockdown Adenovirus	Shanghai Jikai Gene Chemistry Co. China	N/A
Puromycin	Solarbio	P8230
25cm² Rectangular Canted Neck Cell Culture Flask with Vent Cap	Corning	430639
Lipopolysaccharide (MICE)	Solarbio	L8880
Lipopolysaccharide (HUVECs)	Solarbio	IL2020
Evans Blue Stain Solution 0.5%	Solarbio	G1810
HCL (0.1mol/L)	Godow	N/A
TRIzol® Reagent	InvitrogenTM	15596026
RevertAid First Strand cDNA Synthesis Kit	Thermo Scientific	K1622
SYBR® Green real-time PCR master mix	TOYOBO	QPK-201
FITC-Dextran (MW 10000)	MedChemExpress (MCE)	HY-128868
Transwell Permeable Support with 0.4μm Pore Polyester (PET) Membrane	Corning	3470
AnaeroPack-Anaero5%	MITSUBISHI	C-04
2.5L anaerobic culture tank/ culture box	MITSUBISHI	C-31
Oxygen Indicator	MITSUBISHI	C-22
Formamide	LABLEAD	0314

protocol was reviewed and approved by the Animal Experimentation Ethics Committee of the People's Hospital of Peking University (Approval 465 No. 2022PHE058).

2.2 Generation of the ARDS model mice using the HCL/LPS tracheal drip

After inducing general anesthesia and analgesia, the experimental group mice were administered 0.1 ml of HCL (pH = 1.0)/0.1 ml of LPS (10 mg/ml), and the control group mice were administered 0.1 ml of saline through the tracheal drip. After the operation, the mice were carefully transferred to the recovery cages and rewarmed to gain full recovery and consciousness as previously described (16, 17).

2.3 Determination of lung permeability in mice using the Evans blue dye

We first generated the standard curve of the EBD/formamide solution. The lung samples were harvested at 24h after ARDS modeling. Evans blue dye (0.1ml/0.5%) was injected intravenously into the mice 15 min before sampling. The lungs were removed from the chest, and the surface water was dried with filter paper. After removing the surrounding tissues, the lung tissues were cut into smaller pieces, immersed in formamide solution (100 g/20 ml), and incubated at 37°C for 72h in an incubator. After centrifugation, the supernatant was analyzed using a fluorescence spectrophotometer. The amount of Evans blue dye per gram of lung tissue was calculated using the Evans blue-formamide standard curve and reflected pulmonary vascular permeability.

2.4 H&E staining of mouse lung tissue sections

The mice were euthanized after 24h of ARDS modeling. The lung tissue was removed and washed with PBS solution to remove blood. Subsequently, part of the lung tissues were incubated in 4% paraformaldehyde at 4°C overnight. The next day, the tissue samples were dehydrated in 70%–100% ethanol and embedded in paraffin. The paraffin-embedded lung tissues were then sectioned. Subsequently, deparaffinized sections (5 μm thick) were stained with hematoxylin and eosin (H&E) according to standard procedures described previously and photographed under a microscope to observe morphological characteristics, and the Smith scoring method was used to quantify lung injury (Take 10 visual fields and get the average score: Semi-quantitative Analysis of Pulmonary Edema, Alveolar and Interstitial Inflammation, Alveolar and Interstitial Hemorrhage, Atelectasis, and Hyaline Membrane Formation (0–4 Points):0 Points: No injury; 1 Point: Lesion area <25%; 2 Points: Lesion area 25%–50%; 3 Points: Lesion area 50%–75%; 4 Points: Lesion area occupying the entire field of view).

2.5 HUVEC culturing

Human umbilical vein endothelial cells (HUVECs) were cultured in the ECM (ScienCell, USA) medium at 37°C and 5%

CO_2 in a humidified incubator. The cells were regularly assessed for mycoplasma contamination. Cells were passaged twice a week. They were washed with FBS, digested with trypsin (0.05%) solution, and resuspended in ECM medium.

2.6 Generation of HUVECs with stable CMTM3 overexpression

The CMTM3 overexpression lentiviral vector was constructed by the Shanghai Jikai Gene Chemistry Co. Ltd (Shanghai, China). We constructed plasmids carrying the target gene as well as helper plasmids for viral packaging; these plasmids were co-transfected into HEK293T cells using the liposome method. The viral seeds were subsequently harvested and amplified, followed by purification of the virus. Through this process, we successfully generated adenoviruses overexpressing CMTM3 (adCMTM3) and a control adenovirus (with sham virus containing an empty expression vector, adsham). HUVECs were transduced with different concentrations of the adenoviruses particles encoding the *CMTM3* gene to screen for appropriate MOI values (MOI = 10). The transduced cells were screened with ECM medium containing 1 μg/ml puromycin to identify stably transduced strains, which were then used for subsequent experiments.

2.7 Generation of HUVECs with CMTM3 knockdown

To target the CMTM3 gene sequence, shRNA sequences were designed according to RNA interference (RNAi) principles for the construction of shRNA plasmids. The lentiviral backbone used in this study contains a puromycin resistance gene for eukaryotic selection. After obtaining the purified plasmid with confirmed correct sequencing, lentivirus packaging will be carried out using HEK293T cells. Subsequently, HUVECs were co-cultured with different concentrations of lentivirus containing CMTM3 shRNA and a control lentivirus (with sham virus containing an empty expression vector, shsham) after being screened for appropriate MOI values (MOI = 10). The selection of stable transfectants via puromycin resistance and the transduced cells were passaged in the ECM medium for further experiments.

2.8 LPS-stimulated/hypoxia/reoxygenation-stimulated HUVEC models

HUVECs growing exponentially were incubated with different concentrations of LPS, and total cellular RNA was extracted at different time points and analyzed by real-time quantitative reverse transcription polymerase chain reaction (qRT-PCR). After initial screening, subsequent experiments were performed for 6h using 100 ng/ml LPS. Exponentially growing HUVECs were placed in a hypoxia tank (for 4h or 5h) with an AnaeroPack-Anaero5% (to ensure 1% O_2 and 5% CO_2). The cells were reoxygenated for 2h after hypoxic exposure for different time periods (place the hypoxia tank in a normal incubator to ensure the temperature and humidity required for cell growth). Total cellular RNA was extracted from the cells and analyzed by qRT-PCR. After initial screening, the cells were exposed to 4h of hypoxia and 2h of reoxygenation for the subsequent experiments.

2.9 Real-time fluorescence quantitative PCR

Total cellular RNA was extracted using the Trizol method and quantified. Subsequently, cDNA was prepared by reverse transcription using the Revertra Ace qPCR RT Master Mix with gDNA Remover according to the manufacturer's instructions. Then, qPCR was performed using the SYBR® Green Realtime PCR Master Mix. The expression levels of the target genes were estimated relative to GAPDH using the double delta Ct value method ($2^{-\Delta\Delta Ct}$). The qPCR primers are listed in Table 2.

2.10 Estimation of cell permeability using the FITC-dextran assay

The cells were trypsin-digested, harvested, and resuspended in ECM medium. Then, 200 μl (1×10^5) cells were seeded in the upper chamber of the Transwell, 600 μl ECM medium in the down chamber, and cultured cells attached and reached a monolayer cell barrier layer. Then, after LPS-stimulated/hypoxia/

TABLE 2 Quantitative PCR primers.

Gene name	Direction	Primer sequence (5′ to 3′)
Human qPCR primer pair		
CMTM3	Forward	AATGACAAGTGGCAGGGCT
	Reverse	TTGTGGGCTGTGGTCTCAT
IL-6	Forward	AGACAGCCACTCACCTCTTCAG
	Reverse	TTCTGCCAGTGCCTCTTTGCTG
TNF-α	Forward	CTCTTCTGCCTGCTGCACTTTG
	Reverse	ATGGGCTACAGGCTTGTCACTC
GAPDH	Forward	GAAGGTGAAGGTCGGAGTC
	Reverse	GGAAGATGGTGATGGGATTT
Mouse qPCR primer pair		
IL-6	Forward	TACCACTTCACAAGTCGGAGGC
	Reverse	CTGCAAGTGCATCATCGTTGTTC
TNF-α	Forward	GGTGCCTATGTCTCAGCCTCTT
	Reverse	GCCATAGAACTGATGAGAGGGAG
GAPDH	Forward	CATCACTGCCACCCAGAAGACTG
	Reverse	ATGCCAGTGAGCTTCCCGTTCAG

10.3389/fimmu.2025.1544610

reoxygenation-stimulated, 0.1 mg/ml FITC (fluorescein isothiocyanate)-labeled dextran was added to the ECM medium in the upper chamber of the transwell. After 15 min of incubation, medium from the lower chamber of the transwell was collected and the fluorescence signals were estimated using the Fluoroskan Ascent FL plate reader (Thermo Scientific, Waltham, MA) at 485 nm excitation and 538 nm emission. Comparative FITC-dextran concentrations were calculated based on fluorescence intensity to assess the cell layer permeability.

2.11 Transcriptome sequencing

Total RNA was isolated from the CMTM3-knockdown cells using the Trizol reagent. Subsequently, mRNA sample libraries were constructed, and high-throughput sequencing was performed by the Shanghai Zhongke New Life Biotechnology Co. Ltd. (Shanghai, China). Briefly, after quantitation of the total RNA samples, the mRNA was purified by poly-dT oligo-linked magnetic beads. The enriched mRNA fragments were then divided into shorter fragments. The fragmented mRNAs were used as templates for library construction. Once the libraries passed quality control, the sequencing data was generated using the Illumina/BGI platform, and bioinformatics analysis (GOrich, KEGG, PPI) was performed.

2.12 Statistical analysis

Statistical analysis was performed using the GraphPad Prism 8.4.1 software (GraphPad Software Inc., San Diego, CA, USA). Unpaired two-tailed Student's t-test was used for comparisons between two groups. One-way ANOVA and Dunnett's *post hoc* test were used for comparisons between more than two groups. $P < 0.05$ was considered statistically significant.

3 Results

3.1 CMTM3 expression levels are significantly altered in the LPS or hypoxia/reoxygenation-stimulated HUVECs

Initially, we generated *in-vitro* ARDS models in the HUVECs and analyzed CMTM3 expression levels under ARDS inflammatory conditions. To simulate ARDS *in vitro*, we used lipopolysaccharide (LPS) stimulation or hypoxia followed by reoxygenation (hypoxia/reoxygenation). First, we stimulated exponentially growing HUVECs with100 ng/ml of LPS for 2h, 6h, and 24h, and analyzed CMTM3 levels. CMTM3 expression levels were significantly higher in the LPS-stimulated HUVEC cells at all time points compared to the control unstimulated HUVECs, with 6h time point showing the highest level of CMTM3 expression ($p < 0.001$) (Figure 1A). In the hypoxia/reoxygenation ARDS model, HUVEC cells were subjected to hypoxia for 4h followed by reoxygenation for 2h or hypoxia for 5h followed by reoxygenation for 2h Compared with the unstimulated HUVECs, the expression levels of CMTM3 were significantly increased by hypoxia/reoxygenation treatment and were highest in the 4h-hypoxia/2h-reoxygenation-treated HUVECs ($P < 0.001$) (Figure 1B).

3.2 Changes in the permeability of HUVECs with CMTM3 overexpression or knockdown after LPS or hypoxia/reoxygenation stimulation

To investigate the effect of CMTM3 overexpression on the vascular endothelial cell permeability during ARDS-induced inflammatory state, we transfected HUVECs with lentiviruses carrying the CMTM3-overexpressing vector at a MOI of 10 and screened for stably transfected HUVECs overexpressing CMTM3

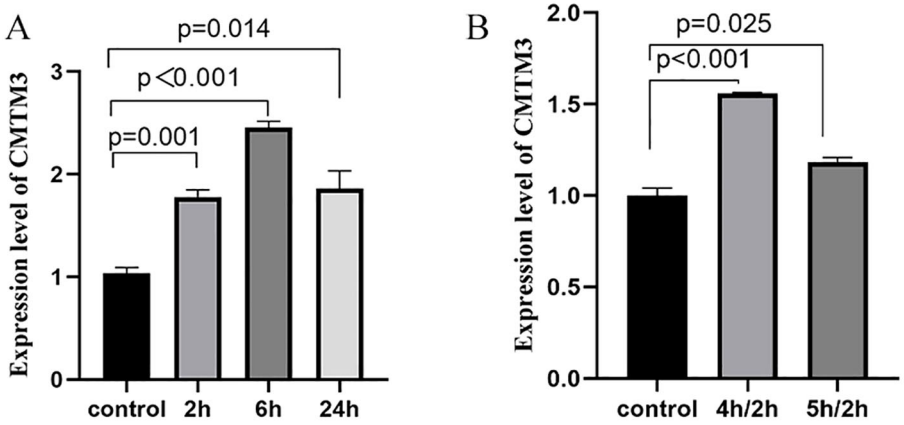

FIGURE 1
(A) The expression levels of CMTM3 transcripts in human umbilical vein endothelial cells (HUVECs) treated with 100 ng/ml LPS for 2h, 6h, and 24h ($n \geq 3$). **(B)** The expression levels of CMTM3 transcripts in HUVECs subjected to stimulation with 4h-hypoxia/2h-reoxygenation and 5h-hypoxia/2h-reoxygenation. Unstimulated HUVECs were used as the control ($n \geq 3$).

(adCMTM3) ($p < 0.0001$) (Figure 2A). Subsequently, we analyzed permeability of the control(adsham) and adCMTM3 HUVECs in the monolayer using the FITC-Dextran assay, adCMTM3HUVECs showed significantly higher endothelial cell permeability (RFI) under unstimulated conditions ($p = 0.0007$, $p = 0.0027$) (Figures 2B, C), as well as when stimulated with 100 ng/ml LPS for 6h ($P = 0.0017$) (Figure 2B) and after 4h hypoxia and 2h of reoxygenation ($p = 0.003$) (Figure 2C) compared with the corresponding controls.

Next, to further investigate the role of CMTM3 in vascular endothelial cell permeability, we transfected HUVECs with lentivirus containing CMTM3 shRNA at a MOI of 10 to knockdown CMTM3 expression levels in the HUVECs and verified the CMTM3 knockdown (shCMTM3-HUVECs) levels against shsham HUVECs ($p < 0.0001$) (Figure 3A). Subsequently, we compared the cell permeability of the control and shCMTM3 HUVECs in the monolayer. FITC-Dextran assay results demonstrated that the permeability of shCMTM3 HUVECs was significantly reduced compared with the shsham HUVECs ($p = 0.0058$, $p = 0.009$) (Figure 3B). Furthermore, when stimulated with 100 ng/ml LPS for 6h, cellular permeability of the shCMTM3-HUVECs was significantly lower than the control group ($P = 0.002$) (Figure 3B). Moreover, when treated with 4h of hypoxia followed by 2h of reoxygenation, cellular permeability of the shCMTM3-HUVECs was significantly lower than the shsham HUVECs ($P < 0.0001$) (Figure 3C).

3.3 Evans blue leakage assay demonstrates reduced lung leakage in the CMTM3 knockout ARDS model mice

To further confirm the *in-vivo* function of CMTM3 in the lung vascular endothelial permeability and ARDS, we generated CMTM3 knockout mice (Figure 4A).

In the HCL-ARDS model, we observed significantly lower leakage of Evans blue dye from the lungs of the CMTM3-KO mice compared to the WT mice as shown in the lung tissue images (Figure 4B).

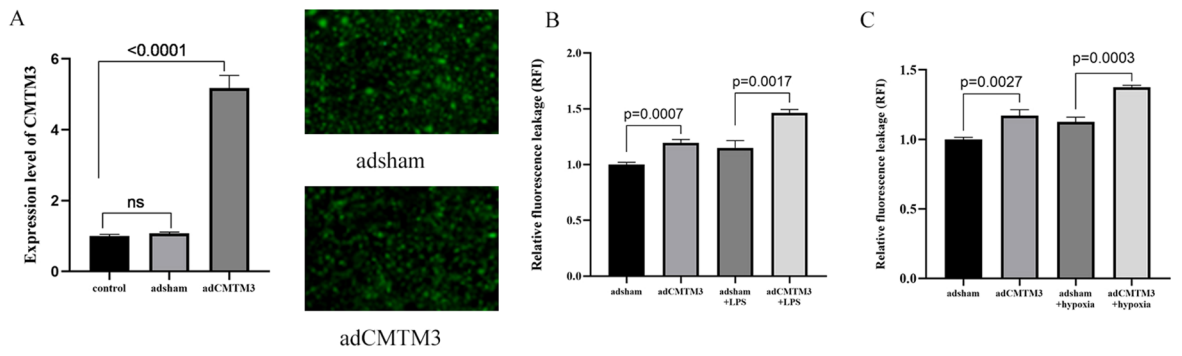

FIGURE 2
CMTM3 overexpression enhances permeability of the human umbilical vein endothelial cells (HUVECs) under *in-vitro* ADRS inflammatory conditions ($n \geqq 3$). **(A)** CMTM3 expression levels in control HUVECs as well as adsham and adCMTM3-transfected HUVECs. **(B)** FITC-dextran assay results show the cellular permeability based on relative fluorescence leakage (RFI) in the adsham- and adCMTM3-transfected HUVECs that were untreated or treated with 100 ng/ml LPS for 6h. **(C)** FITC-Dextran assay results show the cellular permeability based on relative fluorescence leakage (RFI) in the adsham- and adCMTM3-transfected HUVECs that were untreated or treated with 4h-hypoxia/2h-reoxygenation.

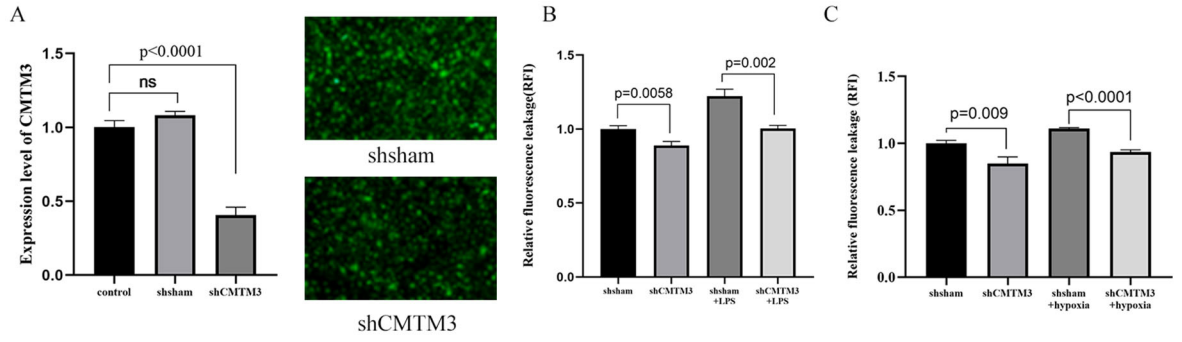

FIGURE 3
CMTM3 knockdown reduces human umbilical vein endothelial cell (HUVEC) permeability under *in-vitro* inflammatory conditions. **(A)** CMTM3 expression levels in the control, shsham, and shCMTM3 HUVECs. **(B)** FITC-dextran assay results show the cellular permeability based on relative fluorescence leakage (RFI) in the shsham and shCMTM3-transfected-HUVECs that were untreated or treated with 100 ng/ml LPS for 6h. **(C)** FITC-dextran assay results show the cellular permeability based on relative fluorescence leakage (RFI) of shsham and shCMTM3-transfected HUVECs that were untreated or treated with 4h-hypoxia/2h-reoxygenation.

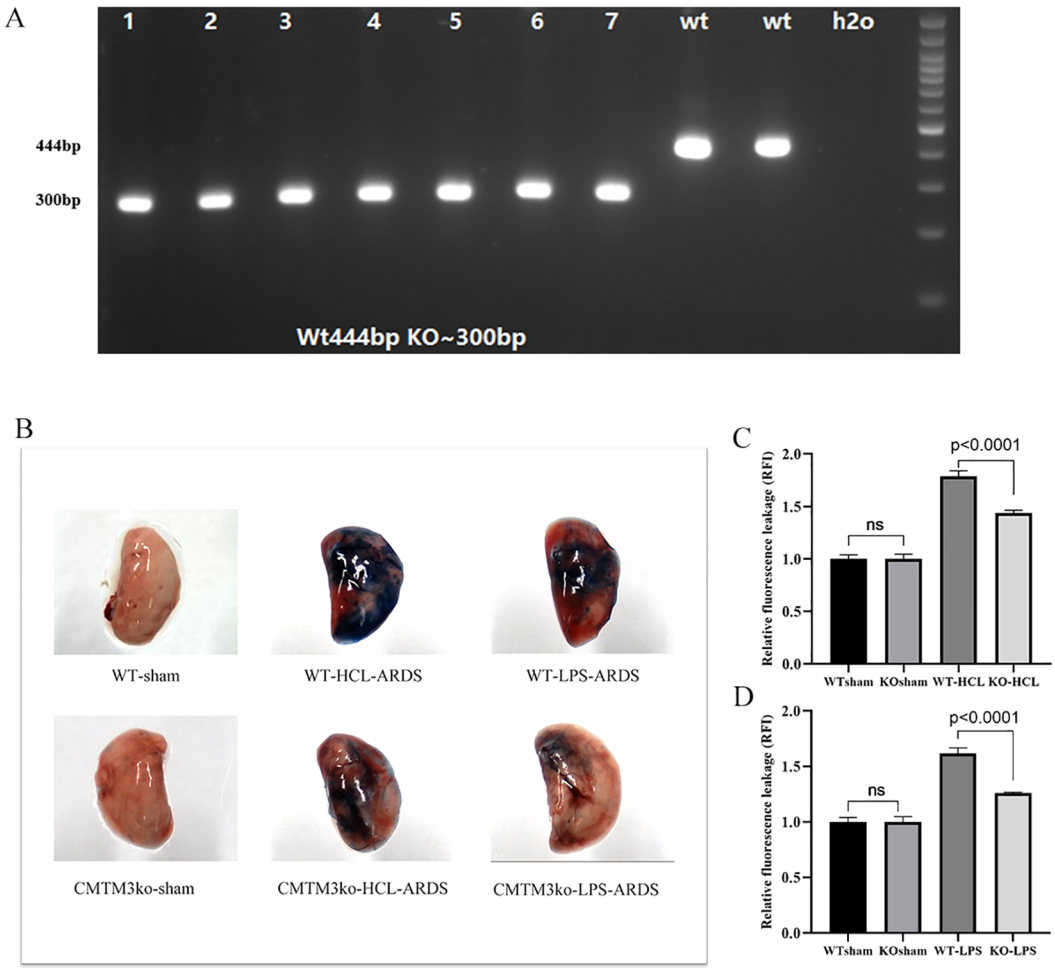

FIGURE 4
In-vivo analysis of lung tissue permeability in the CMTM knockout ARDS model mice (n = 5 per group). **(A)** Polymerase chain reaction (PCR) analysis confirming the genotypes of the in-bred CMTM3 knockout mice. CMTM knockout mice show a 300 bp PCR product compared to the 444 bp product in the wild-type (WT) mice. **(B)** Picture of Evans blue dye leakage analysis of lungs after HCl and lipopolysaccharide (LPS)–based acute respiratory distress syndrome (ARDS) modeling **(C)** Evans blue dye leakage analysis of lungs after HCl-based ARDS modeling of the WT and CMTM knockout mice. **(D)** Evans blue dye leakage analysis of lungs after LPS-based ARDS modeling of the WT and CMTM knockout mice.

Quantification of Evans blue dye fluorescence also showed significantly reduced leakage from the lungs of the CMTM3KO-ARDS model mice compared with the WT-ARDS model mice ($P < 0.0001$, Figure 4C). Similar results were obtained in the LPS-ARDS model. The WT mice showed significantly higher extent of lung injury and EB dye leakage ($p < 0.0001$) (Figure 4D) compared to the CMTM3-KO mice after 24h of ARDS modeling. However, there were no significant differences in the EB dye leakage between the lungs of sham-treated WT and CMTM3-KO mice ($p > 0.05$).

3.4 Effect of CMTM3 on lung inflammation

To investigate the effects of CMTM3 on the inflammatory state in ARDS, we first *in vitro* stimulated HUVECs with LPS for 2h, 6h, and 24h or with hypoxia (4h or 5h)/2h reoxygenation and analyzed the levels of inflammatory cytokines IL-6 and TNF-α. In the LPS model of ARDS, both IL-6 and TNF-α levels increased significantly and reached their peak at the 6h time point ($p < 0.001$ and $p < 0.0001$; Figure 5A). In the hypoxia/reoxygenation model of ARDS, the levels of IL-6 and TNF-α increased significantly compared with the control and reached peak levels when stimulated with hypoxia for 5h followed by 2h of reoxygenation ($p = 0.0146$ and $p = 0.0002$) (Figure 5B).

Subsequently, CMTM3-overexpressing or knockdownHUVECs were treated with LPS to determine the potential effects of CMTM3 expression on the ARDS-related inflammatory state. Compared with the controls, IL-6 and TNF-α levels in the CMTM3-overexpressing HUVECs were significantly elevated when stimulated with LPS ($p = 0.0004$ and $p = 0.0072$; Figure 6A) and 4h/2h hypoxia/reoxygenation ($p < 0.0001$ and $p = 0.0174$; Figure 6B). In contrast, CMTM3-knockdown HUVECs demonstrated significantly reduced levels of IL-6 and TNF-α after stimulation with LPS ($p = 0.0078$ and $p = 0.0068$; Figure 6C) and 4h/2h hypoxia/reoxygenation ($P < 0.0001$ and $p = 0.0006$; Figure 6D).

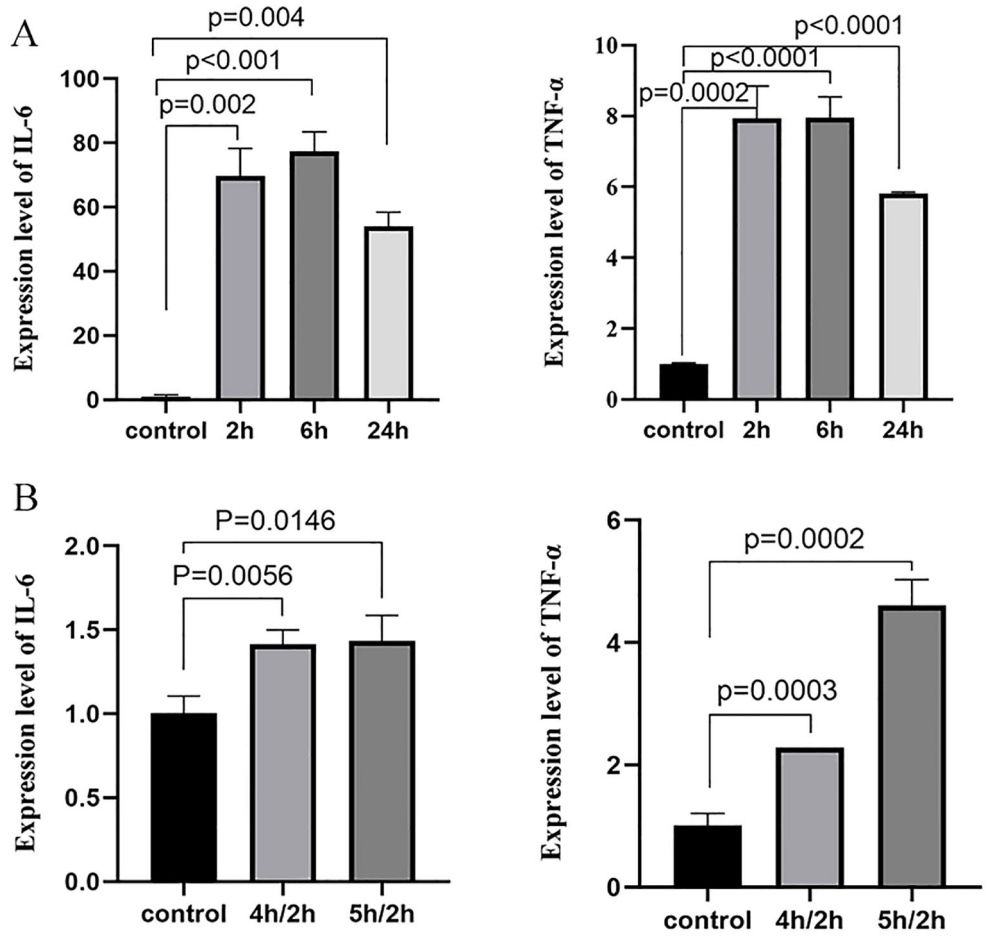

FIGURE 5
IL-6 and TNF-α expression levels after **(A)** stimulation with 100 ng/ml LPS for 2h, 6h, and 24h, and **(B)** stimulation with 4h/2h and 5h/2h hypoxia/reoxygenation. ($n \geq 3$).

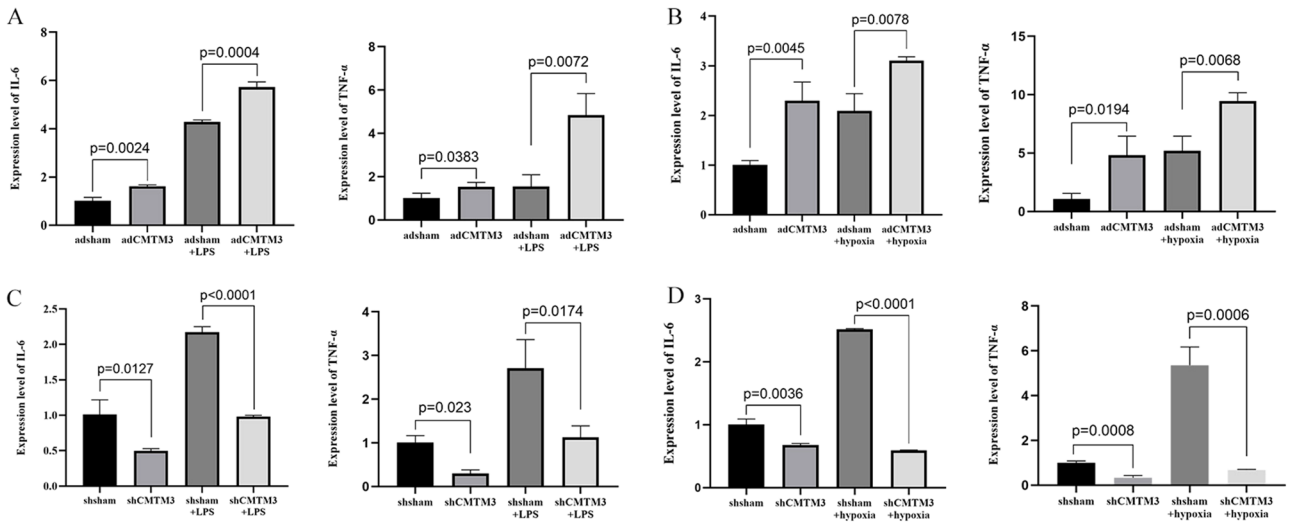

FIGURE 6
The expression levels of IL-6 and TNF-α in the adCMTM3- and shCMTM3-transfected HUVECs after **(A, C)** LPS stimulation for 6 h and **(B, D)** 4h/2h hypoxia/reoxygenation treatment.

3.5 Effect of CMTM3 knockout on the lung inflammatory status in the ARDS model mice

Next, we analyzed the degree of lung injury and inflammation status in the ARDS model CMTM3KO and WT mice. ARDS modeling was performed by two different methods, namely, tracheal drip dilute HCL (WT-HCL-ARDS and CMTM3KO-HCL-ARDS mice) and tracheal drip LPS (WT-LPS-ARDS and CMTM3KO-LPS-ARDS mice). The expression levels of inflammatory factors and lung injury were analyzed in the mice after 24h of modeling. CMTM3KO-HCL-ARDS mice showed reduced lung injury (Figure 7A, p = 0.0017), and significantly lower expression levels of IL-6 and TNF-α (p = 0.0046 and p = 0.0113; Figure 7B) than the WT-HCL-ARDS mice. Furthermore, CMTM3KO-LPS-ARDS mice showed reduced lung injury (Figure 7A, p = 0.0003) and significantly lower expression levels of IL-6 and TNF-α (p = 0.0144 and p = 0.0034; Figure 7C) compared to the WT-LPS-ARDS mice.

3.6 RNA sequencing data analysis

To further determine the role of CMTM3 in the lung endothelial cells during the development of ARDS, we treated shCMTM3-HUVECs and the shsham-HUVECs with LPS for 6h. Subsequently, we harvested total cellular RNA and performed sequencing and RNA transcriptome analysis. Differentially regulated genes (DEGs) were identified between the LPS-treated shCMTM3-HUVECs and shsham-HUVECs. Functional enrichment analysis was performed to determine the upregulated or downregulated KEGG pathways enriched by the DEGs. Our data showed that the TNF signaling pathway and NF-κ B signaling pathway were downregulated in the shCMTM3-HUVECs compared to the shsham group (Figure 8A). Furthermore, compared to the LPS-stimulated shsham-HUVECs, LPS-stimulated shCMTM3-HUVECs showed downregulation of the IL-17 signaling pathway, TNF signaling pathway, and NF-κ B signaling pathway (Figure 8B).

PPI analysis also demonstrated upregulation of VE-calmodulin-dependent factors such as CCL2, CXCL8, and CXCL10 in the shCMTM3-HUVECs compared to the shsham group (Figure 8C). Furthermore, expression levels of CCL2, CXCL8, and CXCL10 were further increased after LPS stimulation in the CMTM3ko-HUVECs (Figure 8D).

3.7 Effect of CMTM3 knockdown on the survival outcomes after ARDS modeling

Finally, we analyzed the effects of CMTM3 knockdown on the survival outcomes of the ARDS model mice. Kaplan–Meier survival curve analysis demonstrated that the survival rate of the CMTM3ko-ARDS model mice was significantly longer than the WT-ARDS model mice (p = 0.0194, Figure 9).

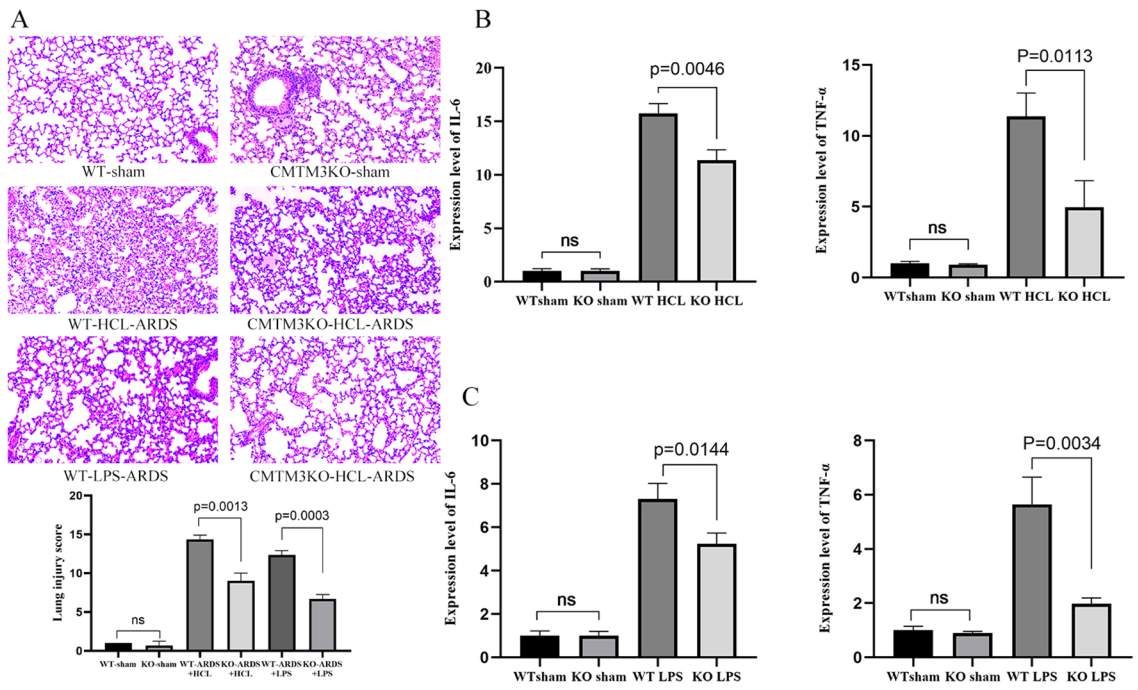

FIGURE 7
(A) Pictures and Smith scoring of lung injury of wild-type (WT) and CMTM3ko mice after tracheal drip dilute HCL/lipopolysaccharide (LPS) modeling (n = 5 per group). **(B)** Lung injury and expression levels of IL-6 and TNF-α in the lungs of the WT and CMTMko mice after tracheal drip dilute HCL modeling (n = 5 per group). **(C)** Lung injury and expression levels of IL-6 and TNF-α in the lungs of the WT and CMTMko mice after tracheal drip LPS modeling (n = 5 per group).

10.3389/fimmu.2025.1544610

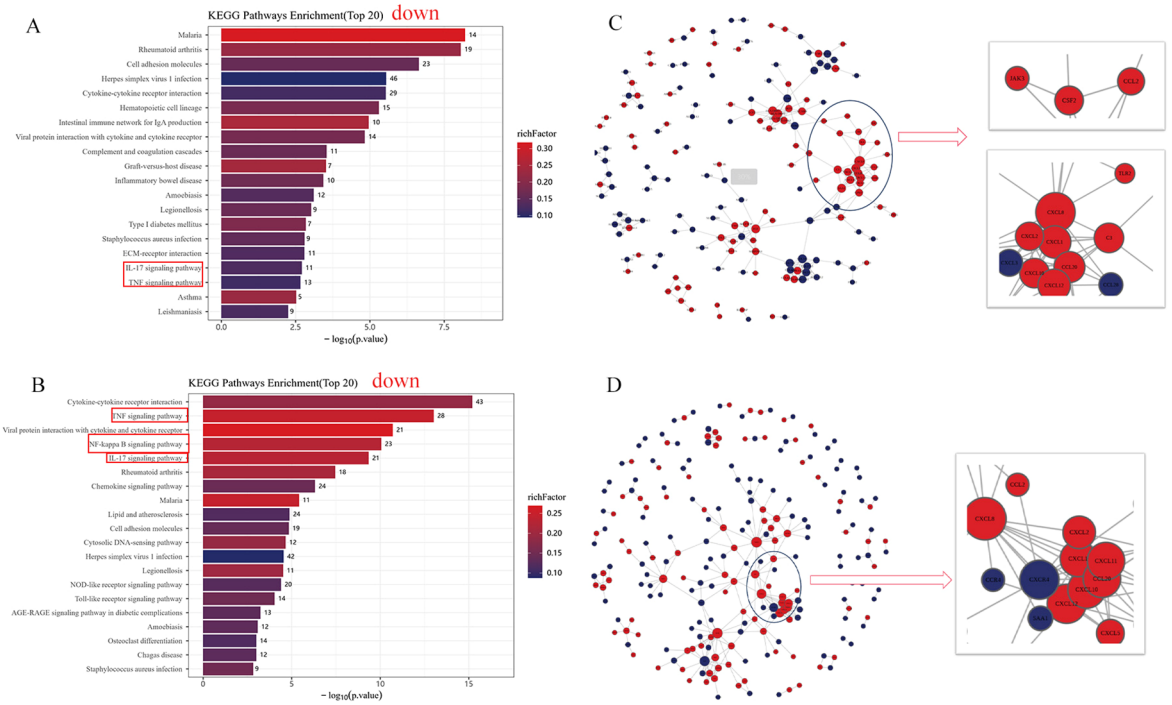

FIGURE 8
RNA sequencing analysis of lipopolysaccharide (LPS)–treated shCMTM3-HUVECs. **(A)** Top 20 KEGG pathways representing DEGs between shCMTM3-HUVECs and shsham- human umbilical vein endothelial cells (HUVECs). **(B)** Top 20 KEGG pathways between LPS-treated shCMTM3-HUVECs and LPS-treated shsham-HUVECs. **(C)** PPI network analysis of DEGs between shCMTM3-HUVECs and shsham-HUVECs. **(D)** PPI network analysis of DEGs between LPS-treated shCMTM3-HUVECs and LPS-treated shsham -HUVECs.

4 Discussion

The pathogenesis of ARDS has not been fully elucidated. In ARDS, systemic inflammatory response triggered by the inflammatory cells leads to the release of excessive amounts of pro-inflammatory mediators and cytokines, which in-turn damages the alveolar-capillary barrier leading to lung injury (18). The alveolar-capillary barrier consists of thin layers of alveolar epithelial cells and capillary endothelial cells separated only by a thin basement membrane to facilitate gas exchange (19). Inflammatory response during ARDS results in the secretion of pro-inflammatory factors, such as TNF-α and IL-6 (20), which promote recruitment of inflammatory cells from the capillaries to the intra- and inter-alveolar compartments. The inflammatory cells produce large amounts of proteolytic enzymes, which extensively damage the alveolar endothelial and epithelial cells. This significantly reduces the levels of alveolar surface-active substances and leads to an increase in permeability and shedding of endothelial surface anticoagulant molecules, including coagulation regulatory proteins and the endothelial cell protein C receptor. Furthermore, upregulation of pro-coagulant molecules contributes to the formation of thrombus in the microvessels and leakage of the plasma fluids into the alveoli and the interstitium. Subsequently, this results in pulmonary edema and formation of hyaline membranes inside the alveoli and atelectasis (21). Throughout the injury process, pulmonary vascular endothelial cells are both damaged as well as activated by various factors. This alters their metabolic and regulatory functions and contributes further to the development and progression of ARDS (22). Damage to the pulmonary endothelial cells impairs endothelial cell-to-cell connectivity and increases vascular endothelial cell permeability, thereby leading to endothelial barrier dysfunction and disease progression (23). Therefore, early identification and intervention of pulmonary endothelial cell damage is necessary to suppress endothelial cell dysfunction and improve the prognosis of ARDS patients.

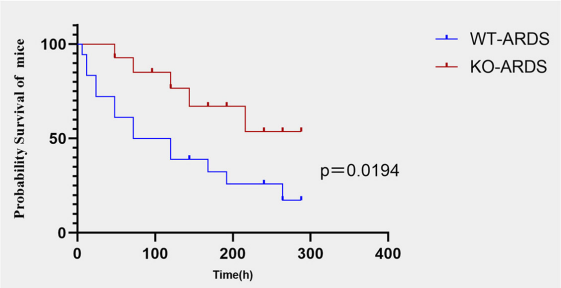

FIGURE 9
Kaplan–Meier survival curve analysis shows survival rates of the CMTM3ko-ARDS and WT-ARDS mice (*n* = 15 per group).

Previous studies have shown that CMTM family members regulate tumor cell growth and migration in different types of cancer (24). Yuan et al. demonstrated that increased CMTM3

expression in gastric cancer cells inhibited tumor cell growth and promoted apoptosis (12). However, the function of CMTM3 in normal cell types has not been studied in detail.

Our study showed that CMTM3 expression was significantly increased in the HUVECs that were treated with LPS or hypoxia/reoxygenation. The highest CMTM3 expression was observed in HUVECs stimulated with LPS for 6h ($p < 0.001$) and 4h of hypoxia followed by 2h of reoxygenation ($p < 0.001$). Furthermore, in the *in vitro* LPS-ARDS modeling experiments, CMTM3-overexpressing HUVECs showed significantly higher permeability ($p = 0.0017$), whereas CMTM3 knockdown HUVECs demonstrated reduced permeability ($p = 0.0003$). Moreover, in the *in-vitro* hypoxia/reoxygenation-ARDS model experiments, CMTM3-overexpressing HUVECs showed increased permeability ($p = 0.002$), whereas CMTM3 knockdown HUVECs showed reduced permeability ($p < 0.0001$).

We also successfully generated CMTM3 knockout mice and induced ARDS using the tracheal drip HCL method or tracheal drip LPS method. After 24h of HCL-ARDS modeling, the EB leakage in the lungs of the CMTM3ko mice was significantly attenuated compared to the WT mice ($p < 0.0001$). Lung injury was more severe in the tracheal drip HCL model compared with the tracheal drip LPS model. However, in the LPS-ARDS model, lung leakage was significantly reduced in the CMTM3ko mice compared to the WT mice ($p < 0.0001$). Chrifi et al. reported that Consistent with the increased monolayer cell permeability of HUVECs after overexpression of CMTM3-overexpressing HUVECs enhanced permeability and endothelial barrier function as shown by transendothelial electrical impedance measurements *in vitro* (15). This suggested that CMTM3 played a key mechanistic role in the endothelial cell dysfunction underlying ARDS by affecting endothelial cell permeability. RNA sequencing data analysis also showed that the expression of CCL2, CXCL8, and CXCL10 was upregulated in the shCMTM3 HUVECs. Furthermore, the expression of CCL2, CXCL8, and CXCL10 was significantly increased in the shCMTM3-HUVECs compared with the shsham group after LPS stimulation. Previous studies have demonstrated that increased expression of CCL2, CXCL8, and CXCL10 is dependent on the expression of VE-Cadherin (25). Maintenance of vascular endothelial integrity is dependent on the vascular endothelial intercellular junctional structures. Vascular endothelial cadherin (VE-cadherin) is located throughout the basement membrane and forms cis-dimers on the cell surface. The homeostatic level of VE-cadherin is dependent on the rate of endocytosis and degradation (26). In the pathological state, VE-cadherin on the cell membrane surface undergoes phosphorylation after stimulation by factors such as VEGF and LPS, and dissociates from the intercellular junctional complex. Subsequently, VE-cadherin is endocytosed by the vesicles and incorporated into the early endosomes. This results in the disruption and increased permeability of the vascular barrier (27). We found that the expression levels of VE-cadherin–dependent genes such as CCL2, CXCL8, and CXCL10 were upregulated in the LPS-stimulated shCMTM3 HUVECs compared with the controls. This suggested that the knockdown of CMTM3 exerted a protective effect against vascular endothelial damage in the LSP-stimulated HUVECs. Therefore, we hypothesize that CMTM3 modulates endothelial cell permeability by affecting endothelial intercellular junctional structure and function via VE-cadherin. CXCL8 (chemokine IL-8) is a pro-inflammatory cytokine with the ability to chemotactically attract neutrophils to sites of inflammation and inhibit neutrophil apoptosis. IL-8 is involved in ARDS mainly through the chemokine receptor CXCR2, which regulates neutrophil migration (28). Furthermore, IL-8 promotes angiogenesis (29). In our study, RNA sequencing analysis showed that the expression levels of IL-8 were elevated in the CMTM3 knockdown HUVECs. However, we did not observe upregulation of the IL-8 pro-inflammatory pathway and the expression of CXCR1/CXCR2, a related receptor. This suggested that upregulation of IL-8 in the CMTM3 knockdown HUVECs may promote angiogenesis, but the specific mechanism of action needs to be explored in further studies.

Inflammatory response is an important mechanism underlying the pathogenesis of ARDS. In the preliminary stages of ARDS, cells of the intrinsic immune system, such as macrophages, neutrophils, and nonspecific T cells, as well as other immune response-related proteins act as first-line effectors to scavenge antigens and induce an inflammatory response at the site of injury. This is followed by effective control of the inflammatory response by specific immune cells such as T cells and B cells (30). TNF-α and IL-6 play an important role as pro-inflammatory factors in the development of ARDS. TNF-α is an early response cytokine that plays a critical role in triggering inflammatory response. Therefore, anti–TNF-α drugs are the earliest interventions to enter clinical trials for ARDS. Toll-like receptor 4 (TLR4)–NF-κB signaling pathway, NF-κB signaling pathway, and p38 mitogen-activated protein kinase (p38MAPK) signaling pathway are the main inflammation-signaling pathways that are associated with the development of ARDS (26, 27, 31). LPS stimulation of HUVECs activates the downstream NF-κB signaling pathway by recognizing and binding transduction signaling receptors on the cell membrane. Furthermore, other inflammatory factors, such as TNF-α can directly act on the upstream protein kinase IKK through one or more signaling pathways. The phosphorylation of NF-κB inhibitory protein (IκB) promotes dissociation of the active NF-κB, which then translocates from the cytoplasm into the nucleus and regulates expression of several inflammation-related genes. In addition, positive feedback activation of NF-κB leads to a dramatic increase in the recruitment of pro-inflammatory and chemokine-mediated inflammatory cells, thereby significantly enhancing the inflammation response (31). In this study, expression levels of inflammatory factors such as IL-6 and TNF-α were significantly elevated in the adCMTM3 HUVECs ($p = 0.0004$ and $p = 0.0072$) and significantly reduced in the shCMTM3 HUVECs ($p < 0.0001$ and $p = 0.0174$) compared with the controls after LPS stimulation. Similarly, expression levels of IL-6 and TNF-α were significantly increased in the adCMTM3 HUVECs ($p = 0.0078$ and $p = 0.0068$) and significantly reduced in the shCMTM3 HUVECs ($p < 0.0001$ and $p = 0.0006$) compared to the controls after hypoxic/reoxygenation stimulation. In the experiments with mice, results from both the tracheal drip HCL and LPS models showed that lung injury was significantly reduced in the CMTM3ko-ARDS mice compared to the WT-ARDS mice.

Furthermore, IL-6 and TNF-α levels were also reduced in the lungs of the CMTM3ko-ARDS mice compared to the WT-ARDS mice ($p < 0.05$) in both the tracheal drip HCL and LPS models. This suggested that CMTM3 knockdown decreased the production of pro-inflammatory factors IL-6 and TNF in the vascular endothelial cells after LPS and hypoxic stimulation, thereby downregulating inflammation in the ARDS mice. Therefore, we performed RNA sequencing analysis of the shsham and shCMTM3 HUVEC cells and observed that the IL-17 signaling pathway, TNF signaling pathway, and NF-κ B signaling pathway were significantly reduced in the shCMTM3 HUVECs compared with the shsham-HUVECs when stimulated by exogenous LPS. This result suggested that CMTM3 knockdown effectively inhibited LPS-induced inflammation in the endothelial cells inflammation. Taken together, this suggested that CMTM3 knockdown may effectively reduce lung damage by inhibiting inflammation and related pathways during the onset of ARDS.

Most importantly, in our *in-vivo* mouse ARDS modeling experiments, the survival rate of the CMTM3ko-ARDS model mice using the tracheal drip LPS method was significantly higher than that of WT ARDS mice ($p = 0.0194$). This suggested that the knockout of the CMTM3 gene not only ameliorated lung injury and inflammation in the ARDS model mice, but also improved the survival outcomes of the mice.

This study has a few limitations. First, we used HUVEC cells instead of lung endothelial cells (HPMECs) as our *in-vitro* model. Although both are endothelial cells, there may be few functional differences between them. Therefore, we plan to follow up by performing similar experiments with the HPMECs regarding the mechanistic action of CMTM3. Second, we used only male mice for the murine ARDS model. Therefore, in the future, to avoid gender bias, we will analyze the function of CMTM3 in female mice through ARDS modeling, and compare data with the male mice. Thirdly, our results suggested that CMTM3 regulated endothelial cell permeability, but the exact molecular mechanisms are unknown. Therefore, we will follow up with co-localization and CO-IP experiments to further investigate the mechanistic role of CMTM3 in ARDS.

In summary, our study suggested that CMTM3 promoted vascular endothelial permeability dysfunction and facilitated inflammation in ARDS. However, knockdown of the CMTM3 gene can effectively protected against vascular endothelial dysfunction and inflammatory lung injury caused by ARDS and improved the survival outcomes in the ARDS mice. Therefore, our study suggested that CMTM3 is novel therapeutic target for ARDS.

Data availability statement

The original contributions presented in the study are included in the article/supplementary material. Further inquiries can be directed to the corresponding author.

Ethics statement

The animal study was approved by Ethics Committee for Animal Experiments of Peking University People's Hospital. The study was conducted in accordance with the local legislation and institutional requirements.

Author contributions

ZX: Conceptualization, Data curation, Writing – original draft, Writing – review & editing. GZ: Conceptualization, Methodology, Writing – original draft. HX: Investigation, Methodology, Supervision, Writing – original draft. LC: Data curation, Supervision, Writing – review & editing. XZ: Methodology, Software, Supervision, Writing – review & editing. SL: Investigation, Project administration, Supervision, Writing – review & editing. CF: Project administration, Software, Supervision, Writing – review & editing. ZW: Data curation, Investigation, Project administration, Writing – review & editing. FZ: Conceptualization, Data curation, Funding acquisition, Investigation, Resources, Software, Supervision, Writing – original draft.

Funding

The author(s) declare that financial support was received for the research and/or publication of this article. 1. Beijing Municipal Natural Science Foundation (7222199). 2. Peking University People's Hospital Scientific Research Development Funds (RDX2022-04, RDJP2023-12, RDGS2023-07). 3. National Natural Science Foundation of China (81971808).

Conflict of interest

The authors declare that the research was conducted in the absence of any commercial or financial relationships that could be construed as a potential conflict of interest.

Generative AI statement

The author(s) declare that no Generative AI was used in the creation of this manuscript.

Publisher's note

References

1. Wang YM, Zheng YJ, Chen Y, Huang YC, Chen WW, Ji R, et al. Effects of fluid balance on prognosis of acute respiratory distress syndrome patients secondary to sepsis. *World J Emerg Med*. (2020) 11:216–22. doi: 10.5847/wjem.j.1920-8642.2020.04.003

2. Rubenfeld GD, Caldwell E, Peabody E, Weaver J, Martin DP, Neff M, et al. Incidence and outcomes of acute lung injury. *N Engl J Med*. (2005) 353:1685–93. doi: 10.1056/NEJMoa050333

3. Piantadosi CA, Schwartz DA. The acute respiratory distress syndrome. *Ann Intern Med*. (2004) 141:460–70. doi: 10.7326/0003-4819-141-6-200409210-00012

4. Shao Z, Li Q, Wang S, Chen Z. Protective effects of PNU-282987 on sepsis-induced acute lung injury in mice. *Mol Med Rep*. (2019) 19:3791–8. doi: 10.3892/mmr.2019.10016

5. Xie J, Wang H, Kang Y, Zhou L, Liu Z, Qin B, et al. The epidemiology of sepsis in Chinese ICUs: a national cross-sectional survey. *Crit Care Med*. (2020) 48:e209–18. doi: 10.1097/CCM.0000000000004155

6. Ragab D, Salah Eldin H, Taeimah M, Khattab R, Salem R. The COVID-19 cytokine storm; what we know so far. *Front Immunol*. (2020) 11:1446. doi: 10.3389/fimmu.2020.01446

7. Thompson BT, Chambers RC, Liu KD. Acute respiratory distress syndrome. *N Engl J Med*. (2017) 377:562–72. doi: 10.1056/NEJMra1608077

8. Dechert RE, Haas CF, Ostwani W. Current knowledge of acute lung injury and acute respiratory distress syndrome. *Crit Care Nurs Clin North Am*. (2012) 24:377–401. doi: 10.1016/j.ccell.2012.06.006

9. Han W, Ding P, Xu M, Wang L, Rui M, Shi S, et al. Identification of eight genes encoding chemokine-like factor superfamily members 1-8 (CKLFSF1-8) by in silico cloning and experimental validation. *Genomics*. (2003) 81:609–17. doi: 10.1016/s0888-7543(03)00095-8

10. Wu J, Li L, Wu S, Xu B. CMTM family proteins 1-8: roles in cancer biological processes and potential clinical value. *Cancer Biol Med*. (2020) 17:528–42. doi: 10.20892/j.issn.2095-3941.2020.0032

11. Sánchez-Pulido L, Martín-Belmonte F, Valencia A, Alonso MA. Marvel: a conserved domain involved in membrane apposition events. *Trends Biochem Sci*. (2002) 27:599–601. doi: 10.1016/s0968-0004(02)02229-6

12. Yuan W, Liu B, Wang X, Li T, Xue H, Mo X, et al. CMTM3 decreases EGFR expression and EGF-mediated tumorigenicity by promoting Rab5 activity in gastric cancer. *Cancer Lett*. (2017) C386:77–86. doi: 10.1016/j.canlet.2016.11.015

13. Yuan W, Li T, Mo X, Wang X, Liu B, Wang W, et al. Knockdown of CMTM3 promotes metastasis of gastric cancer via the STAT3/Twist1/EMT signaling pathway. *Oncotarget*. (2016) 7:29507–19. doi: 10.18632/oncotarget.8789

14. Li W, Zhang S. CKLF-like MARVEL transmembrane domain-containing Member 3 (CMTM3) inhibits the proliferation and Tumorigenisis in hepatocellular carcinoma cells. *Oncol Res*. (2017) 25:285–93. doi: 10.3727/096504016X14732523471442

15. Chrifi I, Louzao-Martinez L, Brandt M, van Dijk CGM, Burgisser P, Zhu C, et al. CMTM3 (CKLF-like marvel transmembrane domain 3) mediates angiogenesis by regulating cell surface availability of VE-cadherin in endothelial adherens junctions. *Arterioscler Thromb Vasc Biol*. (2017) 37:1098–114. doi: 10.1161/ATVBAHA.116.308792

16. Hoegl S, Burns N, Angulo M, Francis D, Osborne CM, Mills TW, et al. Capturing the multifactorial nature of ARDS - "Two-hit" approach to model murine acute lung injury. *Physiol Rep*. (2018) 6:e13648. doi: 10.14814/phy2.13648

17. Kudoh I, Miyazaki H, Ohara M, Fukushima J, Tazawa T, Yamada H. Activation of alveolar macrophages in acid-injured lung in rats: different effects of pentoxifylline on tumor necrosis factor-alpha and nitric oxide production. *Crit Care Med*. (2001) 29:1621–5. doi: 10.1097/00003246-200108000-00020

18. Bux J, Sachs UJH. The pathogenesis of transfusion-related acute lung injury (TRALI). *Br J Haematol*. (2007) 136:788–99. doi: 10.1111/j.1365-2141.2007.06492.x

19. Augustin HG, Koh GY. A systems view of the vascular endothelium in health and disease. *Cell*. (2024) 187:4833–58. doi: 10.1016/j.cell.2024.07.012

20. Saki N, Javan M, Moghimian-Boroujeni B, Kast RE. Interesting effects of interleukins and immune cells on acute respiratory distress syndrome. *Clin Exp Med*. (2023) 23:2979–96. doi: 10.1007/s10238-023-01118-w

21. Su Y, Lucas R, Fulton DJR, Verin AD. Mechanisms of pulmonary endothelial barrier dysfunction in acute lung injury and acute respiratory distress syndrome. *Chin Med J Pulm Crit Care Med*. (2024) 2:80–7. doi: 10.1016/j.pccm.2024.04.002

22. Di A, Mehta D, Malik AB. ROS-activated calcium signaling mechanisms regulating endothelial barrier function. *Cell Calcium*. (2016) 60:163–71. doi: 10.1016/j.ceca.2016.02.002

23. Claesson-Welsh L, Dejana E, McDonald DM. Permeability of the endothelial barrier: identifying and reconciling controversies. *Trends Mol Med*. (2021) 27:314–31. doi: 10.1016/j.molmed.2020.11.006

24. Pei Y, Zhang Z, Tan S. Current opinions on the relationship between CMTM family and hepatocellular carcinoma. *J Hepatocell Carcinoma*. (2023) 10:1411–22. doi: 10.2147/JHC.S417202

25. Zhao Y, Li J, Ting KK, Chen J, Coleman P, Liu K, et al. The VE-cadherin/β-catenin signalling axis regulates immune cell infiltration into tumours. *Cancer Lett*. (2021) 496:1–15. doi: 10.1016/j.canlet.2020.09.026

26. Birukova AA, Tian Y, Meliton A, Leff A, Wu T, Birukov KG. Stimulation of Rho signaling by pathologic mechanical stretch is a "second hit" to Rho-independent lung injury induced by IL-6. *Am J Physiol Lung Cell Mol Physiol*. (2012) 302(9):L965–75. doi: 10.1152/ajplung.00292.2011

27. Mizumura K, Gon Y, Kumasawa F, Onose A, Maruoka S, Matsumoto K, et al. Apoptosis signal-regulating kinase 1-mediated signaling pathway regulates lipopolysaccharide-induced tissue factor expression in pulmonary microvasculature. *Int Immunopharmacol*. (2010) 10:1062–7. doi: 10.1016/j.intimp.2010.06.006

28. Konrad FM, Reutershan J. CXCR2 in acute lung injury. *Mediators Inflammation*. (2012) 2012:740987. doi: 10.1155/2012/740987

29. Fukumoto T, Matsukawa A, Yoshimura T, Edamitsu S, Ohkawara S, Takagi K, et al. IL-8 is an essential mediator of the increased delayed-phase vascular permeability in LPS-induced rabbit pleurisy. *J Leukoc Biol*. (1998) 63:584–90. doi: 10.1002/jlb.63.5.584

30. Lee KY. Pneumonia, Cacute respiratory distress syndrome, and early immune-modulator therapy. *Int J Mol Sci*. (2017) 18:388. doi: 10.3390/ijms18020388

31. Li Y, Zeng Z, Li Y, Huang W, Zhou M, Zhang X, et al. Angiotensin-converting enzyme inhibition attenuates lipopolysaccharide-induced lung injury by regulating the balance between angiotensin-converting enzyme and angiotensin-converting enzyme 2 and inhibiting mitogen-activated protein kinase activation. *Shock*. (2015) 43:395–404. doi: 10.1097/SHK.0000000000000302

frontiers | Frontiers in Pharmacology

TYPE Original Research
PUBLISHED 01 April 2025
DOI 10.3389/fphar.2025.1562535

OPEN ACCESS

EDITED BY
You Shang,
Huazhong University of Science and Technology, China

REVIEWED BY
Shihua Lv,
The Second Affiliated Hospital of Harbin Medical University, China
omali Y. El-khawaga,
Mansoura University, Egypt

*CORRESPONDENCE
Wenjie Jiao,
jiaowj@qduhospital.cn

RECEIVED 17 January 2025
ACCEPTED 24 March 2025
PUBLISHED 01 April 2025

CITATION
Liu H, Wang Z, Qiu T, Du W, Wu Z, Chen S and Jiao W (2025) Dexmedetomidine alleviates lung ischemia-reperfusion injury by inhibiting cuproptosis: an *in vivo* study.
Front. Pharmacol. 16:1562535.
doi: 10.3389/fphar.2025.1562535

Dexmedetomidine alleviates lung ischemia-reperfusion injury by inhibiting cuproptosis: an *in vivo* study

Hanqun Liu[1], Zicheng Wang[1], Tong Qiu[1], Wenxing Du[1], Zhe Wu[1], Sheng Chen[2] and Wenjie Jiao[1]*

[1]Department of Thoracic Surgery, Affiliated Hospital of Qingdao University, Qingdao, Shandong, China, [2]Department of Thoracic Surgery, Peking University People's Hospital, Beijing, Beijing, China

Lung ischemia-reperfusion (I/R) injury represents an inevitable complication in lung transplantation, characterized by the excessive production of oxygen free radicals and toxic substances. Dexmedetomidine (DEX), a widely used anesthetic agent, has been shown to significantly elevate glutathione (GSH) levels, thereby conferring protection against copper influx. This study investigates the protective mechanisms of DEX in lung I/R injury, with a particular focus on cuproptosis. Utilizing a rat I/R model established by clamping the left hilum of lung for 90 min followed by 120 min of reperfusion, we examined the effects of DEX on lung injury scores, GSH content, and the expression of key proteins involved in cuproptosis. In conclusion, cuproptosis is implicated in pulmonary I/R injury, and the protective effect of DEX against lung I/R injury is partly mediated by inhibition of cuproptosis.

KEYWORDS

lung ischemia-reperfusion injury, dexmedetomidine, cuproptosis, rats, *in vitro* experiments

1 Introduction

Lung ischemia-reperfusion (I/R) injury represents a critical complication in thoracic surgeries, including lung transplantation and sleeve pulmonary lobectomy. This pathophysiological process is characterized by excessive generation of oxygen free radicals and cytotoxic metabolites (Ward, 1994), frequently resulting in postoperative pulmonary dysfunction and graft failure. Despite its clinical significance, the precise molecular mechanisms underlying lung I/R injury remain incompletely elucidated. Current research priorities focus on mechanistic exploration and therapeutic development to improve surgical outcomes.

Copper, an essential trace element, serves as a catalytic cofactor in redox reactions and regulates multiple enzymatic systems (Steffens et al., 1987; Harris, 1992; Smith-Mungo and Kagan, 1998; Ash et al., 1984). Beyond its established roles in hemoglobin synthesis, bone formation (Rondanelli et al., 2021), and neuroimmune homeostasis (Gromadzka et al., 2020), emerging evidence implicates copper dysregulation in cellular pathology. Mechanistically, impaired copper metabolism induces proteotoxic stress through ferredoxin 1 (FDX1)-mediated lipoylated protein aggregation, mitochondrial respiratory dysfunction, and depletion of iron-sulfur cluster proteins - a copper-dependent cell death pathway termed cuproptosis (Tsvetkov et al., 2022). This novel regulated cell death

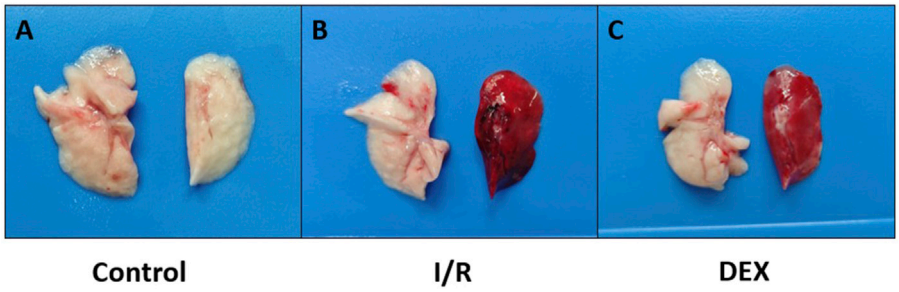

FIGURE 1
Photographs of rat lungs. Lungs were obtained immediately on ice blocks at the end of the experiment. **(A)** lungs in the control group; **(B)** lungs in the I/R group; **(C)** lungs in the DEX group. It was visualized that DEX reduced pulmonary congestion after lung ischemia-reperfusion.

modality has been implicated in both chronic conditions (e.g., Wilson's disease) and acute pathologies, including traumatic spinal cord injury (Li et al., 2023).

Dexmedetomidine (DEX), a selective α2-adrenergic receptor agonist with clinical applications in perioperative sedation, has demonstrated protective effects against pulmonary injury. Preclinical studies revealed its capacity to attenuate oxidative damage through ROS suppression and lipid peroxidation reduction (Fu et al., 2017). Specifically, Zhou et al. (Zhou et al., 2018) documented DEX-mediated mitigation of pulmonary I/R injury in rodent models via modulation of oxidative stress markers (MDA reduction and SOD elevation). While these antioxidant properties are well-documented, the molecular mechanisms underlying DEX's pulmonary protection remain incompletely characterized.

This study investigates the hypothesis that DEX alleviates lung I/R injury through cuproptosis regulation. Utilizing a rat I/R model, we systematically analyze expression profiles of cuproptosis-related proteins and glutathione-mediated antioxidant pathways. Our findings provide novel insights into cuproptosis pathophysiology in pulmonary I/R injury and establish a theoretical framework for developing targeted therapeutic strategies.

2 Methods and materials

2.1 Animals

Male Sprague-Dawley rats (7–8 weeks old; Pengyue, Jinan, China) were housed in a controlled environment with a 12-h light/dark cycle and *ad libitum* access to food and water. All animals underwent a 3-day acclimatization period prior to experimentation. Animal procedures were conducted in accordance with the ARRIVE (Animal Research: Reporting of *In Vivo* Experiments) guidelines and approved by the Institutional Animal Care and Use Committee of the Affiliated Hospital of Qingdao University [AHQU-MAL20230607LH].

2.2 Lung I/R injury model

Body temperature was maintained at 36.5°C–39.0°C using a heating blanket throughout the procedure. Meloxicam (5 mg/kg) was administered subcutaneously for preemptive analgesia 1 h prior to anesthesia induction. Rats were anesthetized via intraperitoneal injection of sodium pentobarbital (60 mg/kg). Following tracheal intubation through a midline cervical incision, mechanical ventilation (initial tidal volume: 10 mL/kg) was initiated using a rodent ventilator. A femoral venous catheter was placed for drug administration.

After thoracotomy, heparin (300 IU/kg) was intravenously injected. Ten minutes post-heparinization, the left pulmonary hilum was occluded at end-expiration using a non-traumatic microvascular clamp. Lidocaine (20 mg) was topically applied to the surgical site for analgesia and phrenic nerve blockade. During ischemia, tidal volume was reduced to 6 mL/kg. Following 90 min of ischemia, clamps were removed and tidal volume restored to 10 mL/kg for 120-min reperfusion. Post-reperfusion, arterial blood was collected for gas analysis, and euthanasia was performed via exsanguination under deep anesthesia. Left lung tissues (Figure 1) and blood samples were harvested for subsequent analyses.

2.3 Experimental groups

Rats were randomly assigned to three groups (n = 6/group): Sham group: Thoracotomy without hilar clamping; I/R group: Full I/R protocol; DEX group: Dexmedetomidine (DEX; Sinopharm Chemical Reagent, 10 μg/kg) administered via femoral vein infusion over 20 min pre-thoracotomy, followed by I/R protocol.

2.4 Histopathological examination and lung injury scoring

Left lung lobes were fixed in 4% paraformaldehyde for 24 h, paraffin-embedded, and sectioned at 6 μm thickness for hematoxylin-eosin (H&E) staining. Histopathological evaluation was performed by a blinded pathologist using light microscopy. Lung injury scores (LIS) were calculated based on four parameters: (1) neutrophil infiltration, (2) interstitial edema, (3) hyaline membrane formation, and (4) hemorrhage. Each parameter was graded 0–4 (0 = normal, 1 = minimal, 2 = mild, 3 = moderate, 4 = severe).

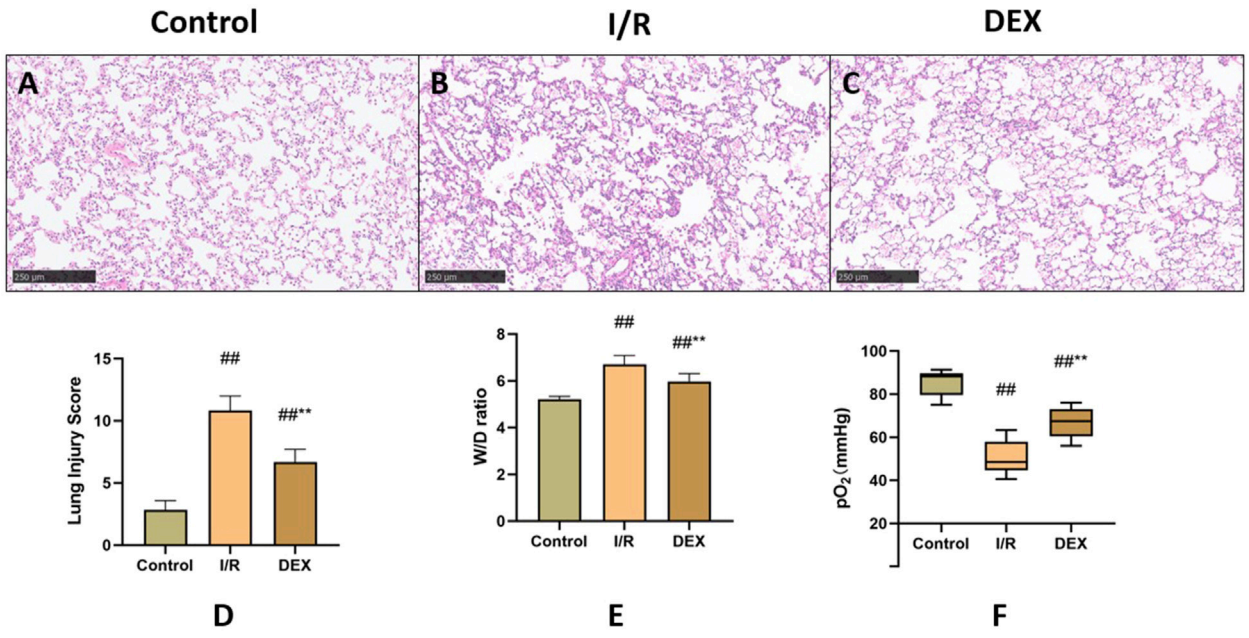

FIGURE 2
Comparison of lung tissue injury. **(A–C)** microscopic images stained with HE. **(D)** Lung injury score (n = 6). **(E)** lung tissue dry-wet weight ratio (n = 6). **(F)** rats' blood gas parameters (n = 6). ## $p < 0.05$ vs. Control group; ** $p < 0.05$ vs. I/R group.

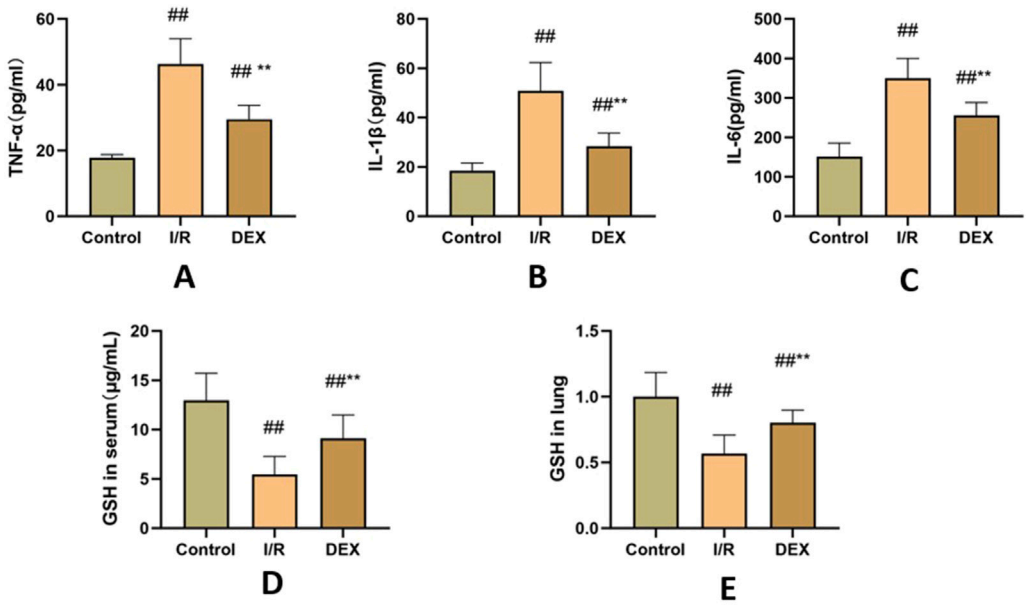

FIGURE 3
Inflammatory factors and GSH. **(A)** concentrations of TNF-α(n = 6). **(B)** concentrations of IL-1β(n = 6). **(C)** concentrations of IL-6 (n = 6). **(D)** concentrations of GSH in serum. **(E)** the ratio of GSH content in lung tissue. ## $p < 0.05$ vs. control group; ** $p < 0.05$ vs. I/R group.

2.5 Wet/dry (W/D) weight ratio

Surface moisture was carefully blotted from fresh lung tissues using filter paper. Wet weights were recorded before desiccation in a 75°C oven for 72 h. Dry weights were measured to calculate the W/D ratio.

2.6 Measurement of inflammatory factors

Blood samples were clotted at room temperature for 2 h, then centrifuged (3,000 × g, 15 min, 4°C) to collect serum. TNF-α, IL-1β, and IL-6 levels were quantified using commercial ELISA kits (Invitrogen) following manufacturer protocols.

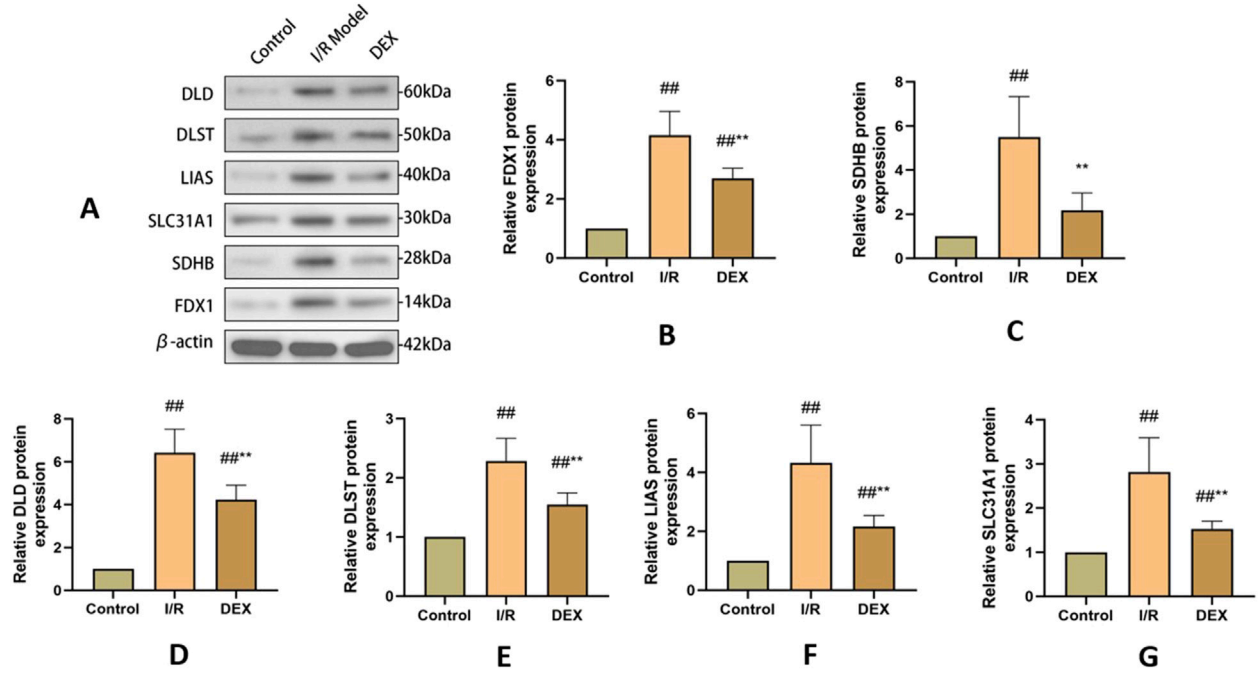

FIGURE 4
WB results of cuproptosis-related protein expression. **(A)** Western blots for FDX 1, SLC 31 A1, LIAS, DLST, DLD, and SDHB in rat lung tissue. **(B–G)** relative levels of FDX 1, SLC 31 A1, LIAS, DLST, DLD, and SDHB in rat lung tissue (n = 3). ## $p < 0.05$ vs. control group; ** $p < 0.05$ vs. I/R group.

2.7 Glutathione (GSH) assay

Lung tissues were homogenized in cold PBS and centrifuged (12,000 × g, 15 min, 4°C). Supernatants were analyzed using GSH assay kits (Elabscience, Wuhan, China). Absorbance at 450 nm was measured for both tissue and serum samples.

2.8 Western blotting

Lung tissues were lysed in RIPA buffer (Elabscience, Wuhan, China) supplemented with protease inhibitors, then sonicated (Sonic Dismembrator, United States). For lipoylated protein analysis, 10 μM TCEP was added prior to 95°C denaturation. Protein concentrations were determined via BCA assay (Elabscience), with equal amounts loaded onto 4%–20% gradient SDS-PAGE gels. Proteins were transferred to PVDF membranes and blocked with 5% non-fat milk. Membranes were incubated overnight at 4°C with primary antibodies against: lipoic acid (Abcam, 1:1,000), FDX1 (Abcam, 1:1,000), LIAS (Proteintech, 1:1,000), SDHB (Proteintech, 1:1,000), DLAT (Proteintech, 1:1,000), DLD (Proteintech, 1:1,000), SLC31A1 (MCE, 1:1,000), DLST (MCE, 1:1,000), and β-actin (Sevier, 1:5,000). After PBST washes, membranes were incubated with HRP-conjugated secondary antibodies (Proteintech, 1:10,000) for 1 h at room temperature. Protein bands were visualized using ECL reagent (Elabscience) and quantified with ImageJ software.

2.9 DLAT oligomerization analysis

Protein samples were prepared with non-reducing loading buffer (Beyotime, China) and minimally heated (70°C, 5 min). Electrophoresis and subsequent procedures followed standard Western blot protocols.

2.10 Immunohistochemical staining

Deparaffinized sections underwent antigen retrieval in citrate buffer (pH 6.0). Endogenous peroxidase was quenched with 3% H_2O_2, followed by blocking with 10% goat serum. Sections were incubated with anti-lipoic acid antibody (Abcam, 1:100) overnight at 4°C, then with HRP-conjugated secondary antibody (37°C, 1 h). Diaminobenzidine (DAB) was used for chromogenic detection. Hematoxylin staining was used to visualize the nuclei.

2.11 Immunofluorescence

After antigen retrieval and blocking, sections were incubated with anti-FDX1 (Abcam, 1:200) and anti-DLAT (Proteintech, 1:500) antibodies overnight at 4°C. Alexa Fluor-conjugated secondary antibodies (Invitrogen, 1:500) were applied for 1 h at room temperature. Nuclei were counterstained with DAPI (5 μg/mL). Images were acquired using an Olympus BX53 fluorescence microscope.

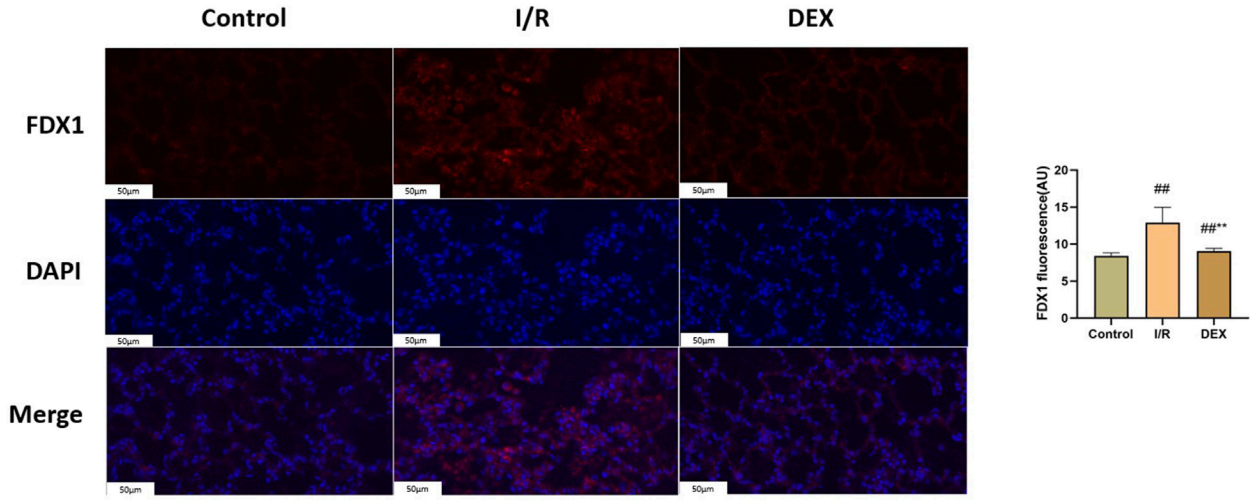

FIGURE 5
Immunofluorescence results of FDX1. Representative images of fluorescence probe for FDX1 and statistical comparison (n = 6). ## $p < 0.05$ vs. control group; ** $p < 0.05$ vs. I/R group.

2.12 Statistical analysis

Data are presented as mean ± SD. Normality was assessed using Shapiro-Wilk test. One-way ANOVA with Tukey's *post hoc* test was performed using Prism 10.1.2 (GraphPad). Statistical significance was set at $p < 0.05$.

3 Results

3.1 DEX attenuated histopathological damage

Histopathological analysis revealed distinct morphological changes among groups (Figures 2A–C). Compared to the sham control, the I/R group demonstrated significantly exacerbated neutrophilic infiltration, interstitial edema, and alveolar hemorrhage. DEX pretreatment markedly improved these pathological alterations. Semi-quantitative assessment of lung injury scores (Figure 2D) confirmed progressive deterioration from control (minimal injury) to I/R groups (severe injury), with DEX intervention showing intermediate protection. The W/D ratio analysis (Figure 2E) paralleled these findings, showing significant elevation in I/R group compared to control, which was effectively reduced by DEX administration ($p = 0.0059$ vs. I/R).

3.2 DEX improved oxygenation parameters

Arterial blood gas analysis (Figure 2F) indicated that lung I/R injury significantly compromised oxygen exchange capacity, as evidenced by decreased PaO_2 levels. DEX treatment partially restored oxygenation parameters, showing statistically significant improvement compared to I/R group ($p = 0.004$).

3.3 DEX suppressed systemic inflammatory response

The I/R procedure induced significant elevation of serum pro-inflammatory cytokines (Figures 3A–C). TNF-α, IL-1β, and IL-6 levels were markedly increased in I/R group versus control ($p < 0.05$ for all comparisons). DEX pretreatment substantially mitigated this inflammatory cascade, demonstrating significant reduction in all measured cytokines compared to I/R group ($p < 0.05$).

3.4 DEX enhanced antioxidant capacity

As shown in Figures 3D, E, I/R injury caused significant depletion of GSH content in both lung tissue and serum compared to control group ($p < 0.05$). DEX administration effectively reversed this trend, restoring GSH levels to values significantly higher than those observed in I/R group ($p < 0.05$).

3.5 DEX modulated cuproptosis-associated proteins

Western blot analysis demonstrated I/R-induced upregulation of key cuproptosis regulators including FDX1, SLC31A1, LIAS, DLST, DLD, and SDHB (Figure 4). DEX treatment significantly attenuated these protein level alterations compared to I/R group ($p < 0.05$). Immunofluorescence quantification confirmed increased FDX1 expression in I/R lungs, which was reduced by DEX intervention (Figure 5).

3.6 DEX inhibited lipoylated protein accumulation

Immunoblot and immunohistochemical analyses revealed significant I/R-induced accumulation of lipoylated DLAT and

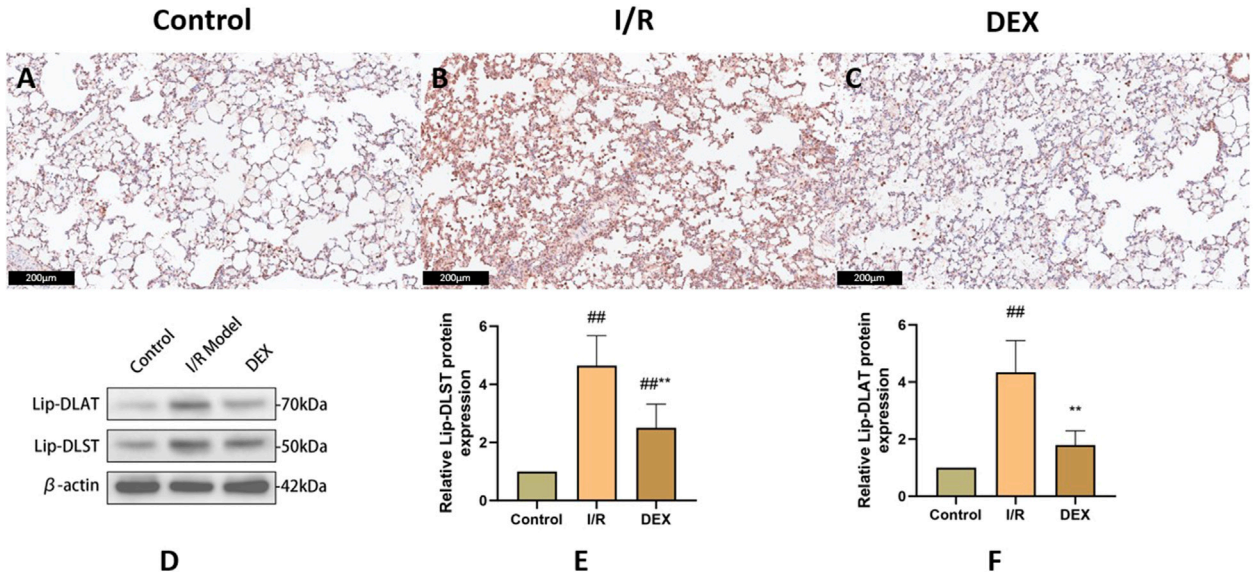

FIGURE 6
Immunohistochemical and WB results of lipoacylated proteins. **(A–C)** representative images of lipoacylated protein immunohistochemical staining in rat lung tissue. **(D)** Western blots for lip-DLAT and lip-DLST. **(E, F)** relative levels of lip-DLAT and lip-DLST in rats lung tissue (n = 3). ## $p < 0.05$ vs. control group; ** $p < 0.05$ vs. I/R group.

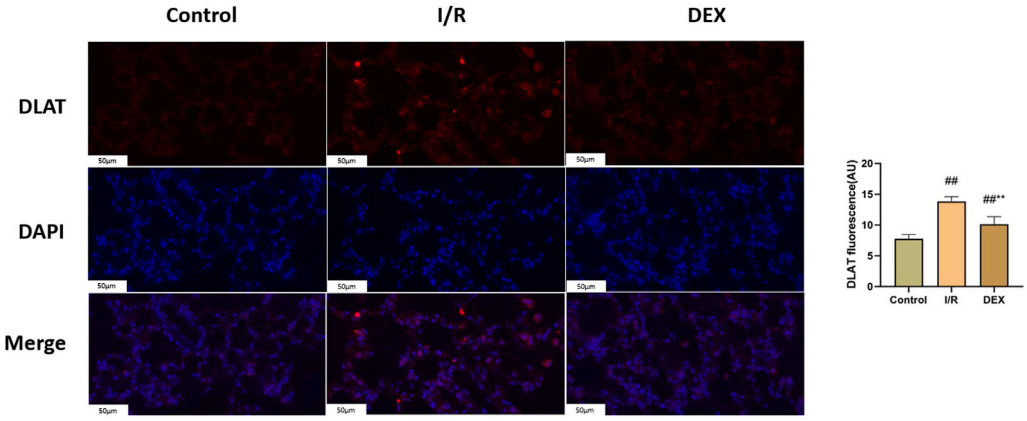

FIGURE 7
Immunofluorescence results of DLAT. Representative images of fluorescence probe for DLAT and statistical comparison (n = 6). ## $p < 0.05$ vs. control group; ** $p < 0.05$ vs. I/R group.

DLST (Figure 6). DEX administration significantly reduced lipoylated protein levels compared to I/R group ($p < 0.05$). Non-reducing Western blot demonstrated prominent DLAT oligomerization in I/R group, which was effectively suppressed by DEX treatment (Figure 7). Immunofluorescence analysis corroborated these findings, showing significant reduction of DLAT aggregates with DEX intervention (Figure 8).

4 Discussion

Our study demonstrates that dexmedetomidine (DEX) administration effectively attenuates lung ischemia-reperfusion (I/R) injury, and this process is accompanied by inhibition of the cuproptosis. The therapeutic effects manifested as improved oxygenation parameters, reduced histopathological damage, and suppression of pro-inflammatory cytokine release.

Copper homeostasis plays pivotal roles in physiological processes, requiring precise regulation through an integrated network of copper-dependent proteins including transporters, chaperones, and enzymes (Zhong et al., 2022; Cobine and Brady, 2022; Bharathi Devi et al., 2016). Central to this regulatory system is solute carrier family 31 member 1 (SLC31A1), the principal copper importer governing cellular copper influx (Qi et al., 2023; Das et al., 2022; Xie et al., 2023). Our findings reveal that DEX significantly downregulates SLC31A1 expression, suggesting direct interference

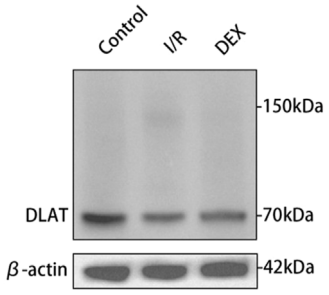

FIGURE 8
Oligomerization of the DLAT protein in WB experiment. DLAT protein oligomerization was observed in the I/R group, but not in the other two groups.

with copper uptake mechanisms. This observation aligns with computational modeling data indicating potential molecular interactions between DEX and SLC31A1, though experimental validation of this binding specificity requires further investigation.

The antioxidant glutathione (GSH) emerged as another critical mediator in DEX's protective mechanism. We observed that DEX administration counteracts I/R-induced GSH depletion in both pulmonary tissue and systemic circulation. Given GSH's established role in copper chelation and detoxification (Saporito-Magriñá et al., 2018), this restoration likely disrupts copper-mediated oxidative cascades. Notably, the coordinated downregulation of SLC31A1 and upregulation of GSH suggests synergistic modulation of copper homeostasis, potentially through adrenergic receptor-dependent signaling pathways warranting further exploration.

Ferredoxin 1 (FDX1), a key reductase facilitating copper redox cycling and protein lipoylation (Tsvetkov et al., 2022), displayed marked overexpression in I/R lungs that was attenuated by DEX treatment. The FDX1 suppression correlated with reduced lipoylated protein accumulation (DLAT/DLST) and diminished DLAT oligomerization - hallmark features of cuproptosis. FDX one results in oxidative stress inside the cell. Oxygen free radicals have been demonstrated to significantly contribute to cell death in organ I/R (Sadrkhanloo et al., 2022). Mechanistically, FDX1 inhibition may preserve cellular redox balance by maintaining GSH/GSSG ratios critical for free radical scavenging (Chen et al., 2022; Poprac et al., 2017). This dual regulation of copper metabolism and oxidative stress pathways positions FDX1 as a crucial nexus in DEX-mediated protection against I/R injury. DEX significantly inhibited FDX1/SLC31A1 expression, reduced copper influx, and restored TCA cycle function. This process may regulate protein post-translational modification through the α2-adrenoceptor mediated PI3K/Akt/mTOR signaling pathway (Zhao et al., 2020; Huang et al., 2024).

Our study has some limitations. First, the absence of cellular models limits mechanistic depth. Genetic manipulation (FDX1 knockout/overexpression) *in vitro* could clarify its regulatory hierarchy and enable mitochondrial functional analyses. Second, the lack of established cuproptosis inhibitors as positive controls prevents direct comparison of DEX's therapeutic efficacy. Future studies should incorporate pharmacological (e.g., tetrathiomolybdate) and genetic interventions to validate target specificity.

5 Conclusion

There is a cuproptosis mechanism in the process of lung ischemia-reperfusion. The protective effect of DEX against lung I/R injury is partly mediated by inhibition of cuproptosis.

Data availability statement

The original contributions presented in the study are included in the article/Supplementary Material, further inquiries can be directed to the corresponding author.

Ethics statement

The animal study was approved by Ethics Committee of Laboratory Animal Welfare, Affiliated Hospital of Qingdao University. The study was conducted in accordance with the local legislation and institutional requirements.

Author contributions

HL: Conceptualization, Data curation, Formal Analysis, Investigation, Methodology, Project administration, Resources, Software, Supervision, Validation, Visualization, Writing – original draft, Writing – review and editing. ZW: Data curation, Formal Analysis, Writing – review and editing. TQ: Funding acquisition, Investigation, Methodology, Project administration, Resources, Writing – review and editing. WD: Data curation, Methodology, Project administration, Resources, Supervision, Validation, Writing – review and editing. ZW: Data curation, Methodology, Supervision, Validation, Visualization, Writing – review and editing. SC: Methodology, Project administration, Validation, Writing – review and editing. WJ: Conceptualization, Funding acquisition, Investigation, Methodology, Project administration, Resources, Software, Validation, Visualization, Writing – review and editing.

Funding

The author(s) declare that financial support was received for the research and/or publication of this article. This study received financial support from National Natural Science Foundation of China, Natural Science Foundation of Shandong Province and Postdoctoral Innovation Project of Shandong Province.

Conflict of interest

The authors declare that the research was conducted in the absence of any commercial or financial relationships that could be construed as a potential conflict of interest.

Generative AI statement

The author(s) declare that no Generative AI was used in the creation of this manuscript.

Publisher's note

All claims expressed in this article are solely those of the authors and do not necessarily represent those of their affiliated organizations, or those of the publisher, the editors and the reviewers. Any product that may be evaluated in this article, or claim that may be made by its manufacturer, is not guaranteed or endorsed by the publisher.

Supplementary material

The Supplementary Material for this article can be found online at: https://www.frontiersin.org/articles/10.3389/fphar.2025.1562535/full#supplementary-material

References

Ash, D. E., Papadopoulos, N. J., Colombo, G., and Villafranca, J. J. (1984). Kinetic and spectroscopic studies of the interaction of copper with dopamine beta-hydroxylase. *J. Biol. Chem.* 259, 3395–3398. doi:10.1016/s0021-9258(17)43105-x

Bharathi Devi, S. R., Dhivya, M. A., and Sulochana, K. N. (2016). Copper transporters and chaperones: their function on angiogenesis and cellular signalling. *J. Biosci.* 41, 487–496. doi:10.1007/s12038-016-9629-6

Chen, G. H., Song, C. C., Pantopoulos, K., Wei, X. L., Zheng, H., and Luo, Z. (2022). Mitochondrial oxidative stress mediated Fe-induced ferroptosis via the NRF2-ARE pathway. *Free Radic. Biol. and Med.* 180, 95–107. doi:10.1016/j.freeradbiomed.2022.01.012

Cobine, P. A., and Brady, D. C. (2022). Cuproptosis: cellular and molecular mechanisms underlying copper-induced cell death. *Mol. cell* 82, 1786–1787. doi:10.1016/j.molcel.2022.05.001

Das, A., Ash, D., Fouda, A. Y., Sudhahar, V., Kim, Y. M., Hou, Y., et al. (2022). Cysteine oxidation of copper transporter CTR1 drives VEGFR2 signalling and angiogenesis. *Nat. cell Biol.* 24, 35–50. doi:10.1038/s41556-021-00822-7

Fu, C., Dai, X., Yang, Y., Lin, M., Cai, Y., and Cai, S. (2017). Dexmedetomidine attenuates lipopolysaccharide-induced acute lung injury by inhibiting oxidative stress, mitochondrial dysfunction and apoptosis in rats. *Mol. Med. Rep.* 15, 131–138. doi:10.3892/mmr.2016.6012

Gromadzka, G., Tarnacka, B., Flaga, A., and Adamczyk, A. (2020). Copper dyshomeostasis in neurodegenerative diseases-therapeutic implications. *Int. J. Mol. Sci.* 21, 9259. doi:10.3390/ijms21239259

Harris, E. D. (1992). Copper as a cofactor and regulator of copper,zinc superoxide dismutase. *J. Nutr.* 122, 636–640. doi:10.1093/jn/122.suppl_3.636

Huang, T., Zhang, Y., Wu, Y., Han, X., Li, L., Guo, Z., et al. (2024). CEBPB dampens the cuproptosis sensitivity of colorectal cancer cells by facilitating the PI3K/AKT/mTOR signaling pathway. *Saudi J. gastroenterology official J. Saudi Gastroenterology Assoc.* 30, 381–388. doi:10.4103/sjg.sjg_169_24

Li, C., Wu, C., Ji, C., Xu, G., Chen, J., Zhang, J., et al. (2023). The pathogenesis of DLD-mediated cuproptosis induced spinal cord injury and its regulation on immune microenvironment. *Front. Cell. Neurosci.* 17, 1132015. doi:10.3389/fncel.2023.1132015

Poprac, P., Jomova, K., Simunkova, M., Kollar, V., Rhodes, C. J., and Valko, M. (2017). Targeting free radicals in oxidative stress-related human diseases. *Trends Pharmacol. Sci.* 38, 592–607. doi:10.1016/j.tips.2017.04.005

Qi, Y., Yao, Q., Li, X., Li, X., Zhang, W., and Qu, P. (2023). Cuproptosis-related gene SLC31A1: prognosis values and potential biological functions in cancer. *Sci. Rep.* 13, 17790. doi:10.1038/s41598-023-44681-8

Rondanelli, M., Faliva, M. A., Infantino, V., Gasparri, C., Iannello, G., Perna, S., et al. (2021). Copper as dietary supplement for bone metabolism: a review. *Nutrients* 13, 2246. doi:10.3390/nu13072246

Sadrkhanloo, M., Entezari, M., Orouei, S., Zabolian, A., Mirzaie, A., Maghsoudloo, A., et al. (2022). Targeting Nrf2 in ischemia-reperfusion alleviation: from signaling networks to therapeutic targeting. *Life Sci.* 300, 120561. doi:10.1016/j.lfs.2022.120561

Saporito-Magriñá, C. M., Musacco-Sebio, R. N., Andrieux, G., Kook, L., Orrego, M. T., Tuttolomondo, M. V., et al. (2018). Copper-induced cell death and the protective role of glutathione: the implication of impaired protein folding rather than oxidative stress. *Metallomics* 10, 1743–1754. doi:10.1039/c8mt00182k

Smith-Mungo, L. I., and Kagan, H. M. (1998). Lysyl oxidase: properties, regulation and multiple functions in biology. *J. Int. Soc. Matrix Biol.* 16, 387–398. doi:10.1016/s0945-053x(98)90012-9

Steffens, G. C., Biewald, R., and Buse, G. (1987). Cytochrome c oxidase is a three-copper, two-heme-A protein. *Eur. J. Biochem.* 164, 295–300. doi:10.1111/j.1432-1033.1987.tb11057.x

Tsvetkov, P., Coy, S., Petrova, B., Dreishpoon, M., Verma, A., Abdusamad, M., et al. (2022). Copper induces cell death by targeting lipoylated TCA cycle proteins. *Science* 375, 1254–1261. doi:10.1126/science.abf0529

Ward, P. A. (1994). Oxygen radicals, cytokines, adhesion molecules, and lung injury. *Environ. health Perspect.* 102 (Suppl. 10), 13–16. doi:10.1289/ehp.94102s1013

Xie, J., Yang, Y., Gao, Y., and He, J. (2023). Cuproptosis: mechanisms and links with cancers. *Mol. cancer* 22, 46. doi:10.1186/s12943-023-01732-y

Zhao, Y., Feng, X., Li, B., Sha, J., Wang, C., Yang, T., et al. (2020). Dexmedetomidine protects against lipopolysaccharide-induced acute kidney injury by enhancing autophagy through inhibition of the PI3K/AKT/mTOR pathway. *Front. Pharmacol.* 11, 128. doi:10.3389/fphar.2020.00128

Zhong, C. C., Zhao, T., Hogstrand, C., Chen, F., Song, C. C., and Luo, Z. (2022). Copper (Cu) induced changes of lipid metabolism through oxidative stress-mediated autophagy and Nrf2/PPARγ pathways. *J. Nutr. Biochem.* 100, 108883. doi:10.1016/j.jnutbio.2021.108883

Zhou, Y., Zhou, X., Zhou, W., Pang, Q., and Wang, Z. (2018). The protective effect of dexmedetomidine in a rat *ex vivo* lung model of ischemia-reperfusion injury. *Acta cir. bras.* 33, 1–13. doi:10.1590/s0102-865020180010000001

frontiers | Frontiers in Cell and Developmental Biology

TYPE Review
PUBLISHED 22 May 2025
DOI 10.3389/fcell.2025.1551138

OPEN ACCESS

EDITED BY
Lulong Bo,
Navy Medical University, China

REVIEWED BY
Wankun Chen,
Fudan University, China
Xiaoting Zhang,
Navy Medical University, China

*CORRESPONDENCE
Shangwen Pan,
pan_shangwen@163.com
Hairong Xiao,
2019xh0141@hust.edu.cn
Huaqing Shu,
huaqing_shu@163.com

†These authors have contributed equally to this work

RECEIVED 24 December 2024
ACCEPTED 08 May 2025
PUBLISHED 22 May 2025

CITATION
Xu X, Zhang Q, Lv Z, Cheng C, Zha J, Shu H, Xiao H and Pan S (2025) Unraveling the deadly dance: endothelial cells and neutrophils in sepsis-induced acute lung injury/acute respiratory distress syndrome.
Front. Cell Dev. Biol. 13:1551138.
doi: 10.3389/fcell.2025.1551138

Unraveling the deadly dance: endothelial cells and neutrophils in sepsis-induced acute lung injury/acute respiratory distress syndrome

Xiujuan Xu[1,2†], Qi Zhang[3†], Zheng Lv[2†], Chuji Cheng[1], Junjing Zha[1], Huaqing Shu[2,4*], Hairong Xiao[4,5,6*] and Shangwen Pan[2,4*]

[1]Department of Critical Medicine, Anqing Municipal Hospital, Anqing, China, [2]Department of Critical Care Medicine, Union Hospital, Tongji Medical College, Huazhong University of Science and Technology, Wuhan, China, [3]Department of General Surgery, Anqing Municipal Hospital, Anqing, China, [4]Institute of Anesthesia and Critical Care Medicine, Union Hospital, Tongji Medical College, Huazhong University of Science and Technology, Wuhan, China, [5]Department of Anesthesiology, Union Hospital, Tongji Medical College, Huazhong University of Science and Technology, Wuhan, China, [6]Key Laboratory of Anesthesiology and Resuscitation, Huazhong University of Science and Technology, Ministry of Education, Wuhan, China

Sepsis-induced acute lung injury (ALI) and acute respiratory distress syndrome (ARDS) are severe complications with high morbidity and mortality rates, characterized primarily by diffuse alveolar damage, endothelial dysfunction, and local inflammatory responses. Neutrophils and endothelial cells (ECs) play crucial roles in the pathogenesis and progression of these diseases. Neutrophils are important regulators of inflammation, while endothelial dysfunction exacerbates vascular permeability and the inflammatory cascade. The interaction between neutrophils and ECs is vital for the development of ALI/ARDS induced by sepsis, driving the pathological processes of inflammation and tissue damage. Despite advancements in treatment strategies such as protective mechanical ventilation and fluid management, effective methods for rapid lung tissue recovery or significant improvement in outcomes remain lacking. Therefore, we comprehensively summarize the current literature to gain deeper insights into the roles of neutrophils, ECs, and their interactions in sepsis-induced ALI/ARDS, hoping to provide critical insights into the mechanisms underlying sepsis-related ALI/ARDS and potential pathways for developing new therapeutic approaches.

KEYWORDS

ALI/ARDS, neutrophils, ECs, Piezo1, sepsis

1 Introduction

Sepsis is a syndrome that is characterized by a dysregulated host response to infection, leading to a series of physiological, pathological, and biological abnormalities (Singer et al., 2016). Although the incidence and mortality rates have declined in recent years due to global efforts, sepsis remains one of

the leading causes of death among patients worldwide. Statistics indicate that in 2017, there were approximately 49 million cases of sepsis globally, with 11 million deaths associated with sepsis, accounting for 19.7% of total global mortality (Rudd et al., 2020).

As a systemic inflammatory response syndrome, acute lung injury (ALI) and acute respiratory distress syndrome (ARDS) are serious complications of sepsis, characterized by high rates of morbidity and mortality. Compared to the common types of ALI/ARDS caused by trauma, pancreatitis, or transfusion of blood products, sepsis-induced ALI/ARDS is driven by a systemic inflammatory response syndrome (SIRS) triggered by infection. This condition is characterized by a more pronounced systemic inflammatory response, accompanied by multiple organ dysfunction syndrome (MODS). In typical ALI/ARDS, the inflammatory response is primarily localized to the lungs, while sepsis-induced ALI/ARDS elicits a robust systemic immune response due to infection, resulting in more severe damage to vascular endothelial cells (ECs) and significantly increased capillary permeability. This exacerbates pulmonary edema, hypotension, and even shock. Although various treatment strategies, including protective mechanical ventilation, restrictive fluid management, and neuromuscular blockade, are widely employed for ARDS induced by sepsis, there is currently no effective method to rapidly repair damaged lung tissue or significantly improve patient prognosis.

The primary histological feature of ARDS is diffuse alveolar damage, with core pathological mechanisms including endothelial dysfunction and localized inflammatory responses (Matthay et al., 2019). Neutrophils play a critical role as key regulators of inflammation in the pathogenesis and progression of ALI/ARDS (Wang et al., 2022). The activation and dysfunction of ECs and neutrophils are not unique to sepsis-induced ALI/ARDS; they also play a crucial role in other types of ALI/ARDS. However, in sepsis-induced ALI/ARDS, the activation and functional abnormalities of ECs and neutrophils are often more pronounced due to the influence of SIRS and infection-related factors. This excessive cellular activation and inflammatory dysregulation further exacerbate lung inflammation and systemic injury, highlighting the distinctive pathological characteristics of sepsis-induced ALI/ARDS. Therefore, this article reviews the roles of ECs, neutrophils, and their interactions in sepsis-induced ALI/ARDS based on existing literature, aiming to enhance understanding of this condition and provide potential insights for exploring clinical treatment avenues.

2 ECs in sepsis-induced ALI/ARDS

ECs, as a monolayer barrier lining the vascular surface and directly interacting with blood, are crucial components of the pulmonary barrier function (Shao et al., 2014). They perform various essential roles, including the regulation of vascular permeability, coagulation, and transcellular transport (substance transport). Activated ECs enhance coagulation activity and increase vascular permeability, leading to capillary thrombosis and pulmonary edema (Gando et al., 2004). Furthermore, activated ECs recruit immune cells to lung tissue, participating in the early inflammatory response and exacerbating lung injury (Qian et al., 2022). During the later stages of lung injury repair, ECs promote their own regeneration and maintain vascular homeostasis by expressing various transcription factors, thereby facilitating lung tissue repair (Liu et al., 2019; Zhao et al., 2020; Zhao et al., 2024). In the following chapters, we will conduct a detailed review of the potential regulatory points of ECs in activation and repair.

2.1 Activation and dysfunction of ECs in sepsis-induced ALI/ARDS

EC activation refers to the process by which these cells are stimulated by various factors, including hypoxia, cytokines, chemokines, thrombin, and bacterial lipopolysaccharides (LPS), as well as through interactions with inflammatory cells (Qiao et al., 2024). ECs express various pattern recognition receptors (PRRs), such as toll-like receptors (TLRs), which can be activated by pathogen-associated molecular patterns (PAMPs) and damage-associated molecular patterns (DAMPs). Once activated, ECs release large amounts of pro-inflammatory mediators, primarily through the NF-κB signaling pathway, exacerbating the inflammatory response by amplifying immune cell recruitment and activation. Functionally, activated ECs also exhibit increased expression of adhesion molecules, which includes P-selectin, E-selectin, intercellular adhesion molecule-1 (ICAM-1), and vascular cell adhesion molecule-1 (VCAM-1). Additionally, the activation of regulators such as tumor necrosis factor receptor-associated factor 6 (TRAF-6) (Lv et al., 2018), TRIM47, and its downstream pathway, including K63-linked TRAF2 (Qian et al., 2022), further promotes lung inflammation in ALI/ARDS by activating NF-κB signaling in ECs.

Upon activation, ECs transition into a pro-inflammatory and pro-coagulant state, which fosters the onset of oxidative stress. This inflammatory response leads to structural alterations in ECs, including damage to the glycocalyx and junctional proteins, as well as EC contraction, all of which contribute to increased vascular permeability and coagulopathy. Glycocalyx damage, driven by enzymes such as heparinase, a disintegrin and metalloproteinases (ADAMs), and matrix metalloproteinases (MMPs), further exacerbates vascular permeability. Notably, the Silent Information Regulator sirtuin 1 (SIRT1) pathway has been shown to protect the endothelial glycocalyx in ALI/ARDS (Duan et al., 2023). Damage to the glycocalyx exposes adhesion molecules that facilitate interactions between blood leukocytes and ECs. In addition, activated ECs secrete cytokines and promote the formation of NETs (Duan et al., 2023), which enhance platelet adhesion and disrupt normal coagulation processes. Simultaneously, the physiological anticoagulant pathways are impaired, further aggravating coagulation dysfunction (Ito et al., 2021).

Myosin light chain kinase (MLCK), which regulates the contraction of the perijunctional actomyosin ring through phosphorylation of the myosin II regulatory light chain, is a key regulator of tight junction permeability (Cunningham and Turner, 2012). The activation of MLCK is also implicated in thrombosis formation and coagulopathy. Specifically, thrombin activates MLCK in a Src-dependent manner, enhancing EC permeability through cell contraction (Kempf et al., 2022).

Oxidative stress is a crucial role in various cellular functions; however, excessive production of ROS can lead to EC dysfunction

and death (Jiang et al., 2020). Extensive EC death is a significant contributor to the pathological progression of ALI/ARDS. Interactions with various blood cells in the bloodstream and responses to cytokines via EC surface receptors further contribute to EC death and the exacerbation of inflammation. Notably, intervention targeting the generation of NETs has been shown to reduce the severity of ferroptosis and pulmonary vascular permeability through the SDC-1/HS/HGF/cMET pathway (Huang et al., 2023). Additionally, low vascular endothelial growth factor (VEGF) levels in lung from ARDS patients have been associated with higher rates of endothelial apoptosis (Abadie et al., 2005). LPS can activate monocytes to induce apoptosis in ECs through both TNF-α-dependent and TNF-α-independent mechanisms (Stefanec, 2000). However, few therapies currently available in clinical practice are capable of effectively reducing endothelial apoptosis at the appropriate stage of disease or as a single-agent treatment in sepsis. Therefore, targeting multiple pathways and implementing timely and effective interventions to block extensive EC death may help contain disease progression. In sepsis-induced ALI, lactic acidemia promotes the release of macrophage-derived extracellular cold-inducible RNA-binding protein (eCIRP), which activates cell death pathways in pulmonary vascular ECs, driving sepsis-related pulmonary complications (Gong et al., 2024; Gong et al., 2024).

2.2 Endothelial regeneration and vascular repair in sepsis-induced ALI/ARDS

Endothelial barrier dysfunction is one of the core factors contributing to the poor prognosis of ALI/ARDS (Tang et al., 2024). The regeneration of ECs and subsequent vascular repair are vital processes in the recovery from these conditions (Huang et al., 2023). This repair process is crucial for maintaining vascular homeostasis and reconstructing the vascular endothelial barrier, involving the participation of many key regulatory factors.

Sox17 is an important regulatory factor in lung ECs regeneration. In LPS-induced lung injury model, Sox17 promotes ECs proliferation by upregulating the expression of Cyclin E1 (Liu et al., 2019). Another key signaling pathway involved in endothelial regeneration is the p110γPI3K signaling pathway, which is essential for activating the reparative transcription factor Forkhead box M1 (FoxM1). Studies have shown that the activation of p110γPI3K is crucial for endothelial regeneration and vascular repair after inflammatory vascular injury. Inhibition of this pathway leads to prolonged lung inflammation and increased vascular permeability, indicating that targeting p110γPI3K maybe a promising therapeutic strategy for enhancing endothelial repair in sepsis-induced ALI/ARDS (Huang et al., 2016). Likewise, the EC regeneration and vascular repair mediated by FoxM1 is considered one of the potential therapeutic pathways for sepsis-induced ARDS (Huang et al., 2023). Upstream of FoxM1, the transcription factor HIF-1α (hypoxia-inducible factor 1-alpha) plays a pivotal role in ECs-mediated vascular repair and inflammation resolution, making it another attractive therapeutic target for sepsis-induced ARDS (Huang et al., 2019). Another important aspect of endothelial repair involves endothelial progenitor cells (EPCs), which are essential for vascular repair and regeneration. Evidence suggests that therapies aimed at increasing the quantity and functionality of EPCs can significantly alleviate lung injury. For example, the administration of Rev-D4F, a high-density lipoprotein mimetic, has been shown to enhance EPC function and numbers, thereby reducing inflammation and promoting vascular repair in LPS-induced ALI models (Yang et al., 2019). Similarly, EPC transplantation could ameliorate ventilator-induced lung injury by improving epithelial permeability and reducing inflammation and apoptosis (Ju et al., 2019). Furthermore, the role of metabolic signaling in ECs is gaining attention as a promising target for therapy. Metabolic pathways in ECs are necessary for both the injury and repair phases of ALI/ARDS. During the repair phase, EC proliferation and junction reannealing are crucial for restoring vascular integrity. Targeting these metabolic pathways could provide novel therapeutic avenues for enhancing endothelial repair and improving outcomes in sepsis-induced ALI/ARDS (Gould et al., 2024). In conclusion, understanding the molecular mechanisms underlying endothelial regeneration and vascular repair in sepsis-induced ALI/ARDS is essential for developing effective therapeutic strategies. Targeting pathways such as p110γPI3K, enhancing EPC function, modulating ECs metabolism, and focusing on transcriptional regulators like Sox17 and HIF-1α represent promising approaches to promote endothelial repair and improve patient outcomes in these critical conditions.

2.3 Pulmonary endothelial heterogeneity—emerging EC subpopulations and their potential roles in sepsis-induced ALI/ARDS

The lung is a complex organ composed of various cell types, with ECs forming a crucial component of the pulmonary vasculature and exhibiting significant heterogeneity. This heterogeneity plays a key role in maintaining normal lung physiology, adapting to environmental changes, and responding to pathophysiological stimuli. During sepsis-induced ALI/ARDS, pulmonary ECs undergo significant alterations. Recent studies have further revealed the diversity of lung ECs, identifying multiple distinct EC subpopulations that may play specific functional roles in the development and progression of sepsis-related ALI/ARDS.

Using single-cell RNA sequencing (scRNA-seq), we have gained a deeper understanding of the heterogeneity of lung microvascular ECs. This research revealed two distinct capillary EC subpopulations: alveolar capillary endothelial cells (aCAPs) and general capillary endothelial cells (gCAPs) (Gillich et al., 2020; Schupp et al., 2021). aCAPs are a lung-specific EC subpopulation primarily responsible for gas exchange and leukocyte trafficking. This subpopulation uniquely expresses carbonic anhydrase 4 (Car4), with its expression dependent on VEGFA secreted by type I alveolar epithelial cells, and constitutes approximately 15% of the total pulmonary ECs (Vila et al., 2020). The characteristics of aCAPs are significantly affected when epithelial cells lose VEGFA; despite the structural integrity of myofibroblasts being maintained, abnormal enlargement of alveolar spaces leads to impaired lung function (Vila et al., 2020).

Unlike aCAPs, gCAPs primarily participate in the regulation of vascular tone and act as important stem/progenitor cells,

maintaining and repairing capillary homeostasis. Through scRNA-seq, Seurat clustering, and differential gene expression analysis, gCAPs were further divided into two main subpopulations: immune-related ECs and development-related ECs. Immune-related ECs highly expressed immune-related genes (e.g., CD74), while development-related ECs were enriched in genes associated with angiogenesis (e.g., Sox17). Studies have report significant differences in gene expression between these two subpopulations at different stages of the inflammatory response, a phenomenon observed in multiple lung injury models (Zhang et al., 2022). During the early stage of inflammation, the expression levels of development-related genes significantly decrease. However, as inflammation resolves and tissue repair commences, these genes gradually return to high levels of expression, promoting EC regeneration (Zhang et al., 2022; Godoy et al., 2023). Furthermore, a novel proliferative EC subpopulation (proECs) was identified during the inflammatory repair phase. This subpopulation is enriched in genes associated with chromosome segregation, mitosis, DNA replication, and the cell cycle, suggesting a crucial role in endothelial regeneration (Liu et al., 2019).

Sox17 is as a key regulator of endothelial regeneration and plays a crucial role in endothelial repair following inflammatory vascular injury. Studies have shown that Sox17 overexpression not only accelerates EC regeneration but also inhibits the expression of pro-inflammatory cytokines, demonstrating its anti-inflammatory potential in the repair process (Zhang et al., 2022). However, the functional division of labor among different pulmonary vascular EC subpopulations during lung injury and repair remains incompletely understood.

In other pathological conditions, a review from Southern Medical University details the updated classification of endothelial dysfunction associated with pulmonary arterial hypertension (PAH) (Shen et al., 2024). Furthermore, research has identified another EC subpopulation closely related to pro-fibrotic processes, characterized by the expression of Cxcl12 (Liu et al., 2021).

In conclusion, the heterogeneity of pulmonary ECs offers novel therapeutic targets for ALI and ARDS. Future studies may further elucidate the functions of different EC subpopulations and their specific roles in inflammation and repair. Targeting the regulation of specific EC subpopulations and their unique responses to inflammation and mechanical stimuli holds promise as a potential strategy for treating these severe lung diseases.

3 Neutrophils in sepsis-induced ALI/ARDS

Neutrophils play a pivotal role in the pathogenesis of sepsis-induced ALI/ARDS. These cells are among the first responders to infection and are crucial for the innate immune response. However, their dysregulated activity can lead to significant tissue damage and exacerbate the condition of ALI/ARDS. The recruitment and activation of neutrophils in the lungs are critical processes that contribute to the progression of these conditions. In sepsis, neutrophils are often found to be dysfunctional, which can lead to impaired migration and excessive accumulation in the lungs, resulting in tissue damage and inflammation (Xu et al., 2024).

3.1 The role of neutrophils in early lung injury

Neutrophils play a pivotal role in the pathogenesis of early sepsis-induced ALI and ARDS. As first responders to infection, these immune cells are essential to the body's defense mechanisms. They contribute to pathogen elimination through the production of antimicrobial peptides, ROS, and inflammatory mediators. However, their dysregulated activation and excessive accumulation in the lungs can exacerbate tissue damage and amplify inflammation, driving the progression of ALI/ARDS. In the early stages of these conditions, neutrophils act as key mediators, striking a delicate balance between protective immune responses and harmful tissue injury, ultimately influencing disease outcomes (Wang et al., 2022).

ARDS is a highly inflammatory disease strongly associated with neutrophil activation. Excessive neutrophil recruitment is a key feature of ARDS, and the released immunomodulatory molecules from these neutrophils induce tissue damage. Studies indicate that inhibiting excessive neutrophil migration or activation can significantly reduce lung injury (Conrad et al., 2022). In the context of sepsis, neutrophils are extensively activated and recruited to the lungs, releasing various cytotoxic substances, including ROS, proteases, and NETs. While intended to combat pathogens, these substances can also damage the alveolar-capillary barrier, leading to increased permeability, edema, and impaired gas exchange, all hallmarks of ALI/ARDS. Furthermore, neutrophil-derived antimicrobial peptides (such as the associated peptide LL-37), in synergy with myeloperoxidase (MPO) and histones, exert significant cytotoxicity on ECs, further exacerbating alveolar and capillary damage, ultimately leading to the development of ALI and ARDS.

Neutrophil recruitment and activation are primarily mediated by various chemokines and cytokines, such as IL-8 and CXCL1. Sustained excessive secretion of these chemokines can trigger an overzealous neutrophil response, leading to lung tissue damage. Furthermore, the formation of NETs, a process known as NETosis, is considered a "double-edged sword" in sepsis-induced ALI/ARDS. While NETs effectively trap and kill pathogens, their excessive production can cause endothelial damage and exacerbate pulmonary inflammation. Research suggests that targeting NET formation or accelerating its clearance may be an effective strategy for mitigating sepsis-induced ALI/ARDS. In ARDS patients, prolonged neutrophil lifespan further amplifies the inflammatory response, whereas promoting neutrophil apoptosis can reduce excessive NET formation and suppress inflammatory processes, thereby alleviating lung injury (Song et al., 2022; Xu et al., 2024). Excessive NET release and impaired clearance are considered significant drivers of persistent inflammation in ARDS (Gregoire et al., 2018). Furthermore, neutrophil-derived exosomal miR-30d-5p activates the NF-κB signaling pathway, inducing M1 macrophage polarization, which in turn triggers pyroptosis and exacerbates the pathological process of sepsis-induced acute lung injury (Jiao et al., 2021).

Neutrophils significantly contribute to sepsis-induced pulmonary microcirculatory dysfunction. During sepsis, excessive neutrophil accumulation in capillaries can lead to localized microcirculatory disturbances, increasing functional dead space and subsequently causing hypoxemia and pulmonary edema. This disruption of pulmonary microcirculation is a crucial factor in hypoxemia associated with ALI and ARDS. Targeting neutrophils to

restore microcirculatory function has demonstrated effectiveness in alleviating hypoxemia and edema, offering a novel research avenue for sepsis-induced ALI/ARDS (Park et al., 2019).

Furthermore, the interplay between neutrophils and other immune cells, such as macrophages and T cells, plays a crucial role in modulating inflammation. These interactions can both amplify inflammatory cascades and, under specific circumstances, promote inflammation resolution (Wang et al., 2022). Investigating the mechanisms of these cellular and molecular interactions is essential for developing targeted therapeutic strategies for sepsis-inducedALI/ARDS.

In summary, while neutrophils are crucial in the initial immune response to sepsis, their dysregulated activity often triggers severe lung injury in ALI/ARDS. Modulating neutrophil function, limiting their overactivation, and targeting related signaling pathways may not only alleviate lung injury but also potentially improve the prognosis of sepsis-induced ALI/ARDS, offering potential therapeutic strategies for these conditions.

3.2 The role of neutrophils in late-stage and lung repair of sepsis-induced ALI/ARDS

Neutrophils participate not only in the early stages of ALI/ARDS but also in the later stages. In these diseases, neutrophils can exacerbate lung injury and initiate repair processes by participating in the clearance of apoptotic cells and debris, resolving inflammation, and restoring tissue homeostasis (Bhatia et al., 2012). First, some molecules can regulate the transition from the initial pro-inflammatory response to an anti-inflammatory state, thereby limiting further tissue damage. For example, neutrophils synthesize and release pro-resolution lipid mediators, including lipoxin A4, resolvin, and protectin, which play a critical role in alleviating lung inflammation (Serhan et al., 2008). Additionally, NETs contribute to the resolution and alleviation of inflammation by degrading excessive cytokines and chemokines (Schauer et al., 2014).

In the late stages of sepsis-induced ALI/ARDS, neutrophils exhibit altered functions, contributing to persistent inflammation and tissue damage. Impaired clearance of apoptotic neutrophils, leading to prolonged inflammation and delayed resolution of lung injury, is partly responsible. Furthermore, NETs, extracellular networks of DNA and antimicrobial proteins, further damage lung tissue by promoting endothelial and epithelial cell death and increasing vascular permeability (Fox et al., 2013; Jin et al., 2023). Dysregulation of neutrophil chemotaxis and migration is another crucial factor in the late phase of sepsis-induced ALI/ARDS. Despite high levels of chemoattractants at the site of infection, neutrophils often fail to migrate effectively, causing them to accumulate in the lungs and release harmful substances, resulting in tissue injury. This impaired migration is associated with dysregulation of signaling pathways, including those involving G protein-coupled receptors (GPCRs), which are critical for neutrophil chemotaxis (Park et al., 2019; Wang et al., 2023).

Furthermore, certain molecules released by neutrophils can directly drive tissue remodeling and repair. For example, MMPs can degrade collagen scars and inflammatory mediators, thereby promoting cell migration and epithelial regeneration (Greenlee et al., 2007; Davey et al., 2011). Furthermore, neutrophils can promote epithelial cell proliferation and repair by activating the Wnt/β-catenin signaling pathway, thereby aiding in the restoration of lung tissue function (Zemans et al., 2011). Neutrophils also actively release growth factors. These factors stimulate the proliferation and migration of epithelial and ECs, promoting the restoration of the alveolar-capillary barrier. VEGF plays a particularly important role in enhancing angiogenesis, which is crucial for regenerating a complete pulmonary microvascular network. Neutrophils can modulate tissue repair by secreting specialized pro-resolution mediators. In addition to lipid mediators like resolvins, they release cytokines and chemokines in a context-dependent manner, transitioning from a pro-inflammatory to a pro-resolving phenotype. For example, TGF-β and amphiregulin released by neutrophils can promote extracellular matrix remodeling and epithelial cell proliferation, thereby repairing damaged alveolar structures. However, excessive TGF-β may lead to aberrant repair and fibrosis, highlighting the need to balance neutrophil activity during the resolution phase.

Upon stimulation by extracellular signals such as angiotensin II or TGF-β, neutrophils can polarize and produce two distinct functional phenotypes (N1 and N2). The N1 phenotype is pro-inflammatory functions and enhanced cytotoxicity, while the N2 phenotype exhibits anti-inflammatory properties and can secrete growth factors and MMPs (such as VEGF and MMP-9), facilitating tissue repair and reconstruction (Fridlender et al., 2009). The involvement of these molecules is crucial for the regeneration of tissue following lung injury.

Moreover, neutrophils can indirectly promote lung repair processes by modulating other immune cells. An effective resolution of the inflammatory response requires macrophages to clear senescent or apoptotic neutrophils. During this process, the macrophage phenotype transitions from one that secretes pro-inflammatory cytokines and chemokines to one that releases anti-inflammatory factors, thus supporting tissue remodeling and repair (Lumbroso et al., 2018).

In summary, while neutrophils exert destructive effects during acute lung injury and inflammation, they also play a crucial role in tissue regeneration and functional recovery through reparative mechanisms, offering new avenues for lung injury treatment research. In the late stages of ARDS, damaged alveoli attempt to restore tissue homeostasis by supporting the reconstruction of alveolar structures, a period characterized by fibroblast proliferation. Neutrophils exacerbate fibrosis by releasing elastase (Takemasa et al., 2012), and NET (Chrysanthopoulou et al., 2014).

3.3 The role of neutrophil death mechanisms in sepsis-induced ALI/ARDS

Neutrophils play a crucial role in the immune response during sepsis, and their different modes of cell death can significantly impact the progression and severity of sepsis-induced ALI/ARDS. In sepsis, neutrophils can undergo various forms of cell death, including apoptosis, necroptosis, and pyroptosis, each of which has distinct implications for inflammation and tissue damage.

The inflammatory response is a fundamental physiological and pathological process, with the inflammasome serving as a key regulator. Inflammasomes recruit and activate caspase-1, which

not only promotes the hydrolytic maturation of IL-1β and IL-18 but also triggers the cleavage of Gasdermin D (GSDMD). The cleaved GSDMD forms pores in the cell membrane, initiating pyroptosis (Broz et al., 2020). During this process, the release of IL-1β, IL-18, and HMGB1 exacerbates local inflammation, causes tissue damage, and transmits danger signals from damaged or dying cells to the surrounding environment. This cascade further stimulates immune cell activity, particularly neutrophil recruitment. While intracellular pathogens are not directly released into the extracellular space during neutrophil pyroptosis, they can form pore-induced intracellular traps. This mechanism, in conjunction with the complement system and clearance receptors, enhances the innate immune response by recruiting neutrophils, which subsequently release ROS or engage in secondary phagocytosis to eliminate pathogens. Notably, neutrophil pyroptosis also serves as a trigger for the formation of NETs.

Necroptosis, a form of programmed necrosis, triggers the release of cellular contents, exacerbating inflammatory responses. Research indicates that this cell death pathway significantly worsens inflammation in sepsis-induced ALI/ARDS, leading to lung injury and dysfunction (Aziz et al., 2014). Specifically, neutrophil necroptosis is often closely associated with the formation of NETs. NET formation induces endothelial dysfunction and increases vascular permeability, thereby aggravating pathological changes (Xu et al., 2024). Furthermore, neutrophil-derived enzymes and ROS released during necroptosis further disrupt the alveolar-capillary barrier, worsening lung damage (Blazquez-Prieto et al., 2018). Notably, the role of autophagy in regulating neutrophil function, including necroptosis, has garnered attention as a potential therapeutic target to mitigate lung injury during sepsis (Park et al., 2017). In summary, neutrophil necroptosis is a crucial factor in the pathogenesis of sepsis-induced ALI/ARDS, significantly contributing to the excessive inflammation and tissue damage.

Apoptosis, a form of programmed cell death, is generally associated with anti-inflammatory effects, unlike other cell death pathways. It is characterized by the orderly dismantling of cells and their clearance by macrophages without the release of inflammatory mediators. Studies have shown that delayed neutrophil apoptosis exacerbates lung injury, while promoting timely apoptosis aids in inflammation resolution (Li et al., 2014; Park et al., 2019). The molecular mechanisms of neutrophil apoptosis are complex, involving the activation of death-associated protein kinase 1 (DAPK1) and caspases, pathways that play a central role in regulating neutrophil apoptosis and inflammation[60–61]. For instance, the lipid mediator protectin D1 has been shown to enhance neutrophil apoptosis, thereby accelerating inflammation resolution. Similarly, research indicates that nanoparticle-induced apoptosis can significantly improve survival rates in sepsis and effectively alleviate lung injury (Paunel-Gorgulu et al., 2012; Li et al., 2014). Furthermore, recent findings suggest that Gasdermin E (GSDME) is a crucial protein regulating the switch between apoptosis and pyroptosis (Ma et al., 2024). Through the action of specific enzymes, such as caspase-3, GSDME modulates the conversion between these cell death pathways, further influencing neutrophil fate and its role in lung inflammation. However, in sepsis, excessive apoptosis of various immune cells, such as neutrophils and macrophages, can lead to immunosuppression, disrupting cellular balance and increasing the risk of secondary lung injury.

In conclusion, the different modes of neutrophil death in sepsis-induced ARDS have profound effects on the inflammatory response and tissue damage. Targeting specific pathways involved in neutrophil death may offer novel therapeutic strategies to improve outcomes (Englert et al., 2019).

3.4 Heterogeneity of neutrophils in the lungs: new subpopulations and their roles in ALI/ARDS

For a long time, neutrophils have been considered key players in the pathogenesis of ALI/ARDS. However, despite significant advancements in neutrophil research, clinical outcomes for ALI/ARDS have not substantially improved. In recent years, neutrophil research has shifted from traditional functional exploration to heterogeneity analysis, revealing their complexity and diversity in disease states. In ALI/ARDS, classically defined neutrophil subtypes participate in inflammatory cascades, pathogen clearance, and tissue repair by initiating and amplifying inflammatory responses, releasing ROS and NETs, and secreting proteases and modulating immune cell interactions. However, other distinct neutrophil subsets may perform a variety of unique functions. Therefore, in-depth investigation of the diversity and functions of neutrophil subsets within the lung microenvironment is crucial for further understanding the complex mechanisms of ALI/ARDS and developing targeted therapeutic strategies.

Using single-cell RNA sequencing (scRNA-seq), researchers identified two distinct neutrophil subpopulations in the lung tissue of an ALI mouse model, namely, *F*th1^{hi} Neu and Prok2^{hi} Neu, which exhibit unique functional and distributional characteristics (Wang et al., 2022). These subpopulations can be clearly distinguished by specific gene expression patterns. *F*th1^{hi} Neu is mainly distributed within and around the airways (e.g., bronchi, alveolar lumen, and interstitial regions), morphologically tending to exhibit multilobed or even hypersegmented nuclei, and displaying aging-associated phenotypic features. Functionally, this subpopulation exhibits strong pro-inflammatory and chemotactic properties, while demonstrating reduced sensitivity to apoptosis and oxidative damage. Prok2^{hi} Neu is primarily found within lung vasculature, characterized by ring-shaped nuclei, and exhibits an immune-activated state. These neutrophils express high levels of antimicrobial peptides, exhibit active glycolysis metabolically, and undergo rapid apoptosis, thereby being promptly cleared by the immune system to avoid excessive inflammation.

In the ALI mouse model, the proportion of *F*th1^{hi} Neu neutrophils is significantly increased, and its level is positively correlated with disease severity. Furthermore, in ARDS patients, neutrophils with high *F*th1 expression and low Prok2 expression may predict poorer clinical outcomes. The study also indicates that the anti-inflammatory cytokine IL-10 can alleviate ALI-induced acute pulmonary inflammation and diffuse alveolar damage by regulating the ratio of *F*th1^{hi} Neu to Prok2^{hi} Neu subpopulations (Wang et al., 2022). These findings suggest that these specific neutrophil subtypes may serve as potential prognostic biomarkers for ARDS patients and provide new ideas for targeted therapy.

Compared to studies on pulmonary ECs, research on neutrophil heterogeneity is relatively limited. However, recent

studies are gradually uncovering the diversity of neutrophils in different pathological states. For instance, Xie et al. used single-cell transcriptomic analysis to reveal the heterogeneity of neutrophils and their coordinated maturation process during homeostasis and bacterial infection (Xie et al., 2020). Furthermore, in cancer research, Liu et al. explored the origin, chemotaxis, and activation regulators of tumor-associated neutrophils, as well as their phenotypes and functions in the tumor microenvironment (Liu et al., 2023).

In conclusion, the diversification of neutrophil subsets plays a significant role in the pathogenesis of ALI/ARDS. The dynamic distribution and functional changes of these subsets offer not only new perspectives for investigating disease mechanisms but also potential applications for clinical intervention and prognostic assessment. With further research, precision therapeutic strategies targeting neutrophil heterogeneity may bring new breakthroughs in the treatment of ALI/ARDS.

4 EC-neutrophil interactions in sepsis-induced ALI/ARDS

Sepsis-induced ALI/ARDS are life-threatening conditions. The complex interplay between ECs and neutrophils is a critical mechanism in this pathological process. ECs form a crucial barrier between the bloodstream and lung tissue, essential for maintaining vascular integrity and regulating immune cell migration. Neutrophils, as the first line of immune defense, play a dual role in combating infection and causing tissue damage during sepsis. This dynamic interaction between these 2 cell types is both a protective mechanism against invading pathogens and a driver of inflammatory dysregulation in sepsis. Understanding these complex interactions is crucial for elucidating the molecular mechanisms of sepsis-induced ALI/ARDS and identifying potential therapeutic targets. In the following sections, we will elaborate on the interaction between ECs and neutrophils.

4.1 Regulation of neutrophil function by ECs

Neutrophil infiltration is a finely regulated multi-step process involving critical phases such as rolling, adhesion, crawling, and transmigration. In this process, activated ECs promote neutrophil rolling and initial adhesion on the vascular endothelium through the expression of surface adhesion molecules, including ICAM-1, VCAM-1, P-selectin, and E-selectin, thereby facilitating neutrophil migration into underlying tissues (Gerhardt and Ley, 2015). During transmigration, neutrophils are activated by chemokines released from ECs, resulting in increased expression of integrins on their surface, which form more stable adhesions with ICAM-1 and VCAM-1, initiating the process of crossing the endothelium to reach damaged tissues (Yuan et al., 2012; Zhong et al., 2018). Additionally, the glycosylated RNA on the neutrophil surface participates in its migration to sites of inflammation by binding to P-selectin on ECs (Zhang et al., 2024). Throughout the transmigration process, the mechanical squeezing force exerted by neutrophils activates signaling pathways in ECs, involving the interaction and activation of Platelet-Endothelial Cell Adhesion Molecule-1 (PECAM-1, or CD31) with the VEGFR2/VE-cadherin mechanotransduction complex in ECs. This interaction increases the intracellular calcium ion concentration in ECs, which further facilitates neutrophil passage across the vascular endothelium (Fu et al., 2023). ROS, and other oxidants generated by activated ECs contribute to tissue damage by neutralizing local antioxidants. In this process, VE-cadherin expression is downregulated, while neutrophil adhesion molecules are upregulated, with increased release of chemokines promoting neutrophil inflammatory migration (Millar et al., 2016). The activated integrin Macrophage-1 antigen (Mac-1) binds to ligands of ECs (e.g., ICAM-1) to promote neutrophil adhesion, crawling, and transmigration across the endothelium (Li et al., 2024). Under the influence of chemokines, the cytoskeleton of ECs undergoes dynamic remodeling, facilitating neutrophil passage through the vascular wall. Furthermore, the levels of Syndecan-4, a key component of the endothelial glycocalyx, are significantly elevated in sepsis-induced ALI/ARDS. Its downregulation, whether in in vivo or *in vitro* models, markedly increases neutrophil adhesion and inflammatory response (Zhu et al., 2023). Thus, ECs engage in the entire process of neutrophil extravasation through multiple mechanisms.

During neutrophil transmigration across ECs, dynamic changes in surface-associated molecules regulate their functional characteristics. Neutrophils experience mechanical forces during transmigration, which have significant implications for their functionality. Among these, the mechanosensory channel protein Piezo1 detects mechanical signals as neutrophils traverse the intercellular junctions of ECs. Activation of Piezo1 induces the upregulation of the Nox4 gene in neutrophils, resulting in increased hydrogen peroxide production, thereby enhancing their bactericidal capacity. Moreover, this shear force, via Piezo1 activation, can also induce NETs, presenting a potential target for studying inflammatory and thrombotic diseases related to NETs (Baratchi et al., 2024).

In addition to facilitating neutrophil migration to inflamed tissues, ECs may induce abnormal transport of neutrophils, resulting in damage to distal tissues. Inflammation-activated ECs release extracellular vehicles (EVs) rich in the transport protein subunit KPNB1, which upregulate neutrophil elastase (NE) activity via STAT signaling, leading to the degradation of junctional adhesion molecule-C (JAM-C). This promotes the reverse transport of neutrophils and induces a phenotypic shift that results in a unique form of reverse trans-endothelial migration (rTEM) activation phenotype (Zi et al., 2024). Reverse migration primarily relies on JAM-C; particularly under ischemic conditions, neutrophils expressing high levels of Mac-1 release elastase to degrade JAM-C, thereby facilitating their reverse migration (Scheiermann et al., 2009). Further studies indicate that neutrophils undergoing reverse migration predominantly transfer to the lungs, where they become sequestered, resulting in lung injury. However, the specific mechanisms underlying this process warrant further exploration. Additionally, not only can EC damage induced by pathogenic infections promote reverse migration of neutrophils, but aging ECs can also enable neutrophils to reverse migrate from localized inflammatory tissues back into the circulation, leading to distal tissue damage, particularly significant in lung tissue (Barkaway et al., 2021). This mechanism of heightened

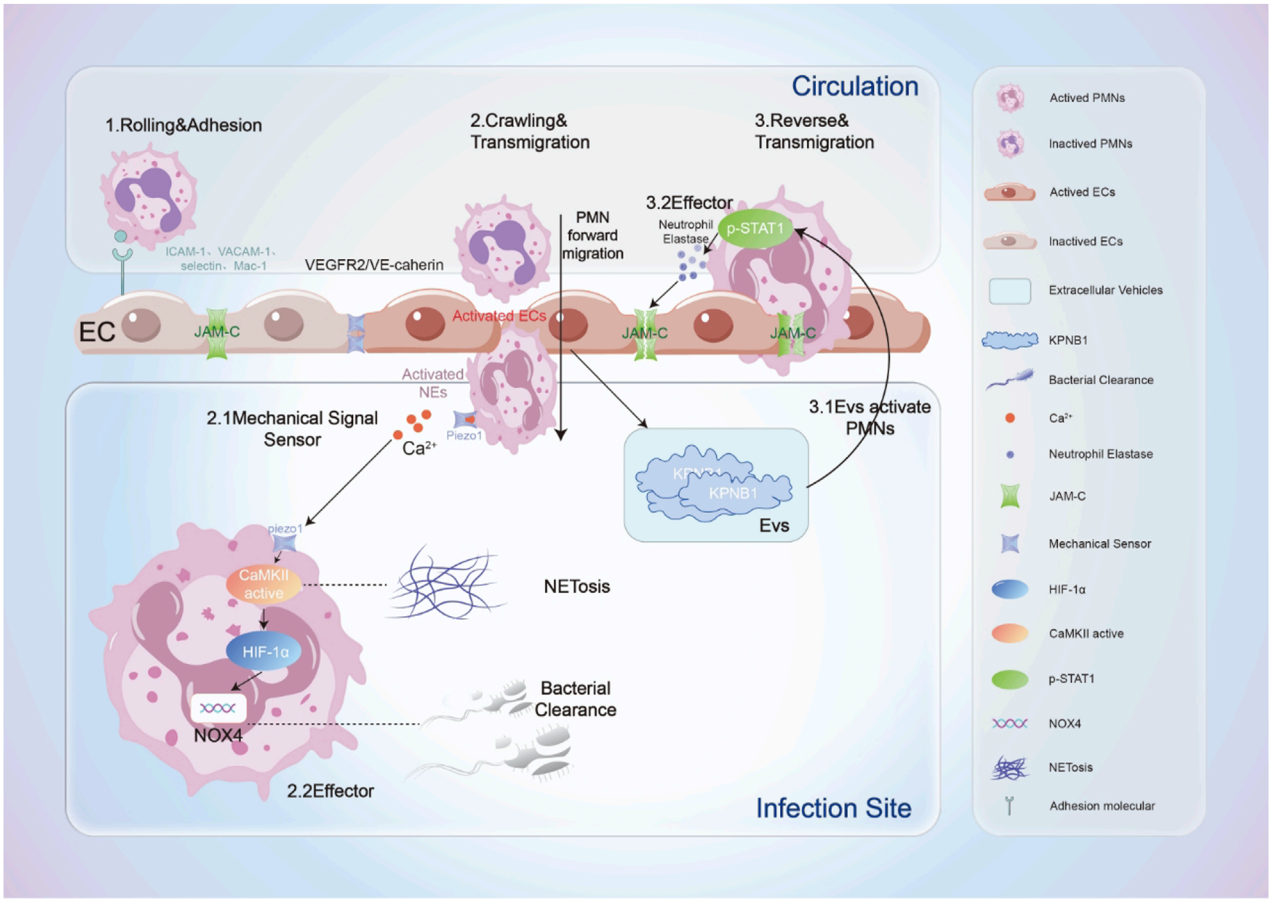

FIGURE 1
The process by which neutrophils interact dynamically with ECs when recruited to sites of inflammation. This includes: 1. Rolling and adhesion: Neutrophils roll along the surface of ECs and establish initial adhesion by binding to adhesion molecules on the endothelial surface; 2. Crawling and transmigration: ECs are activated by mechanical forces and other agents, further facilitating the transendothelial migration of neutrophils. Simultaneously, neutrophils sense mechanical stimuli, leading to the activation of their mechanosensors, which induces cell activation accompanied by an increase in intracellular calcium ion concentration. This activation results in NETosis (formation of extracellular traps) in neutrophils; on the other hand, the upregulation of Nox4 levels enhances the bactericidal capacity of neutrophils; 3. Reverse and transmigration: Activated ECs release extracellular vesicles that stimulate neutrophils to release neutrophil elastase (NE). Neutrophil elastase degrades the JAM-C connections between ECs, prompting neutrophils to undergo reverse transendothelial migration, ultimately leading to damage in distal tissues.

pulmonary susceptibility aligns with the clinically observed phenomenon of a significantly higher incidence of sepsis-induced ARDS compared to other organ injuries. Importantly, while reverse migration of neutrophils reduces the cellularity at the inflammatory sites, potentially mitigating the expansion of local inflammatory responses, the associated damage to distal organs cannot be overlooked. Therefore, precise modulation of neutrophil reverse migration holds considerable therapeutic significance for treating various diseases characterized primarily by neutrophil infiltration as a pathological mechanism (Nourshargh et al., 2016) (Figure 1).

4.2 Regulation of endothelial function by neutrophils

The endothelial barrier primarily consists of three major components: the endothelial glycocalyx, intercellular junctions, and focal adhesion on the basal side. Neutrophils profoundly regulate the integrity and function of the endothelial barrier by altering these structures and their functions. During respiratory bursts, neutrophils generate ROS, and the release of MPO, elastase, cathepsin G, and MMPs during degranulation can cleave the endothelial glycocalyx (Ma et al., 2019). Furthermore, NETs released by neutrophils accelerate the degradation of the glycocalyx (Zhang et al., 2023). Inflammatory cytokines induced by neutrophils, such as IL-6, IL-8, and TNF-α, also contribute to the disruption of glycocalyx structure, significantly increasing endothelial permeability (Schmidt et al., 2012). Once the glycocalyx is compromised, ICAM-1, E-selectin, and other adhesion molecules are exposed on the surface of ECs. This molecular exposure not only triggers a strong inflammatory response but also promotes the rolling and adhesion of leukocytes and platelets, further amplifying inflammation (Becker et al., 2010; Iba and Levy, 2019). Among the intercellular junctions, VE-cadherin is particularly susceptible to degradation by MMPs secreted by neutrophils, leading to the

disruption of the endothelial barrier (Luplertlop et al., 2006; Dejana et al., 2008). Concurrently, TNF-α activates the NF-κB signaling pathway, impairing the tight junction protein claudin-5 at the endothelial junctions, further weakening the barrier function (Clark et al., 2015).

By secreting inflammatory cytokines and chemokines, neutrophils become key mediators in the regulation of endothelial function during ALI. Their derived antimicrobial peptides, such as LL-37, in conjunction with MPO and histones, exert cytotoxic damage on ECs, causing capillary injury and contributing to ALI/ARDS. In sepsis-induced ARDS, the fatty acids halogenated by myeloperoxidase released from neutrophils, specifically 2-chlorofatty acids (2-ClFAs), are closely associated with damage to pulmonary ECs (Meyer et al., 2017). Moreover, neutrophils promote the expression of tissue factor (TF) in ECs, inducing a transition to a pro-inflammatory and pro-coagulant phenotype, further compromising endothelial barrier function (Kim et al., 2016). However, it is noteworthy that during the course of sepsis, neutrophils can also mitigate oxidative stress and endothelial dysfunction by releasing extracellular vesicles carrying superoxide dismutase 2 (SOD2), thus alleviating symptoms of disseminated intravascular coagulation (DIC) (Bao et al., 2022). This protective mechanism highlights the complex role of neutrophils in endothelial barrier function, suggesting future research directions for precision therapies targeting endothelial barrier-related diseases through the modulation of neutrophil function (Figure 1).

5 Outlook

Cell-cell interactions (CCIs) are the basic mechanisms for information exchange and collaborative work between cells in multicellular organisms. Molecular interaction between cells plays the most irreplaceable part. Here, we summarize three research that may have more invaluable discoveries in neutrophil-endothelial interaction in ALI/ARDS (Figure 2).

5.1 The appeal of NETosis

Neutrophils play a crucial role in ALI, with NETs being a common pathogenic mechanism. The process of NET formation and release is termed NETosis. This mechanism involves the release of filamentous extracellular structures by neutrophils in response to external stimuli, capturing pathogens within a network composed of DNA, histones, proteases, and other cytotoxic and inflammatory compounds. As an important innate immune response, NETosis helps protect the body from pathogenic attacks. However, its role is not limited to pathogens; excessive or uncontrolled NETosis can cause significant damage to surrounding tissues. In sepsis-induced ALI/ARDS, the production of NETs is closely related to the severity of the disease (Xu et al., 2024). Research indicates that free DNA within NETs can lead to alveolar dysfunction and epithelial cell damage (Gan et al., 2018). NETosis markedly exacerbates EC damage, enhancing vascular leakage and aggravating sepsis-induced ARDS (Xu et al., 2024). Additionally, PAD4 (protein arginine deiminase 4) is a key enzyme involved in NET formation. Overexpression of PAD4 leads to vascular injury by releasing NETs and inducing the expression of endothelial ICAM-1 and VCAM-1. Experimental studies have shown that complete knockout of PAD4 or the use of PAD4 inhibitors can significantly suppress NET formation, thereby alleviating lung damage (Biron et al., 2018). Furthermore, histones within NETs have been found to induce apoptosis in pulmonary vascular ECs, further exacerbating sepsis-related ALI/ARDS progression (Li et al., 2021). NETosis also disrupts endothelial glycocalyx by releasing and secreting inflammatory cytokines. Simultaneously, NETs can induce macrophages M1 phenotype, leading to the release of more inflammatory cytokines and worsening the inflammatory response (Song et al., 2019). Additionally, NETs promote platelet adhesion, activation, and aggregation, providing scaffolding for thrombus formation. The interaction between platelets and ECs as well as complement further mediates NET generation, triggering immune thrombosis and creating a positive feedback loop in the coagulation process, ultimately resulting in severe endothelial dysfunction (Kumar et al., 2019; Wei et al., 2023).

In summary, in the pathological microenvironment of ALI/ARDS, NETosis significantly impacts alveolar epithelial cells, ECs, macrophages, and platelets. Therapeutic interventions targeting NETs may provide new strategies and directions for treating sepsis-induced ALI/ARDS.

5.2 Immune ECs (IMECs)

ECs possess extensive physiological functions, including facilitating the passage of immune cells across the endothelial barrier, regulating hemostasis and thrombosis, and achieving repair and vascular reconstruction following endothelial injury. Through single-cell transcriptomic studies, several functional subsets of ECs have been identified, one of which is enriched with immune regulation-related genes and is referred to as “immune regulatory ECs” (IMECs).

The lungs, as a highly vascularized organ, primarily consist of microvascular ECs. Because the lungs are directly connected to the external environment, they are exposed to potential pathogenic microorganisms and pollutants, with their primary function being gas exchange. However, the successful completion of this process relies on appropriate immune responses. Research has shown that under physiological conditions, IMECs are rich in MHC II-related genes, which is important in both innate and adaptive immune responses. It is hypothesized that IMECs act as “sentinels,” activating host immune defenses upon sensing airborne pathogens. Furthermore, in lung injury models induced by SARS-CoV-2 and H1N1, immune regulatory ECs exhibited a more rapid and intense inflammatory response, suggesting that the immune regulatory functions of IMECs are critical in addressing pulmonary infections and injuries.

Nevertheless, knowledge about the effects of this specific EC subset on lung injury and repair in ALI/ARDS remains limited. Exploring the immune regulatory functions of IMECs in ALI/ARDS and their contributions to pathogenesis may provide new perspectives for potential therapeutic strategies. This area holds significant frontier research importance.

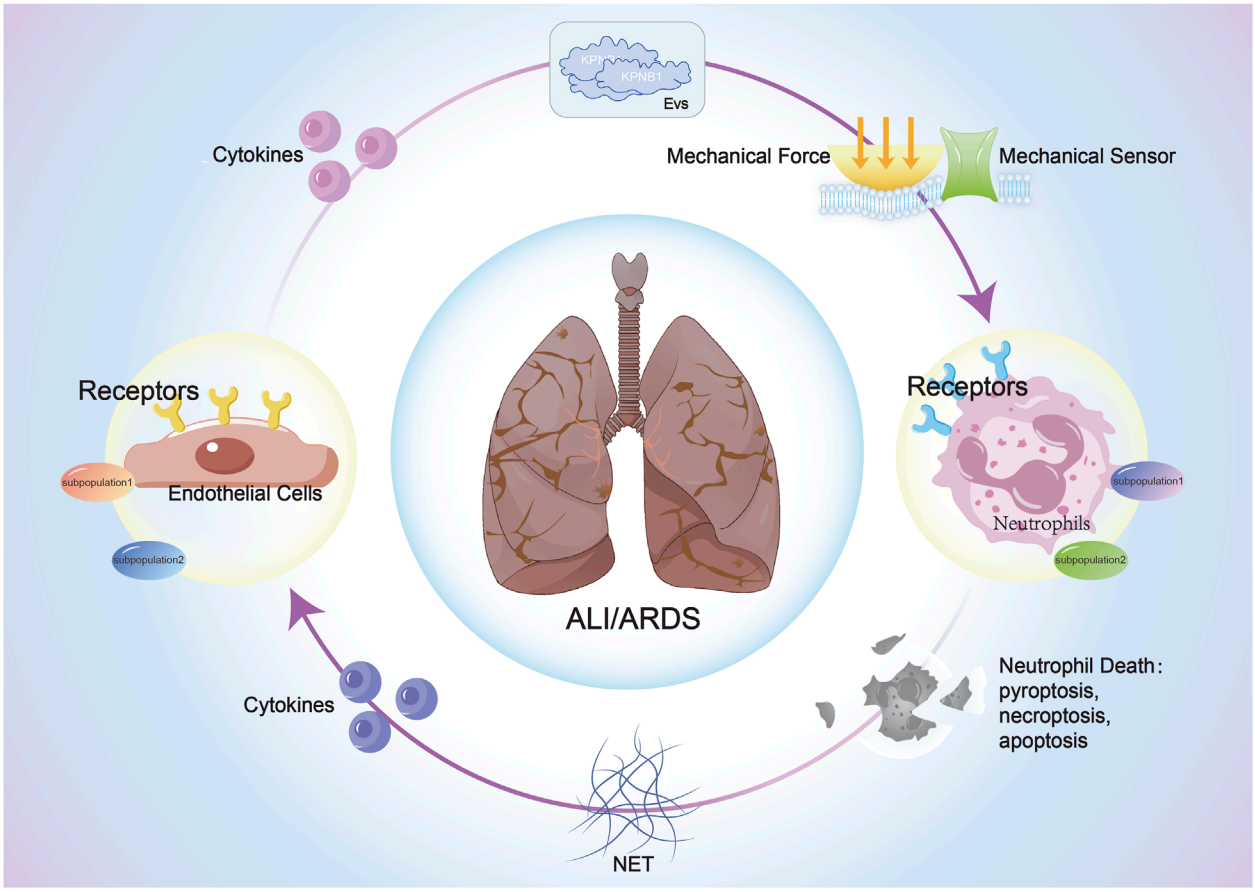

FIGURE 2
The interaction between ECs and neutrophils in sepsis-induced ALI/ARDS: Both cell types activate corresponding signaling pathways through the release of cytokines, extracellular vesicles, and mechanical force changes after stimulation, impacting cellular structure, function, phenotype, and fate, thereby influencing the progression of ALI/ARDS.

5.3 Mechanosensors

The process by which cells sense and respond to mechanical forces, initiating biological activities, is referred to as mechanotransduction. This process has a significant impact on the development and function of organisms, with the groundbreaking discovery of Piezo channels providing a novel perspective for research in this field. Piezo proteins are mechanically sensitive ion channels that can sense biological mechanical forces such as hydrostatic pressure, fluid shear stress, and membrane stretch, transducing mechanical signals into biological signals by regulating calcium ion concentration changes. Piezo proteins are widely distributed in the heart, brain, vasculature, and musculoskeletal systems, participating in various pathophysiological processes (Jia et al., 2024; Lim et al., 2024).

Piezo1 can sense the transmigration of neutrophils across ECs, thereby enhancing their bactericidal ability and participating in immunomodulation (Mukhopadhyay et al., 2024). Concurrently, EC Piezo1 is activated by the synergy between leukocytes and the hemodynamic microenvironment, leading to downstream signaling pathways that disrupt the endothelial barrier and exacerbate leukocyte extravasation. Piezo1, expressed in ECs and type II alveolar cells, may play a detrimental role in regulating pulmonary endothelial barrier function in ventilator-induced lung injury (Friedrich et al., 2019; Liang et al., 2019). In summary, Piezo proteins play a crucial role in intercellular interactions and provide new research directions and potential therapeutic targets for various mechanotransduction-related diseases.

In the pathogenesis of ALI/ARDS, various scenarios involving neutrophils, such as their traversal through ECs, reverse migration, interactions with endothelial adhesion molecules, and the disruption and reconstruction of the endothelial barrier, all entail significant interactions with biomechanical forces. However, current research on these mechanotransduction-related mechanisms still presents substantial room for exploration, particularly regarding the role of Piezo channels in this process, which has not been thoroughly elucidated. Therefore, further investigation into the specific functions and mechanisms of Piezo channels in ALI/ARDS may bring new avenues for the diagnosis and treatment of related diseases.

6 Summary

In this review, we systematically explored the roles of ECs and neutrophils in sepsis-induced ALI/ARDS and their mechanisms of interaction. The interplay between ECs and neutrophils occurs through various pathways, including the recognition and binding of surface molecules, the secretion of cytokines, the release of EVs, the formation of NETs, and interactions involving mechanical forces such as membrane stretching. These interactions can either activate or inhibit corresponding signaling pathways, profoundly affecting cellular functional states and playing a critical role in the pathological progression of ALI/ARDS. These mechanisms not only provide an important basis for understanding the pathogenesis of ALI/ARDS but also indicate directions for exploring novel therapeutic strategies. A deeper understanding of the complex and nuanced interactions between ECs and neutrophils is essential for targeted therapies that regulate inflammatory responses and promote tissue repair.

Author contributions

XX: Writing – original draft. QZ: Writing – original draft. ZL: Writing – original draft. CC: Writing – original draft. JZ: Investigation, Writing – original draft. HS: Writing – review and editing. HX: Writing – review and editing. SP: Writing – review and editing.

Funding

The author(s) declare that no financial support was received for the research and/or publication of this article.

Conflict of interest

The authors declare that the research was conducted in the absence of any commercial or financial relationships that could be construed as a potential conflict of interest.

Generative AI statement

The author(s) declare that no Gen AI was used in the creation of this manuscript.

Publisher's note

References

Abadie, Y., Bregeon, F., Papazian, L., Lange, F., Chailley-Heu, B., Thomas, P., et al. (2005). Decreased VEGF concentration in lung tissue and vascular injury during ARDS. *Eur. Respir. J.* 25, 139–146. doi:10.1183/09031936.04.00065504

Abrams, S. T., Su, D., Sahraoui, Y., Lin, Z., Cheng, Z., Nesbitt, K., et al. (2021). Assembly of alternative prothrombinase by extracellular histones initiates and disseminates intravascular coagulation. *Blood* 137, 103–114. doi:10.1182/blood.2019002973

Aziz, M., Jacob, A., and Wang, P. (2014). Revisiting caspases in sepsis. *Cell Death Dis.* 5, e1526. doi:10.1038/cddis.2014.488

Bao, W., Xing, H., Cao, S., Long, X., Liu, H., Ma, J., et al. (2022). Neutrophils restrain sepsis associated coagulopathy via extracellular vesicles carrying superoxide dismutase 2 in a murine model of lipopolysaccharide induced sepsis. *Nat. Commun.* 13, 4583. doi:10.1038/s41467-022-32325-w

Baratchi, S., Danish, H., Chheang, C., Zhou, Y., Huang, A., Lai, A., et al. (2024). Piezo1 expression in neutrophils regulates shear-induced NETosis. *Nat. Commun.* 15, 7023. doi:10.1038/s41467-024-51211-1

Barkaway, A., Rolas, L., Joulia, R., Bodkin, J., Lenn, T., Owen-Woods, C., et al. (2021). Age-related changes in the local milieu of inflamed tissues cause aberrant neutrophil trafficking and subsequent remote organ damage. *Immunity* 54, 1494–1510.e7. doi:10.1016/j.immuni.2021.04.025

Becker, B. F., Chappell, D., Bruegger, D., Annecke, T., and Jacob, M. (2010). Therapeutic strategies targeting the endothelial glycocalyx: acute deficits, but great potential. *Cardiovasc. Res.* 87, 300–310. doi:10.1093/cvr/cvq137

Bhatia, M., Zemans, R. L., and Jeyaseelan, S. (2012). Role of chemokines in the pathogenesis of acute lung injury. *Am. J. Respir. Cell Mol. Biol.* 46, 566–572. doi:10.1165/rcmb.2011-0392TR

Biron, B. M., Chung, C. S., Chen, Y., Wilson, Z., Fallon, E. A., Reichner, J. S., et al. (2018). PAD4 deficiency leads to decreased organ dysfunction and improved survival in a dual insult model of hemorrhagic shock and sepsis. *J. Immunol.* 200, 1817–1828. doi:10.4049/jimmunol.1700639

Blazquez-Prieto, J., Lopez-Alonso, I., Huidobro, C., and Albaiceta, G. M. (2018). The emerging role of neutrophils in repair after acute lung injury. *Am. J. Respir. Cell Mol. Biol.* 59, 289–294. doi:10.1165/rcmb.2018-0101PS

Broz, P., Pelegrin, P., and Shao, F. (2020). The gasdermins, a protein family executing cell death and inflammation. *Nat. Rev. Immunol.* 20, 143–157. doi:10.1038/s41577-019-0228-2

Chrysanthopoulou, A., Mitroulis, I., Apostolidou, E., Arelaki, S., Mikroulis, D., Konstantinidis, T., et al. (2014). Neutrophil extracellular traps promote differentiation and function of fibroblasts. *J. Pathol.* 233, 294–307. doi:10.1002/path.4359

Clark, P. R., Kim, R. K., Pober, J. S., and Kluger, M. S. (2015). Tumor necrosis factor disrupts claudin-5 endothelial tight junction barriers in two distinct NF-κB-dependent phases. *PLoS One* 10, e0120075. doi:10.1371/journal.pone.0120075

Conrad, C., Yildiz, D., Cleary, S. J., Margraf, A., Cook, L., Schlomann, U., et al. (2022). ADAM8 signaling drives neutrophil migration and ARDS severity. *JCI Insight* 7, e149870. doi:10.1172/jci.insight.149870

Cui, S. N., Chen, L., Yang, Y. Y., Wang, Y. X., Li, S. N., Zhou, T., et al. (2019). Activation of death-associated protein kinase 1 promotes neutrophil apoptosis to accelerate inflammatory resolution in acute respiratory distress syndrome. *Lab. Invest.* 99, 1143–1156. doi:10.1038/s41374-019-0242-9

Cunningham, K. E., and Turner, J. R. (2012). Myosin light chain kinase: pulling the strings of epithelial tight junction function. *Ann. N. Y. Acad. Sci.* 1258, 34–42. doi:10.1111/j.1749-6632.2012.06526.x

Davey, A., McAuley, D. F., and O'Kane, C. M. (2011). Matrix metalloproteinases in acute lung injury: mediators of injury and drivers of repair. *Eur. Respir. J.* 38, 959–970. doi:10.1183/09031936.00032111

Dejana, E., Orsenigo, F., and Lampugnani, M. G. (2008). The role of adherens junctions and VE-cadherin in the control of vascular permeability. *J. Cell Sci.* 121, 2115–2122. doi:10.1242/jcs.017897

Duan, S., Kim, S. G., Lim, H. J., Song, H. R., and Han, M. K. (2023). Interferon-beta alleviates sepsis by SIRT1-mediated blockage of endothelial glycocalyx shedding. *BMB Rep.* 56, 314–319. doi:10.5483/BMBRep.2023-0030

Englert, J. A., Bobba, C., and Baron, R. M. (2019). Integrating molecular pathogenesis and clinical translation in sepsis-induced acute respiratory distress syndrome. *JCI Insight* 4, e124061. doi:10.1172/jci.insight.124061

Fox, E. D., Heffernan, D. S., Cioffi, W. G., and Reichner, J. S. (2013). Neutrophils from critically ill septic patients mediate profound loss of endothelial barrier integrity. *Crit. Care* 17, R226. doi:10.1186/cc13049

Fridlender, Z. G., Sun, J., Kim, S., Kapoor, V., Cheng, G., Ling, L., et al. (2009). Polarization of tumor-associated neutrophil phenotype by TGF-beta: "N1" versus "N2" TAN. *Cancer Cell* 16, 183–194. doi:10.1016/j.ccr.2009.06.017

Friedrich, E. E., Hong, Z., Xiong, S., Zhong, M., Di, A., Rehman, J., et al. (2019). Endothelial cell Piezo1 mediates pressure-induced lung vascular hyperpermeability via disruption of adherens junctions. *Proc. Natl. Acad. Sci. U. S. A.* 116, 12980–12985. doi:10.1073/pnas.1902165116

Fu, T., Sullivan, D. P., Gonzalez, A. M., Haynes, M. E., Dalal, P. J., Rutledge, N. S., et al. (2023). Mechanotransduction via endothelial adhesion molecule CD31 initiates transmigration and reveals a role for VEGFR2 in diapedesis. *Immunity* 56, 2311–2324.e6. doi:10.1016/j.immuni.2023.08.001

Gan, T., Yang, Y., Hu, F., Chen, X., Zhou, J., Li, Y., et al. (2018). TLR3 regulated poly I:C-induced neutrophil extracellular traps and acute lung injury partly through p38 MAP kinase. *Front. Microbiol.* 9, 3174. doi:10.3389/fmicb.2018.03174

Gando, S., Kameue, T., Matsuda, N., Sawamura, A., Hayakawa, M., and Kato, H. (2004). Systemic inflammation and disseminated intravascular coagulation in early stage of ALI and ARDS: role of neutrophil and endothelial activation. *Inflammation* 28, 237–244. doi:10.1023/b:ifla.0000049049.81688.fe

Gerhardt, T., and Ley, K. (2015). Monocyte trafficking across the vessel wall. *Cardiovasc. Res.* 107, 321–330. doi:10.1093/cvr/cvv147

Gillich, A., Zhang, F., Farmer, C. G., Travaglini, K. J., Tan, S. Y., Gu, M., et al. (2020). Capillary cell-type specialization in the alveolus. *Nature* 586, 785–789. doi:10.1038/s41586-020-2822-7

Godoy, R. S., Cober, N. D., Cook, D. P., McCourt, E., Deng, Y., Wang, L., et al. (2023). Single-cell transcriptomic atlas of lung microvascular regeneration after targeted endothelial cell ablation. *eLife* 12, e80900. doi:10.7554/eLife.80900

Gong, T., Wang, Q. D., Loughran, P. A., Li, Y. H., Scott, M. J., Billiar, T. R., et al. (2024). Mechanism of lactic acidemia-promoted pulmonary endothelial cells death in sepsis: role for CIRP-ZBP1-PANoptosis pathway. *Mil. Med. Res.* 11, 71. doi:10.1186/s40779-024-00574-z

Gould, S., Herron, A., Davis, J., Phillips, M., Chakrabarti, M., and Evans, C. E. (2024). Control of inflammatory lung injury and repair by metabolic signaling in endothelial cells. *Curr. Opin. Hematol.* 32, 157–167. doi:10.1097/MOH.0000000000000848

Greenlee, K. J., Werb, Z., and Kheradmand, F. (2007). Matrix metalloproteinases in lung: multiple, multifarious, and multifaceted. *Physiol. Rev.* 87, 69–98. doi:10.1152/physrev.00022.2006

Gregoire, M., Uhel, F., Lesouhaitier, M., Gacouin, A., Guirriec, M., Mourcin, F., et al. (2018). Impaired efferocytosis and neutrophil extracellular trap clearance by macrophages in ARDS. *Eur. Respir. J.* 52, 1702590. doi:10.1183/13993003.02590-2017

Huang, X., Dai, Z., Cai, L., Sun, K., Cho, J., Albertine, K. H., et al. (2016). Endothelial p110γPI3K mediates endothelial regeneration and vascular repair after inflammatory vascular injury. *Circulation* 133, 1093–1103. doi:10.1161/CIRCULATIONAHA.115.020918

Huang, X., Zhang, X., Machireddy, N., Evans, C. E., Trewartha, S. D., Hu, G., et al. (2023). Endothelial FoxM1 reactivates aging-impaired endothelial regeneration for vascular repair and resolution of inflammatory lung injury. *Sci. Transl. Med.* 15, eabm5755. doi:10.1126/scitranslmed.abm5755

Huang, X., Zhang, X., Zhao, D. X., Yin, J., Hu, G., Evans, C. E., et al. (2019). Endothelial hypoxia-inducible factor-1α is required for vascular repair and resolution of inflammatory lung injury through Forkhead box protein M1. *Am. J. Pathol.* 189, 1664–1679. doi:10.1016/j.ajpath.2019.04.014

Iba, T., and Levy, J. H. (2019). Derangement of the endothelial glycocalyx in sepsis. *J. Thromb. Haemost.* 17, 283–294. doi:10.1111/jth.14371

Ito, T., Kakuuchi, M., and Maruyama, I. (2021). Endotheliopathy in septic conditions: mechanistic insight into intravascular coagulation. *Crit. Care* 25, 95. doi:10.1186/s13054-021-03524-6

Jia, S., Liu, W., Zhang, M., Wang, L., Ren, C., Feng, C., et al. (2024). Insufficient mechanical loading downregulates Piezo1 in chondrocytes and impairs fracture healing through ApoE-induced senescence. *Adv. Sci. (Weinh)* 11, e2400502. doi:10.1002/advs.202400502

Jiang, J., Huang, K., Xu, S., Garcia, J., Wang, C., and Cai, H. (2020). Targeting NOX4 alleviates sepsis-induced acute lung injury via attenuation of redox-sensitive activation of CaMKII/ERK1/2/MLCK and endothelial cell barrier dysfunction. *Redox Biol.* 36, 101638. doi:10.1016/j.redox.2020.101638

Jiao, Y., Zhang, T., Zhang, C., Ji, H., Tong, X., Xia, R., et al. (2021). Exosomal miR-30d-5p of neutrophils induces M1 macrophage polarization and primes macrophage pyroptosis in sepsis-related acute lung injury. *Crit. Care* 25, 356. doi:10.1186/s13054-021-03775-3

Jin, H., Aziz, M., Murao, A., Kobritz, M., Shih, A. J., Adelson, R. P., et al. (2023). Antigen-presenting aged neutrophils induce CD4+ T cells to exacerbate inflammation in sepsis. *J. Clin. Invest.* 133, e164585. doi:10.1172/JCI164585

Ju, Y. N., Geng, Y. J., Wang, X. T., Gong, J., Zhu, J., and Gao, W. (2019). Endothelial progenitor cells attenuate ventilator-induced lung injury with large-volume ventilation. *Cell Transpl.* 28, 1674–1685. doi:10.1177/0963689719874048

Kempf, C. L., Sammani, S., Bermudez, T., Song, J. H., Hernon, V. R., Hufford, M. K., et al. (2022). Critical role for the lung endothelial nonmuscle myosin light-chain kinase isoform in the severity of inflammatory murine lung injury. *Pulm. Circ.* 12, e12061. doi:10.1002/pul2.12061

Kim, J. E., Yoo, H. J., Gu, J. Y., and Kim, H. K. (2016). Histones induce the procoagulant phenotype of endothelial cells through tissue factor up-regulation and thrombomodulin down-regulation. *PLoS One* 11, e0156763. doi:10.1371/journal.pone.0156763

Kumar, S., Gupta, E., Kaushik, S., Srivastava, V. K., Saxena, J., Mehta, S., et al. (2019). Quantification of NETs formation in neutrophil and its correlation with the severity of sepsis and organ dysfunction. *Clin. Chim. Acta* 495, 606–610. doi:10.1016/j.cca.2019.06.008

Li, H., Li, Y., Song, C., Hu, Y., Dai, M., Liu, B., et al. (2021). Neutrophil extracellular traps augmented alveolar macrophage pyroptosis via AIM2 inflammasome activation in LPS-induced ALI/ARDS. *J. Inflamm. Res.* 14, 4839–4858. doi:10.2147/JIR.S321513

Li, X., Li, C., Liang, W., Bi, Y., Chen, M., and Dong, S. (2014). Protectin D1 promotes resolution of inflammation in a murine model of lipopolysaccharide-induced acute lung injury via enhancing neutrophil apoptosis. *Chin. Med. J. Engl.* 127, 810–814. doi:10.3760/cma.j.issn.0366-6999.20131104

Li, Y., Xu, X., Wang, H. J., Chen, Y. C., Chen, Y., Chiu, J., et al. (2024). Endoplasmic reticulum protein 72 regulates integrin mac-1 activity to influence neutrophil recruitment. *Arterioscler. Thromb. Vasc. Biol.* 44, e82–e98. doi:10.1161/ATVBAHA.123.319771

Liang, G. P., Xu, J., Cao, L. L., Zeng, Y. H., Chen, B. X., Yang, J., et al. (2019). Piezo1 induced apoptosis of type II pneumocytes during ARDS. *Respir. Res.* 20, 118. doi:10.1186/s12931-019-1083-1

Lim, X. R., Abd-Alhaseeb, M. M., Ippolito, M., Koide, M., Senatore, A. J., Plante, C., et al. (2024). Endothelial Piezo1 channel mediates mechano-feedback control of brain blood flow. *Nat. Commun.* 15, 8686. doi:10.1038/s41467-024-52969-0

Liu, M., Zhang, L., Marsboom, G., Jambusaria, A., Xiong, S., Toth, P. T., et al. (2019). Sox17 is required for endothelial regeneration following inflammation-induced vascular injury. *Nat. Commun.* 10, 2126. doi:10.1038/s41467-019-10134-y

Liu, S., Wu, W., Du, Y., Yin, H., Chen, Q., Yu, W., et al. (2023). The evolution and heterogeneity of neutrophils in cancers: origins, subsets, functions, orchestrations and clinical applications. *Mol. Cancer* 22, 148. doi:10.1186/s12943-023-01843-6

Liu, X., Qin, X., Qin, H., Jia, C., Yuan, Y., Sun, T., et al. (2021). Characterization of the heterogeneity of endothelial cells in bleomycin-induced lung fibrosis using single-cell RNA sequencing. *Angiogenesis* 24, 809–821. doi:10.1007/s10456-021-09795-5

Lumbroso, D., Soboh, S., Maimon, A., Schif-Zuck, S., Ariel, A., and Burstyn-Cohen, T. (2018). Macrophage-derived protein S facilitates apoptotic polymorphonuclear cell clearance by resolution phase macrophages and supports their reprogramming. *Front. Immunol.* 9, 358. doi:10.3389/fimmu.2018.00358

Luplertlop, N., Misse, D., Bray, D., Deleuze, V., Gonzalez, J. P., Leardkamolkarn, V., et al. (2006). Dengue-virus-infected dendritic cells trigger vascular leakage through metalloproteinase overproduction. *EMBO Rep.* 7, 1176–1181. doi:10.1038/sj.embor.7400814

Lv, Y., Kim, K., Sheng, Y., Cho, J., Qian, Z., Zhao, Y. Y., et al. (2018). YAP controls endothelial activation and vascular inflammation through TRAF6. *Circ. Res.* 123, 43–56. doi:10.1161/CIRCRESAHA.118.313143

Ma, F., Ghimire, L., Ren, Q., Fan, Y., Chen, T., Balasubramanian, A., et al. (2024). Gasdermin E dictates inflammatory responses by controlling the mode of neutrophil death. *Nat. Commun.* 15, 386. doi:10.1038/s41467-023-44669-y

Ma, Y., Yang, X., Chatterjee, V., Meegan, J. E., Beard, R. J., and Yuan, S. Y. (2019). Role of neutrophil extracellular traps and vesicles in regulating vascular endothelial permeability. *Front. Immunol.* 10, 1037. doi:10.3389/fimmu.2019.01037

Matthay, M. A., Zemans, R. L., Zimmerman, G. A., Arabi, Y. M., Beitler, J. R., Mercat, A., et al. (2019). Acute respiratory distress syndrome. *Nat. Rev. Dis. Prim.* 5, 18. doi:10.1038/s41572-019-0069-0

Meyer, N. J., Reilly, J. P., Feng, R., Christie, J. D., Hazen, S. L., Albert, C. J., et al. (2017). Myeloperoxidase-derived 2-chlorofatty acids contribute to human sepsis mortality via acute respiratory distress syndrome. *JCI Insight* 2, e96432. doi:10.1172/jci.insight.96432

Millar, F. R., Summers, C., Griffiths, M. J., Toshner, M. R., and Proudfoot, A. G. (2016). The pulmonary endothelium in acute respiratory distress syndrome: insights and therapeutic opportunities. *Thorax* 71, 462–473. doi:10.1136/thoraxjnl-2015-207461

Mukhopadhyay, A., Tsukasaki, Y., Chan, W. C., Le, J. P., Kwok, M. L., Zhou, J., et al. (2024). trans-Endothelial neutrophil migration activates bactericidal function via Piezo1 mechanosensing. *Immunity* 57, 52–67.e10. doi:10.1016/j.immuni.2023.11.007

Nourshargh, S., Renshaw, S. A., and Imhof, B. A. (2016). Reverse migration of neutrophils: where, when, how, and why? *Trends Immunol.* 37, 273–286. doi:10.1016/j.it.2016.03.006

Park, I., Kim, M., Choe, K., Song, E., Seo, H., Hwang, Y., et al. (2019). Neutrophils disturb pulmonary microcirculation in sepsis-induced acute lung injury. *Eur. Respir. J.* 53, 1800786. doi:10.1183/13993003.00786-2018

Park, S. Y., Shrestha, S., Youn, Y. J., Kim, J. K., Kim, S. Y., Kim, H. J., et al. (2017). Autophagy primes neutrophils for neutrophil extracellular trap formation during sepsis. *Am. J. Respir. Crit. Care Med.* 196, 577–589. doi:10.1164/rccm.201603-0596OC

Paunel-Gorgulu, A., Kirichevska, T., Logters, T., Windolf, J., and Flohe, S. (2012). Molecular mechanisms underlying delayed apoptosis in neutrophils from multiple trauma patients with and without sepsis. *Mol. Med.* 18, 325–335. doi:10.2119/molmed.2011.00380

Qian, Y., Wang, Z., Lin, H., Lei, T., Zhou, Z., Huang, W., et al. (2022). TRIM47 is a novel endothelial activation factor that aggravates lipopolysaccharide-induced acute lung injury in mice via K63-linked ubiquitination of TRAF2. *Signal Transduct. Target Ther.* 7, 148. doi:10.1038/s41392-022-00953-9

Qiao, X., Yin, J., Zheng, Z., Li, L., and Feng, X. (2024). Endothelial cell dynamics in sepsis-induced acute lung injury and acute respiratory distress syndrome: pathogenesis and therapeutic implications. *Cell Commun. Signal.* 22, 241. doi:10.1186/s12964-024-01620-y

Rudd, K. E., Johnson, S. C., Agesa, K. M., Shackelford, K. A., Tsoi, D., Kievlan, D. R., et al. (2020). Global, regional, and national sepsis incidence and mortality, 1990-2017: analysis for the Global Burden of Disease Study. *Lancet* 395, 200–211. doi:10.1016/S0140-6736(19)32989-7

Schauer, C., Janko, C., Munoz, L. E., Zhao, Y., Kienhofer, D., Frey, B., et al. (2014). Aggregated neutrophil extracellular traps limit inflammation by degrading cytokines and chemokines. *Nat. Med.* 20, 511–517. doi:10.1038/nm.3547

Scheiermann, C., Colom, B., Meda, P., Patel, N. S., Voisin, M. B., Marrelli, A., et al. (2009). Junctional adhesion molecule-C mediates leukocyte infiltration in response to ischemia reperfusion injury. *Arterioscler. Thromb. Vasc. Biol.* 29, 1509–1515. doi:10.1161/ATVBAHA.109.187559

Schmidt, E. P., Yang, Y., Janssen, W. J., Gandjeva, A., Perez, M. J., Barthel, L., et al. (2012). The pulmonary endothelial glycocalyx regulates neutrophil adhesion and lung injury during experimental sepsis. *Nat. Med.* 18, 1217–1223. doi:10.1038/nm.2843

Schupp, J. C., Adams, T. S., Cosme, C. J., Raredon, M., Yuan, Y., Omote, N., et al. (2021). Integrated single-cell atlas of endothelial cells of the human lung. *Circulation* 144, 286–302. doi:10.1161/CIRCULATIONAHA.120.052318

Serhan, C. N., Chiang, N., and Van Dyke, T. E. (2008). Resolving inflammation: dual anti-inflammatory and pro-resolution lipid mediators. *Nat. Rev. Immunol.* 8, 349–361. doi:10.1038/nri2294

Shao, Y., Cheng, Z., Li, X., Chernaya, V., Wang, H., and Yang, X. F. (2014). Immunosuppressive/anti-inflammatory cytokines directly and indirectly inhibit endothelial dysfunction–a novel mechanism for maintaining vascular function. *J. Hematol. Oncol.* 7, 80. doi:10.1186/s13045-014-0080-6

Shen, Y. H., Ding, D., Lian, T. Y., Qiu, B. C., Yan, Y., Wang, P. W., et al. (2024). Panorama of artery endothelial cell dysfunction in pulmonary arterial hypertension. *J. Mol. Cell. Cardiol.* 197, 61–77. doi:10.1016/j.yjmcc.2024.10.004

Singer, M., Deutschman, C. S., Seymour, C. W., Shankar-Hari, M., Annane, D., Bauer, M., et al. (2016). The third international consensus definitions for sepsis and septic shock (Sepsis-3). *JAMA* 315, 801–810. doi:10.1001/jama.2016.0287

Song, C., Li, H., Li, Y., Dai, M., Zhang, L., Liu, S., et al. (2019). NETs promote ALI/ARDS inflammation by regulating alveolar macrophage polarization. *Exp. Cell Res.* 382, 111486. doi:10.1016/j.yexcr.2019.06.031

Song, C., Li, H., Mao, Z., Peng, L., Liu, B., Lin, F., et al. (2022). Delayed neutrophil apoptosis may enhance NET formation in ARDS. *Respir. Res.* 23, 155. doi:10.1186/s12931-022-02065-y

Stefanec, T. (2000). Endothelial apoptosis: could it have a role in the pathogenesis and treatment of disease? *Chest* 117, 841–854. doi:10.1378/chest.117.3.841

Takemasa, A., Ishii, Y., and Fukuda, T. (2012). A neutrophil elastase inhibitor prevents bleomycin-induced pulmonary fibrosis in mice. *Eur. Respir. J.* 40, 1475–1482. doi:10.1183/09031936.00127011

Tang, F., Zhao, X. L., Xu, L. Y., Zhang, J. N., Ao, H., and Peng, C. (2024). Endothelial dysfunction: pathophysiology and therapeutic targets for sepsis-induced multiple organ dysfunction syndrome. *Biomed. Pharmacother.* 178, 117180. doi:10.1016/j.biopha.2024.117180

Vila, E. L., Cain, M. P., Hutchison, V., Flodby, P., Crandall, E. D., Borok, Z., et al. (2020). Epithelial vegfa specifies a distinct endothelial population in the mouse lung. *Dev. Cell* 52, 617–630.e6. doi:10.1016/j.devcel.2020.01.009

Wang, K., Wang, M., Liao, X., Gao, S., Hua, J., Wu, X., et al. (2022). Locally organised and activated Fth1(hi) neutrophils aggravate inflammation of acute lung injury in an IL-10-dependent manner. *Nat. Commun.* 13, 7703. doi:10.1038/s41467-022-35492-y

Wang, Y., Zhu, C. L., Li, P., Liu, Q., Li, H. R., Yu, C. M., et al. (2023). The role of G protein-coupled receptor in neutrophil dysfunction during sepsis-induced acute respiratory distress syndrome. *Front. Immunol.* 14, 1112196. doi:10.3389/fimmu.2023.1112196

Wei, J. X., Jiang, H. L., and Chen, X. H. (2023). Endothelial cell metabolism in sepsis. *World J. Emerg. Med.* 14, 10–16. doi:10.5847/wjem.j.1920-8642.2023.019

Xie, X., Shi, Q., Wu, P., Zhang, X., Kambara, H., Su, J., et al. (2020). Single-cell transcriptome profiling reveals neutrophil heterogeneity in homeostasis and infection. *Nat. Immunol.* 21, 1119–1133. doi:10.1038/s41590-020-0736-z

Xu, C., Zhang, L., Xu, S., Wang, Z., Han, Q., Lv, Y., et al. (2024). Neutrophil ALDH2 is a new therapeutic target for the effective treatment of sepsis-induced ARDS. *Cell. Mol. Immunol.* 21, 510–526. doi:10.1038/s41423-024-01146-w

Yang, N., Tian, H., Zhan, E., Zhai, L., Jiao, P., Yao, S., et al. (2019). Reverse-D-4F improves endothelial progenitor cell function and attenuates LPS-induced acute lung injury. *Respir. Res.* 20, 131. doi:10.1186/s12931-019-1099-6

Yuan, S. Y., Shen, Q., Rigor, R. R., and Wu, M. H. (2012). Neutrophil transmigration, focal adhesion kinase and endothelial barrier function. *Microvasc. Res.* 83, 82–88. doi:10.1016/j.mvr.2011.06.015

Zemans, R. L., Briones, N., Campbell, M., McClendon, J., Young, S. K., Suzuki, T., et al. (2011). Neutrophil transmigration triggers repair of the lung epithelium via beta-catenin signaling. *Proc. Natl. Acad. Sci. U. S. A.* 108, 15990–15995. doi:10.1073/pnas.1110144108

Zhang, H., Wang, Y., Qu, M., Li, W., Wu, D., Cata, J. P., et al. (2023). Neutrophil, neutrophil extracellular traps and endothelial cell dysfunction in sepsis. *Clin. Transl. Med.* 13, e1170. doi:10.1002/ctm2.1170

Zhang, L., Gao, S., White, Z., Dai, Y., Malik, A. B., and Rehman, J. (2022). Single-cell transcriptomic profiling of lung endothelial cells identifies dynamic inflammatory and regenerative subpopulations. *JCI Insight* 7, e158079. doi:10.1172/jci.insight.158079

Zhang, N., Tang, W., Torres, L., Wang, X., Ajaj, Y., Zhu, L., et al. (2024). Cell surface RNAs control neutrophil recruitment. *Cell* 187, 846–860.e17. doi:10.1016/j.cell.2023.12.033

Zhao, G., Weiner, A. I., Neupauer, K. M., de Mello, C. M., Palashikar, G., Adams-Tzivelekidis, S., et al. (2020). Regeneration of the pulmonary vascular endothelium after viral pneumonia requires COUP-TF2. *Sci. Adv.* 6, eabc4493. doi:10.1126/sciadv.abc4493

Zhao, G., Xue, L., Weiner, A. I., Gong, N., Adams-Tzivelekidis, S., Wong, J., et al. (2024). TGF-βR2 signaling coordinates pulmonary vascular repair after viral injury in mice and human tissue. *Sci. Transl. Med.* 16, eadg6229. doi:10.1126/scitranslmed.adg6229

Zhong, L., Simard, M. J., and Huot, J. (2018). Endothelial microRNAs regulating the NF-κB pathway and cell adhesion molecules during inflammation. *FASEB J.* 32, 4070–4084. doi:10.1096/fj.201701536R

Zhu, Z., Ling, X., Zhou, H., and Xie, J. (2023). Syndecan-4 is the key proteoglycan involved in mediating sepsis-associated lung injury. *Heliyon* 9, e18600. doi:10.1016/j.heliyon.2023.e18600

Zi, S. F., Wu, X. J., Tang, Y., Liang, Y. P., Liu, X., Wang, L., et al. (2024). Endothelial cell-derived extracellular vesicles promote aberrant neutrophil trafficking and subsequent remote lung injury. *Adv. Sci. (Weinh)* 11, e2400647. doi:10.1002/advs.202400647

frontiers | Frontiers in Cell and Developmental Biology

TYPE Review
PUBLISHED 17 June 2025
DOI 10.3389/fcell.2025.1576067

OPEN ACCESS

EDITED BY
Lulong Bo,
Navy Medical University, China

REVIEWED BY
Weijuan Yao,
Peking University, China
Adam Wesley Whisnant,
Julius Maximilian University of Würzburg, Germany

*CORRESPONDENCE
Chengfang Yao,
yaochengfang@sdutcm.edu.cn

RECEIVED 13 February 2025
ACCEPTED 28 May 2025
PUBLISHED 17 June 2025

CITATION
Yang Y, Wang M, Qiu X, Yang R and Yao C (2025) Single-cell RNA sequencing: new insights for pulmonary endothelial cells. *Front. Cell Dev. Biol.* 13:1576067. doi: 10.3389/fcell.2025.1576067

Single-cell RNA sequencing: new insights for pulmonary endothelial cells

Ying Yang[1], Mengyuan Wang[1], Xiao Qiu[1], Rui Yang[2] and Chengfang Yao[1,3]*

[1]Shandong University of Traditional Chinese Medicine, Jinan, China, [2]The Central Hospital Affiliated to Shandong First Medical University, Jinan, China, [3]School of Clinical and Basic Medicine, Shandong First Medical University (Shandong Academy of Medical Sciences), Jinan, China

Pulmonary endothelial cells (PECs) are indispensable for sustaining lung microenvironmental homeostasis and exert significant influence across a spectrum of pulmonary pathologies. Single-cell RNA sequencing (scRNA-seq) has fundamentally transformed conventional paradigms surrounding PECs, unveiling novel perspectives on their roles in both physiological and pathological lung conditions. This technology provides critical insights into the phenotypic diversity and distinct molecular signatures of PECs, underscoring their substantial heterogeneity in structure, function and gene expression, which is contingent upon their spatial localization within the lung microenvironment. The advancements in scRNA-seq have catalyzed remarkable progress in the therapeutic management of pulmonary pathophysiology, facilitating breakthroughs in the identification of cellular subpopulations, functional characterization and discovery of innovative therapeutic targets. In this review, we systematically synthesize the markers and subclusters of PECs as delineated by scRNA-seq, elucidate their applications in normal and pathological lung contexts, and propose future directions regarding molecular mechanisms and therapeutic interventions targeting PECs.

KEYWORDS

single-cell RNA sequencing, pulmonary endothelial cells, biomarkers, subcluster characterization, lung pathology

1 Introduction

Pulmonary endothelial cells (PECs) are pivotal in maintaining physiological lung function and participating in the pathogenesis of various pulmonary diseases (Jambusaria et al., 2020; Goldenberg and Kuebler, 2015). Pulmonary endothelial dysfunction, manifested through multiple interconnected pathological alterations including barrier hyperpermeability, sustained inflammatory activation, ROS-mediated apoptosis, endothelial-mesenchymal transition (EndMT), and metabolic reprogramming constitutes a hallmark of progressive vascular remodeling in both acute and chronic respiratory disorders (Patterson and Lum, 2001; Li et al., 2017; Redetzky et al., 2014). These maladaptive changes synergistically disrupt pulmonary vascular homeostasis, driving disease progression in clinical entities such as coronavirus disease 2019 (COVID-19) (Yamaoka-Tojo, 2020a; Yamaoka-Tojo, 2020b; Bonaventura et al., 2021), lung malignancies (Patterson and Lum, 2001), acute lung injury (Xu and Zhou, 2020), chronic obstructive pulmonary disease (COPD) (Takahashi et al., 2013; Green, 2020; Green and Turner, 2017), pulmonary arterial

hypertension (PAH) (Goyanes et al., 2020; Rounds and Harrington, 2019; Hudson and Farkas, 2021), and idiopathic pulmonary fibrosis (IPF) (Ryter and Rosas, 2022).

PECs constitute a highly heterogeneous and functionally versatile population residing along the luminal surfaces of pulmonary vasculature and lymphatics. While they retain canonical endothelial functions such as maintenance of vascular homeostasis, PECs exhibit lung-specific phenotypic and functional specializations, which include facilitating efficient gas exchange, preserving alveolar-capillary barrier integrity, modulating angiogenic processes, orchestrating immuno-inflammatory responses, and mediating tissue repair following pulmonary injury and infection (Maruhashi et al., 2019; Hennigs et al., 2019; Niethamer et al., 2020; Huertas et al., 2018). Notably, PECs function as an active metabolic and endocrine interface, capable of synthesizing, metabolizing, and secreting a wide repertoire of bioactive molecules such as nitric oxide (NO), prostaglandin E2 (PGE2), arachidonic acid derivatives, von Willebrand factor (vWF), endothelin-1 (ET-1), and intercellular adhesion molecule-1 (ICAM-1), which exert autocrine and paracrine regulatory effects on neighboring cells and systemic physiology (Goldenberg and Kuebler, 2015; Emin et al., 2012). Moreover, PECs express an extensive array of surface receptors, including cytokines, chemokines and growth factors, thereby enabling precise sensing and integration of environmental cues. Insights from single-cell transcriptomic atlases of the human lung reveal that PECs are enriched in signaling molecules such as C-X-C Motif Chemokine Ligand 12 (CXCL12), Ephrin-B2 (EFNB2), Semaphorin-3G (SEMA3G), and Vascular Endothelial Growth Factor A (VEGFA), alongside key components of the nitric oxide signaling axis, including Nitric Oxide Synthase 1 (NOS1), Phosphodiesterase 3A (PDE3A), and Phosphodiesterase 4D (PDE4D), which are critically involved in the fine-tuning of pulmonary vascular tone (Schupp et al., 2021).

PECs play a critical role in mediating the pulmonary immune response (Abedi et al., 2020; Metkus et al., 2022). Under inflammatory stimuli, PECs undergo either Type I or Type II activation, mediated by G-protein-coupled receptors (GPCRs) and pro-inflammatory cytokines such as tumor necrosis factor (TNF) and interleukin-1 (IL-1), respectively (Strassheim et al., 2020). Activated PECs secrete IL-6 and transforming growth factor-beta (TGF-β), which differentially regulate T helper cell populations: IL-6 promotes Th17 cell activation while TGF-β suppresses Th1 cell differentiation (Gao et al., 2020). These activated PECs facilitate leukocyte recruitment and migration, enabling immune cell infiltration into inflammatory foci within the lungs to combat pathogens, neoplasms, or infectious agents (Middleton et al., 2002). The single-cell transcriptome atlas of murine endothelial cells (ECs) has revealed a significant enrichment of immunoregulatory signatures in PECs, notably the overexpression of major histocompatibility complex (MHC) class II genes, suggesting their potential involvement in immune surveillance (Kalucka et al., 2020).

Single-cell RNA sequencing (scRNA-seq) enables transcriptomic profiling at single-cell resolution, allowing for precise quantification of mRNA transcripts, detailed characterization of cellular states and regulatory networks, elucidation of developmental trajectories, and comprehensive deconvolution of cellular heterogeneity within mixed populations (Zieg et al., 2017; Vieira et al., 2019; Shi and Cao, 2023). PECs exhibit striking heterogeneity across morphological architecture, functional profiles and transcriptomic signatures, with these variations being intimately governed by their spatiotemporal anatomical niches and dynamic microenvironmental cues. Elucidating these distinct endothelial identities is essential, as they execute specialized biological functions and contribute decisively to the initiation, progression, and resolution of a broad spectrum of pulmonary pathologies (Gomez-Salinero and Rafii, 2018; Caramelo et al., 2023). Investigating the phenotypic diversity and functional alterations of individual PECs-each possessing unique biological characteristics is imperative for understanding their roles in lung disease progression (Gomez-Salinero and Rafii, 2018; Caramelo et al., 2023). While conventional techniques such as microscopy and flow cytometry enable PEC classification, they fail to provide a comprehensive mechanistic understanding of PEC function (Nishino et al., 2021; Bacon et al., 2023; Neubauer and Zieger, 2022). Through integration with advanced computational and bioinformatic frameworks, scRNA-seq facilitates the identification of novel PECs subpopulations and the dissection of their distinct molecular and functional attributes.

This review offers a comprehensive synthesis of the current understanding of PECs, encompassing their biological characteristics, molecular markers, and subcluster classifications. We further highlight the application of scRNA-seq in elucidating endothelial heterogeneity within the pulmonary microenvironment, with a particular focus on its relevance to both physiological and pathological conditions. Additionally, we explore the translational implications of scRNA-seq-based discoveries for the diagnosis, management, and therapeutic targeting of lung diseases.

2 Markers of PECs in scRNA-seq

2.1 Marker selection for PEC identification

In scRNA-seq studies, precise marker selection is essential to accurately isolate ECs from lung tissue. Typically, multiple endothelial markers are employed simultaneously to define PECs. This article reviews the application of PEC-specific markers across various scRNA-seq studies (Table 1). Schupp et al. compiled six distinct scRNA-seq datasets, identifying 12,563 ECs within an integrated lung dataset based on canonical endothelial markers: Platelet Endothelial Cell Adhesion Molecule 1 (PECAM1)/Cluster of Differentiation 31 (CD31), Cadherin 5 (CDH5)/Vascular Endothelial Cadherin (VE-cadherin), Claudin 5 (CLDN5), and Erythroblast Transformation Specific Related Gene (ERG) (Schupp et al., 2021). In the context of lung adenocarcinoma scRNA-seq analyses, Kim et al. annotated canonical markers such as PECAM1, CLDN5, Fms-like Tyrosine Kinase 1 (FLT1), and Receptor Activity Modifying Protein 2 (RAMP2) to delineate PEC lineages (Kim et al., 2020). In human lung scRNA-seq studies, researchers sorted PECs based on $CD31^+$ expression, epithelial cells via Epithelial Cell Adhesion Molecule positive ($EPCAM^+$), immune cells through $CD45^+$, and stromal populations using $EPCAM^-CD31^-CD45^-$ criteria (Travaglini et al., 2020). Several

TABLE 1 Cell surface markes and subclusters in PECs.

Species	Vivo/vitro	Cells origin	Models	Cells number	Cell surface marker	Subclusters	Ref.
human	vivo	Lung tumor ECs/Peritumor Lung ECs	healthy/tumorous	12,323 hTEC 8,929 hPNEC	CD45 negative, CD31 positive	13 subclusters: arteries, postcapillary, alveolar typeI, Alveolar typeII, scavenging,activated, intermediate,tip cell, immature, activated Pcv,lymphatics hpNEC lymphatics hTEC,patient #5 specific	Goveia et al. (2020)
murine	vivo	lung ECs	normal/tumorous	29,007 mNECs and mTECs	CD45 negative, CD31 positive	16 subclusters: arteries, veins, capillaries typeI, capillaries typeII, lymphatics,TEC capillaries, proliferating,tip cell, immature,large veins, postcap.veins, neophalanx, activated arteries, interferon, breach cell,pre-breach cell	
human	vitro	cuured lung ECs	lung tumor ECs	6,512	CD45 negative, CD31 positive	4 subclusters: Tip EC, proliferating,endothelial-to-mesenchymal transition, intermediate	
human	vivo	lung ECs	datasets	12 563	PECAM1 (CD31), CDH5 (VE-cadherin), CLDN5, ERG	6 subclusters: lymphatic ECs, arterial, capillary (avWFneg/EMCNhigh/EDNRBpos population, avWFpos/EMCNlow/EDN1pos population), venous (COL15A1pos and COL15A1neg) aerocyte	Schupp et al. (2021)
mice	vivo	mice lung vascular cells	healthy	1,504	Cldn5(BAC)-GFP	8 lung ECs subclusters: aEC,cEC1,cEC,cEC2,capilEC,EC1, EC2,LEC	Vila et al. (2020)
mice	vivo	mice lung ECs	healthy and cre recombination	4,278	CD45 negative, CD31 and ICAM2 positive	4 subclusters: Car4 EC, Plvap EC, Vwf EC (Gja5 or Nr2f2), and Prox1 EC	Vila et al. (2020)
human	vivo	lung tumor ECs	healthy/lung adenocarcinoma	2,107	PECAM1,CLDN5,FLT1,RAMP2	5 subclusters: Tumor ECs,Tip-like ECs, Stalk-like ECs, Lymphatic ECs,EPCs	Kim et al. (2020)

(Continued on the following page)

10.3389/fcell.2025.1576067

TABLE 1 (*Continued*) Cell surface markes and subclusters in PECs.

Species	Vivo/vitro	Cells origin	Models	Cells number	Cell surface marker	Subclusters	Ref.
mice	vivo	mice lung ECs	healthy	13,862	Pecam1, Kdr, Cdh5, and Tek (Tie2)	not mentioned	Goveia et al. (2020)
mice	vivo	mice lung ECs	healthy	not mentioned	Pecam1, Cdh5 and excluded Acta2, Col1a1, Hba-a1, Hba-a2, Hbb-bs	5 subclusters: artery, capilary 1, capillary 2, Vein, lymphatic	Kalucka et al. (2020)
mice	vivo	mice lung ECs	RiboTag EC (Cdh5CreERT2/$^{+}$; Rpl22HA/$^{+}$) transgenic mice	1,071	Slc6a1, Slco2a1, Emp2, Atp2a3, Epcam Itgal, Il3ra, St14	not mentioned	Gomez-Salinero and Rafii (2018)
			databases	not mentioned	CD31,CDH5		
human	vivo	hman lung ECs	lung cancer	8,223	not mentioned	6 subclusters: tip cells, high endothelial venules (HEVs),venous ECs,capillary, arterial, lymphatic ECs.	Gillich et al. (2020)
human	vivo	human lung ECs	lung adenocarcinoma	3,381	RAMP2	6 subclusters:extra-alveolar capillary ECs(Endo-C1; Endo-C5),alveolar cECs(Endo-C2),tumor ECs (Endo-C3)arterial ECs (Endo-C4),lymphatic ECs (Endo-C6)	Petegrosso and Kuang (2020)
human	vivo	human lung cells	healthy development	75,000	VWA1,HSPG2	9 subclusters: artery, vein,capillary aerocyte, general capillary cell, capillary intermediate 1 cell, capillary intermediate 2 cell, bronchial vessel 1 cell, bronchial vessel 2 cell, bronchial vessel 1 cell	Jiang et al. (2016)
rat	vivo	lung ECs	healthy/BLM treated	2,181	CD31, CD34, CD144 Vegfr, Vwf, and Pecam1	5 subclusters: cluster a, b, c,d,e	Terpos et al. (2020)

10.3389/fcell.2025.1576067

investigations focused on defining PECs by integrating positive and negative marker expressions. Goveia et al. sequenced 56,771 ECs from human/mouse (peri)-tumoral lung tissues and cultured human lung tumor endothelial cells (TECs) using $CD45^-$and $CD31^+$ markers (Goveia et al., 2020). Research suggests that selecting ECs based on $CD45^-$and $ICAM2^+$ or $CD31^+$ criteria yields more robust results compared to the conventional sole reliance on CD31 (Vila et al., 2020). Kalucka et al. employed PECAM1 and CDH5 as endothelial markers while excluding smooth muscle cell marker—Actin Alpha 2 (Acta2), fibroblast marker—Collagen Type I Alpha 1 Chain (Col1a1), erythrocyte markers—Hemoglobin Subunit Alpha 1 (Hba-a1), Hba-a2, and Hemoglobin Subunit Beta (Hbb-bs), pericyte marker—Platelet Derived Growth Factor Receptor Beta (Pdgfrb), or immune cell marker—Protein Tyrosine Phosphatase Receptor Type C (Ptprc) (Kalucka et al., 2020). In certain studies, lung-specific markers were identified using Green Fluorescent Protein (GFP) in transgenic reporter mice. For instance, Cldn5-Bacterial Artificial Chromosome (BAC)-GFP was utilized to label ECs in mouse brain and lung tissues, while Pdgfrb-BAC-eGFP and Chondroitin Sulfate Proteoglycan 4 (Cspg4)-DsRed labeled mural cells, and Pdgfra-H2B-GFP marked fibroblasts. A total of 147 pan-endothelial marker genes were identified in Cldn5-BAC-GFP-labeled ECs, demonstrating the efficacy of this approach in accurately capturing endothelial populations (He et al., 2018). Jambusaria et al. employed an endothelial-specific RiboTag transgenic mouse model to isolate ECs and investigate their heterogeneity across diverse tissue contexts (Jambusaria et al., 2020).

2.2 Marker utilization for PEC subcluster classification

In scRNA-seq analyses, PECs within distinct subtypes—such as arterial, venous, capillary, and lymphatic ECs—exhibit unique marker profiles for identification. We have compiled a summary of markers corresponding to various PEC subtypes in Table 2. Vila et al. utilized Gap Junction Alpha-5 Protein (Gja5), Nuclear Factor Erythroid 2-Related Factor 2 (Nrf2), and Prospero Homeobox Protein 1 (Prox1) as specific markers for arterial, venous, and lymphatic ECs, respectively (Vila et al., 2020). Goveia et al. employed multiple markers to validate endothelial classification in non-small cell lung cancer, using $CD31^+$/C-X-C Motif Chemokine Receptor 4 (CXCR4), vWF, and EFNB2 to differentiate high-tip cells, veins, and arteries in human TECs. Additionally, Selectin P (SELP) and C-C Motif Chemokine Ligand 14 (CCL14) were identified as signatures for activated postcapillary vein ECs and activated postcapillary vein hTECs, respectively (Goveia et al., 2020).

2.3 Top and novel PEC markers identified via scRNA-seq

ScRNA-seq analyses have revealed top marker genes expressed in distinct tissue contexts, such as Peptidoglycan Recognition Protein 1 (Pglyrp1), Lipocalin 2 (Lcn2), and Transmembrane Protein 100 (Tmem100), which are uniquely enriched in specific tissues like the brain, testis, and lung (Kalucka et al., 2020). Jambusaria et al. identified the top 10 surface markers of PECs, including Solute Carrier Family 6 Member 1 (Slc6a1), Solute Carrier Organic Anion Transporter Family Member 2A1 (Muc1), Lymphotoxin Beta (Ltb), Solute Carrier Organic Anion Transporter 2A1 (Slco2a1), Epithelial Membrane Protein 2 (Emp2), ATPase Sarcoplasmic/Endoplasmic Reticulum Ca^{2+} Transporting 3 (Atp2a3), Epcam, Integrin Subunit Alpha L (Itgal), Interleukin 3 Receptor Subunit Alpha (IL3ra), and Suppression of Tumorigenicity 14 (St14) (Jambusaria et al., 2020). Paik et al. investigated the transcriptional landscapes of ECs across organs via scRNA-seq, identifying top 10 genes expressed in PECs, such as Glycosyltransferase-Like Protein 1 (Grtp1), Adrenoceptor Beta 1 (Adrb1), Sodium Voltage-Gated Channel Alpha Subunit 7 (Scn7a), Tmem100, 15-Hydroxyprostaglandin Dehydrogenase (Hpgd), Forkhead Box F1a (Foxf1a), Non-Catalytic Region of Tyrosine Kinase Adaptor Protein Associated Protein 5 (Nckap5), Ras Guanine Nucleotide Exchange Factor 1A (Rasgef1a), Foxf1 Adjacent Noncoding Developmental Regulatory RNA (Fendrr), and Periaxin (Prx) (Paik et al., 2020). Jambusaria et al. further utilized the RiboTag EC ($Cdh5CreERT2^+$, $Rpl22HA^+$) transgenic model to identify the top 10 most abundant genes in PECs, including AHNAK Nucleoprotein (Ahnak), Microtubule-Actin Crosslinking Factor 1 (Macf1), Actin Beta (Actb), Surfactant Protein C (Sftpc), Spectrin Beta Non-Erythrocytic 1 (Sptbn1), Hypoxia Inducible Factor 2 Alpha (Hif2a), Stearoyl-CoA Desaturase 1 (Scd1), Filamin A (Flna), Adhesion G Protein-Coupled Receptor F5 (Adgrf5), and Low-Density Lipoprotein Receptor Related Protein 1 (Lrp1) (Jambusaria et al., 2020). Additionally, scRNA-seq has uncovered novel pulmonary endothelial markers. Sabbagh et al. identified two new PEC markers, Sodium Voltage-Gated Channel Alpha Subunit 7 (Scn7a) and Sodium Voltage-Gated Channel Beta Subunit 3 (Scn3b), which showed comparable enrichment to angiotensin-converting enzyme (ACE) in PECs, suggesting their potential regulatory roles in ACE function (Sabbagh et al., 2018).

3 Subclusters of PECs in scRNA-seq

3.1 Anatomical location-based classification of PEC subclusters

ECs exhibit inherent heterogeneity, influenced by factors such as tissue-specific biochemical signals, transcriptional programs, mechanical forces, and metabolic processes (Butler and Bhatnagar, 2019; Potente and Makinen, 2017). Similarly, PECs demonstrate distinct heterogeneities based on their anatomical locations. For instance, PECs are categorized into macrovascular endothelium (maEC) and microvascular endothelium (miEC). maECs reside in large arteries and veins responsible for blood transport to and from the lungs, while miECs are located in capillaries surrounding alveoli where gas exchange occurs. These subtypes differ in morphology, permeability, and responsiveness to stimuli (Kostyunina et al., 2023). For example, maECs exhibit enhanced resistance to shear stress and hypoxia, whereas miECs play a more pronounced role in inflammation and angiogenesis (Niethamer et al., 2020; Plebani et al., 2023; Huertas et al., 2013).

TABLE 2 The markers of different subclusters of PECs.

Species	Vivo/vitro	Arterial	Venous	Capillary	Lymphatic	Postcapillary vein ECs	Extra-alveolar capillary ECs	Tip cells	High endothelial venules (HEVs)	Tumor ECs	Ref
human	vivo	GJA5	Nr2f2	not mentioned	PROX1	not mentioned	not mentioned	not mentioned	not mentioned	not mentioned	Vila et al. (2020)
human	vivo	EFNB2	VWF	not mentioned	not mentioned	SELP	not mentioned	CD31+/CXCR4	not mentioned	CCL14	Goveia et al. (2020)
human	vivo	FBLN5, GJA5	SELP	CA4, CD36	PROX1, PDPN	not mentioned	not mentioned	ESM1, NID2	ACKR1	PLVAP IGFBP7	Gillich et al. (2020)
human	vivo	GJA5, FBLN5	SELP	not mentioned	PDPN CCL21	not mentioned	EDN1 SLC6A4, EDN1,CCL2	ESM1,NID2	ACKR1	IGFBP7, PLVAP	Petegrosso and Kuang (2020)
human	vivo	EFNB2, SOX17, BMX, SEMA3, HEY1, LTBP4 FBLN5, GJA5, GJA4	NR2F2, VCAM1 ACKR1, SELP	CA4,PRX, RGCC, SPARC, SGK1, TMEM100	PROX1, LYVE1, FLT4, PDPN	not mentioned	not mentioned	not mentioned	not mentioned	not mentioned	Schupp et al. (2021)
mice	vivo	GJA5,GJA4, CXCL12	COL15A1 VWA1, SELP, Ackr1, NR2F2	Car4,PRX, SGK1	not mentioned	not mentioned	not mentioned	not mentioned	not mentioned	not mentioned	Schupp et al. (2021)

10.3389/fcell.2025.1576067

3.2 Subcluster classification of PECs via scRNA-seq

Beyond broad categories such as lymphatic, capillary, arterial, and venous ECs, scRNA-seq provides a granular classification of PECs and deeper insights into their heterogeneity. We have compiled the subclusters of PECs in Table 1. He et al. described a scRNA-seq dataset delineating vascular and vessel-associated cell subtypes in mouse brain and lung tissues, featuring 1,504 single-cell transcriptomes from mouse lungs. The analysis identified 17 clusters, including eight PEC subclusters: aEC, cEC1, cEC, cEC2, capilEC, EC1, EC2, and LEC, which correspond to arterial, venous, capillary, and lymphatic ECs (He et al., 2018). A recent study reported that PECs in human lung adenocarcinomas consist of multiple subtypes: extra-alveolar capillary ECs divided into two subclusters based on $SLC6A4^+$ and C-C Motif Chemokine Ligand 2 positive ($CCL2^+$) expression, and tumor ECs also divided into two subclusters via $SLC6A4^+$ and $CCL2^+$ expression, including tip ECs and high endothelial venules (HEVs). Furthermore, analysis of highly expressed genes and enriched pathways in each subcluster revealed associations with lymphocyte homing, angiogenesis, and extracellular remodeling (Xing et al., 2021). ScRNA-seq analyses of peritumoral lung tissues in humans and mice, alongside cultured human lung TECs, have explored phenotypic variations across species and models. This study identified 13 subclusters in human PECs, 16 subclusters in mouse PECs, and 4 subclusters in cultured lung tumor ECs. Notably, only tip tumor endothelial cells (tip TECs) exhibited conserved markers consistent across both species and models (Goveia et al., 2020). Several studies have not only delineated PEC subclusters but also characterized their functions based on gene expression profiles within each subpopulation. Specifically, in the lung, veins upregulate distinct metabolic markers, differentiating them from other vascular beds (Kalucka et al., 2020). The heterogeneity observed in control and bleomycin-induced rat lungs was categorized into five clusters: Cluster I exhibited high Neurotrophic Tyrosine Kinase Receptor 2 (Ntkr2) and CXCL12 expression with low Nitric Oxide Synthase 3 (NOS3), Caveolin 1 (CAV1), Matrix Gla Protein (MGP), and SELP levels; Cluster II showed no significant marker gene expression differences; Cluster III displayed notable Atypical Chemokine Receptor 1 (Ackr1), Apolipoprotein L Domain Containing 1 (Apold1), and Vascular Cell Adhesion Molecule 1 (VACM-1) expression expression; Cluster IV was characterized by elevated Nitric Oxide Synthase 3 (Nos3), Caveolin 1 (Cav1), and Matrix Gla Protein (Mgp) with low Ntkr2 and CXCL12 levels; and Cluster V demonstrated high Interleukin 33 (IL33) and SELP expression (Li et al., 2021).

3.3 Novel PEC subclusters expressing specific genes

Certain PEC subclusters are distinguished by the expression of specific genes. Schupp et al. confirmed six human PEC subclusters: pulmonary-venous ECs exhibited Collagen Type XV Alpha 1 Chain negative ($COL15A1^-$) in lung parenchyma and systemic-venous ECs ($COL15A1^+$) in airways and visceral pleura; two capillary EC populations, aerocytes defined by Endothelin Receptor Type B (EDNRB), Sclerostin Domain Containing 1 (SOSTDC1), and T-box Transcription Factor 2 (TBX2) expression, and general capillary ECs (Schupp et al., 2021). Combined scRNA-seq and histological staining revealed that lung capillaries consist of two distinct populations: VWFneg/EMCNhigh/EDNRB1pos and VWFpos/EMCNlow/EDN1pos (Schupp et al., 2021). Niethamer et al. identified a newly described population termed carbonic anhydrase 4 (Car4)-high ECs, which exhibit elevated Car4 expression—a key enzyme catalyzing the reversible hydration of CO_2. These Car4-high ECs cluster with upregulated expressions of Car4, EDNRB, Kdr, and CD34 but comparable levels of other EC markers such as PECAM1, Plvap, Gpihbp1, and Vwf. Car4-high ECs possess a distinct gene signature, with ligand-receptor analysis suggesting their readiness to receive reparative signals from alveolar type I cells. Notably, these cells are predominantly found in regenerating alveolar regions following acute lung injury (Niethamer et al., 2020; Westphalen et al., 2012). Recent reports also indicate that Car4 ECs specifically express Apln, alongside tip EC genes such as Plaur, Serpine1, Sirpa, Piezo2, and Chst1 identified via scRNA-seq. Conversely, Plvap ECs specifically express stalk cell markers like Aplnr and Tek (Tie2). However, the correlation between Car4/Plvap and tip/stalk ECs does not extend to other established markers such as Esm1/Dll4 for tip ECs or Hes1/Flt1 for stalk ECs (Vila et al., 2020). Gillich et al. systematically characterized adult mouse lung PEC diversity via scRNA-seq, concluding that the alveolar capillary network comprises two intermingled yet stable cell types: gCap (general capillary cells) and aCap (aerocytes) (Gillich et al., 2020).

4 Applications of scRNA-seq in normal and diseased lungs

ScRNA-seq is capable of revealing lung disease-related genes and pathways, identifying PEC subclusters linked to pathology, elucidating crosstalk between PECs and other lung cells under pathological conditions, delineating spatial distribution and developmental trajectories of PECs, and detecting rare or transient cell states obscured in bulk analyses, which summaried in Figure 1 (Travaglini et al., 2020; Petegrosso and Kuang, 2020; Jiang et al., 2016).

4.1 Identification of disease-associated genes and pathways in PECs

ScRNA-seq studies have demonstrated that distinct EC genotypes exhibit unique transcriptional profiles and metabolic pathways under health and disease conditions (Qian et al., 2020), identifying aberrant gene expression patterns and specific subclusters in lung diseases, offering valuable references for discovering potential therapeutic targets (Chen et al., 2022). Novel EC surface markers present opportunities for tissue-specific drug delivery (Paik et al., 2020).

Researchers from Belgium employed scRNA-seq to conduct a comprehensive analysis of thousands of ECs in preclinical models of age-related lung cancer and macular degeneration. Their findings revealed consistent upregulation of genes and metabolic pathways during angiogenesis in diseased lungs. Furthermore, they concluded that targeting EC metabolism represents a promising strategy for preventing pathological blood vessel formation, such as in lung

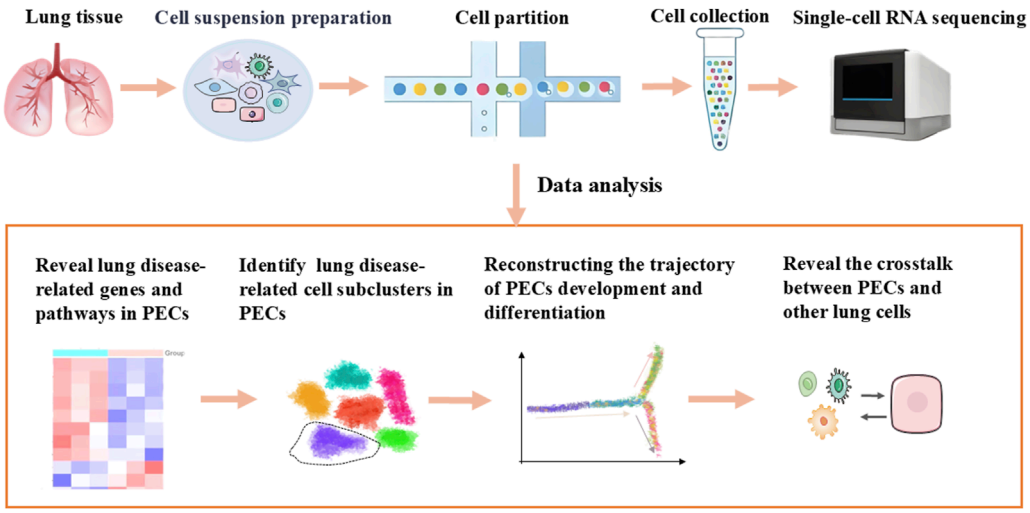

FIGURE 1
Application of scRNA-seq of PECs in normal and diseased lungs.

cancer (Rohlenova et al., 2020). ScRNA-seq analysis of mouse PECs in lung cancer uncovered previously unknown metabolic targets in angiogenesis, specifically Serum Kinase Element (SKE) and Aldehyde Dehydrogenase 18 Family Member A1 (ALDH18A1). Venous lung tumor ECs exhibited upregulation of genes related to prostaglandin metabolism, a critical factor in vascular regulation, sprouting, and inflammation. Additionally, nucleotide catabolism-related genes were upregulated, leading to reduced nucleotide content in interferon-activated TECs (Rohlenova et al., 2020). Numerous RNA-seq studies by Vila et al. revealed downregulation of previously identified sprouting-tip EC markers such as Sirpa and Chst1 in epithelial VEGFa mutant lungs compared to controls (Vila et al., 2020). Jambusaria et al. analyzed the dynamics of EC inflammatory responses across tissues, discovering that lung endothelium exhibited significant upregulation of genes associated with immune-related biological processes, including leukocyte cell-cell adhesion, T cell activation, leukocyte migration, and regulation of immune system functions. They identified the ten most significantly upregulated genes in PECs: Sftpc, Advanced Glycosylation End-Product Specific Receptor (Ager), Slc6a2, Chitinase-Like 3 (Chil3), WAP Four-Disulfide Core Domain 2 (Wfdc2), C-Type Lectin Domain Containing 7A (Clec7a), Muc1, Resistin Like Alpha (Retnla), Lysozyme (Lyz), and Homeobox A5 (Hoxa5) — uncovering the most upregulated inflammatory pathways involving chemokines, early immune response mediators, hematopoiesis genes, and cellular stress responses. *In vitro* scRNA-seq revealed that Lymphocyte Antigen 96 (Ly96) was markedly upregulated while Caspase 6 (Casp6) was strongly downregulated in PECs treated with lipopolysaccharide (LPS) for 6 h. Moreover, Forkhead Box F1 (Foxf1) and Tetraspanin 8 (Tspan8) expression levels significantly decreased in PECs treated with LPS for 6 and 24 h before gradually returning to baseline (Jambusaria et al., 2020). These studies underscore the capacity of scRNA-seq to identify up or downregulated genes in PECs, which hold potential as diagnostic and prognostic markers.

4.2 Identification of disease-related PECs subclusters

ScRNA-seq facilitates precise cell type definition through transcriptome analysis, enabling the identification of novel subclusters and their corresponding marker genes (Perico et al., 2021). ScRNA-seq data analyses have revealed subclusters associated with lung-related diseases. Additionally, the roles of specific disease-associated EC subclusters have been extensively investigated. Research indicates that PECs undergo phenotypic changes in response to various pulmonary pathologies, including IPF, COPD, and COVID-19 (Li et al., 2021; Terpos et al., 2020; Goshua et al., 2020; Delorey et al., 2021).

Vieira, B.F. et al. identified a novel EC population characterized by high expression of interferon-stimulated genes (ISGs), known for their antiviral properties. These ISG^+ ECs were situated near infected epithelial cells, suggesting a potential role in curbing viral spread (Vieira et al., 2019). Travaglini et al. discovered a novel EC population with elevated Programmed Death Ligand 1(PD-L1) expression, a ligand for the immune checkpoint receptor Programmed Death 1 (PD-1). $PD\text{-}L1^+$ ECs were predominantly found in IPF lungs and interacted with $PD\text{-}1^+$ T cells, indicating their potential to modulate immune responses (Travaglini et al., 2020). Hennigs et al. conducted transcriptomic and immunohistochemical analyses, comparing public RNA-seq and protein datasets. This approach unveiled a specific P2 receptor calcium (Ca^{2+}) signalosome in human lung endothelium associated with pulmonary arterial hypertension (Hennigs et al., 2019). In single-cell sequencing analysis of PECs in lung tumors, the study revealed that classical tip and proliferating ECs constituted a minor fraction of the tumor's EC population. Furthermore, it identified distinct subclusters of tumor ECs linked to basement membrane disruption, immune cell recruitment, and semi-professional antigen presentation (Goveia et al., 2020). ScRNA-seq has revealed that approximately 15% of PECs constitute a transcriptionally distinct subpopulation defined by the expression

of Car4. Trajectory analysis further elucidated the developmental divergence of this subset. Functional studies demonstrated that genetic ablation of Car4-expressing ECs, resulting from epithelial-specific deletion of VEGFa, leads to a marked expansion of alveolar spaces, despite the preservation of normal myofibroblast architecture—highlighting the critical role of this endothelial subset in alveolar morphogenesis (Sabbagh et al., 2018).

In the context of lung adenocarcinoma presenting as subsolid pulmonary nodules, scRNA-seq profiling revealed divergent transcriptional programs among endothelial subpopulations. ECs expressing immune-related genes, such as Baculoviral IAP Repeat-Containing 3 (BIRC3), CCL2, CD44, and ICAM1, were enriched in pathways associated with immune activation and lymphocyte recruitment. In contrast, tumor-associated ECs predominantly expressed pro-angiogenic and extracellular matrix remodeling genes, including Heparan Sulfate Proteoglycan 2 (HSPG2) and Periostin (POSTN). Pathway enrichment analysis indicated that Endothelin-1(EDN1)$^{+}$CCL2^{+} endothelial subsets were primarily involved in inflammatory signaling cascades, including TNF-α and interferon-γ (IFN-γ) pathways, whereas tumor-associated endothelial populations exhibited upregulation of biosynthetic and metabolic pathways related to angiogenesis and stromal remodeling (Xing et al., 2021). Additionally, subsets of ECs expressing EDNRB and Interleukin 1 Receptor Like 1 (IL1RL1) demonstrated elevated transcriptional activity of immune-modulatory genes, including ICAM1/2, IL32, and MHC-II molecules, further supporting their role in immune surveillance and activation within the tumor microenvironment. A novel angiogenic pathway centered on collagen modification has also been proposed through the integration of single-cell transcriptomic datasets from multiple human malignancies, corroborated by bulk transcriptome and meta-analytical data as well as functional validation studies. This newly characterized pathway provides mechanistic insight into endothelial remodeling in the tumor vasculature and represents a potential therapeutic target for anti-angiogenic interventions (Goveia et al., 2020). Furthermore, scRNA-seq has identified EC subsets implicated in the pathogenesis of breast cancer, characterized by distinct transcriptional signatures associated with lipid metabolism and immunoregulation. These cells appear to be responsive to metformin, an indirect activator of the PPAR-γ signaling axis, suggesting potential avenues for pharmacological modulation (Geldhof et al., 2022). Collectively, these findings underscore the heterogeneity and functional specialization of PEC subclusters, and highlight their emerging roles in disease pathogenesis, immune regulation, and therapeutic responsiveness. The characterization of these endothelial subsets holds substantial promise for improving diagnostic precision and prognostic assessment in pulmonary and systemic malignancies.

4.3 Elucidating the crosstalk between PECs and other pulmonary cell types

PECs engage in dynamic and reciprocal interactions with various resident cell types within the lung microenvironment, including epithelial cells, immune cells, fibroblasts, and smooth muscle cells. These interactions are mediated through direct cell–cell contact as well as paracrine signaling pathways, and play critical roles in regulating lung development, maintaining tissue homeostasis, and contributing to disease pathogenesis (Kumar and Rao, 2020; Marshall et al., 2018). To dissect the molecular underpinnings of these intercellular communications, single-cell regulatory network inference and clustering analyses have been employed, which summaried in Figure 2. These advanced computational approaches enable the identification of distinct cellular phenotypes and the elucidation of signaling crosstalk between PECs and other pulmonary cell populations, offering novel insights into the complex regulatory networks that govern lung physiology and pathology (Zhang et al., 2020).

4.3.1 Crosstalk between PECs and epithelial cells

PECs and epithelial cells are intricately integrated within the alveolar-capillary unit, a critical anatomical site for efficient gas exchange. Recent scRNA-seq studies have revealed substantial heterogeneity and plasticity within both PEC and epithelial cell populations under physiological and pathological conditions. Notably, transcripts typically associated with epithelial identity, such as Spc and Muc1, have also been detected in PECs, indicating a significant degree of molecular interplay between the pulmonary endothelium and parenchymal epithelium (Jambusaria et al., 2020). In a comprehensive analysis conducted by Vieira et al. scRNA-seq profiling of lung cells from both healthy and influenza-infected murine models identified 58 transcriptionally distinct cell populations, comprising 17 endothelial and 14 epithelial subtypes. Coordinated transcriptional alterations were observed between endothelial and epithelial compartments during infection, suggesting dynamic and functionally relevant intercellular communication between these two lineages (Vieira et al., 2019). PECs and epithelial cells share common developmental origins and are regulated by overlapping molecular pathways, including the Wnt signaling axis, which governs their differentiation, spatial organization, and functional integration. Furthermore, their crosstalk is mediated by a repertoire of secreted factors, such as angiopoietins, VEGFs, and TGF-β, which collectively modulate cellular proliferation, survival, and barrier function (Song et al., 2021).

Importantly, PECs serve as a source of angiocrine signals that actively contribute to alveolar regeneration. Endothelial-derived cues have been shown to promote epithelial repair and regeneration, while postnatal alveologenesis is critically dependent on Forkhead Box F1 (FOXF1) signaling within c-KIT^{+} endothelial progenitor cells (Ding et al., 2011; Ren et al., 2019). These findings underscore the essential role of endothelial–epithelial crosstalk in orchestrating lung development, maintaining tissue homeostasis, and facilitating repair following injury.

4.3.2 Crosstalk between PECs and VSMCs, pericytes, and fibroblasts

PECs engage in multifaceted and highly regulated interactions with vascular smooth muscle cells (VSMCs), pericytes, and fibroblasts, playing an indispensable role in maintaining vascular homeostasis, structural integrity, and orchestrating tissue remodeling. Through the secretion of bioactive vasoactive mediators—such as NO (a key vasodilator), and ET-1 (a potent vasoconstrictor)—PECs exert direct regulatory control over the contractile dynamics and phenotypic

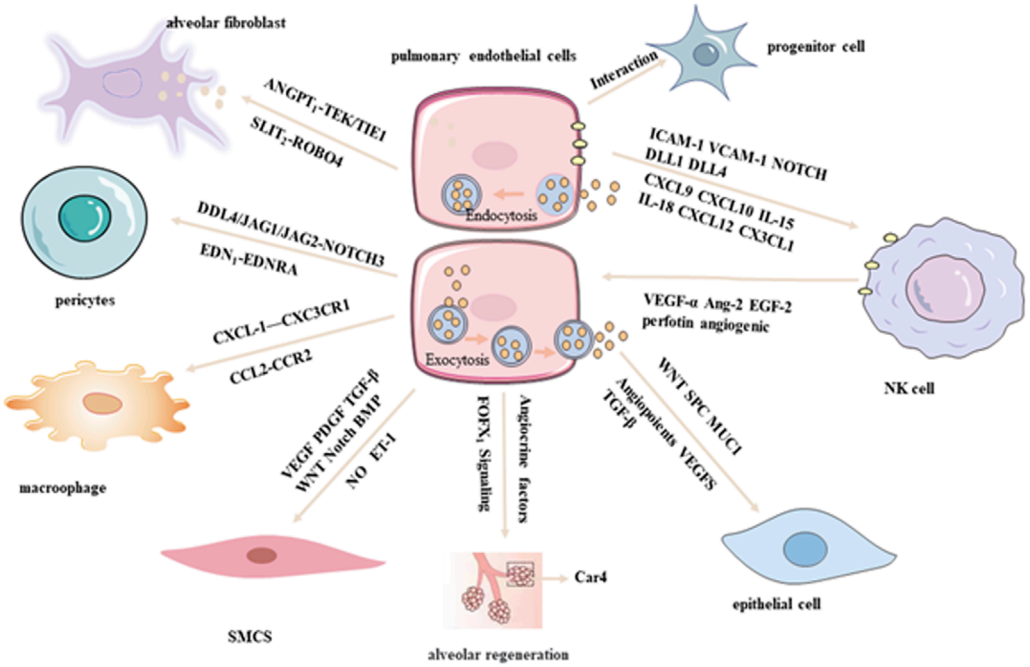

FIGURE 2
Crosstalk between PECs and other lung cells by scRNA-seq analysis.

modulation of VSMCs (Born et al., 2023). In a comprehensive single-cell transcriptomic study, Travaglini et al. profiled lung tissue from three human donors with localized neoplastic lesions, delineating 58 transcriptionally distinct cellular clusters encompassing all major pulmonary lineages, including 10 endothelial and 4 VSMC subtypes. Utilizing the CellPhoneDB algorithm, a robust computational tool for inferring ligand–receptor interactions from high-dimensional gene expression data, the authors identified extensive intercellular communication between ECs and VSMCs mediated via key signaling pathways, including VEGF, PDGF,TGF-β,Wingless/Integrated (WNT), Neurogenic locus notch homolog (NOTCH), and Bone Morphogenetic Protein (BMP).

Notably, pulmonary arterial ECs demonstrated a higher density and complexity of ligand–receptor interactions with VSMCs relative to pulmonary venous ECs, reflecting their discrete developmental origins and functional specialization within the pulmonary vasculature (Travaglini et al., 2020). Building upon these findings, Schupp et al. further elucidated the role of EC subpopulations within the pulmonary cellular interactome, emphasizing critical endotheli–mesenchymal crosstalk. Specifically, arterial ECs were shown to communicate with mural pericytes and VSMCs through the DLL4/JAG1/JAG2–NOTCH3 signaling axis, as well as via the vasoconstrictive EDN1–EDNRA axis. In addition, alveolar fibroblasts were identified as key stromal regulators of endothelial stability, providing essential trophic support to PECs through paracrine signaling pathways including ANGPT1–TEK/TIE1 and SLIT2–ROBO4 (Schupp et al., 2021). Moreover, in the setting of pulmonary fibrosis (PF), scRNA-seq has revealed dysregulated lipid metabolism signatures within specific PEC subsets, suggesting that aberrant endothelial lipid processing may contribute to pathological fibrogenesis. Collectively, these data underscore the complexity and functional relevance of PEC-mediated intercellular communication in the maintenance of vascular architecture and the pathogenesis of pulmonary disease. mmune surveillance and activation.

4.3.3 Crosstalk between PECs and macrophages/progenitor cells

Recent analyses of human control lung tissues using scRNA-seq have revealed intricate interactions between PECs and macrophages, mediated through diverse ligand–receptor pairs such as CX3CL1–CX3CR1 and CCL2–CCR2. These molecular interactions are thought to play a pivotal role in modulating inflammatory responses within the pulmonary microenvironment, thereby contributing to both immune homeostasis and the pathogenesis of lung disease (Schupp et al., 2021). Such findings underscore the power of scRNA-seq in elucidating the complexity of PEC–macrophage communication at single-cell resolution, offering critical insights into the spatial and temporal regulation of immune–endothelial interactions. This growing body of evidence not only enhances our understanding of pulmonary immunobiology but also provides a foundation for the development of targeted therapies aimed at modulating endothelial–immune cell crosstalk in both physiological and pathological contexts. Moreover, the interaction between PECs and progenitor cell populations has garnered increasing attention. Lukowski et al. employed single-cell transcriptomic profiling of the murine aorta to identify two transcriptionally distinct endothelial subpopulations and demonstrated a close association with resident progenitor cell compartments (Lukowski et al., 2019). These observations suggest a fundamental role for PECs in orchestrating vascular repair and regeneration, highlighting their dual function as regulators of both immune responses and vascular progenitor dynamics.

4.3.4 Crosstalk between PECs and NK cells

PECs orchestrate highly specialized and context-dependent interactions with natural killer (NK) cells under a spectrum of physiological and pathological conditions, including viral infections, allergic airway inflammation, pulmonary arterial hypertension, and pulmonary neoplasia. (Zhu et al., 2022; Sauler et al., 2022). PECs play a pivotal immunomodulatory role by regulating NK cell activation, differentiation, and trafficking through both direct intercellular contact and the secretion of soluble mediators. A high-resolution scRNA-seq study conducted by Xing et al. demonstrated that PECs exhibit robust expression of adhesion molecules such as ICAM-1 and vascular cell adhesion molecule-1 (VCAM-1). These molecules interact with integrins on the surface of NK cells, thereby promoting their adhesion to the endothelium and facilitating their transendothelial migration into the pulmonary parenchyma. In addition, PECs secrete chemokines such as CXCL9 and CXCL10, which establish chemotactic gradients that preferentially recruit $CXCR3^+$ NK cell subsets. Beyond recruitment, PECs are also instrumental in modulating NK cell activation states. This is achieved through the induction of activation markers, including CD69 and CD25, via both antigen-independent mechanisms—such as the secretion of pro-inflammatory cytokines like antigen-independent interleukin-15 (IL-15) and interleukin-18 (IL-18) and antigen-dependent interactions involving the presentation of MHC class I molecules. Furthermore, scRNA-seq analyses of subsolid nodules in lung adenocarcinoma have elucidated the presence of transcriptionally distinct PEC subpopulations, some of which express chemotactic ligands such as CXCL12 and CX3CL1. These ligands engage corresponding receptors CXCR4 and CX3CR1 on NK cells, further enhancing immune cell recruitment and spatial organization within the tumor microenvironment (Xing et al., 2021; Cheng et al., 2017). Collectively, these findings underscore the multifaceted role of PECs as critical immunoregulatory sentinels within the lung microenvironment and emphasize the power of single-cell transcriptomic technologies in resolving endothelial heterogeneity with high precision. A more refined understanding of PEC–immune cell crosstalk holds significant potential for identifying novel therapeutic targets aimed at modulating immune dynamics in both pulmonary homeostasis and disease pathogenesis.

4.4 Reconstructing the developmental and differentiation trajectories of PECs

Trajectory analysis represents a powerful application of scRNA-seq in elucidating the lineage hierarchies and dynamic transcriptional landscapes of PECs. By capturing temporal gene expression changes at single-cell resolution, this approach enables the reconstruction of developmental trajectories, thereby offering critical insights into the ontogeny, functional maturation, and phenotypic plasticity of PECs during embryogenesis, tissue homeostasis, and disease progression (Jia et al., 2021). Trajectory inference facilitates the delineation of endothelial differentiation from progenitor cell populations, the acquisition of organ and vascular bed-specific identities, and the cellular responses to pathophysiological stimuli such as inflammation, injury, and EndMT (Won et al., 2022). Notably, a recent study by Li et al. employed trajectory analysis to characterize PECs in murine embryonic lungs across multiple developmental stages. The study identified two ontogenetically distinct progenitor sources—mesodermal and endodermal lineages—contributing to PEC heterogeneity. Mesodermal progenitors predominantly gave rise to arterial and venous endothelial lineages, whereas endodermal progenitors were mainly responsible for the formation of capillary PECs. Moreover, the study elucidated key transcriptional regulators and signaling pathways governing progenitor fate specification and endothelial subtype differentiation (Li et al., 2022).

Among the most widely utilized computational frameworks for trajectory reconstruction are pseudotime analysis and RNA velocity, which enable high-resolution mapping of cellular transitions and directional lineage progression. These methods facilitate the identification of intermediate cell states, regulatory switches, and lineage bifurcations, thereby advancing our understanding of cell fate decisions and endothelial plasticity (Hwang et al., 2018; Slovin et al., 2021). For instance, Monocle-based trajectory analysis revealed that PECs expressing Plvap at embryonic day 17 (E17) undergo progressive maturation, with a subpopulation transitioning into Car4-expressing PECs along a distinct developmental trajectory. This finding supports a model in which $Car4^+$ PECs emerge from $Plvap^+$ precursors by embryonic day 19 (E19), highlighting the temporal dynamics of PEC subtype specification (Vila et al., 2020). Collectively, trajectory analysis provides a robust framework for decoding the molecular events underlying PEC differentiation, enabling the identification of critical regulatory genes and transitional states. These insights are instrumental for advancing our understanding of vascular development and remodeling, as well as for identifying potential therapeutic targets in vascular-associated pulmonary diseases (Papalexi and Satija, 2018).

5 Discussion

Clarifying the biological characteristics of disease-associated cells is essential for a comprehensive understanding of pathophysiological mechanisms (Van de Sande et al., 2023; Wienke et al., 2024). Integrated scRNA-seq profiling facilitates the identification of biochemical functions in PECs, monitoring of transcription factors and markers, prediction of cell targets for circulating hormones, local signaling interactions, immune cell homing, and direct identification of subclusters impacted by lung disease genes or respiratory viruses. The advancement of scRNA-seq techniques has provided novel insights into the pulmonary microenvironment in both health and disease. For instance, scRNA-seq has been instrumental in evaluating pulmonary microenvironmental heterogeneity and the progression of lung-related diseases. In early-stage lung adenocarcinoma, such as ground-glass nodules, scRNA-seq has detected tumor-associated fibroblasts, immature EC populations, and the emergence of tip-like ECs contributing to the pulmonary tumor microenvironment (Kim et al., 2022).

ScRNA-seq is a powerful tool that has unveiled key molecular mechanisms underlying lung development and pathogenesis

(Xia et al., 2023). A deeper understanding of these mechanisms promises to yield predictive models, diagnostic signatures, prognostic biomarkers, and critical information for cancer care, ultimately improving patient outcomes. Furthermore, scRNA-seq will advance prevention strategies and the development of therapeutic agents targeting multiple stages of malignant processes effectively. Current scRNA-seq research is evolving to integrate molecular data not only at the single-cell level but also across diverse cell types and organs with enhanced spatial and temporal precision. Rozenblatt-Rosen et al. developed the Human Tumor Atlas Network (HTAN) based on single-cell resolution, which is poised to significantly contribute to understanding malignancy evolution, metastatic disease, therapeutic responses, and resistance—encompassing both tumor-specific and universal mechanisms (Rozenblatt-Rosen et al., 2020). In the context of precancerous conditions, HTAN is anticipated to facilitate the identification of genetic, epigenetic, and environmental factors associated with early malignancies. This includes distinguishing non-autonomous factors relevant to immune surveillance. In advanced-stage cancers, these atlases may elucidate differences between immune-infiltrated ('hot') and immune-deserted ('cold') tumor microenvironments, provide insights into metastasis drivers more discernible via spatial data compared to genomic data alone, and examine the influence of tumor heterogeneity and microenvironmental ecosystems on therapeutic response and resistance (Rozenblatt-Rosen et al., 2020).

This approach not only enhances our fundamental understanding of lung biology but also aids in developing innovative diagnostic and therapeutic strategies for pulmonary diseases. Single-cell sequencing technology enables the identification of ECs across different organs and discovery of their specific molecular markers (Du et al., 2024). Furthermore, it facilitates the integration of correlations between ECs across various organs, potentially offering new insights into the organism's physiopathological state. For instance, the transcriptional profile of ECs is significantly influenced by their physiological functions and tissue environments in adult stages. Organs with similar functionalities or proximal anatomical locations often exhibit correlated gene expression profiles. For example, ECs in the heart and PECs show notable similarities, likely attributable to their adjacent anatomical positions (Feng et al., 2019).

In the future, integrating scRNA-seq with single-cell Assay for Transposase Accessible Chromatin with high-throughput sequencing (scATAC-seq) and other single-cell techniques such as spatial transcriptomics and proteomics will provide a more comprehensive understanding of molecular and cellular mechanisms underlying lung physiology and pathology. This approach will enable exploration of phenotypic changes in PECs during lung-related diseases, identification of transcriptomic and functional disparities among PEC subclusters, and design of drugs targeting specific PEC phenotypes. Such advancements will be instrumental in developing targeted therapeutic agents.

Author contributions

YY: Conceptualization, Investigation, Project administration, Writing – original draft, Writing – review and editing. MW: Conceptualization, Writing – original draft. XQ: Conceptualization, Investigation, Writing – original draft. RY: Methodology, Writing – original draft. CY: Data curation, Methodology, Project administration, Supervision, Writing – review and editing.

Funding

The author(s) declare that financial support was received for the research and/or publication of this article. This work was supported by grants from the National Nature Science Foundation of China (82074088).

Conflict of interest

The authors declare that the research was conducted in the absence of any commercial or financial relationships that could be construed as a potential conflict of interest.

Generative AI statement

The author(s) declare that no Generative AI was used in the creation of this manuscript.

Publisher's note

References

Abedi, F., Hayes, A. W., Reiter, R., and Karimi, G. (2020). Acute lung injury: the therapeutic role of Rho kinase inhibitors. *Pharmacol. Res.* 155, 104736. doi:10.1016/j.phrs.2020.104736

Bacon, B., Repin, M., Shuryak, I., Wu, H. C., Santella, R. M., Terry, M. B., et al. (2023). High-throughput measurement of double strand break global repair phenotype in peripheral blood mononuclear cells after long-term cryopreservation. *Cytom. A* 103, 575–583. doi:10.1002/cyto.a.24725

Bonaventura, A., Vecchié, A., Dagna, L., Martinod, K., Dixon, D. L., Van Tassell, B. W., et al. (2021). Endothelial dysfunction and immunothrombosis as key pathogenic mechanisms in COVID-19. *Nat. Rev. Immunol.* 21 (5), 319–329. doi:10.1038/s41577-021-00536-9

Born, E., Lipskaia, L., Breau, M., Houssaini, A., Beaulieu, D., Marcos, E., et al. (2023). Eliminating senescent cells can promote pulmonary hypertension development and progression. *Circulation* 147 (8), 650–666. doi:10.1161/CIRCULATIONAHA.122.058794

Butler, P. J., and Bhatnagar, A. (2019). Mechanobiology of the abluminal glycocalyx. *Biorheology* 56 (2-3), 101–112. doi:10.3233/BIR-190212

Caramelo, B., Zagorac, S., Corral, S., Marqués, M., and Real, F. X. (2023). Cancer-associated fibroblasts in bladder cancer: origin, biology, and

therapeutic opportunities. *Eur. Urol. Oncol.* 6, 366–375. doi:10.1016/j.euo.2023.02.011

Chen, S., Zhou, S., Huang, Y. E., Yuan, M., Lei, W., Chen, J., et al. (2022). Estimating metastatic risk of pancreatic ductal adenocarcinoma at single-cell resolution. *Int. J. Mol. Sci.* 23 (23), 15020. doi:10.3390/ijms232315020

Cheng, Y. H., Eby, J. M., LaPorte, H. M., Volkman, B. F., and Majetschak, M. (2017). Effects of cognate, non-cognate and synthetic CXCR4 and ACKR3 ligands on human lung endothelial cell barrier function. *PLoS One* 12 (11), e0187949. doi:10.1371/journal.pone.0187949

Delorey, T. M., Ziegler, C. G. K., Heimberg, G., Normand, R., Yang, Y., Segerstolpe, Å., et al. (2021). COVID-19 tissue atlases reveal SARS-CoV-2 pathology and cellular targets. *Nature* 595 (7865), 107–113. doi:10.1038/s41586-021-03570-8

Ding, B. S., Nolan, D. J., Guo, P., Babazadeh, A. O., Cao, Z., Rosenwaks, Z., et al. (2011). Endothelial-derived angiocrine signals induce and sustain regenerative lung alveolarization. *Cell* 147 (3), 539–553. doi:10.1016/j.cell.2011.10.003

Du, Y., Shi, J., Wang, J., Xun, Z., Yu, Z., Sun, H., et al. (2024). Integration of pan-cancer single-cell and spatial transcriptomics reveals stromal cell features and therapeutic targets in tumor microenvironment. *Cancer Res.* 84 (2), 192–210. doi:10.1158/0008-5472.CAN-23-1418

Emin, M. T., Sun, L., Huertas, A., Das, S., Bhattacharya, J., and Bhattacharya, S. (2012). Platelets induce endothelial tissue factor expression in a mouse model of acid-induced lung injury. *Am. J. Physiol. Lung Cell Mol. Physiol.* 302 (11), L1209–L1220. doi:10.1152/ajplung.00189.2011

Feng, W., Chen, L., Nguyen, P. K., Wu, S. M., and Li, G. (2019). Single cell analysis of endothelial cells identified organ-specific molecular signatures and heart-specific cell populations and molecular features. *Front. Cardiovasc Med.* 6, 165. doi:10.3389/fcvm.2019.00165

Gao, X., Cheng, Y. H., Enten, G. A., DeSantis, A. J., Gaponenko, V., and Majetschak, M. (2020). Regulation of the thrombin/protease-activated receptor 1 axis by chemokine (CXC motif) receptor 4. *J. Biol. Chem.* 295 (44), 14893–14905. doi:10.1074/jbc.RA120.015355

Geldhof, V., de Rooij, L. P. M. H., Sokol, L., Amersfoort, J., De Schepper, M., Rohlenova, K., et al. (2022). Single cell atlas identifies lipid-processing and immunomodulatory endothelial cells in healthy and malignant breast. *Nat. Commun.* 13 (1), 5511. doi:10.1038/s41467-022-33052-y

Gillich, A., Zhang, F., Farmer, C. G., Travaglini, K. J., Tan, S. Y., Gu, M., et al. (2020). Capillary cell-type specialization in the alveolus. *Nature* 586 (7831), 785–789. doi:10.1038/s41586-020-2822-7

Goldenberg, N. M., and Kuebler, W. M. (2015). Endothelial cell regulation of pulmonary vascular tone, inflammation, and coagulation. *Compr. Physiol.* 5 (2), 531–559. doi:10.1002/cphy.c140024

Gomez-Salinero, J. M., and Rafii, S. (2018). Endothelial cell adaptation in regeneration. *Science* 362 (6419), 1116–1117. doi:10.1126/science.aar4800

Goshua, G., Pine, A. B., Meizlish, M. L., Chang, C. H., Zhang, H., Bahel, P., et al. (2020). Endotheliopathy in COVID-19-associated coagulopathy: evidence from a single-centre, cross-sectional study. *Lancet Haematol.* 7 (8), e575–e582. doi:10.1016/S2352-3026(20)30216-7

Goveia, J., Rohlenova, K., Taverna, F., Treps, L., Conradi, L. C., Pircher, A., et al. (2020). An integrated gene expression landscape profiling approach to identify lung tumor endothelial cell heterogeneity and angiogenic candidates. *Cancer Cell* 37 (1), 421–36.e13. doi:10.1016/j.ccell.2020.03.002

Goyanes, A. M., Moldobaeva, A., Marimoutou, M., Varela, L. C., Wang, L., Johnston, L. F., et al. (2020). Functional impact of human genetic variants of col18a1/endostatin on pulmonary endothelium. *Am. J. Respir. Cell Mol. Biol.* 62 (4), 524–534. doi:10.1165/rcmb.2019-0056OC

Green, C. E. (2020). Lung function and endothelial dysfunction: is there a relationship without the presence of lung disease? *Respirology* 25 (1), 49–50. doi:10.1111/resp.13573

Green, C. E., and Turner, A. M. (2017). The role of the endothelium in asthma and chronic obstructive pulmonary disease (COPD). *Respir. Res.* 18 (1), 20. doi:10.1186/s12931-017-0505-1

He, L., Vanlandewijck, M., Mäe, M. A., Andrae, J., Ando, K., Del Gaudio, F., et al. (2018). Single-cell RNA sequencing of mouse brain and lung vascular and vessel-associated cell types. *Sci. Data* 5, 180160. doi:10.1038/sdata.2018.160

Hennigs, J. K., Lüneburg, N., Stage, A., Schmitz, M., Körbelin, J., Harbaum, L., et al. (2019). The P2-receptor-mediated Ca(2+) signalosome of the human pulmonary endothelium - implications for pulmonary arterial hypertension. *Purinergic Signal* 15 (3), 299–311. doi:10.1007/s11302-019-09674-1

Hudson, J., and Farkas, L. (2021). Epigenetic regulation of endothelial dysfunction and inflammation in pulmonary arterial hypertension. *Int. J. Mol. Sci.* 22 (22), 12098. doi:10.3390/ijms222212098

Huertas, A., Das, S. R., Emin, M., Sun, L., Rifkind, J. M., Bhattacharya, J., et al. (2013). Erythrocytes induce proinflammatory endothelial activation in hypoxia. *Am. J. Respir. Cell Mol. Biol.* 48 (1), 78–86. doi:10.1165/rcmb.2011-0402OC

Huertas, A., Guignabert, C., Barberà, J. A., Bärtsch, P., Bhattacharya, J., Bhattacharya, S., et al. (2018). Pulmonary vascular endothelium: the orchestra conductor in respiratory diseases: highlights from basic research to therapy. *Eur. Respir. J.* 51 (4), 1700745. doi:10.1183/13993003.00745-2017

Hwang, B., Lee, J. H., and Bang, D. (2018). Single-cell RNA sequencing technologies and bioinformatics pipelines. *Exp. Mol. Med.* 50 (8), 96–14. doi:10.1038/s12276-018-0071-8

Jambusaria, A., Hong, Z., Zhang, L., Srivastava, S., Jana, A., Toth, P. T., et al. (2020). Endothelial heterogeneity across distinct vascular beds during homeostasis and inflammation. *Elife* 9, e51413. doi:10.7554/eLife.51413

Jia, W., Wang, Z., Gao, C., Wu, J., and Wu, Q. (2021). Trajectory modeling of endothelial-to-mesenchymal transition reveals galectin-3 as a mediator in pulmonary fibrosis. *Cell Death Dis.* 12 (4), 327. doi:10.1038/s41419-021-03603-0

Jiang, L., Chen, H., Pinello, L., and Yuan, G. C. (2016). GiniClust: detecting rare cell types from single-cell gene expression data with Gini index. *Genome Biol.* 17 (1), 144. doi:10.1186/s13059-016-1010-4

Kalucka, J., de Rooij, L. P. M. H., Goveia, J., Rohlenova, K., Dumas, S. J., Meta, E., et al. (2020). Single-cell transcriptome atlas of murine endothelial cells. *Cell* 180 (4), 764–779. doi:10.1016/j.cell.2020.01.015

Kim, E. Y., Cha, Y. J., Lee, S. H., Jeong, S., Choi, Y. J., Moon, D. H., et al. (2022). Early lung carcinogenesis and tumor microenvironment observed by single-cell transcriptome analysis. *Transl. Oncol.* 15 (1), 101277. doi:10.1016/j.tranon.2021.101277

Kim, N., Kim, H. K., Lee, K., Hong, Y., Cho, J. H., Choi, J. W., et al. (2020). Single-cell RNA sequencing demonstrates the molecular and cellular reprogramming of metastatic lung adenocarcinoma. *Nat. Commun.* 11 (1), 2285. doi:10.1038/s41467-020-16164-1

Kostyunina, D. S., Rowan, S. C., Pakhomov, N. V., Dillon, E., Rochfort, K. D., Cummins, P. M., et al. (2023). Shear stress markedly alters the proteomic response to hypoxia in human pulmonary endothelial cells. *Am. J. Respir. Cell Mol. Biol.* 68 (5), 551–565. doi:10.1165/rcmb.2022-0340OC

Kumar, P., and Rao, P. N. (2020). Hepatopulmonary syndrome. *N. Engl. J. Med.* 382 (10), e14. doi:10.1056/NEJMicm1901205

Li, H., He, B., Liu, X., Li, J., Liu, Q., Dong, W., et al. (2017). Regulation on toll-like receptor 4 and cell barrier function by Rab26 siRNA-loaded DNA nanovector in pulmonary microvascular endothelial cells. *Theranostics* 7 (9), 2537–2554. doi:10.7150/thno.17584

Li, P. H., Kong, X. Y., He, Y. Z., Liu, Y., Peng, X., Li, Z. H., et al. (2022). Recent developments in application of single-cell RNA sequencing in the tumour immune microenvironment and cancer therapy. *Mil. Med. Res.* 9 (1), 52. doi:10.1186/s40779-022-00414-y

Liu, X., Qin, X., Qin, H., Jia, C., Yuan, Y., Sun, T., et al. (2021). Characterization of the heterogeneity of endothelial cells in bleomycin-induced lung fibrosis using single-cell RNA sequencing. *Angiogenesis* 24 (4), 809–821. doi:10.1007/s10456-021-09795-5

Lukowski, S. W., Patel, J., Andersen, S. B., Sim, S. L., Wong, H. Y., Tay, J., et al. (2019). Single-cell transcriptional profiling of aortic endothelium identifies a hierarchy from endovascular progenitors to differentiated cells. *Cell Rep.* 27 (9), 2748–2758. doi:10.1016/j.celrep.2019.04.102

Marshall, J. D., Bazan, I., Zhang, Y., Fares, W. H., and Lee, P. J. (2018). Mitochondrial dysfunction and pulmonary hypertension: cause, effect, or both. *Am. J. Physiol. Lung Cell Mol. Physiol.* 314 (5), L782-L796–L796. doi:10.1152/ajplung.00331.2017

Maruhashi, T., Kihara, Y., and Higashi, Y. (2019). Bilirubin and endothelial function. *J. Atheroscler. Thromb.* 26 (8), 688–696. doi:10.5551/jat.RV17035

Metkus, T. S., Kim, B. S., Jones, S. R., Martin, S. S., Schulman, S. P., and Leucker, T. M. (2022). Plasma proprotein convertase subtilisin/kexin type 9 (PCSK9) in the acute respiratory distress syndrome. *Front. Med. (Lausanne)* 9, 876046. doi:10.3389/fmed.2022.876046

Middleton, J., Patterson, A. M., Gardner, L., Schmutz, C., and Ashton, B. A. (2002). Leukocyte extravasation: chemokine transport and presentation by the endothelium. *Blood* 100 (12), 3853–3860. doi:10.1182/blood.V100.12.3853

Neubauer, K., and Zieger, B. (2022). Endothelial cells and coagulation. *Cell Tissue Res.* 387 (3), 391–398. doi:10.1007/s00441-021-03471-2

Niethamer, T. K., Stabler, C. T., Leach, J. P., Zepp, J. A., Morley, M. P., Babu, A., et al. (2020). Defining the role of pulmonary endothelial cell heterogeneity in the response to acute lung injury. *Elife* 9, e53072. doi:10.7554/eLife.53072

Nishino, K., Yoshimatsu, Y., Muramatsu, T., Sekimoto, Y., Mitani, K., Kobayashi, E., et al. (2021). Isolation and characterisation of lymphatic endothelial cells from lung tissues affected by lymphangioleiomyomatosis. *Sci. Rep.* 11 (1), 8406. doi:10.1038/s41598-021-88064-3

Paik, D. T., Tian, L., Williams, I. M., Rhee, S., Zhang, H., Liu, C., et al. (2020). Single-cell RNA sequencing unveils unique transcriptomic signatures of organ-specific endothelial cells. *Circulation* 142 (19), 1848–1862. doi:10.1161/CIRCULATIONAHA.119.041433

Papalexi, E., and Satija, R. (2018). Single-cell RNA sequencing to explore immune cell heterogeneity. *Nat. Rev. Immunol.* 18 (1), 35–45. doi:10.1038/nri.2017.76

Patterson, C. E., and Lum, H. (2001). Update on pulmonary edema: the role and regulation of endothelial barrier function. *Endothelium* 8 (2), 75–105. doi:10.3109/10623320109165319

Perico, L., Benigni, A., Casiraghi, F., Ng, L. F. P., Renia, L., and Remuzzi, G. (2021). Immunity, endothelial injury and complement-induced coagulopathy in COVID-19. *Nat. Rev. Nephrol.* 17 (1), 46–64. doi:10.1038/s41581-020-00357-4

Petegrosso, R. Z.Li, and Kuang, R. (2020). Machine learning and statistical methods for clustering single-cell RNA-sequencing data. *Brief. Bioinform* 21 (4), 1209–1223. doi:10.1093/bib/bbz063

Plebani, R., D'Alessandro, A., Lanuti, P., Simeone, P., Cinalli, M., Righi, I., et al. (2023). Microvascular and macrovascular endothelial cell isolation and purification from lung-derived samples. *J. Vis. Exp.* 192. doi:10.3791/64885

Potente, M., and Makinen, T. (2017). Vascular heterogeneity and specialization in development and disease. *Nat. Rev. Mol. Cell Biol.* 18 (8), 477–494. doi:10.1038/nrm.2017.36

Qian, J., Olbrecht, S., Boeckx, B., Vos, H., Laoui, D., Etlioglu, E., et al. (2020). A pan-cancer blueprint of the heterogeneous tumor microenvironment revealed by single-cell profiling. *Cell Res.* 30 (9), 745–762. doi:10.1038/s41422-020-0355-0

Redetzky, M., Suttorp, H. C. N., and Witzenrath, M. (2014). Dynamics of pulmonary endothelial barrier function in acute inflammation: mechanisms and therapeutic perspectives. *Cell Tissue Res.* 355 (3), 657–673. doi:10.1007/s00441-014-1821-0

Ren, X., Ustiyan, V., Guo, M., Wang, G., Bolte, C., Zhang, Y., et al. (2019). Postnatal alveologenesis depends on FOXF1 signaling in c-KIT(+) endothelial progenitor cells. *Am. J. Respir. Crit. Care Med.* 200 (9), 1164–1176. doi:10.1164/rccm.201812-2312OC

Rohlenova, K., Goveia, J., García-Caballero, M., Subramanian, A., Kalucka, J., Treps, L., et al. (2020). Single-cell RNA sequencing maps endothelial metabolic plasticity in pathological angiogenesis. *Cell Metab.* 31 (4), 862–877. doi:10.1016/j.cmet.2020.03.009

Rounds, H. S., and Harrington, E. O. (2019). Endosomes and autophagy: regulators of pulmonary endothelial cell homeostasis in health and disease. *Antioxid. Redox Signal* 31 (13), 994–1008. doi:10.1089/ars.2019.7817

Rozenblatt-Rosen, O., Regev, A., Oberdoerffer, P., Nawy, T., Hupalowska, A., Rood, J. E., et al. (2020). The human tumor atlas network: charting tumor transitions across space and time at single-cell resolution. *Cell* 181 (2), 236–249. doi:10.1016/j.cell.2020.03.053

Ryter, B. J. S. W., and Rosas, I. O. (2022). Pathogenic mechanisms underlying idiopathic pulmonary fibrosis. *Annu. Rev. Pathol.* 17, 515–546. doi:10.1146/annurev-pathol-042320-030240

Sabbagh, M. F., Heng, J. S., Luo, C., Castanon, R. G., Nery, J. R., Rattner, A., et al. (2018). Transcriptional and epigenomic landscapes of CNS and non-CNS vascular endothelial cells. *Elife* 7, e36187. doi:10.7554/eLife.36187

Sauler, M., McDonough, J. E., Adams, T. S., Kothapalli, N., Barnthaler, T., Werder, R. B., et al. (2022). Characterization of the COPD alveolar niche using single-cell RNA sequencing. *Nat. Commun.* 13 (1), 494. doi:10.1038/s41467-022-28062-9

Schupp, J. C., Adams, T. S., Cosme, C., Jr, Raredon, M. S. B., Yuan, Y., Omote, N., et al. (2021). Integrated single-cell atlas of endothelial cells of the human lung. *Circulation* 144 (4), 286–302. doi:10.1161/CIRCULATIONAHA.120.052318

Shi, J. Y., and Cao, G. (2023). The application of single-cell RNA sequencing in the inflammatory tumor microenvironment. *Biomolecules* 13 (2), 344. doi:10.3390/biom13020344

Slovin, S., Carissimo, A., Panariello, F., Grimaldi, A., Bouché, V., Gambardella, G., et al. (2021). Single-cell RNA sequencing analysis: a step-by-step overview. *Methods Mol. Biol.* 2284, 343–365. doi:10.1007/978-1-0716-1307-8_19

Song, T., Yang, W., Huang, L., Yang, Z., and Jiang, S. (2021). Zearalenone exposure affects the Wnt/β-catenin signaling pathway and related genes of porcine endometrial epithelial cells *in vitro*. *Anim. Biosci.* 34 (6), 993–1005. doi:10.5713/ajas.20.0292

Strassheim, D., Verin, A., Batori, R., Nijmeh, H., Burns, N., Kovacs-Kasa, A., et al. (2020). P2Y purinergic receptors, endothelial dysfunction, and cardiovascular diseases. *Int. J. Mol. Sci.* 21 (18), 6855. doi:10.3390/ijms21186855

Takahashi, T., Kobayashi, S., Fujino, N., Suzuki, T., Ota, C., Tando, Y., et al. (2013). Differences in the released endothelial microparticle subtypes between human pulmonary microvascular endothelial cells and aortic endothelial cells *in vitro*. *Exp. Lung Res.* 39 (4-5), 155–161. doi:10.3109/01902148.2013.784932

Terpos, E., Ntanasis-Stathopoulos, I., Elalamy, I., Kastritis, E., Sergentanis, T. N., Politou, M., et al. (2020). Hematological findings and complications of COVID-19. *Am. J. Hematol.* 95 (7), 834–847. doi:10.1002/ajh.25829

Travaglini, K. J., Nabhan, A. N., Penland, L., Sinha, R., Gillich, A., Sit, R. V., et al. (2020). A molecular cell atlas of the human lung from single-cell RNA sequencing. *Nature* 587 (7835), 619–625. doi:10.1038/s41586-020-2922-4

Van de Sande, B., Lee, J. S., Mutasa-Gottgens, E., Naughton, B., Bacon, W., Manning, J., et al. (2023). Applications of single-cell RNA sequencing in drug discovery and development. *Nat. Rev. Drug Discov.* 22 (6), 496–520. doi:10.1038/s41573-023-00688-4

Vieira, B. F., Kar, G., Berg, M., Carpaij, O. A., Polanski, K., Simon, L. M., et al. (2019). A cellular census of human lungs identifies novel cell states in health and in asthma. *Nat. Med.* 25 (7), 1153–1163. doi:10.1038/s41591-019-0468-5

Vila, E. L., Cain, M. P., Hutchison, V., Flodby, P., Crandall, E. D., Borok, Z., et al. (2020). Epithelial vegfa specifies a distinct endothelial population in the mouse lung. *Dev. Cell* 52 (5), 617–630.e6. doi:10.1016/j.devcel.2020.01.009

Westphalen, K., Monma, E., Islam, M. N., and Bhattacharya, J. (2012). Acid contact in the rodent pulmonary alveolus causes proinflammatory signaling by membrane pore formation. *Am. J. Physiol. Lung Cell Mol. Physiol.* 303 (2), L107–L116. doi:10.1152/ajplung.00206.2011

Wienke, J., Visser, L. L., Kholosy, W. M., Keller, K. M., Barisa, M., Poon, E., et al. (2024). Integrative analysis of neuroblastoma by single-cell RNA sequencing identifies the NECTIN2-TIGIT axis as a target for immunotherapy. *Cancer Cell* 42 (2), 283–300.e8. doi:10.1016/j.ccell.2023.12.008

Won, T., Wood, M. K., Hughes, D. M., Talor, M. V., Ma, Z., Schneider, J., et al. (2022). Endothelial thrombomodulin downregulation caused by hypoxia contributes to severe infiltration and coagulopathy in COVID-19 patient lungs. *EBioMedicine* 75, 103812. doi:10.1016/j.ebiom.2022.103812

Xia, M., Jiao, L., Wang, X. H., Tong, M., Yao, M. D., Li, X. M., et al. (2023). Single-cell RNA sequencing reveals a unique pericyte type associated with capillary dysfunction. *Theranostics* 13 (8), 2515–2530. doi:10.7150/thno.83532

Xing, X., Yang, F., Huang, Q., Guo, H., Li, J., Qiu, M., et al. (2021). Decoding the multicellular ecosystem of lung adenocarcinoma manifested as pulmonary subsolid nodules by single-cell RNA sequencing. *Sci. Adv.* 7 (5), eabd9738. doi:10.1126/sciadv.abd9738

Xu, F., and Zhou, F. (2020). Inhibition of microRNA-92a ameliorates lipopolysaccharide-induced endothelial barrier dysfunction by targeting ITGA5 through the PI3K/Akt signaling pathway in human pulmonary microvascular endothelial cells. *Int. Immunopharmacol.* 78, 106060. doi:10.1016/j.intimp.2019.106060

Yamaoka-Tojo, M. (2020a). Endothelial glycocalyx damage as a systemic inflammatory microvascular endotheliopathy in COVID-19. *Biomed. J.* 43 (5), 399–413. doi:10.1016/j.bj.2020.08.007

Yamaoka-Tojo, M. (2020b). Vascular endothelial glycocalyx damage in COVID-19. *Int. J. Mol. Sci.* 21 (24), 9712. doi:10.3390/ijms21249712

Zhang, L., Li, Z., Skrzypczynska, K. M., Fang, Q., Zhang, W., O'Brien, S. A., et al. (2020). Single-cell analyses inform mechanisms of myeloid-targeted therapies in colon cancer. *Cell* 181 (2), 442–459. doi:10.1016/j.cell.2020.03.048

Zhu, J., Fan, Y., Xiong, Y., Wang, W., Chen, J., Xia, Y., et al. (2022). Delineating the dynamic evolution from preneoplasia to invasive lung adenocarcinoma by integrating single-cell RNA sequencing and spatial transcriptomics. *Exp. Mol. Med.* 54 (11), 2060–2076. doi:10.1038/s12276-022-00896-9

Ziegenhain, C., Vieth, B., Parekh, S., Reinius, B., Guillaumet-Adkins, A., Smets, M., et al. (2017). Comparative analysis of single-cell RNA sequencing methods. *Mol. Cell* 65 (4), 631–643. doi:10.1016/j.molcel.2017.01.023

frontiers | Frontiers in Pharmacology

TYPE Original Research
PUBLISHED 25 June 2025
DOI 10.3389/fphar.2025.1524219

OPEN ACCESS

EDITED BY
Lulong Bo,
Navy Medical University, China

REVIEWED BY
Surya Prakash Pandey,
University of Pittsburgh, United States
Linh Ho,
California Northstate University, United States

*CORRESPONDENCE
Yingying Sun,
liyh1081@163.com

†These authors have contributed equally to this work

RECEIVED 07 November 2024
ACCEPTED 12 June 2025
PUBLISHED 25 June 2025

CITATION
Chen J, Cai Y, Peng X, Xu Y, Chen L, Pan X and Sun Y (2025) Dexmedetomidine reduces acute lung injury caused by LPS through the SIRT3 signaling pathway *in vivo*. *Front. Pharmacol.* 16:1524219. doi: 10.3389/fphar.2025.1524219

Dexmedetomidine reduces acute lung injury caused by LPS through the SIRT3 signaling pathway *in vivo*

Jian Chen[1,2,3†], Yang Cai[1,2,3†], Xiaochun Peng[1,2,3], Yuanling Xu[1,2,3], Liying Chen[1,2,3], Xinxin Pan[1,2,3] and Yingying Sun[1,2,3*]

[1]Department of Anesthesiology, Anhui Provincial children's Hospital, Anhui, China, [2]The Fifth Clinical Medical College of Anhui Medical University, Anhui, China, [3]The Children's Medical Center of Anhui Medical University, Anhui, China

Acute lung injury (ALI) is a clinical syndrome characterized by excessive inflammatory responses. Despite the exploration of various therapeutic approaches, no effective pharmacological treatment is currently available for ALI. In the current study, we investigated the role of SIRT3 in LPS-induced ALI and the potential protective effects of dexmedetomidine (Dex), an agent that activates α2-adrenergic receptors. Histological analysis showed extensive lung damage and increased inflammatory cells in LPS-treated lung samples, with elevated TUNEL+ cells indicating apoptosis ($p < 0.05$). SIRT3 mRNA and protein expression were significantly downregulated following LPS treatment, both *in vivo* and *in vitro* ($p < 0.05$). DEX administration restored protein SIRT3 levels and reduced inflammation, while the SIRT3 inhibitor 3-TYP negated these benefits ($p < 0.05$). Additionally, DEX reduced pro-inflammatory cytokine levels and oxidative stress, effects that were also diminished by 3-TYP ($p < 0.05$). Our findings suggest that DEX exerts its protective effects against LPS-induced ALI via modulation of the SIRT3/LKB1/AMPK signaling pathway, highlighting the critical role of SIRT3 in inflammatory and oxidative stress responses in ALI.

KEYWORDS

acute lung injury, sirt3, dexmedetomidine, inflammation, oxidative stress

Introduction

Acute lung injury (ALI) represents a significant burden in critical care medicine, identified by its high incidence and the profound impact on patient morbidity and mortality (Liu C. et al., 2022; Liu X. et al., 2021). ALI is a clinical syndrome associated with excessive inflammatory responses, which can lead to diffuse alveolar damage, hypoxemic respiratory failure, and significant mortality rates (Yin et al., 2021). The condition is often induced by various factors, including sepsis, pneumonia, and severe trauma, and is marked by the disruption of the alveolar-capillary barrier, leading to protein-rich fluid exudation and impaired gas exchange (Matthay and Zemans, 2011). ALI progression to acute respiratory distress syndrome (ARDS) and the associated increase in mortality rates highlight the urgent need for effective treatments (Xu et al., 2024). The economic and healthcare system burden is substantial, with ALI/ARDS patients often requiring prolonged intensive care, mechanical ventilation, and other

resource-intensive interventions (Rubenfeld et al., 2005). Despite the advancements in intensive care, the available therapies for ALI/ARDS remain largely supportive, such as mechanical ventilation, and do not adequately target the underlying pathophysiological mechanisms (Bellani et al., 2016). The development of gene therapy and the use of therapeutic nucleic acids, such as those discussed in the review by Zhuang et al. (2023), represent a promising direction in modulating the inflammatory response in ALI/ARDS. These approaches aim to target specific genes and molecular pathways involved in the disease process, offering a more precise and potentially more effective treatment modality. Thus, understanding the pathogenesis of ALI/ARDS is critically important for developing targeted therapies to effectively prevent or treat the condition.

SIRT3 has been implicated as a potential therapeutic target in various diseases, including neurodegenerative disorders and cardiovascular diseases (Cao et al., 2022). SIRT3 increases the activity of pyruvate dehydrogenase (PDH) through deacetylation, promoting glucose oxidation and thus playing a role in function and energy production (Chen et al., 2021). SIRT3 deficiency has been associated with proliferation, oxidative stress, inflammation, and fibrosis (Chelladurai et al., 2021). SIRT3/LKB1/AMPK signaling pathway is a key regulator of cellular metabolism and inflammation (Guo et al., 2022). Overexpression of SIRT3 has been shown to increase autophagy level and promote LKB1 phosphorylation, leading to the activation of AMPK and decreased phosphorylation of mTOR, suggesting a role for the LKB1-AMPK-mTOR pathway in the induction of autophagy (Zhang M. et al., 2018). SIRT3 has been reported to be associated with ALI, for example, SIRT3-p53 pathway in sepsis-associated ALI (Gao et al., 2024). However, the role of SIRT3/LKB1/AMPK signaling pathway in ALI remain to be supplemented.

Dexmedetomidine (DEX), an agonist of the α2-adrenergic receptor, is well-known for its properties that reduce inflammation, prevent apoptosis, and provide antioxidant effects. These characteristics have demonstrated considerable advantages in alleviating lung inflammation across different experimental models (Zhang H. et al., 2019; Li et al., 2018; Wang et al., 2019). DEX has the potential to mitigate sepsis-related ALI by influencing macrophage efferocytosis via the ROS/ADAM10/AXL signaling pathway (Li et al., 2024) and our previous results showed that DEX alleviates LPS-induced acute lung injury in rats (Sun et al., 2020). On the other hand, DEX has been shown to ameliorate cardiac ischemia/reperfusion injury that can be improved by promoting autophagy via the AMPK/SIRT3 signaling pathway activation (He et al., 2023), indicating the relationship between DEX and SIRT3 signals. However, whether DEX regulates SIRT3/LKB1/AMPK signaling pathway to modulate ALI needs further exploring.

Herein, the present study aimed to investigate the protective mechanisms of DEX in LPS-induced ALI. Our findings demonstrate that DEX exerts its anti-inflammatory effects through activation of the SIRT3/LKB1/AMPK signaling pathway, thereby providing novel mechanistic insights into its therapeutic potential for ALI and other inflammation-related disorders.

Methods and materials

Animals and ethics

The studies involving animal participants were reviewed and approved by the Ethics Committee of Anhui Medical University. Seven-day-old pathogen-free Sprague-Dawley (DS) rats (male, weighing 250–300 g) were sourced from the Experimental Animal Center of Anhui Medical University (license no. SCXK-2018–031). The rats were housed in standard laboratory cages under controlled conditions, maintaining a 12-h light/dark cycle at 22°C ± 2°C, with free access to food and water.

Sixteen rats were randomly divided into four groups (4 rats/group): a saline control group, a group exposed to LPS (#L2630-100 MG; Sigma Aldrich, United States), a group exposed to both LPS and Dex (#MB4091; Meilunbio Co., Ltd.; 25 μg/kg for rats according to previous reports (Sun et al., 2020; Wang et al., 2018)), and a group treated with LPS and Dex and 3-YTP, SIRT3 inhibitor (#HY-108331; Med chem express, Shanghai, China; 50 mg/kg, ip). The rats were anesthetized through an intraperitoneal injection of pentobarbital sodium at a dose of 40 mg/kg (Merck KGaA; cat. No. 1063180500). Tracheal intubation was performed using a micro-atomizer; the control group received 300 μL saline, whereas the LPS group was given 5 mg/kg LPS. Nebulized solution was given at an oxygen flow rate of 4 L per minute for 25 min. Animals were then fed normally for 30 min without intubation following every 6-hour period. Animals were euthanized by decapitation 12 h later. Lung tissues or bronchoalveolar lavage (BAL) were collected for evaluation, followed by a thoracotomy. The right lung tissue samples were isolated for further experiments.

IHC analysis for lung morphology

For the morphological evaluation of the lungs, freshly collected samples were first weighed to record their wet mass. The samples were then dried overnight at 75°C to assess their dry mass (Herriges and Morrisey, 2014). Hematoxylin/eosin (HE) staining was performed to examine the histological structure of the lungs and assess the inflammatory response after LPS exposure. At designated time points, lung tissues were harvested and fixed in 4% paraformaldehyde, then dehydrated and embedded in paraffin wax. The samples were subsequently sectioned into 5 μm slices. The sections were analyzed using a fluorescence microscope (Olympus IX50; Olympus Corporation) in conjunction with analyzing software (NIS-Elements F3.2). Airspace volume density was determined by dividing the total airspace area by the total area (Plosa et al., 2014). At each time-point, at least 3 randomly selected images from 5 samples per group were analyzed.

Biochemical analysis assay

The levels of SOD, CAT, and MDA were measured in both serum and lung tissue samples, using purchased kits (Beyotime, Shanghai, China). Serum concentrations of tumor necrosis factor-α (TNF-α, ab46070; Abcam), interleukin-1β (IL-1β, # BMS630;

Thermal Fisher Scientific, Waltham, MA, United States) and IL-10 (#ERA23RB; Thermal Fisher Scientific), IL-8 (#EK720269; AFG Scientific, MA, United States) and IL-12 (#EK720274; AFG Scientific), IL-18 (#RAB1147; Merck, United States) and IL-6 (#RAB0311; Merck, United States), IL-5 (#ab267811; Abcam) and IL-17 (#ab119536; Abcam) were quantified using ELISA kits accordingly. A hydrogen peroxide assay kit (#S0051; Beyotime) was applied to measure the levels of hydrogen peroxide (H2O2) and the lucigenin chemiluminescence method was applied to determine the superoxide anion (O2-) levels in lung tissue samples. Briefly, lung tissue samples were homogenized and supernatant after centrifugation was incubated with 5 μM lucigenin in buffer, and then samples were recorded using a Tecan Infinite 200 by light emission. Addition incubation into the medium of 350 U/ml SOD were used to confirm the specificity for O2-. Protein concentrations were determined using a BCA Protein Concentration Assay Kit (Enhanced; #P0010; Beyotime).

Inflammatory cell counts of bronchoalveolar lavage fluid (BALF)

Following treatment, animals were sacrificed, and BALF was obtained by washing the lungs three times with PBS via a tracheal cannula. The samples were centrifuged at 3,000 rpm for 10 min at 4°C, and the pellet of cells was resuspended in PBS for total cell count analysis using a hemocytometer. Cytospin preparations were made for differential cell count, which involved staining with Wright-Giemsa method. The proportions of macrophages, neutrophils, and lymphocytes in the BALF samples were determined by measuring leukocytes under a light microscope.

ELISA assay

Serum samples were collected from administrated animals, and then were subjected to ELISA assay, for the antibodies: TNF-alpha, IL-6, IL-5, IL-1beta, IL-18 and IL-17.

TUNEL analysis

This assay was conducted using a one-step detection kit (#C1086; Beyotime) following the protocol. Tissue samples were deparaffinized in xylene, rehydrated by a graded series of ethanol concentrations, and then heated for antigen retrieval. Hydrogen peroxide of 3% was used to inhibit endogenous peroxidase activity. Subsequently, different dilutions of terminal deoxynucleotidyl transferase in reaction buffer, containing a constant concentration of digoxigenin-labeled nucleotides, were applied to the sections and incubated at 37°C for 1 h, followed by a 10-minute incubation in Stop/Wash buffer. After extensive washing, 50 μL TUNEL detection dilution was applied for 30 min. Then the sections were mounted, and images were captured under the laser wavelength between 450 and 500 nm. The percentage of TUNEL+ cells was quantified and normalized relative to the total number of cells for each group.

RT-qPCR assay

Total RNA was extracted from fresh samples using the Total RNA kit (Omega Bio-Tek, Inc.) and stored on ice, following the manufacturer's protocol. First-strand cDNA synthesis and SYBR® Green qPCR were conducted with the PrimeScript™ RT Reagent kit (Takara Bio, Inc.). Specific primers used in the study for *SIRT3* are listed as follows: F-5′-AAGACATACGGGTGGAGCCT -3′, R-5′ GGACTCAGAGCAAAGGACCC-3'. Real-time PCR was conducted using the SYBR Green kit (TINGEN Biotech, Beijing, China) under the following conditions: denaturation at 95°C for 20 s, annealing at 58°C for 20 s, and extension at 68°C for 30 s mRNA expression levels were measured by the $2^{-\Delta\Delta Cq}$ method and normalized to β-actin level. Levels of *SIRT3* in control group against β-actin were normalized to 100%. The qPCR results represent three independent experiments.

Western blotting assay

This assay was conducted using a standard protocol with polyclonal antibodies specific to SIRT3, LKB1, phosphorylated(p)-LKB1, AMPK and phosphorylated(p)-AMPK. The procedures for protein extraction and immunoblotting were previously detailed. Protein samples were extracted from lung tissue homogenates using RIPA buffer (Beyotime, Shanghai, China), supplemented with inhibitors of protease and phosphatase. Protein concentrations were then determined using the BCA assay. The proteins were separated using 10% SDS-PAGE and subsequently transferred to a PVDF membrane. Following a blocking step with 5% non-fat milk, the membrane was incubated overnight at 4°C with antibodies targeting SIRT3 (1:1,000; #ab217319; Abcam), LKB1 (1:1,000; #ab199970), phosphorylated(p)-LKB1 (1:500; #ab63473; Abcam), AMPK (1:1,000; #ab32047; Abcam) and Anti-AMPK alpha 1 (phospho T183) + AMPK alpha 2 (phospho T172) antibody (1:1,000; #ab133448; Abcam) in TBS buffer. GAPDH was used as a loading control (1:2,000; #5174; CST, MA, United States). Following incubation with secondary antibodies, either HRP goat anti-rabbit (1:1,000; # A0208; Beyotime) or anti-mouse IgG (1:1,000; #A0216; Beyotime)—the blots were developed using the BeyoECL Star ECL (P0018AM; Beyotime) and imaged. Band intensities were quantified using ImageJ (NIH, United States). Levels in control group against GAPDH were normalized to 100%. The Western blot results represent three independent experiments.

Statistical analysis

Statistical analyses and graph construction were conducted by the software package (version 10.0; GraphPad Software, Inc.). Data are expressed as mean ± standard deviation (SD) from a minimum of three independent experiments. To assess significant differences between control and treatment groups, one-way ANOVA followed by Tukey's *post hoc* test or unpaired Student's t-test were employed. A p-value of less than 0.05 was regarded as statistically significant.

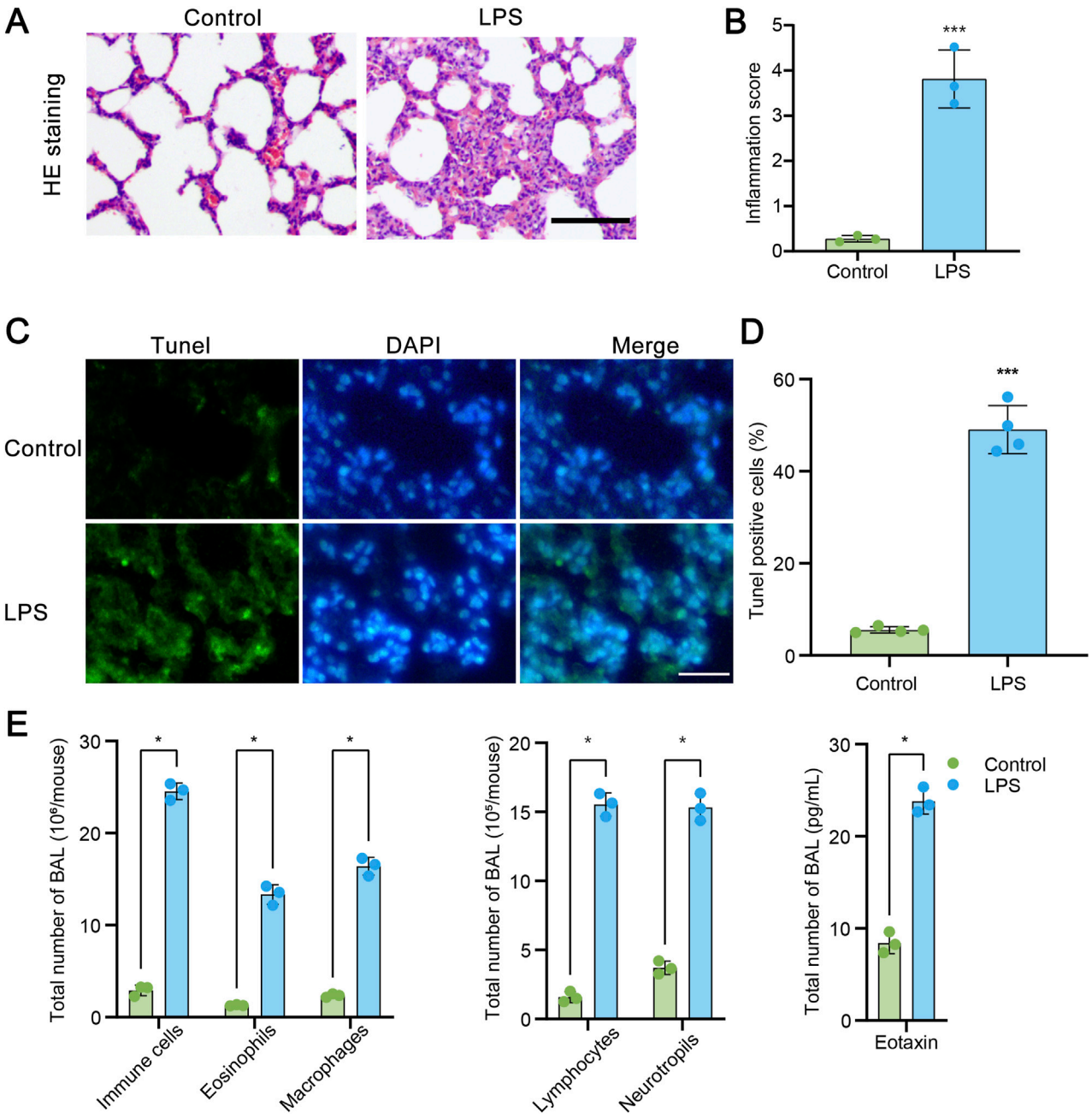

FIGURE 1
LPS administration induces to acute lung injury (ALI). **(A)** Hematoxylin and eosin (HE) staining of transverse lung sections from rats in the control and LPS-treated groups. **(B)** Quantification of the inflammatory response based on HE staining (n = 3). **(C)** TUNEL staining of transverse lung sections from the control and LPS-treated groups. **(D)** The number of TUNEL-positive cells relative to the total cells in lung tissue from the control and LPS-treated groups (n = 4). **(E)** Assessment of total cells, neutrophils, lymphocytes, macrophages, eosinophils, and Eotaxin levels in bronchoalveolar lavage fluid (BAL) by Wright-Giemsa (n = 3). Scale bars = 100 μm. Data are presented as mean ± SD. *P < 0.05 vs control; ***P < 0.001 vs control.

Results

LPS induces acute lung injury (ALI)

We first constructed a commonly used acute lung injury model using LPS. As described in the methods, rats were treated with LPS and then samples were collected and subjected to HE staining. Histological characteristics of the sections were observed. As illustrated in Figure 1A, LPS administration significantly caused the diffuse damage in the alveoli, alveolar tubes, alveolar sacs, bronchi, and alveolar septa. The quantified data of inflammation score shown in Figure 1B revealed that numerous inflammatory cells were observed in the alveolar septa after LPS exposure. Furthermore, samples were subjected to TUNEL assay. The results in Figure 1C showed that LPS administration markedly increased the number of TUNEL-positive pulmonary cells in lung samples. The quantified data were shown in Figure 1D. Then, we conducted bronchoalveolar lavages (BAL) assay to reveal the inflammatory cell infiltration by

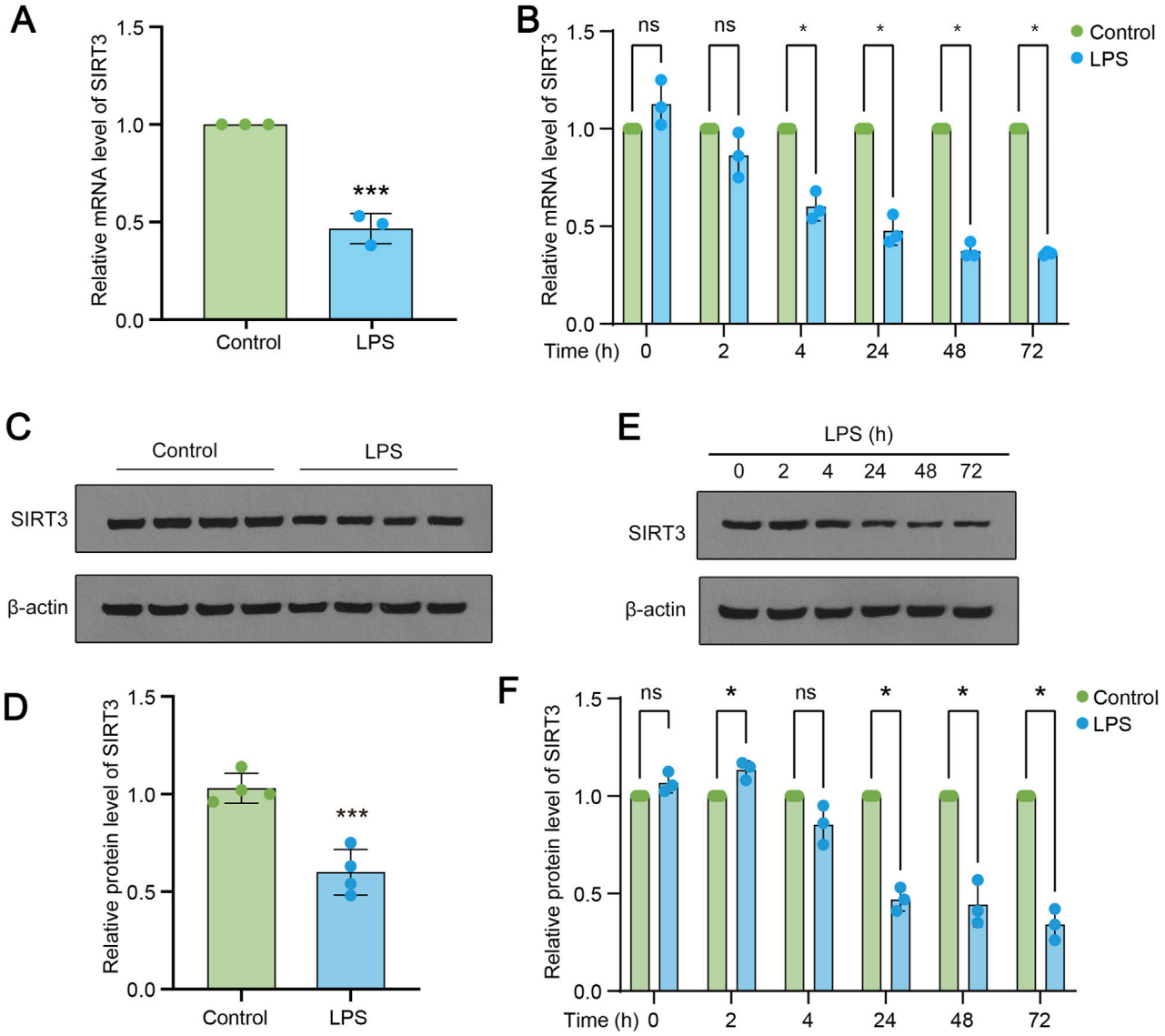

FIGURE 2
SIRT3 is downregulated during LPS induced ALI. **(A)** mRNA expression levels of SIRT3 in control and LPS-treated rats. **(B)** mRNA levels of SIRT3 in LPS-induced rat lung endothelial cells at 2, 4, 24, 48, and 72 h **(C–D)** Protein levels of SIRT3 in lung tissue samples (n = 4) from LPS-treated and control rats. **(E–F)** Protein levels of SIRT3 in lung endothelial cells at 2, 4, 24, 48, and 72 h (n = 3). Data are expressed as mean ± SD (n = 3 or 4). *P < 0.05 vs control; ***P < 0.001 vs control.

Wright-Giemsa method. As shown in Figure 1E, LPS administration significantly resulted in the increasement of immune cells, eosinophils, macrophages, lymphocytes and neutrophils. Furthermore, in LPS treated lung samples, the BAL eotaxin level was also increased. These data indicate that LPS administration significantly induced acute lung injury.

Dexmedetomidine (DEX) regulates the SIRT3/LKB1/AMPK signaling pathway in LPS-induced acute lung injury

Next, we tried to ask whether SIRT3 was involved in LPS-induced ALI. Samples from LPS treated rats were subjected to RT-qPCR and the levels of SIRT3 were measured. As shown in Figure 2A, the levels of SIRT3 were significantly reduced in LPS group, compared to control rats. Then cultured lung epithelial cells were treated with LPS of indicated time points (2, 4, 24, 48 and 72 h). The data revealed that the mRNA levels of SIRT3 were gradually decreasing along the time points (Figure 2B). Samples of LPS treated rats and cultured cells administrated with LPS were subjected to Western blotting assay. The data showed that SIRT3 protein levels were also markedly decreased upon LPS treatment (Figures 2C,D). Also, the levels of SIRT3 protein were gradually downregulated in LPS-treated lung endothelial cells, same trend as the mRNA levels (Figures 2E,F).

We have previously reported that DEX could alleviate LPS-induced acute lung injury (Sun et al., 2020). Since SIRT3 was

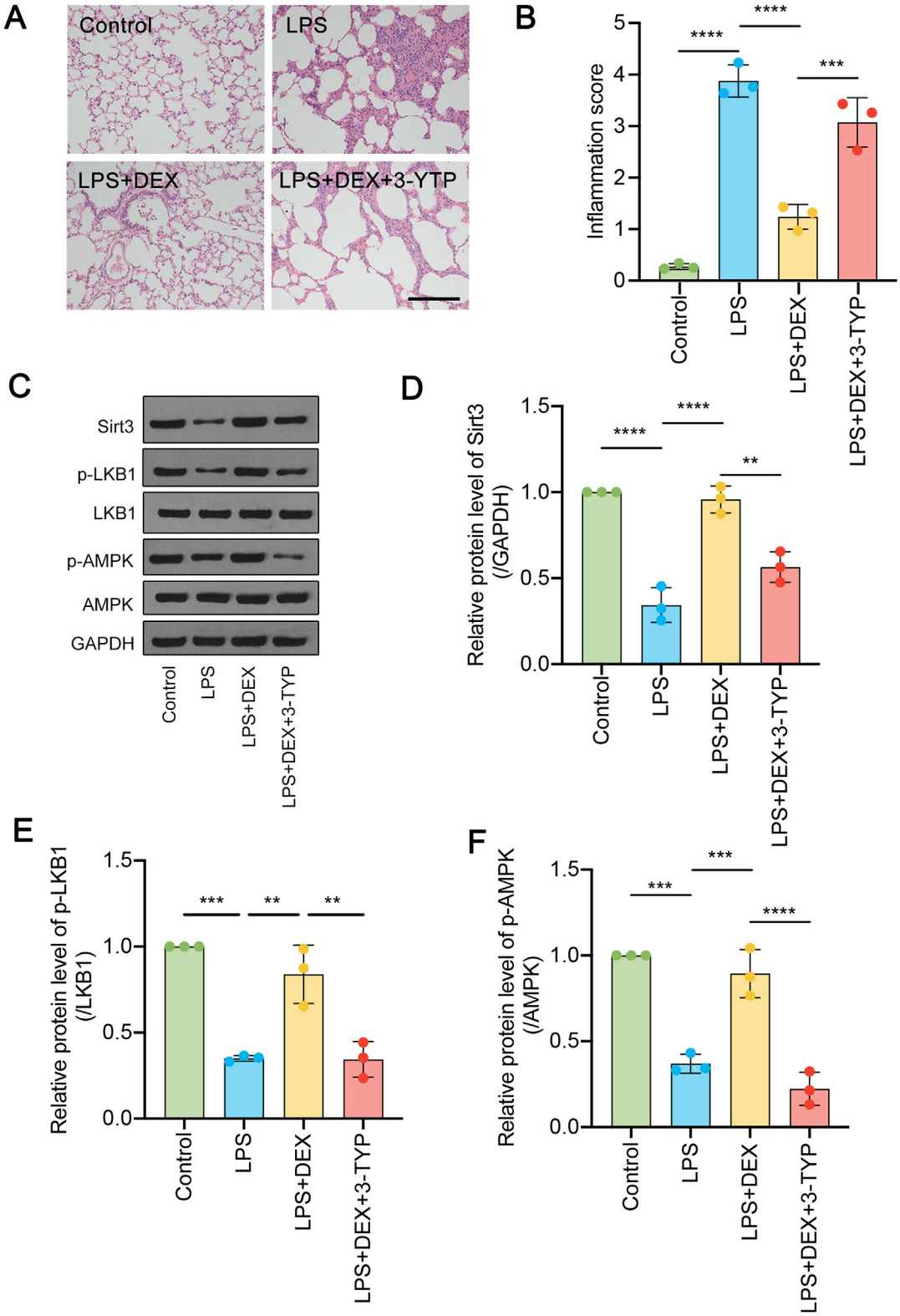

FIGURE 3
Dexmedetomidine (DEX) regulates the SIRT3/LKB1/AMPK signaling pathway in LPS-induced ALI. **(A)** HE-staining of transverse lung sections from rats in the control and LPS-treated groups, LPS + DEX, LPS + DEX+3-YTP (inhibitor of SIRT3) was performed. **(B)** The inflammation score was quantified for **(A)**. **(C)** The protein levels of total SIRT3, phosphorylated and total LKB1 and phosphorylated and total AMPK were determined. **(D–F)** The quantified data were shown. The data are represented as mean ± SD (n = 3). **P < 0.01; ***P < 0.001; ****P < 0.0001.

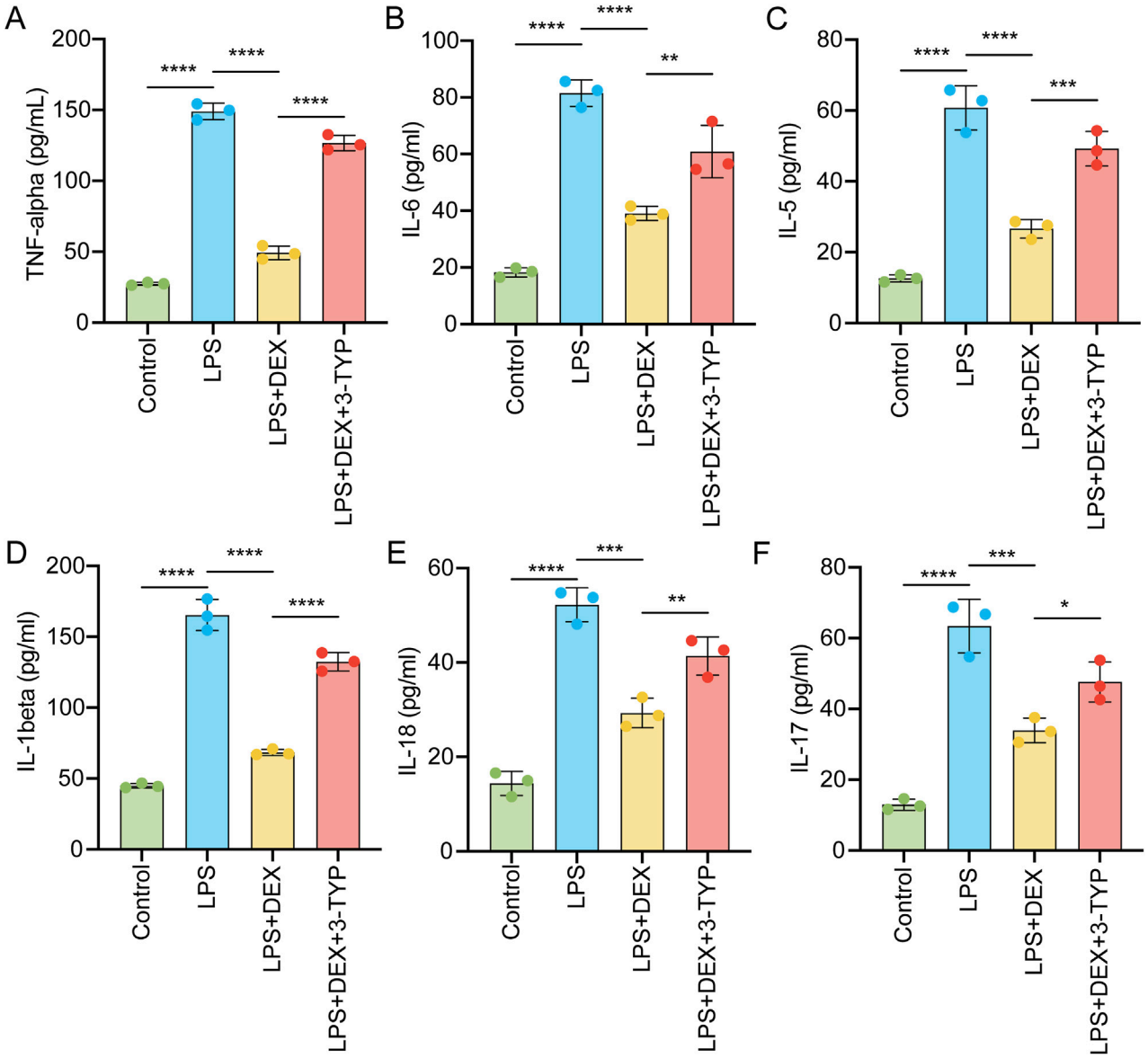

FIGURE 4
Inhibition of SIRT3 signaling abolishes the protective effect of DEX during pro-inflammatory cytokine release induced by LPS. Animals were treated as in Figure 3 and then serum pro-inflammatory cytokines were measured by ELISA, including **(A)** tumor necrosis factor-α (TNF-α), **(B)** interleukin-6 (IL-6), **(C)** IL-5, **(D)** IL-1β, **(E)** IL-18 and **(F)** IL-17. The data are presented as mean ± SD (n = 3). *P < 0.05; **P < 0.01; ***P < 0.001; ****P < 0.0001.

involved in LPS-induced ALI, we asked whether DEX would function via the regulation of SIRT3 signaling pathway. LPS-administrated rats were treated with DEX, or the SIRT3 inhibitor 3-TYP. Firstly, we performed immunohistochemistry assay to reveal the histological characteristics of the sections under different treatment. As shown in Figure 3A, LPS-induced inflammation was significantly suppressed by DEX treatment, however, this process could be restored by SIRT3 inhibitor. The diffuse damage in the alveoli, alveolar tubes, alveolar sacs, bronchi, and alveolar septa showed the same trend as inflammation response, which was quantified in Figure 3B. Next, LPS administration significantly decreased the SIRT3 protein levels (Figures 3C,D), which could be rescued by the treatment of DEX. However, the addition of SIRT3 inhibitor 3-TYP further alleviated the restored level of SIRT3 protein (Figure 3B). Furthermore, when compared to the total level, the phosphorylated level of LKB1 and AMPK proteins were also shown the same trend as SIRT3 protein (Figures 3E,F). These results suggest that SIRT3 signaling pathway is involved in LPS-induced AKL, which could be modulated by DEX treatment.

Inhibition of SIRT3 signaling alleviates the protective effect of DEX against pro-inflammatory cytokine release and oxidative stress during LPS-induced ALI

To investigate whether the pro-inflammatory response evoked by LPS could be mitigated by DEX through the SIRT3 signaling

10.3389/fphar.2025.1524219

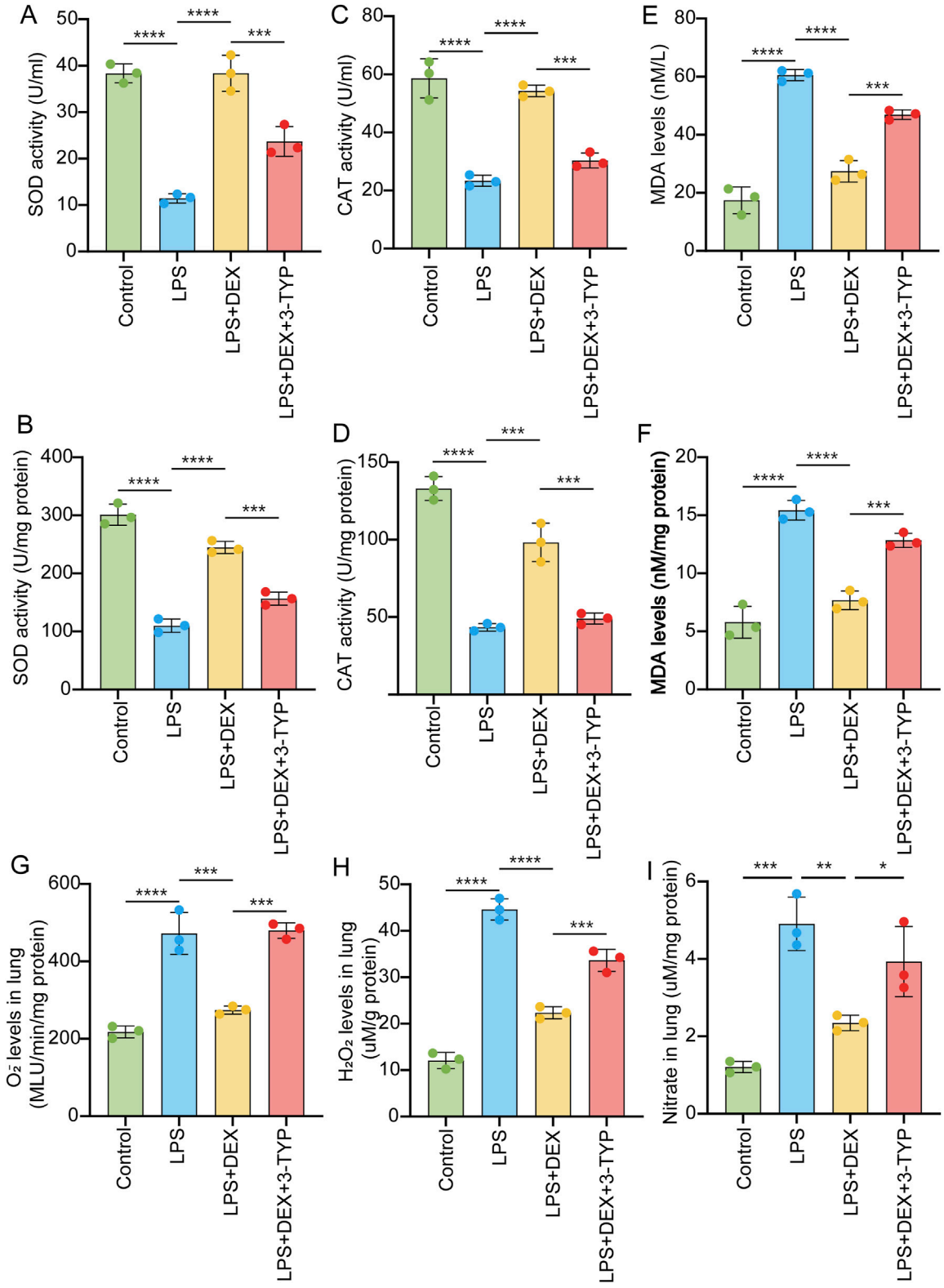

FIGURE 5
Inhibition of SIRT3 signaling abolishes the protective effect of DEX during oxidative stress induced by LPS. Rats were administered as in Figure 3. The collected samples were subjected to oxidative stress detection. SOD activity **(A,B)**, CAT activity **(C,D)** and MDA **(E,F)** levels measured in the serum or in the lung tissue samples of LPS-treated rats, with or without DEX or 3-YTP. O2- **(G)** and H2O2 **(H)**, and nitrate levels **(I)** in the LPS-induced lung tissue samples were measured. The data are presented as mean ± SD (n = 3). *P < 0.05; **P < 0.01; ***P < 0.001; ****P < 0.0001.

pathway, we administered rats with LPS, DEX, or the SIRT3 inhibitor 3-TYP. We then assessed the levels of pro-inflammatory cytokines in their serum. As depicted in Figure 4, exposure to LPS markedly upregulated the serum levels of TNF-α (Figure 4A), IL-6 (Figure 4B), IL-5 (Figure 4C), IL-1β (Figure 4D), IL-18 (Figure 4E), and IL-17 (Figure 4F). However, the administration of DEX notably attenuated these cytokine levels, an effect that was nullified by the additional treatment with 3-TYP (Figure 4). Collectively, these findings indicate that pharmacological inhibition of the SIRT3 pathway undermines the protective role of DEX in LPS-induced inflammation in ALI.

Oxidative stress, closely related to SIRT3 signaling pathway (Zheng et al., 2023), is critical for ALI (Zhong et al., 2024). To elucidate the role of SIRT3 in the generation of ROS in LPS-induced acute lung injury, we measured the activities of SOD and CAT in serum and lung tissue samples after LPS treatment. As depicted in Figures 5A–D, LPS induction significantly decreased the levels of SOD activity (Figures 5A,B) and CAT activity (Figures 5C,D). However, DEX administration notably reversed these reductions in SOD and CAT activities, an effect that was abrogated by the addition of the SIRT3 inhibitor 3-TYP (Figures 5A–D). In contrast, the level of MDA was upregulated by LPS treatment, but this increase was attenuated by DEX and further restored with the additional treatment of 3-TYP (Figures 5E,F). Moreover, we observed that the levels of oxidants such as O2−, H2O2, and nitrate in LPS-induced lung tissue samples were elevated following LPS treatment, but DEX treatment reduced these levels (Figures 5G–I). The addition of 3-TYP significantly inhibited the mitigating effect of DEX. Token together, these findings suggest that the inhibition of the SIRT3 pathway impairs the protective function of DEX against LPS-induced oxidative stress in ALI.

Discussion

In general, we examined the effects of LPS on acute lung injury and the role of SIRT3 in mediating these effects. We established a rat model of ALI using LPS, observing significant damage to alveolar structures, increased inflammatory cell infiltration, and heightened apoptosis as indicated by TUNEL assays. Quantitative analysis revealed a marked upregulation of pro-inflammatory cytokines and a decrease in antioxidant enzyme activities, indicative of oxidative stress. We found that LPS administration resulted in a significant downregulation of SIRT3 at both the mRNA and protein levels in lung tissues and cultured epithelial cells. Treatment with DEX effectively restored SIRT3 levels and improved lung pathology. However, the use of the SIRT3 inhibitor 3-TYP undermined DEX's protective effects, leading to elevated pro-inflammatory cytokines and oxidative stress markers.

ALI is characterized by an intense inflammatory response within the lung tissue. A systematic review and meta-analysis has indicated a significant association between ALI and elevated levels of certain inflammatory biomarkers, including angiopoietin-2 (ANG-2), interleukin (IL)-1β, IL-6, and tumor necrosis factor (TNF)-α (Liu Z. et al., 2022). These biomarkers are thought to play a crucial role in the pathogenesis of ALI, contributing to the severity of the condition and the subsequent development of acute respiratory distress syndrome (ARDS) (Mokra and Kosutova, 2015). The interaction between immune cells and vascular endothelial cells is another key aspect of the inflammatory process in ALI. These interactions lead to chemotaxis and adhesion of immune cells, which can exacerbate lung injury (Wu et al., 2022). For example, neutrophils, a type of white blood cell, migrating to the site of injury is a critical aspect of ALI pathophysiology, leading to further tissue damage and inflammation (Li et al., 2023). Furthermore, oxidative stress is intricately linked with acute lung injury, as it can lead to cellular damage, inflammation, and the exacerbation of lung tissue damage through the production of reactive oxygen species and the activation of inflammatory pathways (Bezerra et al., 2023). Oxidative stress not only causes direct tissue damage but also upregulates multiple inflammatory cytokines, perpetuating a cycle of damage and inflammation (Liu et al., 2023). Oxidants, such as ROS, act as inflammatory signaling molecules, activating pathways like NF-κB and NLRP3, which exacerbate ALI/ARDS (Ward, 2010). Here, we used LPS to construct the ALI model in rats. As we previously reported (Sun et al., 2020), LPS administration significantly induced severe damage in rat lungs (Figure 1). However, the detailed mechanism underlying inflammatory response during ALI need to be further explored.

The SIRT3/LKB1/AMPK signaling pathway plays a critical role in the regulation of cellular metabolism, energy homeostasis, and stress response, including its relationship with acute lung injury (ALI). SIRT3, a mitochondrial deacetylase, regulates proteins that are involved in ROS production, primarily by altering the acetylation of SOD2, which increases its activity and influences ROS homeostasis (Xi et al., 2024). SIRT3 abolishes sepsis-induced ALI via pyroptosis inhibition, which are crucial in mitigating inflammation and oxidative stress in ALI (Wu et al., 2023). Melatonin protects against ALI via SIRT3-dependent deacetylation of SOD2 (Ning et al., 2022). SIRT3 inhibition exacerbates mitochondrial dynamic imbalance and pro-inflammatory polarization, aggravating sepsis-induced ALI (Sun et al., 2024). Here, we found that LPS administration markedly downregulated the mRNA and protein levels of SIRT3, phosphorylated LKB1, and phosphorylated AMPK in lung samples. Dex treatment rescued these protein levels but could be suppressed by the additional administration of SIRT3 inhibitor 3-YTP (Figure 3). This finding suggests that the SIRT3/LKB1/AMPK signaling pathway is protective in ALI, which is consistent with above reports.

Dexmedetomidine (DEX) has been studied for its potential protective effects on ALI. Dexmedetomidine reduces systemic inflammation and lung injury by promoting Treg cells proliferation through the AMPK/SIRT1 signaling pathway (Zhang et al., 2023). DEX reduces LPS-induced ALI by targeting miR-381/NLRP3 axis (Zhang et al., 2018b). DEX mitigates IL-17-induced lung injury through a dose-dependent anti-inflammatory effect (Zhang et al., 2018c). DEX mitigates hyperoxia-induced ALI by inhibiting the activation of the NLRP3 inflammasome (Zhang et al., 2017). DEX protects against lung injury by influencing mitochondrial dynamics and promoting oxygen consumption (Zhang JR. et al., 2019), or via the PKC-alpha/HO-1 pathway (Song et al., 2022). DEX alleviates LPS-induced ALI in rats by regulating Nrf2/Keap1 and Akt signals (Yan et al., 2017). DEX alleviates pulmonary edema in LPS-induced ALI by upregulating AQP1 and AQP5 expression (Jiang et al., 2015). On the other hand,

SIRT3 is involved in DEX regulated diseases. For example, DEX helps protect enteric glial cells from mitochondrial damage and cell death during experimental intestinal ischemia/reperfusion injury by utilizing a SIRT3-dependent pathway (Zhang et al., 2021). DEX safeguards the heart against ischemia-reperfusion injury by boosting autophagy via the AMPK/SIRT3 pathway, thereby reducing oxidative stress, inflammation, and improving cardiac function and mitochondrial integrity (He et al., 2023). DEX protects against nephritis by upregulating SIRT3 expression, which mitigates inflammation, oxidative stress, and apoptosis in renal cells both *in vivo* and *in vitro* (Lu et al., 2024). Here, in the current study, we found that DEX could also alleviate the LPS-induced inflammation and also DEX modulate SIRT3 signaling pathway to execute the protective function during ALI.

Dexmedetomidine is associated with several side effects, particularly hemodynamic and respiratory complications, which clinicians must monitor closely. Dexmedetomidine is associated with a significant decrease in heart rate compared to propofol, indicating potential bradycardia as a side effect (Nicholson et al., 2021). Dexmedetomidine has been noted to cause respiratory depression and hypoxia, particularly in combination with other sedatives (Liu S. et al., 2021). Despite its favorable respiratory profile, dexmedetomidine may still lead to severe circulatory complications in adults (Su and Hammer, 2011). The combination of dexmedetomidine with propofol in younger patients was associated with reduced mortality, while increasing dexmedetomidine doses correlated with increased mortality (Shehabi et al., 2023). While it shows efficacy in sedation and analgesia, its safety profile compared to other sedatives like propofol and olanzapine suggests a need for careful consideration in its use, especially in vulnerable populations.

In conclusion, the present study suggests that DEX mitigates LPS-induced ALI primarily through the SIRT3/LKB1/AMPK signaling pathway, reinforcing the importance of SIRT3 in the inflammatory and oxidative responses associated with ALI. These findings may offer insights into therapeutic strategies targeting SIRT3 in lung inflammatory diseases.

Data availability statement

The original contributions presented in the study are included in the article/supplementary material, further inquiries can be directed to the corresponding author.

Ethics statement

All animal procedures adhered to international animal welfare standards and complied with the regulations set by the committee at Anhui Medical University. Seven-day-old pathogen-free Sprague-Dawley (DS) rats (male, weighing 250–300 g) were sourced from the Experimental Animal Center of Anhui Medical University (license no. SCXK-2018–031). The rats were housed in standard laboratory cages under controlled conditions, maintaining a 12-hour light/dark cycle at 22°C ± 2°C, with free access to food and water. The study was conducted in accordance with the local legislation and institutional requirements.

Author contributions

JC: Data curation, Writing – original draft. YC: Writing – original draft, Writing – review and editing. XP: Writing – review and editing. YX: Writing – review and editing. LC: Writing – review and editing. XP: Writing – review and editing. YS: Conceptualization, Writing – review and editing.

Funding

The author(s) declare that financial support was received for the research and/or publication of this article. This works was supported by Clinical Science Foundation from Anhui Medical University (No. 2022xkj244), Excellent Young Academic Leader Training Program of Anhui Provincial Children's Hospital (No. eyrc014), the key project of Anhui Provincial University Scientific Research Project (No. 2023AH050654) and Clinical Medical Research Transformation Project of Anhui Provincial (No. 202304295107020068).

Conflict of interest

The authors declare that the research was conducted in the absence of any commercial or financial relationships that could be construed as a potential conflict of interest.

Generative AI statement

The author(s) declare that no Generative AI was used in the creation of this manuscript.

Publisher's note

References

Bellani, G., Laffey, J. G., Pham, T., Fan, E., Brochard, L., Esteban, A., et al. (2016). Epidemiology, patterns of care, and mortality for patients with acute respiratory distress syndrome in intensive care units in 50 countries. *JAMA* 315, 788–800. doi:10.1001/jama.2016.0291

Bezerra, F. S., Lanzetti, M., Nesi, R. T., Nagato, A. C., Silva, C. P. E., Kennedy-Feitosa, E., et al. (2023). Oxidative stress and inflammation in acute and chronic lung injuries. *Antioxidants (Basel)* 12, 548. doi:10.3390/antiox12030548

Cao, M., Zhao, Q., Sun, X., Qian, H., Lyu, S., Chen, R., et al. (2022). Sirtuin 3: emerging therapeutic target for cardiovascular diseases. *Free Radic. Biol. Med.* 180, 63–74. doi:10.1016/j.freeradbiomed.2022.01.005

Chelladurai, P., Boucherat, O., Stenmark, K., Kracht, M., Seeger, W., Bauer, U. M., et al. (2021). Targeting histone acetylation in pulmonary hypertension and right ventricular hypertrophy. *Br. J. Pharmacol.* 178, 54–71. doi:10.1111/bph.14932

Chen, X., Hao, B., Li, D., Reiter, R. J., Bai, Y., Abay, B., et al. (2021). Melatonin inhibits lung cancer development by reversing the warburg effect *via* stimulating the SIRT3/PDH axis. *J. Pineal Res.* 71, e12755. doi:10.1111/jpi.12755

Gao, N., Liu, X. Y., Chen, J., Hu, T. P., Wang, Y., and Zhang, G. Q. (2024). Menaquinone-4 alleviates sepsis-associated acute lung injury *via* activating SIRT3-p53/SLC7A11 pathway. *J. Inflamm. Res.* 17, 7675–7685. doi:10.2147/JIR.S486984

Guo, Z., Tuo, H., Tang, N., Liu, F. Y., Ma, S. Q., An, P., et al. (2022). Neuraminidase 1 deficiency attenuates cardiac dysfunction, oxidative stress, fibrosis, inflammatory *via* AMPK-SIRT3 pathway in diabetic cardiomyopathy mice. *Int. J. Biol. Sci.* 18, 826–840. doi:10.7150/ijbs.65938

He, H., Liu, P., and Li, P. (2023). Dexmedetomidine ameliorates cardiac ischemia/reperfusion injury by enhancing autophagy through activation of the AMPK/SIRT3 pathway. *Drug Des. Devel Ther.* 17, 3205–3218. doi:10.2147/DDDT.S428024

Herriges, M., and Morrisey, E. E. (2014). Lung development: orchestrating the generation and regeneration of a complex organ. *Development* 141, 502–513. doi:10.1242/dev.098186

Jiang, Y. X., Dai, Z. L., Zhang, X. P., Zhao, W., Huang, Q., and Gao, L. K. (2015). Dexmedetomidine alleviates pulmonary edema by upregulating AQP1 and AQP5 expression in rats with acute lung injury induced by lipopolysaccharide. *J. Huazhong Univ. Sci. Technol. Med. Sci.* 35, 684–688. doi:10.1007/s11596-015-1490-6

Li, F., Bai, Y., Guan, Z., Ji, X., Zhan, X., Gao, Y., et al. (2024). Dexmedetomidine attenuates sepsis-associated acute lung injury by regulating macrophage efferocytosis through the ROS/ADAM10/AXL pathway. *Int. Immunopharmacol.* 142, 112832. doi:10.1016/j.intimp.2024.112832

Li, J., Chen, Q., He, X., Alam, A., Ning, J., Yi, B., et al. (2018). Dexmedetomidine attenuates lung apoptosis induced by renal ischemia-reperfusion injury through α2AR/PI3K/Akt pathway. *J. Transl. Med.* 16, 78. doi:10.1186/s12967-018-1455-1

Li, Y., Jiang, Y., Zhang, H., Zhang, J., Ma, J., Yang, Z., et al. (2023). Research on acute lung injury inflammatory network. *Int. J. Clin. Pharmacol. Ther.* 61, 394–403. doi:10.5414/CP204438

Liu, C., Xiao, K., and Xie, L. (2022a). Progress in preclinical studies of macrophage autophagy in the regulation of ALI/ARDS. *Front. Immunol.* 13, 922702. doi:10.3389/fimmu.2022.922702

Liu, S., Zhao, R., Yang, R., Zhao, H., Ji, C., Duan, M., et al. (2021b). Are dexmedetomidine and olanzapine suitable to control delirium in critically ill elderly patients? A retrospective cohort study. *Biomed. Pharmacother.* 139, 111617. doi:10.1016/j.biopha.2021.111617

Liu, X., Wang, L., Xing, Q., Li, K., Si, J., Ma, X., et al. (2021a). Sevoflurane inhibits ferroptosis: a new mechanism to explain its protective role against lipopolysaccharide-induced acute lung injury. *Life Sci.* 275, 119391. doi:10.1016/j.lfs.2021.119391

Liu, Y., Li, H., Ouyang, Y., Zhang, Y., and Pan, P. (2023). Exploration of the role of oxidative stress-related genes in LPS-Induced acute lung injury *via* bioinformatics and experimental studies. *Sci. Rep.* 13, 21804. doi:10.1038/s41598-023-49165-3

Liu, Z., Liu, D., Wang, Z., Zou, Y., Wang, H., Li, X., et al. (2022b). Association between inflammatory biomarkers and acute respiratory distress syndrome or acute lung injury risk: a systematic review and meta-analysis. *Wien Klin. Wochenschr* 134, 24–38. doi:10.1007/s00508-021-01971-3

Lu, K., Li, X., and Wu, J. (2024). Sirtuin 3 is required for the dexmedetomidine-mediated alleviation of inflammation and oxidative stress in nephritis. *Immun. Inflamm. Dis.* 12, e1135. doi:10.1002/iid3.1135

Matthay, M. A., and Zemans, R. L. (2011). The acute respiratory distress syndrome: pathogenesis and treatment. *Annu. Rev. Pathol.* 6, 147–163. doi:10.1146/annurev-pathol-011110-130158

Mokra, D., and Kosutova, P. (2015). Biomarkers in acute lung injury. *Respir. Physiol. Neurobiol.* 209, 52–58. doi:10.1016/j.resp.2014.10.006

Nicholson, C. R., Mullen, C., Frazee, L. A., and Cucci, M. D. (2021). Hemodynamic adverse effects of dexmedetomidine and propofol in a critically ill trauma and surgical population: a retrospective cohort. *J. Trauma Nurs.* 28, 149–158. doi:10.1097/JTN.0000000000000576

Ning, L., Rui, X., Guorui, L., Tinglv, F., Donghang, L., Chenzhen, X., et al. (2022). A novel mechanism for the protection against acute lung injury by melatonin: mitochondrial quality control of lung epithelial cells is preserved through SIRT3-dependent deacetylation of SOD2. *Cell Mol. Life Sci.* 79, 610. doi:10.1007/s00018-022-04628-0

Plosa, E. J., Young, L. R., Gulleman, P. M., Polosukhin, V. V., Zaynagetdinov, R., Benjamin, J. T., et al. (2014). Epithelial β1 integrin is required for lung branching morphogenesis and alveolarization. *Development* 141, 4751–4762. doi:10.1242/dev.117200

Rubenfeld, G. D., Caldwell, E., Peabody, E., Weaver, J., Martin, D. P., Neff, M., et al. (2005). Incidence and outcomes of acute lung injury. *N. Engl. J. Med.* 353, 1685–1693. doi:10.1056/NEJMoa050333

Shehabi, Y., Serpa Neto, A., Bellomo, R., Howe, B. D., Arabi, Y. M., Bailey, M., et al. (2023). Dexmedetomidine and propofol sedation in critically ill patients and dose-associated 90-Day mortality: a secondary cohort analysis of a randomized controlled trial (SPICE III). *Am. J. Respir. Crit. Care Med.* 207, 876–886. doi:10.1164/rccm.202206-1208OC

Song, K., Shi, J., Zhan, L., Gao, Q., Yang, J., Dong, S., et al. (2022). Dexmedetomidine modulates mitochondrial dynamics to protect against endotoxin-induced lung injury *via* the protein kinase C-α/haem oxygenase-1 signalling pathway. *Biomarkers* 27, 159–168. doi:10.1080/1354750X.2021.2023219

Su, F., and Hammer, G. B. (2011). Dexmedetomidine: pediatric pharmacology, clinical uses and safety. *Expert Opin. Drug Saf.* 10, 55–66. doi:10.1517/14740338.2010.512609

Sun, M., Li, Y., Xu, G., Zhu, J., Lu, R., An, S., et al. (2024). Sirt3-Mediated Opa1 deacetylation protects against sepsis-induced acute lung injury by inhibiting alveolar macrophage pro-inflammatory polarization. *Antioxid. Redox Signal* 41, 1014–1030. doi:10.1089/ars.2023.0322

Sun, Y., Xia, Y., Liu, X., Liu, J., He, W., Ye, H., et al. (2020). Dexmedetomidine alleviates LPS-Induced acute lung injury *via* regulation of the p38/HO-1 pathway. *Mol. Med. Rep.* 22, 2442–2450. doi:10.3892/mmr.2020.11330

Wang, D. S., Kaneshwaran, K., Lei, G., Mostafa, F., Wang, J., Lecker, I., et al. (2018). Dexmedetomidine prevents excessive gamma-Aminobutyric acid type A receptor function after anesthesia. *Anesthesiology* 129, 477–489. doi:10.1097/ALN.0000000000002311

Wang, J., Yi, X., Jiang, L., Dong, H., Feng, W., Wang, S., et al. (2019). Protective effects of dexmedetomidine on lung in rats with one-lung ventilation. *Exp. Ther. Med.* 17, 187–192. doi:10.3892/etm.2018.6952

Ward, P. A. (2010). Oxidative stress: acute and progressive lung injury. *Ann. N. Y. Acad. Sci.* 1203, 53–59. doi:10.1111/j.1749-6632.2010.05552.x

Wu, B., Xu, M. M., Fan, C., Feng, C. L., Lu, Q. K., Lu, H. M., et al. (2022). STING inhibitor ameliorates LPS-Induced ALI by preventing vascular endothelial cells-mediated immune cells chemotaxis and adhesion. *Acta Pharmacol. Sin.* 43, 2055–2066. doi:10.1038/s41401-021-00813-2

Wu, Z., Wang, Y., Lu, S., Yin, L., and Dai, L. (2023). SIRT3 alleviates sepsis-induced acute lung injury by inhibiting pyroptosis *via* regulating the deacetylation of FoxO3a. *Pulm. Pharmacol. Ther.* 82, 102244. doi:10.1016/j.pupt.2023.102244

Xi, S., Chen, W., and Ke, Y. (2024). Advances in SIRT3 involvement in regulating autophagy-related mechanisms. *Cell Div.* 19, 20. doi:10.1186/s13008-024-00124-y

Xu, Y., Xin, J., Sun, Y., Wang, X., Sun, L., Zhao, F., et al. (2024). Mechanisms of sepsis-induced acute lung injury and advancements of natural small molecules in its treatment. *Pharm. (Basel)* 17, 472. doi:10.3390/ph17040472

Yan, X., Cheng, X., Zhou, L., He, X., Zheng, W., and Chen, H. (2017). Dexmedetomidine alleviates lipopolysaccharide-induced lung injury in wistar rats. *Oncotarget* 8, 44410–44417. doi:10.18632/oncotarget.17899

Yin, X., Zhu, G., Wang, Q., Fu, Y. D., Wang, J., and Xu, B. (2021). Ferroptosis, a new insight into acute lung injury. *Front. Pharmacol.* 12, 709538. doi:10.3389/fphar.2021.709538

Zhang, H., Sha, J., Feng, X., Hu, X., Chen, Y., Li, B., et al. (2019a). Dexmedetomidine ameliorates LPS induced acute lung injury *via* GSK-3β/STAT3-NF-κB signaling pathway in rats. *Int. Immunopharmacol.* 74, 105717. doi:10.1016/j.intimp.2019.105717

Zhang, J. R., Lin, Q., Liang, F. Q., and Xie, T. (2019b). Dexmedetomidine attenuates lung injury by promoting mitochondrial fission and oxygen consumption. *Med. Sci. Monit.* 25, 1848–1856. doi:10.12659/MSM.913239

Zhang, M., Deng, Y. N., Zhang, J. Y., Liu, J., Li, Y. B., Su, H., et al. (2018a). SIRT3 protects rotenone-induced injury in SH-SY5Y cells by promoting autophagy through the LKB1-AMPK-mTOR pathway. *Aging Dis.* 9, 273–286. doi:10.14336/AD.2017.0517

Zhang, Q., Liu, X. M., Hu, Q., Liu, Z. R., Liu, Z. Y., Zhang, H. G., et al. (2021). Dexmedetomidine inhibits mitochondria damage and apoptosis of enteric glial cells in experimental intestinal ischemia/reperfusion injury *via* SIRT3-dependent PINK1/HDAC3/p53 pathway. *J. Transl. Med.* 19, 463. doi:10.1186/s12967-021-03027-6

Zhang, Q., Wu, D., Yang, Y., Liu, T., and Liu, H. (2017). Dexmedetomidine alleviates hyperoxia-induced acute lung injury *via* inhibiting NLRP3 inflammasome activation. *Cell Physiol. Biochem.* 42, 1907–1919. doi:10.1159/000479609

Zhang, Y., Jia, S., Gao, T., Zhang, R., Liu, Z., and Wang, Y. (2018c). Dexmedetomidine mitigate acute lung injury by inhibiting IL-17-induced inflammatory reaction. *Immunobiology* 223, 32–37. doi:10.1016/j.imbio.2017.10.017

Zhang, Y., Wang, X., Liu, Z., and Yu, L. (2018b). Dexmedetomidine attenuates lipopolysaccharide induced acute lung injury by targeting NLRP3 *via* miR-381. *J. Biochem. Mol. Toxicol.* 32, e22211. doi:10.1002/jbt.22211

Zhang, Z. T., Xie, K., Luo, R. J., Zhang, D. Y., He, Z. W., Li, K. F., et al. (2023). Dexmedetomidine alleviates acute lung injury by promoting tregs differentiation *via* activation of AMPK/SIRT1 pathway. *Inflammopharmacology* 31, 423–438. doi:10.1007/s10787-022-01117-5

Zheng, Y., Wang, S., Wu, J., and Wang, Y. (2023). Mitochondrial metabolic dysfunction and non-alcoholic fatty liver disease: new insights from pathogenic mechanisms to clinically targeted therapy. *J. Transl. Med.* 21, 510. doi:10.1186/s12967-023-04367-1

Zhong, Y., Xia, S., Wang, G., Liu, Q., Ma, F., Yu, Y., et al. (2024). The interplay between mitophagy and mitochondrial ROS in acute lung injury. *Mitochondrion* 78, 101920. doi:10.1016/j.mito.2024.101920

Zhuang, C., Kang, M., and Lee, M. (2023). Delivery systems of therapeutic nucleic acids for the treatment of acute lung injury/acute respiratory distress syndrome. *J. Control Release* 360, 1–14. doi:10.1016/j.jconrel.2023.06.018

frontiers | Frontiers in Cell and Developmental Biology

TYPE Review
PUBLISHED 07 July 2025
DOI 10.3389/fcell.2025.1564627

OPEN ACCESS

EDITED BY
Guochang Hu,
University of Illinois Chicago, United States

REVIEWED BY
Mosharraf Sarker,
Liverpool John Moores University,
United Kingdom
Vigneshwaran Vellingiri,
University of Illinois Chicago, United States

*CORRESPONDENCE
Diana Klein,
diana.klein@uk-essen.de

RECEIVED 21 January 2025
ACCEPTED 26 June 2025
PUBLISHED 07 July 2025

CITATION
Klein D (2025) The vascular endothelium as decision maker in lung injury.
Front. Cell Dev. Biol. 13:1564627.
doi: 10.3389/fcell.2025.1564627

The vascular endothelium as decision maker in lung injury

Diana Klein*

Institute of Cell Biology (Cancer Research), University Hospital, University of Duisburg-Essen, Essen, Germany

The vascular endothelium is the largest organ in the human body, capable of performing a wide range of cellular signaling and synthetic functions. It is also subjected to considerable mechanical stress due to the shear forces generated by blood flow, which amounts to approximately 10,000 L per day. The endothelial layer plays a crucial role in regulating vascular tone locally and controlling the extravasation of certain blood components. Additionally, it is integral to the coagulation process. The endothelium serves as the entry point for immune cells, which migrate from the bloodstream to surrounding tissues by passing through the endothelial layer. This underscores the importance of proper endothelial function for the health of the body's tissues and organs. When the endothelium fails to perform these functions adequately, leading to endothelial dysfunction, pathological conditions are more likely to develop. Notably, acute lung injury and its severe form, acute respiratory distress syndrome (ARDS), are often associated with endothelial dysfunction. ARDS refers to pulmonary edema with increased vascular permeability resulting from various pulmonary or systemic insults. In most cases, an exaggerated inflammatory and pro-thrombotic response to the initial insult causes disruption of the alveolar–capillary membrane and leakage of vascular fluid. This review emphasizes the central role of the vascular endothelium in acute conditions and seeks to clarify the concepts and interplay between endothelial activation, dysfunction, and damage.

KEYWORDS

vascular dysfunction, damage, endothelial activation, pulmonary endothelium, lung injury, inflammation

Introduction

In a normal, healthy state, the endothelium is the innermost layer of blood vessels and is considered quiescent; that is, it maintains a state in which endothelial cells are resting, awaiting stimulation and activation signals. However, it is now clear that even a quiescent endothelium is highly active, and this state must be actively regulated (Ricard et al., 2021). The overall characteristics of healthy endothelial cells were recently summarized in an elegant review (Augustin and Koh, 2024), with the "life cycle" characteristics encompassing the mechanisms of vasculogenesis, angiogenesis, maintenance and quiescence during adulthood, and changes during aging. Further key characteristics of endothelial cells include their responsive and relaying functions, such as barrier function, cell trafficking control, perfusion permeability, and blood pressure regulation, as well as triggering coagulation. Additionally, they perform instructive functions such as mechanotransduction and metabolic regulation, particularly in an

organ-specific manner (Augustin and Koh, 2024). In contrast, endothelial cells are critically involved in various life-threatening and chronic diseases, including cancer (De Palma and Hanahan, 2024; Klein, 2018), arterial diseases (e.g., cardiovascular disease, atherosclerosis, and hypertension) (Gallo et al., 2021; Xu et al., 2021; Wang and He, 2020), coagulation, and inflammation (van Hinsbergh, 2012), as well as in cerebral disorders (Sashindranath and Nandurkar, 2021) and aging (Franceschi et al., 2018). Thus, it has become clear that the vascular endothelium should be more widely appreciated as a systemically distributed organ with vital regulatory roles and instructive gatekeeper functions crucial for the maintenance of organ and system homeostasis (Augustin and Koh, 2024; Aug et al., 2017). A disruption of endothelial integrity and thus of endothelial barrier function represents the most striking pathophysiological change in acute lung injury (ALI), a life-threatening inflammatory lung disease usually caused by local or systemic inflammation and, in its most severe form, clinically manifesting as acute respiratory distress syndrome (ARDS) (Orfanos et al., 2006; Maniatis et al., 2008). Damage to the alveolar endothelium is accompanied by impairment of the alveolar epithelium, resulting in an overall dysfunction of the alveolar-capillary membrane barriers, which allows the exudation of protein-rich fluid into the alveolar space ultimately leading to pulmonary edema (Gu et al., 2024; Zhao et al., 2017). In addition, endothelial inflammation following endothelial activation leads to increased leukocyte adhesion, platelet aggregation and coagulation activation, which in turn can lead to endothelial cell damage and cell death, as well as microthrombosis and fibrin deposition further increasing vascular permeability (endothelial dysfunction). Here, the prevailing current concepts regarding the pulmonary endothelium are presented and an attempt is made to shed more light on the concepts and interactions between endothelial activation, dysfunction and damage.

The pulmonary endothelium

The pulmonary circulation is unique among all vascular beds, because it receives all of the cardiac output while maintaining low vascular pressures (Hough et al., 2024). In combination with the formation of sufficiently thin endothelial-epithelial barriers, the blood-air barrier, this enables the main function of the lungs, the gas exchange (Mora Massad et al., 2025). Generally, three primary endothelial cell types are generally distinguished in lungs: pulmonary microvascular, pulmonary artery, and pulmonary vein endothelial cells (Przysinda et al., 2020; Aird, 2007). But the lung vascular bed is predominantly made up of microvascular endothelium, which facilitates the gas exchange between the bloodstream on the apical side and the air in the alveoli on the basal side (Amersfoort et al., 2022). And particularly pulmonary capillary endothelial cells harbor unique properties, which are the large numbers of caveolae, the expression of activated leukocyte cell adhesion molecule (ALCAM, also known as CD166) and the clotting factor (factor VIII) together with and the high expression levels of Angiotensin I–converting enzyme (ACE) (Aird, 2007) as well as the overall low permeability (compared to pulmonary arteries) (Aird, 2007; Qiao and Bhattacharya, 1985).

Among the capillary endothelium, two distinct endothelial subpopulations have been identified: aerocytes and general capillary endothelial cells, with aerocytes being rarer in the human lung than general capillary endothelial cells (Schupp et al., 2021; Sikkema et al., 2023; Travaglini et al., 2020). Aerocytes are described as expansive and intimately associated with type 1 pneumocytes. This capillary cell type exhibits a specialized gene repertoire, reflecting their roles in gas exchange and leukocyte trafficking, while the intermingled general capillary cells show the most significant changes in inflammatory signaling and stress responses in pulmonary diseases (Gillich et al., 2020). General capillary endothelial cells were shown to interact with aerocytes along the capillary axis and expressing N-cadherin, which forms heterotypic adhesions with surrounding pericytes. This capillary cell type is specialized to regulate vasomotor tone and may function as stem/progenitor cell in capillary homeostasis and repair (Gillich et al., 2020; Trimm and Red-Horse, 2023). The advent of single-cell analysis technologies has enabled further specification and identification of distinct endothelial subpopulations within the given organ and provided insights into how these cells respond to inflammatory stimuli (Zhang et al., 2022; Niethamer et al., 2020; Schupp et al., 2021). Carbonic anhydrase four-positive aerocytes in the alveolus, for example, display an atypically large “Swiss cheese”-like morphology, spreading over the thin alveolar type 1 epithelium. These cells receive reparative signals from alveolar type I cells, particularly in damaged alveoli during ALI (Niethamer et al., 2020). Single-cell RNA sequencing of lung endothelial cells, obtained after (lipopolysaccharide-induced) inflammatory lung injury, identified two major subpopulations within the lung microvascular endothelium. One subpopulation was characterized by enriched expression of immune response genes, such as MHC genes (designated as immune endothelial cells), and the other by increased expression of vascular development genes, such as Sox17, designated as developmental endothelial cells. The former exhibited a strong propensity for inflammatory signaling, while the latter showed a greater tendency for endothelial regeneration (Zhang et al., 2022). Both endothelial cell types appeared to align with the previously identified aerocyte and general capillary cell phenotypes. Angiocrine signals derived from the endothelium influence the fate of other lung progenitor cells, suggesting that pulmonary capillary endothelial cells instruct neoalveologenesis to restore gas exchange function in regenerating lungs, at least to some extent (Rafii et al., 2016). Consequently, the high regenerative potential of the lung microvasculature facilitates the efficient replacement of damaged or lost endothelial cells, contributing to the maintenance of (though impaired) vascular homeostasis following exposure to endothelial toxins or other environmental stresses (Taha et al., 2017). Furthermore, blood vessels harbor niches of endothelial progenitor and stem cells, which play essential roles in vascular repair and regeneration (Ergun et al., 2011; Klein et al., 2010). Particularly in the lungs, highly proliferative resident microvascular endothelial progenitor cells, capable of reconstituting the entire proliferative hierarchy of pulmonary microvascular endothelial cells, have been identified (Alvarez et al., 2008). However, the functions of individual endothelial cells and the full extent of heterogeneity among all lung endothelial cells remain incompletely understood despite the discovery of new endothelial cell types. In a more systematic approach, human lung scRNA-seq data were analyzed, and endothelial cell

populations were characterized through iterative clustering and subsequent differential expression analysis (Schupp et al., 2021). This study identified two previously indistinguishable endothelial populations: pulmonary venous endothelial cells localized in the lung parenchyma and systemic venous endothelial cells found in the airways and visceral pleura (Schupp et al., 2021).

In summary, pulmonary endothelial cells, due to their strategic location at the interface between the bloodstream and lung tissue, play a key role not only in optimizing gas exchange and controlling barrier integrity and function but also in regulating the pulmonary vascular tone. Inhaled air exposes the lungs—the first point of contact—to various pathogens and pollutants. The pulmonary endothelium functions as an active and dynamic receptor-effector tissue, responding to various chemical, physical, and mechanical stimuli by secreting the appropriate substances to maintain vasomotor balance and vascular tissue homeostasis. As a vital part of the respiratory system, changes in the pulmonary endothelium play a central role in the pathogenesis of both acute and chronic lung diseases, a role emphasized by the term "orchestra conductor in respiratory diseases" (Huertas et al., 2018). Lung inflammation and its consequences, such as ALI and ARDS, present particular challenges in pulmonary and intensive care medicine. Although most ALI cases lack definitive identification of causative pathogens, respiratory viruses, common Gram-negative or Gram-positive bacteria, and mycobacteria are known to cause acute respiratory infections (Long et al., 2022; Matthay et al., 2019). The central processes involve endothelial cell activation, endothelial dysfunction, and the potential loss of endothelial cells, which, in turn, exacerbate the impairment of the structural integrity of lung endothelial barriers.

Endothelial quiescence in normal lung homeostasis

Endothelial quiescence, and thus proper endothelial barrier function, is maintained through restricted permeability of the interendothelial connections formed by the adhesive properties of proteins that constitute tight and adherens junctions. In tight junctions, the extracellular domains of occludins, claudins, and junctional adhesion molecules create close and very tight endothelial cell–cell adhesions. Organotypic and vessel type-specific variations in claudin-5 expression, for example, contribute to the maintenance of varying degrees of barrier function in continuous vascular beds (Richards et al., 2022). Adherens junctions are mediated by the transmembrane protein vascular endothelium cadherin (VE-CAD), which facilitates homophilic adhesion between neighboring endothelial cells. The intracellular domains of these connecting proteins provide junctional stability through their interaction with the actin cytoskeleton *via* α-, β-, and p120-catenin or zona occludens-1/2/3 proteins (Van et al., 2008). P120, a multidomain intracellular protein, which mediates various cellular functions, including stabilization of cell-cell transmembrane cadherin complexes, contributes to endothelial permeability changes through its association with Rho GTPase activating protein (p190RhoGAP) and Rac1, whereby Rac1 activation by p190RhoGAP results in a reduction of RhoA activity to counteract increased permeability (Tian et al., 2013). Junctional barriers are generally dynamic structures with varying baseline differences in the organization of endothelial cell–cell junction components and protein expression, depending on the vascular bed (Brandon et al., 2024). An interendothelial or paracellular crossing of the endothelium occurs through small intercellular spaces between adjacent cells, allowing restricted passage of macromolecules larger than 3 nm in diameter through interendothelial junctions, while permitting convective and diffusive transport of smaller molecules under 3 nm in diameter (Van et al., 2008; Simionescu et al., 1978).

Immune cell recruitment requires endothelial activation

Inflammatory processes depend on the ability of leukocytes to enter tissues from the bloodstream; this transendothelial migration of leukocytes, also known as leukodiapedesis, is essential for the immune response. An increased expression of immune-relevant adhesion molecules serves as a guide for leukocytes to the appropriate exit sites on the endothelium. This process is regulated by a coordinated action between endothelial cells and leukocytes, with endothelial cells activating leukocytes and guiding them to extravasation sites, which, in turn, instruct endothelial cells to create a path for transmigration (Vestweber, 2015). Lectin-like adhesion molecules, such as selectins, initially mediate the docking of leukocytes on the endothelial surface. Leukocytes slow down, allowing firm adhesion mediated by integrins and immunoglobulin-like adhesion molecules. This step initiates the regulated transmigration of the recruited cells, while simultaneously maintaining the integrity of the endothelial layer. Diapedesis of leukocytes mainly occurs intercellularly through the regulated temporary opening of interendothelial cell junctions; however, in certain cases, cells can also migrate transcellularly through individual endothelial cells. Prior to leukocyte transmigration, endothelial cells can extend membrane structures on their apical surface, forming clusters of endothelial adhesion receptors at exit sites, which are described as intracellular adhesion molecule I (ICAM-1)- and vascular cell adhesion molecule I (VCAM-1)-enriched "transmigratory cups" (Vestweber, 2015; Carman and Springer, 2004). The diapedesis process involves multiple functions of both leukocytes and endothelial cells, particularly the loosening of interendothelial cell contacts while preventing plasma leakage, active leukocyte migration through the junctional cleft, and sealing of the junction after diapedesis (Vestweber, 2015). These processes are not completely resolved in detail. The movement of leukocytes through the opened junctions between endothelial cells depends on adhesion molecules ICAM-1 and VCAM-1, which trigger tyrosine phosphorylation in VE-cadherin and/or component enrichment in platelet endothelial cell adhesion molecule 1 (PECAM-1), the diapedesis-mediating receptor CD99, and junctional adhesion molecules (JAM), particularly JAM-A. This may be supported by a multivesicular compartment, termed the lateral border recycling compartment (Vestweber, 2015; Muller, 2011; Mamdouh et al., 2003; Muller, 2014). Chronic exposure to inflammation further increases the endothelial production of matrix-degrading enzymes, such as matrix metalloproteinases (MMPs) and disintegrin and metalloproteinases (e.g., ADAM10), remodeling the basement membrane and facilitating leukocyte exit from the bloodstream into

the tissue (Pruessmeyer et al., 2014). Increased intracellular calcium concentrations further contribute to increased vascular permeability following the activation of ADAM10, an extracellular sheddase that proteolytically cleaves VE-CAD, thereby reducing productive lateral endothelial contacts (Schulz et al., 2008). Increased cellular stress in general and particularly reactive oxygen species (ROS) production in endothelial cells are known to activate p38/MAPK signaling. Resulting (Rho/ROCK signaling-dependent) cytoskeletal (actin) rearrangements leading to the formation of stress fibers resulting in increased contractility caused retraction of junctional adhesion molecules (e.g., PECAM-1) away from the junction finally causing gaps between endothelial cells (Wang et al., 2024). ZO-1 and VE-cadherin can even be downregulated following p38/MAPK in the lung epithelium. Beside the dominating paracellular pathway, crossing the endothelium from the blood to the interstitium can also occur through the endothelial cell (also called transcytosis) as vesicle-mediated transport of macromolecules, e.g., plasma proteins, across the endothelial barrier in a caveolae-dependent manner (transcellular pathway) (Van et al., 2008). Increases in endothelial permeability were even linked to decreased expression levels of aquaporin 1, a protein involved in water and hydrogen peroxide balance through transcytosis, with accompanied increses in lung edema (Wang et al., 2024). Given the critical importance of continuously maintaining vascular homeostasis and integrity, hyperpermeability (vascular leakage) is associated with many pathological conditions. It can exaggerate disease severity and can lead to edema, reduced vascular perfusion, and finally impaired drug delivery (Figure 1).

Endothelial activation

Immunomodulation by endothelial cells are of particular importance to ensure lung homeostasis and dampen immune activation following lung damage thereby promoting immunity (Amersfoort et al., 2022). It has long been established that inflammatory cytokines, such as interleukins (ILs) or tumor necrosis factors (TNFs), and bacterial products, such as Gram-negative endotoxins, modulate the adhesive properties of blood leukocytes in cultured human endothelial cells (Bevilacqua et al., 1985). Pathogen-associated molecular patterns (PAMPs) released from microorganisms during infections or damage-associated molecular patterns (DAMPs) released from injured tissue cells during tissue damage stimulate endothelial cells either directly, or even indirectly through activating cells of the innate immune system (such as mast cells, macrophages and dendritic cells), which then secrete cytokines and other pro-inflammatory mediators that in turn activate nearby endothelial cells of the microvasculature (Vestweber, 2015).

Endothelial activation represents a shift from quiescence and, thus, from immune surveillance to a phenotype that facilitates host defense reactions (inflammatory responses) (Klein, 2018). Endothelial activation is defined by the expression of cell-surface adhesion molecules following stimuli that facilitate the recruitment and attachment of circulating leukocytes to blood vessels. The upregulation of adhesive endothelial surface antigens includes human leukocyte antigen (HLA) molecules, particularly leukocyte adhesion molecules (e.g., E-selectin, ICAM-1/2, and VCAM-1). Additionally, other adhesion proteins have been identified in the endothelium, including immunoglobulin-containing and proline-rich receptor-1 (IGPR-1), and PECAM-1 (also known as CD31) (Wang et al., 2016). Beyond the upregulation of adhesive properties, endothelial activation also leads to an increase in the production of immuno-attractive cytokines (e.g., IL-6, IL-8, and MCP-1), while the loss of surface anticoagulant molecules, such as thrombomodulin and heparan sulfate induces pro-thrombotic changes in endothelial cells and/or alterations in vascular tone (e.g., deregulated production and/or bioavailability of nitric oxide, NO). Therefore, five core changes have been defined for endothelial cell activation: loss of vascular integrity, expression of leukocyte adhesion molecules, a shift in phenotype from antithrombotic to pro-thrombotic, cytokine production, and upregulation of HLA (Hunt and Jurd, 1998).

Primary inflammatory cytokines typically include TNFs and ILs, released from resident memory T and sentinel cells, such as mast cells, macrophages, and dendritic cells (DCs), to attract circulating blood to sites of tissue injury and infection. The primary goal of this process is to mitigate the initial inflammatory trigger and initiate tissue repair (Wang and He, 2020; Long et al., 2022). Similarly, inflammation-related and recruited white blood cells, including mast cells, are an important source of cytokines that affect the endothelium, including vascular endothelial growth factor (VEGF), leukotrienes, prostaglandins, cathepsins, interleukins, tryptases, platelet-activating factor, TNF-alpha, and other growth factors (e.g., FGF2, TGF-beta), which are released following secretion or from dying cells (Kunder et al., 2011; Giri et al., 2024). These substances, in turn, affect the local endothelium and inflammation and may foster systemic inflammation by delivering inflammatory factors into the blood circulation. Among the proinflammatory cytokines, TNF-alpha is one of the best known pleiotropic cytokines, whereby elevated concentrations under pathophysiological conditions induce an accumulation of inflammatory cells, stimulate the production of inflammatory mediators and can cause oxidative and nitrosative stress (Mukhopadhyay et al., 2006; Malaviya et al., 2017). TNF-alpha is mainly synthesized by macrophages and monocytes and exerts its effect *via* tumor necrosis factor receptors that can subsequently activate NF-κB/MAPK-mediated inflammation and/or induce apoptosis in the course of various complex formations (Mannel and Echtenacher, 1999). TNF-alpha mediated inflammation promotion in endothelial cells includes upregulation of adhesion molecules that are important for leukocyte transport to sites of inflammation as well as stimulation the release of eicosanoids, platelet-activating factor and other vasoconstrictors (e.g., endothelin-1), which in turn promote inflammation further through vasodilation, adhesion and migration of leukocytes (Malaviya et al., 2017). At the same time, TNF-alpha increases the permeability, which is based on endothelial barrier disruption *via* destabilization of adherens and tight junctions finally leading to pulmonary edema and hypoxemia (Ng et al., 2025). In addition to these activating cytokines, PAMPs, DAMPs, ROS, reactive nitogen species (RNS) and oxidized low-density lipoproteins (LDL) are known to directly and indirectly activate endothelial cells (Long et al., 2022; Liao, 2013). Beside these numerous biochemical stimuli, biomechanical stimuli (e.g., pulsatile blood flow, fluid shear stress, hydrostatic pressure, and cyclic stretching), can foster altered gene expressions in the endothelium finally causing endothelial activation (Gimbrone et al., 1997).

Endothelial activation can also result from indirect mechanisms, such as increased cellular stress and subsequent paracrine signaling

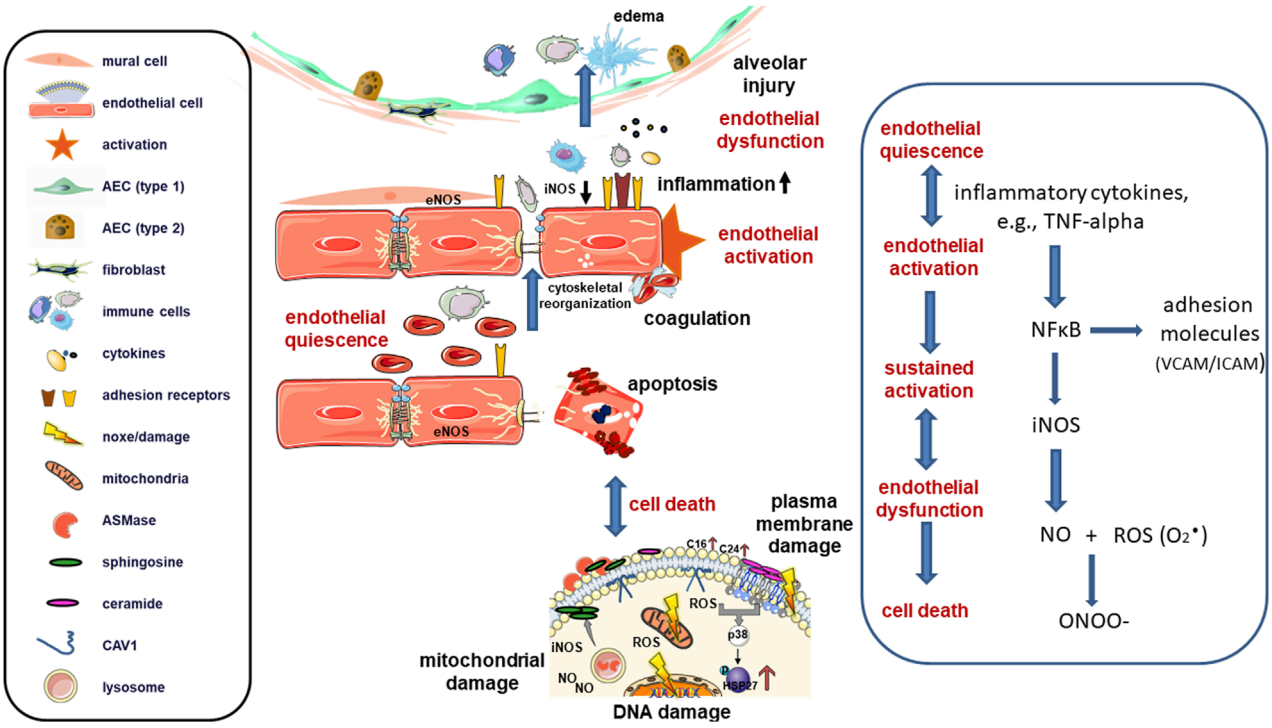

FIGURE 1
In a healthy state, mature endothelial cells (represented as red cells) are quiescent while performing a semi-permeable barrier function that regulates the supply of nutrients and oxygen to tissues and the removal of carbon dioxide and waste products. Nitric oxide (NO) produced through endothelial nitric oxide synthase (eNOS) is the primary regulator of blood flow and pressure. Upon activation, such as in response to pro-inflammatory cytokines and chemokines (e.g., TNF-alpha) or bacterial pathogens during lung infection or injury, inducible nitric oxide synthase (iNOS) becomes activated and generates high concentrations of NO through the activation of inducible nuclear factors, including NF-κB. Activated endothelial cells then upregulate cell adhesion molecules (selectins and integrins) to enhance leukocyte-endothelial cell interactions, facilitating the capture of circulating immune cells, such as neutrophils and monocytes, before extravasation into interstitial and alveolar spaces. Simultaneously, alterations in tight and adherens junctions allow excess extravasation of proteins, increasing endothelial permeability and leakage of bloodstream components. NO can reduce endothelial activation through inhibition of the transcription factor NF-κB and loss of NO increases endothelial cell activation. Endothelial activation can revert to its pre-inflammatory state, but prolonged/sustained activation can lead to irreversible endothelial dysfunction. Endothelial dysfunction in turn, leads to further increased permeability and transmigration of leukocytes through the endothelium, as well as to platelet activation and cytokine release. Together, these processes create a detrimental microenvironment, which damages the endothelial lining that can ultimately lead to endothelial cell death. Induced (sublethal) DNA damage and/or DNA repair deficiencies may also cause an activated endothelial state through activation of the genotoxic stress-induced NF-κB signaling pathway ("intrinsic" endothelial activation). In addition to endothelial DNA damage, the release of damage-associated molecular patterns (DAMPs) and the generation of reactive oxygen/nitrogen species (ROS/RNS) can further promote NF-κB activation. Superoxide (O_2•) as primary ROS/RNS species can rapidly react with NO to form peroxynitrite (ONOO–). Peroxynitrite in turn can cause multiple deleterious effects including tyrosine nitration of proteins and antioxidants inactivation finally mediating cell death and lung damage. Severe endothelial cell loss can occur as a long-term complication when the DNA-damaged and activated endothelial cells begin to proliferate. In most cases, endothelial cell death is apoptotic and involves the activation of acid sphingomyelinase (ASMase) and the subsequent formation of ceramides. In ALI, damage to both the vascular endothelium and alveolar epithelium occurs in response to systemic and local production of pro-inflammatory cytokines, resulting in the destruction of the endothelial and epithelial barriers in the lungs and the accumulation of edematous fluid and debris in the alveolar spaces.

from neighboring cells, including epithelial cells, fibroblasts, or infiltrating immune cells, or in response to genotoxic stressors. For example, genotoxic stress induced by radiation treatment in the lungs leads to senescence of the respiratory epithelium, a central process for the initiation and progression of lung diseases, particularly pneumonitis and fibrosis, both of which are strongly associated with endothelial dysfunction (Hansel et al., 2021; Hansel et al., 2020; Klein et al., 2017; Wiesemann et al., 2019). The pro-inflammatory and pro-oxidative senescence-associated secretory phenotype (SASP) of the epithelium impairs the microenvironment and affects the function of neighboring cells in a paracrine manner. Thus, the otherwise quiescent, healthy endothelium, which typically provides an efficient barrier to liquids and cell extravasation, becomes activated in response to certain epithelial-derived SASP factors (e.g., the chemokine MCP-1/CCL2). The resulting increased endothelial permeability causes leakage of bloodstream components into the lung interstitium, thereby fostering inflammation and/or metastais formation (acute reactions) (Hansel et al., 2021; Klein et al., 2017; Wiesemann et al., 2019). These effects could be efficiently reduced, thus protecting the endothelial compartment, when either induced epithelial senescence is limited or associated SASP factors are reduced (Hansel et al., 2021; Wiesemann et al., 2019). Supporting evidence arose from *in vitro* studies showing that radiation increases the permeability of the endothelial barrier by reducing the levels of proteins required for endothelial cell–cell contacts. Endothelial cell loss, contributing to long-term complications, was observed when irradiated, DNA-damaged endothelial cells began to proliferate following SASP factor

stimulation (Wiesemann et al., 2019), a well-known phenomenon where radiation-induced endothelial changes were sustained and even progressive from months to years after the initial damage (late effects) (Satyamitra et al., 2016).

In addition to extrinsic stimulation, endothelial activation can also occur "from within" the endothelial cells due to intrinsic stimuli, e.g., following genotoxic stress. Genotoxic stress induced by radiation treatment, for example, can increase the production of ROS in endothelial cells, ultimately leading to DNA, mitochondrial, and/or plasma membrane damage, which results in severe endothelial activation. The induced expression of adhesion molecules and the release of inflammatory cytokines cause a similar (indistinguishable) activated endothelial phenotype in the irradiated endothelium as is caused by circulating factors (e.g., TNF-alpha and IL-6) or shear stress, the latter specifically due to turbulent blood flow. Thus, genotoxic stress-induced endothelial damage can lead to endothelial activation, followed by endothelial dysfunction and potential endothelial cell loss, contributing to severe adverse effects on the lungs (Wiesemann et al., 2019; Sharma and Himburg, 2022). This progression, initiated by intrinsic endothelial cell damage, might not be reversible. Endothelial activation, therefore, leads to changes in endothelial surface molecules, with the resulting functional alterations being expected to be reversible upon return to quiescence once the activating factors are removed.

Sustained endothelial activation, dysfunction, and cell loss

Endothelial activation should be distinguished from endothelial dysfunction or cell damage, which may result from prolonged activation and can even progress to endothelial cell death (Klein, 2018; Butcher and Warner-Lambert/Parke-Davis Award lecture, 1990; Hunt and Jurd, 1998). Sustained endothelial activation has also been observed in lung injury, particularly during the development of pulmonary fibrosis (Fließer et al., 2024; Raslan et al., 2024). In fibrotic regions, a reduced barrier strength of the endothelium was found, as well as an increased sensitivity of the fibrotic endothelial cells to TNF-alpha or IFN-gamma, which in turn was associated with elevated immune cell adhesion and was based on an increase in the integrity markers PECAM-1/CD31, VE-CAD, thrombomodulin, and the VEGF receptor 2 (VEGFR-2/KDR) in different endothelial subpopulations (Fließer et al., 2024). It has been shown that a convergent signaling axis between the transcriptional regulator YAP and the tropomyosin-related kinase receptor B (TrkB) acts as a putative regulatory hub in persistently activated pulmonary endothelial cells (Raslan et al., 2024). A modulation of this axis, e.g., by brain-derived neurotrophic factor (BDNF), a ligand available from regenerating alveolar type I cells that act on the TrkB receptor of activated endothelial cells, could in turn promote endothelial morphogenesis (Raslan et al., 2024). Likewise, the transcriptional regulator FOXF1, a member of the forkhead box (FOX) family of transcription factors that is highly enriched in lung endothelial cells compared to endothelial cells of other organs, turned out to be a critical regulator of the transition from normal to fibrosis-associated endothelial cells (Bian et al., 2023). Decreases in endothelial FOXF1 in the course of pulmonary fibrosis was accompanied by increased endothelial permeability that contributed to aberrant inflammation and increased fibrosis. Therefore, restoring endothelial cell homeostasis and function, i.e., normalizing the pulmonary vascular bed, could represent an innovative therapeutic option for fibrotic lung diseases. An excellent review summarizing the transcriptional factors that mediate the transition from homeostasis to an activated endothelial cell state and the pathogenesis of (lung) diseases and which could serve as future therapeutic targets has just been published (Fließer et al., 2025).

Endothelial dysfunction is a pathological condition of the endothelium that encompasses a broader spectrum of phenotypes associated with heterogeneous changes in vascular permeability and inflammation, as well as vasoconstriction and thrombosis, thus leading to the loss of endothelial homeostatic functions (Alexander et al., 2021; Naderi-Meshkin and Setyaningsih, 2024). The timing of endothelial cell dysfunction turned out to be crucial, with endothelial activation and thus increased expression of adhesion molecules and increased vascular permeability being among the early events. Accordingly, markers associated with endothelial dysfunction enabling early diagnosis of the disease include acute-phase cytokines (such as IL-6, IL-1, and TNF-alpha) and adhesion molecules, particularly ICAM-1, VCAM-1, and E-selectin, which are involved in the adherence of inflammatory cells. Of note, similar pattern of cytokines and markers was also found for COVID-19 and septic patients, highlighting the importance of endothelial dysfunction here and further suggesting that the endothelium should be further evaluated as a therapeutic target for the disease (Libby, 2024; Xu et al., 2023; Hokama et al., 2022). Within sustained chronic activation and thus endothelial dysfunction (but also within acute activating conditions), the nuclear transcription factors NF-κB should be considered as key regulator of most cytokines and adhesion molecules induced in the endothelial cells (Guo et al., 2024; Hallahan et al., 1998; Poulos et al., 2016; Sonveaux et al., 2017). *Among the various cytokines,* TNF-alpha and thrombin have been shown to be the most potent activators of NF-κB signaling in endothelial cells (Soh et al., 2010; Mussbacher et al., 2019). TNF-alpha binds to its receptors (TNFR-1 and TNFR-2), mediating the plasma membrane assembly of TNFR1-RIP-TRADD-TRAF2 complexes (Guo et al., 2024). As a specific binding partner of TNFR1, epidermal growth factor receptor (EGFR) activation has been shown to mediate enhanced recruitment of TNFR-associated factor 2 (TRAF2) to the TNFR1 complex and to increase phosphorylation of receptor-interacting protein 1 (RIP1) in endothelial cells, ultimately increasing NF-κB/MAPK-mediated inflammation (Zhang et al., 2023). MMPs, for example, are targets of NF-κB signaling and promote transendothelial extravasation as well as shaping of the microenvironment (John and Tuszynski, 2001) and even impact on mitochondrial dynamics in endothelial cells (Herke et al., 2020). Protease-activated receptor 1 (PAR1) is the predominant thrombin receptor in endothelial cells (van den Eshof et al., 2017). Both ligand-receptor interactions downstream induce NF-κB signaling *via* activation of the IKKα/IKKβ/NEMO (IKKγ) complex, with synergistic effects (Tiruppathi et al., 2001). In addition to NF-κB-driven activation and resulting vascular dysfunction, the local stress-response processes in endothelial cells generally depend on the function of endothelial Weibel–Palade bodies, which are members of the family of lysosome-related organelles, harbouring proteins involved in inflammation and thrombosis such as coagulation factor

VIII, von Willebrand factor, or P-selectin (Goligorsky et al., 2009). Following signal transduction from ligands as diverse as thrombin, histamine, growth factors (e.g., VEGF), and superoxide anions, exocytosis of Weibel–Palade bodies occurs, with membrane fusion and content release (Mussbacher et al., 2019; Goligorsky et al., 2009). Osteoprotegerin (OPG), a member of the TNF receptor superfamily, is a receptor activator of nuclear factor kappa-B ligand (RANKL), and TRAIL (TNF-related apoptosis-inducing ligand) mediates endothelial cell apoptosis inhibition by inhibiting TRAILR1/2 signaling (Rochette et al., 2018). At the same time, OPG has been shown to induce vascular dysfunction by promoting reactive ROS production (Le et al., 2022). ROS, in turn, are known to directly activate redox-sensitive transcription factors such as nuclear factor (erythroid-derived 2)-like 2 (NRF2) and activator protein 1 (AP-1) (Tiruppathi et al., 2001; Goligorsky et al., 2009).

Concerning the (chronic) endothelial activation-dysfunction interconnection, it has been mechanistically revealed that endothelium-derived NO generally prevents endothelial activation prior to endothelial dysfunction through inhibition of the transcription factor NF-κB (Liao, 2013; Baeuerle, 1998). Accordingly, endothelial dysfunction has been defined as the decreased synthesis, release, and/or activity of endothelium-derived NO (Liao, 2013), following the observation that eNOS inhibitor treatment increases the number of adherent and emigrated leukocytes to mesenteric venules (Kubes et al., 1991). Endothelial cells usually utilize NO production to regulate vascular tension *via* vasoconstriction and vasodilation to meet cellular oxygen demands. Increased NO levels lead to elevated cGMP and cAMP levels, which activate cellular kinase cascades, such as protein kinase A (PKA) or protein kinase G (PKG), leading to smooth muscle relaxation. NO also increases platelet cAMP levels and serves as an important platelet aggregation inhibitor, a mechanism that is impaired during endothelial dysfunction. The shift from a non-adhesive endothelial surface, which supports unrestricted blood flow by inhibiting platelet aggregation and fibrin formation, to an adhesive surface that captures circulating blood cells following endothelial activation (Naß et al., 2021) also causes damage to the coagulation system (Qiao et al., 2024). Endothelial cells regulate the balance between coagulation and fibrinolysis through the release of tissue factor pathway inhibitor (TFPI), the activated protein C (APC) system, expression of thrombomodulin, and the synthesis and release of tissue plasminogen activator (t-PA). Activated endothelial cells and leukocytes release tissue factor (also called coagulation factor III) into the bloodstream to trigger acute intravascular thrombus formation following interaction with other coagulation factors, mainly factor VII. Furtheron, downregulation of the surface receptor thrombomodulin, an anticoagulant cofactor, increases free thrombin and activates platelets, creating a pro-thrombotic state (Giri et al., 2024). Similarly, fibrinolysis inhibitors, such as plasminogen activator inhibitor-1 (PAI-1) and thrombin-activatable fibrinolysis inhibitor (TAFI), can be detected following prolonged vascular stress in septic conditions, which can lead to abnormal blood clotting throughout the body's blood vessels, resulting in disseminated intravascular coagulation (Papageorgiou et al., 2018). Endothelial dysfunction further impacts endothelial morphology, including endothelial hypertrophy associated with the reorganization of actin filaments and detachment from the basement membrane, ultimately causing vascular constrictions, thrombosis due to hypercoagulation, platelet aggregation, and rupture of microvascular walls (Fajardo et al., 2008). The latter contributes to an increase in chronic permeability.

Beside the reduced production of NO, endothelial dysfunction has been linked to mitochondrial damage and dysfunction mediated by the (chronic) overproduction of ROS or impaired energy production (Wang et al., 2023). The imbalance of NO and ROS, generally promoting endothelial dysfunction can be roughly summarized as oxidative stress (Higashi et al., 2014; Lugrin et al., 2014). The formation of ROS is actually an inevitable consequence of living in an oxygen-rich environment. However, excessive formation of oxygen radicals under pathological conditions can cause severe damage to the pulmonary endothelium, which has been summarized in a very elegant review (Kellner et al., 2017). In addition to endothelial cells, vascular wall cells and interstitial fibroblasts, immune cells such as neutrophils, eosinophils and alveolar macrophages as well as alveolar epithelial cells are the cellular ROS and also RNS generators. On molecular level, activation of nicotinamide–adenine dinucleotide phosphate (NADPH) oxidase, xanthine oxidase, cyclooxygenase, and uncoupled endothelial nitric oxide synthase (eNOS) and mitochondrial electron transport lead to an increase in ROS production, particularly in production of the superoxide radical ($O_2^{\cdot -}$) (Higashi et al., 2014; Kellner et al., 2017). Inactivation of the antioxidant system (e.g., superoxide dismutase, glutathione peroxidase and catalase), and thus a reduction in ROS degradation could further contribute to enhanced levels. The ROS dependent expression of adhesion molecules by endothelial cells in turn fosters immune cell recruitment to the site of inflammation that themselves generate high levels of ROS thereby contributing to the oxidative stress levels (Kellner et al., 2017). The simultaneous generation of NO, a highly reactive, gaseous free radical, by eNOS, can locally interact with $O_2^{\cdot -}$ to make peroxynitrite (ONOO−), a RNS. eNOS is the main source of NO with strong vasodilatory, anti-inflammatory, and antioxidant properties in healthy (pulmonary) endothelium, which is constitutively expressed at low levels (in the picomole range) and requires increased intracellular Ca2+ for activation. Inducible NOS (iNOS), on the other hand, acts calcium-independent and is the main NOS producer in response to conditions of stress and inflammation (Lowry et al., 2013). Furthermore, iNOS was systematically localized predominantly in the lungs (Pitt and Croix, 2002). iNOS was shown to be widely distributed in the airway epithelium and vascular smooth muscles, and was especially found to be expressed by expressed by inflammatory cells such as neutrophils and macrophages (Geller and Billiar, 1998; Golden et al., 2021). Furthermore, immunoreactive iNOS was found within the lung endothelium in areas of chronic inflammation and even seems to be constitutively expressed in upper and lower airway epithelium in normal lung tissue. (Kobzik et al., 1993; Pitt and Croix, 2002; Uetani et al., 2001; Farahani et al., 2025). Generally, NOS catalyze the production of NO and L-citrulline from L-arginine and O_2, using electrons donated from NADPH, a process termed coupled eNOS activity (Cyr et al., 2020). In the uncoupled process, electrons are passed directly to O_2, generating superoxide, which can ultimately combine with locally produced NO to generate peroxynitrite. Generated peroxynitrite then induces nitrasative stress on cells by nitrating proteins and thus, together with the promotion of oxidation of biomolecules

via secondary oxidants (e.g., nitrogen dioxide radical ($\cdot NO_2$) and hydroxyl radical ($\cdot OH$)) alters signaling pathways thereby promoting tissue damage (Beckman and Koppenol, 1996; Bartesaghi and Radi, 2017). Certain growth factor in addition, for example, TNF-alpha, were shown to induce a peroxynitrite-dependent increase in pulmonary endothelial permeability that is associated with generation of nitrated beta-actin, which alters actin-polymerization dynamics and thus ultimately barrier function (Neumann et al., 2006). Depending on production rates, endogenous antioxidant levels and exposure time, peroxynitrite can even induce both cellular apoptosis and necrosis (Szabó et al., 2007). Within that scenario, mitochondrial depolarization and loss of redox capacity have been described as (early) targets for both nitric oxide and peroxynitrite-mediated cellular effects. Herein, nitric oxide primarily inhibits cytochrome oxidase (complex IV) and potential interactis with iron sulfur proteins, whereas peroxynitrite inhibits complexes I-III finally resulting in the collapse of the mitochondrial membrane potential and the in a severe decline in energy production (Gow et al., 1998; Szabo et al., 2007; Haddad et al., 1994). In contrast, endothelial cells have been described to be equipped with fewer mitochondrial organells (Parra-Bonilla et al., 2010), which coincides with the observation that concerning the metabolsim glycolytic pathways have primacy over mitochondrial respiration (Stevens et al., 2021; Li et al., 2019). This means that pulmonary lung endothelial cells produce their energy, i.e., ATP, primarily through aerobic glycolysis, despite being exposed to higher oxygen concentrations than other cells. This metabolic strategy is thought to facilitate oxygen diffusion to neighboring cells by minimizing their own oxygen consumption and reducing the formation of ROS (Mora Massad et al., 2025; Pi et al., 2018; Leung and Shi, 2022). Although impaired glycolysis under pathological conditions may lead to the activation of alternative metabolic pathways to maintain energy balance, this would be accompanied by increased oxidative stress, which can then lead to dysfunction and ultimately the death of endothelial cells (Mora Massad et al., 2025; Pi et al., 2018; Leung and Shi, 2022). In addition, lung microvascular endothelial cells appear to have a predominately socalled fission phenotype of the mitochondria, which make emdothelial cells more sensitive to metabolic disturbances under diseased conditions (Pokharel et al., 2024).

Severe endothelial cell stress, caused by vascular dysfunction or direct endothelial cell damage, particularly in response to genotoxic stress, promotes endothelial cell death. Induced (sublethal) DNA damage and/or DNA repair deficiencies may contribute to the activated endothelial cell state through the activation of the genotoxic stress-induced NF-κB signaling machinery (Hellweg, 2015; Liu et al., 2017). Intrinsic endothelial activation following oxidative stress, namely, the activation of the endothelium to a pro-inflammatory state in the absence of typical endogenous factors or pathogens, is known as "sterile inflammation" (Baselet et al., 2019). Altered metabolic products of dying or stressed (neighboring) cells can also serve as danger signals to activate innate immune cells. When released DAMPs bind to endothelial cells, they subsequently upregulate pro-inflammatory signaling pathways, leading to NF-κB, MAPK, and interferon regulatory factor 3 (IRF3) signaling (Liu et al., 2017; Zindel et al., 2020). Severe endothelial cell loss is hypothesized to occur as a long-term complication, as irradiated, DNA-damaged, and further activated endothelial cells start to proliferate, which subsequently leads to apoptosis (Klein et al., 2017; Wiesemann et al., 2019). Endothelial apoptotic cell death following severe endothelial stress can be mediated by either p53 or the p53-independent sphingomyelin ceramide pathway (Chopra et al., 2022). The activation of p53 *via* phosphorylation (e.g., following DNA damage induction) triggers endothelial cell cycle arrest. Insufficient DNA damage repair initiates apoptotic cell death *via* the intrinsic cytochrome c-mediated mitochondrial pathway, the extrinsic TNF death receptor pathway, or the activation of the sphingomyelin ceramide pathway (Venkatesulu et al., 2018). Endothelial cell death has been closely linked to acid sphingomyelinase (ASMase)-induced ceramide production, which occurs through the proteolytic cleavage of sphingomyelin present in the outer leaflet of the plasma membrane. The resulting plasma membrane alterations and generated lipid rafts cause clustering of receptors, including death receptors (Hernández-Corbacho et al., 2015; Pilátová et al., 2023). Mechanistically, induced ASMase activity and subsequent ceramide generation foster the formation of large lipid platforms, ultimately altering p38 mitogen-activated protein kinase (MAPK)/heat-shock protein 27 (HSP27)/AKT (protein kinase B, PKB) signaling to enhance apoptotic processes (Wiesemann et al., 2019).

Conclusion

As part of normal tissue homeostasis, the initiation of endothelial activation directs immune cells to sites of tissue injury, mediating protective effects of endogenous anti-inflammatory systems. The main feature of the activation and subsequent dysfunction of the pulmonary endothelium is increased permeability, which leads to the development of a pro-inflammatory phenotype characterized by increased expression of adhesion molecules to recruit inflammatory cells, by activation of pro-inflammatory transcription factors, and by release of inflammatory mediators. These changes can result in vascular leakage and edema formation. Additionally, increased oxidative stress, an altered balance between vasoconstriction and vasodilation, and a thrombotic phenotype have been implicated in the loss of endothelial homeostatic function. Depending on the nature, extent, duration, and combination of pro-inflammatory stimuli, this physiological activation can progress to detrimental pathological activation, resulting in endothelial dysfunction. Further progression to the death of pulmonary endothelial cells, along with dysfunction or even death of alveolar epithelial cells, can lead to the disruption of the alveolar-capillary barrier, a process that characterizes ALI and its clinical manifestation, ARDS. Although significant progress has been made in understanding pulmonary endothelial dysfunction, the triggers, mechanisms, and consequences of a dysfunctional endothelium in acute and chronic lung diseases are still not fully understood. A better understanding of these key aspects will help identify new disease biomarkers and/or therapeutic targets to maintain homeostasis in response to injury and disease.

Author contributions

DK: Conceptualization, Formal Analysis, Funding acquisition, Investigation, Supervision, Visualization, Writing – original draft, Writing – review and editing.

Funding

The author(s) declare that financial support was received for the research and/or publication of this article. This work was supported by the Federal Ministry of Education and Research (BMBF) (LuOrgNTT: 16LW0293 to DK). We acknowledge the support from the Open Access Publication Fund of the University of Duisburg-Essen.

Conflict of interest

The author declares that this research was conducted in the absence of any commercial or financial relationships that could be construed as potential conflicts of interest.

Generative AI statement

The author(s) declare that no Generative AI was used in the creation of this manuscript.

Publisher's note

References

Aird, W. C. (2007). Phenotypic heterogeneity of the endothelium: II. Representative vascular beds. *Circulation Res.* 100, 174–190. doi:10.1161/01.RES.0000255690.03436.ae

Alexander, Y., Osto, E., Schmidt-Trucksäss, A., Shechter, M., Trifunovic, D., Duncker, D. J., et al. (2021). Endothelial function in cardiovascular medicine: a consensus paper of the European Society of Cardiology Working Groups on Atherosclerosis and Vascular Biology, Aorta and Peripheral Vascular Diseases, Coronary Pathophysiology and Microcirculation, and Thrombosis. *Cardiovasc Res.* 117, 29–42. doi:10.1093/cvr/cvaa085

Alvarez, D. F., Huang, L., King, J. A., ElZarrad, M. K., Yoder, M. C., and Stevens, T. (2008). Lung microvascular endothelium is enriched with progenitor cells that exhibit vasculogenic capacity. *Am. J. Physiol. Lung Cell Mol. Physiol.* 294, L419–L430. doi:10.1152/ajplung.00314.2007

Amersfoort, J., Eelen, G., and Carmeliet, P. (2022). Immunomodulation by endothelial cells — partnering up with the immune system? *Nat. Rev. Immunol.* 22, 576–588. doi:10.1038/s41577-022-00694-4

Augustin, H. G., and Koh, G. Y. (2017). Organotypic vasculature: from descriptive heterogeneity to functional pathophysiology. *Science* 357, eaal2379. doi:10.1126/science.aal2379

Augustin, H. G., and Koh, G. Y. (2024). A systems view of the vascular endothelium in health and disease. *Cell* 187, 4833–4858. doi:10.1016/j.cell.2024.07.012

Baeuerle, P. A. (1998). IkappaB-NF-kappaB structures: at the interface of inflammation control. *Cell* 95, 729–731. doi:10.1016/s0092-8674(00)81694-3

Bartesaghi, S., and Radi, R. (2017). Fundamentals on the biochemistry of peroxynitrite and protein tyrosine nitration. *Redox Biol.* 14, 618–625. doi:10.1016/j.redox.2017.09.009

Baselet, B., Sonveaux, P., Baatout, S., and Aerts, A. (2019). Pathological effects of ionizing radiation: endothelial activation and dysfunction. *Cell Mol. Life Sci.* 76, 699–728. doi:10.1007/s00018-018-2956-z

Beckman, J. S., and Koppenol, W. H. (1996). Nitric oxide, superoxide, and peroxynitrite: the good, the bad, and ugly. *Am. J. Physiol.* 271, C1424–C1437. doi:10.1152/ajpcell.1996.271.5.C1424

Bevilacqua, M. P., Pober, J. S., Wheeler, M. E., Cotran, R. S., and Gimbrone, M. A., Jr. (1985). Interleukin 1 acts on cultured human vascular endothelium to increase the adhesion of polymorphonuclear leukocytes, monocytes, and related leukocyte cell lines. *J. Clin. Invest.* 76, 2003–2011. doi:10.1172/JCI112200

Bian, F., Lan, Y.-W., Zhao, S., Deng, Z., Shukla, S., Acharya, A., et al. (2023). Lung endothelial cells regulate pulmonary fibrosis through FOXF1/R-Ras signaling. *Nat. Commun.* 14, 2560. doi:10.1038/s41467-023-38177-2

Brandon, K. D., Frank, W. E., and Stroka, K. M. (2024). Junctions at the crossroads: the impact of mechanical cues on endothelial cell-cell junction conformations and vascular permeability. *Am. J. Physiol. Cell Physiol.* 327, C1073–c1086. doi:10.1152/ajpcell.00605.2023

Butcher, E. C., and Warner-Lambert/Parke-Davis Award lecture (1990). Cellular and molecular mechanisms that direct leukocyte traffic. *Am. J. Pathol.* 136, 3–11.

Carman, C. V., and Springer, T. A. (2004). A transmigratory cup in leukocyte diapedesis both through individual vascular endothelial cells and between them. *J. Cell Biol.* 167, 377–388. doi:10.1083/jcb.200404129

Chopra, S., Shankavaram, U., Bylicky, M., Dalo, J., Scott, K., Aryankalayil, M. J., et al. (2022). Profiling mRNA, miRNA and lncRNA expression changes in endothelial cells in response to increasing doses of ionizing radiation. *Sci. Rep.* 12, 19941. doi:10.1038/s41598-022-24051-6

Cyr, A. R., Huckaby, L. V., Shiva, S. S., and Zuckerbraun, B. S. (2020). Nitric oxide and endothelial dysfunction. *Crit. Care Clin.* 36, 307–321. doi:10.1016/j.ccc.2019.12.009

De Palma, M., and Hanahan, D. (2024). Milestones in tumor vascularization and its therapeutic targeting. *Nat. Cancer* 5, 827–843. doi:10.1038/s43018-024-00780-7

Ergun, S., Tilki, D., and Klein, D. (2011). Vascular wall as a reservoir for different types of stem and progenitor cells. *Antioxid. Redox Signal* 15, 981–995. doi:10.1089/ars.2010.3507

Fajardo, L. F. L. G. (2008). "Ionizing radiation and the endothelium," in *Late effects of cancer treatment on normal tissues*. Editors P. Rubin, L. S. Constine, L. B. Marks, and P. Okunieff (Berlin, Heidelberg: Springer Berlin Heidelberg), 19–22.

Farahani, A., Farahani, A., Kashfi, K., and Ghasemi, A. (2025). Inducible nitric oxide synthase (iNOS): more than an inducible enzyme? Rethinking the classification of NOS isoforms. *Pharmacol. Res.* 216, 107781. doi:10.1016/j.phrs.2025.107781

Fließer, E., Jandl, K., Chen, S.-H., Wang, M.-T., Schupp, J. C., Kuebler, W. M., et al. (2025). Transcriptional signatures of endothelial cells shape immune responses in cardiopulmonary health and disease. *JCI Insight* 10, e191059. doi:10.1172/jci.insight.191059

Fließer, E., Jandl, K., Lins, T., Birnhuber, A., Valzano, F., Kolb, D., et al. (2024). Lung fibrosis is linked to increased endothelial cell activation and dysfunctional vascular barrier integrity. *Am. J. Respir. Cell Mol. Biol.* 71, 318–331. doi:10.1165/rcmb.2024-0046OC

Franceschi, C., Garagnani, P., Parini, P., Giuliani, C., and Santoro, A. (2018). Inflammaging: a new immune–metabolic viewpoint for age-related diseases. *Nat. Rev. Endocrinol.* 14, 576–590. doi:10.1038/s41574-018-0059-4

Gallo, G., Volpe, M., and Savoia, C. (2021). Endothelial dysfunction in hypertension: current concepts and clinical implications. *Front. Med. (Lausanne)* 8, 798958. doi:10.3389/fmed.2021.798958

Geller, D. A., and Billiar, T. R. (1998). Molecular biology of nitric oxide synthases. *Cancer Metastasis Rev.* 17, 7–23. doi:10.1023/a:1005940202801

Gillich, A., Zhang, F., Farmer, C. G., Travaglini, K. J., Tan, S. Y., Gu, M., et al. (2020). Capillary cell-type specialization in the alveolus. *Nature* 586, 785–789. doi:10.1038/s41586-020-2822-7

Gimbrone, M. A., Jr., Nagel, T., and Topper, J. N. (1997). Biomechanical activation: an emerging paradigm in endothelial adhesion biology. *J. Clin. Invest.* 99, 1809–1813. doi:10.1172/JCI119346

Giri, H., Biswas, I., and Rezaie, A. R. (2024). Thrombomodulin: a multifunctional receptor modulating the endothelial quiescence. *J. Thromb. Haemost.* 22, 905–914. doi:10.1016/j.jtha.2024.01.006

Golden, T. N., Venosa, A., and Gow, A. J. (2021). Cell origin and iNOS function are critical to macrophage activation following acute lung injury. *Front. Pharmacol.* 12, 761496. doi:10.3389/fphar.2021.761496

Goligorsky, M. S., Patschan, D., and Kuo, M.-C. (2009). Weibel–Palade bodies—sentinels of acute stress. *Nat. Rev. Nephrol.* 5, 423–426. doi:10.1038/nrneph.2009.87

Gow, A. J., Thom, S. R., and Ischiropoulos, H. (1998). Nitric oxide and peroxynitrite-mediated pulmonary cell death. *Am. J. Physiology-Lung Cell. Mol. Physiology* 274, L112–L118. doi:10.1152/ajplung.1998.274.1.L112

Gu, W., Zeng, Q., Wang, X., Jasem, H., and Ma, L. (2024). Acute lung injury and the NLRP3 inflammasome. *J. Inflamm. Res.* 17, 3801–3813. doi:10.2147/jir.s464838

Guo, Q., Jin, Y., Chen, X., Ye, X., Shen, X., Lin, M., et al. (2024). NF-κB in biology and targeted therapy: new insights and translational implications. *Signal Transduct. Target. Ther.* 9, 53. doi:10.1038/s41392-024-01757-9

Haddad, I. Y., Pataki, G., Hu, P., Galliani, C., Beckman, J. S., and Matalon, S. (1994). Quantitation of nitrotyrosine levels in lung sections of patients and animals with acute lung injury. *J. Clin. Invest.* 94, 2407–2413. doi:10.1172/JCI117607

Hallahan, D. E., Virudachalam, S., and Kuchibhotla, J. (1998). Nuclear factor kappaB dominant negative genetic constructs inhibit X-ray induction of cell adhesion molecules in the vascular endothelium. *Cancer Res.* 58, 5484–5488.

Hansel, C., Barr, S., Schemann, A. V., Lauber, K., Hess, J., Unger, K., et al. (2021). Metformin protects against radiation-induced acute effects by limiting senescence of bronchial-epithelial cells. *Int. J. Mol. Sci.* 22, 7064. doi:10.3390/ijms22137064

Hansel, C., Jendrossek, V., and Klein, D. (2020). Cellular senescence in the lung: the central role of senescent epithelial cells. *Int. J. Mol. Sci.* 21, 3279. doi:10.3390/ijms21093279

Hellweg, C. E. (2015). The nuclear factor κB pathway: a link to the immune system in the radiation response. *Cancer Lett.* 368, 275–289. doi:10.1016/j.canlet.2015.02.019

Herkenne, S., Ek, O., Zamberlan, M., Pellattiero, A., Chergova, M., Chivite, I., et al. (2020). Developmental and tumor angiogenesis requires the mitochondria-shaping protein Opa1. *Cell Metab.* 31, 987–1003. doi:10.1016/j.cmet.2020.04.007

Hernández-Corbacho, M. J., Canals, D., Adada, M. M., Liu, M., Senkal, C. E., Yi, J. K., et al. (2015). Tumor necrosis factor-α (TNFα)-induced ceramide generation *via* ceramide synthases regulates loss of focal adhesion kinase (FAK) and programmed cell death. *J. Biol. Chem.* 290, 25356–25373. doi:10.1074/jbc.M115.658658

Higashi, Y., Maruhashi, T., Noma, K., and Kihara, Y. (2014). Oxidative stress and endothelial dysfunction: clinical evidence and therapeutic implications. *Trends Cardiovasc. Med.* 24, 165–169. doi:10.1016/j.tcm.2013.12.001

Hokama, L. T., Veiga, A. D. M., Menezes, M. C. S., Sardinha Pinto, A. A., de Lima, T. M., Ariga, S. K. K., et al. (2022). Endothelial injury in COVID-19 and septic patients. *Microvasc. Res.* 140, 104303. doi:10.1016/j.mvr.2021.104303

Hough, R. F., Alvira, C. M., Bastarache, J. A., Erzurum, S. C., Kuebler, W. M., Schmidt, E. P., et al. (2024). Studying the pulmonary endothelium in health and disease: an official American Thoracic Society Workshop Report. *Am. J. Respir. Cell Mol. Biol.* 71, 388–406. doi:10.1165/rcmb.2024-0330ST

Huertas, A., Guignabert, C., Barberà, J. A., Bärtsch, P., Bhattacharya, J., Bhattacharya, S., et al. (2018). Pulmonary vascular endothelium: the orchestra conductor in respiratory diseases: highlights from basic research to therapy. *Eur. Respir. J.* 51, 1700745. doi:10.1183/13993003.00745-2017

Hunt, B. J., and Jurd, K. M. (1998). Endothelial cell activation. A central pathophysiological process. *Bmj* 316, 1328–1329. doi:10.1136/bmj.316.7141.1328

John, A., and Tuszynski, G. (2001). The role of matrix metalloproteinases in tumor angiogenesis and tumor metastasis. *Pathology Oncol. Res.* 7, 14–23. doi:10.1007/BF03032599

Kellner, M., Noonepalle, S., Lu, Q., Srivastava, A., Zemskov, E., and Black, S. M. (2017). "ROS signaling in the pathogenesis of acute lung injury (ALI) and acute respiratory distress syndrome (ARDS)," in *Pulmonary vasculature redox signaling in health and disease*. Editor Y.-X. Wang (Cham: Springer International Publishing), 105–137.

Klein, D. (2018). The tumor vascular endothelium as decision maker in cancer therapy. *Front. Oncol.* 8, 367. doi:10.3389/fonc.2018.00367

Klein, D., Hohn, H. P., Kleff, V., Tilki, D., and Ergün, S. (2010). Vascular wall-resident stem cells. *Histol. Histopathol.* 25, 681–689. doi:10.14670/HH-25.681

Klein, D., Steens, J., Wiesemann, A., Schulz, F., Kaschani, F., Rock, K., et al. (2017). Mesenchymal stem cell therapy protects lungs from radiation-induced endothelial cell loss by restoring superoxide dismutase 1 expression. *Antioxid. Redox Signal* 26, 563–582. doi:10.1089/ars.2016.6748

Kobzik, L., Bredt, D. S., Lowenstein, C. J., Drazen, J., Gaston, B., Sugarbaker, D., et al. (1993). Nitric oxide synthase in human and rat lung: immunocytochemical and histochemical localization. *Am. J. Respir. Cell Mol. Biol.* 9, 371–377. doi:10.1165/ajrcmb/9.4.371

Kubes, P., Suzuki, M., and Granger, D. N. (1991). Nitric oxide: an endogenous modulator of leukocyte adhesion. *Proc. Natl. Acad. Sci. U. S. A.* 88, 4651–4655. doi:10.1073/pnas.88.11.4651

Kunder, C. A., St John, A. L., and Abraham, S. N. (2011). Mast cell modulation of the vascular and lymphatic endothelium. *Blood* 118, 5383–5393. doi:10.1182/blood-2011-07-358432

Le, N. T., Olmsted-Davis, E. A., and Abe, J. I. (2022). Paradoxical effects of osteoprotegerin on vascular function: inhibiting inflammation while promoting oxidative stress? *Clin. Sci. (Lond)* 136, 379–382. doi:10.1042/CS20211096

Leung, S. W. S., and Shi, Y. (2022). The glycolytic process in endothelial cells and its implications. *Acta Pharmacol. Sin.* 43, 251–259. doi:10.1038/s41401-021-00647-y

Li, X., Sun, X., and Carmeliet, P. (2019). Hallmarks of endothelial cell metabolism in health and disease. *Cell Metab.* 30, 414–433. doi:10.1016/j.cmet.2019.08.011

Liao, J. K. (2013). Linking endothelial dysfunction with endothelial cell activation. *J. Clin. Invest.* 123, 540–541. doi:10.1172/JCI66843

Libby, P. (2024). Endothelial inflammation in COVID-19. *Science* 386, 972–973. doi:10.1126/science.add2962

Liu, T., Zhang, L., Joo, D., and Sun, S.-C. (2017). NF-κB signaling in inflammation. *Signal Transduct. Target. Ther.* 2, 17023. doi:10.1038/sigtrans.2017.23

Long, M. E., Mallampalli, R. K., and Horowitz, J. C. (2022). Pathogenesis of pneumonia and acute lung injury. *Clin. Sci. (Lond)* 136, 747–769. doi:10.1042/CS20210879

Lowry, J. L., Brovkovych, V., Zhang, Y., and Skidgel, R. A. (2013). Endothelial nitric-oxide synthase activation generates an inducible nitric-oxide synthase-like output of nitric oxide in inflamed endothelium. *J. Biol. Chem.* 288, 4174–4193. doi:10.1074/jbc.M112.436022

Lugrin, J., Rosenblatt-Velin, N., Parapanov, R., and Liaudet, L. (2014). The role of oxidative stress during inflammatory processes. *Biol. Chem.* 395, 203–230. doi:10.1515/hsz-2013-0241

Malaviya, R., Laskin, J. D., and Laskin, D. L. (2017). Anti-TNFα therapy in inflammatory lung diseases. *Pharmacol. Ther.* 180, 90–98. doi:10.1016/j.pharmthera.2017.06.008

Mamdouh, Z., Chen, X., Pierini, L. M., Maxfield, F. R., and Muller, W. A. (2003). Targeted recycling of PECAM from endothelial surface-connected compartments during diapedesis. *Nature* 421, 748–753. doi:10.1038/nature01300

Maniatis, N. A., Kotanidou, A., Catravas, J. D., and Orfanos, S. E. (2008). Endothelial pathomechanisms in acute lung injury. *Vasc. Pharmacol.* 49, 119–133. doi:10.1016/j.vph.2008.06.009

Mannel, D. N., and Echtenacher, B. (1999). TNF in the inflammatory response. *Chem. Immunol.* 74, 141–161. doi:10.1159/000058757

Matthay, M. A., Zemans, R. L., Zimmerman, G. A., Arabi, Y. M., Beitler, J. R., Mercat, A., et al. (2019). Acute respiratory distress syndrome. *Nat. Rev. Dis. Prim.* 5, 18. doi:10.1038/s41572-019-0069-0

Mora Massad, K., Dai, Z., Petrache, I., Ventetuolo, C. E., and Lahm, T. (2025). Lung endothelial cell heterogeneity in health and pulmonary vascular disease. *Am. J. Physiol. Lung Cell Mol. Physiol.* 328, L877–L884. doi:10.1152/ajplung.00296.2024

Mukhopadhyay, S., Hoidal, J. R., and Mukherjee, T. K. (2006). Role of TNFalpha in pulmonary pathophysiology. *Respir. Res.* 7, 125. doi:10.1186/1465-9921-7-125

Muller, W. A. (2011). Mechanisms of leukocyte transendothelial migration. *Annu. Rev. Pathology Mech. Dis.* 6, 323–344. doi:10.1146/annurev-pathol-011110-130224

Muller, W. A. (2014). How endothelial cells regulate transmigration of leukocytes in the inflammatory response. *Am. J. Pathol.* 184, 886–896. doi:10.1016/j.ajpath.2013.12.033

Mussbacher, M., Salzmann, M., Brostjan, C., Hoesel, B., Schoergenhofer, C., Datler, H., et al. (2019). Cell type-specific roles of NF-κB linking inflammation and thrombosis. *Front. Immunol.* 10, 85. doi:10.3389/fimmu.2019.00085

Naderi-Meshkin, H., and Setyaningsih, W. A. W. (2024). Endothelial cell dysfunction: onset, progression, and consequences. *Front. Biosci. (Landmark Ed)* 29, 223. doi:10.31083/j.fbl2906223

Naß, J., Terglane, J., and Gerke, V. (2021). Weibel Palade bodies: unique secretory organelles of endothelial cells that control blood vessel homeostasis. *Front. Cell Dev. Biol.* 9, 813995. doi:10.3389/fcell.2021.813995

Neumann, P., Gertzberg, N., Vaughan, E., Weisbrot, J., Woodburn, R., Lambert, W., et al. (2006). Peroxynitrite mediates TNF-α-induced endothelial barrier dysfunction and nitration of actin. *Am. J. Physiology-Lung Cell. Mol. Physiology* 290, L674–L684. doi:10.1152/ajplung.00391.2005

Ng, C. T., Fong, L. Y., Tan, J. J., and Abdullah, M. N. H. (2025). Endothelial barrier disruptive effect of IFN-Ɣ and TNF-α: synergism of pro-inflammatory cytokines. *Cytokine* 190, 156922. doi:10.1016/j.cyto.2025.156922

Niethamer, T. K., Stabler, C. T., Leach, J. P., Zepp, J. A., Morley, M. P., Babu, A., et al. (2020). Defining the role of pulmonary endothelial cell heterogeneity in the response to acute lung injury. *Elife* 9, e53072. doi:10.7554/eLife.53072

Orfanos, S. E., Mavrommati, I., Korovesi, I., and Roussos, C. (2006). "Pulmonary endothelium in acute lung injury: from basic science to the critically ill," in *Applied physiology in intensive care medicine*. Editors M. R. Pinsky, L. Brochard, and J. Mancebo (Berlin, Heidelberg: Springer Berlin Heidelberg), 171–183.

Papageorgiou, C., Jourdi, G., Adjambri, E., Walborn, A., Patel, P., Fareed, J., et al. (2018). Disseminated intravascular coagulation: an update on pathogenesis, diagnosis, and therapeutic strategies. *Clin. Appl. Thromb. Hemost.* 24, 8S–28s. doi:10.1177/1076029618806424

Parra-Bonilla, G., Alvarez, D. F., Al-Mehdi, A. B., Alexeyev, M., and Stevens, T. (2010). Critical role for lactate dehydrogenase A in aerobic glycolysis that sustains pulmonary microvascular endothelial cell proliferation. *Am. J. Physiol. Lung Cell Mol. Physiol.* 299, L513–L522. doi:10.1152/ajplung.00274.2009

Pi, X., Xie, L., and Patterson, C. (2018). Emerging roles of vascular endothelium in metabolic homeostasis. *Circ. Res.* 123, 477–494. doi:10.1161/CIRCRESAHA.118.313237

Pilátová, M. B., Solárová, Z., Mezencev, R., and Solár, P. (2023). Ceramides and their roles in programmed cell death. *Adv. Med. Sci.* 68, 417–425. doi:10.1016/j.advms.2023.10.004

Pitt, B. R., and Croix, C. M.St. (2002). Complex regulation of iNOS in lung. *Am. J. Respir. Cell Mol. Biol.* 26, 6–9. doi:10.1165/ajrcmb.26.1.f224

Pokharel, M. D., Garcia-Flores, A., Marciano, D., Franco, M. C., Fineman, J. R., Aggarwal, S., et al. (2024). Mitochondrial network dynamics in pulmonary disease: bridging the gap between inflammation, oxidative stress, and bioenergetics. *Redox Biol.* 70, 103049. doi:10.1016/j.redox.2024.103049

Poulos, M. G., Ramalingam, P., Gutkin, M. C., Kleppe, M., Ginsberg, M., Crowley, M. J. P., et al. (2016). Endothelial-specific inhibition of NF-κB enhances functional haematopoiesis. *Nat. Commun.* 7, 13829. doi:10.1038/ncomms13829

Pruessmeyer, J., Hess, F. M., Alert, H., Groth, E., Pasqualon, T., Schwarz, N., et al. (2014). Leukocytes require ADAM10 but not ADAM17 for their migration and inflammatory recruitment into the alveolar space. *Blood* 123, 4077–4088. doi:10.1182/blood-2013-09-511543

Przysinda, A., Feng, W., and Li, G. (2020). Diversity of organism-wide and organ-specific endothelial cells. *Curr. Cardiol. Rep.* 22, 19. doi:10.1007/s11886-020-1275-9

Qiao, R. L., and Bhattacharya, J. (1985). Segmental barrier properties of the pulmonary microvascular bed. *J. Appl. Physiol.* 71, 2152–2159. doi:10.1152/jappl.1991.71.6.2152

Qiao, X., Yin, J., Zheng, Z., Li, L., and Feng, X. (2024). Endothelial cell dynamics in sepsis-induced acute lung injury and acute respiratory distress syndrome: pathogenesis and therapeutic implications. *Cell Commun. Signal* 22, 241. doi:10.1186/s12964-024-01620-y

Rafii, S., Butler, J. M., and Ding, B.-S. (2016). Angiocrine functions of organ-specific endothelial cells. *Nature* 529, 316–325. doi:10.1038/nature17040

Raslan, A. A., Pham, T. X., Lee, J., Kontodimas, K., Tilston-Lunel, A., Schmottlach, J., et al. (2024). Lung injury-induced activated endothelial cell states persist in aging-associated progressive fibrosis. *Nat. Commun.* 15, 5449. doi:10.1038/s41467-024-49545-x

Ricard, N., Bailly, S., Guignabert, C., and Simons, M. (2021). The quiescent endothelium: signalling pathways regulating organ-specific endothelial normalcy. *Nat. Rev. Cardiol.* 18, 565–580. doi:10.1038/s41569-021-00517-4

Richards, M., Nwadozi, E., Pal, S., Martinsson, P., Kaakinen, M., Gloger, M., et al. (2022). Claudin5 protects the peripheral endothelial barrier in an organ and vessel-type-specific manner. *Elife* 11. doi:10.7554/elife.78517

Rochette, L., Meloux, A., Rigal, E., Zeller, M., Cottin, Y., and Vergely, C. (2018). The role of osteoprotegerin in the crosstalk between vessels and bone: its potential utility as a marker of cardiometabolic diseases. *Pharmacol. Ther.* 182, 115–132. doi:10.1016/j.pharmthera.2017.08.015

Sashindranath, M., and Nandurkar, H. H. (2021). Endothelial dysfunction in the brain: setting the stage for stroke and other cerebrovascular complications of COVID-19. *Stroke* 52, 1895–1904. doi:10.1161/STROKEAHA.120.032711

Satyamitra, M. M., DiCarlo, A. L., and Taliaferro, L. (2016). Understanding the pathophysiology and challenges of development of medical countermeasures for radiation-induced vascular/endothelial cell injuries: report of a NIAID workshop, August 20, 2015. *Radiat. Res.* 186, 99–111. doi:10.1667/RR14436.1

Schulz, B., Pruessmeyer, J., Maretzky, T., Ludwig, A., Blobel, C. P., Saftig, P., et al. (2008). ADAM10 regulates endothelial permeability and T-cell transmigration by proteolysis of vascular endothelial cadherin. *Circulation Res.* 102, 1192–1201. doi:10.1161/CIRCRESAHA.107.169805

Schupp, J. C., Adams, T. S., Cosme, C., Jr., Raredon, M. S. B., Yuan, Y., Omote, N., et al. (2021). Integrated single-cell atlas of endothelial cells of the human lung. *Circulation* 144, 286–302. doi:10.1161/CIRCULATIONAHA.120.052318

Sharma, G. P., and Himburg, H. A. (2022). Organ-specific endothelial dysfunction following total body irradiation exposure. *Toxics* 10, 747. doi:10.3390/toxics10120747

Sikkema, L., Ramírez-Suástegui, C., Strobl, D. C., Gillett, T. E., Zappia, L., Madissoon, E., et al. (2023). An integrated cell atlas of the lung in health and disease. *Nat. Med.* 29, 1563–1577. doi:10.1038/s41591-023-02327-2

Simionescu, N., Simionescu, M., and Palade, G. E. (1978). Open junctions in the endothelium of the postcapillary venules of the diaphragm. *J. Cell Biol.* 79, 27–44. doi:10.1083/jcb.79.1.27

Soh, U. J., Dores, M. R., Chen, B., and Trejo, J. (2010). Signal transduction by protease-activated receptors. *Br. J. Pharmacol.* 160, 191–203. doi:10.1111/j.1476-5381.2010.00705.x

Sonveaux, P., Aerts, A., Baselet, B., Ramadan, R., Benotmane, A. M., and Baatout, S. (2017). "Selected endothelial responses after ionizing radiation exposure," in *Endothelial dysfunction - old concepts and new challenges*. Editor H. Lenasi (Rijeka: IntechOpen).

Stevens, R. P., Paudel, S. S., Johnson, S. C., Stevens, T., and Lee, J. Y. (2021). Endothelial metabolism in pulmonary vascular homeostasis and acute respiratory distress syndrome. *Am. J. Physiol. Lung Cell Mol. Physiol.* 321, L358–l376. doi:10.1152/ajplung.00131.2021

Szabó, C., Ischiropoulos, H., and Radi, R. (2007). Peroxynitrite: biochemistry, pathophysiology and development of therapeutics. *Nat. Rev. Drug Discov.* 6, 662–680. doi:10.1038/nrd2222

Taha, M., Cadete, V. J., and Stewart, D. J. (2017). Macro- and micro-heterogeneity of lung endothelial cells: they May not be smooth, but they got the moves. *Pulm. Circ.* 7, 755–757. doi:10.1177/2045893217743710

Tian, Y., Tian, X., Gawlak, G., Higginbotham, K., Reynolds, A., Birukova, A., et al. (2013). Interaction of p190RhoGAP with C-terminal domain of p120-catenin modulates endothelial cytoskeleton and permeability. *J. Biol. Chem.* 288, 18290–18299. doi:10.1074/jbc.M112.432757

Tiruppathi, C., Naqvi, T., Sandoval, R., Mehta, D., and Malik, A. B. (2001). Synergistic effects of tumor necrosis factor-alpha and thrombin in increasing endothelial permeability. *Am. J. Physiol. Lung Cell Mol. Physiol.* 281, L958–L968. doi:10.1152/ajplung.2001.281.4.L958

Travaglini, K. J., Nabhan, A. N., Penland, L., Sinha, R., Gillich, A., Sit, R. V., et al. (2020). A molecular cell atlas of the human lung from single-cell RNA sequencing. *Nature* 587, 619–625. doi:10.1038/s41586-020-2922-4

Trimm, E., and Red-Horse, K. (2023). Vascular endothelial cell development and diversity. *Nat. Rev. Cardiol.* 20, 197–210. doi:10.1038/s41569-022-00770-1

Uetani, K., Thomassen, M. J., and Erzurum, S. C. (2001). Nitric oxide synthase 2 through an autocrine loop *via* respiratory epithelial cell-derived mediator. *Am. J. Physiol. Lung Cell Mol. Physiol.* 280, L1179–L1188. doi:10.1152/ajplung.2001.280.6.L1179

Vandenbroucke, E., Mehta, D., Minshall, R., and Malik, A. B. (2008). Regulation of endothelial junctional permeability. *Ann. N. Y. Acad. Sci.* 1123, 134–145. doi:10.1196/annals.1420.016

van den Eshof, B. L., Hoogendijk, A. J., Simpson, P. J., van Alphen, F. P. J., Zanivan, S., Mertens, K., et al. (2017). Paradigm of biased PAR1 (Protease-Activated Receptor-1) activation and inhibition in endothelial cells dissected by phosphoproteomics. *Arteriosclerosis, Thrombosis, Vasc. Biol.* 37, 1891–1902. doi:10.1161/ATVBAHA.117.309926

van Hinsbergh, V. W. (2012). Endothelium–role in regulation of coagulation and inflammation. *Semin. Immunopathol.* 34, 93–106. doi:10.1007/s00281-011-0285-5

Venkatesulu, B. P., Mahadevan, L. S., Aliru, M. L., Yang, X., Bodd, M. H., Singh, P. K., et al. (2018). Radiation-induced endothelial vascular injury: a review of possible mechanisms. *JACC Basic Transl. Sci.* 3, 563–572. doi:10.1016/j.jacbts.2018.01.014

Vestweber, D. (2015). How leukocytes cross the vascular endothelium. *Nat. Rev. Immunol.* 15, 692–704. doi:10.1038/nri3908

Wang, J., Liu, Y., Guo, Y., Liu, C., Yang, Y., Fan, X., et al. (2024). Function and inhibition of P38 MAP kinase signaling: targeting multiple inflammation diseases. *Biochem. Pharmacol.* 220, 115973. doi:10.1016/j.bcp.2023.115973

Wang, L., Rivas, R., Wilson, A., Park, Y. M., Walls, S., Yu, T., et al. (2023). Dose-dependent effects of radiation on mitochondrial morphology and clonogenic cell survival in human microvascular endothelial cells. *Cells* 13, 39. doi:10.3390/cells13010039

Wang, X., and He, B. (2020). Endothelial dysfunction: molecular mechanisms and clinical implications. *MedComm* 5, e651. doi:10.1002/mco2.651

Wang, Y. H. W., Meyer, R. D., Bondzie, P. A., Jiang, Y., Rahimi, I., Rezazadeh, K., et al. (2016). IGPR-1 is required for endothelial cell-cell adhesion and barrier function. *J. Mol. Biol.* 428, 5019–5033. doi:10.1016/j.jmb.2016.11.003

Wiesemann, A., Ketteler, J., Slama, A., Wirsdorfer, F., Hager, T., Rock, K., et al. (2019). Inhibition of radiation-induced Ccl2 signaling protects lungs from vascular dysfunction and endothelial cell loss. *Antioxid. Redox Signal* 30, 213–231. doi:10.1089/ars.2017.7458

Xu, S., Ilyas, I., Little, P. J., Li, H., Kamato, D., Zheng, X., et al. (2021). Endothelial dysfunction in atherosclerotic cardiovascular diseases and beyond: from mechanism to pharmacotherapies. *Pharmacol. Rev.* 73, 924–967. doi:10.1124/pharmrev.120.000096

Xu, S.-w., Ilyas, I., and Weng, J.-p. (2023). Endothelial dysfunction in COVID-19: an overview of evidence, biomarkers, mechanisms and potential therapies. *Acta Pharmacol. Sin.* 44, 695–709. doi:10.1038/s41401-022-00998-0

Zhang, H., Zhang, X., Ling, C., Liu, C., Hua, S., Xiong, Z., et al. (2023). EGFR-TNFR1 pathway in endothelial cell facilitates acute lung injury by NF-κB/MAPK-mediated inflammation and RIP3-dependent necroptosis. *Int. Immunopharmacol.* 117, 109902. doi:10.1016/j.intimp.2023.109902

Zhang, L., Gao, S., White, Z., Dai, Y., Malik, A. B., and Rehman, J. (2022). Single-cell transcriptomic profiling of lung endothelial cells identifies dynamic inflammatory and regenerative subpopulations. *JCI Insight* 7, e158079. doi:10.1172/jci.insight.158079

Zhao, Y., Ridge, K., and Zhao, J. (2017). Acute lung injury, repair, and remodeling: pulmonary endothelial and epithelial biology. *Mediat. Inflamm.* 2017, 9081521. doi:10.1155/2017/9081521

Zindel, J., and Kubes, P. (2020). DAMPs, PAMPs, and LAMPs in immunity and sterile inflammation. *Annu. Rev. Pathol.* 15, 493–518. doi:10.1146/annurev-pathmechdis-012419-032847

frontiers | Frontiers in Cell and Developmental Biology

TYPE Review
PUBLISHED 09 July 2025
DOI 10.3389/fcell.2025.1569346

OPEN ACCESS

EDITED BY
Bilal Çiğ,
Ahi Evran University Medicine Faculty
Department of Physiology, Türkiye

REVIEWED BY
Seiji Yamamoto,
University of Toyama, Japan
Nirupama Ramadas,
University of North Carolina at Chapel Hill,
United States
Shamima Akhtar,
All India Institute of Medical Sciences, India

*CORRESPONDENCE
Meitang Wang,
meitangwang@smmu.edu.cn
Lulong Bo,
bartbo@smmu.edu.cn

†These authors have contributed equally to this work and share first authorship

RECEIVED 31 January 2025
ACCEPTED 16 June 2025
PUBLISHED 09 July 2025

CITATION
Wang S, Zhang X, Zhang Y, Wu N, Bo L and Wang M (2025) The pathogenesis and therapeutic strategies of heat stroke-induced endothelial injury.
Front. Cell Dev. Biol. 13:1569346.
doi: 10.3389/fcell.2025.1569346

The pathogenesis and therapeutic strategies of heat stroke-induced endothelial injury

Shaokang Wang[1†], Xiaoting Zhang[2†], Yongqi Zhang[1], Nannan Wu[1], Lulong Bo[2*] and Meitang Wang[1*]

[1]Department of Emergency, Changhai Hospital, Naval Medical University, Shanghai, China, [2]Faculty of Anesthesiology, Changhai Hospital, Naval Medical University, Shanghai, China

Heat stroke is a severe and life-threatening condition characterized by elevated core body temperature and central nervous system dysfunction, often accompanied by multi-organ damage. The incidence and mortality of heat stroke are increasing due to global warming and more frequent heatwaves. This review aims to summarize the recent progress in understanding the pathogenesis of heat stroke-induced endothelial injury and explore potential therapeutic strategies. The vascular endothelium plays a crucial role in maintaining vascular homeostasis, and its dysfunction is a key factor in the development of heat stroke complications. The pathogenesis of heat stroke-induced endothelial injury involves multiple mechanisms, including degradation of the endothelial glycocalyx, impaired vascular tone regulation, disruption of intercellular junctional proteins, and activation of regulated cell death pathways. Biomarkers such as syndecan-1, endothelin-1, and von Willebrand factor are associated with endothelial injury and can predict disease severity and outcomes. Potential interventions include early fluid resuscitation, heat acclimation, and targeted therapies to inhibit specific cell death pathways or protect the endothelial glycocalyx. Further research is needed to elucidate the detailed mechanisms and develop targeted therapeutic interventions to reduce the morbidity and mortality of heat stroke.

KEYWORDS

heat stroke, heat stress, endothelial dysfunction, vascular barrier, glycocalyx

1 Introduction

The frequency, duration, and intensity of heat waves have increased worldwide under enhanced global warming, especially over the past two decades (Perkins-Kirkpatrick and Lewis, 2020; Watts et al., 2021). The Lancet-Planet Health shows Globally, 5,083,173 deaths were associated with non-optimal temperatures per year, accounting for 9.43% of all deaths (0.91% were heat-related) (Zhao et al., 2021). Heat stroke (HS) is the most hazardous condition in a spectrum of illnesses progressing from heat exhaustion to heat stroke, clinically characterized by a core temperature of >40.5°C and abnormalities of the central nervous system, including changes in mental status, convulsions or coma and accompanied by life threatening multiple organ damage. The primary pathogenic mechanism of heat stroke involves an imbalance between heat production by and dissipation from the body caused by exposure to a hot environment and/or intense exercise. Depending on its cause and degree of susceptibility within the population,

HS may be categorized as either classic (passive) or exertional heat stroke. Although substantial progress has been achieved in the treatment of HS, the mortality of HS is still high. Between 2015 and 2017, the incidence of heat stroke in Japan during the period from June to September was 37.5 cases per 100,000 population (95% CI, 36.8–38.2), and in 2018, it was 74.4 cases per 100,000 population (95% CI, 72.7–76.1) (Ogata et al., 2021). Based on a Japanese cross-sectional survey, out of 763 patients admitted with heat illness (56.9% non-exertional heat stroke and 40.0% exertional heat stroke), the mortality rate was 4.6% (Shimazaki et al., 2020). Comprehending the etiology and pathophysiological mechanisms underlying HS is crucial for identifying prospective therapeutic targets.

The vascular endothelium, comprising endothelial cells (ECs), forms a monolayer barrier along the innermost structure of the arteries, capillaries and veins. Healthy endothelial cells are essential for important physiological functions, including barrier functions, immune response, vascular permeability, coagulation, and angiogenesis (Trimm and Red-Horse, 2023). Damage to ECs in the lungs, brain, heart and liver has been documented in primate models and patients suffered from heat stroke (Abdullah et al., 2024). Heat stress induces ECs injury through direct thermal cytotoxic effects and secondary excessive systemic inflammatory response syndrome. The injury is supported by the finding of increased serum endothelial cell damage biomarkers, such as intercellular adhesion molecular-1 (ICAM-1), soluble endothelial cell leukocyte adhesion molecule 1, endothelin, von Willebrand factor-antigen and endothelial glycocalyx component syndecan-1 (SDC-1) in the heat stroke models of experimental animals and patients (Tong et al., 2014; Umemura et al., 2018). This ECs overactivation impair vascular integrity and barrier function, leading to increased permeability, coagulopathy, and inflammation of heat stroke. The lung emerges as a particularly vulnerable target organ in instances of heat stroke. Impairment of vascular integrity precipitates severe disruptions in the process of gas exchange, which may ultimately culminate in the development of acute lung injury (ALI) and, in more severe cases, progress to acute respiratory distress syndrome (ARDS). Damage and dysfunction to ECs can precipitate injury to other vital organs, such as acute liver injury, acute kidney injury, encephalopathy, and disseminated intravascular coagulation (DIC). During hospital stays, 20% of inpatients require mechanical ventilation and 2% received renal replacement therapy (Kaewput et al., 2021). Consequently, it is of paramount importance to elucidate the specific mechanisms underlying EC dysfunction in the context of heat stroke.

In this review, we summarized the recent research progress on the potential underlying mechanisms and fundamental management principles associated with heat stroke and heat stroke-induced endothelial injury. This comprehensive analysis serves to establish a theoretical foundation and delineate future research directions in the study of heat stroke and its associated endothelial complications.

Abbreviations: HS, heat stroke; EC, endothelial cell; ICAM-1, intercellular adhesion molecular-1; SDC-1, syndecan-1; ALI, acute lung injury; ARDS, acute respiratory distress syndrome; DIC, disseminated intravascular coagulation; VCAM-1, vascular cell adhesion molecule-1; IL, interleukin; ZO-1, zonula occludens-1; vWF, von Willebrand factor; BMDMs, Bone marrow-derived mononuclear cells; DEX, dexmedetomidine; ET-1, endothelin-1; TNF-α, tumor necrosis factor-alpha; ROS, reactive oxygen species; NO, nitric oxide; NOS, nitric oxide synthase; HMGB1, high mobility group box-1 protein; HSP, heat shock protein; GCX, glycocalyx.

2 Related mechanisms of heat stroke-induced endothelial injury

The endothelial glycocalyx, cell junctions, and intracellular homeostasis are of vital importance for maintaining the structure and function of endothelial cells, as well as preventing the adhesion of inflammatory cells (Vestweber et al., 2009; Foote et al., 2022). The shedding of the glycocalyx, compromised structural-barrier integrity, and regulated cell death of endothelial cell have been observed in the heat stroke model, and all of which contribute the coagulopathy and inflammation associated with heat stroke (Figure 1) (Roberts et al., 2005; Peng et al., 2023).

2.1 Damage to the glycocalyx

The glycocalyx is an endovascular barrier structure that covers the surface of endothelial cells. The main components include sulfated proteoglycans (syndecan and glypican), glycosaminoglycans (heparan sulfate, chondroitin sulfate, hyaluronic acid, and dermatan sulfate), and plasma proteins (albumin and antithrombin). It plays important physiological roles, including maintaining barrier function, exerting antithrombotic and anti-inflammatory effects, and regulating vascular permeability. The degradation of the endothelial glycocalyx directly exposes endothelial surface adhesion molecules, including ICAM-1 and vascular cell adhesion molecule-1 (VCAM-1), thereby amplifying leukocyte-endothelial adhesion and subsequent inflammatory infiltration (Petrovich et al., 2016; Van Steen et al., 2023). Concurrently, the liberation of stored chemokines such as interleukin-8 (IL-8) and monocyte chemoattractant protein-1 (MCP-1) activates the NF-κB signaling pathway, resulting in upregulation of pro-inflammatory cytokine expression (Graham et al., 2019; Akhtar and Sharma, 2022). Glycocalyx impairment further disrupts endothelial barrier integrity through abnormal phosphorylation of tight junction proteins, particularly zonula occludens-1 (ZO-1) and occludin (Li J. et al., 2021; Cao et al., 2023).

Experimental evidence indicates that heparan sulfate degradation compromises antithrombin III binding capacity, compromising endogenous anticoagulant mechanisms disrupting endogenous anticoagulant mechanisms and promoting microthrombus formation (Chappell et al., 2014a; Nordling et al., 2015). In addition, pro-inflammatory cytokines stimulate neutrophils to release neutrophil extracellular traps (NETs), these chromatin-DNA-protein complexes entrap platelets and activate coagulation factor XII, thereby amplifying thrombogenesis through reciprocal activation of inflammatory and coagulatory cascades (McDonald et al., 2017; Zhang et al., 2022). These interconnected mechanisms collectively establish a pathological cascade that perpetuates endothelial dysfunction, systemic inflammation, and coagulopathy in heat stroke progression.

The shedding of glycocalyx is mediated by various specific enzymes, with hyaluronidase activity being significantly elevated

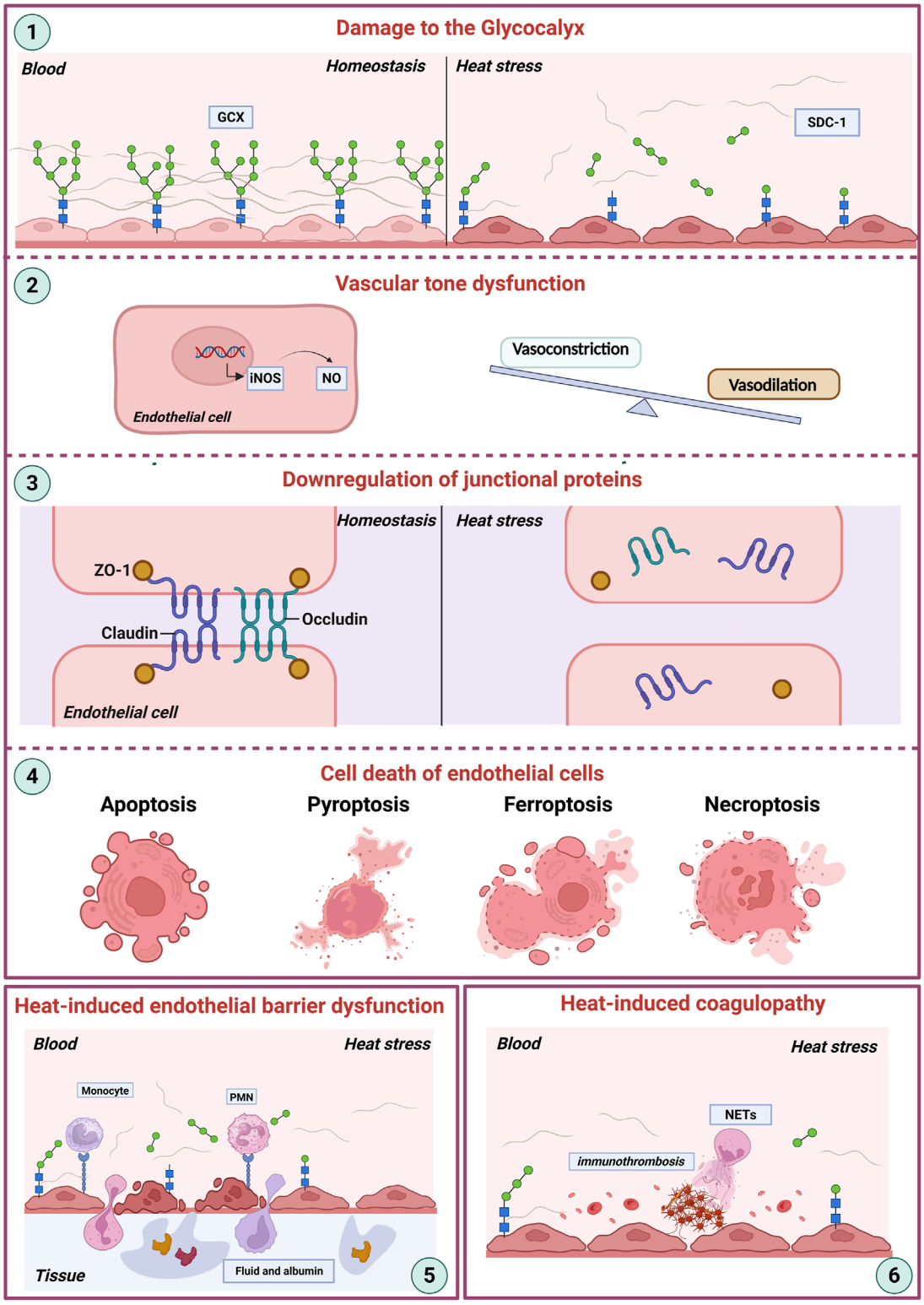

FIGURE 1
Heat stroke-induced endothelial dysfunction. This schematic illustrates the key mechanisms contributing to endothelial damage during heat stroke. (1) Damage to the Glycocalyx: Heat stress directly disrupts the endothelial glycocalyx (GEX), a critical surface layer maintaining vascular homeostasis between the blood and the vessel wall. (2) Vascular Tone Dysfunction: Damaged endothelial cells show dysregulated nitric oxide (NO) production, often via increased inducible nitric oxide synthase (iNOS) expression. This imbalance disrupts the normal equilibrium between vasoconstriction and vasodilation. (3) Downregulation of Junctional Proteins: Heat stress impairs endothelial barrier integrity by downregulating essential tight junction proteins (ZO-1, Occludin, Claudin), further compromising vascular homeostasis. (4) Endothelial Cell Death: Severe heat stress triggers various pathways of endothelial cell death, including apoptosis, pyroptosis, ferroptosis, and necroptosis. (5) Endothelial Barrier Dysfunction: Cumulative damage
(*Continued*)

FIGURE 1 (Continued)
encompassing glycocalyx degradation, junctional disruption, and cell death culminates in severe barrier failure, manifesting as increased vascular permeability and extravasation of fluid and albumin into tissues, ultimately contributing to organ dysfunction. (6) Coagulation system: NETs and other inflammatory processes drive pathological clot formation, culminating in disseminated intravascular coagulation (DIC). Abbreviations: GCX, glycocalyx; SDC-1, syndecan-1; iNOS, inducible nitric oxide synthase; NO, nitric oxide; ZO-1, zonula occludens-1. NETs, neutrophil extracellular traps; DIC, disseminated intravascular coagulation.

under heat stress conditions (Clay and Adler, 1967). The degradation of the glycocalyx layer leads to the release of its components, such as SDC-1, heparan sulfate, hyaluronic acid, and chondroitin sulfate, into the plasma. In experimental heat stroke models, the degradation of the glycocalyx layer results in a thinner and more sparse structure, which allows the translocation of plasma proteins and fluid across the vascular wall, thereby contributing to the formation of tissue edema, such as cerebral edema or pulmonary edema. Heat stress induces glycocalyx shedding, as evidenced by fluorescence staining revealing diminished expression of glypican-1 (GPC-1) and SDC-1 in pulmonary vascular endothelia following heat stroke. And ELISA quantification demonstrated elevated plasma levels of both GPC-1 and SDC-1 post-thermal challenge. In heat stroke rat models (ambient temperature: 40°C ± 2°C; relative humidity: 65% ± 5%), pretreatment of heparanase - the enzyme responsible for cleaving heparan sulfate side chains - significantly potentiated heat stress-induced vascular hyperpermeability and exacerbated endothelial dysfunction. This pathological progression was associated with enhanced pulmonary tissue apoptosis, inflammatory responses, and oxidative stress. Notably, therapeutic intervention with unfractionated heparin effectively mitigated thermal stress-mediated glycocalyx damage (Cao et al., 2023). Upon transmission electron microscopy examination of the pulmonary capillaries in heat stroke rats, it was found that the endothelial glycocalyx began to shed following the induction of heat stress, with this shedding becoming more obvious and even absent by 24 h post-induction. Plasma SDC-1 and hyaluronic acid, which are components of the endothelial glycocalyx, gradually increased after the onset of heat stroke and peaked at 24 h. The levels of plasma SDC-1 and hyaluronic acid were positively correlated with the circulating levels of coagulation markers, including von Willebrand factor (vWF), thrombin-antithrombin complex, and plasmin-antiplasmin, and endothelin-1 (ET-1), as well as pro-inflammatory cytokines such as IL-6 and tumor necrosis factor-alpha (TNF-α).

In heat stroke, vascular endothelial cells generated excessive reactive oxygen species (ROS), a key mediator of endothelial glycocalyx degradation. Notably, N-acetyl cysteine protected against endothelial glycocalyx injury by reducing ROS production in heat-stressed vascular endothelial cells (Peng et al., 2023). Inhalation of 2% hydrogen gas significantly mitigated heat stroke-induced shedding of the vascular endothelial glycocalyx in rat models. This protective effect was mediated by its dual mechanisms of antioxidant and anti-inflammatory mechanisms (Truong et al., 2021; Zang et al., 2024). Multiple evidence suggested that bone marrow-derived mononuclear cells (BMDMs) had host-protective paracrine properties, and they were reported to reduce organ dysfunction caused by ischemic reperfusion and systemic inflammation in several animal studies. In a rat model of heat stroke, administration of BMDMs significantly attenuated the elevation of SDC-1 at 6 and 12 h after heat stress. Moreover, BMDMs intervention markedly suppressed serum levels of pro-inflammatory cytokines, including TNF-α and IL-6 (Umemura et al., 2018).

Dexmedetomidine (DEX), a sedative that acts on the α2 adrenergic receptor, is frequently utilized in intensive care settings. Studies have demonstrated that DEX can attenuate the levels of serum inflammatory cytokines in critically ill patients and exhibit anti-inflammatory and anti-apoptotic effect in sepsis. Heat stroke elicits a sepsis-like inflammatory response, and DEX can attenuate heat stroke-induced intestinal barrier disruption in rats, mitigate sepsis-associated inflammation and multi-organ damage, and enhance survival rates by modulating the NF-κB pathway (Xia et al., 2017). Heat stroke leads to a reduction in the glycocalyx thickness, an effect that can be mitigated by the administration of DEX. This intervention also results in a decrease in the elevation of plasma SDC-1 levels induced by heat stroke (Kobayashi et al., 2018).

2.2 Vascular tone dysfunction

Vascular tone, defined as the balance between the degree of constriction of the blood vessel and its maximum dilation, is modulated by the release of relaxing and constricting factors derived from the endothelium (Ajoolabady et al., 2024). The endothelium exerts significant influence on the regulation of vascular tone through the synthesis and release of a diverse array of endothelium-derived factors. These factors encompass vasodilatory substances such as prostacyclin and nitric oxide (NO), as well as endothelium-dependent hyperpolarization factors. Additionally, the endothelium also produces endothelium-derived contracting factors, thereby modulating vascular tone in a multifaceted manner (Godo and Shimokawa, 2017; Ajoolabady et al., 2024).)

The mean concentration of NO in heat stroke patients was significantly elevated compared to that in control subjects. Furthermore, non-survivors exhibited higher NO levels than survivors. Additionally, NO concentration demonstrated a positive correlation with the Acute Physiology and Chronic Health Evaluation II (APACHE II) score (Warsy et al., 1999; Cheng and MacDonald, 2019). Under heat stress conditions, elevated NO levels augment cutaneous blood flow, thereby enhancing heat dissipation and providing protection against various heat-related disorders. However, excessive NO production may excessively reduce blood pressure, potentially giving rise to complications (Gostimirovic et al., 2020; Suschek et al., 2022). Nitric oxide synthase (NOS) can be classified into three types: endothelial nitric oxide synthase (eNOS), neuronal nitric oxide synthase (nNOS), and inducible nitric oxide synthase (iNOS), these enzymes facilitate the conversion of l-arginine into citrulline and NO. iNOS has been shown to be upregulated by lipopolysaccharide, IL-1, and TNF-α, all of which are elevated in heat stroke, thereby resulting in the

production of substantial quantities of NO (Quirino et al., 2013; Lim, 2018; Snipe et al., 2018).

However, heat stroke is characterized by a paradoxical duality in vascular tone regulation, encompassing both systemic vasodilation for thermolysis and localized vasoconstrictive responses that exacerbate end-organ injury. Notably, clinical and experimental evidence suggests that hyperthermia-induced vasoconstriction of the carotid artery, resulting in cerebral ischemia and subsequent brain damage. *In vitro* studies using rabbit carotid artery strips demonstrated that stepwise heating from 37°C to 47°C elicited reproducible, temperature-proportional contractions in a graded manner. Specifically, heating decreased the contractile responses to norepinephrine and electrical field stimulation but increased contraction in response to KCl. Notably, these effects were not abolished by pretreatment with the neuronal blocker tetrodotoxin (Mustafa et al., 2004; Mustafa et al., 2007). Additionally, ethanol was found to potentiate heat-induced contraction (Mustafa and Ismael, 2017). Clinically, these findings underscore the therapeutic rationale for targeted cooling, particularly of the neck region, to mitigate temperature-sensitive vasoconstrictive responses. However, the interplay between hyperthermia, endothelial injury, and smooth muscle reactivity remains incompletely elucidated, necessitating further research to delineate tissue-specific vascular responses and optimize hemodynamic management in heat stroke.

2.3 Downregulation of junctional proteins

The integrity of the endothelial barrier is crucial for maintaining vascular homeostasis and regulating the passage of fluids, solutes, and cells between the bloodstream and tissues. The junctional proteins, including ZO-1, claudin-5, JAM-A, VE-cadherin, and occludin, are essential for maintaining the structural and functional integrity of endothelial cell-cell junctions, and their disruption can have profound pathological consequences.

Heat stress activates various inflammatory pathways, including the p38 MAPK pathway, which plays a pivotal role in endothelial barrier dysfunction. The activation of p38 MAPK leads to the phosphorylation of heat shock protein 27 (HSP27) (Mertenskötter et al., 2013; Huang J. et al., 2022). Which in turn affects the cytoskeletal dynamics and tight junction integrity of endothelial cells. The phosphorylation of HSP27 and other cytoskeletal proteins under heat stress conditions leads to the reorganization of the actin cytoskeleton. This reorganization results in increased endothelial permeability and barrier disruption.

Recent studies have demonstrated that heat stress can induce the expression of protease-activated receptor 1 (PAR1) in endothelial cells and disrupt endothelial barrier function through the activation of the PAR1 signaling pathway. The specific mechanisms involve the release of matrix metalloproteinase-1 (MMP-1) from endothelial cells, leading to the rearrangement of F-actin and actin phosphorylation, which subsequently increases endothelial permeability (Xu et al., 2015a; Zhang et al., 2017). Furthermore, inhibition of PAR1 using specific inhibitors and neutralizing antibodies can significantly reduce heat stress-induced endothelial permeability (Xu et al., 2015b). The increase in endothelial permeability results in pulmonary edema, increased alveolar-capillary permeability, and leukocyte infiltration, which contribute to the development of ALI and ARDS. Additionally, the traditional Chinese medicine Xuebijing injection has been proven to protect endothelial barrier function by inhibiting the PAR1-moesin signaling pathway (Epstein and Yanovich, 2019). These findings highlight the potential therapeutic role of PAR1 inhibitors and traditional Chinese medicine in mitigating heat stress-induced endothelial dysfunction and associated pulmonary complications.

2.4 Cell death of endothelial cells

Heat stress, as a physical stimulus, can cause instantaneous and catastrophic cell death when intense. Additionally, the pathogenesis of heat stroke-induced cell death involves multiple mechanisms, including apoptosis, pyroptosis, necroptosis, ferroptosis, and PANoptosis (Shi et al., 2017; Bertheloot et al., 2021; Wang Z. et al., 2024). These regulated cell death pathways play distinct roles in modulating the progression of heat stroke and the associated multi-organ dysfunction at various levels.

Pyroptosis is a form of regulated cell death characterized by the formation of pores in the cell membrane, primarily composed of gasdermin D (GSDMD), leading to cell swelling, lysis, and the release of inflammatory cytokines such as IL-1β and IL-18. Research indicates that the high mobility group box-1 protein (HMGB1) signaling is activated during heat stroke, leading to cell pyroptosis. Elevated levels of HMGB1 are consistently observed in patients with heat stroke who exhibit significantly higher mortality rates (Lu et al., 2004; Tong et al., 2011; Dehbi et al., 2012). Endothelial cells cultured at 43°C exhibit cytoskeletal disorganization and become unclear, accompanied by cell swelling. Heat stress induces the cleavage of caspase-1 from precursor form (procaspase-1) into the active caspase-1. The levels of active caspase-1 increase progressively over a specific temperature range, peaking at 43°C, 4 h after the induction of heat stress. Heat stress-induced pyroptosis in human umbilical vein endothelial cells can be effectively mitigated by siRNA targeting GSDMD (Pei et al., 2018). Exertional heat stroke (EHS) triggers endothelial pyroptosis, leading to HMGB1 release, which enhence macrophage pyroptosis and induces immune dysregulation. Neutralizing HMGB1 antibodies significantly reduce tissue damage and systemic inflammation following EHS (Deng et al., 2018; Yu et al., 2024). Recent studies have demonstrated that exosomes derived from mesenchymal stem cells can mitigate organ damage and reduce inflammation in both cellular and animal models of heat stroke. These therapeutic effects are achieved through the inhibition of the HMGB1/NLRP3 inflammasome activation and the pyroptosis pathway. Additionally, miR-548x-3p plays a crucial role in these processes (Wang et al., 2022; Pei et al., 2023).

Ferroptosis is characterized by increased accumulated iron, lipid peroxidation and ROS levels (Xie et al., 2016; Xie et al., 2021 S.). During heat stroke, iron metabolism is disrupted, characterized by elevated iron concentrations in the damaged hippocampus and increased hepcidin levels. Notably, ferroportin 1 expression is significantly downregulated in the hippocampus (Liu et al., 2019). SIRT1-mediated p53 deacetylation can inhibit ferroptosis and

alleviate heat stress-induced lung epithelial cell damage (Chen et al., 2022; Zhu et al., 2024). EHS causes an increase in serum myoglobin concentrations, which can induce acute kidney injury through ferroptosis. Baicalein, a natural flavonoid compound, can mitigate heat stress-induced renal injury by reducing the elevation of ROS caused by heat stress, accompanied by changes in ferroptosis-related proteins (Luan et al., 2023). Recent study suggested that ACSL4 was a key molecule driving rhabdomyolysis following EHS in mice. Evidence includes increased ACSL4, iron accumulation, lipid peroxidation, GPX4 decrease, and reduced survival death with ferroptosis inhibitors. Targeting ACSL4, either genetically or pharmacologically, significantly reduced muscle cell death and rhabdomyolysis biomarkers both *in vitro* and *in vivo*, suggesting ACSL4 inhibition is a promising therapeutic strategy to prevent EHS-induced rhabdomyolysis (He et al., 2022). Currently, research on the impact of heat stress on ferroptosis in endothelial cells remains limited.

Necroptosis is primarily mediated by the necrosome complex, which includes receptor-interacting protein kinase 1 (RIPK1), RIPK3, and mixed lineage kinase domain-like protein (MLKL) (Gao et al., 2022). In heat stroke, the activation of these proteins leads to the formation of pores in the cell membrane, causing cell swelling and eventual rupture (Yuan et al., 2022; Cai et al., 2023; Li F. et al., 2023; Ai et al., 2024). ZBP1, Z-nucleic acid receptor, was identified to mediate heat stroke via necroptosis by triggering RIPK3-dependent cell death. Deletion of ZBP1, RIPK3, caspase-8, and MLKL can reduce heat stress-induced injuries, including cell death, circulatory failure, and organ damage (Yuan et al., 2022). ROS play a crucial role in heat stroke-induced necroptosis. The clearance of ROS significantly inhibits HS-induced RIPK1/RIPK3-dependent necroptosis both *in vivo* and *in vitro*, thereby alleviating inflammatory responses and multi-organ dysfunction (Li et al., 2020; Xie W. et al., 2021; Huang W. et al., 2022). *In vitro*, pretreatment with necrostatin-1, a RIPK1 inhibitor, attenuated heat stress-induced necroptosis in pulmonary microvascular endothelial cells and inhibited the nuclear-to-cytoplasmic translocation of HMGB1 via the MAPK, NF-κB, and c-Jun signaling pathways (Figure 2) (Huang et al., 2020).

3 Roles of endothelial dysfunction in HS

Under heat stress, endothelial cells are subjected to various challenges, including oxidative stress, barrier dysfunction, and cell death, which collectively impair their normal function. The endothelial dysfunction not only affects local blood flow but can also contribute to systemic complications such as multi-organ failure and cardiovascular diseases. Patient mortality with multiple organ dysfunction syndrome reaches 85%, with the respiratory system as the most commonly affected organ system at 85.7% (Varghese et al., 2005). Full understanding of the pathogenesis of endothelial injury requires knowledge of the host thermoregulatory and heat stress responses to extreme heat stress. In addition, understanding the roles of endothelial dysfunction in heat stress is crucial for developing effective interventions to mitigate the adverse effects of heat exposure on human health.

3.1 Role of heat-induced endothelial barrier dysfunction

Endothelial barrier dysfunction is intricately linked to the development and progression of various diseases, including ALI, ARDS, and atherosclerosis. Recent advancements in the understanding of heat stress mechanisms have unveiled that heat stress can disrupt endothelial barrier function through multiple signaling pathways and molecular mechanisms. This disruption is a crucial factor in the pathogenesis of heat stroke.

The development of heat stroke involves a transition from a compensatory phase, where thermoregulatory mechanisms attempt to maintain core body temperature, to a decompensatory phase where heat production exceeds heat dissipation. During the compensatory phase, the body attempts to dissipate heat through mechanisms such as vasodilation of cutaneous blood vessels and increased sweating. However, as heat stress continues, the circulatory system becomes overwhelmed, leading to a reduction in circulating blood volume and a subsequent decrease in cardiac output. When the heart can no longer meet the demands of thermoregulation, heat stroke ensues (Epstein and Yanovich, 2019). Heat stress disrupts the integrity of endothelial tight junctions, leading to increased permeability and leakage of plasma proteins. This results in a reduction of intravascular volume and the accumulation of fluid in tissues, causing edema. In addition, heat stress induces endothelial injury, leading to increased vascular permeability, reduced blood volume, tissue edema, and the migration of inflammatory cells. These changes further exacerbate circulatory failure and multi-organ dysfunction.

3.2 Role of heat-induced coagulopathy

In severe heat stroke cases, clinical studies have reported a 48% incidence of DIC as a life-threatening complication (Huisse et al., 2008; Hemmelgarn and Gannon, 2013; Hifumi et al., 2018). Critically, patients who develop DIC exhibit significantly higher rates of multiorgan dysfunction and heat stroke-related mortality compared to those without coagulopathy. The pathophysiology of heat-induced coagulopathy is complex and not fully understood. However, it is believed that heat stress can trigger the release of various procoagulant factors, such as vWF and factor VIII, from vascular endothelial cells. These factors promote intravascular thrombosis by enhancing platelet aggregation and activation (da Cruz et al., 2019). Additionally, heat stress can lead to endothelial dysfunction, characterized by the loss of anticoagulant properties and increased expression of adhesion molecules, further contributing to the prothrombotic state. Inflammatory activation also plays a crucial role in the development of heat-induced coagulopathy. Heat stress can induce the release of pro-inflammatory cytokines, such as IL-6 and TNF-α, which in turn activate the coagulation system (Pennings et al., 2022). This interaction between inflammation and coagulation creates a self-amplifying loop, leading to the formation of microthrombi and further endothelial damage (Sylman et al., 2015). Despite its clinical significance, the precise pathophysiological mechanisms underlying heat stroke-induced coagulopathy remain incompletely characterized. Further mechanistic investigations are necessary to identify potential therapeutic targets.

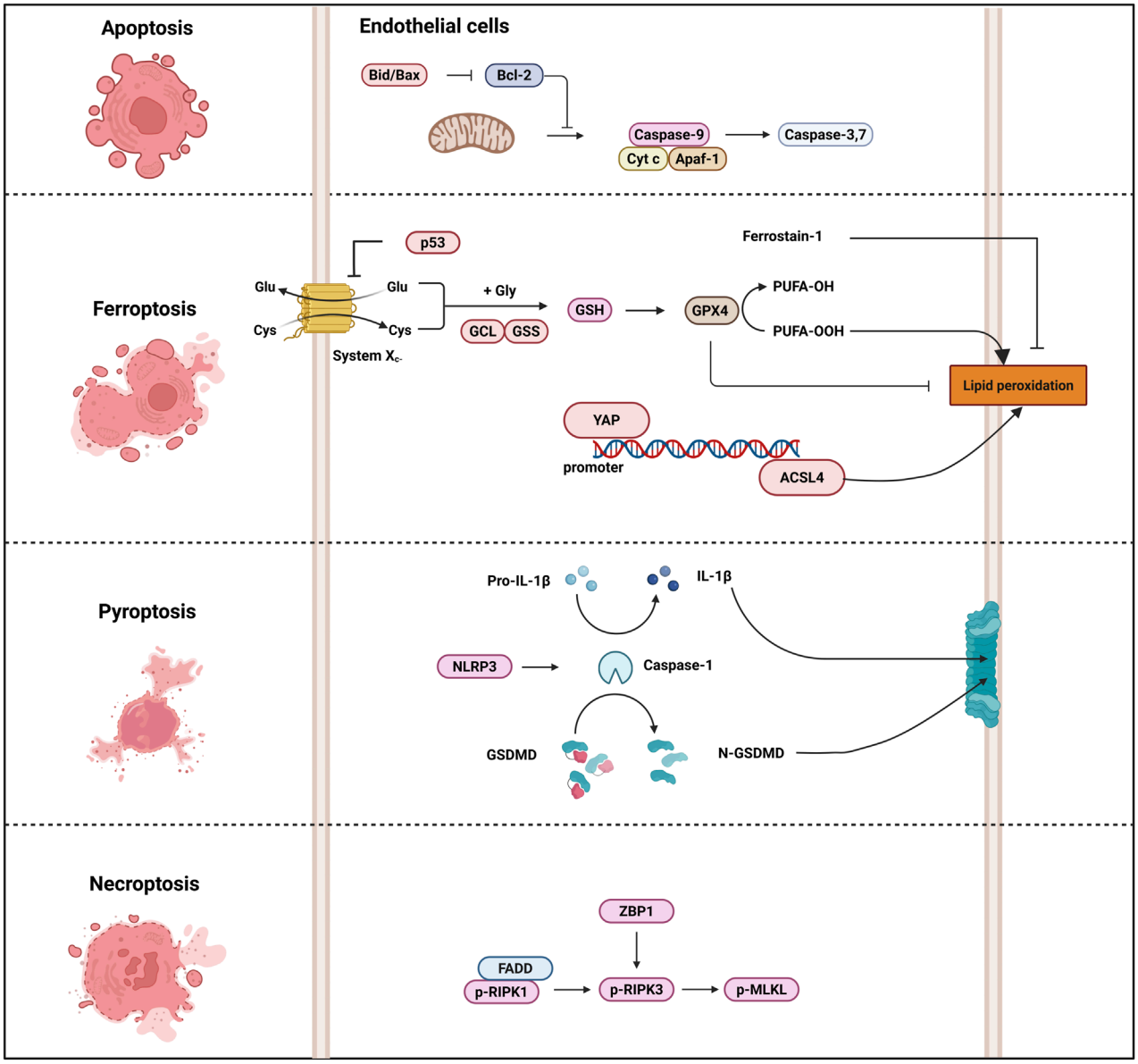

FIGURE 2
Heat stroke-induced cell death pathway. Several cell death-associated markers are implicated in the pathogenesis of heatstroke. For instance, ACSL4 regulates ferroptosis, caspase-1 and GSDMD execute pyroptosis, and RIPK and MLKL mediate necroptosis. In animal models of heat stroke, therapeutic administration of specific cell death inhibitors attenuates heat-induced organ injury. Excessive activation of these cell death pathways can precipitate cardiovascular collapse, MODS, DIC, and death in heat stroke. Abbreviations: ACSL4, Acyl-CoA synthetase long chain family member 4; GSDMD, Gasdermin-D; RIPK, receptor-interacting protein kinase; MLKL, mixed lineage kinase domain-like protein; MODS, multiple organ dysfunction syndrome; DIC, disseminated intravascular coagulation.

4 Biomarkers and potential interventions for endothelial injury in HS

4.1 Biomarkers for endothelial injury in HS

As mentioned above, the glycocalyx plays multiple roles in vascular homeostasis. Glycocalyx fragments shed into the bloodstream during sepsis may serve as clinically relevant biomarkers (Uchimido et al., 2019). Numerous preclinical and clinical investigations have established a significant correlation between pro-inflammatory cytokines and biomarkers indicative of glycocalyx degradation. In addition, preclinical and clinical investigations have demonstrated that hypervolemia triggers the secretion of atrial natriuretic peptide from cardiac atrial chambers, a response mediated by mechanical wall stress secondary to atrial distension. Emerging evidence implicates hypervolemia as a contributory factor in glycocalyx degradation through mechanotransduction pathways (Chappell et al., 2014b; Sukudom et al., 2024). Emerging studies reveal pathognomonic

elevation of glycocalyx degradation products (specifically SDC-1, heparan sulfate, and hyaluronan) in both experimental heat stroke models and human patient plasma. These circulating biomarkers demonstrate significant associations with multiple clinical parameters, including Sequential Organ Failure Assessment scores, inflammatory cytokine levels, and mortality rates (Kobayashi et al., 2018; Umemura et al., 2018; Truong et al., 2021; Cao et al., 2023; Peng et al., 2023).

Other indicators of endothelial cell activation and compromised integrity include the detachment of endothelial cells and their subsequent release into the peripheral circulation. An increasement in circulating endothelial cells has been observed in an experimental heat stroke rat model, indicating its potential utility as a marker for endothelial injury (Tong et al., 2014).

Endothelins, predominantly ET-1, are potent vasoactive peptides synthesized by endothelial cells that regulate vascular tone and tissue perfusion through endothelin A/endothelin B receptor-mediated signaling. While essential for hemodynamic homeostasis, pathological ET-1 overproduction under stress conditions (e.g., hyperthermia, inflammation) drives microvascular dysfunction, endothelial hyperpermeability, and multiorgan injury, positioning it as both a pathophysiological mediator and therapeutic target in critical illnesses (Banecki and Dora, 2023; Kanai and Clouthier, 2023; Schiffrin and Pollock, 2024). Experimental studies in rodent heat stroke models demonstrate significant elevation of circulating ET-1 levels, with mechanistic analyses revealing that selective ET-1 receptor antagonism ameliorates thermoregulatory failure by attenuating TNF-α production. This therapeutic intervention preserves hemodynamic stability by maintaining mean arterial pressure within physiological thresholds and normalizing cerebral perfusion parameters during heat stroke, suggesting its potential for mitigating blood-brain barrier disruption in hyperthermia-induced encephalopathy (Liu et al., 2004; Chen et al., 2023; Xu et al., 2023).

The pathogenesis of heat stroke is characterized by a significant elevation in biomarkers of endothelial injury, particularly vWF, plasminogen activator inhibitor-1 and soluble thrombomodulin (TM), which are prominently increased in plasma during heat stroke (Bergonzelli and Kruithof, 1991; Shieh et al., 1995; Rücker et al., 2006; Kawasaki et al., 2014). These biomarkers exhibit a strong correlation with the severity of coagulopathy and mortality risk, reflecting the dual activation of thrombo-inflammatory pathways and failure of anticoagulant mechanisms (Shieh et al., 1995; Roberts et al., 2008; Li Y. et al., 2023; Wan et al., 2023). TM confers both anticoagulant and anti-inflammatory properties, thereby enhancing the survival outcomes in patients with septic shock. The administration of thrombomodulin has been shown to alleviate heat stroke-induced multi-barrier dysfunction by mitigating intestinal hyperpermeability and blood-brain barrier disruption. This therapeutic effect is achieved through the suppression of complement activation, endotoxin release, and HMGB1 protein (Hagiwara et al., 2010; Kawasaki et al., 2014; Lin et al., 2024). In patients or animal models of heat stroke, elevated levels of HMGB1, extracellular histone H3, and circulating heat shock proteins (e.g., HSP70) have been observed in plasma (Geng et al., 2015; Schlader et al., 2022). These non-endothelial-specific markers of injury originate from necrotic cells, neutrophil extracellular traps, and stressed parenchymal cells. Collectively, they amplify systemic inflammation through the activation of TLR4/RAGE and NLRP3 inflammasome pathways (Dehbi et al., 2010; Dehbi et al., 2012; Bruchim et al., 2016; Bruchim et al., 2017; Li Y. et al., 2021; Du et al., 2022; Yin et al., 2022).

4.2 Potential interventions for endothelial injury in HS

Heat acclimatization is a physiological adaptation process that occurs in response to repeated heat exposure. This process involves a series of physiological changes in the body, including improved cardiovascular function, enhanced sweating efficiency, and better thermoregulation. It was reported that heat acclimatization can enhance the viability and resilience of vascular endothelial cells following heat stress. It also partially restores the normal function of these cells. This protective effect is likely associated with the upregulation of HSP70 expression (Wen et al., 2024).

During passive heat stress, significant augmentation of cutaneous blood flow is primarily supported by a coordinated increase in cardiac output and a concomitant decrease in vascular conductance within non-cutaneous vascular beds (Crandall and Wilson, 2014; Cramer et al., 2022). However, this reflex cutaneous vasodilation is markedly attenuated in healthy older adults (≥60 years), a phenomenon attributed to impairments in both central sympathetic outflows directed to the cutaneous circulation and cutaneous microvascular endothelial function (Kriebel-Gasparro, 2024; Kriebel-Gasparro, 2024). Notably, these age-related deficits may be exacerbated by hypercholesterolemia - particularly elevated low-density lipoprotein levels, a well-established risk factor for atherosclerotic cardiovascular disease. Experimental evidence demonstrates that hypercholesterolemia independently associates with dysregulated sympathetic control and impaired microvascular endothelial responsiveness (Eikelis et al., 2017). In experimental settings using whole-body heating via water-perfused suits to simulate thermal stress, researchers have identified that the diminished reflex vasodilation in older adults result from combined dysfunction in both central sympathetic regulation and peripheral microvascular mechanisms. Importantly, while older adults with untreated hypercholesterolemia demonstrate significant impairment in heat-induced cutaneous vasodilation, this deficit is normalized in age-matched counterparts receiving statin therapy. This therapeutic effect suggests that statins may mitigate cholesterol-related microvascular dysfunction through lipid-independent pleiotropic mechanisms (Greaney et al., 2019).

Heat stroke-induced thermoregulatory deficits and mortality may arise from ischemic and oxidative damage to the hypothalamus, the primary thermoregulatory center in the mammalian brain (Cramer et al., 2022). Compared to normothermic controls, mice exposed to heat stress exhibit significantly elevated levels of cellular ischemia markers (such as glutamate and the lactate-to-pyruvate ratio) in the hypothalamus (Chang et al., 2007; Chen et al., 2009; Zhang et al., 2023). Studies demonstrated that heat stroke triggers intestinal villi injury accompanied by enhanced epithelial cell apoptosis and elevated HIF-1α expression. The intervention of HIF-1α overexpression can suppress eIF2α/ATF4/CHOP pathway, ultimately attenuating heat stroke-mediated intestinal damage. Hypobaric hypoxia preconditioning is a temporary condition triggered by short periods of sublethal hypoxia, which activate

various endogenous atrophic signals and provide strong protection against future lethal challenges (Liu et al., 2021; Torosyan et al., 2021). Twenty minutes after heat stress, rats exposed to heat without hypoxia preconditioning (HHP) treatment showed significantly higher core and hypothalamic temperatures, hypothalamic MMP-9 levels, and counts of apoptotic neurons in the hypothalamus, compared to control rats not exposed to heat. These heat-exposed rats also exhibited significantly lower mean blood pressure, hypothalamic blood flow, and PaO_2 values. However, in rats exposed to heat, HHP significantly increased the hypothalamic levels of HIF-1α, HSP-72, and HO-1, and effectively alleviated hypothalamic hyperthermia, hypotension, hypothalamic ischemia, hypoxia, neuronal apoptosis, and degeneration (Chen et al., 2009; Chao et al., 2020). Once hydroxylated by prolyl hydroxylase, HIF-1α undergoes rapid degradation via the ubiquitin-proteasome pathway (Kim and Yang, 2015). Roxadustat, a hypoxia-inducible factor prolyl hydroxylase inhibitor, can enhance the production of endogenous erythropoietin to treat anemia in chronic kidney disease patients through the activation of the HIF-1α pathway (Chen et al., 2019). Roxadustat pretreatment significantly enhanced renal function, thermotolerance, and survival rate in mice subjected to heat stroke. This protective effect is attributed to the activation of BNIP3-mediated mitophagy, which shields renal tubular epithelial cells from inflammation and apoptosis. Conversely, genetic ablation of BNIP3 not only weakened roxadustat-induced mitophagy but also nullified the renal protective effects mediated by roxadustat (Wang L. et al., 2024).

5 Conclusion

Heat stroke-induced endothelial injury is a complex pathological process involving multiple mechanisms, including glycocalyx degradation, vascular tone dysfunction, junctional protein disruption, and regulated cell death pathways. These changes contribute to systemic complications such as multi-organ failure and cardiovascular diseases. Understanding the detailed mechanisms underlying endothelial dysfunction in heat stroke is crucial for developing targeted therapeutic strategies. Potential interventions, such as early fluid resuscitation, heat acclimation, and pharmacological agents targeting specific pathways, show promise in mitigating heat stroke-induced endothelial injury and improving patient outcomes. Future research should focus on further elucidating the pathophysiological mechanisms and identifying more effective biomarkers and therapeutic targets to reduce the high mortality and morbidity associated with heat stroke.

Author contributions

SW: Conceptualization, Data curation, Writing – original draft. XZ: Conceptualization, Writing – original draft, Writing – review and editing. YZ: Resources, Writing – review and editing. NW: Writing – review and editing. LB: Conceptualization, Funding acquisition, Resources, Supervision, Writing – review and editing. MW: Conceptualization, Funding acquisition, Resources, Supervision, Writing – review and editing.

Funding

The author(s) declare that financial support was received for the research and/or publication of this article. This study was supported by the Fund Project of "Basic Research Subject" of Changhai Hospital, Naval Medical University (2023PY16).

Conflict of interest

The authors declare that the research was conducted in the absence of any commercial or financial relationships that could be construed as a potential conflict of interest.

Generative AI statement

The author(s) declare that no Generative AI was used in the creation of this manuscript.

Publisher's note

All claims expressed in this article are solely those of the authors and do not necessarily represent those of their affiliated organizations, or those of the publisher, the editors and the reviewers. Any product that may be evaluated in this article, or claim that may be made by its manufacturer, is not guaranteed or endorsed by the publisher.

References

Abdullah, M., Ehaideb, S., Roberts, G., and Bouchama, A. (2024). Insights into pathophysiology and therapeutic strategies for heat stroke: lessons from a baboon model. *Exp. Physiol.* 109, 484–501. doi:10.1113/EP091586

Ai, Y., Meng, Y., Yan, B., Zhou, Q., and Wang, X. (2024). The biochemical pathways of apoptotic, necroptotic, pyroptotic, and ferroptotic cell death. *Mol. Cell* 84, 170–179. doi:10.1016/j.molcel.2023.11.040

Ajoolabady, A., Pratico, D., and Ren, J. (2024). Endothelial dysfunction: mechanisms and contribution to diseases. *Acta Pharmacol. Sin.* 45, 2023–2031. doi:10.1038/s41401-024-01295-8

Akhtar, S., and Sharma, A. (2022). Endothelial dysfunction sustains immune response in atherosclerosis: potential cause for ineffectiveness of prevailing drugs. *Int. Rev. Immunol.* 41, 123–134. doi:10.1080/08830185.2020.1866568

Banecki, K. M. R. M., and Dora, K. A. (2023). Endothelin-1 in health and disease. *Int. J. Mol. Sci.* 24, 11295. doi:10.3390/ijms241411295

Bergonzelli, G. E., and Kruithof, E. K. (1991). Induction of plasminogen activator inhibitor 1 biosynthesis by hyperthermia. *J. Cell. Physiol.* 148, 306–313. doi:10.1002/jcp.1041480217

Bertheloot, D., Latz, E., and Franklin, B. S. (2021). Necroptosis, pyroptosis and apoptosis: an intricate game of cell death. *Cell. Mol. Immunol.* 18, 1106–1121. doi:10.1038/s41423-020-00630-3

Bruchim, Y., Ginsburg, I., Segev, G., Mreisat, A., Avital, Y., Aroch, I., et al. (2017). Serum histones as biomarkers of the severity of heatstroke in dogs. *Cell Stress Chaperones* 22, 903–910. doi:10.1007/s12192-017-0817-6

Bruchim, Y., Segev, G., Kelmer, E., Codner, C., Marisat, A., and Horowitz, M. (2016). Hospitalized dogs recovery from naturally occurring heatstroke; does serum heat shock protein 72 can provide prognostic biomarker? *Cell Stress Chaperones* 21, 123–130. doi:10.1007/s12192-015-0645-5

Cai, H., Qin, D., Liu, Y., Guo, X., Liu, Y., Ma, B., et al. (2023). Remodeling of gut microbiota by probiotics alleviated heat stroke-induced necroptosis in Male germ cells. *Mol. Nutr. Food Res.* 67, 2300291. doi:10.1002/mnfr.202300291

Cao, J., Ding, C., Huang, J., Chen, Y., and Chen, Y. (2023). Pulmonary vascular endothelial glycocalyx degradation contributes to acute lung injury in experiencing heatstroke. *Shock* 59, 966–972. doi:10.1097/SHK.0000000000002130

Chang, C.-K., Chang, C.-P., Liu, S.-Y., and Lin, M.-T. (2007). Oxidative stress and ischemic injuries in heat stroke. *Prog. Brain Res.* 162, 525–546. doi:10.1016/S0079-6123(06)62025-6

Chao, C.-M., Chen, C.-L., Niu, K.-C., Lin, C.-H., Tang, L.-Y., Lin, L.-S., et al. (2020). Hypobaric hypoxia preconditioning protects against hypothalamic neuron apoptosis in heat-exposed rats by reversing hypothalamic overexpression of matrix metalloproteinase-9 and ischemia. *Int. J. Med. Sci.* 17, 2622–2634. doi:10.7150/ijms.47560

Chappell, D., Brettner, F., Doerfler, N., Jacob, M., Rehm, M., Bruegger, D., et al. (2014a). Protection of glycocalyx decreases platelet adhesion after ischaemia/reperfusion: an animal study. *Eur. J. Anaesthesiol.* 31, 474–481. doi:10.1097/EJA.0000000000000085

Chappell, D., Bruegger, D., Potzel, J., Jacob, M., Brettner, F., Vogeser, M., et al. (2014b). Hypervolemia increases release of atrial natriuretic peptide and shedding of the endothelial glycocalyx. *Crit. Care* 18, 538. doi:10.1186/s13054-014-0538-5

Chen, H., Lin, X., Yi, X., Liu, X., Yu, R., Fan, W., et al. (2022). SIRT1-mediated p53 deacetylation inhibits ferroptosis and alleviates heat stress-induced lung epithelial cells injury. *Int. J. Hyperth.* 39, 977–986. doi:10.1080/02656736.2022.2094476

Chen, J., Ding, C., Cao, J., Tong, H., and Chen, Y. (2023). Heat stress combined with lipopolysaccharide induces pulmonary microvascular endothelial cell glycocalyx inflammatory damage *in vitro*. *Immun. Inflamm. Dis.* 11, e1034. doi:10.1002/iid3.1034

Chen, N., Hao, C., Liu, B.-C., Lin, H., Wang, C., Xing, C., et al. (2019). Roxadustat treatment for anemia in patients undergoing long-term dialysis. *N. Engl. J. Med.* 381, 1011–1022. doi:10.1056/NEJMoa1901713

Chen, Z.-C., Wu, W.-S., Lin, M.-T., and Hsu, C.-C. (2009). Protective effect of transgenic expression of porcine heat shock protein 70 on hypothalamic ischemic and oxidative damage in a mouse model of heatstroke. *BMC Neurosci.* 10, 111. doi:10.1186/1471-2202-10-111

Cheng, J. L., and MacDonald, M. J. (2019). Effect of heat stress on vascular outcomes in humans. *J. Appl. Physiol. Bethesda Md 1985* 126, 771–781. doi:10.1152/japplphysiol.00682.2018

Clay, M. M., and Adler, M. W. (1967). Alterations in hyaluronidase activity and serum protein electrophoretic patterns after chronic heat stress. *J. Pharm. Sci.* 56, 765–767. doi:10.1002/jps.2600560627

Cramer, M. N., Gagnon, D., Laitano, O., and Crandall, C. G. (2022). Human temperature regulation under heat stress in health, disease, and injury. *Physiol. Rev.* 102, 1907–1989. doi:10.1152/physrev.00047.2021

Crandall, C. G., and Wilson, T. E. (2014). "Human cardiovascular responses to passive heat stress," in *Comprehensive physiology*. Editor R. Terjung (Wiley), 17–43. doi:10.1002/cphy.c140015

da Cruz, D. B., Helms, J., Aquino, L. R., Stiel, L., Cougourdan, L., Broussard, C., et al. (2019). DNA-bound elastase of neutrophil extracellular traps degrades plasminogen, reduces plasmin formation, and decreases fibrinolysis: proof of concept in septic shock plasma. *FASEB J.* 33, 14270–14280. doi:10.1096/fj.201901363RRR

Dehbi, M., Baturcam, E., Eldali, A., Ahmed, M., Kwaasi, A., Chishti, M. A., et al. (2010). Hsp-72, a candidate prognostic indicator of heatstroke. *Cell Stress Chaperones* 15, 593–603. doi:10.1007/s12192-010-0172-3

Dehbi, M., Uzzaman, T., Baturcam, E., Eldali, A., Ventura, W., and Bouchama, A. (2012). Toll-like receptor 4 and high-mobility group box 1 are critical mediators of tissue injury and survival in a mouse model for heatstroke. *PloS One* 7, e44100. doi:10.1371/journal.pone.0044100

Deng, M., Tang, Y., Li, W., Wang, X., Zhang, R., Zhang, X., et al. (2018). The endotoxin delivery protein HMGB1 mediates Caspase-11-Dependent lethality in sepsis. *Immunity* 49, 740–753.e7. doi:10.1016/j.immuni.2018.08.016

Du, D., Lv, W., Jing, X., Yu, C., Wuen, J., and Hasi, S. (2022). Camel whey protein alleviates heat stress-induced liver injury by activating the Nrf2/HO-1 signaling pathway and inhibiting HMGB1 release. *Cell Stress Chaperones* 27, 449–460. doi:10.1007/s12192-022-01277-x

Eikelis, N., Lambert, E. A., Phillips, S., Sari, C. I., Mundra, P. A., Weir, J. M., et al. (2017). Muscle sympathetic nerve activity is associated with elements of the plasma lipidomic profile in young Asian adults. *J. Clin. Endocrinol. Metab.* 102, 2059–2068. doi:10.1210/jc.2016-3738

Epstein, Y., and Yanovich, R. (2019). Heatstroke. *N. Engl. J. Med.* 380, 2449–2459. doi:10.1056/NEJMra1810762

Foote, C. A., Soares, R. N., Ramirez-Perez, F. I., Ghiarone, T., Aroor, A., Manrique-Acevedo, C., et al. (2022). Endothelial glycocalyx. *Compr. Physiol.* 12, 3781–3811. doi:10.1002/cphy.c210029

Gao, W., Wang, X., Zhou, Y., Wang, X., and Yu, Y. (2022). Autophagy, ferroptosis, pyroptosis, and necroptosis in tumor immunotherapy. *Signal Transduct. Target. Ther.* 7, 196. doi:10.1038/s41392-022-01046-3

Geng, Y., Ma, Q., Liu, Y.-N., Peng, N., Yuan, F.-F., Li, X.-G., et al. (2015). Heatstroke induces liver injury via IL-1β and HMGB1-induced pyroptosis. *J. Hepatol.* 63, 622–633. doi:10.1016/j.jhep.2015.04.010

Godo, S., and Shimokawa, H. (2017). Endothelial functions. *Arterioscler. Thromb. Vasc. Biol.* 37, e108–e114. doi:10.1161/ATVBAHA.117.309813

Gostimirovic, M., Novakovic, R., Rajkovic, J., Djokic, V., Terzic, D., Putnik, S., et al. (2020). The influence of climate change on human cardiovascular function. *Arch. Environ. Occup. Health* 75, 406–414. doi:10.1080/19338244.2020.1742079

Graham, G. J., Handel, T. M., and Proudfoot, A. E. I. (2019). Leukocyte adhesion: reconceptualizing chemokine presentation by glycosaminoglycans. *Trends Immunol.* 40, 472–481. doi:10.1016/j.it.2019.03.009

Greaney, J. L., Stanhewicz, A. E., and Kenney, W. L. (2019). Chronic statin therapy is associated with enhanced cutaneous vascular responsiveness to sympathetic outflow during passive heat stress. *J. Physiol.* 597, 4743–4755. doi:10.1113/JP278237

Hagiwara, S., Iwasaka, H., Goto, K., Ochi, Y., Mizunaga, S., Saikawa, T., et al. (2010). Recombinant thrombomodulin prevents heatstroke by inhibition of high-mobility group box 1 protein in sera of rats. *Shock Augusta Ga* 34, 402–406. doi:10.1097/SHK.0b013e3181d492e4

He, S., Li, R., Peng, Y., Wang, Z., Huang, J., Meng, H., et al. (2022). ACSL4 contributes to ferroptosis-mediated rhabdomyolysis in exertional heat stroke. *J. Cachexia Sarcopenia Muscle* 13, 1717–1730. doi:10.1002/jcsm.12953

Hemmelgarn, C., and Gannon, K. (2013). Heatstroke: thermoregulation, pathophysiology, and predisposing factors. *Compend. Contin. Educ. Vet.* 35, E4.

Hifumi, T., Kondo, Y., Shimazaki, J., Oda, Y., Shiraishi, S., Wakasugi, M., et al. (2018). Prognostic significance of disseminated intravascular coagulation in patients with heat stroke in a nationwide registry. *J. Crit. Care* 44, 306–311. doi:10.1016/j.jcrc.2017.12.003

Huang, J., Chai, X., Wu, Y., Hou, Y., Li, C., Xue, Y., et al. (2022a). β-Hydroxybutyric acid attenuates heat stress-induced neuroinflammation via inhibiting TLR4/p38 MAPK and NF-κB pathways in the hippocampus. *FASEB J.* 36, e22264. doi:10.1096/fj.202101469RR

Huang, W., Mao, L., Xie, W., Cai, S., Huang, Q., Liu, Y., et al. (2022b). Impact of UCP2 depletion on heat stroke-induced mitochondrial function in human umbilical vein endothelial cells. *Int. J. Hyperth.* 39, 287–296. doi:10.1080/02656736.2022.2032846

Huang, W., Xie, W., Gong, J., Wang, W., Cai, S., Huang, Q., et al. (2020). Heat stress induces RIP1/RIP3-dependent necroptosis through the MAPK, NF-κB, and c-Jun signaling pathways in pulmonary vascular endothelial cells. *Biochem. Biophys. Res. Commun.* 528, 206–212. doi:10.1016/j.bbrc.2020.04.150

Huisse, M.-G., Pease, S., Hurtado-Nedelec, M., Arnaud, B., Malaquin, C., Wolff, M., et al. (2008). Leukocyte activation: the link between inflammation and coagulation during heatstroke. A study of patients during the 2003 heat wave in Paris. *Crit. Care Med.* 36, 2288–2295. doi:10.1097/CCM.0b013e318180dd43

Kaewput, W., Thongprayoon, C., Petnak, T., Cato, L. D., Chewcharat, A., Boonpheng, B., et al. (2021). Inpatient burden and mortality of heatstroke in the United States. *Int. J. Clin. Pract.* 75, e13837. doi:10.1111/ijcp.13837

Kanai, S. M., and Clouthier, D. E. (2023). Endothelin signaling in development. *Dev. Camb. Engl.* 150, dev201786. doi:10.1242/dev.201786

Kawasaki, T., Okamoto, K., Kawasaki, C., and Sata, T. (2014). Thrombomodulin improved liver injury, coagulopathy, and mortality in an experimental heatstroke model in mice. *Anesth. Analg.* 118, 956–963. doi:10.1213/ANE.0000000000000170

Kim, S. Y., and Yang, E. G. (2015). Recent advances in developing inhibitors for hypoxia-inducible factor prolyl hydroxylases and their therapeutic implications. *Mol. Basel Switz.* 20, 20551–20568. doi:10.3390/molecules201119717

Kobayashi, K., Mimuro, S., Sato, T., Kobayashi, A., Kawashima, S., Makino, H., et al. (2018). Dexmedetomidine preserves the endothelial glycocalyx and improves survival in a rat heatstroke model. *J. Anesth.* 32, 880–885. doi:10.1007/s00540-018-2568-7

Kriebel-Gasparro, Dr. A. (2024). Case discussion: the effect of extreme temperatures on an older adult. *Geriatr. Nur. (Lond.)* 58, 525–528. doi:10.1016/j.gerinurse.2024.07.016

Li, F., Deng, J., He, Q., and Zhong, Y. (2023a). ZBP1 and heatstroke. *Front. Immunol.* 14, 1091766. doi:10.3389/fimmu.2023.1091766

Li, J., Qi, Z., Li, D., Huang, X., Qi, B., Feng, J., et al. (2021a). Alveolar epithelial glycocalyx shedding aggravates the epithelial barrier and disrupts epithelial tight junctions in acute respiratory distress syndrome. *Biomed. Pharmacother.* 133, 111026. doi:10.1016/j.biopha.2020.111026

Li, L., Tan, H., Zou, Z., Gong, J., Zhou, J., Peng, N., et al. (2020). Preventing necroptosis by scavenging ROS production alleviates heat stress-induced intestinal injury. *Int. J. Hyperth.* 37, 517–530. doi:10.1080/02656736.2020.1763483

Li, Y., Li, H., Ma, W., Maegele, M., Tang, Y., and Gu, Z. (2023b). Proteomic profiling of serum exosomes reveals acute phase response and promotion of inflammatory and platelet activation pathways in patients with heat stroke. *PeerJ* 11, e16590. doi:10.7717/peerj.16590

Li, Y., Liu, Z., Shi, X., Tong, H., and Su, L. (2021b). Prognostic value of plasma exosomal levels of histone H3 protein in patients with heat stroke. *Exp. Ther. Med.* 22, 922. doi:10.3892/etm.2021.10354

Lim, C. L. (2018). Heat sepsis precedes heat toxicity in the pathophysiology of heat stroke—A new paradigm on an ancient disease. *Antioxidants* 7, 149. doi:10.3390/antiox7110149

Lin, C.-H., Tang, L.-Y., Wang, L.-Y., and Chang, C.-P. (2024). Thrombomodulin improves cognitive deficits in heat-stressed mice. *Int. J. Neuropsychopharmacol.* 27, pyae027. doi:10.1093/ijnp/pyae027

Liu, C.-C., Chen, Z.-C., Cheng, B.-C., and Lin, M.-T. (2004). Prior antagonism of Endothelin-1A receptors alleviates circulatory shock and cerebral ischemia during rat heatstroke. *J. Pharmacol. Sci.* 96, 177–187. doi:10.1254/jphs.FP0040203

Liu, J., Gu, Y., Guo, M., and Ji, X. (2021). Neuroprotective effects and mechanisms of ischemic/hypoxic preconditioning on neurological diseases. *CNS Neurosci. Ther.* 27, 869–882. doi:10.1111/cns.13642

Liu, J., Wan, M., Zhang, Y., Zhang, S., Zhang, H., and Wu, S. (2019). Dysfunction of iron metabolism and iron-regulatory proteins in the rat hippocampus after heat stroke. *Shock* 51, 780–786. doi:10.1097/SHK.0000000000001182

Lu, K.-C., Wang, J.-Y., Lin, S.-H., Chu, P., and Lin, Y.-F. (2004). Role of circulating cytokines and chemokines in exertional heatstroke. *Crit. Care Med.* 32, 399–403. doi:10.1097/01.CCM.0000108884.74110.D9

Luan, Y., Huang, E., Huang, J., Yang, Z., Zhou, Z., Liu, Y., et al. (2023). Serum myoglobin modulates kidney injury via inducing ferroptosis after exertional heatstroke. *J. Transl. Intern. Med.* 11, 178–188. doi:10.2478/jtim-2023-0092

McDonald, B., Davis, R. P., Kim, S.-J., Tse, M., Esmon, C. T., Kolaczkowska, E., et al. (2017). Platelets and neutrophil extracellular traps collaborate to promote intravascular coagulation during sepsis in mice. *Blood* 129, 1357–1367. doi:10.1182/blood-2016-09-741298

Mertenskötter, A., Keshet, A., Gerke, P., and Paul, R. J. (2013). The p38 MAPK PMK-1 shows heat-induced nuclear translocation, supports chaperone expression, and affects the heat tolerance of Caenorhabditis elegans. *Cell Stress Chaperones* 18, 293–306. doi:10.1007/s12192-012-0382-y

Mustafa, S., and Ismael, H. N. (2017). Ethanol potentiates heat response in the carotid artery via TRPV1. *Life Sci.* 188, 83–86. doi:10.1016/j.lfs.2017.08.037

Mustafa, S., Thulesius, O., Elgazzar, A. H., and Ismael, H. N. (2007). Synergistic effects of ethanol and hyperthermia on carotid artery vasoconstriction. *Clin. Physiol. Funct. Imaging* 27, 185–190. doi:10.1111/j.1475-097X.2007.00733.x

Mustafa, S., Thulesius, O., and Ismael, H. N. (2004). Hyperthermia-induced vasoconstriction of the carotid artery, a possible causative factor of heatstroke. *J. Appl. Physiol.* 96, 1875–1878. doi:10.1152/japplphysiol.01106.2003

Nordling, S., Hong, J., Fromell, K., Edin, F., Brännström, J., Larsson, R., et al. (2015). Vascular repair utilising immobilised heparin conjugate for protection against early activation of inflammation and coagulation. *Thromb. Haemost.* 113, 1312–1322. doi:10.1160/TH14-09-0724

Ogata, S., Takegami, M., Ozaki, T., Nakashima, T., Onozuka, D., Murata, S., et al. (2021). Heatstroke predictions by machine learning, weather information, and an all-population registry for 12-hour heatstroke alerts. *Nat. Commun.* 12, 4575. doi:10.1038/s41467-021-24823-0

Pei, Y., Geng, Y., and Su, L. (2018). Pyroptosis of HUVECs can be induced by heat stroke. *Biochem. Biophys. Res. Commun.* 506, 626–631. doi:10.1016/j.bbrc.2018.10.051

Pei, Y., Ma, W., Wang, H., Chen, F., Xiao, W., Fan, M., et al. (2023). Mesenchymal stem cell-derived exosomal miR-548x-3p inhibits pyroptosis of vascular endothelial cells through HMGB1 in heat stroke. *Genomics* 115, 110719. doi:10.1016/j.ygeno.2023.110719

Peng, N., Geng, Y., Ouyang, J., Liu, S., Yuan, F., Wan, Y., et al. (2023). Endothelial glycocalyx injury is involved in heatstroke-associated coagulopathy and protected by N-acetylcysteine. *Front. Immunol.* 14, 1159195. doi:10.3389/fimmu.2023.1159195

Pennings, G. J., Reddel, C. J., Traini, M., Lam, M., Kockx, M., Chen, V. M., et al. (2022). Rapid release of Interleukin-1β from human platelets is independent of NLRP3 and caspase. *Thromb. Haemost.* 122, 517–528. doi:10.1055/s-0041-1731288

Perkins-Kirkpatrick, S. E., and Lewis, S. C. (2020). Increasing trends in regional heatwaves. *Nat. Commun.* 11, 3357. doi:10.1038/s41467-020-16970-7

Petrovich, E., Feigelson, S. W., Stoler-Barak, L., Hatzav, M., Solomon, A., Bar-Shai, A., et al. (2016). Lung ICAM-1 and ICAM-2 support spontaneous intravascular effector lymphocyte entrapment but are not required for neutrophil entrapment or emigration inside endotoxin-inflamed lungs. *FASEB J.* 30, 1767–1778. doi:10.1096/fj.201500046

Quirino, I. E. P., Cardoso, V. N., Santos, R. D. G. C. D., Evangelista, W. P., Arantes, R. M. E., Fiúza, J. A., et al. (2013). The role of l-arginine and inducible nitric oxide synthase in intestinal permeability and bacterial translocation. *J. Parenter. Enter. Nutr.* 37, 392–400. doi:10.1177/0148607112458325

Roberts, G. T., Chishti, M. A., Al-Mohanna, F. H., El-Sayed, R. M., and Bouchama, A. (2005). Vascular endothelium is severely perturbed and undergoes apoptosis in experimental heatstroke in Primates. *Blood* 106, 3972. doi:10.1182/blood.V106.11.3972.3972

Roberts, G. T., Ghebeh, H., Chishti, M. A., Al-Mohanna, F., El-Sayed, R., Al-Mohanna, F., et al. (2008). Microvascular injury, thrombosis, inflammation, and apoptosis in the pathogenesis of heatstroke: a study in baboon model. *Arterioscler. Thromb. Vasc. Biol.* 28, 1130–1136. doi:10.1161/ATVBAHA.107.158709

Rücker, M., Schäfer, T., Scheuer, C., Harder, Y., Vollmar, B., and Menger, M. D. (2006). Local heat shock priming promotes recanalization of thromboembolized microvasculature by upregulation of plasminogen activators. *Arterioscler. Thromb. Vasc. Biol.* 26, 1632–1639. doi:10.1161/01.ATV.0000223144.65958.c3

Schiffrin, E. L., and Pollock, D. M. (2024). Endothelin system in hypertension and chronic kidney disease. *Hypertens. Dallas Tex 1979* 81, 691–701. doi:10.1161/HYPERTENSIONAHA.123.21716

Schlader, Z. J., Davis, M. S., and Bouchama, A. (2022). Biomarkers of heatstroke-induced organ injury and repair. *Exp. Physiol.* 107, 1159–1171. doi:10.1113/EP090142

Shi, J., Gao, W., and Shao, F. (2017). Pyroptosis: gasdermin-mediated programmed necrotic cell death. *Trends biochem. Sci.* 42, 245–254. doi:10.1016/j.tibs.2016.10.004

Shieh, S.-D., Shiang, J.-C., Lin, Y.-F., Shiao, W.-Y., and Wang, J.-Y. (1995). Circulating Angiotensin-Converting Enzyme, Von Willebrand Factor Antigen and Thrombomodulin in Exertional Heat Stroke. *Clin. Sci.* 89, 261–265. doi:10.1042/cs0890261

Shimazaki, J., Hifumi, T., Shimizu, K., Oda, Y., Kanda, J., Kondo, Y., et al. (2020). Clinical characteristics, prognostic factors, and outcomes of heat-related illness (heatstroke study 2017–2018). *Acute Med. Surg.* 7, e516. doi:10.1002/ams2.516

Snipe, R. M. J., Khoo, A., Kitic, C. M., Gibson, P. R., and Costa, R. J. S. (2018). The impact of exertional-heat stress on gastrointestinal integrity, gastrointestinal symptoms, systemic endotoxin and cytokine profile. *Eur. J. Appl. Physiol.* 118, 389–400. doi:10.1007/s00421-017-3781-z

Sukudom, S., Smart, L., and Macdonald, S. (2024). Association between intravenous fluid administration and endothelial glycocalyx shedding in humans: a systematic review. *Intensive Care Med. Exp.* 12, 16. doi:10.1186/s40635-024-00602-1

Suschek, C. V., Feibel, D., von Kohout, M., and Opländer, C. (2022). Enhancement of nitric oxide bioavailability by modulation of cutaneous nitric oxide stores. *Biomedicines* 10, 2124. doi:10.3390/biomedicines10092124

Sylman, J. L., Artzer, D. T., Rana, K., and Neeves, K. B. (2015). A vascular injury model using focal heat-induced activation of endothelial cells. *Integr. Biol. Quant. Biosci. Nano Macro* 7, 801–814. doi:10.1039/c5ib00108k

Tong, H., Wan, P., Zhang, X., Duan, P., Tang, Y., Chen, Y., et al. (2014). Vascular endothelial cell injury partly induced by mesenteric lymph in heat stroke. *Inflammation* 37, 27–34. doi:10.1007/s10753-013-9708-x

Tong, H.-S., Tang, Y.-Q., Chen, Y., Qiu, J.-M., Wen, Q., and Su, L. (2011). Early elevated HMGB1 level predicting the outcome in exertional heatstroke. *J. Trauma Inj. Infect. Crit. Care* 71, 808–814. doi:10.1097/TA.0b013e318220b957

Torosyan, R., Huang, S., Bommi, P. V., Tiwari, R., An, S. Y., Schonfeld, M., et al. (2021). Hypoxic preconditioning protects against ischemic kidney injury through the IDO1/kynurenine pathway. *Cell Rep.* 36, 109547. doi:10.1016/j.celrep.2021.109547

Trimm, E., and Red-Horse, K. (2023). Vascular endothelial cell development and diversity. *Nat. Rev. Cardiol.* 20, 197–210. doi:10.1038/s41569-022-00770-1

Truong, S. K., Katoh, T., Mimuro, S., Sato, T., Kobayashi, K., and Nakajima, Y. (2021). Inhalation of 2% hydrogen improves survival rate and attenuates shedding of vascular endothelial glycocalyx in rats with heat stroke. *Shock* 56, 593–600. doi:10.1097/SHK.0000000000001797

Uchimido, R., Schmidt, E. P., and Shapiro, N. I. (2019). The glycocalyx: a novel diagnostic and therapeutic target in sepsis. *Crit. Care Lond. Engl.* 23, 16. doi:10.1186/s13054-018-2292-6

Umemura, Y., Ogura, H., Matsuura, H., Ebihara, T., Shimizu, K., and Shimazu, T. (2018). Bone marrow-derived mononuclear cell therapy can attenuate systemic inflammation in rat heatstroke. *Scand. J. Trauma Resusc. Emerg. Med.* 26, 97. doi:10.1186/s13049-018-0566-2

Van Steen, A. C. I., Grönloh, M. L. B., Joosten, S., Van Alphen, F., Van Den Biggelaar, M., Nolte, M. A., et al. (2023). Endothelial ICAM-1 adhesome recruits CD44 for optimal transcellular migration of human CTLs. *J. Immunol.* 211, 377–388. doi:10.4049/jimmunol.2200761

Varghese, G. M., John, G., Thomas, K., Abraham, O. C., and Mathai, D. (2005). Predictors of multi-organ dysfunction in heatstroke. *Emerg. Med. J. EMJ* 22, 185–187. doi:10.1136/emj.2003.009365

Vestweber, D., Winderlich, M., Cagna, G., and Nottebaum, A. F. (2009). Cell adhesion dynamics at endothelial junctions: VE-cadherin as a major player. *Trends Cell Biol.* 19, 8–15. doi:10.1016/j.tcb.2008.10.001

Wan, L., Shi, X., Yang, J., Qian, J., Wang, F., Chen, R., et al. (2023). Construction and Validation of the Nomogram Based on von Willebrand Factor Predicting

Mortality in Patients with Heatstroke. *Ther. Hypothermia Temp. Manag.* 13, 191–199. doi:10.1089/ther.2022.0059

Wang, L., Song, Y., Zhang, P., Chen, W., Xiao, F., Zhou, P., et al. (2024a). Hypoxia-inducible factor prolyl hydroxylase inhibitor alleviates heatstroke-induced acute kidney injury by activating BNIP3 -mediated mitophagy. *FASEB J.* 38, e23723. doi:10.1096/fj.202400047R

Wang, Y., Fang, J., Liu, B., Shao, C., and Shi, Y. (2022). Reciprocal regulation of mesenchymal stem cells and immune responses. *Cell Stem Cell* 29, 1515–1530. doi:10.1016/j.stem.2022.10.001

Wang, Z., Zhu, J., Zhang, D., Lv, J., Wu, L., and Liu, Z. (2024b). The significant mechanism and treatments of cell death in heatstroke. *Apoptosis* 29, 967–980. doi:10.1007/s10495-024-01979-w

Warsy, A. S., Ansari, Z., Zhang, H., Vincent, J.-L., Alzeer, A. H., and Al-Arifi, A. (1999). Nitric oxide production is enhanced in patients with heat stroke. *Intensive Care Med.* 25, 58–62. doi:10.1007/s001340050787

Watts, N., Amann, M., Arnell, N., Ayeb-Karlsson, S., Beagley, J., Belesova, K., et al. (2021). The 2020 report of the lancet countdown on health and climate change: responding to converging crises. *Lancet* 397, 129–170. doi:10.1016/S0140-6736(20)32290-X

Wen, J., Lin, Z., Cheng, J., Li, C., Wang, L., Zou, Y., et al. (2024). Heat acclimation alleviates the heat stress-induced impairment of vascular endothelial cells. *Tissue Cell* 90, 102520. doi:10.1016/j.tice.2024.102520

Xia, Z.-N., Zong, Y., Zhang, Z.-T., Chen, J.-K., Ma, X.-J., Liu, Y.-G., et al. (2017). Dexmedetomidine protects against multi-organ dysfunction induced by heatstroke via sustaining the intestinal integrity. *Shock* 48, 260–269. doi:10.1097/SHK.0000000000000826

Xie, S., Sun, W., Zhang, C., Dong, B., Yang, J., Hou, M., et al. (2021a). Metabolic control by heat stress determining cell fate to ferroptosis for effective cancer therapy. *ACS Nano* 15, 7179–7194. doi:10.1021/acsnano.1c00380

Xie, W., Huang, W., Cai, S., Chen, H., Fu, W., Chen, Z., et al. (2021b). NF-κB/IκBα signaling pathways are essential for resistance to heat stress-induced ROS production in pulmonary microvascular endothelial cells. *Mol. Med. Rep.* 24, 814. doi:10.3892/mmr.2021.12454

Xie, Y., Hou, W., Song, X., Yu, Y., Huang, J., Sun, X., et al. (2016). Ferroptosis: process and function. *Cell Death Differ.* 23, 369–379. doi:10.1038/cdd.2015.158

Xu, J., Strasburg, G. M., Reed, K. M., Bello, N. M., and Velleman, S. G. (2023). Differential effects of temperature and mTOR and Wnt-planar cell polarity pathways on syndecan-4 and CD44 expression in growth-selected Turkey satellite cell populations. *PloS One* 18, e0281350. doi:10.1371/journal.pone.0281350

Xu, Q., Guo, X., Liu, J., Chen, B., Liu, Z., and Su, L. (2015a). Blockage of protease-activated receptor 1 ameliorates heat-stress induced intestinal high permeability and bacterial translocation. *Cell Biol. Int.* 39, 411–417. doi:10.1002/cbin.10408

Xu, Q., Liu, J., Wang, Z., Guo, X., Zhou, G., Liu, Y., et al. (2015b). Heat stress-induced disruption of endothelial barrier function is via PAR1 signaling and suppressed by xuebijing injection. *PLOS ONE* 10, e0118057. doi:10.1371/journal.pone.0118057

Yin, H., Wu, M., Lu, Y., Wu, X., Yu, B., Chen, R., et al. (2022). HMGB1-activatied NLRP3 inflammasome induces thrombocytopenia in heatstroke rat. *PeerJ* 10, e13799. doi:10.7717/peerj.13799

Yu, C., Huang, Y., Xie, J., Duan, C., Liu, S., Zhao, W., et al. (2024). HMGB1 released from pyroptotic vascular endothelial cells promotes immune disorders in exertional heatstroke. *Int. J. Hyperth.* 41, 2378867. doi:10.1080/02656736.2024.2378867

Yuan, F., Cai, J., Wu, J., Tang, Y., Zhao, K., Liang, F., et al. (2022). Z-DNA binding protein 1 promotes heatstroke-induced cell death. *Science* 376, 609–615. doi:10.1126/science.abg5251

Zang, Y., Zhang, B., Zhang, G., Hu, J., Shu, D., Han, J., et al. (2024). Effects of combined treatment with hydrogen-rich electrolyzed water and tea polyphenols on oxidative stress, intestinal injury and intestinal flora disruption in heat-stressed mice. *J. Therm. Biol.* 123, 103921. doi:10.1016/j.jtherbio.2024.103921

Zhang, S., Liu, Y., Wang, Z., Liu, J., Gu, Z., Xu, Q., et al. (2017). PAR1-mediated c-Jun activation promotes heat stress-induced early stage apoptosis of human umbilical vein endothelial cells. *Mol. Med. Rep.* 15, 2595–2603. doi:10.3892/mmr.2017.6303

Zhang, X., Wang, D., and Liu, J. (2023). Hypoxia-inducible factor-1α is involved in the response to heat stress in lactating dairy cows. *J. Therm. Biol.* 112, 103460. doi:10.1016/j.jtherbio.2023.103460

Zhang, Y., Deng, X., Zhang, J., Zhang, L., Akram, Z., Zhang, B., et al. (2022). A potential driver of disseminated intravascular coagulation in heat stroke mice: neutrophil extracellular traps. *Int. J. Environ. Res. Public. Health* 19, 12448. doi:10.3390/ijerph191912448

Zhao, Q., Guo, Y., Ye, T., Gasparrini, A., Tong, S., Overcenco, A., et al. (2021). Global, regional, and national burden of mortality associated with non-optimal ambient temperatures from 2000 to 2019: a three-stage modelling study. *Lancet Planet. Health* 5, e415–e425. doi:10.1016/S2542-5196(21)00081-4

Zhu, J., Jin, P., Zhou, T., Zhang, D., Wang, Z., Tang, Z., et al. (2024). SIRT1 modulates microglia phenotypes via inhibiting drp1 phosphorylation reduces neuroinflammation in heatstroke. *Brain Res. Bull.* 218, 111101. doi:10.1016/j.brainresbull.2024.111101

frontiers | Frontiers in Immunology

TYPE Mini Review
PUBLISHED 22 July 2025
DOI 10.3389/fimmu.2025.1567980

OPEN ACCESS

EDITED BY
Lulong Bo,
Navy Medical University, China

REVIEWED BY
Hao Zhang,
Fudan University, China

*CORRESPONDENCE
Yi Wang
w_yi2022@163.com
Xiaobo Huang
drhuangxb@163.com
Siyuan Song
si-yuan.song@bcm.edu

†These authors have contributed equally to this work

RECEIVED 28 January 2025
ACCEPTED 07 July 2025
PUBLISHED 22 July 2025

CITATION
Yao M, Liao J, Liu Z, Zhao W, Song S, Huang X and Wang Y (2025) Ferroptosis: a key driver and therapeutic target in the pathogenesis of acute respiratory distress syndrome.
Front. Immunol. 16:1567980.
doi: 10.3389/fimmu.2025.1567980

Ferroptosis: a key driver and therapeutic target in the pathogenesis of acute respiratory distress syndrome

Mingjun Yao[1†], Jinfeng Liao[2†], Zheng Liu[3†], Wei Zhao[1†], Siyuan Song[3*], Xiaobo Huang[4*] and Yi Wang[4,5*]

[1]School of Medicine, University of Electronic Science and Technology of China, Chengdu, China, [2]Department of Dermatology, Sichuan Provincial People's Hospital, University of Electronic Science and Technology of China, Chengdu, Sichuan, China, [3]Department of Neuroscience, Baylor College of Medicine, Houston, TX, United States, [4]Department of Critical Care Medicine, Sichuan Provincial People's Hospital, University of Electronic Science and Technology of China, Chengdu, Sichuan, China, [5]Translational Clinical Immunology Medicine Key Laboratory of Sichuan Province, Center of Organ Transplantation, Sichuan Academy of Medical Science and Sichuan Provincial People's Hospital, Chengdu, Sichuan, China

Acute Respiratory Distress Syndrome (ARDS) is a severe inflammatory lung condition often triggered by infections or sepsis, characterized by diffuse alveolar damage, pulmonary edema, and impaired gas exchange. Despite advances in supportive care, ARDS continues to have a high mortality rate. The pathogenesis of ARDS involves an exaggerated immune response leading to tissue damage and inflammation. Regulatory cell death pathways, particularly ferroptosis, an iron-dependent form of cell death driven by lipid peroxidation and oxidative stress, play a critical role in ARDS progression. Ferroptosis is characterized by the accumulation of lipid peroxides and is regulated by enzymes such as glutathione peroxidase 4 (GPX4) and the system Xc- antiporter. Dysregulation of these pathways exacerbates oxidative stress and tissue damage in ARDS. In the context of ARDS, ferroptosis contributes to the destruction of alveolar and endothelial cells, leading to increased vascular permeability, pulmonary edema, and impaired gas exchange. Immune cells like macrophages and neutrophils, while essential for pathogen clearance, can also contribute to lung injury when overactivated, highlighting the need for therapeutic strategies to modulate ferroptosis. Therapeutic targeting of ferroptosis in ARDS includes the use of antioxidants, GPX4 activators, iron chelators, and inhibitors of lipid peroxidation. These approaches aim to reduce oxidative stress, restore antioxidant defenses, and prevent iron-driven cell death. Future research must address challenges in identifying reliable biomarkers, understanding subphenotype-specific mechanisms, and integrating ferroptosis inhibitors into existing therapeutic frameworks. By targeting ferroptosis, it may be possible to mitigate ARDS severity and improve patient outcomes, offering new hope for the management of this devastating condition.

KEYWORDS

cell death pathways, immune homeostasis, acute respiratory distress syndrome, ferroptosis, immune cytokines

1 Introduction

Acute respiratory distress syndrome (ARDS) is a severe, life-threatening inflammatory condition of the lungs commonly triggered by infections such as bacterial pneumonia, viral pathogens (e.g., influenza and SARS-CoV-2), and systemic sepsis (1). Hallmarked by diffuse alveolar damage, pulmonary edema, hypoxemia, and impaired gas exchange, ARDS frequently necessitates mechanical ventilation in intensive care units (ICUs) (1, 2). Despite advancements in supportive care, infection-driven ARDS continues to have a high mortality rate of 30–50% (3).

The pathogenesis of ARDS involves an exaggerated immune response that damages alveolar structures, disrupts the alveolar-capillary barrier, and promotes excessive inflammation, vascular leakage, and oxygenation failure (4, 5). Immune cells like macrophages and neutrophils, while essential for pathogen clearance, contribute to lung injury when overactivated (6, 7). This highlights the critical need to maintain immune homeostasis to mitigate disease progression (8).

Regulated cell death pathways, such as apoptosis, pyroptosis, necroptosis, and ferroptosis, play pivotal roles in controlling inflammation and maintaining tissue integrity. However, their dysregulation can exacerbate inflammation and tissue damage in ARDS (9, 10). Among these, ferroptosis, an iron-dependent form of cell death driven by lipid peroxidation, oxidative stress, and glutathione depletion, has garnered significant attention (11). In ARDS, ferroptosis contributes to the destruction of alveolar and endothelial cells, thereby exacerbating lung injury (12).

Given the central role of oxidative stress and lipid peroxidation in ARDS, targeting ferroptosis represents a promising therapeutic strategy (13). This review explores the mechanisms of ferroptosis, its role in ARDS progression, and its potential as a target for therapeutic interventions.

2 Ferroptosis in infection and ARDS development

Cell death pathways play critical roles in immune homeostasis, infection defense, and inflammation resolution. In ARDS, an imbalance between these pathways contributes to exaggerated immune responses, tissue damage, and disease progression (14) Among these pathways, ferroptosis has emerged as a key player in infection-induced lung injury, offering new therapeutic insights for ARDS management (12).

2.1 Ferroptosis: a central player in ARDS pathogenesis

Ferroptosis is a regulated, iron-dependent form of cell death distinguished by oxidative damage and lipid peroxidation. It plays a dual role in infection and inflammation. While ferroptosis helps eliminate infected or damaged cells, its dysregulation exacerbates inflammation, tissue injury, and alveolar-capillary barrier dysfunction in ARDS (15). Understanding the mechanisms of ferroptosis offers opportunities for therapeutic intervention, especially in targeting oxidative stress and iron dysregulation.

2.2 Key molecular mechanisms of ferroptosis

Ferroptosis is characterized by the iron-dependent accumulation of lipid peroxides, driven by dysregulated oxidative stress and impaired antioxidant defenses. A central player in this process is glutathione peroxidase 4 (GPX4), an enzyme responsible for neutralizing lipid peroxides. When GPX4 is inhibited or depleted, lipid peroxidation spirals out of control, leading to cell death (16). The system Xc^-, which imports cystine for glutathione (GSH) synthesis, also plays a crucial role. Dysfunction of system Xc^- depletes GSH, further compromising the cell's ability to counteract oxidative damage (17).

Iron metabolism is another critical factor in ferroptosis. Excess free iron, often resulting from inflammation-induced disruption of iron homeostasis, generates reactive oxygen species (ROS) through the Fenton reaction (18). These ROS amplify lipid peroxidation, particularly in cell membranes rich in polyunsaturated fatty acids (PUFAs). Enzymes like ACSL4 (acyl-CoA synthetase long-chain family member 4) facilitate the incorporation of PUFAs into membrane phospholipids, increasing their vulnerability to peroxidation (19). Together, these mechanisms underscore the intricate interplay of oxidative stress, lipid metabolism, and iron dysregulation in driving ferroptosis (Figure 1).

2.3 Triggers and amplifiers of ferroptosis in ARDS

The pathological environment of ARDS provides multiple triggers for ferroptosis, exacerbating lung injury and inflammation. Oxidative stress is a hallmark of ARDS, with elevated ROS levels initiating and propagating lipid peroxidation (20–22). Mitochondrial dysfunction, a frequent feature in ARDS, further contributes to ROS generation and disrupts cellular redox balance, creating a vicious cycle of oxidative damage (22).

Inflammation also amplifies ferroptosis through cytokine-mediated pathways. Pro-inflammatory mediators, such as TNF-α and IL-1β, enhance iron dysregulation by promoting ferritin degradation and releasing free iron into the cytosol. This excess iron accelerates lipid peroxidation, aggravating tissue damage (22). Additionally, systemic inflammation and vascular leakage in ARDS disrupt iron transport and storage mechanisms, further compounding the pro-ferroptotic state (23). These interconnected triggers highlight the multifactorial nature of ferroptosis in ARDS and its significant role in disease progression.

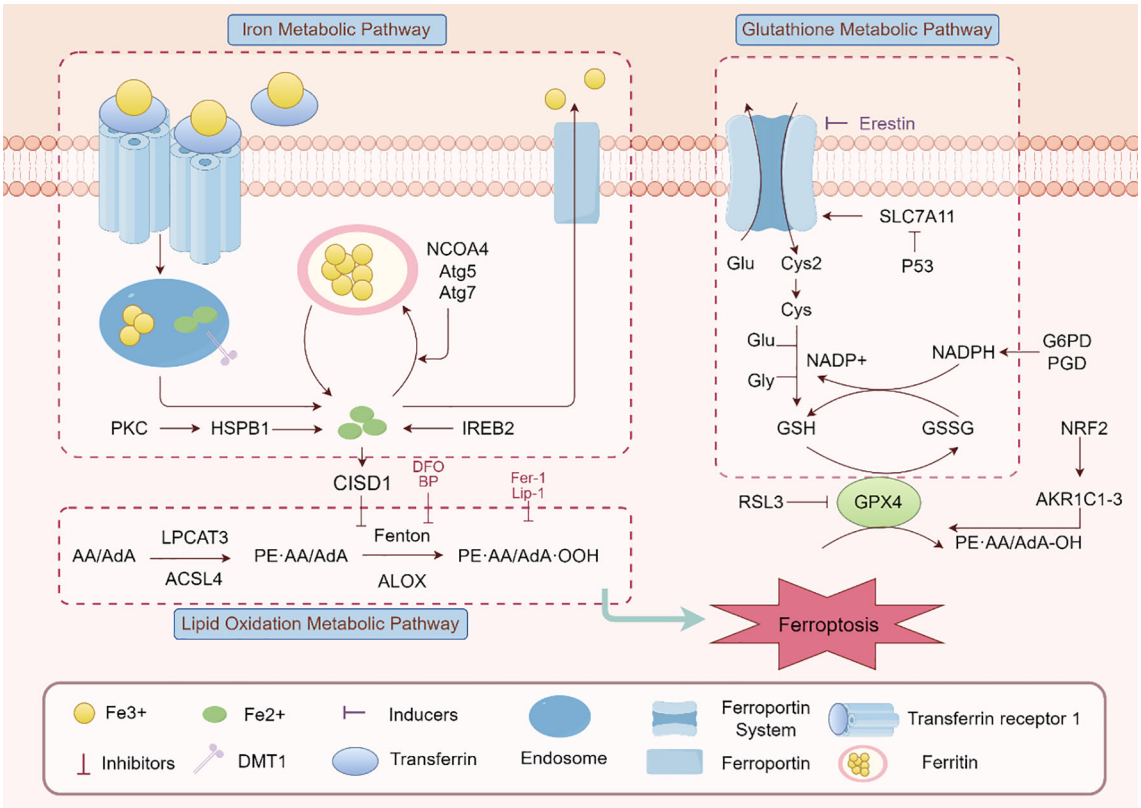

FIGURE 1
Ferroptosis signaling pathway. The main elements and interactions of ferroptosis, a type of controlled cell death marked by iron-dependent lipid peroxidation, are depicted in this figure. The pathway includes lipid oxidation (e.g., ALOX, LPCAT3), glutathione metabolism (e.g., GSH/GSSG, GPX4), and iron metabolism (e.g., transferrin receptor, ferroportin). Ferroptosis modulation is greatly aided by regulatory proteins like as Nrf2, p53, and SLC7A11. Additionally shown are ferroptosis inducers (like RSL3) and inhibitors (like Fer-1), emphasizing the harmony between pro- and anti-ferroptotic elements.

2.4 The role of hypoxia in ferroptosis induced ARDS

A common ARDS symptom, hypoxia, worsens lung damage in a number of ways. It is becoming more widely acknowledged that ferroptosis, a newly identified kind of controlled cell death triggered by iron-dependent lipid peroxidation, plays a major role in the pathophysiology of ARDS (24). A defining feature of ARDS is hypoxia, which is brought on by compromised gas exchange as a result of edema and alveolar injury (25). Pulmonary vasoconstriction, endothelial dysfunction, and the production of inflammatory cytokines are among the physiological and pathological alterations brought on by hypoxia. The hypoxia-inducible factor (HIF) pathway, which controls genes related to energy metabolism and iron homeostasis, is activated by the hypoxic environment in ARDS (26). Lung damage may be exacerbated by this pathway's ability to alter the equilibrium between the oxidative and antioxidant systems (Figure 2). In the context of ARDS, recent research has emphasized the link between ferroptosis and hypoxia. Ferroptosis can be facilitated by hypoxia in a number of ways. First of all, ferroptosis may be impacted by the overexpression of genes related to iron metabolism, such as HO-1, caused by the activation of HIF-1α in hypoxic environments (27). Second, oxidative stress brought on by hypoxia can deplete antioxidants such as glutathione, increasing the vulnerability of cells to ferroptosis and lipid peroxidation (28). For instance, via activating the Nrf2/HO-1 pathway and preventing ferroptosis, ferulic acid was demonstrated to mitigate alveolar epithelial barrier failure in sepsis-induced acute lung damage (29). This implies that one possible treatment approach for ARDS patients may be to target ferroptosis to reduce the damage that hypoxia causes to the lungs (Figure 3).

2.5 Crosstalk of ferroptosis with other cell death

The onset and progression of ARDS are significantly influenced by ferroptosis as well as other types of controlled cell death, including apoptosis, necroptosis, and pyroptosis (30).

Despite being two different types of cell death, ferroptosis and apoptosis have several regulatory mechanisms in common. Iron-dependent lipid peroxidation is the main cause of ferroptosis, which results in the buildup of lipid peroxides and cell death. Apoptosis, on the other hand, is distinguished by the cleavage of certain substrates and the activation of caspases. Recent research,

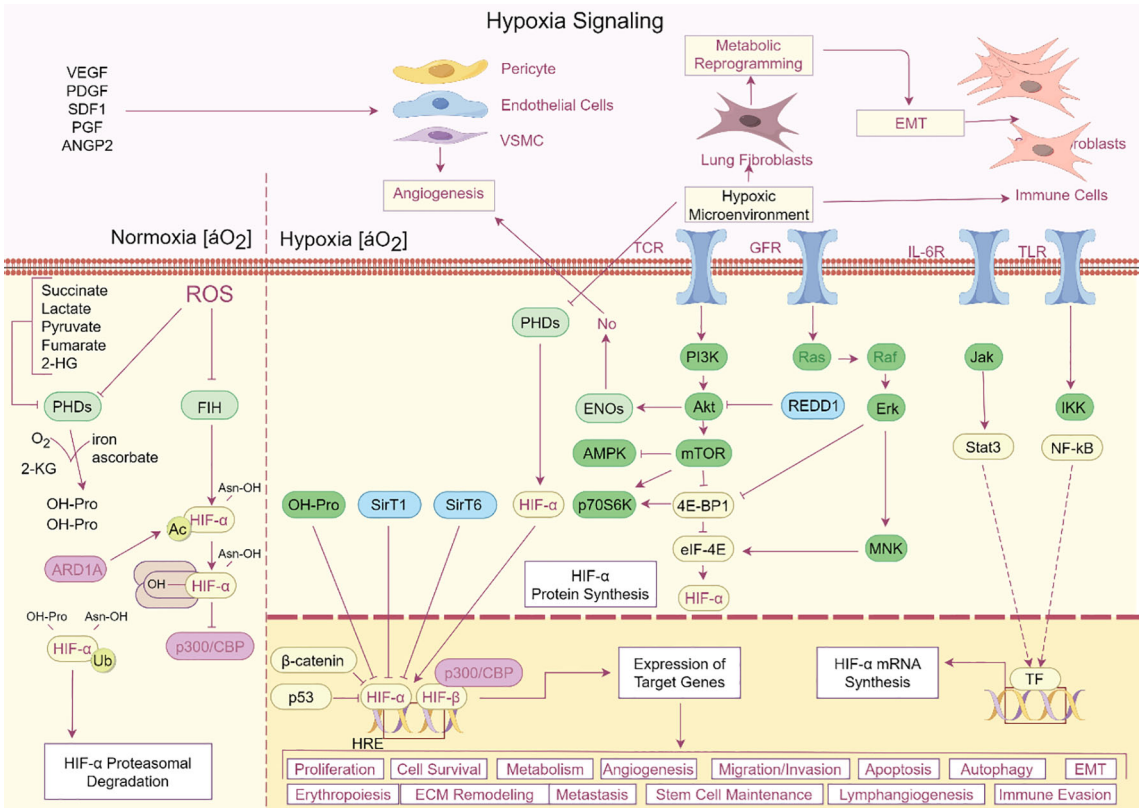

FIGURE 2
Hypoxia signaling pathway in ARDS. The complex hypoxia signaling cascade and its various impacts on cellular functions are depicted in this image. Oxygen levels fall in hypoxic environments, stabilizing HIF-α, which then dimerizes with HIF-β to bind HRE elements and control the expression of target genes. Numerous biological processes, including as cell division, survival, metabolism, angiogenesis, erythropoiesis, extracellular matrix remodeling, metastasis, and immune evasion, are impacted by this system. HIF-α is further stabilized by metabolic alterations such as increased lactate and succinate synthesis, which block PHDs and FIH. Angiogenesis and immune cell recruitment are encouraged by the upregulation of signaling molecules like VEGF, PDGF, and SDF-1. Hypoxia also affects stem cell maintenance, the epithelial-mesenchymal transition (EMT), and cell migration/invasion. Important regulators that interact with HIF-α to modify cellular responses are also highlighted in the picture, including PI3K, mTOR, AMPK, and NF-kB. This intricate network emphasizes how important hypoxia is in influencing the cellular microenvironment and triggering adaptive reactions in a range of healthy and pathological settings.

however, has demonstrated that apoptosis and ferroptosis can interact and affect one another. For instance, iron may be released from mitochondria as a result of apoptosis activation, which may subsequently encourage ferroptosis. Furthermore, apoptosis can be attenuated by inhibiting ferroptosis since it lowers the production of pro-apoptotic proteins (31, 32).

The necrosome, a complex made up of receptor-interacting protein kinase (RIPK) 1 and RIPK3, is responsible for regulating necrosis, or necroptosis (33). When necroptosis is triggered, mixed lineage kinase domain-like pseudokinase (MLKL) is phosphorylated, creating holes in the cell membrane and ultimately resulting in cell death (34). Ferroptosis and necroptosis can interact and affect one another, according to recent research. For example, iron may be released from injured cells as a result of necroptosis activation, which may subsequently encourage ferroptosis. The release of damage-associated molecular patterns (DAMPs), which are known to cause necroptosis, can be decreased by inhibiting ferroptosis (35).

Inflammasome activation causes pro-inflammatory cytokines, including IL-1β and IL-18 to be released during pyroptosis, a type of programmed cell death. Ferroptosis and pyroptosis can interact and affect one another, according to recent research. For instance, in deadly polymicrobial sepsis, gasdermin D-mediated pyroptosis can be triggered by lipid peroxidation during ferroptosis. Furthermore, ferroptosis suppression can attenuate pyroptosis by lowering the release of pro-inflammatory cytokines (9).

Numerous important molecular pathways are involved in the crosstalk between ferroptosis, necroptosis, and pyroptosis. The control of lipid peroxidation and iron metabolism is one important mechanism. Cell death may result from lipid peroxidation brought on by iron excess. Enzymes like glutathione peroxidase 4 (GPX4), which lowers lipid hydroperoxides and inhibits lipid peroxidation, control this process. Ferroptosis results from increased lipid peroxidation caused by GPX4 deficiency (36). The tumor suppressor p53 and its downstream targets regulate ferroptosis, which is another significant mechanism. By upregulating genes related to lipid peroxidation and iron absorption, p53 can cause ferroptosis (37). Furthermore, the Nrf2/ARE pathway, which controls redox homeostasis, is essential for preventing ferroptosis in cells. Nrf2 helps sustain cellular viability by transcriptionally activating anti-ferroptotic genes, including SLC7A11 and HO-1 (38).

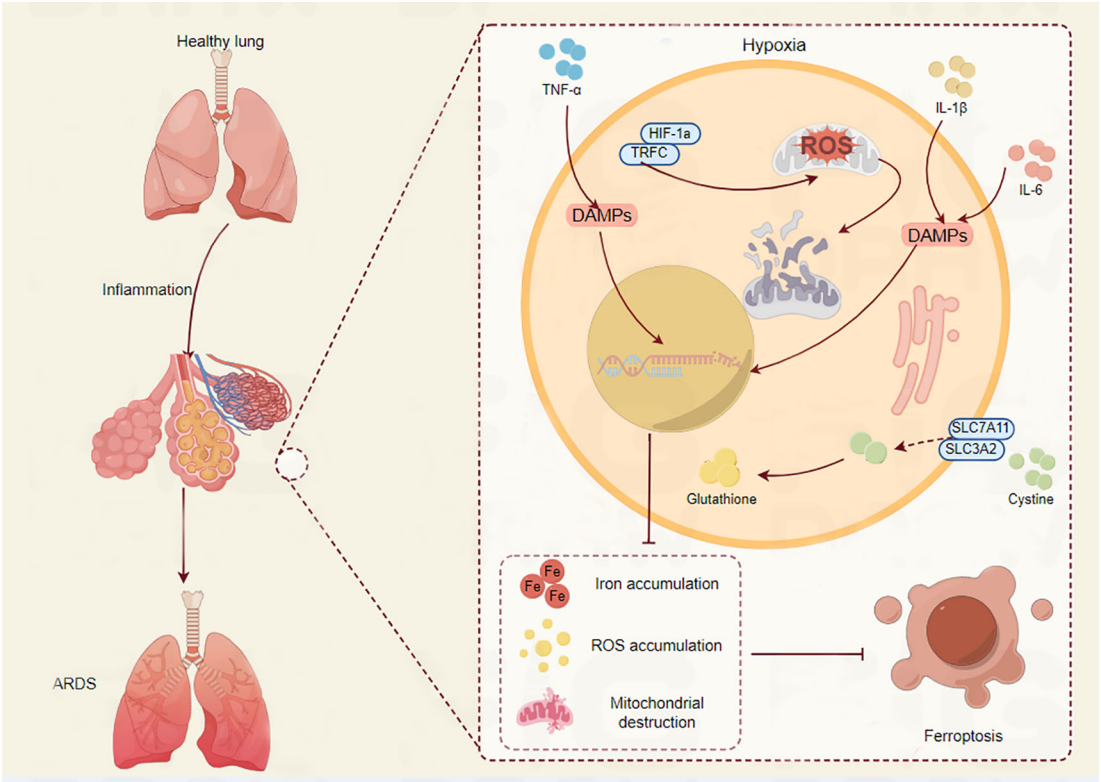

FIGURE 3
The crucial role of ferroptosis in ARDS progression. The connection between ferroptosis and hypoxia in relation to lung injury is depicted. The lung maintains homeostasis under normal circumstances. On the other hand, TNF-α and IL-1β levels rise during hypoxia, which causes HIF-1α to stabilize. This sets off a series of events that include the release of damage-associated molecular patterns (DAMPs), which fuel inflammation, and the generation of reactive oxygen species (ROS). By raising glutathione levels, the xCT cystine-glutamate antiporter's components SLC7A11 and SLC3A2 are upregulated in an effort to combat oxidative stress. But this is frequently not enough. The condition is made worse by the buildup of iron and ROS, which ultimately results in the loss of mitochondria. Acute respiratory distress syndrome (ARDS) is a result of these alterations, which ultimately lead to ferroptosis, a type of controlled cell death. The intricate relationship between ferroptosis, inflammation, and hypoxia in lung pathology is depicted in this image.

3 Ferroptosis in the development of ARDS

3.1 Alveolar epithelial cell damage

The distinct functions of ferroptosis in alveolar type I (AT1) and type II (AT2) epithelial cells have been brought to light by recent research, offering information about possible treatment targets (39).

AT1 cells regulate gas exchange and preserve alveolar shape (40). These cells are especially prone to ferroptosis because of their exposure to oxidative stress and role in maintaining the alveolar-capillary membrane (41). However, the majority of studies focused on AT2 cells. AT2 cells are essential for the synthesis of surfactants and alveolar healing. Particularly in diseases like sepsis and ischemia-reperfusion injury, ferroptosis in AT2 cells has been linked to the pathophysiology of ARDS (42). AT2 cells displayed ferroptotic symptoms, such as mitochondrial contraction and ruptured mitochondrial membranes, in a study on sepsis-induced ALI/ARDS (43). The study also emphasized how regulatory elements like MUC1 suppress ferroptosis by modulating the GSK3β/KEAP1-Nrf2-GPX4 axis. MUC1 has been demonstrated to prevent ferroptosis in AT2 cells by promoting Nrf2 nuclear translocation, increasing GSK3β phosphorylation, decreasing KEAP1 expression, and raising GPX4 levels (44).

Ferroptosis in alveolar epithelial cells is caused by a number of important processes and regulatory variables. One important mechanism that controls redox homeostasis and guards against ferroptosis is the Nrf2/ARE pathway (45). Anti-ferroptotic genes, including SLC7A11 and HO-1, are transcriptionally activated by Nrf2, promoting cellular survival. According to a study on intestinal ischemia-reperfusion (IIR)-induced ALI/ARDS, Nrf2 inhibits oxidative stress and attenuates ferroptosis via controlling the amounts of ferroptosis-related proteins, such as SLC7A11 and GPX4. Additional regulatory elements include PCTR1, circEXOC5, and AUF1. The mRNA-binding protein AUF1 reduces sepsis-associated ALI damage by negatively affecting ATF3 and positively regulating Nrf2, which in turn controls ferroptosis (46). Through the enhancement of ATF3 mRNA degradation and the reduction of GPX4 levels, CircEXOC5 controls the IGF2BP2/ATF3 axis to promote ferroptosis (47). The potential of PCTR1, a protectin compound, as a therapeutic target has been highlighted by its ability to control ferroptosis in alveolar epithelial cells (48).

Ferroptosis inhibitors have been shown in preclinical research to lessen lung damage in ARDS animals. Ferrostatin-1 and Liproxstatin-1, two well-known inhibitors of ferroptosis, for instance, have demonstrated protective benefits in both ARDS and ALI models (49). These inhibitors prevent cell death by lowering lipid peroxidation. In a study that used an LPS-induced ALI model, ferrostatin-1 therapy successfully decreased inflammation and lung damage (50). Likewise, it has been demonstrated that ginseng diol (Px), which is extracted from the root of ginseng, reduces LPS-induced ALI/ARDS via activating the KEAP1/Nrf2/HO-1 pathway (51).

3.2 Endothelial cell dysfunction

One characteristic of ARDS is endothelial cell dysfunction, which exacerbates lung injury by disrupting the alveolar-capillary barrier. One important mechanism behind endothelial cell dysfunction in ARDS is ferroptosis, a kind of cell death caused by iron-dependent lipid peroxidation (52) (Figure 4).

Iron-dependent lipid peroxidation, which causes lipid peroxides to build up and ultimately cause cell death, is a hallmark of ferroptosis. Because endothelial cells are subjected to severe oxidative stress in ARDS, this mechanism is especially pertinent. ARDS patients have been found to have dysregulated iron metabolism, as evidenced by elevated levels of total and non-heme iron in plasma and bronchoalveolar lavage fluid (BALF) when compared to healthy controls. Ferroptosis's involvement is reinforced by the recent finding of lipid hydroperoxides in the pulmonary drainage fluid of ARDS patients (53).

Lipid peroxidation, the glutathione (GSH)/GPX4 axis, and iron metabolism comprise the central signaling mechanism of ferroptosis. The Fenton reaction, in which iron catalyzes the production of reactive oxygen species (ROS) that target

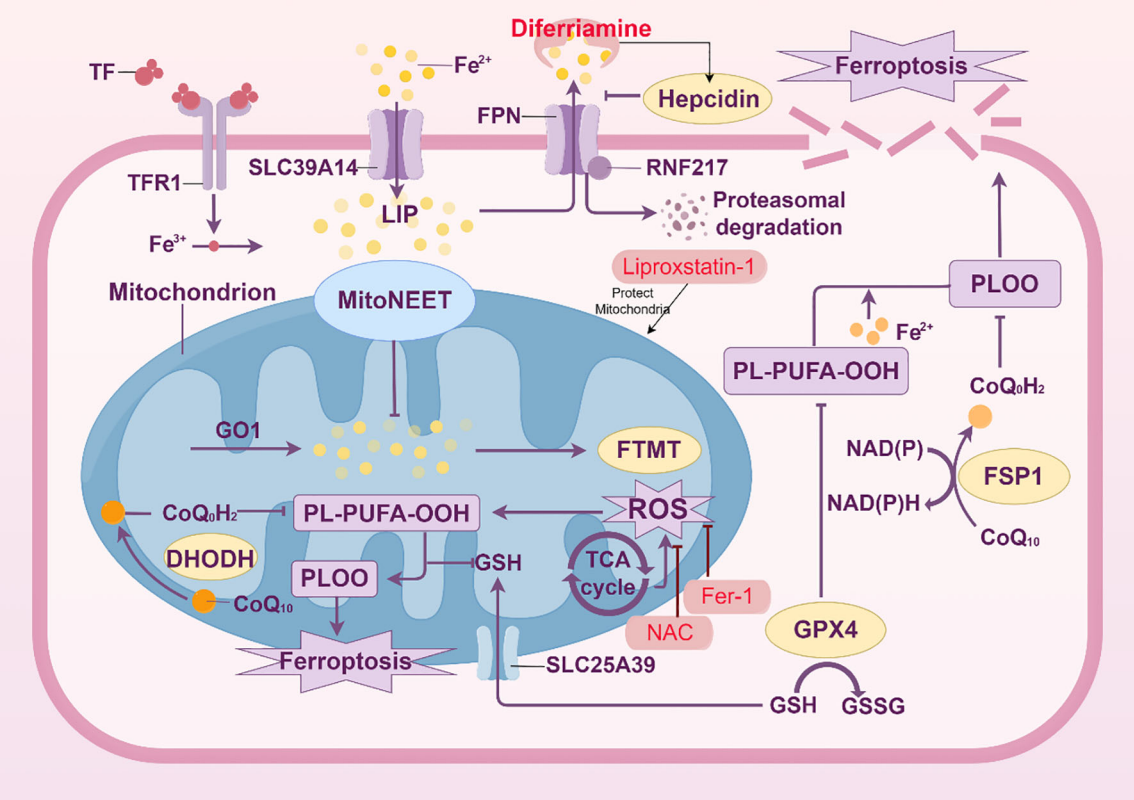

FIGURE 4
Mechanisms of ferroptosis in endothelial cells. The intricate metabolic and signaling processes involved in ferroptosis, a type of controlled cell death marked by iron-dependent lipid peroxidation, particularly in endothelial cells, are depicted in this picture. Iron buildup triggers ferroptosis, which is controlled by ferroportin (FPN) and hepcidin and mediated by the transferrin receptor (TFR1). Increased labile iron pool (LIP) from iron overload catalyzes the Fenton reaction, which produces lipid reactive oxygen species (ROS) and peroxidation products (such PL-PUFA-OOH). Several important defense mechanisms against ferroptosis are highlighted in the figure. By converting CoQ10 to ubiquinol (CoQoH2), which scavenges ROS, the mitochondrial protein MitoNEET and the ferroptosis suppressor protein 1 (FSP1) have been demonstrated to preserve mitochondria. Lipid peroxide detoxification relies heavily on the glutathione (GSH) system, which includes the enzyme GPX4 and the GSH/GSSG balance. Furthermore, the function of the mitochondrial GSH transporter SLC25A39 in preserving mitochondrial GSH levels is highlighted. The effectiveness of ferroptosis inhibitors, including Liproxstatin-1 and Fer-1, to stop lipid peroxidation and stop cell death is highlighted. On the other hand, it has been demonstrated that ferroptosis inducers such as RSL3 interfere with these defenses. The role of NAD(P)H and the elements of the electron transport chain (such as CoQ10 and DHODH) in preserving redox homeostasis is also depicted in the picture. The balance between pro- and anti-ferroptotic components is highlighted in this picture, which offers a thorough summary of the molecular pathways and regulatory mechanisms that control ferroptosis in endothelial cells.

polyunsaturated fatty acids (PUFAs) in cell membranes, can cause ferroptosis in endothelial cells. Lipid peroxides produced by this mechanism have the potential to cause cell death. One important aspect of lipid peroxidation is the generation of hydroxyl radicals (OH•), which can be fatal to cells if they accumulate excessively (54).

Through an array of procedures, ferroptosis contributes to endothelial cell damage as ARDS progresses (55). Patients with ARDS may have elevated iron levels in their lungs, which may lead to oxidative stress while stimulating lipid peroxidation (56). As a result, the alveolar-capillary barrier collapses, vascular permeability increases, and pulmonary edema develops. Ferroptosis inhibitors, including ferrostatin-1 and lipostatin-1, have been demonstrated in studies that reduce lung damage in ARDS models by decreasing lipid peroxidation and inhibiting cell death. In the meantime, ferroptosis in endothelial cells during ARDS is modulated by a number of regulatory variables and pathways. In order to maintain a redox state of equilibrium and prevent ferroptosis, the transcription factor Nrf2 is essential. Anti-ferroptotic genes, including SLC7A11 and HO-1, which support cellular survival, have their transcription activated by Nrf2. According to a study on LPS-induced ARDS, Nrf2 inhibits oxidative stress and attenuates ferroptosis via controlling the amounts of ferroptosis-related proteins, such as SLC7A11 and GPX4. Additional regulatory elements include PCTR1 (48), circEXOC5 (47), and AUF1 (46). The mRNA-binding protein AUF1 reduces sepsis-associated ALI damage by negatively affecting ATF3 and positively regulating Nrf2, which in turn controls ferroptosis. Through the enhancement of ATF3 mRNA degradation and the reduction of GPX4 levels, CircEXOC5 controls the IGF2BP2/ATF3 axis to promote ferroptosis (47).

3.3 Fibroblast

The survival controls for ARDS fibroblasts differ from those for healthy lung fibroblasts. They have a higher fibroproliferative capacity and can divide *in vitro* without the need for extra growth factors. If this increased proliferative ability is not appropriately controlled, it may result in excessive fibrosis. During the resolution phase of ARDS, ferroptosis has been identified as a method to limit fibroblast proliferation and eliminate surplus cells (57).

Ferroptosis in fibroblasts is caused by a number of important processes and regulatory variables. The control of lipid peroxidation and iron metabolism is one important mechanism. Cell death may result from lipid peroxidation brought on by iron excess. Enzymes like glutathione peroxidase 4 (GPX4), which lowers lipid hydroperoxides and inhibits lipid peroxidation, control this process. Ferroptosis results from increased lipid peroxidation caused by GPX4 deficiency. The tumor suppressor p53 and its downstream targets regulate ferroptosis, which is another significant mechanism. By upregulating genes related to lipid peroxidation and iron absorption, p53 can cause ferroptosis. Furthermore, fibroblasts are shielded against ferroptosis by the Nrf2/ARE pathway, which controls redox homeostasis. Anti-ferroptotic genes, including SLC7A11 and HO-1, are transcriptionally activated by Nrf2, promoting cellular survival. More information on the function of ferroptosis in fibroblasts during ARDS has been revealed by recent investigations. One study showed, for example, that fibroblasts from ARDS patients are more prone to ferroptosis than normal fibroblasts themselves (9). Higher iron and lipid peroxidation markers are linked to this heightened vulnerability. Inhibiting ferroptosis in fibroblasts has been demonstrated in another study to decrease fibroproliferation and enhance lung function in ARDS animals (58).

3.4 Immune cell dysregulation

Immune cells, including macrophages, neutrophils, T cells, and B cells, play a dual role in ARDS pathogenesis. Ferroptosis in these cells disrupts immune homeostasis and contributes to inflammation and tissue injury (Figure 5).

3.4.1 Macrophages

In response to environmental stimuli, macrophages can polarize into different phenotypes, demonstrating their extraordinary adaptability. M1 (classically activated) and M2 (alternatively activated) macrophages are the two primary phenotypes. While M2 macrophages are anti-inflammatory and support tissue healing and inflammation, M1 macrophages are pro-inflammatory and participate in eliminating infections and tissue damage. By changing the cellular environment and the accessibility of iron, which is essential for macrophage activity, ferroptosis might affect macrophage polarization. In diseases like ARDS, iron excess can exacerbate tissue damage by skewing macrophage polarization toward a pro-inflammatory M1 phenotype. On the other hand, suppressing ferroptosis might enhance an M2 phenotype that is anti-inflammatory, which may help decrease tissue damage and inflammation (59).

Depletion of glutathione peroxidase 4 (GPX4), an enzyme that lowers lipid hydroperoxides and inhibits lipid peroxidation, is the main cause of ferroptosis in macrophages (60). Cell death results from increased lipid peroxidation caused by GPX4 deficiency. The excessive accumulation of iron, which triggers the Fenton reaction and produces reactive oxygen species (ROS), makes this process more severe. Macrophages in ARDS are more vulnerable to ferroptosis because they are subjected to greater amounts of oxidative stress and iron overload. Ferroptotic macrophages can intensify the inflammatory response by releasing pro-inflammatory cytokines and damage-associated molecular patterns (DAMPs). For example, ferroptotic macrophages have the ability to generate HMGB1, a DAMP that triggers the release of pro-inflammatory cytokines, including IL-1β and IL-18, and activates the inflammasome (61).

By increasing inflammation and blocking tissue healing, ferroptosis in macrophages in ARDS increases the severity of lung damage. Ferroptotic macrophages can trigger a systemic inflammatory response by releasing DAMPs and pro-inflammatory cytokines that can activate the inflammasome. This

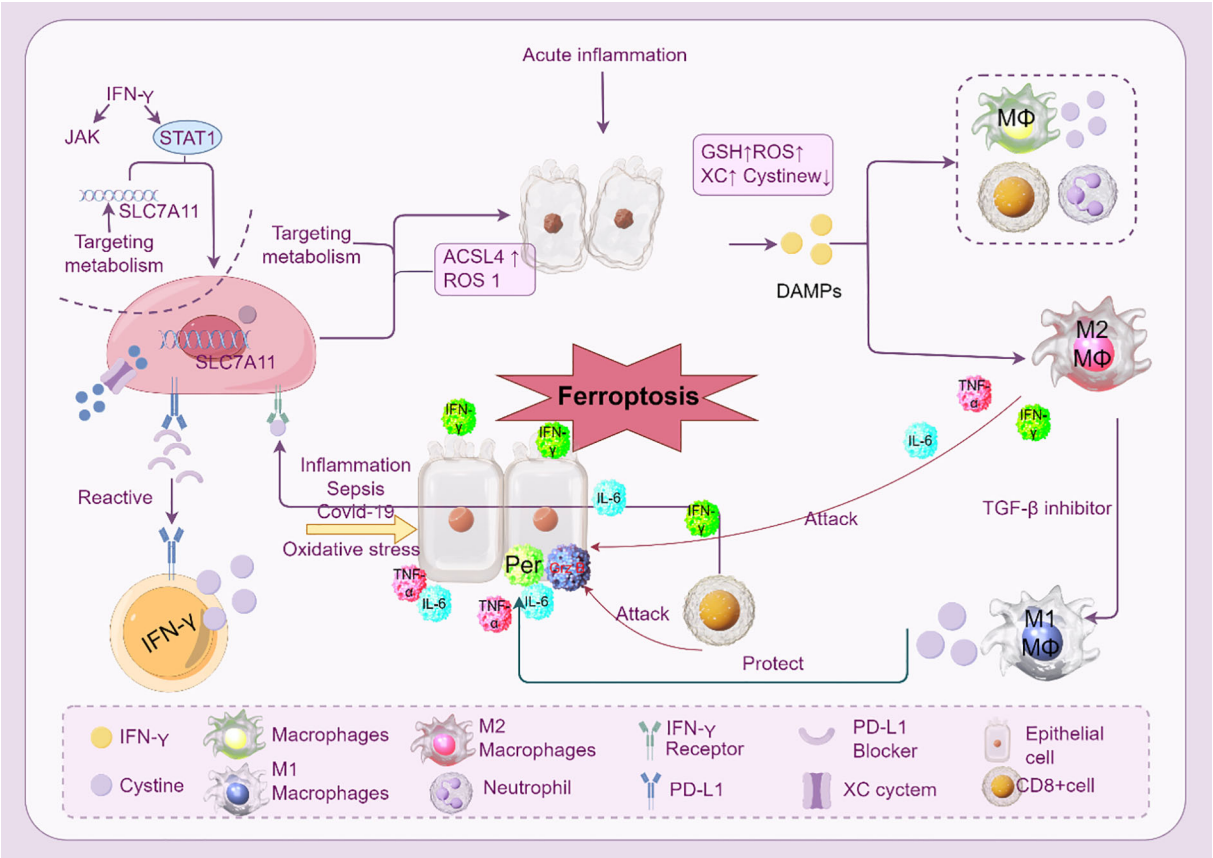

FIGURE 5
Ferroptosis and immune cells in ARDS. The interaction between immune cells and ferroptosis during acute inflammation and sepsis-induced ARDS is depicted. Numerous immune cells and cytokines control ferroptosis, which is typified by iron-dependent lipid peroxidation. By producing cytokines like IL-6 and TNF-α, macrophages (M1 and M2) are essential in controlling ferroptosis. By downregulating the cystine-glutamate antiporter (SLC7A11) and upregulating the generation of ROS and ACSL4, IFN-γ, which is generated by CD8+ T cells, can cause ferroptosis in macrophages. By producing ROS and DAMPs, neutrophils also aid in ferroptosis. The image emphasizes the role of metabolic pathways (like GSH and ROS) and the consequences of using inhibitors to target these pathways (such ferroptosis inhibitors and SLC7A11 targeting). Furthermore, the function of epithelial cells in triggering ferroptosis via receptor blockage and PD-L1 expression is illustrated.

contributes to the pathophysiology of ARDS by generating a self-amplifying loop of inflammation. Furthermore, ferroptosis may disrupt macrophage function by decreasing their capacity to eliminate infections and their phagocytic activity. This may result in a persistent inflammatory reaction and a delayed recovery from lung damage. Research has demonstrated that in ARDS models, preventing macrophage ferroptosis may minimize tissue damage and inflammation (62).

A potential treatment approach to reduce inflammation and tissue damage in ARDS is to target ferroptosis in macrophages. It has been demonstrated that ferroptosis inhibitors, such as ferrostatin-1 (Fer-1) and lipostatin-1, lower lipid peroxidation and arrest macrophage death. These inhibitors may improve ARDS outcomes by regulating the inflammatory response (63). Furthermore, enhancing cellular antioxidant defenses by targeting the Nrf2 pathway may offer a viable strategy for reducing macrophage dysfunction and improving ARDS outcomes (64). Anti-ferroptotic genes, including SLC7A11 and HO-1, which support cellular survival, have their transcription activated by Nrf2.

3.4.2 Neutrophils

The most prevalent kind of white blood cells, neutrophils, are among the first to arrive at areas of inflammation and infection (65). They play a crucial role in the phagocytosis of pathogens, the release of reactive oxygen species (ROS), and antimicrobial peptides. However, by releasing oxidants, proteases, and other inflammatory mediators, neutrophils can cause tissue damage in diseases like ARDS. Numerous triggers, such as infection, ischemia-reperfusion injury, and exposure to pro-inflammatory cytokines, can cause neutrophils to undergo ferroptosis. Increased iron absorption, lipid peroxidation, and the buildup of lipid peroxides, which results in cell death, are the hallmarks of the process. This type of cell death differs from necrosis and apoptosis in that it involves particular morphological changes and metabolic processes (66).

Numerous important pathways and regulatory variables are involved in the molecular mechanisms that underlie neutrophil ferroptosis. The reduction of glutathione peroxidase 4 (GPX4), an enzyme that lowers lipid hydroperoxides and inhibits lipid peroxidation, is one important mechanism (67). Cell death results

from increased lipid peroxidation caused by GPX4 deficiency. Furthermore, iron buildup exacerbates oxidative stress and lipid peroxidation by catalyzing the Fenton reaction, which produces ROS. The Nrf2/ARE pathway, which controls redox homeostasis and fights against ferroptosis, is another regulatory component. Anti-ferroptotic genes, including SLC7A11 and HO-1, are transcriptionally activated by Nrf2, promoting cellular survival. These pathways are crucial for neutrophil survival and function since blocking them can make individuals more susceptible to ferroptosis (66).

Neutrophils are frequently detected in a highly active state in ARDS, which exacerbates lung injury and causes the release of pro-inflammatory cytokines. Neutrophils that undergo ferroptosis may die and emit damage-associated molecular patterns (DAMPs), which intensifies the inflammatory response (68). For example, HMGB1, a DAMP that triggers the inflammasome and promotes the release of pro-inflammatory cytokines including IL-1β and IL-18, can be released by ferroptotic neutrophils. This exacerbates ARDS by generating a self-reinforcing cycle of inflammation. Furthermore, ferroptosis can hinder neutrophil function by decreasing their capacity to eliminate infections and engage in phagocytic activity. This may result in a protracted inflammatory reaction and a delayed recovery from lung damage. In ARDS models, studies have demonstrated that preventing neutrophil ferroptosis can lessen tissue damage and inflammation (69).

3.4.3 T cells

The inflammatory response and tissue damage seen in ARDS are largely caused by T cells, which are essential elements of the adaptive immune system (70). Here, we provide an overview of the connection between ferroptosis and T cell function, with particular attention to the roles that several T cell subtypes, including Th1, Th2, Th17, Th22, Treg, γδ T cells, effector T cells, and memory T cells, in ARDS (70).

Pro-inflammatory Th1 cells generate cytokines including TNF-α and IFN-γ, which are essential for combating intracellular infections. Through the secretion of these cytokines, Th1 cells in ARDS may be involved in tissue destruction. Th1 cells that undergo ferroptosis may perish and emit damage-associated molecular patterns (DAMPs), which intensifies the inflammatory response. Research has demonstrated that in ARDS models, preventing Th1 cell ferroptosis can lessen tissue damage and inflammation (71). Th2 cells are known to produce cytokines, including IL-4, IL-5, and IL-13, and are important in the immune response towards external infections. Th2 cells are useful in tissue regeneration and inflammation resolution in ARDS. Th2 cells that undergo ferroptosis might function less effectively and cause a prolonged inflammatory response (72). It may be possible to sustain Th2 cells' anti-inflammatory properties and enhance ARDS results by preventing ferroptosis (71). Th17 cells are essential for the immune response against extracellular bacteria and fungi because they generate IL-17. Th17 cells can cause tissue damage in ARDS by releasing IL-17, which encourages neutrophil activation and recruitment. Th17 cell ferroptosis can result in DAMP release and cell death, which exacerbates inflammation (73, 74). Th17 cell ferroptosis inhibition could mitigate tissue damage along with improving ARDS outcomes (72). IL-22, which is important in barrier function and tissue repair, is produced by Th22 cells, a subgroup of T helper cells. Th22 cells may assist in tissue regeneration and inflammation resolution in ARDS. Th22 cells that undergo ferroptosis have reduced function and cause a lengthy inflammatory response (75). A distinct subgroup of T cells known as γδ T cells is capable of identifying and reacting to a broad variety of infections. γδ T cells may help in tissue healing and the immune response in ARDS. A protracted inflammatory response can result from ferroptosis in γδ T cells, which can affect their function (76).

Preventing excessive inflammation and preserving immunological tolerance depend on Treg cells. Treg cells may assist in tissue healing and inflammatory response modulation in ARDS (77). Treg cell ferroptosis can affect the extent to which they function and cause unchecked inflammation. Treg cell ferroptosis inhibition may preserve immunological tolerance and enhance ARDS outcomes (70).

Activated T cells that have undergone differentiation to carry out specific activities, such as cytotoxicity or cytokine production, are known as effector T cells (78). Effector T cells can cause tissue damage in ARDS by releasing cytotoxic and pro-inflammatory cytokines (79). Effector T cell ferroptosis can result in DAMP release and cell death, which intensifies the inflammatory response. Reducing tissue damage and improving outcomes in ARDS may be achieved by inhibiting effector T cell ferroptosis.

3.4.4 B cells

The adaptive immune system's main constituents, B cells, are essential for the tissue damage and immunological response seen in ARDS (80). Depletion of glutathione peroxidase 4 (GPX4), an enzyme that lowers lipid hydroperoxides and inhibits lipid peroxidation, is the main cause of ferroptosis in B cells (81). Cell death results from increased lipid peroxidation caused by GPX4 deficiency. Furthermore, iron buildup exacerbates oxidative stress and lipid peroxidation by catalyzing the Fenton reaction, which produces reactive oxygen species (ROS).

Generating an adaptive immune response requires naive B cells, which are the progenitors of effector and memory B cells. Naive B cells may become fewer in number and less able to react to antigens if ferroptosis is induced in them. Since effector B cells are necessary for the creation of antibodies and other immunological processes, this can subsequently impair the immune response as a whole (82). According to studies, p53-mediated reactions and the stimulation of polyamine metabolism can cause ferroptosis in naive B cells. Spermidine/spermine N (1)-acetyltransferase (SAT1) is upregulated in this process, and it interacts with p53-mediated ferroptotic reactions to promote polyamine metabolism (83). Effector B cells are activated B cells that have undergone differentiation to carry out particular tasks, such as producing antibodies. By releasing pro-inflammatory cytokines and antibodies, effector B cells in ARDS can cause tissue damage. DAMPs are released when effector B cells undergo ferroptosis, which can result in cell death and intensify the inflammatory response (84). Inhibiting effector B cell ferroptosis may reduce tissue damage and enhance ARDS results. When re-exposed

to a pathogen, memory B cells, the long-lived B cells, offer a strong and quick defense. Memory B cells can support tissue healing and the immune response in ARDS (81). A subpopulation of B cells known as Bregs is essential for preserving immunological tolerance and limiting excessive inflammation. Bregs with ferroptosis may have impaired function and uncontrolled inflammation. According to research, Breg activity can be inhibited by downregulating the expression of the thioredoxin (TXN) gene, which encourages the development of pro-inflammatory B cells and causes systemic inflammation (85). On the other hand, in illness models, elevated TXN expression can reduce lung tissue damage and raise survival rates (82). Ferroptosis in B cells is controlled by similar signaling mechanisms (81).

3.5 Other cells

For lung regeneration and repair, pulmonary endogenous stem cells are essential. These cells are essential for preserving lung homeostasis because they have the ability to develop into a variety of lung cell types, such as endothelial and alveolar epithelial cells (86). Significant damage is done to the lung tissue in ARDS, and tissue regeneration and repair depend on endogenous stem cell activation. According to recent research, ARDS patients frequently exhibit downregulated expression levels of pulmonary endogenous stem cells, which may hinder the lung's capacity for self-healing. Multipotent stromal cells called mesenchymal stem cells (MSCs) have the ability to differentiate into a variety of cell types, such as adipocytes, osteoblasts, and chondrocytes. Because of their immunomodulatory and tissue-repair capabilities, MSCs have demonstrated potential in the treatment of ARDS. MSCs can release growth factors and anti-inflammatory cytokines, which aid in tissue repair and inflammation reduction in the lungs (87). Furthermore, MSCs can improve the viability and function of injured lung cells by transferring mitochondria to them. One important way that MSCs lessen lung damage in ARDS is by this mitochondrial translocation (88).

MSCs, ferroptosis, and pulmonary endogenous stem cells interact in a complicated and multidimensional way. Both MSCs and pulmonary endogenous stem cells have the ability to alter the lung's inflammatory milieu, which can affect how vulnerable lung cells are to ferroptosis. MSCs, for instance, have the ability to release substances that prevent ferroptosis, shielding lung cells from iron-dependent lipid peroxidation (89). Furthermore, pulmonary endogenous stem cell activation can encourage tissue healing and lessen the need for ferroptosis-induced cell replacement. Novel therapeutic approaches for ARDS may be offered by focusing on the inhibition of ferroptosis of MSCs and pulmonary endogenous stem cells. Enhancing the activity of MSCs and pulmonary endogenous stem cells, for example, may encourage lung healing and lessen the severity of ARDS. Furthermore, preventing ferroptosis may prevent the death of vital lung cells, maintaining lung function. MSC therapy for ARDS has demonstrated encouraging outcomes in recent clinical trials, underscoring the cells' capacity to reduce inflammation and encourage tissue repair (68).

4 Ferroptosis and ARDS progression

4.1 Oxidative stress and ROS amplification

Oxidative stress is a hallmark of ARDS and plays a pivotal role in driving ferroptosis. The excessive production of ROS during ARDS creates an environment conducive to ferroptotic cell death. In alveolar epithelial cells and endothelial cells, mitochondrial dysfunction serves as a major source of ROS. Damage to the mitochondrial electron transport chain increases ROS leakage, further amplifying oxidative stress (12). This ROS overproduction, compounded by elevated iron levels, enhances lipid peroxidation, a key feature of ferroptosis.

Lipid peroxidation forms a feedback loop that exacerbates ferroptosis and ARDS progression. Lipid hydroperoxides accumulate in the cellular membranes of lung cells, destabilizing the barrier functions of alveolar epithelial and endothelial cells. The inability of antioxidant systems, such as GPX4-dependent pathways, to counteract ROS amplifies ferroptotic damage (90). This cycle of ROS generation and lipid peroxidation perpetuates oxidative injury, worsening inflammation, vascular permeability, and respiratory dysfunction in ARDS patients (91).

4.2 Iron overload and dysregulated metabolism

Iron overload is a critical factor that drives ferroptosis and worsens ARDS pathology. In ARDS, disrupted iron homeostasis leads to the accumulation of free iron, increasing the availability of $Fe2^{+}$ for the Fenton reaction. This reaction generates hydroxyl radicals, a highly reactive form of ROS, which accelerates lipid peroxidation and cell death. Elevated levels of ferritin and transferrin, markers of iron dysregulation, have been observed in clinical ARDS cases, linking iron metabolism to disease severity (12).

Mitochondrial dysfunction exacerbates iron-driven ferroptosis by impairing the organelle's ability to sequester and regulate iron levels. Mitochondrial iron accumulation further disrupts redox homeostasis, amplifying oxidative stress and contributing to persistent cellular injury (92). Dysregulated iron metabolism not only promotes ferroptosis but also disrupts essential metabolic processes required for tissue repair, highlighting its role in ARDS progression (53).

4.3 Fibrosis and long-term outcomes

The chronic inflammation and unresolved ferroptosis associated with ARDS contribute significantly to lung fibrosis and long-term complications. Persistent ferroptosis in alveolar and endothelial cells triggers pro-fibrotic signaling pathways, such as those involving TGF-β and connective tissue growth factor (CTGF), which drive ECM deposition and fibroproliferation. This fibroproliferative response compromises lung elasticity, impairs

alveolar regeneration, and leads to irreversible remodeling of lung tissue (93).

Unresolved ferroptosis also hinders the recovery of injured lung cells. By depleting populations of functional alveolar epithelial cells, ferroptosis prevents the repair of the alveolar-capillary barrier, leaving the lung vulnerable to further injury (94). In survivors of ARDS, this impaired regenerative capacity manifests as pulmonary fibrosis, characterized by reduced lung compliance and chronic respiratory dysfunction. These long-term consequences underscore the need for therapeutic strategies that can effectively mitigate ferroptosis and its downstream effects.

5 Therapeutic targeting of ferroptosis in ARDS

Given the central role of ferroptosis in ARDS pathogenesis, therapeutic strategies targeting ferroptotic pathways offer promising avenues to mitigate disease severity and improve outcomes. Interventions aimed at regulating oxidative stress, restoring antioxidant defenses, chelating iron, and preventing lipid peroxidation are at the forefront of these efforts (Figure 6).

5.1 Antioxidants and ROS inhibitors

Oxidative stress drives ferroptosis and contributes to the lung injury observed in ARDS. Antioxidants and ROS inhibitors aim to reduce oxidative damage by restoring redox balance. NAC serves as a precursor for glutathione (GSH) synthesis, a critical antioxidant that neutralizes ROS and protects cells from lipid peroxidation. By replenishing intracellular GSH levels, NAC helps restore the antioxidant capacity of lung cells and mitigate oxidative stress-induced ferroptosis (95, 96). MitoTEMPO: This mitochondrial-targeted antioxidant scavenges mitochondrial ROS, which play a significant role in initiating ferroptosis. MitoTEMPO's targeted action protects mitochondrial function and reduces lipid ROS formation, safeguarding both alveolar epithelial and endothelial cells from ferroptotic cell death (97). Emerging antioxidants designed to specifically target ROS in the lung microenvironment may provide further benefits in managing ARDS.

5.2 GPX4 activators

As a key regulator of ferroptosis, glutathione peroxidase 4 (GPX4) plays a critical role in preventing lipid peroxidation and maintaining

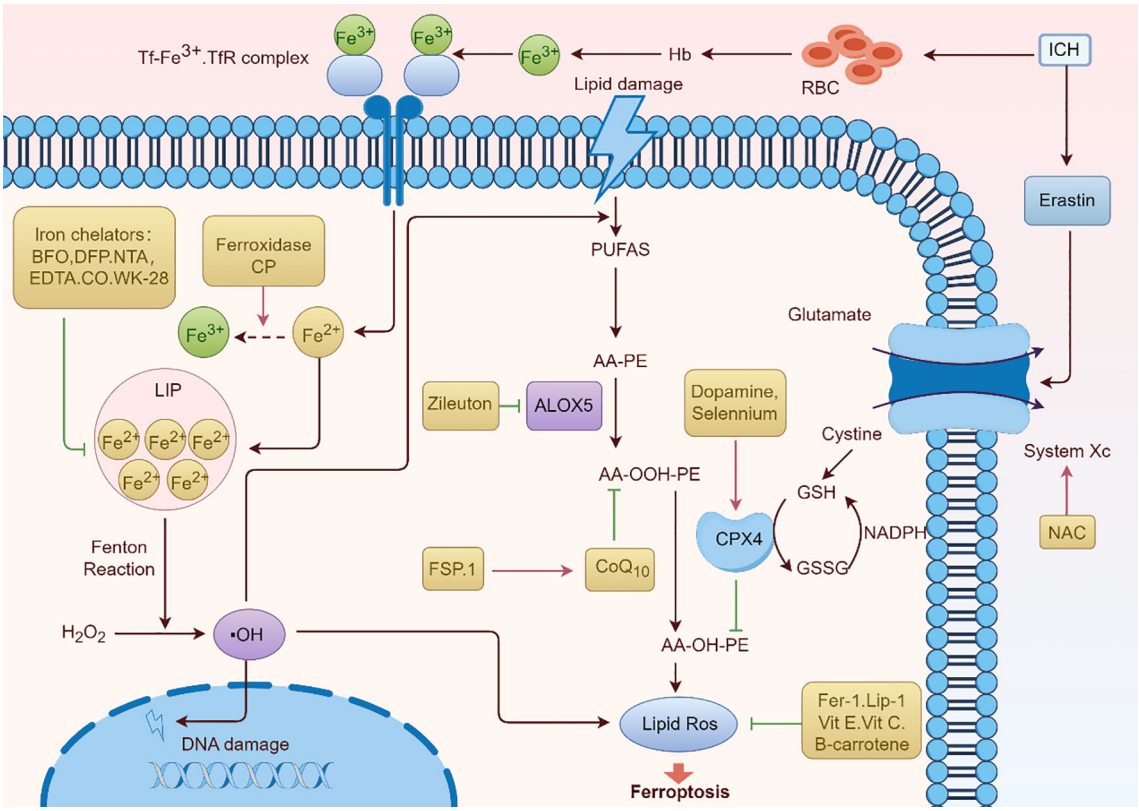

FIGURE 6
Ferroptosis pathway and potential therapeutic drugs for ARDS. The processes and mechanisms underlying ferroptosis, a type of controlled cell death marked by iron-dependent lipid peroxidation, are shown in Figure 6. Important elements like the Tf-Fe3+.TfR complex, which promotes iron absorption, and the function of hemoglobin (Hb) and red blood cells (RBC) in iron-related processes are highlighted in the image. It also demonstrates how lipid damage is involved and how iron chelators (like EDTA and DFP) and antioxidants (such NAC, vitamin E, and vitamin C) can protect against it. The figure depicts the contribution of enzymes such as ALOX5 and FSP.1 to lipid peroxidation, as well as the roles of glutathione (GSH) and NADPH in antioxidant defense. A thorough summary of the molecular processes underpinning ferroptosis is given in this graphic.

cellular homeostasis. GPX4 activators have shown promise in halting ferroptosis in preclinical studies. Ferrostatins (e.g., Fer-1)is the small molecules that inhibit lipid peroxidation by stabilizing GPX4 activity, thus preventing the ferroptotic death of lung cells (98). Fer-1 has been demonstrated to protect against oxidative injury in lung tissues by limiting the accumulation of toxic lipid hydroperoxides (99). RSL3 is a GPX4 inhibitor that drives ferroptosis by reducing the enzyme's activity. Therapeutics that block RSL3-mediated GPX4 inactivation may provide a targeted approach to preserving antioxidant capacity in ARDS patients, reducing the extent of ferroptosis-driven lung damage (13).

5.3 Iron chelators

Iron overload exacerbates ferroptosis by fueling ROS production and lipid peroxidation, making iron chelation a viable therapeutic approach. Deferoxamine is the first one. It is clinically established iron chelator binds excess free iron, thereby reducing its availability for the Fenton reaction and subsequent ROS generation. Deferoxamine has demonstrated efficacy in preclinical models of ARDS, where it mitigates iron-driven oxidative damage and inflammation (100). Another potent iron chelator, deferiprone, offers the advantage of oral administration. By limiting iron availability, it curtails ferroptotic damage in lung cells and supports redox balance during ARDS progression (101). Iron chelation therapies may also modulate downstream pro-inflammatory and pro-fibrotic effects linked to ferroptosis, underscoring their therapeutic potential in ARDS.

5.4 Targeting lipid peroxidation

Preventing lipid peroxidation is critical to halting ferroptosis in ARDS, as peroxidized lipids drive cellular dysfunction and death. Acyl-CoA synthetase long-chain family member 4 (ACSL4) facilitates the incorporation of PUFAs into membrane phospholipids, increasing their susceptibility to peroxidation. Inhibitors of ACSL4 reduce this vulnerability, preserving membrane integrity and protecting lung cells from ferroptotic injury (102). Therefore, ACSL4 inhibitor might be a potential therapeutic drug for ARDS. There is another one targeting lipid ROS scavengers. Compounds like liproxstatin-1 neutralize lipid peroxides, preventing their accumulation and halting ferroptosis. Liproxstatin-1 has shown potential in preclinical models of lung injury by reducing oxidative damage, inflammation, and vascular permeability (103). Future research may focus on optimizing the delivery of lipid ROS scavengers to the lungs, ensuring precise targeting of injured tissues while minimizing systemic side effects (Table 1).

6 Future directions and challenges

Despite significant advancements in understanding the role of ferroptosis in ARDS, several challenges remain in translating these findings into effective clinical strategies. Future research must address the gaps in biomarkers, subphenotype-specific mechanisms, and the integration of ferroptosis-targeted therapies into standard care.

6.1 Biomarkers of ferroptosis in ARDS

The identification of reliable biomarkers is critical for diagnosing ferroptosis-driven ARDS, stratifying patients for treatment, and monitoring therapeutic responses. Potential candidates include lipid peroxidation byproducts, such as malondialdehyde (MDA) and 4-hydroxynonenal (4-HNE), which are indicative of oxidative damage (104). Additionally, the measurement of glutathione peroxidase 4 (GPX4) activity and reduced glutathione (GSH) levels may serve as functional markers of ferroptosis susceptibility (105). Advanced lipidomic profiling and transcriptomic approaches could further refine biomarker discovery, enabling the differentiation of ferroptosis from other cell death pathways, such as apoptosis and necroptosis, in ARDS. The establishment of standardized protocols for biomarker assessment in clinical settings remains an ongoing challenge.

TABLE 1 Ferroptosis inhibitors and therapeutic potential in ARDS.

Inhibitor name	Dose	Cell/Animal model	Targeted cells	Molecular mechanisms
Dipyridamole (DIPY)	Not specified	LPS-induced acute lung injury mouse model, CLP-induced sepsis mouse model, Human airway organoids (HAOs)	Lung epithelial and endothelial cells	Downregulates heme oxygenase 1 (HMOX1) by binding to and activating superoxide dismutase 1 (SOD1), inhibiting the CREB1/HMOX1 pathway
Ferrostatin-1 (Fer-1)	2.5 μM/kg	LPS-induced ARDS mouse model	Alveolar epithelial cells	Inhibits ferroptosis, reduces lipid peroxidation, and protects against lung injury
Ferrostatin-1 (Fer-1)	Not specified	Sepsis mouse model, MLE-12 cells	Alveolar epithelial cells	Increases GPX4 expression, reduces lipid peroxidation, and inhibits ferroptosis
Hepcidin	Not specified	LPS-induced ARDS mouse model	Lung cells	Upregulates ferritin heavy chain (FTH) to reduce labile iron pool (LIP) and inhibit ferroptosis
Liproxstatin-1	Not specified	LPS/IL-13-induced bronchial epithelial cell injury and neutrophilic asthma mouse model	Bronchial epithelial cells	Inhibits ferroptosis and reduces inflammation
Panaxydol	Not specified	LPS-induced acute lung injury mouse model	Lung cells	Activates Keap1-Nrf2/HO-1 pathway to inhibit ferroptosis

6.2 Role of ferroptosis in ARDS subphenotypes

ARDS is a heterogenous syndrome with distinct subphenotypes, including hyperinflammatory and hypoinflammatory forms, which differ in pathophysiology, clinical presentation, and response to treatment. Investigating whether ferroptosis contributes differentially to these subphenotypes could provide valuable insights for personalized therapies. For instance, hyperinflammatory ARDS, characterized by excessive cytokine release and oxidative stress, may exhibit higher ferroptosis activity than hypoinflammatory ARDS. Identifying these differences through advanced molecular and imaging techniques could help tailor ferroptosis-targeted interventions to specific subphenotypes, optimizing therapeutic efficacy. Further exploration of animal models and patient-derived organoid systems may facilitate these investigations.

6.3 Combining ferroptosis inhibition with standard therapies

Integrating ferroptosis-targeted therapies with existing ARDS interventions, such as corticosteroids, immunomodulators, or mechanical ventilation, presents both opportunities and challenges. While corticosteroids may alleviate inflammation, they could interact with ferroptosis inhibitors in unpredictable ways, necessitating careful evaluation of combinatorial effects. Additionally, mechanical ventilation, a cornerstone of ARDS management, may influence ferroptosis through ventilation-induced oxidative stress, further complicating treatment strategies. Future clinical trials should investigate the safety, timing, and dosing of ferroptosis inhibitors when combined with standard-of-care therapies. Preclinical studies exploring the synergistic effects of such combinations are also essential for advancing this approach.

Efforts to optimize drug delivery systems, such as nanoparticle-based carriers, may enhance the precision and efficacy of ferroptosis inhibitors while minimizing off-target effects. Furthermore, addressing the challenges of patient heterogeneity, drug resistance, and adverse effects will be critical for the successful translation of ferroptosis-targeted therapies into clinical practice.

7 Conclusion

Maintaining a balance between cell survival and regulated cell death pathways is fundamental to preserving tissue integrity and immune homeostasis in ARDS. While apoptosis plays a protective role in clearing infected cells in a controlled manner, its dysregulation can lead to immune overactivation, exacerbating inflammation and tissue damage. In contrast, ferroptosis has emerged as a key driver of ARDS pathogenesis, contributing to epithelial and endothelial cell injury, oxidative stress, and immune dysfunction.

Therapeutic targeting of ferroptosis holds great promise for mitigating ARDS severity. Antioxidants and ROS inhibitors reduce oxidative damage, iron chelators limit iron-mediated toxicity, and GPX4 activators preserve cellular antioxidant capacity, collectively offering a multifaceted approach to suppressing ferroptosis in the injured lung. However, several challenges remain, including the identification of reliable biomarkers, understanding subphenotype-specific mechanisms, and integrating ferroptosis inhibitors into existing therapeutic frameworks.

Future research should prioritize addressing these challenges to enhance the clinical translation of ferroptosis-targeted therapies. Combining these innovative approaches with personalized medicine strategies may not only improve outcomes for ARDS patients but also provide valuable insights into the broader implications of ferroptosis in critical illness. By bridging gaps in knowledge and practice, therapeutic targeting of ferroptosis offers the potential to transform ARDS management and improve patient survival.

Author contributions

MY: Writing – original draft. ZL: Writing – original draft. WZ: Writing – original draft. SS: Conceptualization, Investigation, Supervision, Writing – review & editing. XH: Conceptualization, Funding acquisition, Investigation, Project administration, Supervision, Writing – review & editing. YW: Conceptualization, Investigation, Project administration, Supervision, Validation, Writing – review & editing. JL: Writing – original draft.

Funding

The author(s) declare that financial support was received for the research and/or publication of this article. This research was supported by the National Natural Science Foundation of China This study was supported by the National Natural Science Foundation of China (81802504), the Sichuan Science and Technology Program (2025YFHZ0123), Chengdu Science and Technology Program (2024-YF05-01315-SN), and a grant from Shenzhen Weixin (2024HX008) for YW.

Acknowledgments

All the figures are drawn by FigDraw (www.figdraw.com).

Conflict of interest

The authors declare that the research was conducted in the absence of any commercial or financial relationships that could be construed as a potential conflict of interest.

Generative AI statement

The author(s) declare that no Generative AI was used in the creation of this manuscript.

Publisher's note

References

1. Bos LDJ, Ware LB. Acute respiratory distress syndrome: causes, pathophysiology, and phenotypes. *Lancet*. (2022) 400:1145–56. doi: 10.1016/S0140-6736(22)01485-4

2. Gorman EA, O'Kane CM, McAuley DF. Acute respiratory distress syndrome in adults: diagnosis, outcomes, long-term sequelae, and management. *Lancet*. (2022) 400:1157–70. doi: 10.1016/S0140-6736(22)01439-8

3. Matthay MA, Zemans RL, Zimmerman GA, Arabi YM, Beitler JR, Mercat A, et al. Acute respiratory distress syndrome. *Nat Rev Dis Primers*. (2019) 5:18. doi: 10.1038/s41572-019-0069-0

4. Swenson KE, Swenson ER. Pathophysiology of acute respiratory distress syndrome and COVID-19 lung injury. *Crit Care Clin*. (2021) 37:749–76. doi: 10.1016/j.ccc.2021.05.003

5. Xu Z, Shi L, Wang Y, Zhang J, Huang L, Zhang C, et al. Pathological findings of COVID-19 associated with acute respiratory distress syndrome. *Lancet Respir Med*. (2020) 8:420–2. doi: 10.1016/S2213-2600(20)30076-X

6. Potey PM, Rossi AG, Lucas CD, Dorward DA. Neutrophils in the initiation and resolution of acute pulmonary inflammation: understanding biological function and therapeutic potential. *J Pathol*. (2019) 247:672–85. doi: 10.1002/path.5221

7. Liu C, Xiao K, Xie L. Progress in preclinical studies of macrophage autophagy in the regulation of ALI/ARDS. *Front Immunol*. (2022) 13:922702. doi: 10.3389/fimmu.2022.922702

8. Huppert LA, Matthay MA, Ware LB. Pathogenesis of acute respiratory distress syndrome. *Semin Respir Crit Care Med*. (2019) 40:31–9. doi: 10.1055/s-0039-1683996

9. Zheng Y, Huang Y, Xu Y, Sang L, Liu X, Li Y. Ferroptosis, pyroptosis and necroptosis in acute respiratory distress syndrome. *Cell Death Discov*. (2023) 9:91. doi: 10.1038/s41420-023-01369-2

10. Yuan C, Ma Z, Xie J, Li W, Su L, Zhang G, et al. The role of cell death in SARS-CoV-2 infection. *Signal Transduct Target Ther*. (2023) 8:357. doi: 10.1038/s41392-023-01580-8

11. Wang S, Guo Q, Zhou L, Xia X. Ferroptosis: A double-edged sword. *Cell Death Discov*. (2024) 10:265. doi: 10.1038/s41420-024-02037-9

12. Qu M, Zhang H, Chen Z, Sun X, Zhu S, Nan K, et al. The role of ferroptosis in acute respiratory distress syndrome. *Front Med (Lausanne)*. (2021) 8:651552. doi: 10.3389/fmed.2021.651552

13. Ma TL, Zhou Y, Wang C, Wang L, Chen JX, Yang HH, et al. Targeting ferroptosis for lung diseases: exploring novel strategies in ferroptosis-associated mechanisms. *Oxid Med Cell Longev*. (2021) 2021:1098970. doi: 10.1155/2021/1098970

14. Matute-Bello G, Martin TR. Science review: apoptosis in acute lung injury. *Crit Care*. (2003) 7:355–8. doi: 10.1186/cc1861

15. Yan HF, Zou T, Tuo QZ, Xu S, Li H, Belaidi AA, et al. Ferroptosis: mechanisms and links with diseases. *Signal Transduct Target Ther*. (2021) 6:49. doi: 10.1038/s41392-020-00428-9

16. Feng H, Stockwell BR. Unsolved mysteries: How does lipid peroxidation cause ferroptosis? *PloS Biol*. (2018) 16:e2006203. doi: 10.1371/journal.pbio.2006203

17. Feng S, Tang D, Wang Y, Li X, Bao H, Tang C, et al. The mechanism of ferroptosis and its related diseases. *Mol Biomed*. (2023) 4:33. doi: 10.1186/s43556-023-00142-2

18. Ru Q, Li Y, Chen L, Wu Y, Min J, Wang F. Iron homeostasis and ferroptosis in human diseases: mechanisms and therapeutic prospects. *Signal Transduct Target Ther*. (2024) 9:271. doi: 10.1038/s41392-024-01969-z

19. Zhou Q, Meng Y, Le J, Sun Y, Dian Y, Yao L, et al. Ferroptosis: mechanisms and therapeutic targets. *MedComm (2020)*. (2024) 5:e70010. doi: 10.1002/mco2.70010

20. Kellner M, NooNepalle S, Lu Q, Srivastava A, Zemskov E, Black SM. ROS signaling in the pathogenesis of acute lung injury (ALI) and acute respiratory distress syndrome (ARDS). *Adv Exp Med Biol*. (2017) 967:105–37. doi: 10.1007/978-3-319-63245-2_8

21. Endale HT, Tesfaye W, Mengstie TA. ROS induced lipid peroxidation and their role in ferroptosis. *Front Cell Dev Biol*. (2023) 11:1226044. doi: 10.3389/fcell.2023.1226044

22. Gao M, Yi J, Zhu J, Minikes AM, Monian P, Thompson CB, et al. Role of mitochondria in ferroptosis. *Mol Cell*. (2019) 73:354–63.e3. doi: 10.1016/j.molcel.2018.10.042

23. Huang Q, Le Y, Li S, Bian Y. Signaling pathways and potential therapeutic targets in acute respiratory distress syndrome (ARDS). *Respir Res*. (2024) 25:30. doi: 10.1186/s12931-024-02678-5

24. Chen J, Zhu H, Chen Q, Yang Y, Chen M, Huang J, et al. The role of ferroptosis in chronic intermittent hypoxia-induced lung injury. *BMC Pulm Med*. (2022) 22:488. doi: 10.1186/s12890-022-02262-x

25. Cherian SV, Kumar A, Akasapu K, Ashton RW, Aparnath M, Malhotra A. Salvage therapies for refractory hypoxemia in ARDS. *Respir Med*. (2018) 141:150–8. doi: 10.1016/j.rmed.2018.06.030

26. Chen L, Yang J, Zhang M, Fu D, Luo H, Yang X. SPP1 exacerbates ARDS via elevating Th17/Treg and M1/M2 ratios through suppression of ubiquitination-dependent HIF-1alpha degradation. *Cytokine*. (2023) 164:156107. doi: 10.1016/j.cyto.2022.156107

27. Liu XQ, Shi MZ, Bai YT, Su XL, Liu YM, Wu JC, et al. Hypoxia and ferroptosis. *Cell Signal*. (2024) 122:111328. doi: 10.1016/j.cellsig.2024.111328

28. Wang B, Wang Y, Zhang J, Hu C, Jiang J, Li Y, et al. ROS-induced lipid peroxidation modulates cell death outcome: mechanisms behind apoptosis, autophagy, and ferroptosis. *Arch Toxicol*. (2023) 97:1439–51. doi: 10.1007/s00204-023-03476-6

29. Tang X, Liu J, Yao S, Zheng J, Gong X, Xiao B. Ferulic acid alleviates alveolar epithelial barrier dysfunction in sepsis-induced acute lung injury by activating the Nrf2/HO-1 pathway and inhibiting ferroptosis. *Pharm Biol*. (2022) 60:2286–94. doi: 10.1080/13880209.2022.2147549

30. Lee YS, Lee DH, Choudry HA, Bartlett DL, Lee YJ. Ferroptosis-induced endoplasmic reticulum stress: cross-talk between ferroptosis and apoptosis. *Mol Cancer Res*. (2018) 16:1073–6. doi: 10.1158/1541-7786.MCR-18-0055

31. Su LJ, Zhang JH, Gomez H, Murugan R, Hong X, Xu D, et al. Reactive oxygen species-induced lipid peroxidation in apoptosis, autophagy, and ferroptosis. *Oxid Med Cell Longev*. (2019) 2019:5080843. doi: 10.1155/2019/5080843

32. Yang J, Hu S, Bian Y, Yao J, Wang D, Liu X, et al. Targeting cell death: pyroptosis, ferroptosis, apoptosis and necroptosis in osteoarthritis. *Front Cell Dev Biol*. (2021) 9:789948. doi: 10.3389/fcell.2021.789948

33. Tang R, Xu J, Zhang B, Liu J, Liang C, Hua J, et al. Ferroptosis, necroptosis, and pyroptosis in anticancer immunity. *J Hematol Oncol*. (2020) 13:110. doi: 10.1186/s13045-020-00946-7

34. Qu M, Wang Y, Qiu Z, Zhu S, Guo K, Chen W, et al. Necroptosis, pyroptosis, ferroptosis in sepsis and treatment. *Shock*. (2022) 57:161–71. doi: 10.1097/SHK.0000000000001936

35. Minagawa S, Yoshida M, Araya J, Hara H, Imai H, Kuwano K. Regulated necrosis in pulmonary disease. A focus on necroptosis and ferroptosis. *Am J Respir Cell Mol Biol*. (2020) 62:554–62. doi: 10.1165/rcmb.2019-0337TR

36. Liu Y, Wan Y, Jiang Y, Zhang L, Cheng W. GPX4: The hub of lipid oxidation, ferroptosis, disease and treatment. *Biochim Biophys Acta Rev Cancer*. (2023) 1878:188890. doi: 10.1016/j.bbcan.2023.188890

37. Kang R, Kroemer G, Tang D. The tumor suppressor protein p53 and the ferroptosis network. *Free Radic Biol Med*. (2019) 133:162–8. doi: 10.1016/j.freeradbiomed.2018.05.074

38. Baiskhanova D, Schafer H. The role of Nrf2 in the regulation of mitochondrial function and ferroptosis in pancreatic cancer. *Antioxidants (Basel)*. (2024) 13(6):696. doi: 10.3390/antiox13060696

39. Qi X, Luo Y, Xiao M, Zhang Q, Luo J, Ma L, et al. Mechanisms of alveolar type 2 epithelial cell death during acute lung injury. *Stem Cells*. (2023) 41:1113–32. doi: 10.1093/stmcls/sxad074

40. Wang Y, Wang L, Ma S, Cheng L, Yu G. Repair and regeneration of the alveolar epithelium in lung injury. *FASEB J*. (2024) 38:e23612. doi: 10.1096/fj.202400088R

41. Wang Y, Duan H, Zhang J, Wang Q, Peng T, Ye X, et al. YAP1 protects against PM2.5-induced lung toxicity by suppressing pyroptosis and ferroptosis. *Ecotoxicol Environ Saf*. (2023) 253:114708. doi: 10.1016/j.ecoenv.2023.114708

42. Cheng H, Feng D, Li X, Gao L, Tang S, Liu W, et al. Iron deposition-induced ferroptosis in alveolar type II cells promotes the development of pulmonary fibrosis. *Biochim Biophys Acta Mol Basis Dis*. (2021) 1867:166204. doi: 10.1016/j.bbadis.2021.166204

43. Jiang W, Ren J, Zhou H, He R, Li D, Xiong R, et al. TMEM16A deficiency in alveolar type 2 epithelial cells protected against endoplasmic reticulum stress-induced ferroptosis during acute lung injury. *Int Immunopharmacol*. (2023) 125:111208. doi: 10.1016/j.intimp.2023.111208

44. Zhang W, Sun Z, Cheng W, Li X, Zhang J, Li Y, et al. Impaired GPX4 activity elicits ferroptosis in alveolar type II cells promoting PHMG-induced pulmonary

fibrosis development. *Ecotoxicol Environ Saf*. (2024) 281:116680. doi: 10.1016/j.ecoenv.2024.116680

45. Chen Z, Tang H, Gan S, Yang C, Li S, Li J, et al. Ferroptosis mediates airway epithelial E-cadherin dysfunction in LPS-induced acute lung injury. *Pulm Pharmacol Ther*. (2024) 84:102284. doi: 10.1016/j.pupt.2023.102284

46. Wang Y, Chen D, Xie H, Jia M, Sun X, Peng F, et al. AUF1 protects against ferroptosis to alleviate sepsis-induced acute lung injury by regulating NRF2 and ATF3. *Cell Mol Life Sci*. (2022) 79:228. doi: 10.1007/s00018-022-04248-8

47. Wang W, Xu R, He P, Xiong Y, Zhao H, Fu X, et al. CircEXOC5 aggravates sepsis-induced acute lung injury by promoting ferroptosis through the IGF2BP2/ATF3 axis. *J Infect Dis*. (2024) 229:522–34. doi: 10.1093/infdis/jiad337

48. Lv Y, Chen D, Tian X, Xiao J, Xu C, Du L, et al. Protectin conjugates in tissue regeneration 1 alleviates sepsis-induced acute lung injury by inhibiting ferroptosis. *J Transl Med*. (2023) 21:293. doi: 10.1186/s12967-023-04111-9

49. Chen X, Shen J, Jiang X, Pan M, Chang S, Li J, et al. Characterization of dipyridamole as a novel ferroptosis inhibitor and its therapeutic potential in acute respiratory distress syndrome management. *Theranostics*. (2024) 14:6947–68. doi: 10.7150/thno.102318

50. Liu Y, Zhang X, Cao Y, Chen X, Zhu J, Zou Y. Ferrostatin-1 ameliorated oxidative lipid damage in LPS-induced acute lung injury. *J Surg Res*. (2023) 290:266–75. doi: 10.1016/j.jss.2023.05.006

51. Li J, Lu K, Sun F, Tan S, Zhang X, Sheng W, et al. Panaxydol attenuates ferroptosis against LPS-induced acute lung injury in mice by Keap1-Nrf2/HO-1 pathway. *J Transl Med*. (2021) 19:96. doi: 10.1186/s12967-021-02745-1

52. Su Y, Lucas R, Fulton DJR, Verin AD. Mechanisms of pulmonary endothelial barrier dysfunction in acute lung injury and acute respiratory distress syndrome. *Chin Med J Pulm Crit Care Med*. (2024) 2:80–7. doi: 10.1016/j.pccm.2024.04.002

53. Yang L, Cao LM, Zhang XJ, Chu B. Targeting ferroptosis as a vulnerability in pulmonary diseases. *Cell Death Dis*. (2022) 13:649. doi: 10.1038/s41419-022-05070-7

54. Zheng D, Liu J, Piao H, Zhu Z, Wei R, Liu K. ROS-triggered endothelial cell death mechanisms: Focus on pyroptosis, parthanatos, and ferroptosis. *Front Immunol*. (2022) 13:1039241. doi: 10.3389/fimmu.2022.1039241

55. Zou X, Liu C, Huang Z, Xiang S, Li K, Yuan Y, et al. Inhibition of STEAP1 ameliorates inflammation and ferroptosis of acute lung injury caused by sepsis in LPS-induced human pulmonary microvascular endothelial cells. *Mol Biol Rep*. (2023) 50:5667–74. doi: 10.1007/s11033-023-08403-7

56. Ghio AJ, Carter JD, Richards JH, Richer LD, Grissom CK, Elstad MR. Iron and iron-related proteins in the lower respiratory tract of patients with acute respiratory distress syndrome. *Crit Care Med*. (2003) 31:395–400. doi: 10.1097/01.CCM.0000050284.35609.97

57. Xing L, Dong W, Chen Y, Dai W, Xiao X, Liu Z, et al. Fibroblast ferroptosis is involved in periodontitis-induced tissue damage and bone loss. *Int Immunopharmacol*. (2023) 114:109607. doi: 10.1016/j.intimp.2022.109607

58. Cheng HP, Feng DD, Li XH, Gao LH, Qiu YJ, Liang XY, et al. NMDA receptor activation induces damage of alveolar type II cells and lung fibrogenesis through ferroptosis. *Biochim Biophys Acta Mol Cell Res*. (2023) 1870:119535. doi: 10.1016/j.bbamcr.2023.119535

59. Feng Z, Meng F, Huo F, Zhu Y, Qin Y, Gui Y, et al. Inhibition of ferroptosis rescues M2 macrophages and alleviates arthritis by suppressing the HMGB1/TLR4/STAT3 axis in M1 macrophages. *Redox Biol*. (2024) 75:103255. doi: 10.1016/j.redox.2024.103255

60. Jiang Q, Wan R, Jiang J, Li T, Li Y, Yu S, et al. Interaction between macrophages and ferroptosis: Metabolism, function, and diseases. *Chin Med J (Engl)*. (2024) 138:509–22. doi: 10.1097/CM9.0000000000003189

61. Yang Y, Wang Y, Guo L, Gao W, Tang TL, Yan M. Interaction between macrophages and ferroptosis. *Cell Death Dis*. (2022) 13:355. doi: 10.1038/s41419-022-04775-z

62. Wu J, Liu Q, Zhang X, Tan M, Li X, Liu P, et al. The interaction between STING and NCOA4 exacerbates lethal sepsis by orchestrating ferroptosis and inflammatory responses in macrophages. *Cell Death Dis*. (2022) 13:653. doi: 10.1038/s41419-022-05115-x

63. Jiao Y, Yong C, Zhang R, Qi D, Wang D. Hepcidin alleviates LPS-induced ARDS by regulating the ferritin-mediated suppression of ferroptosis. *Shock*. (2022) 57:274–81. doi: 10.1097/SHK.0000000000001941

64. Xu W, Wu Y, Wang S, Hu S, Wang Y, Zhou W, et al. Melatonin alleviates septic ARDS by inhibiting NCOA4-mediated ferritinophagy in alveolar macrophages. *Cell Death Discov*. (2024) 10:253. doi: 10.1038/s41420-024-01991-8

65. Kim R, Hashimoto A, Markosyan N, Tyurin VA, Tyurina YY, Kar G, et al. Ferroptosis of tumour neutrophils causes immune suppression in cancer. *Nature*. (2022) 612:338–46. doi: 10.1038/s41586-022-05443-0

66. Zhang H, Liu J, Zhou Y, Qu M, Wang Y, Guo K, et al. Neutrophil extracellular traps mediate m(6)A modification and regulates sepsis-associated acute lung injury by activating ferroptosis in alveolar epithelial cells. *Int J Biol Sci*. (2022) 18:3337–57. doi: 10.7150/ijbs.69141

67. Li P, Jiang M, Li K, Li H, Zhou Y, Xiao X, et al. Glutathione peroxidase 4-regulated neutrophil ferroptosis induces systemic autoimmunity. *Nat Immunol*. (2021) 22:1107–17. doi: 10.1038/s41590-021-00993-3

68. Wang T, Zhang Z, Deng Z, Zeng W, Gao Y, Hei Z, et al. Mesenchymal stem cells alleviate sepsis-induced acute lung injury by blocking neutrophil extracellular traps formation and inhibiting ferroptosis in rats. *PeerJ*. (2024) 12:e16748. doi: 10.7717/peerj.16748

69. Wen Q, Liu J, Kang R, Zhou B, Tang D. The release and activity of HMGB1 in ferroptosis. *Biochem Biophys Res Commun*. (2019) 510:278–83. doi: 10.1016/j.bbrc.2019.01.090

70. Risso K, Kumar G, Ticchioni M, Sanfiorenzo C, Dellamonica J, Guillouet-de Salvador F, et al. Early infectious acute respiratory distress syndrome is characterized by activation and proliferation of alveolar T-cells. *Eur J Clin Microbiol Infect Dis*. (2015) 34:1111–8. doi: 10.1007/s10096-015-2333-x

71. Yang B, Hou S, Huang S, Li H, Li Y. Ferroptosis inhibitor regulates the disease progression of systematic lupus erythematosus mice model through Th1/Th2 ratio. *Curr Mol Med*. (2023) 23:799–807. doi: 10.2174/1566524022666220525144630

72. Ma L, He Y, Xie H, Wang J, Chen J, Song S, et al. Ferroptotic alveolar epithelial type II cells drive T(H)2 and T(H)17 mixed asthma triggered by birch pollen allergen Bet v 1. *Cell Death Discov*. (2024) 10:96. doi: 10.1038/s41420-024-01861-3

73. Liu Y, Zhang W, Wang H, Liu H, Yu Q, Luo X, et al. Fine particulate matter potentiates Th17-cell pathogenicity in experimental autoimmune uveitis via ferroptosis. *Ecotoxicol Environ Saf*. (2024) 284:116979. doi: 10.1016/j.ecoenv.2024.116979

74. Zhang J, Ding W, Yin Z, Liu S, Zhao M, Xu Y, et al. Interleukin-12p40 deficiency attenuates myocardial ferroptosis in doxorubicin-induced chronic cardiomyopathy by inhibiting Th17 differentiation and interleukin-17A production. *Cardiovasc Res*. (2024) 120:2117–33. doi: 10.1093/cvr/cvae208

75. Lu KC, Tsai KW, Wang YK, Hu WC. Types of cell death and their relations to host immunological pathways. *Aging (Albany NY)*. (2024) 16:11755–68. doi: 10.18632/aging.206035

76. Hu Y, Chen D, Hong M, Liu J, Li Y, Hao J, et al. Apoptosis, pyroptosis, and ferroptosis conspiringly induce immunosuppressive hepatocellular carcinoma microenvironment and gammadelta T-cell imbalance. *Front Immunol*. (2022) 13:845974. doi: 10.3389/fimmu.2022.845974

77. Li GG, Cao YH, Run Y, Xu RX, Zheng ZD. Inhibition of CD8(+) T cells and elimination of myeloid cells by CD4(+) Foxp3(-) T regulatory type 1 cells in acute respiratory distress syndrome. *Clin Exp Pharmacol Physiol*. (2016) 43:1191–8. doi: 10.1111/1440-1681.12656

78. Wang W, Green M, Choi JE, Gijon M, Kennedy PD, Johnson JK, et al. CD8(+) T cells regulate tumour ferroptosis during cancer immunotherapy. *Nature*. (2019) 569:270–4. doi: 10.1038/s41586-019-1170-y

79. Anft M, Paniskaki K, Blazquez-Navarro A, Doevelaar A, Seibert FS, Holzer B, et al. COVID-19-induced ARDS is associated with decreased frequency of activated memory/effector T cells expressing CD11a(+). *Mol Ther*. (2020) 28:2691–702. doi: 10.1016/j.ymthe.2020.10.001

80. Aziz M, Ode Y, Zhou M, Ochani M, Holodick NE, Rothstein TL, et al. B-1a cells protect mice from sepsis-induced acute lung injury. *Mol Med*. (2018) 24:26. doi: 10.1186/s10020-018-0029-2

81. Chen Q, Xiang M, Gao Z, Lvu F, Sun Z, Wang Y, et al. The role of B-cell ferroptosis in the pathogenesis of systemic lupus erythematosus. *Clin Immunol*. (2023) 256:109778. doi: 10.1016/j.clim.2023.109778

82. Dang Q, Sun Z, Wang Y, Wang L, Liu Z, Han X. Ferroptosis: a double-edged sword mediating immune tolerance of cancer. *Cell Death Dis*. (2022) 13:925. doi: 10.1038/s41419-022-05384-6

83. Ou Y, Wang SJ, Li D, Chu B, Gu W. Activation of SAT1 engages polyamine metabolism with p53-mediated ferroptotic responses. *Proc Natl Acad Sci U S A*. (2016) 113:E6806–E12. doi: 10.1073/pnas.1607152113

84. Chen F, Tang H, Cai X, Lin J, Kang R, Tang D, et al. DAMPs in immunosenescence and cancer. *Semin Cancer Biol*. (2024) 106-107:123–42. doi: 10.1016/j.semcancer.2024.09.005

85. Bradford HF, McDonnell TCR, Stewart A, Skelton A, Ng J, Baig Z, et al. Thioredoxin is a metabolic rheostat controlling regulatory B cells. *Nat Immunol*. (2024) 25:873–85. doi: 10.1038/s41590-024-01798-w

86. Saguil A, Fargo MV. Acute respiratory distress syndrome: diagnosis and management. *Am Fam Physician*. (2020) 101:730–8.

87. Cao JK, Hong XY, Feng ZC, Li QP. Mesenchymal stem cells-based therapies for severe ARDS with ECMO: a review. *Intensive Care Med Exp*. (2024) 12:12. doi: 10.1186/s40635-024-00596-w

88. Antebi B, Mohammadipoor A, Batchinsky AI, Cancio LC. The promise of mesenchymal stem cell therapy for acute respiratory distress syndrome. *J Trauma Acute Care Surg*. (2018) 84:183–91. doi: 10.1097/TA.0000000000001713

89. Lin F, Chen W, Zhou J, Zhu J, Yao Q, Feng B, et al. Mesenchymal stem cells protect against ferroptosis via exosome-mediated stabilization of SLC7A11 in acute liver injury. *Cell Death Dis*. (2022) 13:271. doi: 10.1038/s41419-022-04708-w

90. Liu M, Kong XY, Yao Y, Wang XA, Yang W, Wu H, et al. The critical role and molecular mechanisms of ferroptosis in antioxidant systems: a narrative review. *Ann Transl Med*. (2022) 10:368. doi: 10.21037/atm-21-6942

91. Bezerra FS, Lanzetti M, Nesi RT, Nagato AC, Silva CPE, Kennedy-Feitosa E, et al. Oxidative stress and inflammation in acute and chronic lung injuries. *Antioxidants (Basel)*. (2023) 12(3):548. doi: 10.3390/antiox12030548

92. Li J, Jia YC, Ding YX, Bai J, Cao F, Li F. The crosstalk between ferroptosis and mitochondrial dynamic regulatory networks. *Int J Biol Sci*. (2023) 19:2756–71. doi: 10.7150/ijbs.83348

93. Hu Y, Huang Y, Zong L, Lin J, Liu X, Ning S. Emerging roles of ferroptosis in pulmonary fibrosis: current perspectives, opportunities and challenges. *Cell Death Discov*. (2024) 10:301. doi: 10.1038/s41420-024-02078-0

94. Yin X, Zhu G, Wang Q, Fu YD, Wang J, Xu B. Ferroptosis, a new insight into acute lung injury. *Front Pharmacol*. (2021) 12:709538. doi: 10.3389/fphar.2021.709538

95. Atkuri KR, Mantovani JJ, Herzenberg LA, Herzenberg LA. N-Acetylcysteine–a safe antidote for cysteine/glutathione deficiency. *Curr Opin Pharmacol*. (2007) 7:355–9. doi: 10.1016/j.coph.2007.04.005

96. Li Q, Liao J, Chen W, Zhang K, Li H, Ma F, et al. NAC alleviative ferroptosis in diabetic nephropathy via maintaining mitochondrial redox homeostasis through activating SIRT3-SOD2/Gpx4 pathway. *Free Radic Biol Med*. (2022) 187:158–70. doi: 10.1016/j.freeradbiomed.2022.05.024

97. Guo J, Zhou Y, Liu D, Wang M, Wu Y, Tang D, et al. Mitochondria as multifaceted regulators of ferroptosis. *Life Metab*. (2022) 1:134–48. doi: 10.1093/lifemeta/loac035

98. Skouta R, Dixon SJ, Wang J, Dunn DE, Orman M, Shimada K, et al. Ferrostatins inhibit oxidative lipid damage and cell death in diverse disease models. *J Am Chem Soc*. (2014) 136:4551–6. doi: 10.1021/ja411006a

99. Liu P, Feng Y, Li H, Chen X, Wang G, Xu S, et al. Ferrostatin-1 alleviates lipopolysaccharide-induced acute lung injury via inhibiting ferroptosis. *Cell Mol Biol Lett*. (2020) 25:10. doi: 10.1186/s11658-020-00205-0

100. Ameri A, Pourseyedi F, Davoodian P, Safa O, Hassanipour S, Fathalipour M. Efficacy and safety of deferoxamine in moderately ill COVID-19 patients: An open label, randomized controlled trial. *Med (Baltimore)*. (2024) 103:e39142. doi: 10.1097/MD.0000000000039142

101. Kontoghiorghes GJ. Deferiprone: A forty-year-old multi-targeting drug with possible activity against COVID-19 and diseases of similar symptomatology. *Int J Mol Sci*. (2022) 23(12):6735. doi: 10.3390/ijms23126735

102. Liu Y, Bao D, She H, Zhang Z, Shao S, Wu Z, et al. Role of Hippo/ACSL4 axis in ferroptosis-induced pericyte loss and vascular dysfunction in sepsis. *Redox Biol*. (2024) 78:103353. doi: 10.1016/j.redox.2024.103353

103. Zhao J, Li J, Wei D, Gao F, Yang X, Yue B, et al. Liproxstatin-1 alleviates lung transplantation-induced cold ischemia-reperfusion injury by inhibiting ferroptosis. *Transplantation*. (2023) 107:2190–202. doi: 10.1097/TP.0000000000004638

104. Stojkovic L, Djordjevic A, Stefanovic M, Stankovic A, Dincic E, Djuric T, et al. Circulatory indicators of lipid peroxidation, the driver of ferroptosis, reflect differences between relapsing-remitting and progressive multiple sclerosis. *Int J Mol Sci*. (2024) 25 (20):11024. doi: 10.3390/ijms252011024

105. Zhang W, Liu Y, Liao Y, Zhu C, Zou Z. GPX4, ferroptosis, and diseases. *BioMed Pharmacother*. (2024) 174:116512. doi: 10.1016/j.biopha.2024.116512

Frontiers in
Cell and Developmental Biology

Explores the fundamental biological processes of life, covering intracellular and extracellular dynamics.

The world's most cited developmental biology journal, advancing our understanding of the fundamental processes of life. It explores a wide spectrum of cell and developmental biology, covering intracellular and extracellular dynamics.

Discover the latest Research Topics

See more →

Frontiers

Avenue du Tribunal-Fédéral 34
1005 Lausanne, Switzerland
frontiersin.org

Contact us

+41 (0)21 510 17 00
frontiersin.org/about/contact